Title

Utilization of the beta-Lactam Core Towards the Preparation of Chiral Ring-Fused Lactams and Preparation and Application of Synthetic Peptide Libraries Toward the Discovery and Understanding of Membrane-Permeable Macrocycles

Author

Hewitt, William Merton

Publication Date

2014

Peer reviewed|Thesis/dissertation

UNIVERSITY OF CALIFORNIA

SANTA CRUZ

Utilization of the β-Lactam Core Towards the Preparation of Chiral Ring-Fused Lactams and Preparation and Application of Synthetic Peptide Libraries Toward the Discovery and Understanding of Membrane-Permeable Macrocycles

A dissertation submitted in partial satisfaction
of the requirements for the degree of

DOCTOR OF PHILOSOPHY

in

CHEMISTRY AND BIOCHEMISTRY

by

William Merton Hewitt

December 2014

The Dissertation of William Merton Hewitt
is approved:

_____
Professor R. Scott Lokey, Advisor

_____
Professor Joseph P. Konopelski, Chair

_____
Professor Roger Linington

_____
Tyrus Miller
Vice Provost and Dean of Graduate Studies

Table of Contents

Chapter 2: Cell-permeable cyclic peptides from synthetic libraries inspired by natural products.

Chapter 3: Investigation of the Influence of Lipophilicity and Molecular Weight on Passive Membrane Permeation of Cyclic Peptides

List of Figures

List of Schemes

List of Tables

Abstract

Title: Utilization of the β-Lactam Core Towards the Preparation of Chiral Ring-Fused Lactams and Preparation and Application of Synthetic Peptide Libraries Toward the Discovery and Understanding of Membrane-Permeable Macrocycles.

Author: William Merton Hewitt

The β-lactam synthon method is an established technique utilizing β-lactams in natural product synthesis. Through application of our previously described novel β-lactam preparation, we describe the C3 functionalization and application of previously described and novel β-lactams towards the synthesis of pactamycin—a densely functionalized cyclopentane natural product—and non-natural analogs of salinosporamide A—a proteasome inhibitor currently in clinical trials for treatment of multiple myeloma.

Additionally, we present a methodology for the discovery of geometrically diverse, membrane permeable cyclic peptide scaffolds based on the synthesis and permeability screening of a combinatorial library, followed by deconvolution of membrane-permeable scaffolds to identify cyclic peptides with good to excellent passive cell permeabilities. We use a combination of experimental and computational approaches to investigate structure-permeability relationships in one of these scaffolds, and uncover structural and conformational factors that govern passive membrane diffusion in a related set of cyclic peptide diastereomers. Further, we investigate the dependency of permeability on side chain identity of one of these scaffolds through single-point diversifications to show the adaptability of these scaffolds towards development of permeability-biased libraries suitable for bioactivity screens. Overall, our results demonstrate that many novel, cell

permeable scaffolds exist beyond those found in extant natural products, and that such scaffolds can be rapidly identified using a combination of synthesis and deconvolution which can, in principle, be applied to any type of macrocyclic template.

Finally, we report the application of this "split-pool" synthetic library approach towards the extension of known physical models of passive membrane permeation—in particular, the barrier domain model—to larger molecular weight chemical space. We show that the membrane permeability of macrocycles is governed by lipophilicity and solubility and that the window between the two narrows with increasing molecular size. We recognize this brings into question again the origin of intrinsic permeability of natural membrane-permeable macrocycles such as cyclosporin A.

Dedicated to my loving wife Kristy, who supported me through the good times, the bad times, and the ugly times.

Acknowledgements

The text of this dissertation includes reprint of the following previously published material:

Chapter 1:

Hewitt, W.M.; Egger, M.; Zuckermann, N.B.; Konopelski, J.P. "Preparation of fused β-lactams through Weinreb amide α-anions." *Tetrahedron*, **2014**, *70*, 5283-5290.

The following co-authors are acknowledged for their contributions to the published work reprinted in this chapter:

Dr. Michael Egger for assisting in the development of the synthesis for compound **1.54** from L-Methionine and for his assistance in initial investigations towards optimizing the C-N oxidative bond formation in the synthesis of **1.59**; Dr. Nathaniel B. Zuckermann in the initial preparation of **1.24** and for growing x-ray quality crystals thereof; and Dr. Joseph P. Konopelski, who directed and supervised the research which forms the basis for this dissertation chapter.

Chapter 1: Utilization of the β-Lactam Core in Natural Product Synthesis: Towards the Synthesis of Chiral Ring-Fused β-Lactams

Introduction

Azetidin-2-ones (β-lactams) are among the most highly investigated heterocyclic ring systems (Figure 1). Beyond the obvious impact on antibiotic research and treatment,[1] β-lactams have expressed biological activity in cholesterol absorption[2] and as a target of viral proteases.[3] As reagents, β-lactams offer a well-defined stereochemical relationship between the adjacent sp^3 centers and an amide carbonyl that is reactive by virtue of the 4-membered ring strain.[4-5] In peptide chemistry β-lactams have been employed as turn mimics[6-7] and as precursors to β-amino acids[8-9] and their related polymers (β-foldamers)[10-12] that have been the focus of much study. New synthetic methods for the preparation of this ring system continue to appear in the literature with great frequency.[13-14]

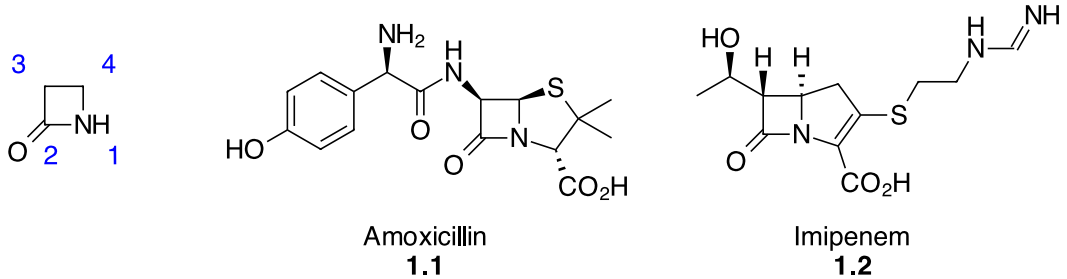

Figure 1.1. Generic azetidin-2-one (β-lactam) with ring numbering and selected β-lactam antibiotics Amoxicillin and Imipenem.

In the arena of synthetic organic chemistry, β-lactams have been used as building blocks in the synthesis of non-β-lactam containing targets.[15] This so-called "β-lactam synthon" method is gaining popularity in the literature.[16] In one example (Scheme 1.1), De

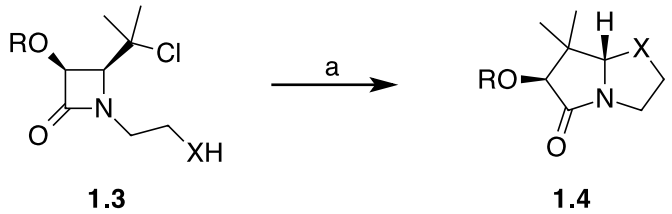

Scheme 1.1. Synthesis of bicyclic γ-lactams (X = O, NBoc) **1.4** by Dekeukeleire *et al.* from β-lactam **1.3**. Conditions: a) $AgBF_4$, pyridine, refluxing toluene.

Kimpe and coworkers synthesized complex bicyclic γ-lactams **1.4** from the β-lactam**1.3** via ring expansion and intramolecular attack on an intermediate acyliminium ion.[17]

In addition, several groups have employed the chirality of β-lactam products towards the synthesis of β-lactam fused polycyclic systems and stereochemically elaborate heterocycles. Van Brabandt *et al.* synthesized enantiopure morpholine and piperazine based bicyclic β-lactams **1.6** from the 4-formyl-*N*-haloalkyl β-lactam **1.5** (Scheme 1.2).[18] Additionally, Leemans *et al.* showed that chiral 2-(dihydroxyethyl)-piperidines **1.9** can be prepared with diastereoselectivity from β-lactams **1.7** via the azabicycle **1.8** after tributyltin-mediated radical cyclization.[19] These substituted piperidines are important building blocks in the synthesis of etoxadrol (**1.10**) and dexoxadrol (**1.11**), NMDA receptor

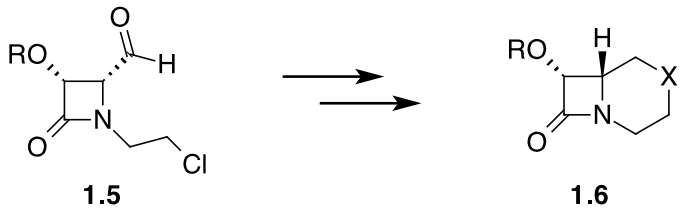

Scheme 1.2. Synthesis of decorated piperazines (X = NH) and morpholines (X = O) **1.6** via formation of bicyclic β-lactam intermediates by Van Brabandt *et al.*

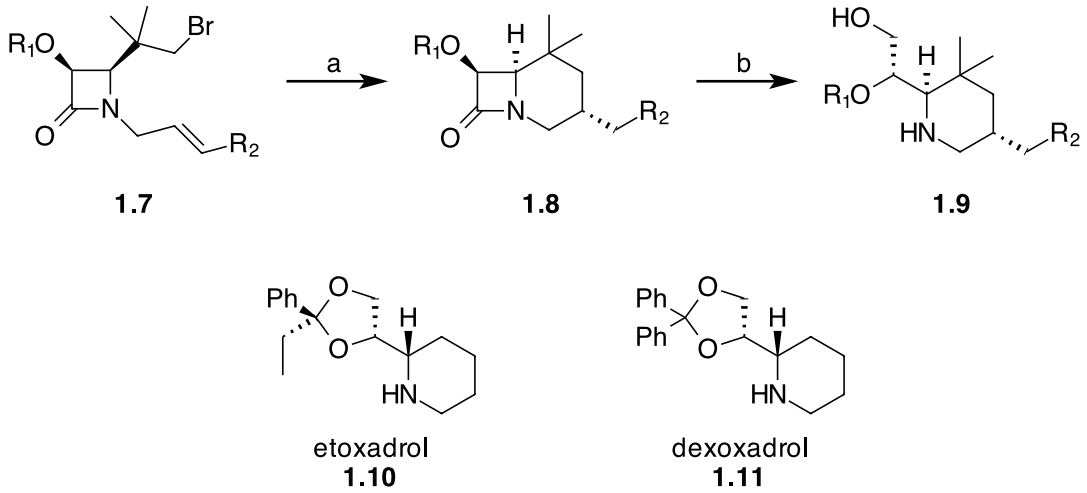

Scheme 1.3. Synthesis of diastereomerically pure piperidines **1.9** from β-lactams **1.7**, important intermediates in the synthesis of etaxodrol and dexoxadrol. Conditions: a) Bu_3SnH, AIBN, toluene, Δ; b) $LiAlH_4$, Et_2O, Δ.

antagonists (Scheme 1.3).[20] The same authors later reported the diastereoselective synthesis of a disubstituted *cis*-oxolane **1.14** via the 3,4-fused bicyclic β-lactam **1.13**.[21] This structural unit bears similarity to the oxolane core of chryscandin (**1.15**), a peptidyl nucleoside antibiotic (Scheme 1.4).[22]

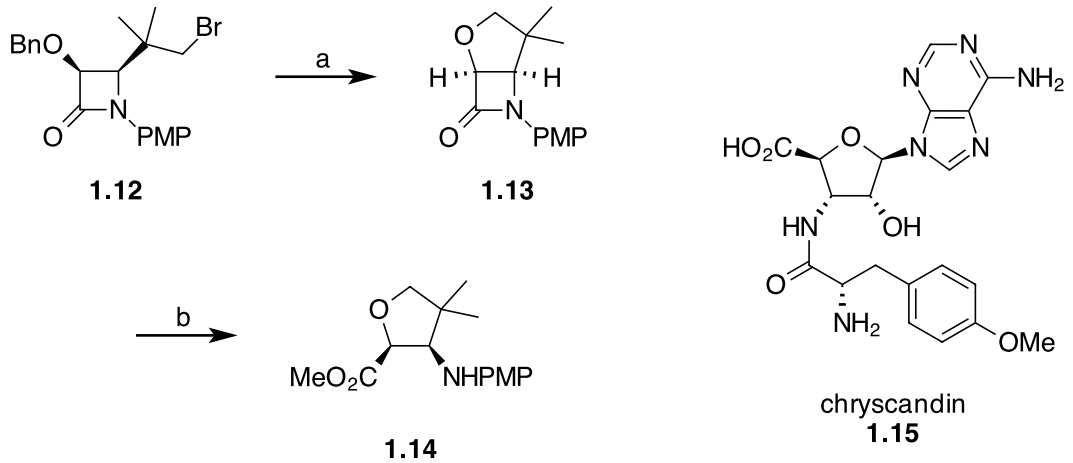

Scheme 1.4. Synthesis of a tetrahydrofuran-based *cis*-β-amino acid **1.14** from β-lactam **1.12** via a C3-C4 fused bicyclic β-lactam **1.13**. This β-amino acid product represents a structural subunit present within the natural product chryscandin. Conditions: a) Pd/C, H_2, MeOH, then NEt_3, C_6H_6, Δ; b) HCl, MeOH, Δ.

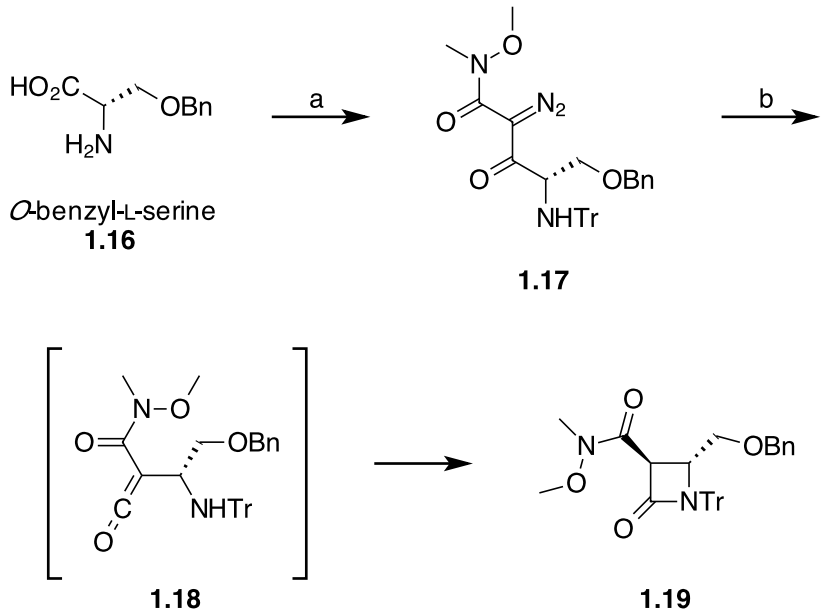

Scheme 1.5. Synthesis of the previously described *O*-benzyl protected β-lactam **1.19** from *O*-benzyl-L-serine. Conditions: a) *i*. Me_3SiCl, then TrCl, NEt_3; *ii*. CDI, THF; *iii*. LHMDS, $CH_3CON(Me)OMe$, THF; *iv*. MsN_3, DBU, CH_3CN. b) hν, toluene.

These oxolane-based *cis*-β-amino acids pose a significant challenge to the synthetic community.

We recently presented a new route to enantiomerically pure β-lactams, including **1.19** (Scheme 1.5), from commercially available α-amino acids in a process that is efficient in the use of photochemistry for the key reaction and in the dearth of chromatographic separations.[23] In addition, we have demonstrated the reactivity of the Weinreb amide functionality in its ability to effectively undergo reactions with Grignard and alkyllithium reagents without opening of the β-lactam nucleus due to the steric presence of the *N*-trityl group. In an effort to extend this work, we saw the opportunity to employ the rigid and bulky *N*-trityl protected β-lactam in a bicyclic system for employment as a chiral directing group to invoke stereoselective introduction of functionalities and to allow rapid and

divergent analogue synthesis of biologically relevant natural and non-natural products. We began by exploring the reactive capabilities for functionalization at carbon 3 of the four-membered ring, followed by explorations in the synthesis of sterically constrained β-lactam-fused ring systems. We report our progress towards the application of this strategy towards the synthesis of the natural product pactamycin. In addition, we present our results on the oxidative coupling of the dianion formed from deprotonation of the C3 position and a C4 pendant N-H amide functionality, resulting in the formation of a diazabicyclo[3.2.0]heptane structure, a potential precursor to β-lactam based proteasome inhibitors with a similar mechanism of action as that of the natural product salinosporamide A.

C-3 Elaboration Through Weinreb Amide α-Anions

Generally, Weinreb amides have not been effective α-anion-stabilizing functionalities;[24] they are more often introduced into the molecule of interest and directly reacted with alkyllithium or Grignard reagents, or hydride reducing agents to furnish the corresponding ketones and aldehydes, respectively. Indeed, our published work documents this technology within the context of β-lactam **1.19**. Given the generally modest results when standard strong bases have been employed for Weinreb amide α-deprotonation, we decided to employ KH, a base that we have used effectively in the past.[25] Our first attempts involved introduction of an electrophile with a synthetic handle close to the quaternary center (Scheme 1.6). To this end, we attempted lead (IV) mediated vinylation. However, subjection of **1.19** under standard conditions returned only starting material. Similar results were obtained when attempting alkylation with ethylene sulfate or ethylene oxide towards **1.21** and **1.22**, respectively. Gratifyingly, alkylation of the anion of **1.19** with both EtI and

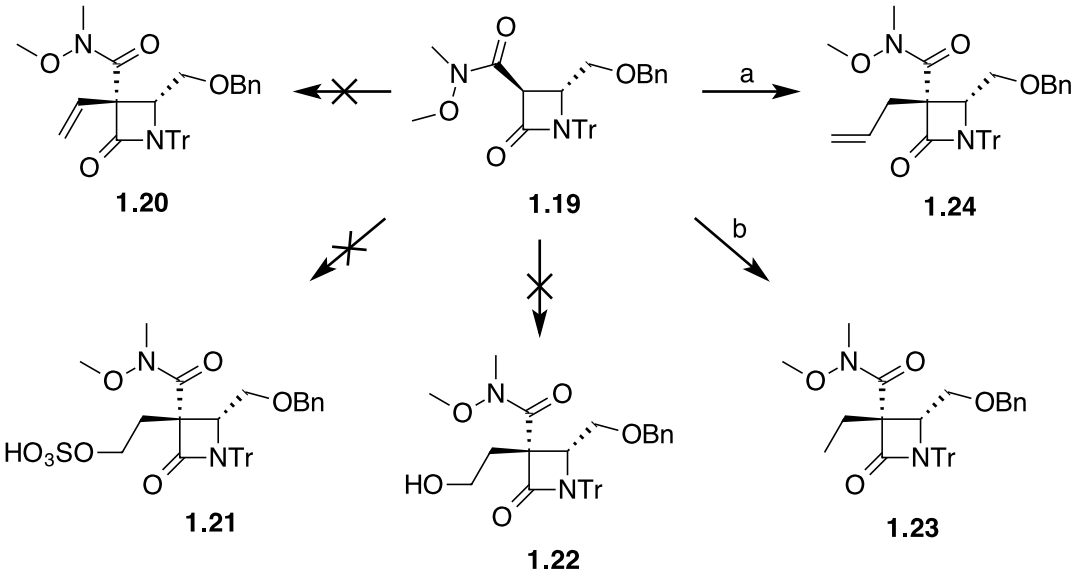

Scheme 1.6. Exploration of reactivity towards C3 elaboration of the β-lactam nucleus. Conditions: a) KH, allyl bromide, NaI, THF, 93%, *dr* = 6:1; b) KH, EtI, THF, 73%, *dr* = 2.3:1.

allylbromide/NaI afforded the expected products **1.23** and **1.24**, respectively, in good yield. The major product arose from approach of the electrophile from the least hindered face, opposite to the $-CH_2OBn$ group, as evidenced by single crystal X-ray analysis of **1.24**.[26]

To demonstrate the utility of this scaffold despite the neighboring quaternary center, we investigated its reactivity at various positions. Reduction of the Weinreb amide with MeLi proceeded in excellent yield in the presence of the adjacent quaternary center, affording methyl ketone **1.25**. Elaboration of the allyl functionality in **1.24** proceeded by treatment with catalytic OsO_4 followed by $NaIO_4$ to provide the chain-shortened aldehyde **1.26**, which was reduced in good yield with $NaBH_4$ to afford the corresponding alcohol **1.27** (Scheme 1.7).

Having established the ability to manipulate this scaffold, we sought to apply this system to a β-lactam synthon strategy towards the synthesis of natural products.

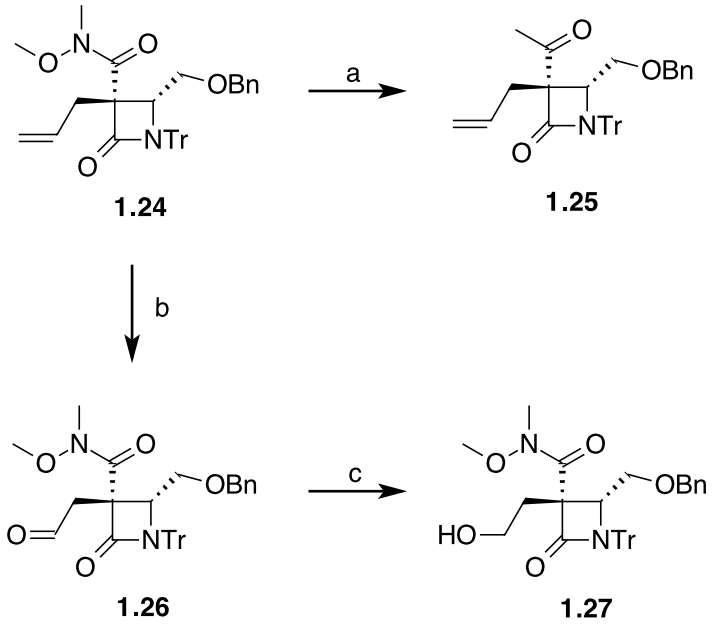

Scheme 1.7. Synthetic elaboration around the quaternary C3 center. Conditions: a) MeLi, THF, 96%; b) OsO_4, H_2O / tBuOH, then $NaIO_4$, acetone / H_2O, 81%; c) $NaBH_4$, MeOH, 69%.

Preparation of Bicyclic β-Lactams and Application Towards the Synthesis of Pactamycin

Pactamycin (**1.28**) is a densely functionalized cyclopentane natural product first discovered in 1961.[28] This unique natural product displays antitumor, antiviral, antimicrobial, and antiprotozoal activity through ribosomal inhibition[29] and binds to the E-site by mimicking a unit of RNA through π-stacking of its aromatic groups (Figure 1.2).[30] Although this site in the ribosome is evolutionarily conserved, studies have shown that some pactamycin derivatives show reduced toxicity, suggesting its potential for drug development.[31] In addition to its intriguing biological activity, **1.28** bears a significant challenge to the synthetic community. The natural product bears six contiguous stereocenters, three of which are quaternary carbons. For this reason, **1.28** has been the target of total synthesis for many years.

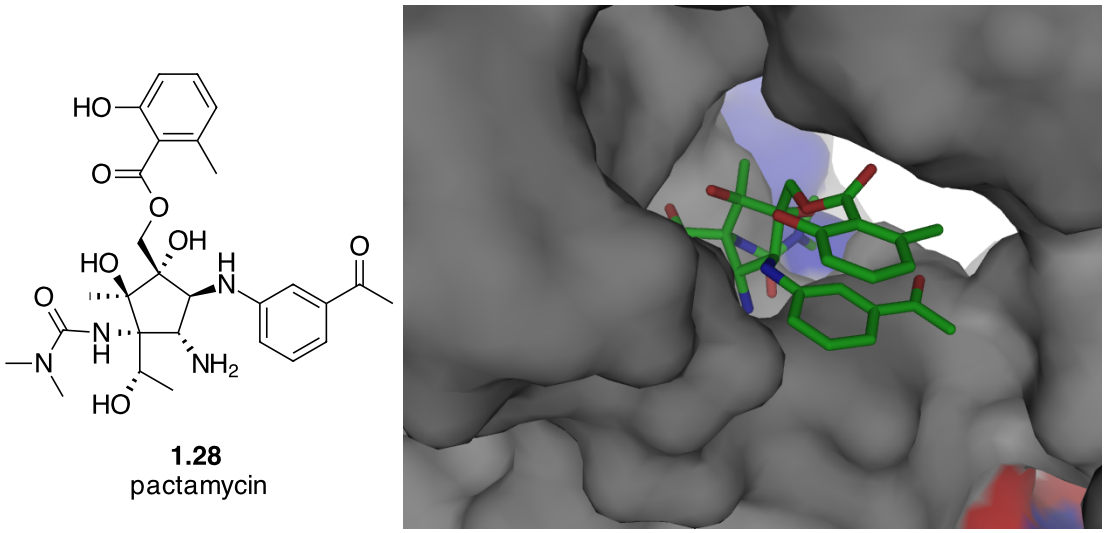

Figure 1.2. The structure of pactamycin (**1.28**) and a crystal structure of the natural product in the E-site of the ribosome.

Several approaches toward pactamycin have been published since the initial reports of its discovery and until recently has eluded synthetic endeavors for five decades.[32] In 2011, Hanessian and coworkers reported the first total synthesis of this synthetically challenging natural product from the known L-threonine-derived oxazoline **1.29** serving as a natural source for the C1 / C7 stereocenters (Scheme 1.8).[33] They utilized a titanium-mediated intramolecular aldol condensation to access a cyclopentenone intermediate **1.31**. The overall stereochemistry was later established by x-ray crystallography of the fully oxygenated cyclopentane precursor **1.32**. Although the published synthesis is riddled with protection group problems and stereochemical challenges across the lengthy 29 steps, this serves as a landmark publication providing the first ever synthesis of this natural product in an overall 3.0 % yield.

More recently, Malinowski *et al.* disclosed an impressive 15-step synthesis to **1.28** (Scheme 1.9).[34] Their strategy begins with an asymmetric Mannich reaction with

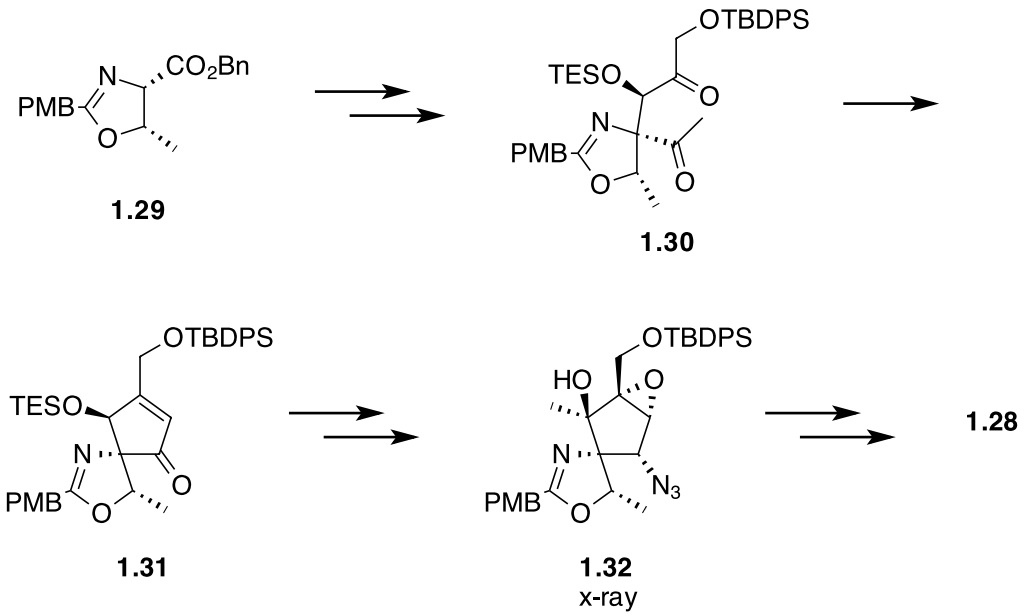

Scheme 1.8. Summary of Hanessian's synthesis of **1.28** from oxazolidine **1.29** derived from L-threonine. Highlighted (**1.30** to **1.31**) is a titanium-mediated intramolecular aldol condensation / elimination sequence, forming the cyclopentane core.

dimethyluredo-2,5-dipentanone to access **1.33**, thus choosing to incorporate the dimethylurea functionality in its native form from early in the synthesis. They also utilize an intramolecular aldol condensation to access a similar cyclopentenone intermediate **1.35**. Further elaboration furnishes the fully oxygenated pactamycin core **1.36**, for which stereochemistry is confirmed through x-ray analysis.

We sought to utilize an enantiopure β-lactam as both a chiral directing group and as a masked form of the C1 urea and C2 nitrogen functionalities (Scheme 1.10). Upon late-stage opening of the β-lactam, the C1 urea can be produced via Curtius rearrangement, followed by *in situ* trapping of the generated isocyanate. Use of this approach will allow rapid divergent synthesis of pactamycin analogues from a common intermediate **1.37** to allow exploration of structure-activity relationships and selectivity of its bioactivity. This

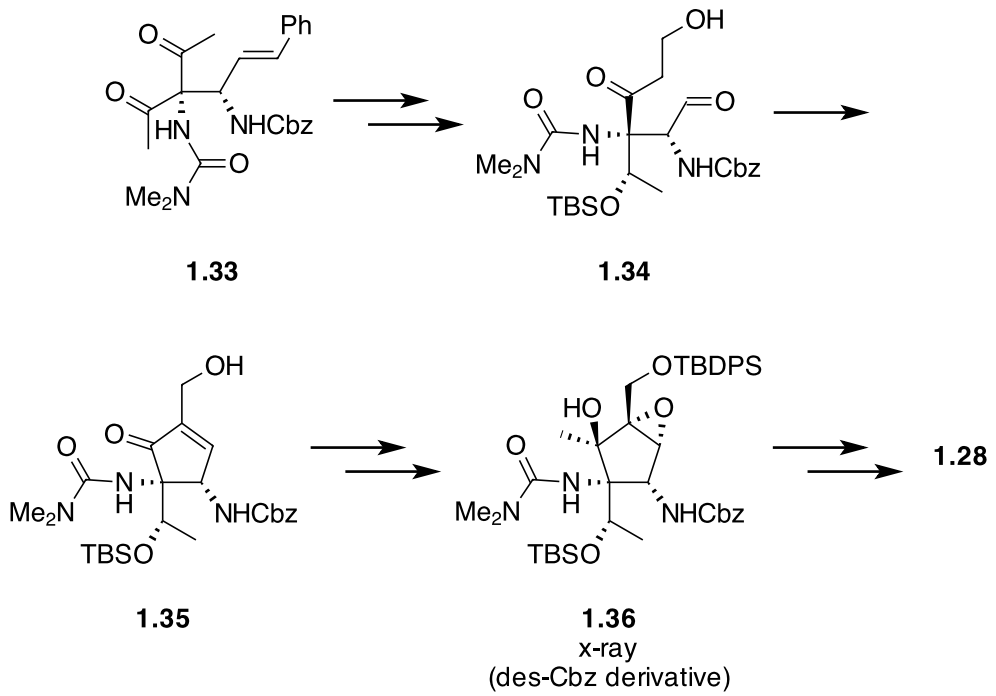

Scheme 1.9. Johnson's synthesis of **1.28** featuring a methoxide-mediated aldol condensation to form the cyclopentane core.

intermediate is envisioned to arise from appropriate elaboration of a protected serine-derived β-lactam similar to that previously described.

As discussed earlier, we have shown that C3-C4 *trans*-disubstituted β-lactams such as **1.19** are easily elaborated through C3-substitution and can be manipulated despite the neighboring quaternary center, as exemplified in the synthesis of **1.25**. However, our inability to remove the benzyl group of **1.25** in the presence of the allyl double bond under a variety of published conditions necessitated a change in the C4 protection strategy.

Our initial investigations were turned towards the chemically similar, yet orthogonal *p*-methoxybenzyl (PMB) group. We have previously reported the standard deprotection of **1.19** to provide **1.38** by action of Pearlman's catalyst in high yield (Scheme 1.11). Reprotection of the alcohol as the PMB ether followed by allylation proceeded smoothly to

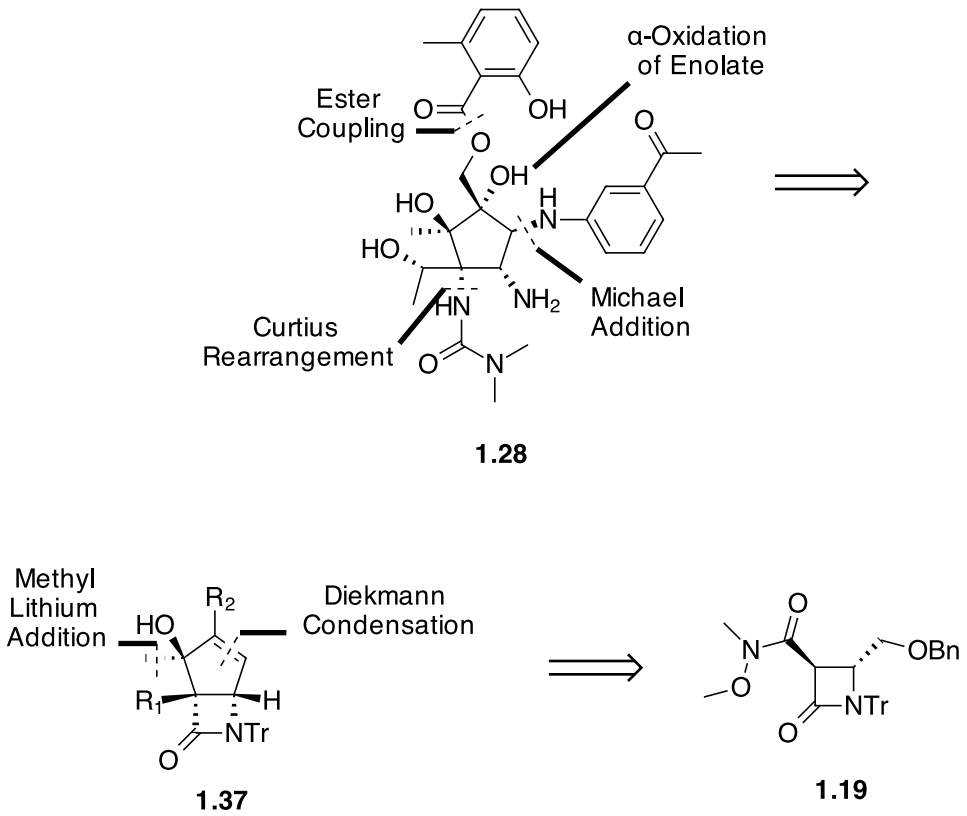

Scheme 1.10. Retrosynthetic analysis of natural product **1.28**.

give intermediate **1.42**, whose relative configuration was confirmed by 1D-NOE experiments. However, attempts to remove the PMB group of methyl ketone **1.45** by standard oxidative conditions (DDQ, DCM / H_2O) proved sluggish, providing the product in a dissatisfying 11% yield. It is postulated that the sluggishness of the reaction arises from π-stacking of the PMB aromatic system with the neighboring *N*-trityl group, a phenomenon known to effectively deter PMB removal.[27]

We next turned our attention to a silyl-based protection scheme. Introduction of both the –TBS and the –TBDPS groups on the primary alcohol proceeded in excellent yield to

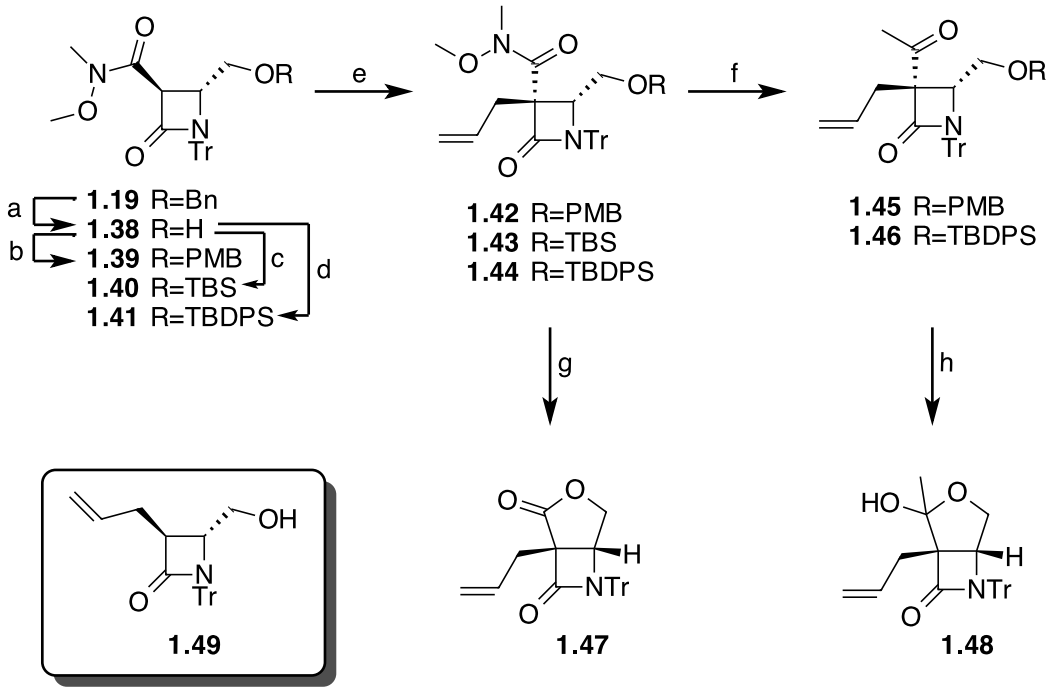

Scheme 1.11. Protection group evaluation and access to bicyclic lactone **1.47** and lactol **1.48**. Conditions: a) $Pd(OH)_2$, H_2, MeOH, quant.; b) *p*-methoxybenzyl 2,2,2-trichloroacetimidate, pTSA, CH_2Cl_2, 83%; c) TBSCl, imidazole, DMF, 86%; d) TBDPSCl, imidazole, NEt_3, DMF, 60°C, quant.; e) KH, allyl bromide, NaI, 22-82%; f) MeLi, THF, -41°C, 86-89%; g) for R=TBDPS, TBAF, THF, 65°C, 60%; h) TBAF, AcOH, THF, 65°C, 69%.

give **1.40** (86%) and **1.41** (>99%), respectively. However, allyl introduction employing the same methodology as previously described afforded vastly different yields, with **1.40** providing only 22% yield of the expected product **1.43** while **1.41** returned **1.44** in 82% as a single diastereomer. Deprotection of **1.44** with TBAF in refluxing THF afforded fused bicyclic lactone **1.47**, thereby confirming the *cis* relationship between the Weinreb amide and hydroxymethyl side chain. Compound **1.47** was also identified in the reaction mixture that produced **1.43**, suggesting instability of the –TBS group to the allylation conditions. Ketone production from **1.44** via methyllithium treatment proceeded without incident to deliver **1.46**. Interestingly, the deprotection of the silyl ether proved nontrivial. Reaction of the TBDPS ether with TBAF proved sluggish when run at room temperature. When the

temperature was raised to 65 °C, or when performed under basic conditions (NaOH / MeOH), the degredation product **1.49** was isolated, presumably via a retroaldol pathway. However, employing the use of TBAF under buffered conditions led smoothly to furnish lactol **1.48**.

We envisioned access to a cyclopenteneone core similar to **1.31** and **1.35** fused with our β-lactam nucleus via an intramolecular aldol approach. However, all attempts to oxidize the primary alcohol component of lactol **1.48** proved unsuccessful.

Application to the Synthesis of a Library of Proteasome Inhibitors

Salinosporamide A (**1.50**, Figure 1.3) belongs to a family of β-lactone-based marine natural products. Following its discovery in 2003,[35] biological evaluation revealed its activity as a proteasome inhibitor. This discovery led to its clinical development for the treatment of multiple myeloma.

Following Corey's initial total synthesis of the natural product in 2004,[36] **1.50** has been the focus of synthetic endeavors for nearly a decade, leading to over 22 total and formal syntheses, along with access to numerous additional natural and non-natural analogues through synthesis and natural product isolation. This work has lead to an extensive understanding of the structure-activity relationship (SAR) of this class of natural products.[37]

In 2005, the synthesis of a non-natural analogue (**1.51**) related the natural **1.50** incorporating a β-lactam core was reported.[38] In this work, they showed the analogue also inhibits the proteasome by the same mechanism as its parent natural product, but with

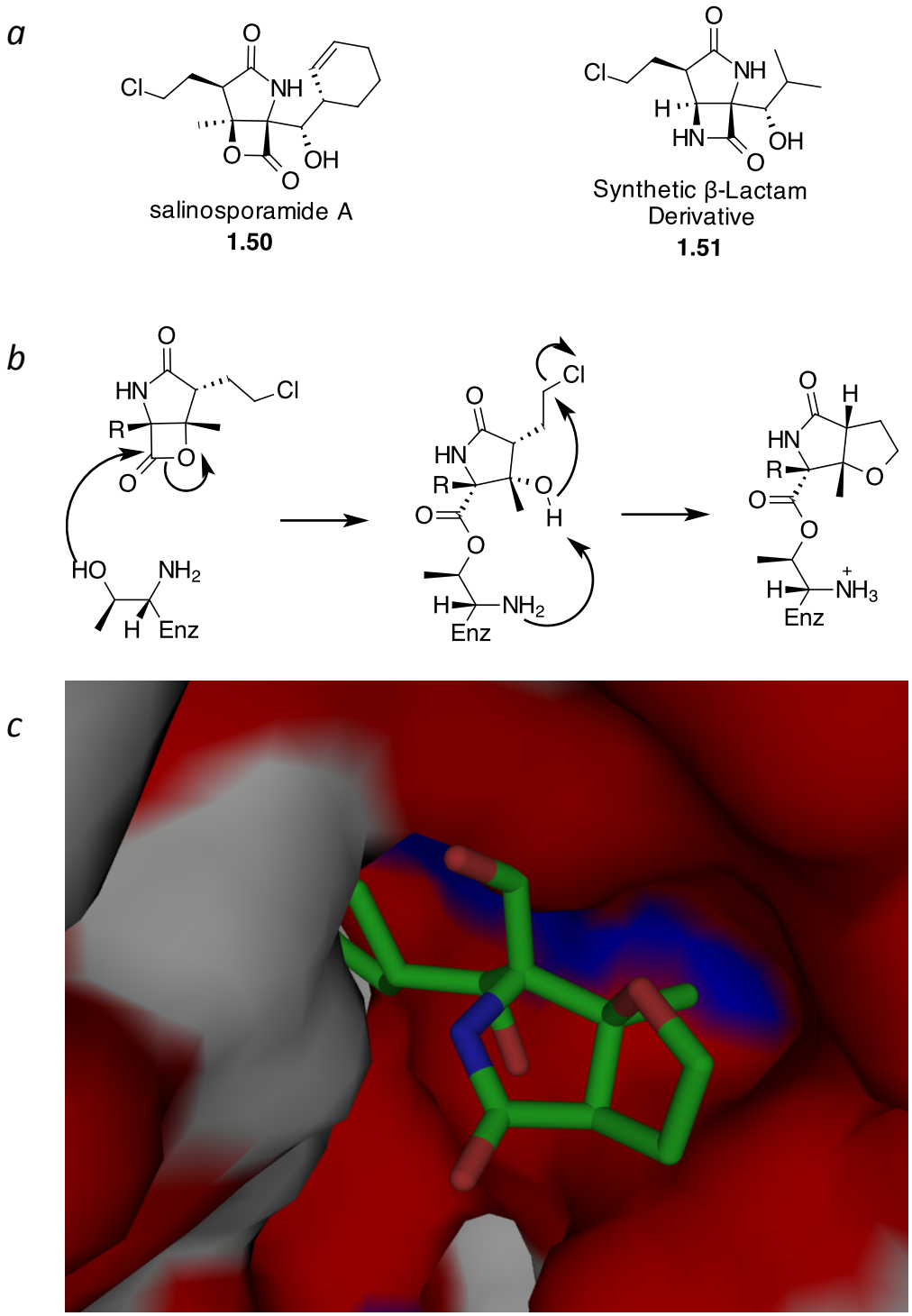

Figure 1.3. a) Structures of Salinosporamide A (**1.50**) and a synthetic β-lactam-based derivative (**1.51**). b) Mechanism of action for proteasome inhibition by Salinosporamide-like small molecules. c) **1.50** covalently bound to the active site of the 20S proteasome.

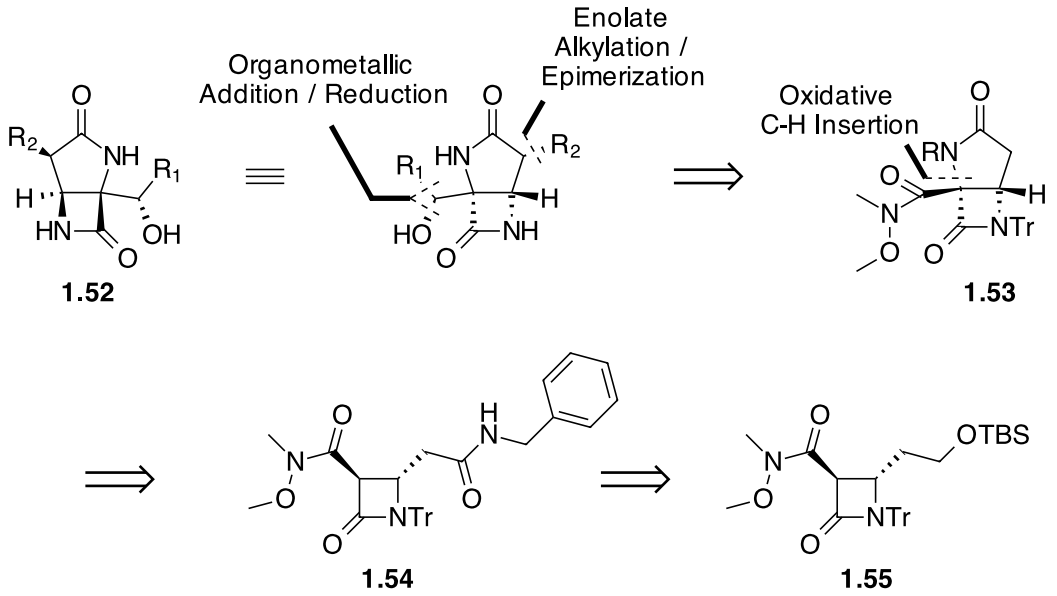

Scheme 1.12. Retrosynthetic analysis of β-lactam-based proteasome inhibitors.

greater aqueous and shelf stability, suggesting it to be a better candidate for drug development. Unfortunately, the synthetic approach is not amenable to the development of analogues, as all the structural elements contributing to the molecule's activity and selectivity are installed relatively early in the synthesis.

We decided to utilize our approach to the synthesis of enantiomerically pure β-lactams to the synthesis of this unique natural product analogue. Our approach (Scheme 1.12) involves initial β-lactam formation, followed by a C3 oxidative C-N bond formation to establish the bicyclic core. The incorporation of the Weinreb amide allows the divergent synthesis of a diverse set of functionalities at this center. In addition, the late-stage introduction of the chloroethyl group will allow additional variation. In short, this approach incorporates late-stage introduction of activity-essential structural elements allowing divergent synthesis of a library of compounds.

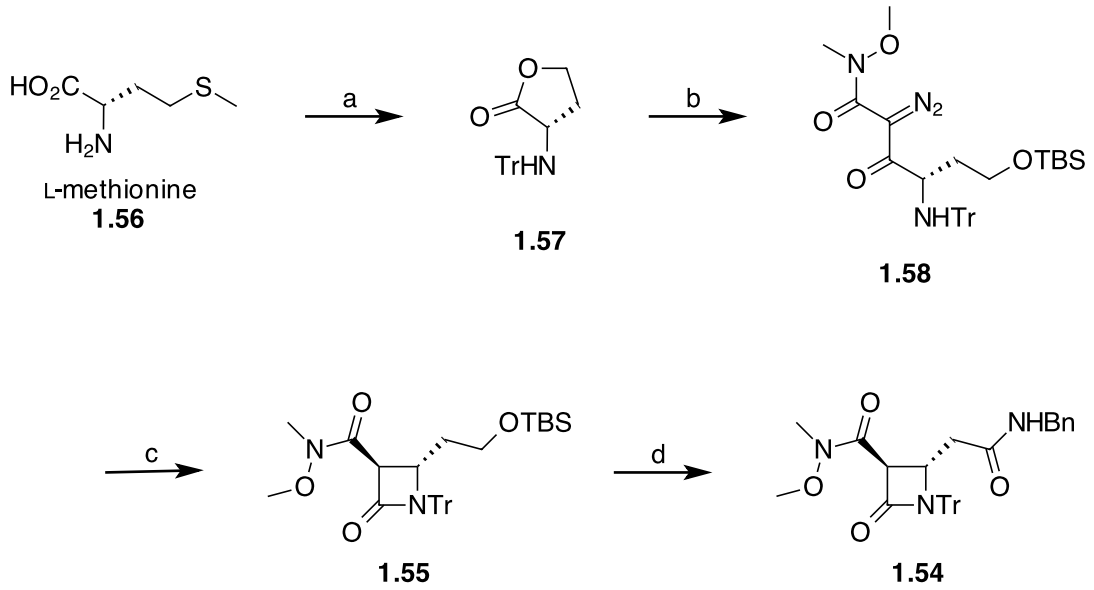

Scheme **1.13**. Synthesis of oxidative cyclization precursor **1.54**. Conditions: a) Bromoacetic acid, H_2O / iPrOH, Δ, then TrCl, NEt_3, DCM, 69% (two steps); b) *i.* nBuLi, $CH_3CON(Me)OMe$, THF / DMPU; *ii*. TBSCl, imidazole, DMF; *iii*. MsN_3, DBU, CH_3CN, 89% (three steps). c) hν, DBU, toluene (92%) or DBU, toluene, Δ (89%). d) *i.* TBAF, THF; *ii*. $RuCl_3$-*x*H_2O, $NaIO_4$, CCl_4 / CH_3CN / H_2O; *iii*. CDI, DCM, then benzylamine, 80% (three steps).

The preparation of the β-lactam core proceeded from the known *N*-trityl protected γ-lactam **1.57**, derived from L-methionine in a two-step process.[39] The Weinreb amide functionality was introduced via the enolate addition of *N*-methoxy-*N*-methylacetamide, followed by *O*-TBS protection and diazo-transfer to furnish intermediate **1.58**. Interestingly, *O*-TBS protection of the free alcohol intermediate proved non-trivial and necessitated the use of freshly purified *N,N*-dimethylformamide to prevent the formation of an undesired bis-protected side-product.

Decomposition of the reactive α-diazo-β-ketoamide intermediate **1.58** via UV light or heat led to the desired *O*-TBS protected β-lactam **1.55**. This unique β-lactam was easily *O*-deprotected and oxidized to the corresponding carboxylic acid with ruthenium tetroxide. Amide formation proceeded smoothly via activation by CDI to give the desired oxidative-

Table 1.1. Optimization of oxidative C-N bond formation

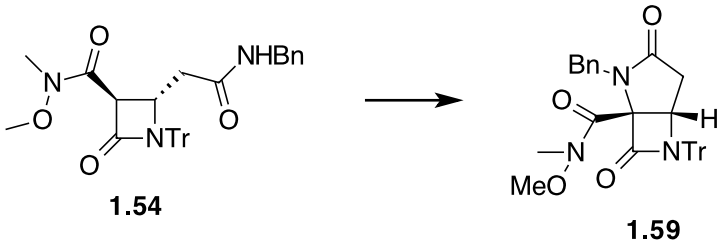

Entry	Reagents	Conditions	Yield
1	$PhI(OAc)_2$	CH_3CN, rt	NR
2	PhIO, TBAI	toluene, rt	5%
3	LHMDS, then $PhI(OAc)_2$	THF, -78 to 0°C	5%
4	LHMDS, then I_2	THF, -78 to 0°C	32%
5	LHMDS, then $Cu(OAc)_2$	THF, -78 to 0°C	NR
6	LHMDS, then $Fe(OAc)_3$	THF, -78 to 0°C	NR
7	LHMDS, then NBS	THF, -78 to 0°C	28%

coupling precursor **1.54** in 7 steps and 66% yield from known lactone **1.57**.

We next turned our attention towards the C—N bond formation, a key step in this synthesis and important towards the development of this potentially divergent synthesis of Salinosporamide-like small molecules. While there are numerous examples of C–C bond formation through oxidative coupling,[40] fewer C–N bond forming events have been described.[41] The Hofmann-Löffler-Freytag (HLF) reaction is one such reaction offering this type of transformation.[42] However, these conditions typically require decomposition of a pre-halogenated electron-poor nitrogen. In addition, a wide variety of variations of the HLF reaction have been reported.[43] Of these, the Suarez modification utilizes hypervalent iodine-based oxidants. Based on this literature precedence, we decided to first pursue oxidants of this nature. Unfortunately, reaction of intermediate amide **1.54** with either iodosobenzene diacetate (IBDA) or iodosylbenzene gave minimal conversion.

Extensive work in this area has been performed by Sarpong and coworkers.[41] They have reported several successful C—N bond forming oxidations. Typical conditions investigated involve reaction of preformed dianions with iodine-based oxidants in the presence of an additive. Following this protocol, we screened several known oxidants in the presence of the preformed dianion with minimal success. Gratifyingly, we found that reaction of the dianion with either molecular iodine or *N*-bromosuccinimide at low temperatures furnished the desired bicyclic product **1.59**, albeit in low yield. Although this transformation requires further optimization, these results establish precedence for further investigations towards the divergent synthesis of β-lactam based proteasome inhibitors.

Conclusion

We have demonstrated that β-lactams such as **1.19** are amenable to α-alkylation of the Weinreb amide functionality, generating a quaternary center with predictable stereochemistry. The functional groups at C3 and C4 of the resultant β-lactams are transformed under standard conditions to provide synthetic handles for future ventures in natural product synthesis. We also reported results of our utilization of this scaffold to gain access to a cyclopentane intermediate towards the synthesis of pactamycin. In addition, the dianion of **1.54**, prepared from L-methionine in high yield, has been shown to undergo oxidative coupling through the use of the α-anion of a Weinreb amide to furnish the corresponding diazabicyclo[3.2.0] heptane **1.59**.

General Methods

Melting point determinations are uncorrected. Infrared spectra were recorded as thin films on salt plates, with ν-max in inverse centimeters (cm^{-1}). High-resolution mass measurements were obtained on an ESITOF mass spectrometer.

Flash chromatography was performed on Silica Gel 60, 40-63 mesh using EtOAc/hexanes mixtures as solvent unless otherwise indicated. Thin layer chromatography (TLC) was carried out on silica gel plates with UV detection. Proton (^{1}H NMR) and carbon (^{13}C NMR) magnetic resonance spectra where obtained in $CDCl_3$ at 500 MHz and 125 MHz, respectively, unless otherwise noted. The following abbreviations were utilized to describe peak patterns: br = broad, s = singlet, d = doublet, t = triplet, q = quartet, quin = quintet, sex = sextet, app = apparent, and m = multiplet.

All air and moisture sensitive reactions were carried out under an atmosphere of dry nitrogen using oven-dried or flame-dried glassware and standard syringe techniques. Triethylamine (NEt_3), *N*,*N*-dimethylpropyleneurea (DMPU), benzylamine, and hexamethyldisilizane (HMDS) were distilled from calcium hydride. Allyl bromide was passed through a column of basic alumina immediately before use. *N*,*N*-dimethylformamide was distilled sequentially from calcium hydride, then calcium oxide to remove trace amounts of dimethylamine. *N*-bromosuccinimide was recrystallized from water. Tetrahydrofuran (THF), acetonitrile (CH_3CN), methylene chloride (CH_2Cl_2) and toluene were freshly obtained from the solvent purification system. Compounds **1.19**[23] and **1.57**[39] were prepared according to literature procedures. *N*-methoxy-*N*-methylacetamide[44] and *p*-methoxybenzyl 2,2,2-trichloroacetimidate[45] were prepared by procedures described in the literature.

Single-crystal data were recorded using a Bruker SMART APEX II CCD area detector X-ray diffractometer using graphite monochromated Mo-Kα radiation (λ = 0.71073 Å). The structures were solved by direct methods and expanded routinely. The models were refined by full-matrix least-squares analysis of F2 against all reflections. All non-hydrogen atoms were refined with anisotropic thermal displacement parameters. Thermal parameters for the hydrogen atoms were tied to the isotropic thermal parameter of the atom to which they are bonded. Programs used: APEX-II v2.1.4;[46] SHELXTL v6.14.[47-48]

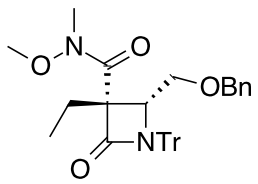

(2*R*,3*R*)-2-(Benzyloxymethyl)-3-ethyl-*N*-methoxy-*N*-methyl-4-oxo-1-tritylazetidine-3-carboxamide (1.23). To a suspension of potassium hydride (141 mg, 1.056 mmol, 1.1 equiv) in THF (10 mL) at -78°C was added the *trans*-β-lactam **1.19** (500 mg, 0.960 mmol, 1 equiv). The solution was stirred for 30 min, after which ethyl iodide (84 µL, 1.06 mmol, 1.1 equiv) was added. The resulting solution was stirred overnight while slowly warming to room temperature, after which TLC (30% EtOAc / Hexanes) indicated consumption of starting material. The reaction was quenched with sat. NH_4Cl (10 mL) and the aqueous phase extracted with dichloromethane (3 x 10 mL). The combined organics were washed with brine (5 mL), dried ($MgSO_4$), and purified by flash chromatography (30% EtOAc / Hexanes to 70% EtOAc / Hexanes)S to obtain the title compound (268 mg) and its C3 epimer (116 mg) as colorless solids (*dr* = 2.3:1, 73% combined yield). Major isomer: mp = 118-122°C; $[\alpha]_D^{24}$ = +62.8 (c = 0.382, CH_2Cl_2) ^{1}H NMR (500 MHz, $CDCl_3$): δ (ppm) 7.30-7.17 (m, 20H), 4.09 (d, *J* = 11 Hz, 1H), 3.90 (d, *J* = 11.5 Hz, 1H), 3.55 (s, 1H), 3.39 (s, 3H), 3.17 (m, 1H), 2.92 (s, 3H), 2.34-2.22 (m, 2H), 1.76 (m, 1H), 1.00 (t, *J* = 7.5 Hz, 3H); ^{13}C NMR (125 MHz, $CDCl_3$): δ (ppm) 168.3, 142.9,

138.0, 130.2, 128.3, 127.9, 127.8, 127.6, 127.5, 73.7, 73.2, 66.1, 64.4, 62.1, 61.8, 33.1, 29.9, 9.5; IR (thin film) [cm^{-1}]: ν = 3056, 2879, 1748, 1639, 1452, 1275, 1104, 749, 699; HRMS for $C_{35}H_{36}N_2O_4Na$ [M+Na] calcd., 571.2567, found, 571.2539 (Error = -4.88 ppm).

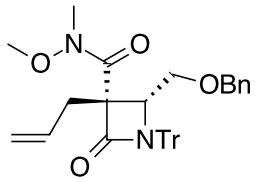

(2*R*,3*R*)-3-Allyl-2-((benzyloxy)methyl)-*N*-methoxy-*N*-methyl-4-oxo-1-tritylazetidine-3-carboxamide (1.24). To a suspension of potassium hydride (110 mg, 0.960 mmol, 2 equiv) and sodium iodide (7 mg, 0.096 mmol, 0.1 equiv) in tetrahydrofuran (10 mL) at room temperature was added β-lactam **1.19**. The solution was stirred for 30 min, then cooled to -78 °C and allyl bromide (45 µL, 0.502 mmol, 1.1 equiv) was added. The solution was stirred overnight while slowly being allowed to warm to room temperature. TLC (50%EtOAc/Hex) indicated complete consumption of starting material. The reaction was quenched with sat. NH_4Cl (20 mL). The mixture was concentrated and extracted with EtOAc (3 x 20 mL) and the combined organic layers were washed with brine (50 mL) and dried ($MgSO_4$). Concentration and purification by flash chromatography (50% EtOAc/Hex) afforded 215 mg of **1.24** as a colorless solid and 34 mg of its C3-epimer as a colorless solid (93% combined yield, *dr* = 6:1). mp = 118-120 °C; $[\alpha]_D^{24}$ = +16.9 (c = 4.5, CH_2Cl_2); ^{1}H NMR (500 MHz, $CDCl_3$): δ (ppm) 7.37-7.25 (m, 20H), 5.97 (app. sex, *J* = 8.0 Hz, 1H), 5.13 (d, *J* = 17.0 Hz, 1H), 5.05 (d, *J* = 10.0 Hz, 1H), 4.17 (d, *J* = 11.0 Hz, 1H), 4.00 (d, *J* = 11.0 Hz, 1H), 3.69 (s, 1H), 3.45 (s, 3H), 3.24 (d, *J* = 6.0 Hz, 1H), 2.98 (m, 4H), 2.57 (d, *J* = 6.0 Hz, 1H), 2.36 (app. s, 1H); ^{13}C NMR (125 MHz, $CDCl_3$): δ (ppm) 167.6, 142.8, 138.0, 132.9, 130.2, 128.3, 128.0, 127.8, 127.7, 127.5, 118.9, 74.0, 73.2, 66.1, 63.6, 61.8, 61.3, 40.3, 33.1; IR (thin film) [cm^{-1}]: ν = 3062, 3032, 2931, 1751, 1640, 1599, 1493,

1449, 730, 700; HRMS for $C_{36}H_{37}N_2O_4$ [M+H] calcd., 561.2748, found, 561.2738 (Error = -1.75 ppm). X-ray quality crystals were obtained by recrystallization.

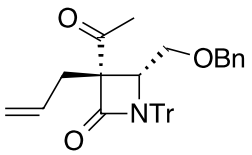

(3*S*,4*R*)-3-Acetyl-3-allyl-4-(benzyloxymethyl)-1-tritylazetidin-2-one (1.25). To a solution of allyl β-lactam **1.24** (612 mg, 1.09 mmol, 1 equiv) in THF (11 mL) at -41°C was added methyllithium (as a 1.6 M solution in ether, 1.87 mL, 2 equiv). The solution was stirred for 30 min, after which TLC (30% EtOAc/hexane) showed complete consumption of starting material. The solution was quenched with methanol, warmed to room temperature, and concentrated. The residue was partitioned between dichloromethane (25 mL) and sat. NH_4Cl (25 mL) and the aqueous layer extracted with dichloromethane (2 x 15 mL). The combined organic layers were washed with brine (25 mL), dried ($MgSO_4$) and concentrated to obtain the product (539 mg, 96% yield) as a colorless solid. mp = 96-99 °C; $[\alpha]_D^{26}$ = -35.7 (c = 0.28, CH_2Cl_2); ^{1}H NMR (500 MHz, $CDCl_3$): δ (ppm) 7.37-7.22 (m, 20H), 5.96 (dddd, *J* = 6.7, 8.1, 10.1, 16.9 Hz, 1H), 5.12 (d, *J* = 17.0 Hz, 1H), 5.07 (d, *J* = 10.5 Hz, 1H), 4.03 (d, *J* = 10.0 Hz, 1H), 3.86 (d, *J* = 10.5 Hz, 1H), 3.73 (s, 1H), 3.12 (d, *J* = 10.5 Hz, 1H), 2.71 (dd, *J* = 8.5, 14.0 Hz, 1H), 2.60 (dd, *J* = 6.5, 13.5 Hz, 1H), 2.19 (s, 3H), 1.97 (d, *J* = 10.0 Hz, 1H); ^{13}C NMR (125 MHz, $CDCl_3$): δ (ppm) 205.2, 168.6, 142.7, 137.1, 132.3, 130.2, 129.0, 128.5, 128.2, 127.8, 127.7, 119.4, 74.1, 73.2, 65.2, 64.0, 39.2, 31.2; IR (thin film) [cm^{-1}]: ν = 3063, 3032, 2926, 2867, 1747, 1705, 1640, 1598, 1494, 1444, 1350, 699; HRMS for $C_{35}H_{33}NO_3Na$ [M+Na] calcd., 538.2353, found, 538.2362 (Error = 1.66 ppm).

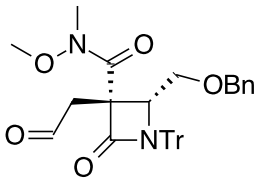

(2*R*,3*R*)-2-((Benzyloxy)methyl)-*N*-methoxy-*N*-methyl-4-oxo-3-(2-oxoethyl)-1-tritylazetidine-3-carboxamide (1.26). To a solution of allyl β-lactam **1.24** (149 mg, 0.27 mmol) in acetone/H_2O (2.5 mL, 9:1) was added *N*-methylmorpholine-*N*-oxide (53 mg, 0.45 mmol, 1.7 equiv) and osmium tetroxide (as a solution in *t*-BuOH, 67 µL, 5.3 µmol, 0.02 equiv) and the resulting solution was allowed to stir overnight in the dark. TLC (50% EtOAc/hexane) showed complete consumption of starting material. Sodium periodate (114 mg, 0.53 mmol, 2 equiv) was added and the solution was stirred for an additional 2.5 h. The suspended solid was removed by vacuum filtration and the solution concentrated under vacuum. The residue was resuspended in water (10 mL) and extracted with EtOAc (3 x 15 mL). The combined organic layers were washed with sat. sodium thiosulfate (30 mL), brine (30 mL), dried ($MgSO_4$), and concentrated to obtain **1.26** (120 mg, 81% yield) as a colorless solid. mp = 56 °C (decomposition); $[\alpha]_D^{25}$ = +38.1 (c = 0.173, CH_2Cl_2); ^{1}H NMR (500 MHz, $CDCl_3$): δ (ppm) 9.83 (dd, *J* = 1.0, 2.5 Hz, 1H), 7.37-7.26 (m, 20H), 4.18 (d, *J* = 11.0 Hz, 1H), 4.10 (d, *J* = 11.0 Hz, 1H), 3.99 (dd, *J* = 2.0, 5.5 Hz, 1H), 3.54 (s, 3H), 3.06 (s, 3H), 2.98 (d, *J* = 9.5 Hz, 1H), 2.92 (d, *J* = 16.0 Hz, 1H), 2.87-2.82 (m, 2H); ^{13}C NMR (125 MHz, $CDCl_3$): δ (ppm) 198.5, 168.2, 166.4, 142.4, 137.5, 129.8, 128.3, 127.9, 127.7, 127.6, 74.0, 73.3, 66.4, 63.0, 61.8, 58.9, 47.1, 32.9; IR (thin film) [cm^{-1}]: ν = 3060, 2925, 1754, 1723, 1638, 1493, 1449, 1339, 751, 735, 700; HRMS for $C_{35}H_{34}N_2O_5Na$ [M+Na] calcd., 585.2366, found, 585.2377 (Error = 1.88 ppm).

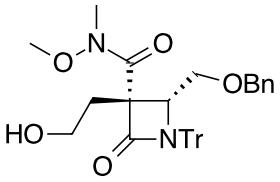

(2*R*,3*R*)-2-((Benzyloxy)methyl)-3-(2-hydroxyethyl)-*N*-methoxy-*N*-methyl-4-oxo-1-tritylazetidine-3-carboxamide (1.27). To a

solution of aldehyde **1.26** (118 mg, 0.210 mmol, 1 equiv) in MeOH (2 mL) at 0 °C was added sodium borohydride (24 mg, 0.631 mmol, 3 equiv). The solution was stirred for 30 min and concentrated to dryness. The residue was redissolved in CH_2Cl_2 (10 mL), washed with sat NH_4Cl (3 x 10 mL), brine (10 mL), dried ($MgSO_4$), and concentrated to afford the product **1.27** as a colorless solid (82 mg, 69% yield). mp = 80-83 °C; $[\alpha]_D^{24}$ = +50.4 (c = 0.222, CH_2Cl_2); ^{1}H NMR (500 MHz, $CDCl_3$): δ (ppm) 7.37-7.26 (m, 20H), 4.13 (d, *J* = 11.0 Hz, 1H), 4.02 (br-s, 1H), 3.95 (d, *J* = 11.0 Hz, 1H), 3.75-3.71 (m, 3H), 3.39 (s, 3H), 3.32 (d, *J* = 10.5 Hz, 1H), 2.61(ddd, *J* = 2.0, 4.5, 14.0 Hz, 1H), 2.22 (d, *J* = 10.0 Hz, 1H), 2.12 (ddd, *J* = 4.0, 9.0, 13.5 Hz, 1H); ^{13}C NMR (125 MHz, $CDCl_3$): δ (ppm) 169.5, 169.4, 142.2, 137.7, 130.0, 128.3, 128.1, 127.9, 127.7, 74.0, 73.2, 65.5, 64.3, 61.7, 61.2, 60.1, 39.1, 33.1; IR (thin film) [cm^{-1}]: ν = 3436, 3059, 2925, 1749, 1641, 1493, 1445, 1357, 752, 700; HRMS for $C_{35}H_{37}N_2O_5$ [M+H] calcd., 565.2697, found, 565.2707 (Error = 1.77 ppm).

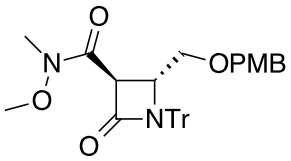

(2*R*,3*S*)-2-(((4-methoxybenzyl)oxy)methyl)-*N*-methoxy-*N*-methyl-4-oxo-1-tritylazetidine-3-carboxamide (1.39). To a solution of β-lactam **1.38** (176 mg, 0.409 mmol, 1 equiv) in dichloromethane (1.5 mL) was added freshly prepared *p*-methoxybenzyl 2,2,2-trichloroacetimidate (693 mg, 2.45 mmol, 6 equiv) and PTSA (8 mg, 0.041 mmol, 0.1 equiv). The resulting solution was stirred overnight, after which TLC (50% EtOAc/Hexane) showed consumption of starting material. The solution was diluted with dichloromethane to 10 mL, washed with sat. $NaHCO_3$ (3 x 10 mL), brine (2 mL), dried ($MgSO_4$) and concentrated. The residue was purified by flash chromatography (30% EtOAc/Hexane to 100% EtOAc) to afford 187 mg (83% yield) of product **1.39** as a colorless solid. mp = 161-165°C; $[\alpha]_D^{23}$ = +12.5° (c =

0.4, CH_2Cl_2); ^{1}H NMR (500 MHz, $CDCl_3$): δ (ppm) 7.31-7.27 (m, 15H), 7.16 (d, *J* = 8.5 Hz, 2H), 6.88 (d, *J* = 8.5 Hz, 2H), 4.58 (s, 1H), 4.36 (s, 1H), 4.11 (m, 2H), 3.82 (s, 3H), 3.79 (s, 3H), 3.24 (s, 3H), 3.00 (d, *J* = 10.5 Hz, 1H), 2.21 (dd, *J* = 2.0, 10.5 Hz, 1H); ^{13}C NMR (125 MHz, $CDCl_3$): δ (ppm) 167.7, 163.6, 159.5, 142.2, 130.1, 129.7, 128.2, 127.9, 127.6, 113.9, 74.1, 72.9, 67.2, 62.7, 56.1, 55.5, 51.9, 32.5; IR (thin film) [cm^{-1}]: ν = 3044, 2937, 2852, 1754, 1654, 1513, 1444, 701; HRMS for $C_{34}H_{35}N_2O_5$ [M+H] calcd., 551.2540, found, 551.2565 (Error = 4.45 ppm)

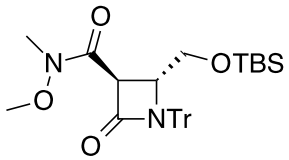

(2*R*,3*S*)-2-((*tert*-Butyldimethylsilyloxy)methyl)-*N*-methoxy-*N*-methyl-4-oxo-1-tritylazetidine-3-carboxamide (1.40). To a solution of β-lactam **1.38** (301 mg, 0.699 mmol, 1 equiv) in dimethylformamide (1 mL) was added *tert*-butyldimethylsilyl chloride (158 mg, 1.05 mmol, 1.5 equiv) and imidazole (143 mg, 2.10 mmol, 3 equiv). The solution was stirred overnight, after which TLC (50% EtOAc/Hex) indicated complete consumption of starting material. The solution was diluted with water (25 mL) and extracted with EtOAc (3 x 25 mL). The combined organic layers were washed with water (3 x 50 mL), brine (50 mL), dried ($MgSO_4$), and concentrated. The resulting residue was purified by flash chromatography (15% EtOAc/Hex to 30% EtOAc/Hex) to obtain 328 mg (86% yield) of product **1.40** as a colorless solid. mp = 82-84°C; $[\alpha]_D^{23}$ = +10 (c = 0.8, CH_2Cl_2); ^{1}H NMR (500 MHz, $CDCl_3$): δ (ppm) 7.34-7.29 (m, 15H), 4.56 (s, 1H), 4.28 (s, 1H), 3.80 (s, 3H), 3.25 (s, 3H), 3.13 (d, *J* = 11.5 Hz, 1H), 2.45 (d, *J* = 11.5 Hz, 1H), 0.88 (s, 9H), -0.06 (s, 3H), -0.07 (s, 3H); ^{13}C NMR (125 MHz, $CDCl_3$): δ (ppm) 167.9, 163.7, 142.2, 130.1, 127.9, 127.6, 74.1, 62.5, 60.7, 57.6, 51.1, 32.4, 25.9, 25.8, 18.4, -5.3, -5.7; IR (thin film) [cm^{-1}]: ν = 3060, 3033, 2954, 2930, 2857, 1755, 1658, 1445,

1348, 735, 701; HRMS for $C_{32}H_{40}N_2O_4SiNa$ [M+Na] calcd., 567.2655, found, 567.2681 (Error = 4.58 ppm).

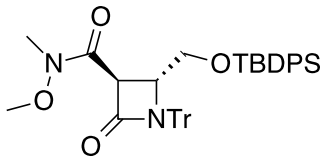

(2*R*,3*S*)-2-(((*tert*-Butyldiphenylsilyl)oxy)methyl)-*N*-methoxy-*N*-methyl-4-oxo-1-tritylazetidine-3-carboxamide (1.41). To a solution of β-lactam **1.38** (682 mg, 1.58 mmol, 1 equiv) in dimethylformamide (1.5 mL) was added *tert*-butyldiphenylsilyl chloride (1.24 µL, 4.75 mmol, 3 equiv), imidazole (324 mg, 4.75 mmol, 3 equiv), and triethylamine (662 µL, 4.75 mmol, 3 equiv). The solution was stirred for 10 h at 60 °C, after which TLC (50% EtOAc/Hex) indicated complete consumption of starting material. The solution was diluted with water (15 mL) and extracted with CH_2Cl_2 (3 x 15 mL). The combined organic layers were washed with water (3 x 30 mL), brine (5 mL), dried ($MgSO_4$), and concentrated. The resulting residue was purified by flash chromatography (10% EtOAc/Hex to 30% EtOAc/Hex) to obtain 1.065 g (100% yield) of product **1.41** as a colorless solid. mp = 74-77 °C; $[\alpha]_D^{25}$ = +34.8 (c = 3.0, CH_2Cl_2); ^{1}H NMR (500 MHz, $CDCl_3$): δ (ppm) 7.54-7.24 (m, 25H), 4.73 (s, 1H), 4.32 (s, 1H), 3.78 (s, 3H), 3.25 (s, 3H), 3.07 (d, *J* = 12.0 Hz, 1H), 2.81 (dd, *J* = 4.0, 12.0 Hz, 1H), 1.07 (s, 9H); ^{13}C NMR (125 MHz, $CDCl_3$): δ (ppm) 167.7, 163.8, 142.3, 135.8, 135.7, 132.9, 132.7, 130.1, 129.9, 128.0, 127.8, 127.6, 74.2, 62.7, 61.8, 57.6, 51.4, 32.5, 27.1, 19.4; IR (thin film) [cm^{-1}]: ν = 3057, 2932, 2858, 1755, 1657, 1445, 1428, 1347, 739, 701; HRMS for $C_{42}H_{45}N_2O_4Si$ [M+H] calcd., 669.3143, found, 669.3163 (Error = 3.01 ppm).

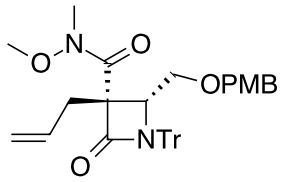

(2*R*,3*R*)-3-Allyl-2-(((4-methoxybenzyl)oxy)methyl)-*N*-methoxy-*N*-methyl-4-oxo-1-tritylazetidine-3-carboxamide (1.42). To a suspension of potassium hydride (106 mg, 0.920 mmol, 3 equiv) and sodium iodide (5 mg, 0.0308 mmol, 0.1 equiv) in THF at 0 °C was added the *trans*-β-lactam **1.39** (170 mg, 0.308 mmol, 1 equiv). The solution was stirred for 30 min, after which allyl bromide (29 µL, 0.339 mmol, 1.1 equiv) was added. The resulting solution was warmed to room temperature and stirred overnight, after which TLC (30% EtOAc / Hexanes) indicated consumption of starting material. The reaction was quenched with methanol and concentrated and the residue purified by silica gel chromatography (30% EtOAc to 70% EtOAc) to obtain the title compound (77 mg) and its C3 epimer (33 mg) as colorless solids. (*dr* = 2.3:1, 60% combined yield). mp = 82-85°C; $[\alpha]_D^{25}$ = +25.3° (c = 6.2, CH_2Cl_2); ^{1}H NMR (500 MHz, $CDCl_3$): δ (ppm) 7.40-7.23 (m, 17H), 6.91 (d, *J* = 8.0 Hz, 2H), 6.00 (app. dq, *J* = 16.7, 8.4 Hz, 1H), 5.16 (d, *J* = 17.0 Hz, 1H), 5.07 (d, *J* = 9.5 Hz, 1H), 4.13 (d, *J* = 11.0 Hz, 1H), 3.96 (d, *J* = 11.0 Hz, 1H), 3.86 (s, 3H), 3.71 (s, 1H), 3.47 (s, 3H), 3.23-3.22 (m, 1H), 3.02-2.98 (m, 4H), 2.60-2.58 (m, 1H), 2.38-2.37 (m, 1H); ^{13}C NMR (125 MHz, $CDCl_3$): δ (ppm) 169.5, 167.6, 159.2, 142.8, 132.8, 130.1, 129.5, 127.7, 127.5, 118.8, 113.6, 73.9, 72.8, 65.8, 63.6, 61.8, 61.2, 55.4, 40.2, 33.1; IR (thin film) [cm^{-1}]: ν = 3059, 2933, 1752, 1641, 1614, 1515, 1493, 1444, 1339, 1303, 754, 728, 701, 640, 624; HRMS for $C_{37}H_{38}N_2O_5Na$ [M+Na] calcd., 613.2673, found, 613.2588 (Error = -13.9 ppm)

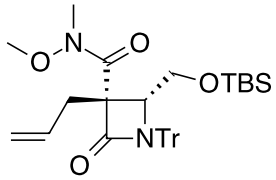

(2*R*,3*R*)-3-Allyl-2-((*tert*-butyldimethylsilyloxy)methyl)-*N*-methoxy-*N*-methyl-4-oxo-1-tritylazetidine-3-carboxamide (1.43).

To a suspension of KH (147 mg, 1.10 mmol, 2 equiv) and NaI (8 mg, 0.055 mmol, 0.1 equiv) in THF (5 mL) at 0 °C was added *trans*-β-lactam **1.40** (300 mg, 0.551 mmol, 1 equiv). The solution was stirred for 1 h, after which allyl bromide (52 µL, 0.606 mmol, 1.1 equiv) was added. The reaction mixture was allowed to stir overnight while warming to room temperature. The solution was quenched with sat. NH_4Cl (10 mL) and the aqueous layer extracted with dichloromethane (2 x 10 mL). The combined organic layers were washed with brine (5 mL), dried ($MgSO_4$), concentrated, and the residue purified by flash chromatography (gradient, 30% EtOAc/hexane to 70% EtOAc/hexane) to afford the title compound as a colorless solid (70 mg, 22% yield), along with the fused lactone / lactam **1.47** (22 mg, 10% yield) as a colorless solid. Analytical data for **1.43**: mp = 69-72°C; $[\alpha]_D^{25}$ = +30.6 (c = 5.8, CH_2Cl_2); ^{1}H NMR (500 MHz, $CDCl_3$): δ (ppm) 7.29 (app. s, 15H), 6.03 (ddt, *J* = 10.0, 17.0, 7.0 Hz, 1H), 5.16 (dd, *J* = 2.0, 17.0 Hz, 1H), 5.05 (dd, *J* = 2.0, 10.0 Hz, 1H), 3.70 (dd, *J* = 3.0, 6.5 Hz, 1H), 3.50 (s, 3H), 3.20 (s, 4H), 3.07 (dd, *J* = 7.0, 14.0 Hz, 1H), 3.03 (app. s, 1H), 2.68 (dd, *J* = 7.0, 14.0 Hz, 1H), 0.79 (s, 9H), -0.16 (s, 6H); ^{13}C NMR (125 MHz, $CDCl_3$): δ (ppm) 167.6, 143.1, 133.6, 130.1, 127.9, 127.6, 118.4, 73.8, 65.5, 61.9, 60.9, 60.1, 40.5, 33.1, 26.0, 18.3, -5.2, -5.5; IR (thin film) [cm^{-1}]: ν = 3060, 2930, 1754, 1653, 1599, 1493, 1449, 776, 755, 734, 701; HRMS for $C_{35}H_{44}N_2O_4SiNa$ [M+Na] calcd., 607.2968, found, 607.2990 (Error = 3.62 ppm).

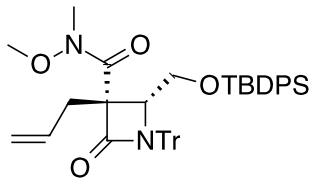

(2*R*,3*R*)-3-Allyl-2-(((*tert*-butyldiphenylsilyl)oxy)methyl)-*N*-methoxy-*N*-methyl-4-oxo-1-tritylazetidine-3-carboxamide (1.44). To a suspension of potassium hydride (367 mg, 3.21 mmol, 3 equiv) and sodium iodide (16 mg, 0.11 mmol, 0.1 equiv) in THF at 0 °C was added

the *trans*-β-lactam **1.41** (715 mg, 1.07 mmol, 1 equiv). The solution was stirred for 30 min, after which allyl bromide (185 µL, 2.14 mmol, 2 equiv) was added. The resulting solution was warmed to room temperature and stirred overnight, after which TLC (30% EtOAc / Hexanes) indicated consumption of starting material. The reaction was quenched with sat. NH_4Cl (1 mL) and the aqueous phase extracted with EtOAc (3 x 1 mL). The combined organics were washed with brine (5 mL), dried ($MgSO_4$), and concentrated to obtain the title compound **1.44** (621 mg, 82% yield) as a single diastereomer. mp = 60-63 °C; $[\alpha]_D^{25}$ = +33.6 (c = 3.65, CH_2Cl_2); ^{1}H NMR (500 MHz, $CDCl_3$): δ (ppm) 7.46-7.32 (m, 10H), 7.17-7.13 (m, 15H), 6.06 (app. ddt, *J* = 7.0, 10.0, 17.0 Hz, 1H), 5.23 (d, *J* = 17.0 Hz, 1H), 5.09 (d, *J* = 10.0 Hz, 1H), 3.76 (dd, *J* = 3.5, 10.0 Hz, 1H), 3.68 (app. t, *J* = 10 Hz, 1H), 3.41 (s, 3H), 3.20 (dd, *J* = 7.0, 14.0 Hz, 1H), 3.15 (s, 3H), 2.82 (dd, *J* = 3.5, 10.0 Hz, 1H), 2.66 (dd, *J* = 7.0, 14.0 Hz, 1H), 0.94 (s, 9H); ^{13}C NMR (125 MHz, $CDCl_3$): δ (ppm) 167.7, 167.0, 142.8, 135.9, 134.0, 133.6, 133.5, 129.7, 129.6, 127.8, 127.6, 127.4, 118.5, 73.7, 65.0, 62.3, 61.7, 60.8, 39.7, 32.9, 26.8, 19.2; IR (thin film) [cm^{-1}]: ν = 3071, 2933, 2858, 1754, 1653, 736, 701; HRMS for $C_{45}H_{48}N_2O_4SiNa$ [M+Na] calcd., 731.3281, found, 731.3301 (Error = 2.73 ppm).

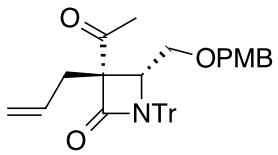

(3*S*,4*R*)-3-acetyl-3-allyl-4-(((4-methoxybenzyl)oxy)methyl)-1-tritylazetidin-2-one (1.45). To a solution of allyl β-lactam **1.42** (310 mg, 0.521 mmol, 1 equiv) in THF (5 mL) at -41°C was added methyllithium (as a 1.6M solution in ether, 0.90 mL, 2 equiv). The solution was stirred for 30 min, after which TLC (30% EtOAc/hexane) showed complete consumption of starting material. The solution was quenched with methanol, warmed to room temperature, and concentrated. The residue was partitioned between dichloromethane (10 mL) and sat.

NH_4Cl (10 mL) and the aqueous layer extracted with dichloromethane (2 x 10 mL). The combined organic layers were washed with brine (25 mL), dried ($MgSO_4$) and concentrated to obtain the product **1.45** (246 mg, 86% yield) as a colorless solid. $[\alpha]_D^{26}$ = +1.0° (c = 1.17, CH_2Cl_2); ^{1}H NMR (500 MHz, $CDCl_3$): δ (ppm) 7.31-7.25 (m, 15H), 7.16 (d, *J* = 8.0 Hz, 2H), 6.89 (d, *J* = 8.0 Hz, 2H), 5.96 (m, 1H), 5.12 (d, *J* = 17.0 Hz, 1H), 5.07 (d, *J* = 10.0 Hz, 1H), 3.96 (d, *J* = 10.0 Hz, 1H), 3.85 (s, 3H), 3.80 (d, *J* = 10.0 Hz, 1H), 3.72 (s, 1H), 3.08 (d, *J* = 10.5 Hz, 1H), 2.71 (dd, *J* = 8.0, 13.5 Hz, 1H), 2.59 (dd, *J* = 6.5, 13.5 Hz, 1H), 2.18 (s, 3H), 1.93 (d, *J* = 10.5 Hz, 1H); ^{13}C NMR (125 MHz, $CDCl_3$): δ (ppm) 205.2, 168.6, 159.6, 142.7, 132.3, 130.5, 130.3, 130.1, 127.8, 127.7, 119.4, 113.8, 74.1, 72.7, 65.2, 64.9, 64.0, 55.5, 39.2, 31.3; IR (thin film) [cm^{-1}]: ν = 3060, 2931, 2863, 1747, 1706, 1613, 1515, 1493, 1444, 755, 701; HRMS for $C_{36}H_{35}NO_4Na$ [M+] calcd., 568.2458, found, 568.2379 (Error = -13.9 ppm)

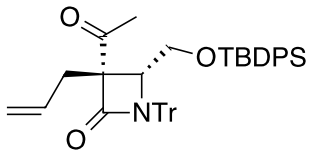

(3*S*,4*R*)-3-acetyl-3-allyl-4-(((*tert*-butyldiphenylsilyl)oxy)methyl)-1-tritylazetidin-2-one (1.46). To a solution of allyl β-lactam **1.44** (50 mg, 70.5 µmol, 1 equiv) in THF (1 mL) at -41 °C was added methyllithium (as a 1.6M solution in ether, 0.26 mL, 6 equiv). The solution was stirred for 30 min, after which TLC (30% EtOAc/hexane) showed complete consumption of starting material. The solution was quenched with methanol, warmed to room temperature, and concentrated. The residue was partitioned between CH_2Cl_2 (5 mL) and sat. aq. NH_4Cl (5 mL) and the aqueous layer extracted with CH_2Cl_2 (2 x 5 mL). The combined organic layers were washed with brine (5 mL), dried ($MgSO_4$) and concentrated to obtain the product **1.46** (42 mg, 89% yield) as a colorless solid. mp = 63-67 °C; $[\alpha]_D^{26}$ = +11.8 (c = 3.35, CH_2Cl_2); ^{1}H NMR (500 MHz, $CDCl_3$): δ (ppm) 7.47-7.45 (m, 5H),

7.41-7.34 (m, 5H), 7.21-7.12 (m, 15H), 5.90 (ddt, *J* = 10.0, 17.0, 7.0 Hz, 1H), 5.20 (dd, *J* = 1.0, 17.0 Hz, 1H), 5.12 (d, *J* = 10.0 Hz, 1H), 3.78 (dd, *J* = 7.8, 3.7 Hz, 1H), 3.41 (dd, *J* = 10.8, 7.9 Hz, 1H), 2.97 (dd, *J* = 10.9, 3.7 Hz, 1H), 2.83 (dd, *J* = 7.1, 14.0 Hz, 1H), 2.74 (dd, *J* = 7.2, 14.0 Hz, 1H), 2.36 (s, 3H), 0.99 (d, *J* = 9.5 Hz, 9H).; ^{13}C NMR (125 MHz, $CDCl_3$): δ (ppm) 204.8, 168.2, 142.5, 135.8, 132.8, 129.89, 129.74, 127.89, 127.76, 127.5, 119.4, 74.6, 67.0, 63.5, 61.3, 37.6, 30.3, 27.1, 19.3; IR (thin film) [cm^{-1}]: ν = 3070, 2926, 2855, 1755, 1712, 1590, 1491, 1449, 822, 741, 701; HRMS for $C_{44}H_{45}NO_3SiNa$ [M+Na] calcd., 686.3061, found, 686.3063 (Error = 0.27 ppm).

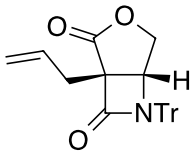

(1*R*,5*R*)-1-Allyl-6-trityl-3-oxa-6-azabicyclo[3.2.0]heptane-2,7-dione (1.47). To a solution of β-lactam **1.44** (101 mg, 0.14 mmol, 1 equiv) in THF (0.57 mL) was added TBAF (1 M solution in THF, 0.43 mL, 3 equiv). The resulting solution was refluxed for 16 h. The solution was quenched with sat. aq. NH_4Cl (5 mL) and extracted with EtOAc (3 x 5 mL). The combined organic layers were washed with brine (10 mL), dried over $MgSO_4$, and concentrated. Flash chromatography (15% EtOAc/Hex to 50% EtOAc/Hex) afforded the title compound **1.47** (35 mg, 60% yield) as a colorless solid. mp = 158-160 °C; $[\alpha]_D^{24}$ = +105.5 (c = 1.83, CH_2Cl_2); ^{1}H NMR (500 MHz, $CDCl_3$): δ (ppm) 7.35-7.34 (m, 9H), 7.14-7.12 (m, 6H), 5.82 (ddt, *J* = 10.0, 17.0, 7.5 Hz, 1H), 5.26 (dd, *J* = 1.0, 17.0 Hz, 1H), 5.20 (dd, *J* = 1.0, 10.0 Hz, 1H), 4.45 (d, *J* = 4.5 Hz, 1H), 3.74 (dd, *J* = 4.5, 11.5 Hz, 1H), 3.25 (d, *J* = 11.5 Hz, 1H), 2.80 (d, *J* = 7.5 Hz, 2H); ^{13}C NMR (125 MHz, $CDCl_3$): δ (ppm) 171.4, 162.6, 141.7, 131.5, 129.7, 128.5, 128.3, 120.4, 74.8, 68.6, 62.8, 58.4; IR (thin film) [cm^{-1}]: ν = 3060, 2928, 2856, 1787, 1751, 1598, 1492, 1445, 741, 700; HRMS for $C_{27}H_{24}NO_3$ [M+H] calcd., 410.1756, found, 410.1764 (Error = 1.95 ppm).

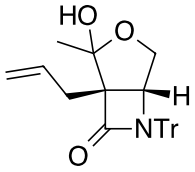

(1*S*,5*R*)-1-Allyl-2-hydroxy-2-methyl-6-trityl-3-oxa-6-azabicyclo[3.2.0]heptan-7-one (1.48). To a solution of lactam **1.46** (401 mg, 0.60 mmol, 1 equiv) in THF (2.2 mL) was added TBAF (1M solution in THF, 1.8 mL, 3 equiv) and acetic acid (0.26 mL, 4.53 mmol, 7.5 equiv). The solution was stirred at reflux for 4 h, after which TLC (30% EtOAc/hexane) showed consumption of starting material. The solution was quenched with sat. aq. $NaHCO_3$ (10 mL) and extracted with EtOAc (3 x 10 mL). The combined organic layers were washed with brine (15 mL), dried over $MgSO_4$, and concentrated. The residue was purified by silica gel chromatography (25% EtOAc/Hex to 50% EtOAc/Hex) to afford the title compound **1.48** (177 mg, 69% yield) as a colorless solid. mp = 174-177 °C; $[\alpha]_D^{24}$ = +66.7 (c = 2.0, CH_2Cl_2); ^{1}H NMR (500 MHz, $CDCl_3$): δ (ppm) 7.29 (app. s, 9H), 7.16 (app. s, 6H), 6.03 (app. dp, *J* = 7.5, 9.7 Hz, 1H), 5.25 (d, *J* = 16.9 Hz, 1H), 5.15 (d, *J* = 9.7 Hz, 1H), 4.11 (d, *J* = 2.0 Hz, 1H), 3.47 (dd, *J* = 10.7, 2.0 Hz, 1H), 2.75 (d, *J* = 10.7 Hz, 1H), 2.66-2.57 (m, 2H), 2.09 (s, 1H), 1.59 (s, 3H); ^{13}C NMR (125 MHz, $CDCl_3$): δ (ppm) 168.1, 142.7, 134.3, 130.1, 127.9, 127.7, 118.9, 102.5, 74.4, 67.8, 65.4, 63.2, 30.8, 23.5; IR (thin film) [cm^{-1}]: ν = 3411, 3060, 2984, 2935, 1730, 1642, 1598, 1493, 1445, 737, 701; HRMS for $C_{28}H_{27}NO_3$ [M+H] calcd., 426.2064, found, 426.2072 (Error = 2.02 ppm).

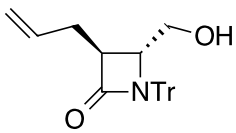

(3*S*,4*R*)-3-allyl-4-(hydroxymethyl)-1-tritylazetidine-2-one (1.49). ^{1}H NMR (500 MHz, $CDCl_3$): δ (ppm) 7.24-7.21 (m, 15H), 5.78 (ddt, *J* = 10.1, 17.0, 6.9 Hz, 1H), 5.06 (d, *J* = 17.1 Hz, 1H), 4.99 (d, *J* = 10.1 Hz, 1H), 3.52 (dt, *J* = 4.3, 2.1 Hz, 1H), 3.03 (ddd, *J* = 9.3, 5.2, 2.0 Hz, 1H), 2.94 (dd, *J* = 11.8, 2.0 Hz, 1H), 2.60 (dd, *J* = 11.9, 4.6 Hz, 1H), 2.57-2.53 (m, 1H), 2.35 (dt, *J* = 15.0, 7.8 Hz, 1H); ^{13}C NMR

(125 MHz, $CDCl_3$): δ (ppm) 170.5, 142.7, 135.0, 129.8, 128.1, 127.7, 117.3, 73.8, 61.6, 60.7, 49.5, 32.9

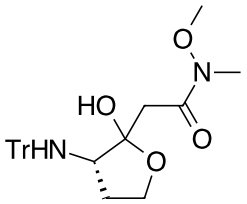

2-((3*S*)-2-Hydroxy-3-(tritylamino)tetrahydrofuran-2-yl)-*N*-methoxy-*N*-methylacetamide. Hexamethyldisilazane (14.0 mL, 67.0 mmol, 2.3 equiv) was dissolved in dry THF (50 mL) and cooled to 0 °C. A solution of n-BuLi (2.5 M solution in hexanes, 25.6 mL, 64.1 mmol, 2.2 equiv) was added and the mixture was stirred for 15 min at 0 °C. The solution was cooled to-78 °C and *N*-methoxy-*N*-methylacetamide (6.5 mL, 61.2 mmol, 2.1 equiv) was added dropwise. The mixture was stirred for 45 min at -78 °C and *N*,*N*-dimethylpropyleneurea (DMPU, 50 mL) was added. After stirring for an additional 15 min, a solution of lactone **1.57** (10.0 g, 29.1 mmol, 1 equiv) in THF (50 mL) was added, resulting in a deeply red solution. The cooling bath was replaced by an ice bath and the solution was allowed to warm to 0 °C and stirred for 2 h. The reaction was quenched with a saturated aqueous solution of NH_4Cl, extracted with EtOAc, washed with brine, dried ($MgSO_4$) and concentrated. The resulting residue was dissolved in a minimal amount of CH_2Cl_2 and applied to a silica plug. The plug was first washed with 10% EtOAc/Hex. The product was then eluted with EtOAc, and the EtOAc was concentrated to obtain the title compound as a colorless solid and was employed in the next reaction without purification. mp = 60-64 °C; $[\alpha]_D^{25}$ = -12.5 (c = 53, CH_2Cl_2); ^{1}H NMR (500 MHz, $CDCl_3$): δ (ppm) 7.57 (d, *J* = 7.5 Hz, 6H), 7.26 (app. t, *J* = 7.5 Hz, 6H), 7.18 (t, *J* = 7.5 Hz, 3H), 3.81 (app. dt, *J* = 3.5, 9.0 Hz, 1H), 3.66 (s, 3H), 3.48 (app. q, *J* = 8.0 Hz, 1H), 3.20 (s, 3H), 2.96 (dd, *J* = 8.0, 8.5 Hz, 1H), 2.70 (d, *J* = 15.5 Hz, 1H), 2.56 (d, *J* = 15.5 Hz, 1H), 2.39 (br-s, 1H), 1.35 (app. quin, *J* = 9.0 Hz, 1H), 1.22 (m, 1H); ^{13}C NMR (125 MHz, $CDCl_3$): δ (ppm) 173.2,

147.1, 129.0, 128.0, 126.5, 102.8, 70.5, 64.9, 61.6, 60.2, 36.7, 31.9, 31.2; IR (thin film) [cm^{-1}]: ν = 3347, 3057, 2939, 2891, 1632, 1596, 1489, 1448, 1389, 771, 736, 709; HRMS for $C_{27}H_{31}N_2O_4$ [M+H] calcd., 447.2278, found, 447.2263 (Error = -3.34 ppm).

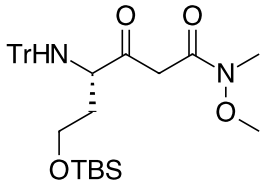

(*S*)-6-((*tert*-Butyldimethylsilyl)oxy)-*N*-methoxy-*N*-methyl-3-oxo-4-(tritylamino)hexanamide. To a solution of the above lactol (2.384 g, 5.01 mmol, 1 equiv) in freshly distilled dimethylformamide (5 mL) was added *tert*-butyldimethylsilyl chloride (1.133 g, 7.52 mmol, 1.5 equiv) and imidazole (682 mg, 10.0 mmol, 3 equiv). The resulting solution was stirred overnight, after which TLC (30% EtOAc/Hex) indicated complete consumption of starting material. The solution was diluted in water (25 mL) and extracted with EtOAc (3 x 50 mL) and the combined organics washed with water (3 x 75 mL), brine (75 mL), dried ($MgSO_4$), and concentrated to afford 2.60 g of the title compound (92% yield) as a thick oil and was used without further purification. An analytically pure sample was obtained by flash chromatography (25% EtOAc/Hex to 50% EtOAc/Hex) as a mixture of keto and enol tautomers (approx.. 2.5:1 ratio; ^{1}H NMR data shown with major isomer H-count in whole integers and minor isomer H-count as decimals). $[\alpha]_D^{26}$ = +7.3 (c = 3, CH_2Cl_2); ^{1}H NMR (500 MHz, $CDCl_3$): δ (ppm) 7.52-7.49 (m, 2.4H), 7.47-7.44 (m, 6H), 7.28-7.13 (m, 12.6H), 5.05 (s, 0.4H), 3.80-3.61 (m, 3.8H), 3.60 (s, 1.2H), 3.54 (s, 3H), 3.46-3.41 (m, 2H), 3.34-3.28 (m, 0.4H), 3.27-3.23 (m, 1H), 3.13 (s, 1.2H), 3.12 (s, 3H), 3.07 (s, 0.4H), 3.04-3.01 (m, 0.4H), 1.90-1.82 (m, 1.4H), 1.67-1.60 (m, 1H), 1.53-1.46 (m, 0.4H), 0.85 (s, 9H), 0.82 (s, 3.6H), 0.05 (s, 3H), 0.03 (s, 3H), 0.01 (s, 2.4H); ^{13}C NMR (125 MHz, $CDCl_3$): δ (ppm) 207.4, 178.3, 171.7, 168.2, 146.9, 146.4, 129.2, 128.0, 127.8, 126.7, 126.4, 87.4, 71.5, 61.4, 61.3, 60.7, 60.0, 59.8, 55.1, 44.2, 37.1, 36.2, 32.0, 26.0, 25.9,

18.3, -5.4; IR (thin film) [cm^{-1}]: ν = 3435, 2954, 2856, 2102, 1633, 1471, 1447, 1254; HRMS for $C_{33}H_{44}N_2O_4NaSi$ [M+Na] calcd., 583.2963, found, 583.2978 (Error = 2.6 ppm).

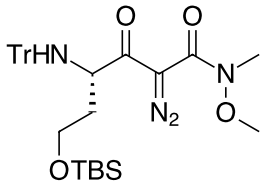

(*S*)-6-((*tert*-Butyldimethylsilyl)oxy)-2-diazo-*N*-methoxy-*N*-methyl-3-oxo-4-(tritylamino)hexanamide (1.58). To a solution of the above β-ketoamide (6.3 g, 11.2 mmol) in acetonitrile (140 mL) was added methanesulfonyl azide (1.5 mL, 16.9 mmol, 1.5 equiv) and 1,8-diazabicyclo[2.2.0]undec-1-ene (DBU, 2.2 mL, 14.6 mmol, 1.3 equiv). The mixture was stirred at room temperature under nitrogen for 4 h, concentrated and filtered over a plug of silica (elution with hexanes/EtOAc 3:1). The clear solution was again concentrated and the remaining solid was crystallized from CH_2Cl_2/hexanes to obtain 6.4 g (97% yield) of **1.58** as a colorless solid. mp = 124 °C (decomposition); $[\alpha]_D^{25}$ = -28.0 (c = 3.8, CH_2Cl_2); ^{1}H NMR (500 MHz, $CDCl_3$): δ (ppm) 7.50-7.52 (m, 6H), 7.20-7.23 (m, 6H), 7.13-7.16 (m, 3H), 4.64-4.71 (m, 1H), 3.85 (app. t, *J* = 7.4 Hz, 2H), 3.61 (s, 3H), 3.48 (d, *J* = 10.6 Hz, 1H), 3.12 (s, 3H), 1.98-2.05 (m, 1H), 1.83-1.90 (m, 1H), 0.90 (s, 9H), 0.07 (s, 3H), 0.06 (s, 3H); ^{13}C NMR (125 MHz, $CDCl_3$): δ (ppm) 196.1, 162.3, 146.6, 129.2, 127.8, 126.4, 71.2, 61.2, 60.3, 56.7, 38.0, 33.7, 26.0, 18.4, -5.2; IR (thin film) [cm^{-1}]: ν = 3310, 3057, 2953, 2929, 2114, 1641, 1362, 1187, 1091; HRMS for $C_{33}H_{43}N_4O_4Si$ [M+H] calcd., 587.3048, found, 587.3069 (Error = 3.6 ppm).

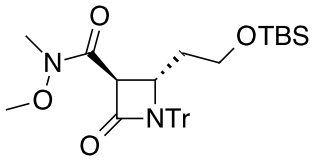

(2*S*,3*S*)-2-(2-((*tert*-Butyldimethylsilyl)oxy)ethyl)-*N*-methoxy-*N*-methyl-4-oxo-1-tritylazetidine-3-carboxamide (1.55). Method A: A degassed solution of α-diazo-β-ketoamide **1.58** (5.7 g, 9.7 mmol, 1 equiv) in dry toluene (1 L), was cooled to 0 °C and irradiated with a medium

pressure mercury vapor lamp for 4.5 h. DBU (7.2 mL, 48.5 mmol, 5 equiv) was added and the mixture was stirred at room temperature overnight, concentrated and filtered over a plug of silica (elution with EtOAc/hexanes 1:1). After removal of the solvents the remaining oil was redissolved in EtOAc, washed with saturated aqueous NH_4Cl, water and brine and dried over $MgSO_4$. Concentration afforded **1.55** as a white foam (5.0 g, 92% yield) which was used for the next step without further purification. Analytical data were obtained from the crystalline solid after purification by flash chromatography on silica gel (elution with hexanes/EtOAc 2:1, 1:1).

Method B: To a degassed solution of α-diazo-β-ketoamide **1.58** (2.46 g, 4.19 mmol, 1 equiv) in dry toluene (1 L) was added DBU (3.1 mL, 21.0 mmol, 5 equiv). The resulting solution was refluxed under N_2 for 1 h. After cooling to room temperature, the solution was washed with aq. 5% citric acid (3 x 100 mL), brine (50 mL), dried over $MgSO_4$, and concentrated to afford the title compound (2.09 g, 89% yield) as a colorless solid which was used for the next step without further purification. mp = 92-94 °C; $[\alpha]_D^{26}$ = +2.0 (c = 2.6, CH_2Cl_2); ^{1}H NMR (500 MHz, $CDCl_3$): δ (ppm) 7.26-7.34 (m, 15H), 4.39 (br d, *J* = 10.6 Hz, 1H), 4.35 (br s, 1H), 3.82 (s, 3H), 3.42-3.46 (m, 1H), 3.33-3.38 (m, 1H), 3.26 (s, 3H), 1.43-1.50 (m, 1H), 0.97-1.02 (m, 1H), 0.82 (s, 9H), -0.06 (s, 3H), -0.07 (s, 3H); ^{13}C NMR (125 MHz, $CDCl_3$): δ (ppm) 167.6, 163.9, 142.4, 129.9, 128.0, 127.6, 74.0, 62.6, 60.3, 56.3, 35.6, 32.3, 25.9, 18.3, -5.6, -5.7; IR (thin film) [cm^{-1}]: ν = 3059, 2953, 2928, 2856, 1752, 1657, 1445, 1101; HRMS for $C_{33}H_{43}N_2O_4Si$ [M+H] calcd., 559.2987, found, 559.2982 (Error = -0.8 ppm).

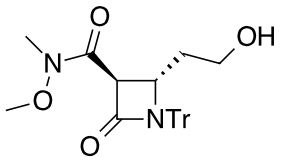

(2*S*,3*S*)-2-(2-Hydroxyethyl)-*N*-methoxy-*N*-methyl-4-oxo-1-tritylazetidine-3-carboxamide. TBAF (1 M in THF, 10.8 mL, 1.5 equiv) was added to a solution of lactam **1.55** (4.0 g, 7.2 mmol, 1 equiv) in THF (4 mL) at room temperature. The mixture was stirred for 2 h and concentrated under a stream of nitrogen. The residue was dissolved in EtOAc, washed with saturated aqueous NH_4Cl, water and brine, dried (Na_2SO_4) and concentrated. Purification by flash chromatography on silica gel (elution with EtOAc/hexanes 6:1 to 8:1) yielded the title compound as a white foam (2.9 g, 91%). mp = 113-115 °C; $[\alpha]_D^{25}$ = +13.6 (c = 3.3, CH_2Cl_2); ^{1}H NMR (500 MHz, $CDCl_3$): δ (ppm) 7.27-7.34 (m, 15H), 4.40 (br d, *J* = 10.5 Hz, 1H), 4.28 (br s, 1H), 3.81 (s, 3H), 3.39-3.50 (m, 2H), 3.27 (s, 3H), 1.47-1.54 (m, 1H), 1.36 (br s, 1H), 0.96-1.03 (m, 1H); ^{13}C NMR (125 MHz, $CDCl_3$): δ (ppm) 167.6, 163.5, 142.3, 128.9, 128,1, 127.6, 74.1, 62.6, 59.7, 56.5, 55.9, 35.4, 32.4; IR (thin film) [cm^{-1}]: ν = 3466, 3058, 2941, 1747, 1651, 1492, 1445; HRMS for $C_{27}H_{29}N_2O_4$ [M+H] calcd., 445.2122, found, 445.2116 (Error = -1.4 ppm).

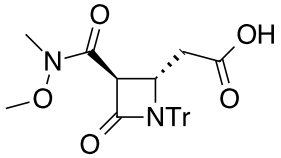

2-((2*S*,3*S*)-3-(Methoxy(methyl)carbamoyl)-4-oxo-1-tritylazetidin-2-yl)acetic acid (23). To a biphasic solution of the previous primary alcohol (748 mg, 1.683 mmol, 1 equiv) in CCl_4 / CH_3CN / H_2O (11.2 mL, 2:2:3) was added $NaIO_4$ (1.080 g, 5.049 mmol, 3 equiv) and $RuCl_3$-*x*H_2O (10 mg, 0.034 mmol, 0.02 equiv) and the resulting solution was stirred vigorously overnight at room temp. The resulting brownish suspension was quenched with brine / sat. $Na_2S_2O_3$ (1:1, 50 mL) and extracted with CH_2Cl_2 (3 x 50 mL). The combined organics were dried ($MgSO_4$) and concentrated to obtain 680 mg (90%) of a slightly brownish solid which was

recrystallized from EtOAc. mp = 82 °C (decomposition); $[\alpha]_D^{25}$ = +27.5 (c = 0.79, CH_2Cl_2); ^{1}H NMR (500 MHz, DMSO-d_6): δ (ppm) 12.24 (br-s, 1H), 7.39-7.34 (m, 9H), 7.19 (d, *J* = 7.0 Hz, 6H), 4.41 (s, 1H), 4.22 (app. dt, *J* = 3.0, 11.0 Hz, 1H), 3.70 (s, 3H), 3.20 (s, 3H), 2,46 (dd, *J* = 10.5, 16.5 Hz, 1H), 1.31 (dd, *J* = 3.5, 17.0 Hz, 1H); ^{13}C NMR (125 MHz, DMSO-d_6): δ (ppm) 171.3, 166.8, 163.1, 141.7, 129.4, 127.9, 127.6, 73.3, 61.7, 54.9, 53.0, 36.0, 31.8; IR (thin film) [cm^{-1}]: ν = 3143, 3059, 2973, 2940, 1750, 1737, 1655, 1492, 1446, 736, 701; HRMS for $C_{27}H_{27}N_2O_5$ [M+H] calcd., 459.1914, found, 459.1944 (Error = 6.4 ppm).

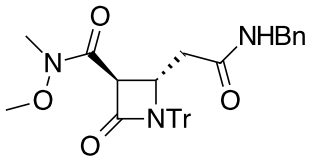

(2*S*,3*S*)-2-(2-(Benzylamino)-2-oxoethyl)-*N*-methoxy-*N*-methyl-4-oxo-1-tritylazetidine-3-carboxamide (1.54). To a solution of the previous carboxylic acid (250 mg, 0.545 mmol, 1 equiv) in CH_2Cl_2 (5.5 mL, 0.1 M) was added 1,1'-carbonyldiimidazole (97 mg, 0.60 mmol, 1.1 equiv). The resulting solution was stirred for 15 min, after which benzylamine (117 mg, 1.090 mmol, 2 equiv) was added and the solution was allowed to stir at room temperature overnight. The reaction mixture was diluted to 10 mL with CH_2Cl_2, washed with sat. NH_4Cl (3 x 10 mL), brine (10 mL) and dried ($MgSO_4$). Concentration afforded the desired compound **1.54** (294 mg, 98 % yield) as a colorless solid which was recrystallized from EtOAc. mp = 91 °C (decomposition); $[\alpha]_D^{25}$ = +16.6 (c = 1.2, CH_2Cl_2); ^{1}H NMR (500 MHz, DMSO-d_6): δ (ppm) 8.19 (t, *J* = 5.5 Hz, 1H), 7.39-7.13 (m, 20H), 4.34-4.33 (m, 2H), 4.17 (dd, *J* = 6.0, 15.0 Hz, 1H), 4.09 (dd, *J* = 6.0, 15.5 Hz, 1H), 3.62 (s, 3H), 3.18 (s, 3H), 2.35 (dd, *J* = 11.5, 15.0 Hz, 1H), 1.45 (dd, *J* = 3.0, 14.0 Hz, 1H); ^{13}C NMR (125 MHz, DMSO-d_6): δ (ppm) 168.4, 166.5, 162.8, 141.6, 139.0, 129.2, 128.1, 127.8, 127.4, 127.0, 126.6, 73.2, 61.6, 54.5, 53.9, 41.8, 37.8, 31.7; IR (thin film)

[cm^{-1}]: ν = 3424, 3061, 2929, 1754, 1657, 1652, 1543, 1494, 1446, 735, 700; HRMS for $C_{34}H_{33}N_3O_4Na$ [M+H] calcd., 548.2544, found, 548.2555 (Error = 1.08 ppm).

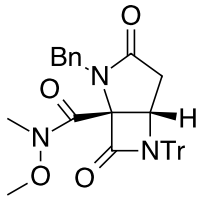

(1*R*,5*S*)-2-Benzyl-*N*-methoxy-*N*-methyl-3,7-dioxo-6-trityl-2,6-diazabicyclo[3.2.0]heptane-1-carboxamide (1.59). General Procedure: A solution of the above secondary amide **1.54** (55 mg, 0.10 mmol) in THF (1 mL) was cooled to -78 °C. A freshly prepared solution of LHMDS (0.17 mL, 1 M Solution in THF, 2.2 equiv) was added and the solution was stirred at -78 °C for 1 h. An oxidant (0.2 mmol, 2 equiv) was then added. The solution was warmed to 0 °C and allowed to stir for an additional 2 h before being quenched with aq. sat. $NaHCO_3$ (2 mL) and aq. sat. $Na_2S_2O_3$ (2 mL). After stirring for 5 min, the aqueous layer was extracted with EtOAc (3 x 5 mL). The combined organic layers were washed with aq. sat. NH_4Cl (3 x 10 mL), Brine (10 mL), and dried over $MgSO_4$. The crude residue was then purified by flash chromatography (30% EtOAc / Hex to 100% EtOAc) to afford the desired product **1.59** as a colorless solid. mp = 80 °C (decomposition); $[\alpha]_D^{25}$ = +60.0 (c = 0.72, CH_2Cl_2); ^{1}H NMR (500 MHz, $CDCl_3$): δ (ppm) 7.46-7.02 (m, 20H), 4.71 (d, *J* = 14.5 Hz, 1H), 4.62 (d, *J* = 14.5 Hz, 1H), 4.44 (d, *J* = 6.5 Hz, 1H) 3.40 (s, 3H), 3.02 (s, 3H), 2.16 (dd, *J* = 6.5, 18.5 Hz, 1H), 1.72 (d, *J* = 18.5 Hz, 1H); ^{13}C NMR (125 MHz, $CDCl_3$): δ (ppm) 173.8, 163.2, 142.0, 136.1, 129.9, 129.8, 128.8, 128.3, 128.1, 127.8, 74.4, 61.3, 56.1, 46.8, 44.8, 34.7, 32.7; IR (thin film) [cm^{-1}]: ν = 3061, 3027, 2934, 1765, 1702, 1662, 1494, 1445, 755, 733, 700; HRMS for $C_{34}H_{32}N_3O_4$ [M+H] calcd., 546.2387, found, 546.2408 (Error = 3.89 ppm).

Crystal data for **1.24** $C_{36}H_{36}N_2O_4$; M_r = 560.67; Hexagonal; space group P6(5); *a* = 9.3384(13) Å; *b* = 9.3384(13) Å; *c* = 59.687(10) Å; α = 90°; β = 90°; γ = 120°; V = 4507.7(12) $Å^3$; Z = 6; T = 150(2) K; λ(Mo-Kα) = 0.71073 Å; μ(Mo-Kα) = 0.081 mm^{-1}; d_{calc} = 1.239g.cm^{-3}; 49903 reflections collected; 7189 unique (R_{int} = 0.0411); giving R_1 = 0.0377, wR_2 = 0.0916 for 6788 data with [I>2σ(I)] and R_1 = 0.0403, wR_2 = 0.0934 for all 7189 data. Residual electron density (e^-.$Å^{-3}$) max/min: 0.183/-0.212. An arbitrary sphere of data were collected on a colorless blade-like crystal, having approximate dimensions of 0.18 × 0.07 × 0.06 mm, on a Bruker APEX-II diffractometer using a combination of ω- and ϕ-scans of 0.3°. Data were corrected for absorption and polarization effects and analyzed for space group determination. The structure was solved by direct methods and expanded routinely. The model was refined by full-matrix least-squares analysis of F^2 against all reflections. All non-hydrogen atoms were refined with anisotropic thermal displacement parameters. Unless otherwise noted, hydrogen atoms were included in calculated positions. Thermal parameters for the hydrogens were tied to the isotropic thermal parameter of the atom to which they are bonded (1.5 X for methyl, 1.2 for all others).

Table 1. Crystal data and structure refinement for **1.24**.

Identification code	xsc1031a	
Empirical formula	C36 H36 N2 O4	
Formula weight	560.67	
Temperature	150(2) K	
Wavelength	0.71073 Å	
Crystal system	Hexagonal	
Space group	P6(5)	
Unit cell dimensions	*a* = 9.3384(13) Å	α = 90°
	b = 9.3384(13) Å	β = 90°
	c = 59.687(10) Å	γ = 120°
Volume	4507.7(12) $Å^3$	
Z	6	
Density (calculated)	1.239 $g.cm^{-3}$	
Absorption coefficient (μ)	0.081 mm^{-1}	
F(000)	1788	
Crystal size	0.18 × 0.07 × 0.06 mm^3	
ω range for data collection	2.05 to 27.88°	
Index ranges	$-12 \leq h \leq 12$, $-12 \leq k \leq 12$, $-78 \leq l \leq 78$	
Reflections collected	49903	
Independent reflections	7189 [R_{int} = 0.0411]	
Completeness to θ = 27.88°	100.0 %	
Absorption correction	Empirical	
Max. and min. transmission	0.7459 and 0.6913	
Refinement method	Full-matrix least-squares on F^2	
Data / restraints / parameters	7189 / 1 / 387	
Goodness-of-fit on F^2	1.039	
Final R indices [I>2σ(I)]	R_1 = 0.0377, wR_2 = 0.0916	
R indices (all data)	R_1 = 0.0403, wR_2 = 0.0934	
Absolute structure parameter	-0.3(7)	
Largest diff. peak and hole	0.183 and -0.212 $e^-.Å^{-3}$	

Table 2. Atomic coordinates and equivalent isotropic displacement parameters ($Å^2$) for **1.24**. U(eq) is defined as one third of the trace of the orthogonalized U_{ij} tensor.

	x	y	z	U(eq)
N(1)	1.03288(14)	1.32310(15)	0.03897(2)	0.019(1)
C(23)	1.18693(17)	1.54517(18)	0.01249(2)	0.020(1)
C(2)	1.03944(17)	1.36710(18)	0.01471(2)	0.019(1)
C(11)	0.87474(17)	1.35697(17)	0.00849(2)	0.019(1)
C(28)	1.48058(19)	1.7342(2)	0.01742(3)	0.029(1)
C(12)	0.79865(18)	1.29579(19)	-0.01220(2)	0.023(1)
C(17)	1.06671(19)	1.2477(2)	-0.00028(2)	0.023(1)
C(22)	0.9789(2)	1.0776(2)	0.00370(3)	0.031(1)
C(24)	1.16793(19)	1.67975(19)	0.00696(3)	0.026(1)
C(18)	1.1660(2)	1.3051(2)	-0.01943(3)	0.031(1)
C(27)	1.34641(19)	1.5748(2)	0.01708(2)	0.025(1)
C(26)	1.4592(2)	1.8678(2)	0.01259(3)	0.033(1)
C(16)	0.80210(19)	1.4178(2)	0.02336(3)	0.026(1)
C(13)	0.6540(2)	1.2958(2)	-0.01789(3)	0.031(1)
C(14)	0.5846(2)	1.3583(2)	-0.00316(3)	0.036(1)
C(29)	0.8354(2)	1.6399(2)	0.08681(3)	0.031(1)
C(25)	1.3036(2)	1.8397(2)	0.00691(3)	0.033(1)
C(30)	0.7567(2)	1.5536(2)	0.10606(3)	0.038(1)
C(1)	1.0091(2)	1.6787(2)	0.08221(4)	0.041(1)
C(33)	0.5911(2)	1.6525(3)	0.07730(3)	0.039(1)
C(21)	0.9927(3)	0.9685(2)	-0.01088(3)	0.040(1)
C(34)	0.5137(2)	1.5662(2)	0.09649(3)	0.037(1)
C(32)	0.7505(2)	1.6884(2)	0.07239(3)	0.036(1)
C(15)	0.6592(2)	1.4191(2)	0.01755(3)	0.033(1)
C(19)	1.1768(2)	1.1936(3)	-0.03402(3)	0.041(1)
C(20)	1.0906(3)	1.0266(3)	-0.02978(3)	0.046(1)
C(31)	0.5972(2)	1.5178(2)	0.11092(3)	0.039(1)
O(3)	1.08936(15)	1.39599(15)	0.10722(2)	0.033(1)
O(2)	0.78550(14)	1.07436(14)	0.04595(2)	0.032(1)

N(2)	0.82680(18)	1.19371(18)	0.10363(2)	0.032(1)
C(4)	0.91584(18)	1.19380(18)	0.05127(2)	0.022(1)
C(9)	1.16239(17)	1.56993(18)	0.06547(2)	0.021(1)
C(6)	0.98134(19)	1.2878(2)	0.09556(2)	0.024(1)
C(10)	1.0995(2)	1.1363(2)	0.07737(3)	0.027(1)
C(8)	1.14553(17)	1.40656(17)	0.05830(2)	0.019(1)
C(7)	1.1708(2)	1.0982(2)	0.05724(3)	0.031(1)
C(5)	1.02662(18)	1.25122(18)	0.07250(2)	0.021(1)
O(4)	1.00206(13)	1.54456(13)	0.06997(2)	0.022(1)
O(1)	0.71954(16)	1.05095(16)	0.09179(2)	0.040(1)
C(35)	0.7860(3)	1.1928(3)	0.12712(3)	0.042(1)
C(36)	0.5850(3)	1.0683(4)	0.08342(5)	0.070(1)
C(3)	1.3307(3)	1.1608(3)	0.05390(4)	0.046(1)
H(28A)	1.5875	1.7521	0.0210	0.035
H(12A)	0.8461	1.2537	-0.0225	0.028
H(22A)	0.9090	1.0359	0.0165	0.037
H(24A)	1.0616	1.6623	0.0032	0.031
H(18A)	1.2265	1.4202	-0.0225	0.037
H(27A)	1.3630	1.4842	0.0200	0.030
H(26A)	1.5505	1.9774	0.0132	0.039
H(16A)	0.8513	1.4586	0.0376	0.031
H(13A)	0.6028	1.2526	-0.0320	0.038
H(14A)	0.4868	1.3597	-0.0071	0.043
H(25A)	1.2891	1.9301	0.0029	0.040
H(30A)	0.8127	1.5187	0.1160	0.045
H(1A)	1.0684	1.7820	0.0734	0.049
H(1B)	1.0692	1.6941	0.0965	0.049
H(33A)	0.5348	1.6874	0.0674	0.047
H(21A)	0.9344	0.8533	-0.0078	0.048
H(34A)	0.4037	1.5402	0.0998	0.044
H(32A)	0.8024	1.7467	0.0590	0.043
H(15A)	0.6118	1.4618	0.0277	0.040
H(19A)	1.2444	1.2338	-0.0470	0.049
H(20A)	1.0983	0.9517	-0.0398	0.055

H(31A)	0.5449	1.4596	0.1243	0.047
H(9A)	1.2321	1.6114	0.0791	0.026
H(9B)	1.2156	1.6530	0.0534	0.026
H(10A)	1.1871	1.1894	0.0889	0.033
H(10B)	1.0110	1.0310	0.0837	0.033
H(8A)	1.2558	1.4153	0.0561	0.023
H(7A)	1.0965	1.0249	0.0463	0.037
H(35A)	0.8668	1.2976	0.1341	0.063
H(35B)	0.7886	1.1012	0.1348	0.063
H(35C)	0.6752	1.1789	0.1284	0.063
H(36A)	0.5082	0.9684	0.0751	0.104
H(36B)	0.6280	1.1643	0.0734	0.104
H(36C)	0.5268	1.0841	0.0960	0.104
H(3A)	1.413(3)	1.235(3)	0.0648(4)	0.053(7)
H(3B)	1.375(3)	1.136(3)	0.0399(5)	0.069(8)

Table 3. Anisotropic displacement parameters $(Å)^2$ for **1.24**. The anisotropic displacement factor exponent takes the form: $-2\pi^2[h^2 a^{*2} U_{11} + ... + 2 h k a^* b^* U_{12}]$

	U_{11}	U_{22}	U_{33}	U_{23}	U_{13}	U_{12}
N(1)	0.0177(5)	0.0202(6)	0.0184(5)	-0.0022(4)	-0.0032(4)	0.0095(5)
C(23)	0.0195(7)	0.0255(7)	0.0148(6)	0.0000(5)	0.0009(5)	0.0106(6)
C(2)	0.0198(6)	0.0253(7)	0.0153(6)	-0.0017(5)	-0.0016(5)	0.0135(6)
C(11)	0.0179(6)	0.0213(6)	0.0191(6)	-0.0006(5)	-0.0015(5)	0.0105(5)
C(28)	0.0196(7)	0.0401(9)	0.0230(7)	0.0020(6)	0.0014(6)	0.0107(7)
C(12)	0.0233(7)	0.0283(7)	0.0198(7)	-0.0036(6)	-0.0031(5)	0.0144(6)
C(17)	0.0247(7)	0.0330(8)	0.0203(6)	-0.0062(6)	-0.0075(5)	0.0209(7)
C(22)	0.0401(9)	0.0320(8)	0.0278(8)	-0.0087(6)	-0.0093(7)	0.0234(7)
C(24)	0.0248(7)	0.0299(8)	0.0235(7)	0.0019(6)	-0.0027(6)	0.0142(6)
C(18)	0.0278(8)	0.0476(10)	0.0230(7)	-0.0066(7)	-0.0034(6)	0.0239(8)
C(27)	0.0232(7)	0.0344(8)	0.0191(7)	0.0009(6)	0.0012(5)	0.0158(6)
C(26)	0.0281(8)	0.0293(8)	0.0286(8)	0.0032(6)	0.0006(6)	0.0052(7)
C(16)	0.0259(7)	0.0377(8)	0.0202(7)	-0.0054(6)	-0.0044(6)	0.0200(7)
C(13)	0.0283(8)	0.0457(10)	0.0243(8)	-0.0089(7)	-0.0098(6)	0.0214(8)
C(14)	0.0270(8)	0.0547(11)	0.0360(9)	-0.0091(8)	-0.0085(7)	0.0287(8)
C(29)	0.0250(8)	0.0233(7)	0.0440(10)	-0.0133(7)	-0.0028(7)	0.0126(6)
C(25)	0.0369(9)	0.0270(8)	0.0328(8)	0.0029(6)	-0.0033(7)	0.0139(7)
C(30)	0.0342(9)	0.0312(9)	0.0522(11)	0.0007(8)	-0.0074(8)	0.0196(7)
C(1)	0.0262(8)	0.0302(9)	0.0646(13)	-0.0219(8)	-0.0012(8)	0.0132(7)
C(33)	0.0311(9)	0.0495(11)	0.0380(10)	0.0021(8)	-0.0069(7)	0.0205(8)
C(21)	0.0561(12)	0.0403(10)	0.0385(10)	-0.0147(8)	-0.0163(9)	0.0346(9)
C(34)	0.0271(8)	0.0452(10)	0.0380(9)	-0.0020(8)	0.0018(7)	0.0185(8)
C(32)	0.0308(9)	0.0393(9)	0.0293(8)	-0.0020(7)	0.0012(7)	0.0116(7)
C(15)	0.0289(8)	0.0486(10)	0.0331(8)	-0.0101(7)	-0.0046(7)	0.0277(8)
C(19)	0.0407(10)	0.0694(13)	0.0261(8)	-0.0148(8)	-0.0043(7)	0.0377(10)
C(20)	0.0604(13)	0.0677(14)	0.0357(9)	-0.0250(9)	-0.0165(9)	0.0520(12)
C(31)	0.0369(9)	0.0401(10)	0.0381(9)	0.0049(8)	0.0024(7)	0.0177(8)
O(3)	0.0345(6)	0.0407(7)	0.0209(5)	-0.0043(5)	-0.0044(5)	0.0157(6)
O(2)	0.0243(6)	0.0274(6)	0.0297(6)	-0.0011(4)	-0.0044(4)	0.0029(5)

N(2)	0.0322(7)	0.0359(8)	0.0246(6)	0.0019(6)	0.0070(5)	0.0154(6)
C(4)	0.0218(7)	0.0243(7)	0.0210(7)	-0.0016(5)	-0.0012(5)	0.0120(6)
C(9)	0.0192(7)	0.0237(7)	0.0202(6)	-0.0026(5)	-0.0016(5)	0.0098(6)
C(6)	0.0285(7)	0.0313(8)	0.0178(7)	0.0021(6)	-0.0001(6)	0.0187(7)
C(10)	0.0322(8)	0.0290(8)	0.0254(7)	0.0037(6)	-0.0011(6)	0.0187(7)
C(8)	0.0177(6)	0.0229(7)	0.0170(6)	-0.0015(5)	-0.0023(5)	0.0108(5)
C(7)	0.0387(9)	0.0306(8)	0.0310(8)	0.0006(6)	-0.0005(7)	0.0229(7)
C(5)	0.0200(7)	0.0233(7)	0.0191(6)	-0.0001(5)	-0.0008(5)	0.0111(6)
O(4)	0.0200(5)	0.0238(5)	0.0251(5)	-0.0074(4)	-0.0038(4)	0.0123(4)
O(1)	0.0293(6)	0.0373(7)	0.0431(7)	-0.0024(6)	0.0071(5)	0.0090(5)
C(35)	0.0510(11)	0.0517(11)	0.0300(9)	0.0082(8)	0.0151(8)	0.0307(10)
C(36)	0.0320(11)	0.112(2)	0.0646(16)	-0.0284(15)	-0.0030(10)	0.0361(14)
C(3)	0.0423(11)	0.0506(12)	0.0559(13)	0.0007(10)	0.0083(10)	0.0314(10)

Table 4. Bond lengths [Å] for **1.24**.

atom-atom	distance	atom-atom	distance
N(1)-C(4)	1.3680(19)	N(1)-C(8)	1.4917(17)
N(1)-C(2)	1.4979(18)	C(23)-C(24)	1.394(2)
C(23)-C(27)	1.399(2)	C(23)-C(2)	1.546(2)
C(2)-C(11)	1.5384(19)	C(2)-C(17)	1.5471(19)
C(11)-C(12)	1.3964(19)	C(11)-C(16)	1.399(2)
C(28)-C(27)	1.386(2)	C(28)-C(26)	1.389(3)
C(12)-C(13)	1.393(2)	C(17)-C(22)	1.396(2)
C(17)-C(18)	1.399(2)	C(22)-C(21)	1.394(2)
C(24)-C(25)	1.394(2)	C(18)-C(19)	1.399(2)
C(26)-C(25)	1.383(3)	C(16)-C(15)	1.385(2)
C(13)-C(14)	1.383(2)	C(14)-C(15)	1.393(2)
C(29)-C(30)	1.384(3)	C(29)-C(32)	1.390(3)
C(29)-C(1)	1.501(2)	C(30)-C(31)	1.384(3)
C(1)-O(4)	1.4227(19)	C(33)-C(34)	1.379(3)
C(33)-C(32)	1.384(3)	C(21)-C(20)	1.381(3)
C(34)-C(31)	1.381(3)	C(19)-C(20)	1.374(3)
O(3)-C(6)	1.226(2)	O(2)-C(4)	1.2119(19)
N(2)-C(6)	1.349(2)	N(2)-O(1)	1.395(2)
N(2)-C(35)	1.452(2)	C(4)-C(5)	1.552(2)
C(9)-O(4)	1.4196(17)	C(9)-C(8)	1.515(2)
C(6)-C(5)	1.528(2)	C(10)-C(7)	1.500(2)
C(10)-C(5)	1.559(2)	C(8)-C(5)	1.564(2)
C(7)-C(3)	1.319(3)	O(1)-C(36)	1.434(3)

Symmetry transformations used to generate equivalent atoms:

Table 5. Bond angles [°] for **1.24**.

atom-atom-atom	angle	atom-atom-atom	angle
C(4)-N(1)-C(8)	95.15(11)	C(4)-N(1)-C(2)	131.74(12)
C(8)-N(1)-C(2)	133.06(12)	C(24)-C(23)-C(27)	118.09(14)
C(24)-C(23)-C(2)	122.92(13)	C(27)-C(23)-C(2)	118.94(13)
N(1)-C(2)-C(11)	108.30(11)	N(1)-C(2)-C(23)	105.67(11)
C(11)-C(2)-C(23)	111.79(11)	N(1)-C(2)-C(17)	111.11(11)
C(11)-C(2)-C(17)	109.63(11)	C(23)-C(2)-C(17)	110.28(12)
C(12)-C(11)-C(16)	118.45(13)	C(12)-C(11)-C(2)	121.82(12)
C(16)-C(11)-C(2)	119.66(12)	C(27)-C(28)-C(26)	120.21(15)
C(13)-C(12)-C(11)	120.74(14)	C(22)-C(17)-C(18)	118.35(14)
C(22)-C(17)-C(2)	120.46(14)	C(18)-C(17)-C(2)	120.86(14)
C(21)-C(22)-C(17)	120.58(17)	C(25)-C(24)-C(23)	120.59(15)
C(17)-C(18)-C(19)	120.29(18)	C(28)-C(27)-C(23)	121.11(15)
C(25)-C(26)-C(28)	119.29(15)	C(15)-C(16)-C(11)	120.65(14)
C(14)-C(13)-C(12)	120.24(15)	C(13)-C(14)-C(15)	119.48(15)
C(30)-C(29)-C(32)	118.71(16)	C(30)-C(29)-C(1)	119.20(17)
C(32)-C(29)-C(1)	122.09(18)	C(26)-C(25)-C(24)	120.58(16)
C(31)-C(30)-C(29)	120.57(17)	O(4)-C(1)-C(29)	108.23(13)
C(34)-C(33)-C(32)	120.23(17)	C(20)-C(21)-C(22)	120.50(19)
C(33)-C(34)-C(31)	119.50(17)	C(33)-C(32)-C(29)	120.61(17)
C(16)-C(15)-C(14)	120.43(15)	C(20)-C(19)-C(18)	120.69(18)
C(19)-C(20)-C(21)	119.58(17)	C(34)-C(31)-C(30)	120.38(18)
C(6)-N(2)-O(1)	117.71(13)	C(6)-N(2)-C(35)	122.74(15)
O(1)-N(2)-C(35)	115.02(14)	O(2)-C(4)-N(1)	131.55(14)
O(2)-C(4)-C(5)	136.14(14)	N(1)-C(4)-C(5)	91.88(11)
O(4)-C(9)-C(8)	108.39(11)	O(3)-C(6)-N(2)	120.37(14)
O(3)-C(6)-C(5)	119.33(14)	N(2)-C(6)-C(5)	120.12(13)
C(7)-C(10)-C(5)	114.34(13)	N(1)-C(8)-C(9)	115.83(11)
N(1)-C(8)-C(5)	86.92(10)	C(9)-C(8)-C(5)	116.69(12)
C(3)-C(7)-C(10)	123.70(18)	C(6)-C(5)-C(4)	126.99(12)
C(6)-C(5)-C(10)	104.52(11)	C(4)-C(5)-C(10)	111.07(12)
C(6)-C(5)-C(8)	115.37(12)	C(4)-C(5)-C(8)	85.38(10)
C(10)-C(5)-C(8)	112.83(12)	C(9)-O(4)-C(1)	111.68(11)
N(2)-O(1)-C(36)	108.64(16)		

Symmetry transformations used to generate equivalent atoms:

Table 6. Torsion angles [°] for **1.24**.

atom-atom-atom-atom	angle	atom-atom-atom-atom	angle
C(4)-N(1)-C(2)-C(11)	48.79(19)	C(8)-N(1)-C(2)-C(11)	-127.96(15)
C(4)-N(1)-C(2)-C(23)	168.71(14)	C(8)-N(1)-C(2)-C(23)	-8.04(19)
C(4)-N(1)-C(2)-C(17)	-71.67(19)	C(8)-N(1)-C(2)-C(17)	111.59(15)
C(24)-C(23)-C(2)-N(1)	-113.59(14)	C(27)-C(23)-C(2)-N(1)	63.78(16)
C(24)-C(23)-C(2)-C(11)	4.01(18)	C(27)-C(23)-C(2)-C(11)	-178.62(12)
C(24)-C(23)-C(2)-C(17)	126.25(14)	C(27)-C(23)-C(2)-C(17)	-56.39(16)
N(1)-C(2)-C(11)-C(12)	-141.83(14)	C(23)-C(2)-C(11)-C(12)	102.15(15)
C(17)-C(2)-C(11)-C(12)	-20.46(19)	N(1)-C(2)-C(11)-C(16)	41.39(17)
C(23)-C(2)-C(11)-C(16)	-74.63(16)	C(17)-C(2)-C(11)-C(16)	162.76(14)
C(16)-C(11)-C(12)-C(13)	0.2(2)	C(2)-C(11)-C(12)-C(13)	-176.66(15)
N(1)-C(2)-C(17)-C(22)	43.92(18)	C(11)-C(2)-C(17)-C(22)	-75.75(17)
C(23)-C(2)-C(17)-C(22)	160.76(13)	N(1)-C(2)-C(17)-C(18)	-142.87(14)
C(11)-C(2)-C(17)-C(18)	97.46(16)	C(23)-C(2)-C(17)-C(18)	-26.03(18)
C(18)-C(17)-C(22)-C(21)	1.2(2)	C(2)-C(17)-C(22)-C(21)	174.59(14)
C(27)-C(23)-C(24)-C(25)	-2.5(2)	C(2)-C(23)-C(24)-C(25)	174.87(14)
C(22)-C(17)-C(18)-C(19)	-0.4(2)	C(2)-C(17)-C(18)-C(19)	-173.72(14)
C(26)-C(28)-C(27)-C(23)	-1.7(2)	C(24)-C(23)-C(27)-C(28)	3.7(2)
C(2)-C(23)-C(27)-C(28)	-173.80(13)	C(27)-C(28)-C(26)-C(25)	-1.6(2)
C(12)-C(11)-C(16)-C(15)	-0.8(2)	C(2)-C(11)-C(16)-C(15)	176.06(15)
C(11)-C(12)-C(13)-C(14)	0.7(3)	C(12)-C(13)-C(14)-C(15)	-0.9(3)
C(28)-C(26)-C(25)-C(24)	2.8(3)	C(23)-C(24)-C(25)-C(26)	-0.7(2)
C(32)-C(29)-C(30)-C(31)	-0.6(3)	C(1)-C(29)-C(30)-C(31)	179.16(17)
C(30)-C(29)-C(1)-O(4)	88.9(2)	C(32)-C(29)-C(1)-O(4)	-91.4(2)
C(17)-C(22)-C(21)-C(20)	-1.5(3)	C(32)-C(33)-C(34)-C(31)	0.9(3)
C(34)-C(33)-C(32)-C(29)	-0.8(3)	C(30)-C(29)-C(32)-C(33)	0.6(3)
C(1)-C(29)-C(32)-C(33)	-179.12(17)	C(11)-C(16)-C(15)-C(14)	0.6(3)
C(13)-C(14)-C(15)-C(16)	0.2(3)	C(17)-C(18)-C(19)-C(20)	-0.2(3)
C(18)-C(19)-C(20)-C(21)	-0.2(3)	C(22)-C(21)-C(20)-C(19)	1.0(3)
C(33)-C(34)-C(31)-C(30)	-0.8(3)	C(29)-C(30)-C(31)-C(34)	0.7(3)
C(8)-N(1)-C(4)-O(2)	-179.77(17)	C(2)-N(1)-C(4)-O(2)	2.6(3)
C(8)-N(1)-C(4)-C(5)	-6.51(11)	C(2)-N(1)-C(4)-C(5)	175.88(14)
O(1)-N(2)-C(6)-O(3)	-166.28(15)	C(35)-N(2)-C(6)-O(3)	-11.4(2)
O(1)-N(2)-C(6)-C(5)	8.8(2)	C(35)-N(2)-C(6)-C(5)	163.73(15)
C(4)-N(1)-C(8)-C(9)	-111.81(13)	C(2)-N(1)-C(8)-C(9)	65.76(19)
C(4)-N(1)-C(8)-C(5)	6.46(11)	C(2)-N(1)-C(8)-C(5)	-175.97(14)
O(4)-C(9)-C(8)-N(1)	55.18(15)	O(4)-C(9)-C(8)-C(5)	-44.99(16)
C(5)-C(10)-C(7)-C(3)	107.3(2)	O(3)-C(6)-C(5)-C(4)	-147.14(15)
N(2)-C(6)-C(5)-C(4)	37.7(2)	O(3)-C(6)-C(5)-C(10)	81.57(17)
N(2)-C(6)-C(5)-C(10)	-93.59(16)	O(3)-C(6)-C(5)-C(8)	-42.92(19)
N(2)-C(6)-C(5)-C(8)	141.92(14)	O(2)-C(4)-C(5)-C(6)	-62.6(3)

N(1)-C(4)-C(5)-C(6)	124.71(15)	O(2)-C(4)-C(5)-C(10)	66.2(2)
N(1)-C(4)-C(5)-C(10)	-106.50(13)	O(2)-C(4)-C(5)-C(8)	178.92(19)
N(1)-C(4)-C(5)-C(8)	6.20(11)	C(7)-C(10)-C(5)-C(6)	-173.58(14)
C(7)-C(10)-C(5)-C(4)	46.45(18)	C(7)-C(10)-C(5)-C(8)	-47.48(18)
N(1)-C(8)-C(5)-C(6)	-134.72(12)	C(9)-C(8)-C(5)-C(6)	-17.25(17)
N(1)-C(8)-C(5)-C(4)	-5.69(10)	C(9)-C(8)-C(5)-C(4)	111.78(13)
N(1)-C(8)-C(5)-C(10)	105.24(12)	C(9)-C(8)-C(5)-C(10)	-137.29(13)
C(8)-C(9)-O(4)-C(1)	164.76(14)	C(29)-C(1)-O(4)-C(9)	-178.37(14)
C(6)-N(2)-O(1)-C(36)	-115.87(19)	C(35)-N(2)-O(1)-C(36)	87.3(2)

Symmetry transformations used to generate equivalent atoms:

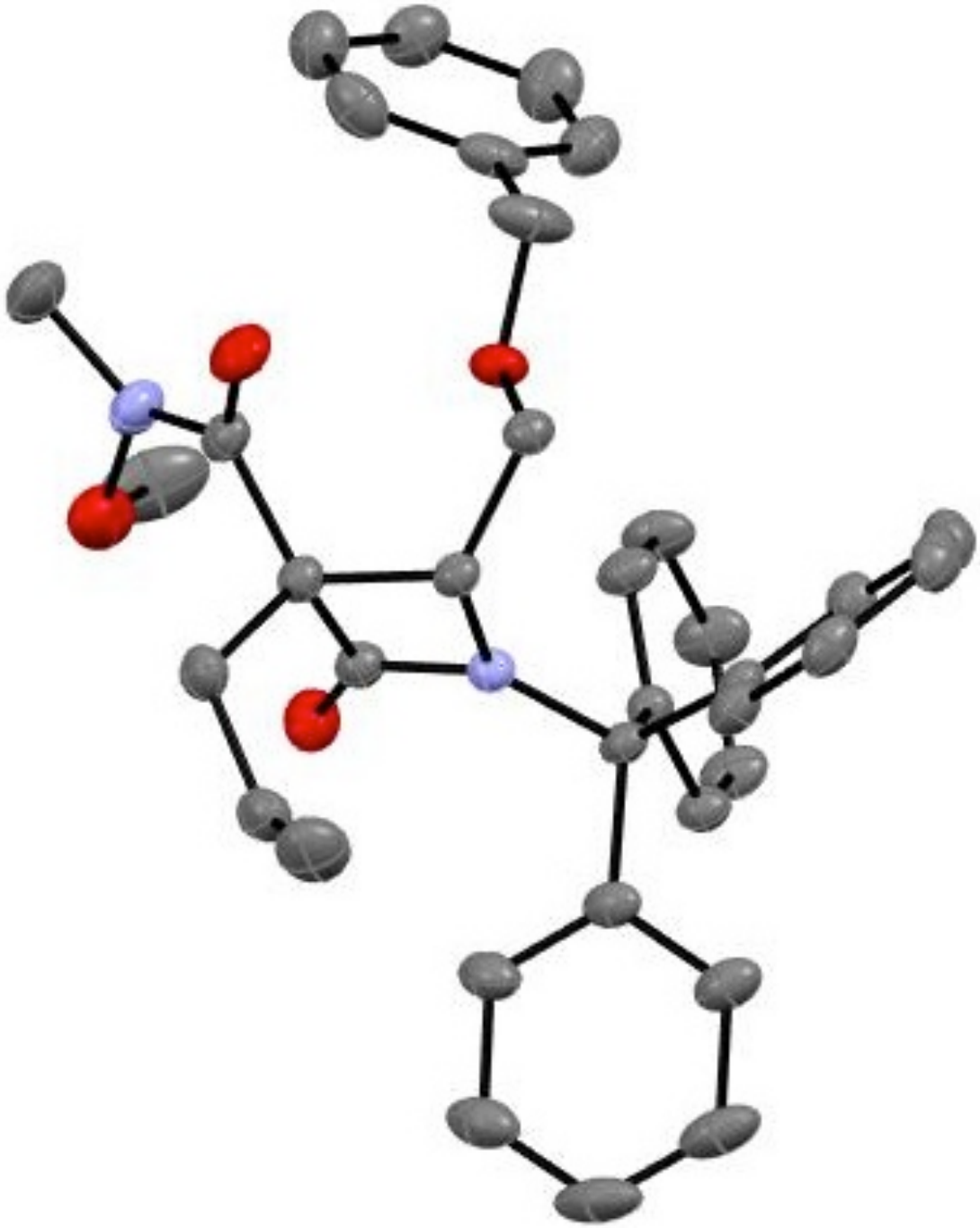

ORTEP of **1.24**

References

1. Von Nussbaum, F.; Brands, M.; Hinzen, B.; Weigand, S.; Häbich, D. *Angew. Chem. Int. Ed.* **2006**, *45*, 5072-5129.
2. Kværnø, L.; Werder, M.; Hauser, H.; Carreira, E. *J. Med. Chem.* **2005**, *48*, 6035-6053.
3. Gerona-Navarro, G.; de Vega, M. J. P.; García-López, M. T.; Andrei, G.; Snoeck, R.; De Clercq, E.; Balzarini, J.; González-Muñiz, R. *J. Med. Chem.* **2005**, *48*, 2612-2621.
4. Alcaide, B.; Almendros, P. *Chem. Soc. Rev.* **2001**, *30*, 226-240.
5. Alcaide, B.; Almendros, P.; Aragoncillo, C. *Chem Rev.* **2007**, 107, 4437-4492.
6. Maier, T. C.; Frey, W. U.; Podlech, J. *Eur. J. Org. Chem.* **2002**, 2686-2689.
7. Palomo, C.; Aizpurua, J. M.; Balentová, E.; Jimenez, A.; Oyarbide, J.; Fratila, R. M.; Miranda, J. I. *Org. Lett.* **2007**, *9*, 101-104.
8. a) Juraisti, E. *Enantioselective Synthesis of* β-*Amino Acids*, Wiley-VCH: New York, 1997. b) Juraisti, E.; Soloshonok, V. *Enantioselective Synthesis of* β-*Amino Acids*, 2nd ed.; Wiley: New York, 2005.
9. a) Palomo, C.; Aizpurua, J. M.; Ganboa, I., "The Synthesis of β-Amino Acids and Their Derivatives from β-Lactams," in reference 8a, Chapter 14. b) Palomo, C.; Aizpurua, J. M.; Ganboa, I.; Oiarbide, M., "The Synthesis of β-Amino Acids and Their Derivatives from β-Lactams: Update," in reference 8b, Chapter 20.
10. Fülöp, F.; Forró, E.; Tóth, G. K. *Org. Lett.* **2004**, *6*, 4239-4241.
11. a) Gelman, M. A.; Gellman, S. H., "Using Constrained β-Amino Acid Residues to Control *b*-Peptide Shape and Function," in reference 8b, Chapter 22. b) Campo, M. A.; Escalante, J.; Šebesta, R., "β^2-Amino Acids with Proteinogenic Side Chains and

Corresponding Peptides: Synthesis, Secondary Structure, and Biological Activity," in reference 8b, Chapter 23.

12. Seebach, D.; Kimmerlin, T.; Šebesta, R.; Campo, M. A.; Beck, A. K. *Tetrahedron* **2004**, *60*, 7455-7506.
13. Singh, G. S. *Tetrahedron* **2003**, *59*, 7631-7649.
14. France, S.; Weatherwax, A.; Taggi, A. E.; Lectka, T. *Acc. Chem. Res.* **2004**, *37*, 592-600.
15. D'hooghe, M.' Dekeukeleire, S.; Leemans, E.; De Kimpe, N. *Pure Appl. Chem.* **2010**, *82*, 1749-1759.
16. a) Ojima, I. *The Organic Chemistry of β-Lactams*; Georg, G. I., Ed.; VCH Publishers: New York, 1992; 197-255. b) Ojima, I. *Acc. Chem. Res.* **1995**, *28*, 383-389.
17. Dekeukeleire, S.; D'hooghe, M.; De Kimpe, N. *Pure Appl. Chem.* **2005**, *77*, 2061
18. Van Brabandt, W.; Vanwalleghem, M.; D'hooghe, M.; De Kimpe, N. *J. Org. Chem.* **2006**, *71*, 7083.
19. Leemans, E.; D'hooghe, M.; Dejaegher, Y.; Törnroos, K.W.; De Kimpe, N. *J. Org Chem.* **2008**, *73*, 1422.
20. a) Thurkauf, A.; Mattson, M.V.; Huguenin, P.N.; Rice, K.C.; Jacobson, A.E. *FEBS Lett.* **1988**, *238*, 369. b) Sax, M.; Ebert, K.; Schepmann, D.; Wibbeling, B.; Wünsch, B. *Bioorg. Med. Chem.* **2006**, *14*, 5955.
21. Leemans, E.; D'hooghe, M.; Dejaegher, Y.; Törnroos, K.W.; De Kimpe, N. *Eur. J. Org. Chem.* **2010**, 352
22. Yamashita, M.; Tsurumi, Y.; Hosoda, J.; Komori, T.; Kohsaka, M.; Imanaka, H. *J. Antibiot.* **1984**, *37*, 1279.

23. Mimieux Vaske, Y. S.; Mahoney, M. E.; Konopelski, J. P.; Rogow, D. L.; McDonald, W. J. *J. Am. Chem. Soc.* **2010**, *132*, 11379-11385.

24. Davies, S. G.; Fletcher, A. M.; Thomson, J. E. *Chem Commun.* **2013**, *49*, 8586-8598

25. (a) Konopelski, J. P.; Boehler, M. A. *J. Am. Chem. Soc.* **1989**, *111*, 4515-4517; (b) Zuckerman, N. B.; Myers, A. S.; Quan, T. K.; Bray, W. M.; Lokey, R. S.; Hartzog, G. A.; Konopelski, J. P. *ChemMedChem* **2012**, *7*, 761-765.

26. CCDC No. 996120; special thanks to Dr. Nathaniel B. Zuckermann for providing X-ray quality crystals for analysis.

27. Hotoda, H.; Takahashi, M.; Tanzawa, K.; Takahashi, S.; Kaneko, M. *Tetrahedron Lett.* **1995**, *36*, 5037.

28. a) Bhuyan, B.K.; Dietz, A.; Smith, C.G. *Antimicrob. Agents Chemother.* **1961**, 184-190. b) Argoudelis, A.D.; Jahnke, H.K.; Fox, J.A. *Antimicrob. Agents Chemother.* **1961**, 191-197. c) Brodasky, T.F.; Lummis, W.L. *Antimicrob. Agents Chemother.* **1961**, 198-204.

29. a) Wiley, P.F.; Jahnke, H.K.; MacKellar, F.; Kelly, R.B., Argoudelis, A.D. *J. Org. Chem.* **1970**, *35*, 1420. b) Duchamp, D.J. abstract no. 23 presented at the American Crystallographic Association Winter Meeting, Albuquerque, NM, 3 to 7 April 1972. c) Weller, D.D.; Haber, A.; Rinehart, K.L. Jr.; Wiley, P.F. *J. Antibiot.* **1978**, *31*, 997. d) Dinos, G.; Wilson, D.N.; Teraoka, Y.; Szaflarski, W.; Fucini, P.; Kalpaxis, D.; Nierhaus, K.H. *Mol. Cell* **2004**, *13*, 113-124.

30. Brodersen, D.E.; Clemons, W.M. Jr.; Carter, A.P.; Morgan-Warren, R.J.; Wimberly, B.T.; Ramakrishnan, V. *Cell* **2000**, *103*, 1143-1154.

31. a) Dobashi, K. *et al.*; *J. Antibiot.* **1986**, *39*, 1779. b) Otoguro, K.; Iwatsuki, M.; Ishiyama, A.; Namatame, M.; Nishihara-Tukashima, A.; Shibahara, S.; Kondo, S.;

Yamada, H.; Ŏmura, S. *J. Antibiot.* **2010**, *63*, 381. c) Lu, W.; Roongsawang, N.; Mahmud, T. *Chem. Biol.* **2011**, *18*, 425. d) Iwatsuki, M.; Nishihara-Tsukashima, A.; Ishiyama, A.; Namatame, M.; Watanabe, Y.; Handasah, S.; Pranamuda, H.; Marwota, B.; Matsumoto, A.; Takahashi, Y.; Otoguro, K.; Ŏmura, S. *J. Antibiot.* **2012**, *65*, 169.

32. a) Tsujimoto, T.; Nishikawa, T.; Urabe, D.; Isobe, M. *Synlett* **2005**, *3*, 433-436. b) Knapp, S.; Yu, Y. *Org. Lett.* **2007**, *9*, 1359-1362. c) Malinowski, J.T.; McCarver, S.J.; Johnson, J.S. *Org. Lett.* **2012**, *14*, 2878-2881. d) Looper, R.E.; Haussener, T.J. *Org. Lett.* **2012**, *14*, 3632-3635. e) Matsumoto, N.; Tsujimoto, T.; Nakazaki, A.; Isobe, M.; Nishikawa, T. *RSC Adv.* **2012**, *2*, 9448-9462.
33. a) Hanessian, S.; Vakiti, R.R.; Dorich, S.; Banerjee, S.; Lecomte, F.; DelValle, J.R.; Zhang, J.; Deschênes-Simard, B. *Angew. Chem. Int. Ed.* **2011**, *50*, 3497-3500 b) Hanessian, S.; Vakiti, R.R.; Dorich, S.; Banerjee, S.; Deschênes-Simard, B. *J. Org. Chem.* **2012**, *77*, 9458-9472.
34. a) Malinowski, J.T.; Sharpe, R.J.; Johnson, J.S. *Science* **2013**, *340*, 180-182. b) Kisunzu, J.K.; Sarpong, R. *Angew. Chem. Int. Ed.* **2013**, *52*, 10694-10696. c) Sharpe, R.J.; Malinowski, J.T.; Johnson, J.S. *J. Am. Chem. Soc.* **2013**, *135*, 17990-17998.
35. Feling, R.H.; Buchanan, G.O.; Mincer, T.J.; Kauffman, C.A.; Jensen, P.R.; Fenical, W. *Angew. Chem. Int. Ed.* **2003**, *42*, 355-357.
36. Reddy, L.R.; Saravanan, P.; Corey, E.J. *J. Am. Chem. Soc.* **2004**, *126*, 6230-6231.
37. For a recent review, see Ma, Y.; Qu, L.; Liu, Z.; Zhang, L.; Yang, Z.; Zhang, L. *Curr. Top. Med. Chem.* **2011**, *11*, 2906-2922.
38. Hogan, P. C.; Corey, E. J., *J. Am. Chem. Soc.* **2005**, *127*, 15386-15387.

39. a) Lee, J.-H.; Evans, B. S.; Li, G.; Kelleher, N. L.; van der Donk, W. A. *Biochemistry* **2009**, *48*, 5054-5056. b) Baldwin, J. E.; North, M.; Flinn, A. *Tetrahedron* **1988**, *44*, 637-642.

40. Yeung, C.S.; Dong, V.M. *Chem. Rev.*, **2011**, *111*, 1215–1292

41. Jeffrey, J.L.; Bartlett, E.S.; Sarpong, R. *Angew. Chem. Int. Ed.* **2013**, *52*, 2194–2197 and references therein

42. Wolff, M.E. *Chem. Rev.* **1963**, *63*, 55-64.

43. a) Baldwin, S.W.; Doll, T.J. *Tetrahedron Lett.* **1979**, *20*, 3275-3278; b) Ban, Y.; Kimura, M.; Oishi, T. *Chem. Pharm. Bull.* **1976**, *24*, 1490-1496; c) Kimura, M.; Ban, Y. *Synthesis* **1976**, 201-202; d) Chow, Y.L.; Mojelsky, T.W.; Magdzinski, L.J.; Tichy, M. *Can. J. Chem.* **1985**, *63*, 2197-2202; e) Nikishin, G.I.; Troyansky, E.I.; Lazareva, M.I. *Tetrahedron Lett.* **1985**, *26*, 3743-3744; f) Hernández, R.; Rivera, A.; Salazar, J.A.; Suárez, E. *Chem. Commun.* **1980**, *20*, 958-959; g) De Armas, P.; Francisco, C.G.; Hernández, R.; Salazar, J.A.; Suárez, E. *J. Chem. Soc. Perkin Trans.* **1988**, *1*, 3255-3265; h) Carrau, R.; Hernández, R.; Suárez, E.; Betancor, C. *J. Chem. Soc. Perkin Trans.* **1987**, *1*, 937-943; i) Francisco, C.G.; Herrera, A.J.; Suárez, E. *J. Org. Chem.* **2003**, *68*, 1012-1017; j) Betancor, C.; Conceptión, J.I.; Hernández, R.; Salazar, J.A.; Suárez, E. *J. Org. Chem.* **1983**, *48*, 4430-4432; k) De Armas, P.; Carrau, R.; Conceptión, J.I.; Francisco, C.G.; Hernández, R.; Suárez, E. *Tetrahedron Lett.* **1985**, *26*, 2493-2496.

44. Verron, J.; Malherbe, P.; Prinssen, E.; Thomas, A.W.; Nock, N.; Masciadri, R. *Tetrahedron Lett.* **2007**, *48*, 377-380.

45. Bourgeois, D.; Craig, D.; Grellepois, F.; Mondford, D.M.; Stewart, A.J.W. *Tetrahedron* **2006**, *62*, 483-495

46. Bruker-AXS APEX-II, 2.1.4, Madison, WI, 2007.

47. SHELXTL Crystal Structure Determination Package; Bruker Analytical X-ray Systems: Madison, WI, 1995-1999.

48. Crystallographic data for structure **1.24** have been deposited with the Cambridge Crystallographic Data Centre as supplementary publication No. CCDC 996120. Copies of the data can be obtained, free of charge, on application to CCDC, 12 Union Road, Cambridge CB2 1EZ, UK (fax: !44-(0)1223e336033 or email: deposit@ccdc.cam.ac.uk).

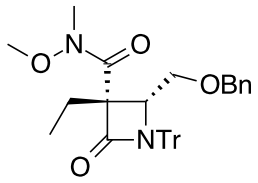

1.23

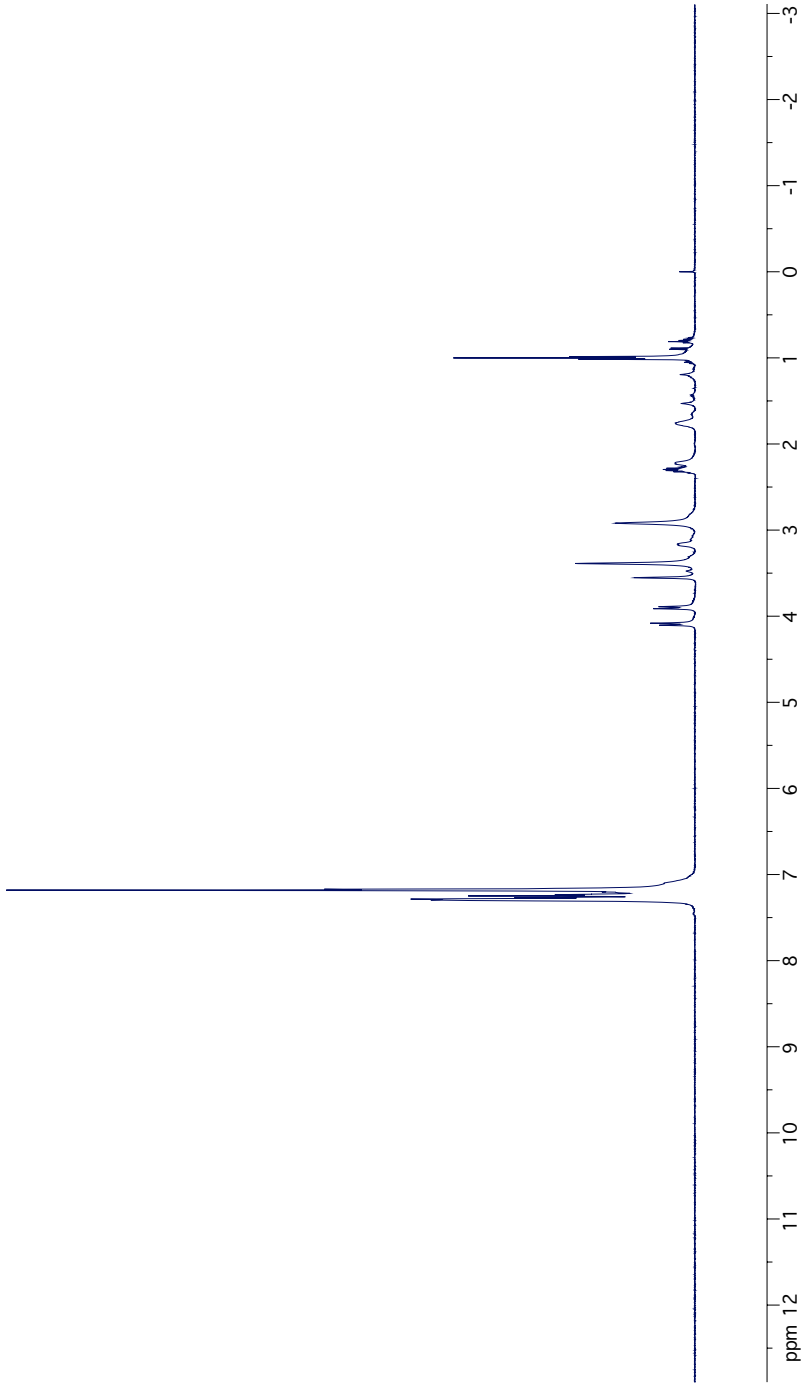

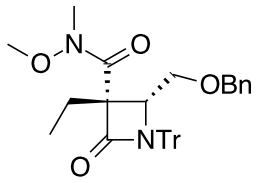

1.23

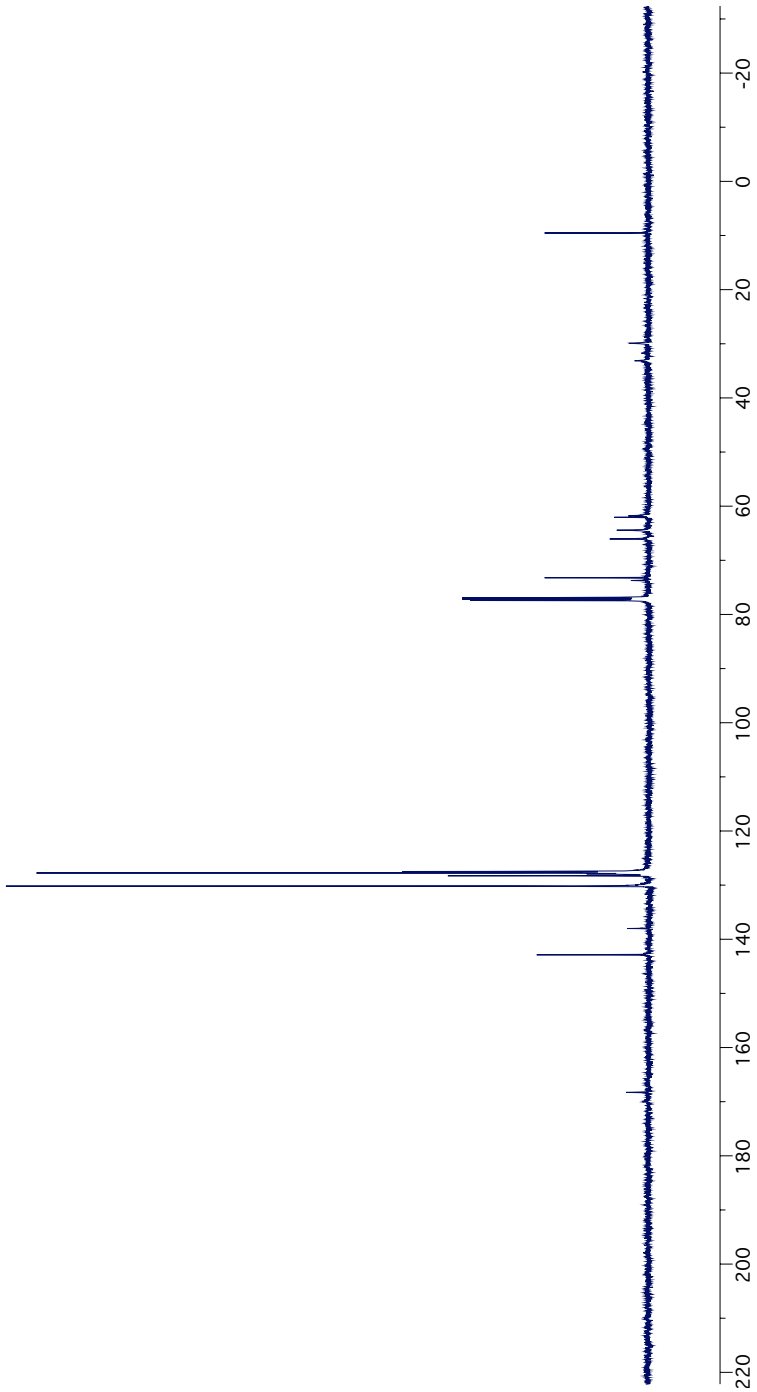

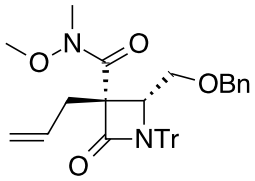

1.24

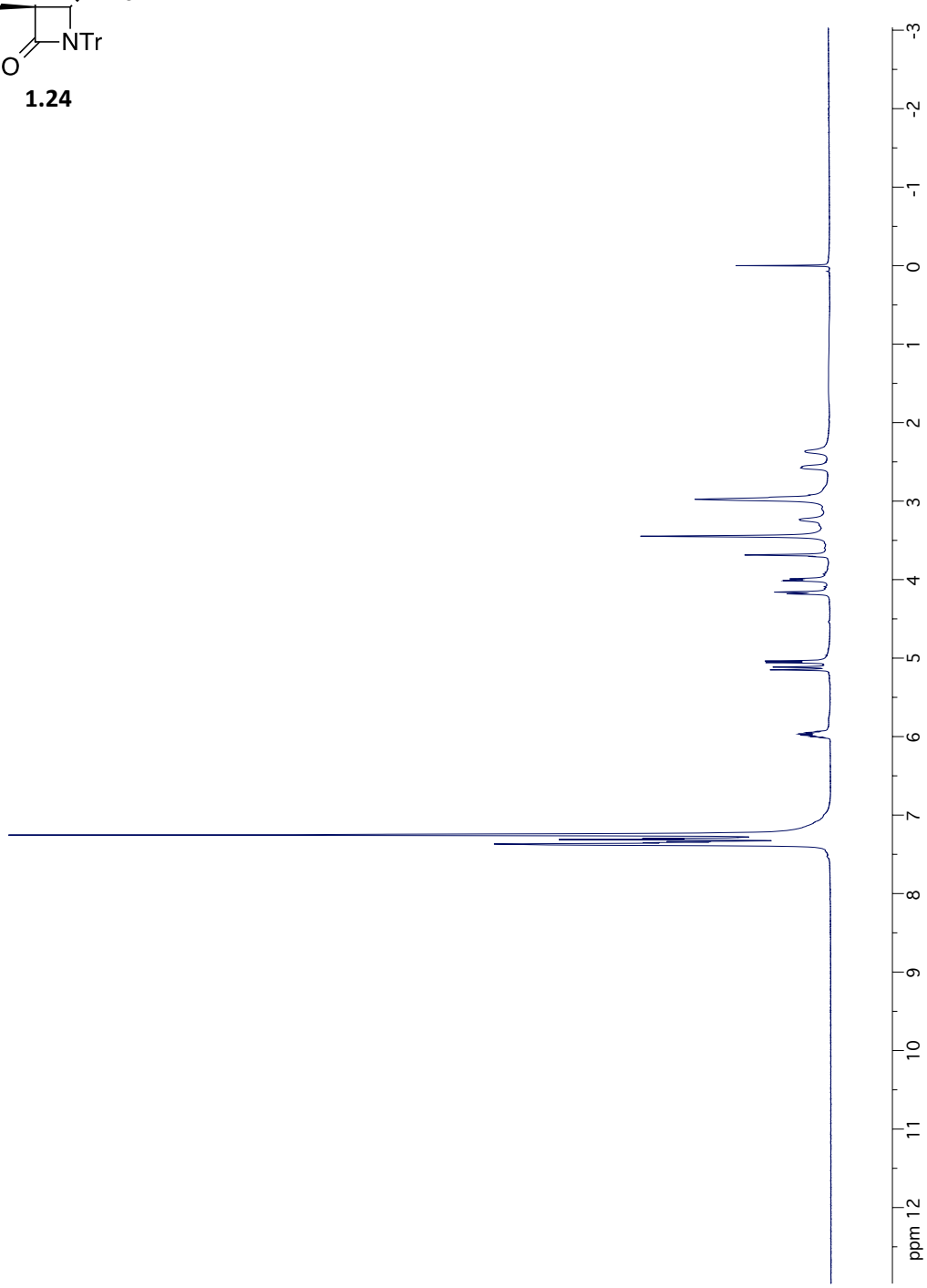

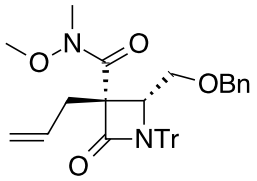

1.24

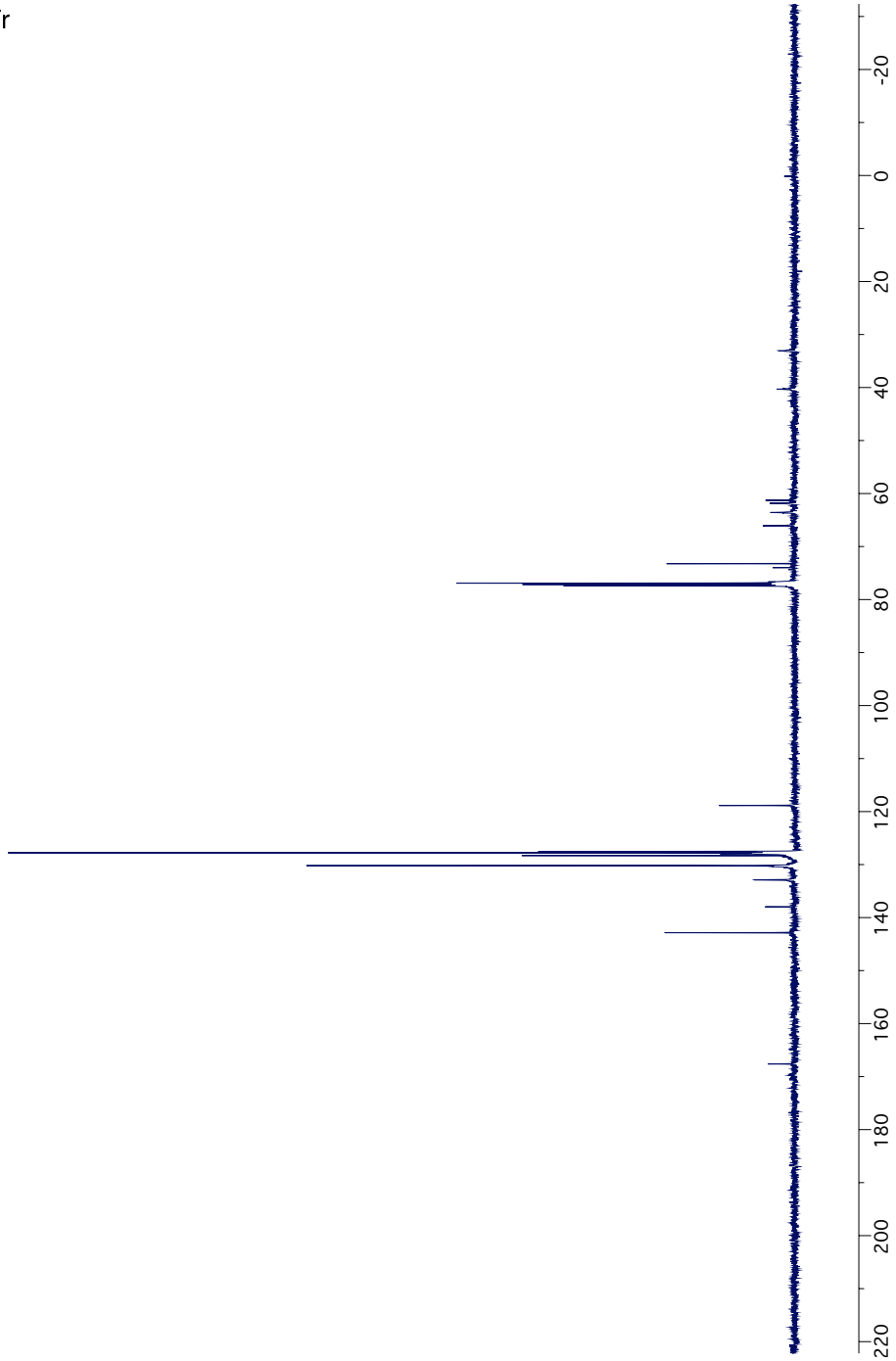

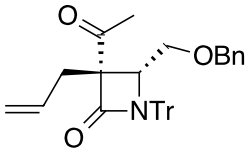

1.25

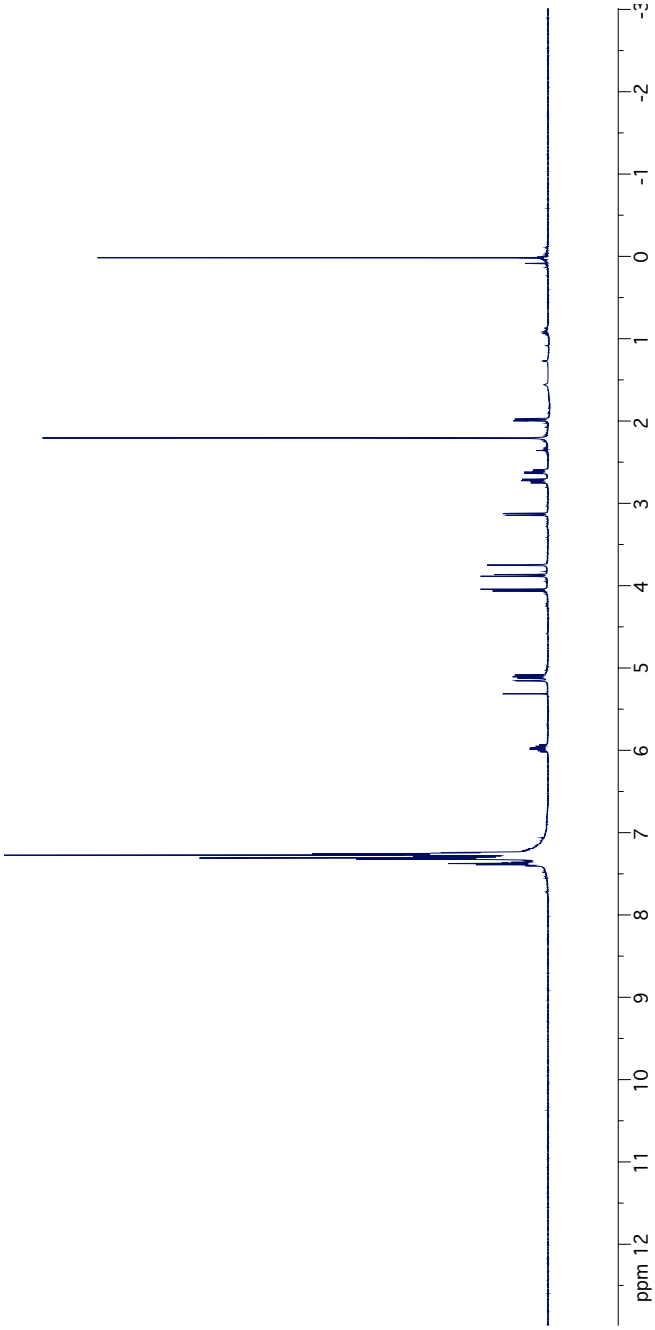

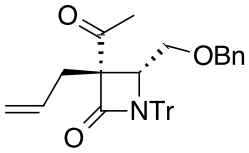

1.25

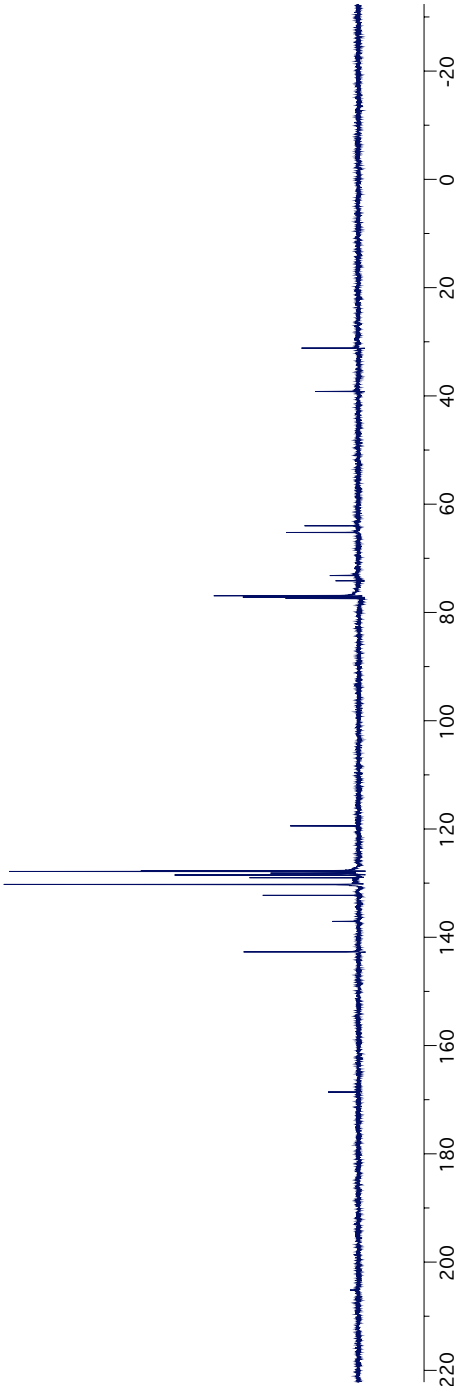

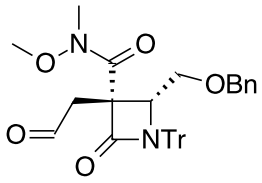

1.26

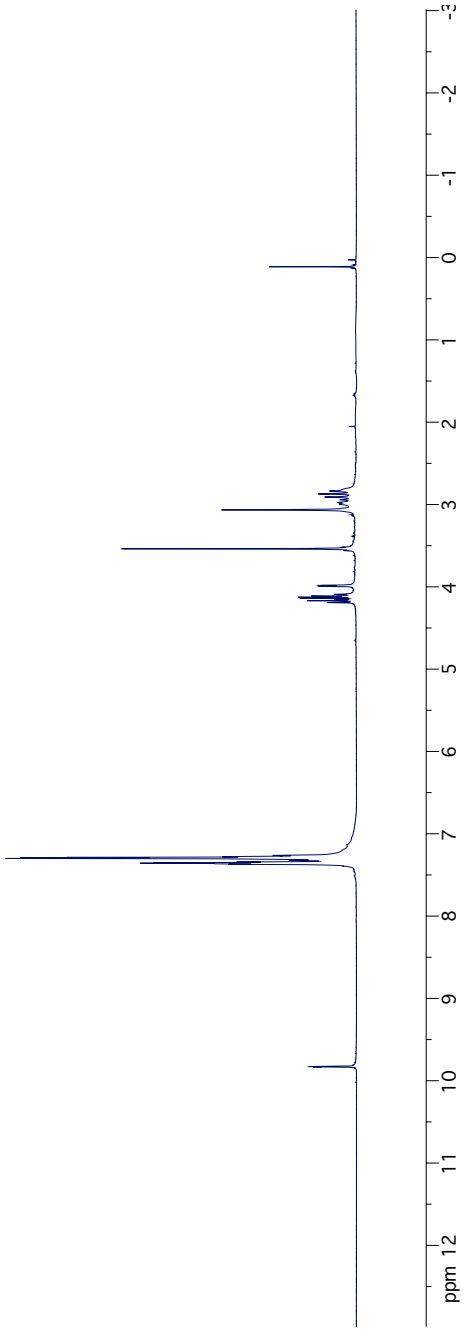

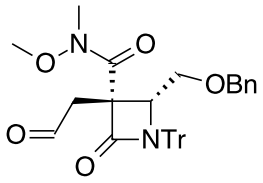

1.26

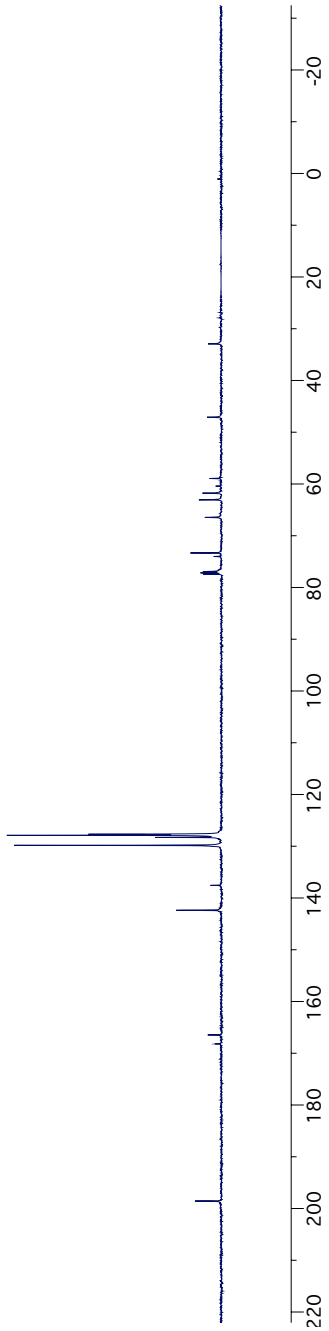

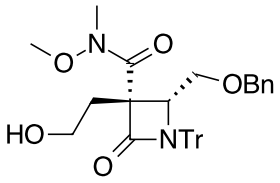

1.27

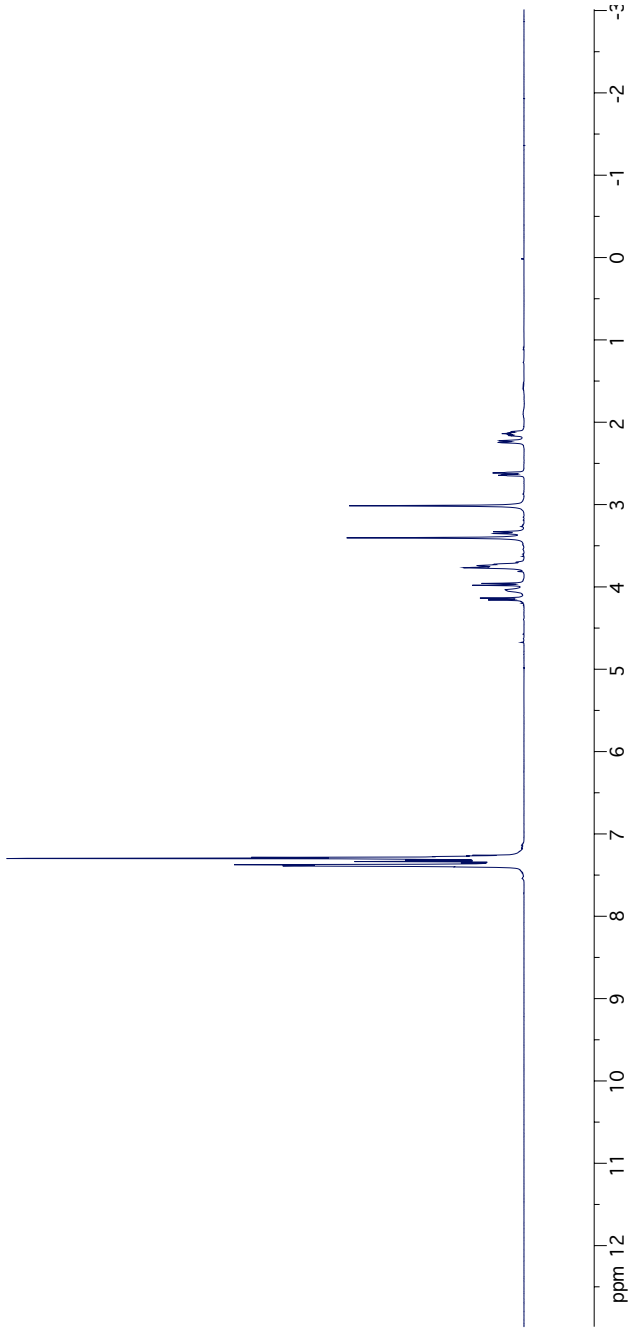

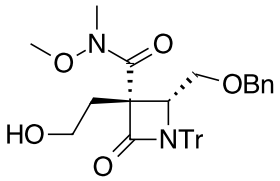

1.27

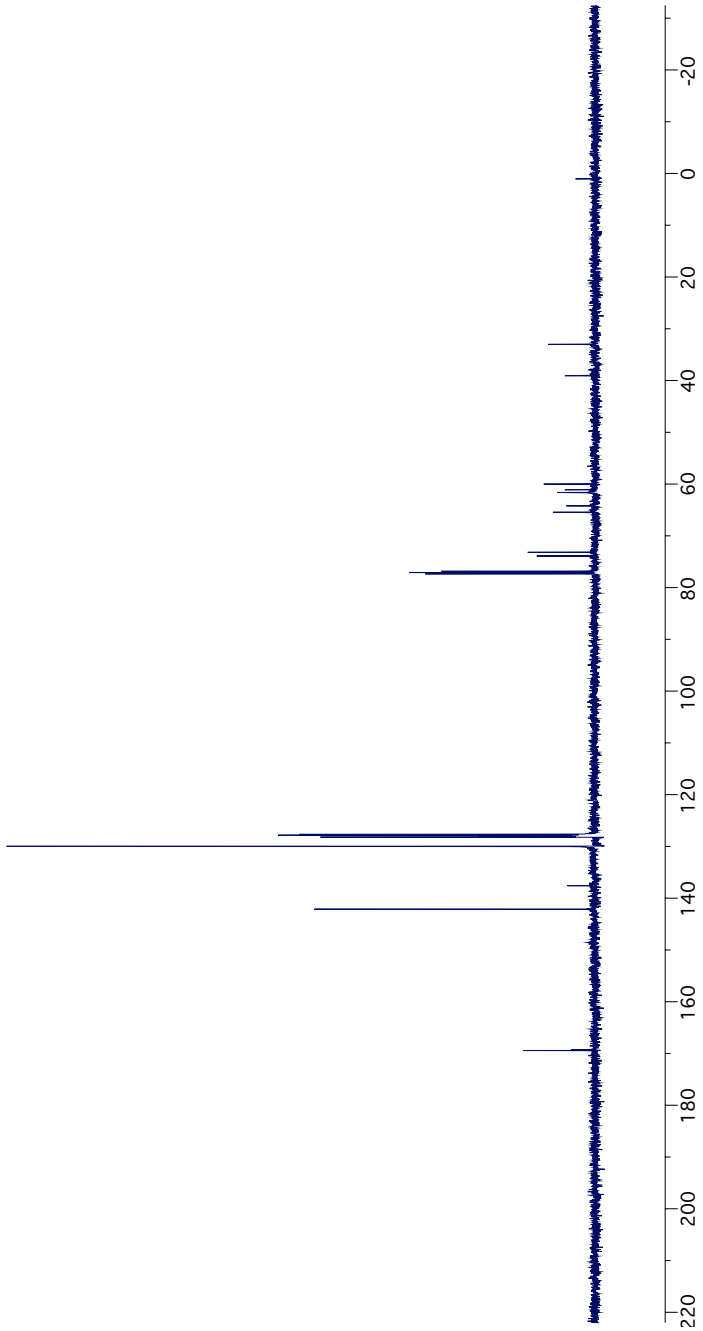

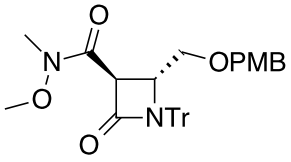

1.39

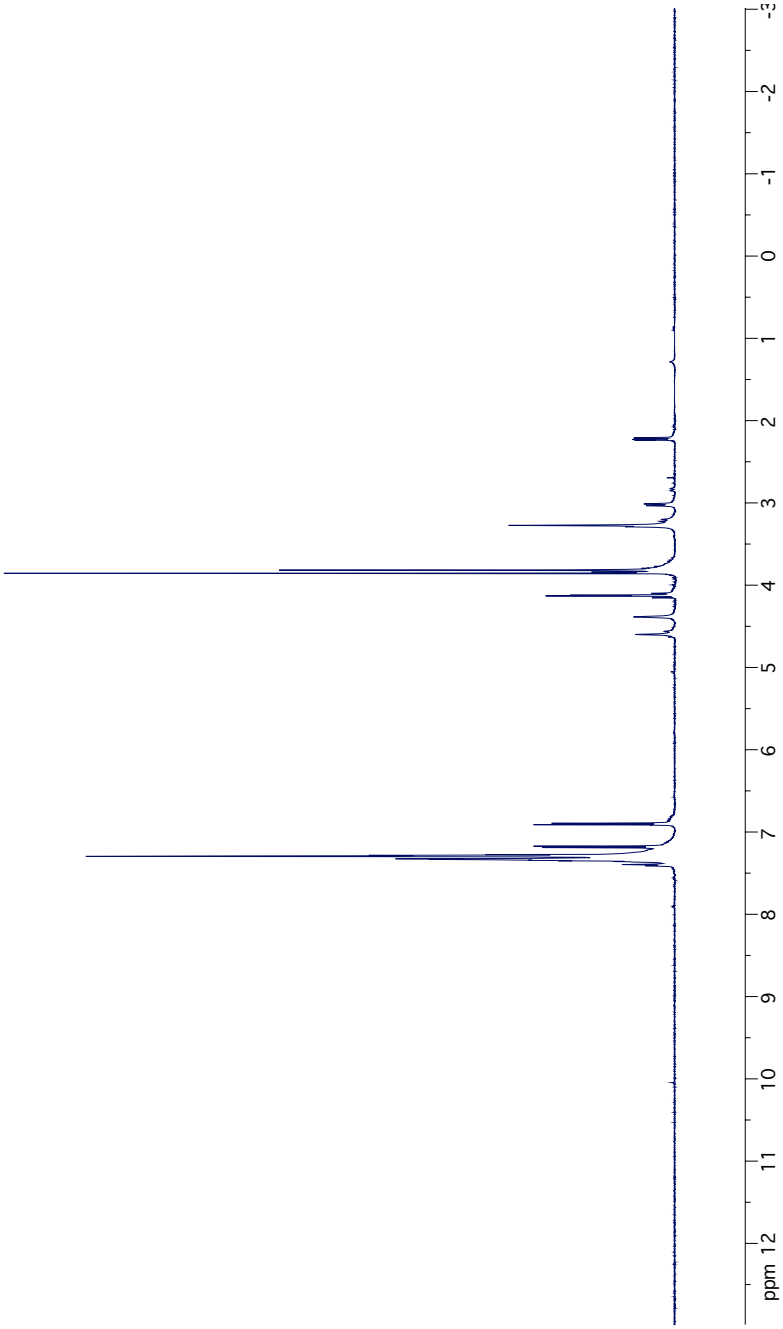

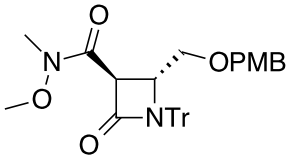

1.39

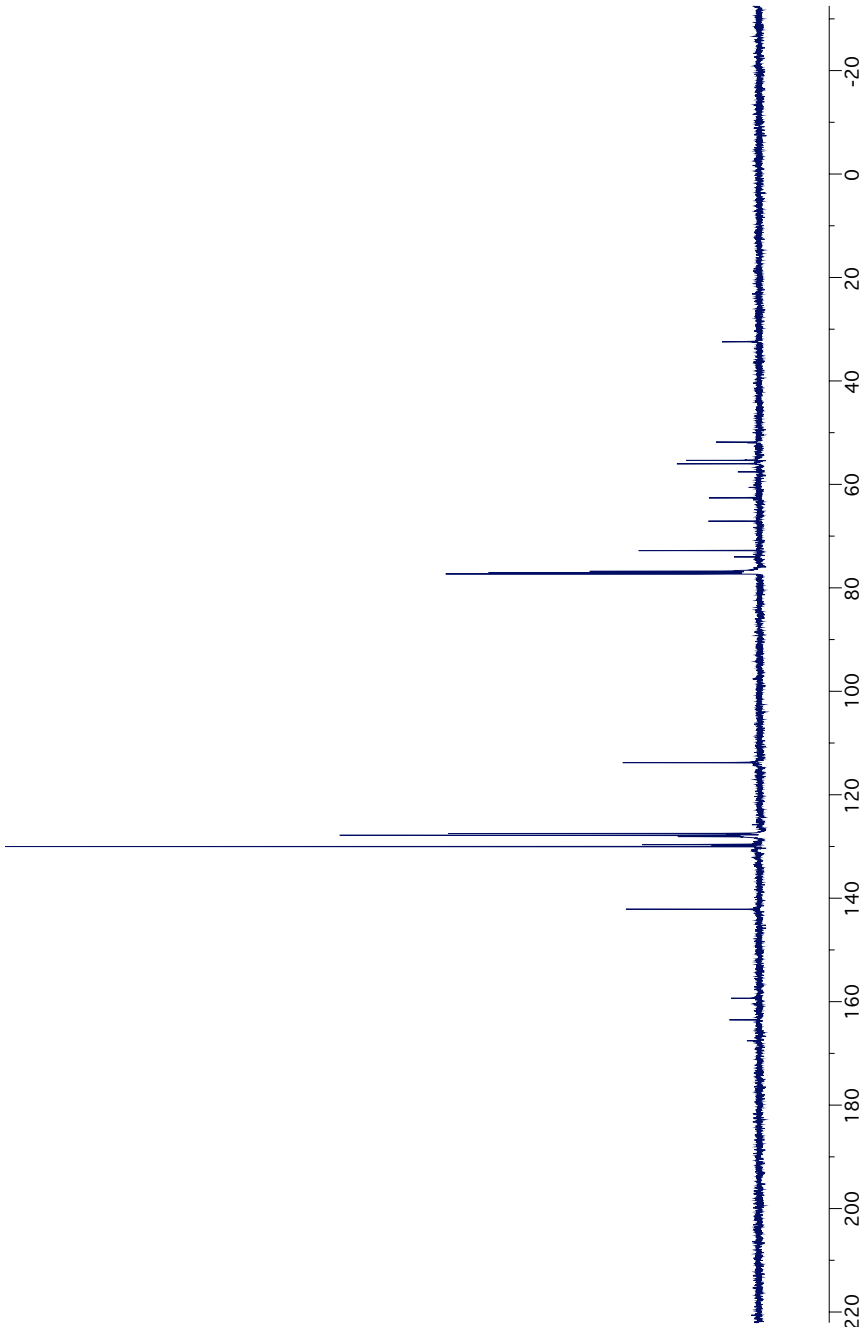

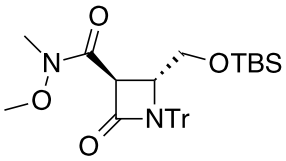

1.40

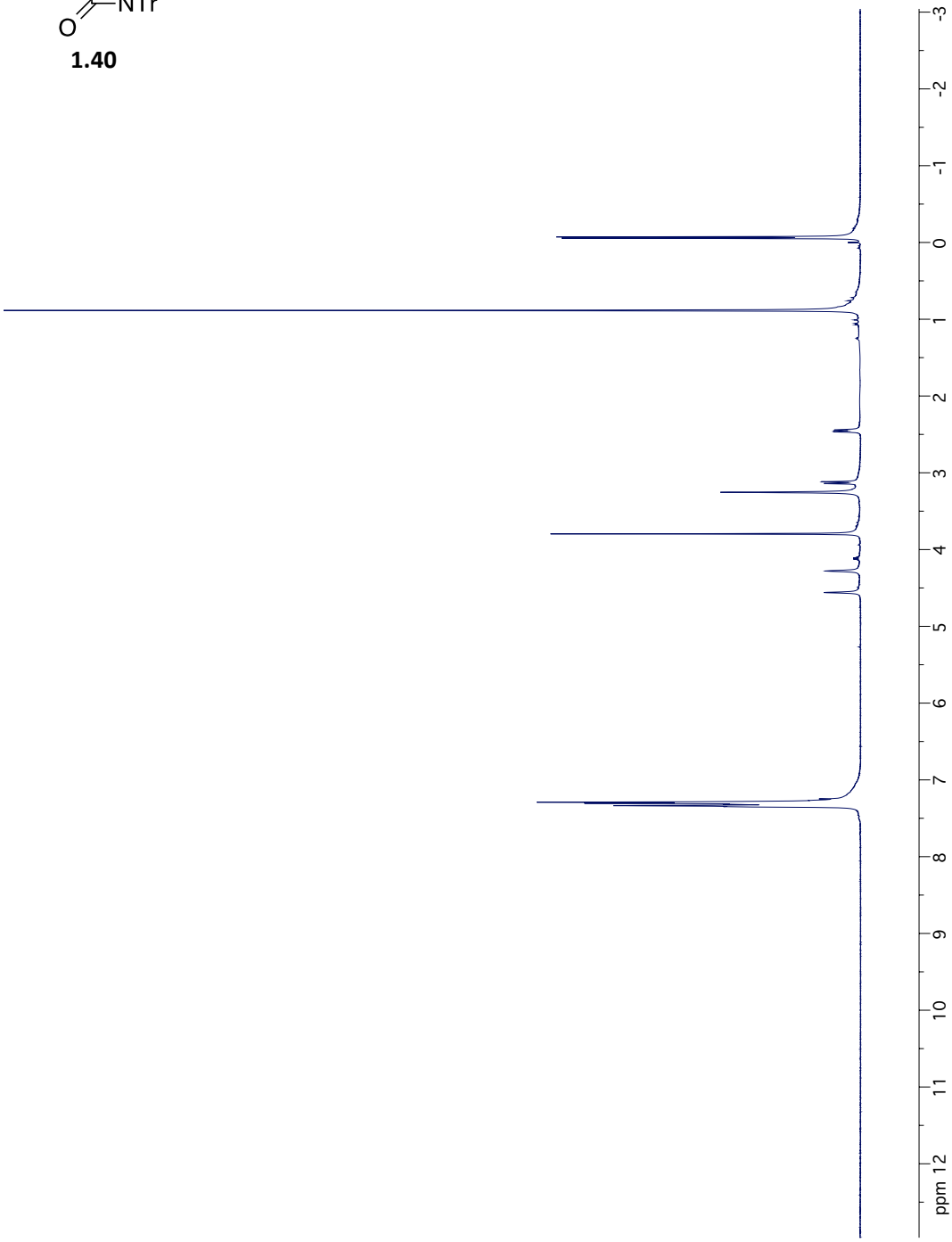

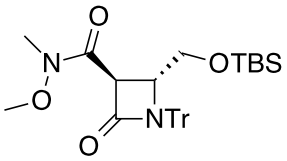

1.40

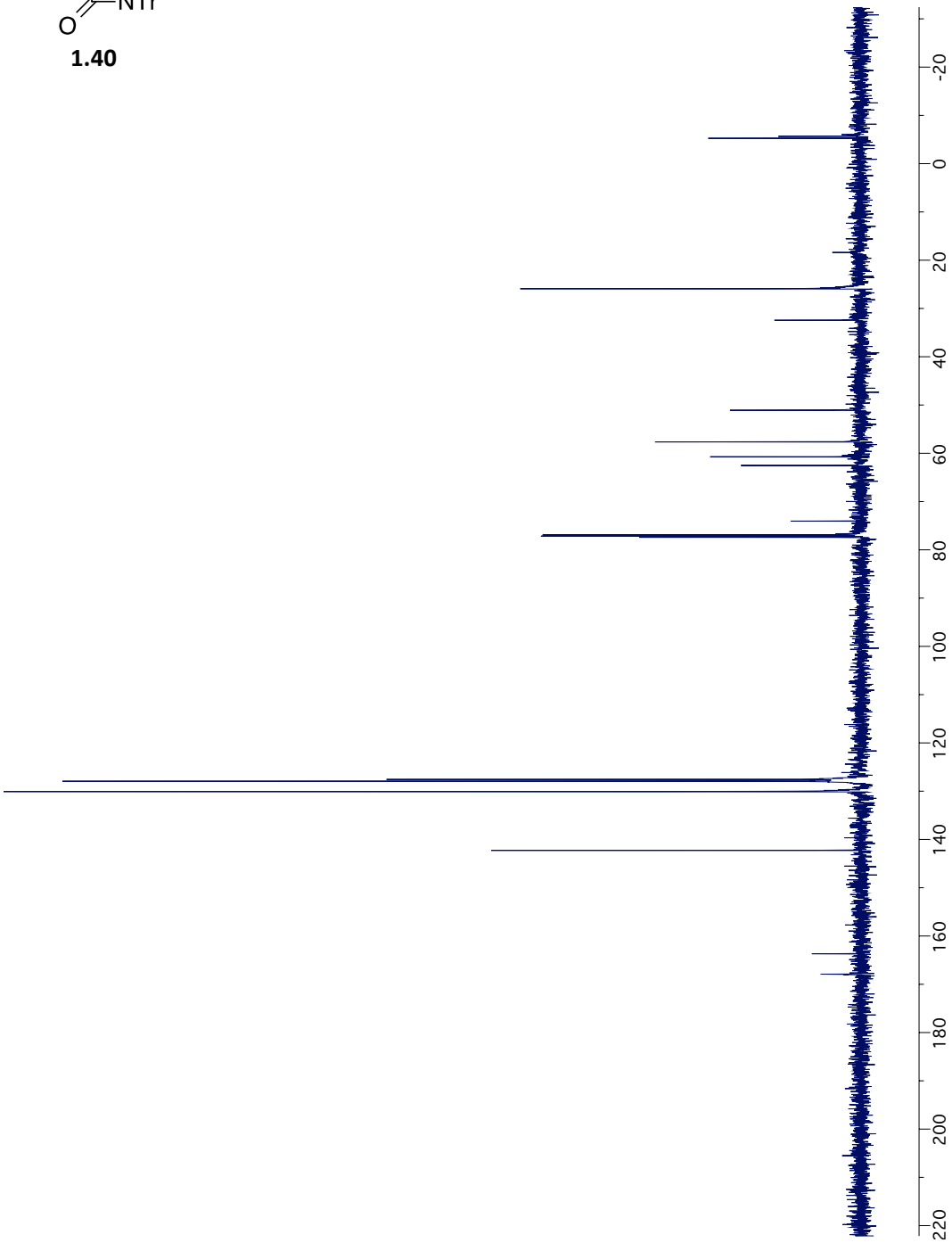

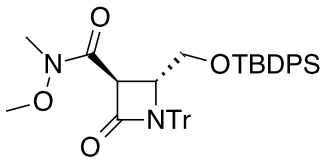

1.41

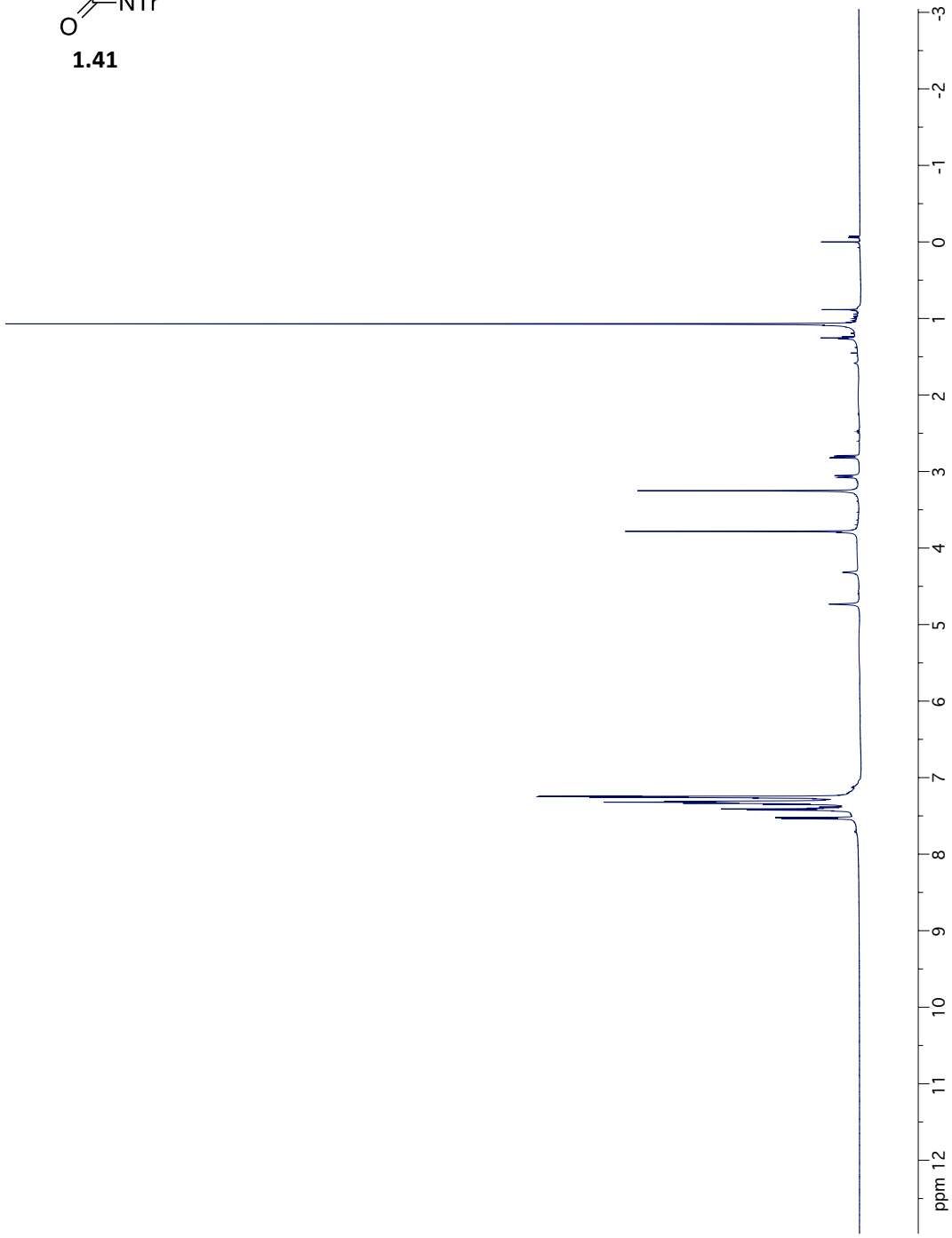

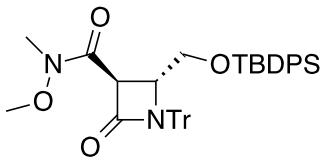

1.41

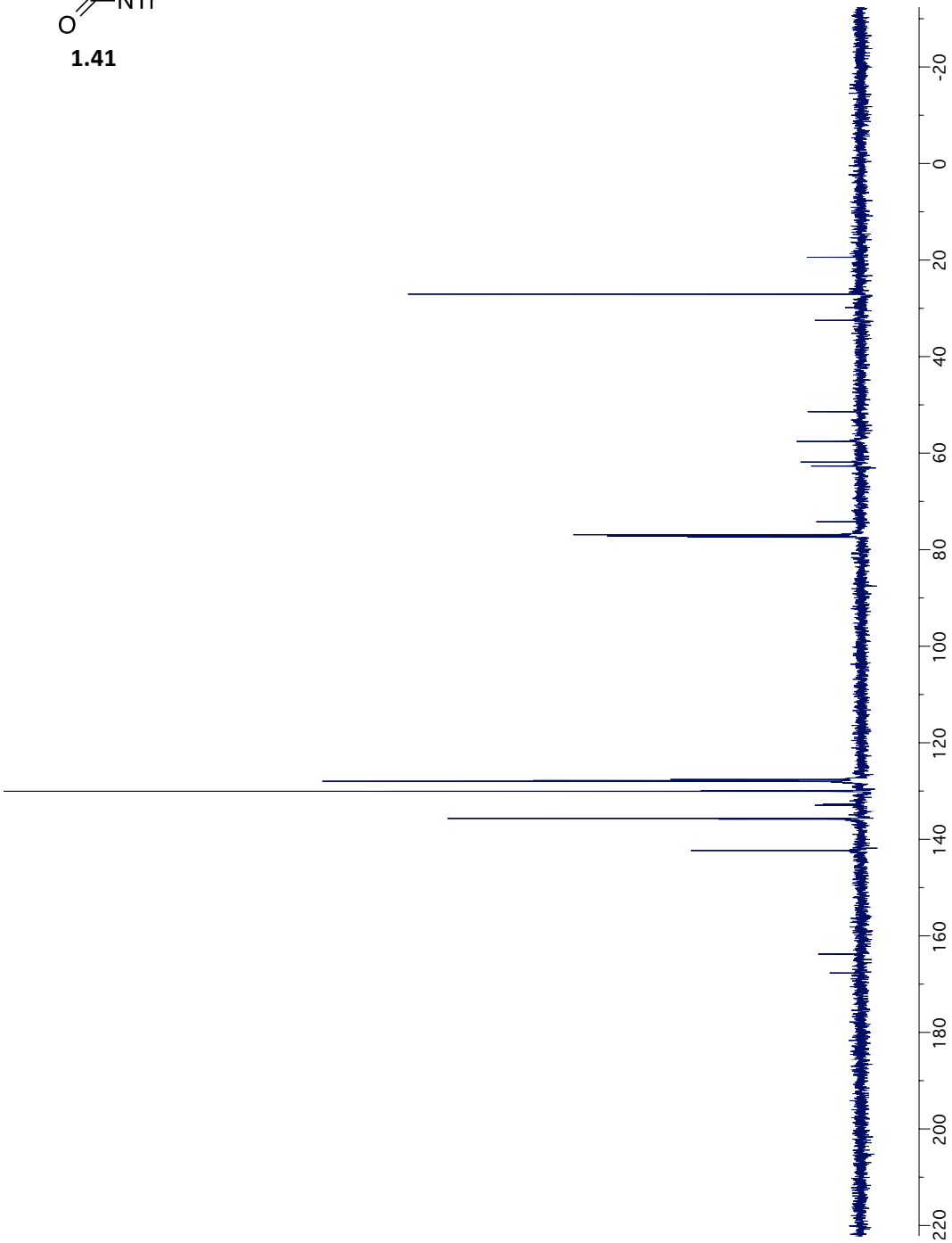

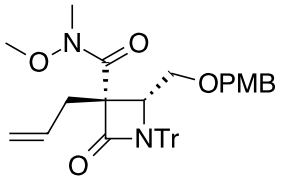

1.42

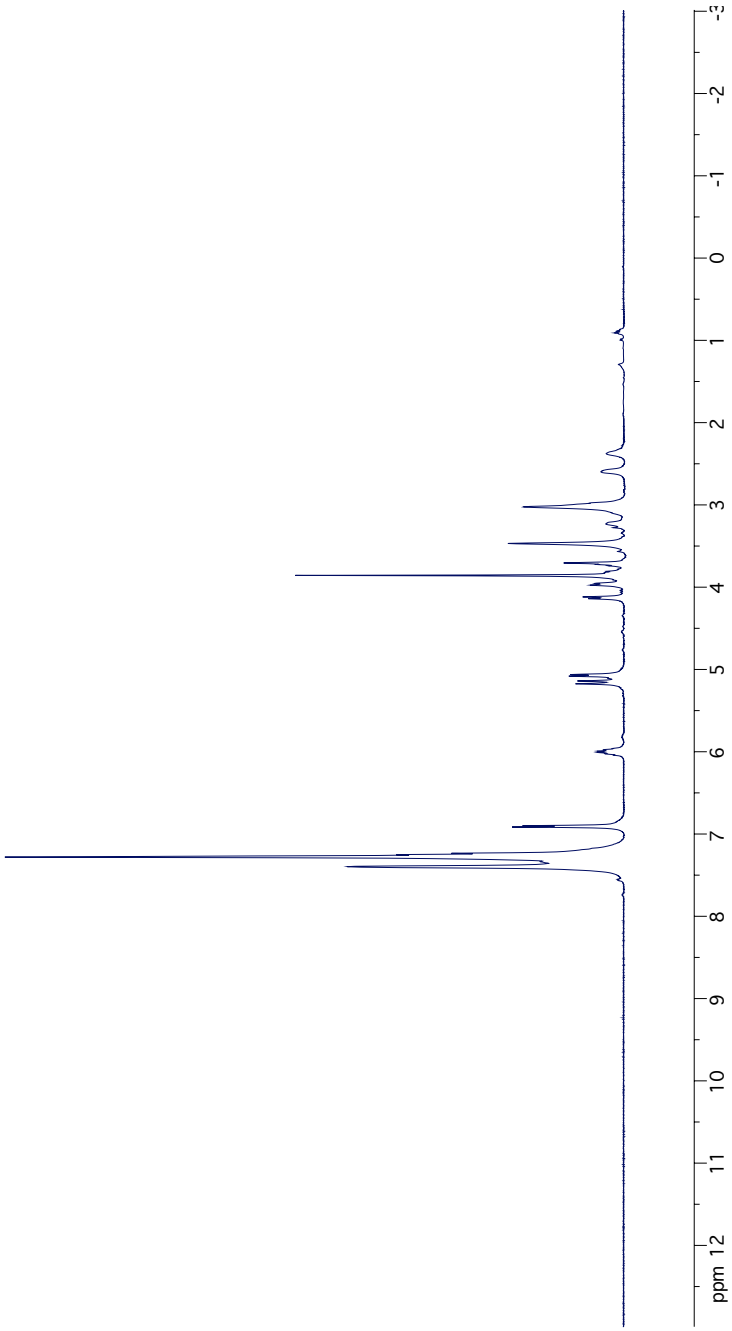

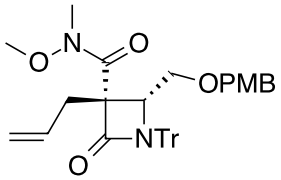

1.42

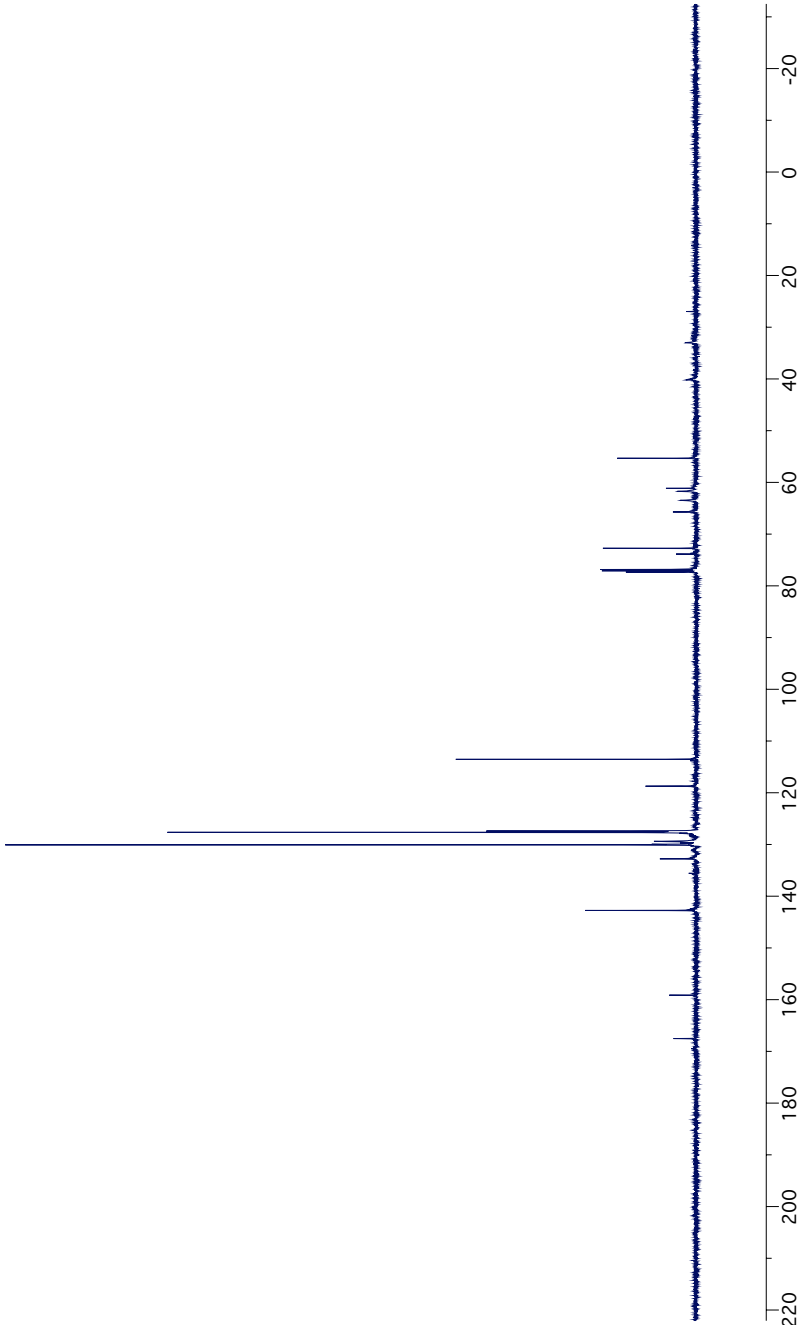

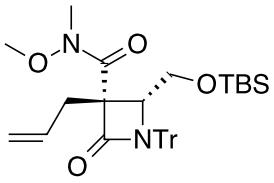

1.43

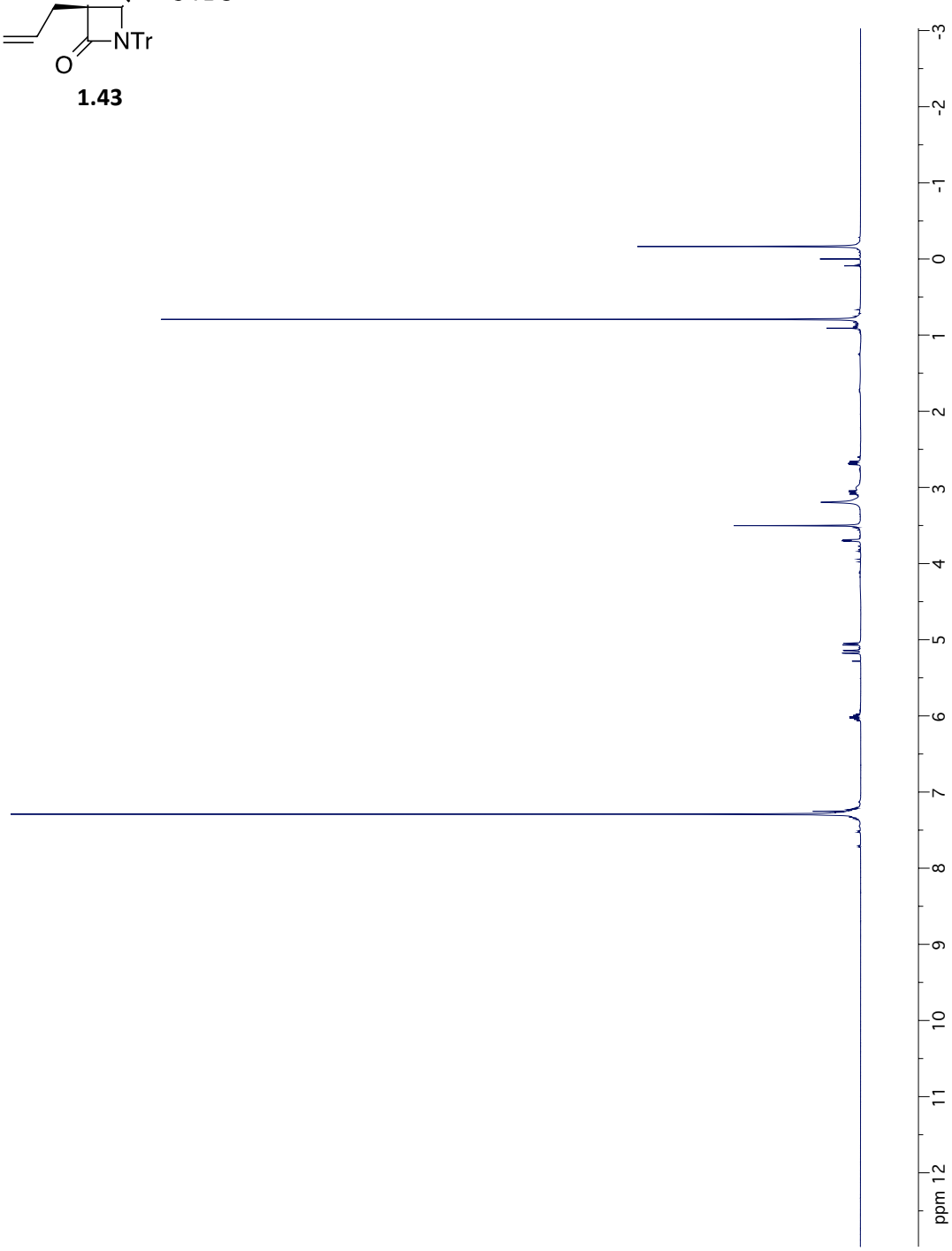

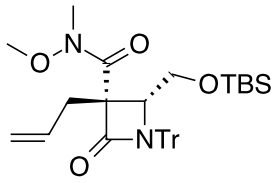

1.43

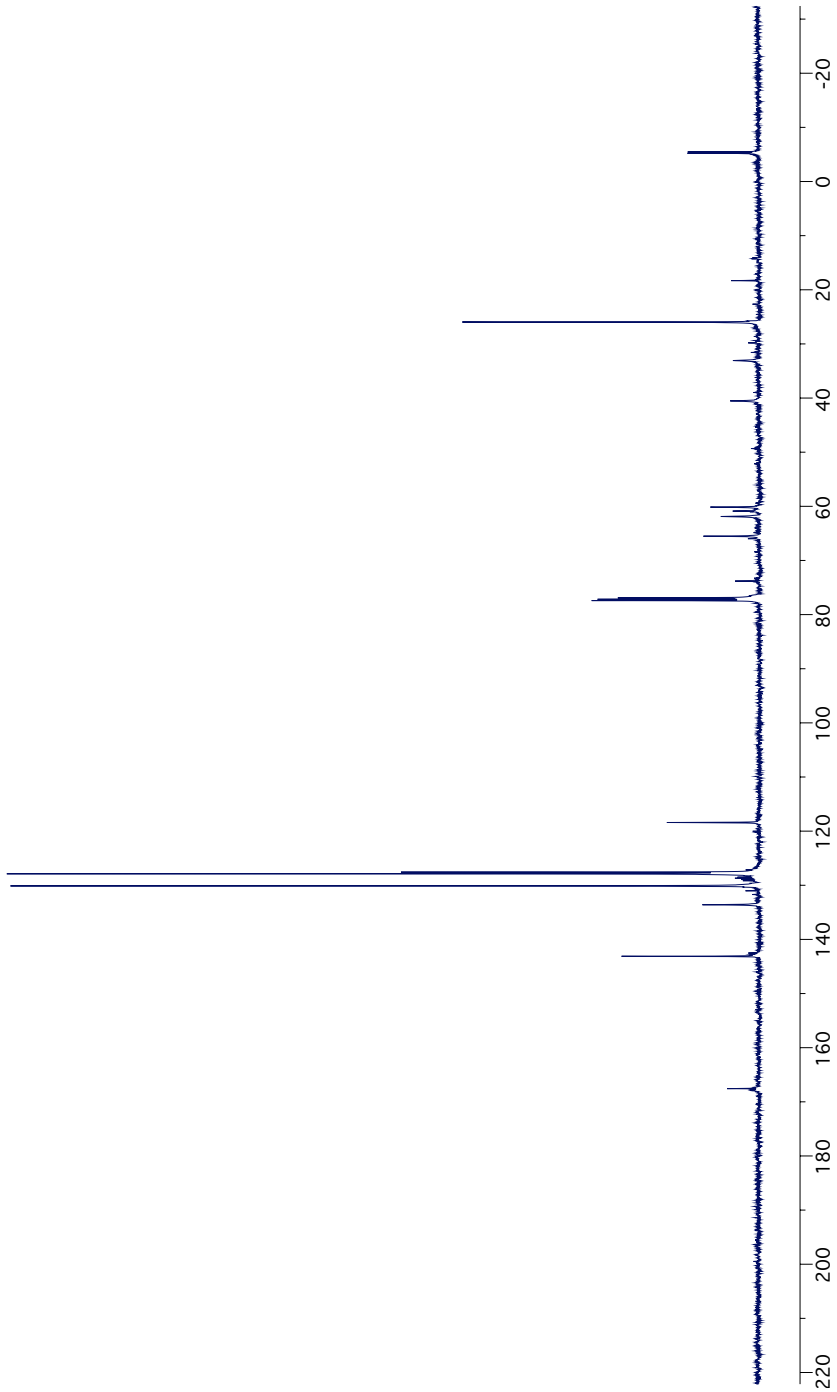

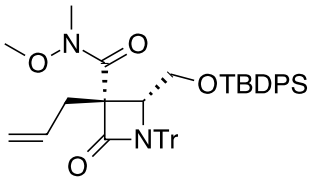

1.44

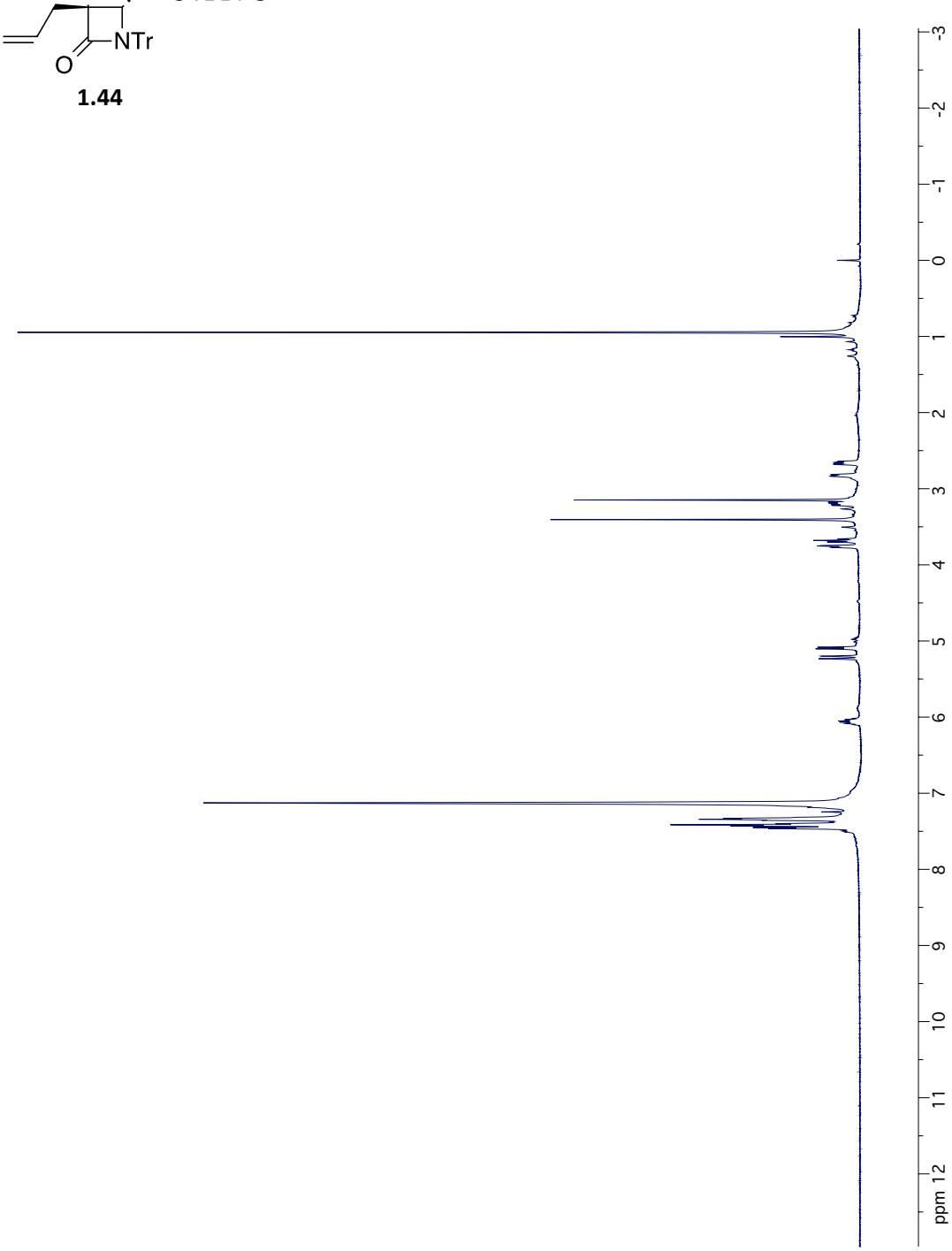

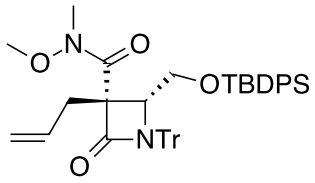

1.44

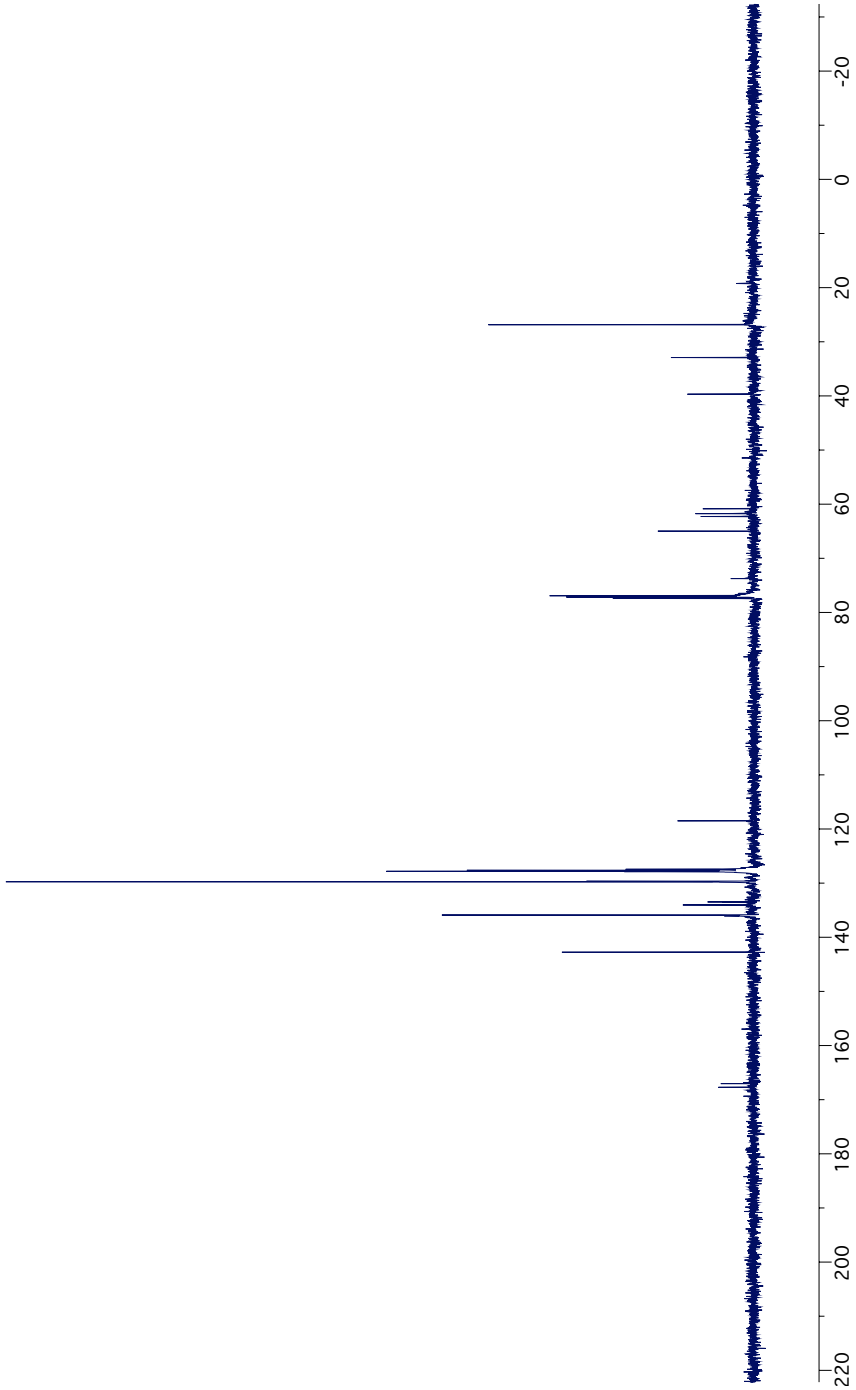

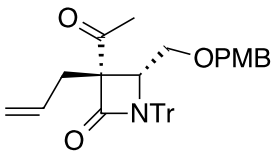

1.45

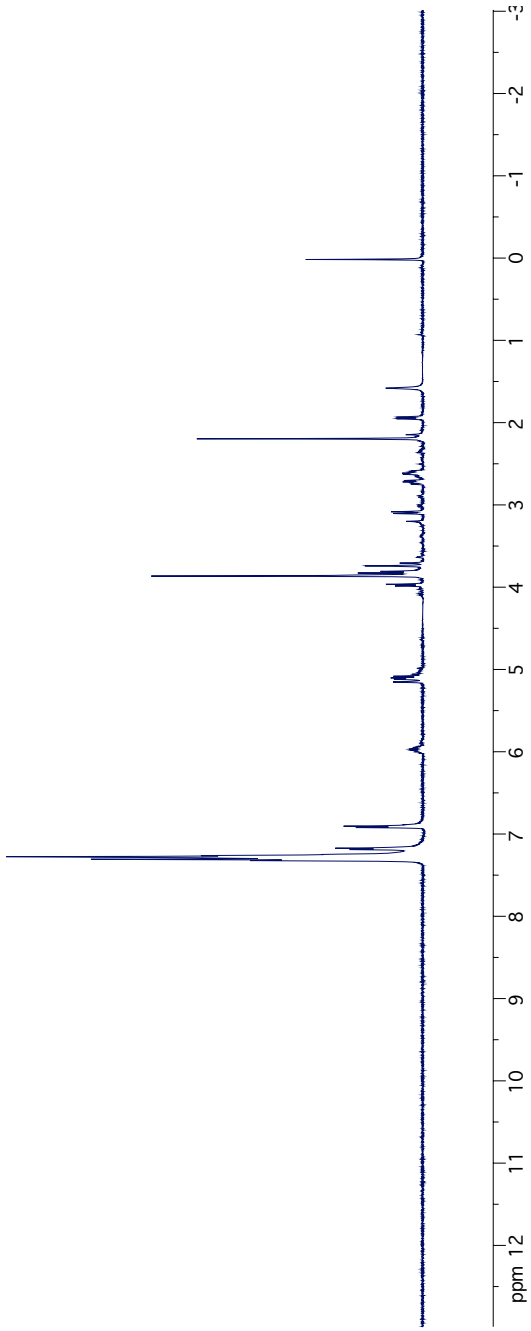

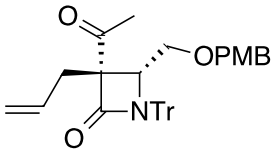

1.45

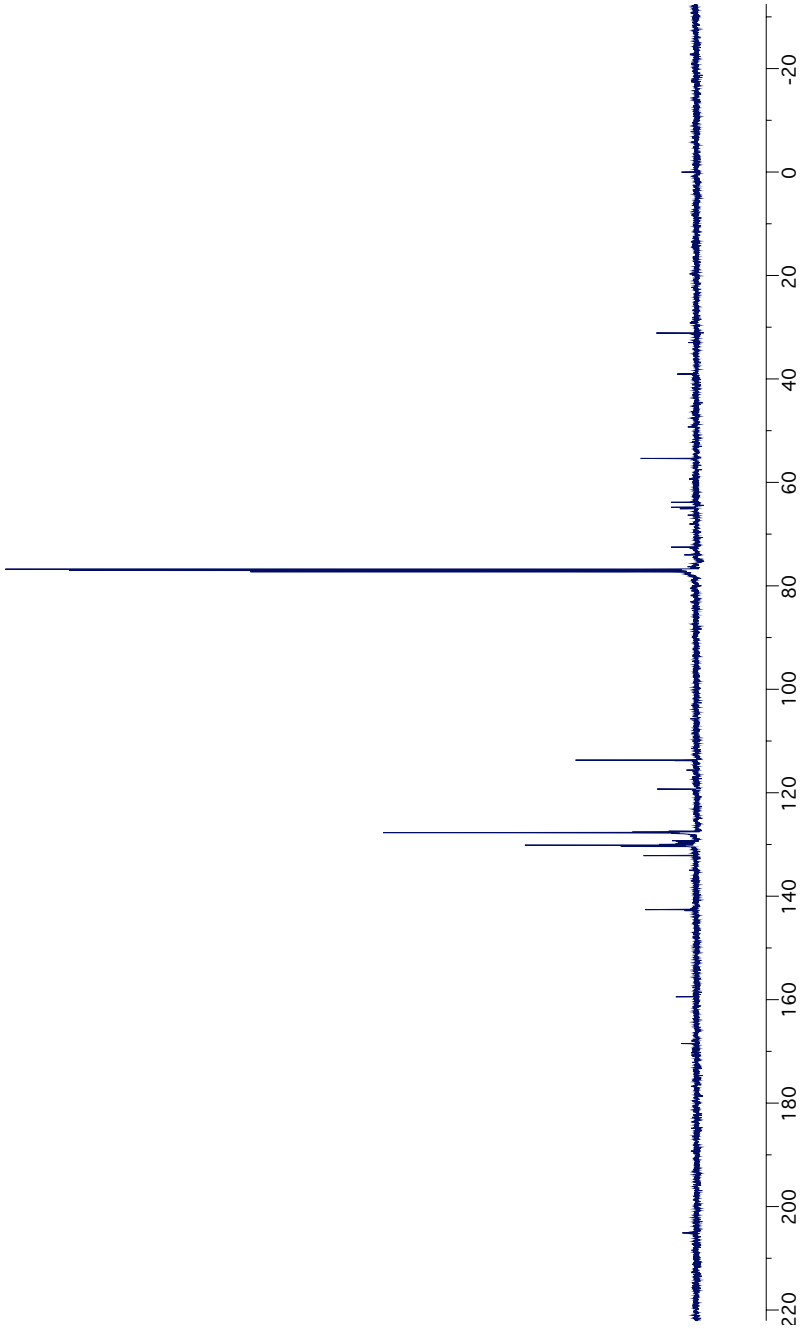

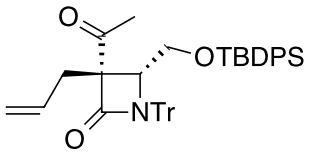

1.46

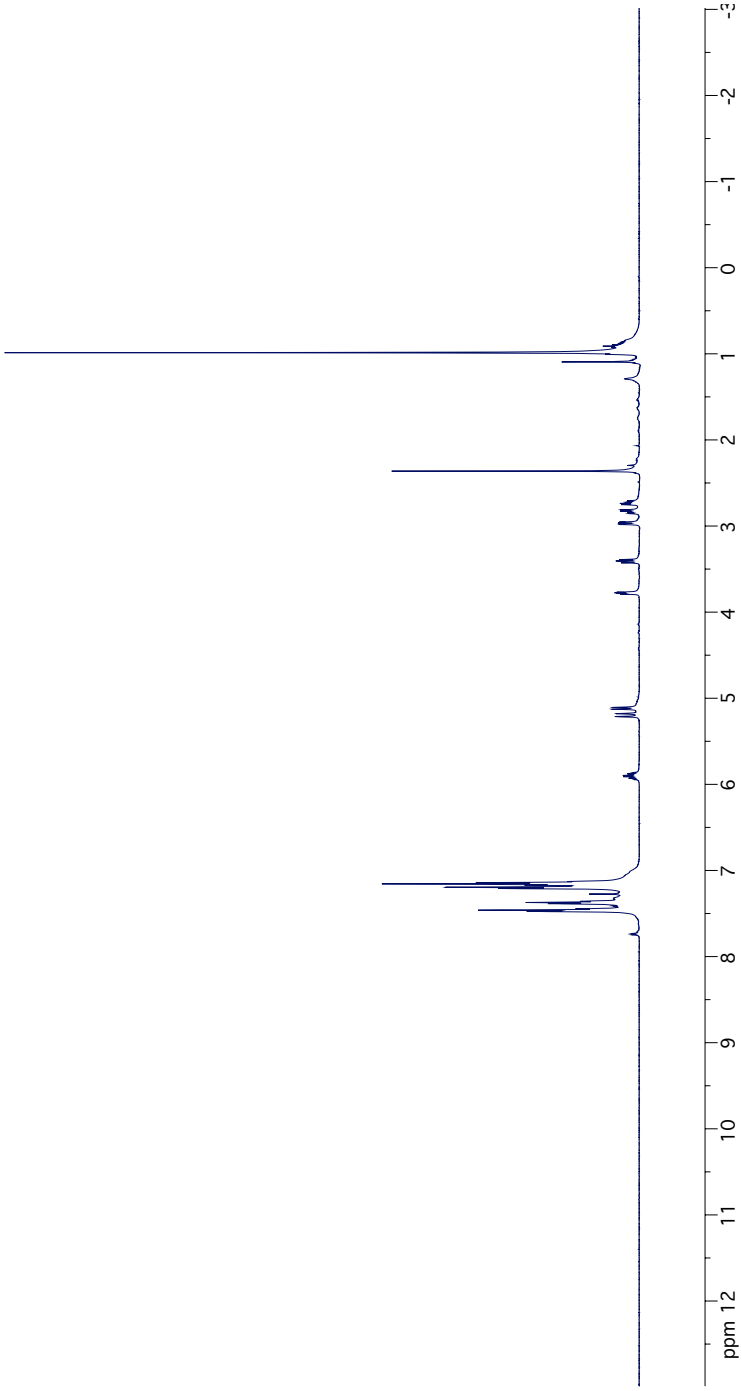

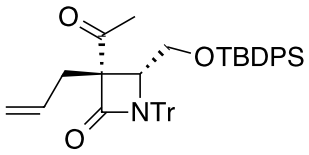

1.46

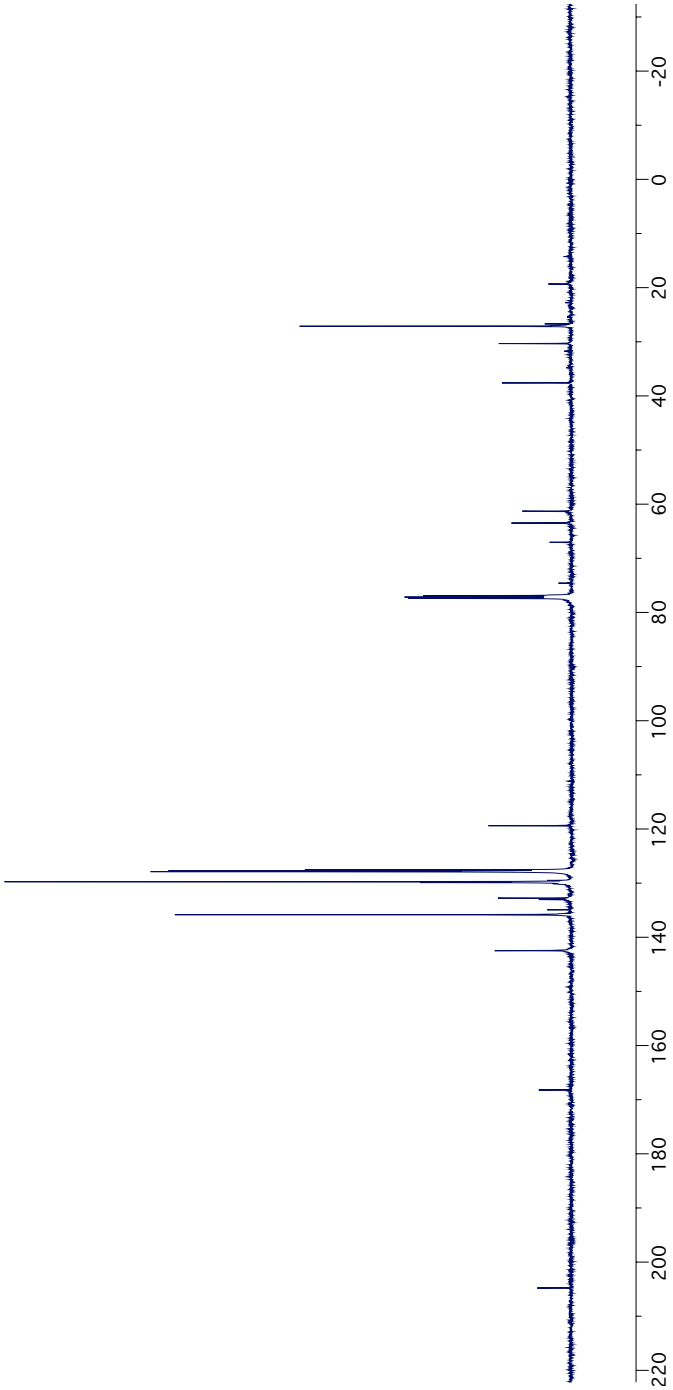

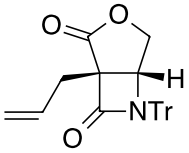

1.47

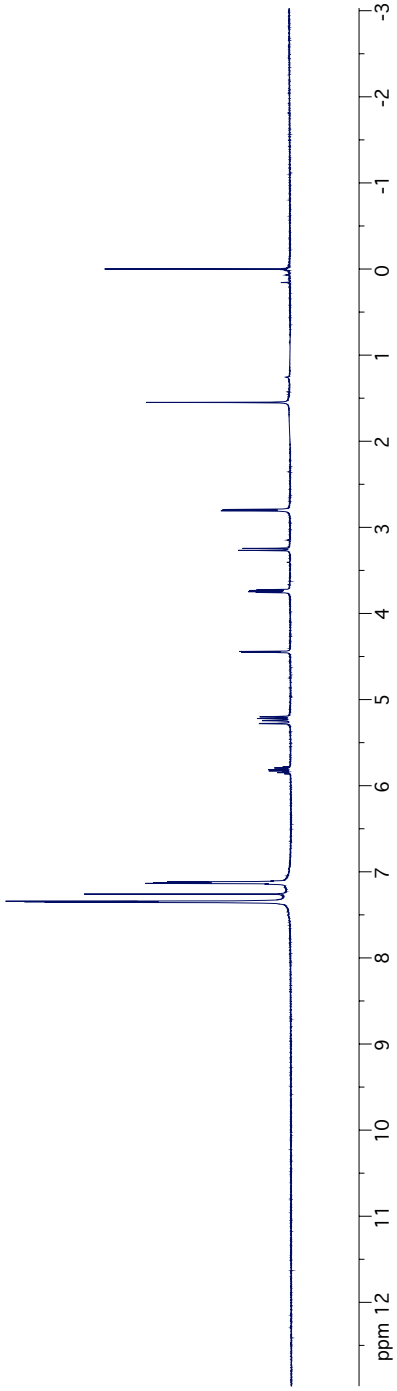

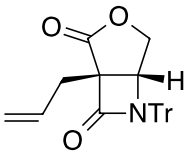

1.47

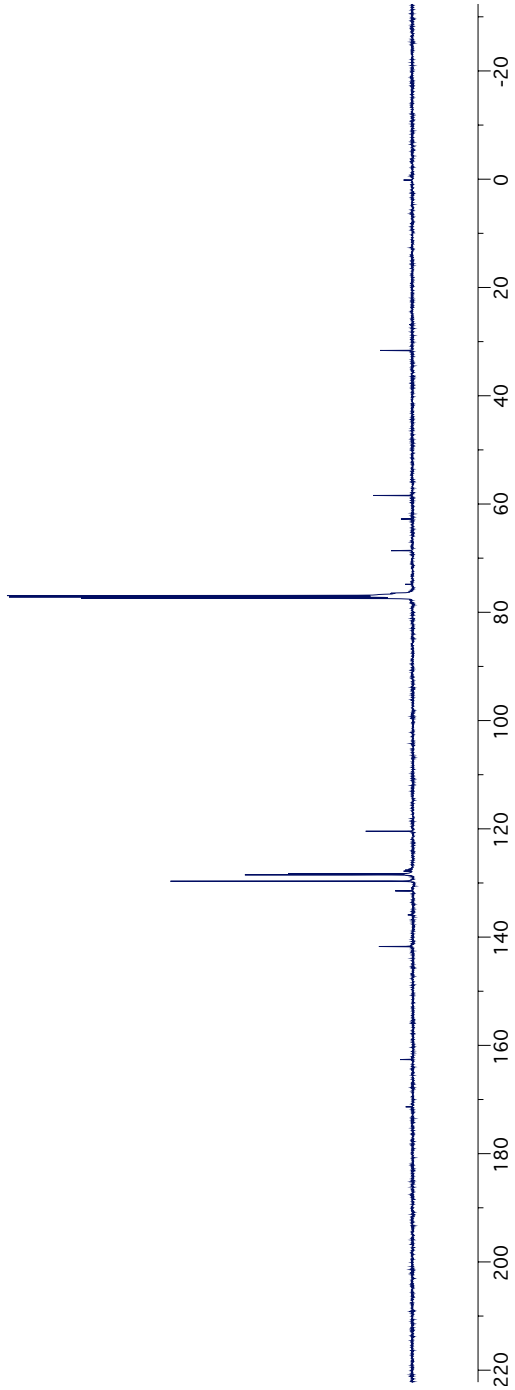

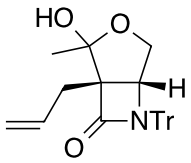

1.48

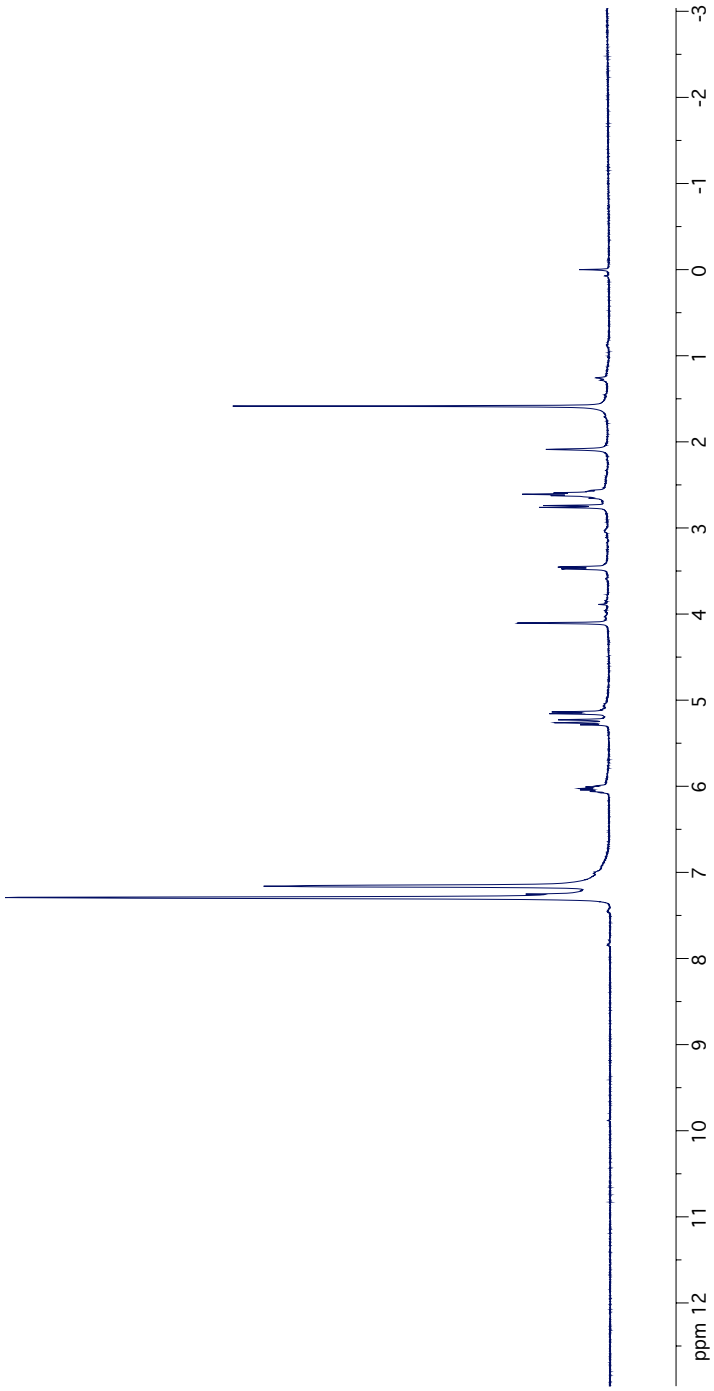

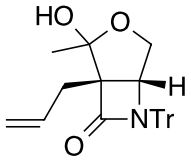

1.48

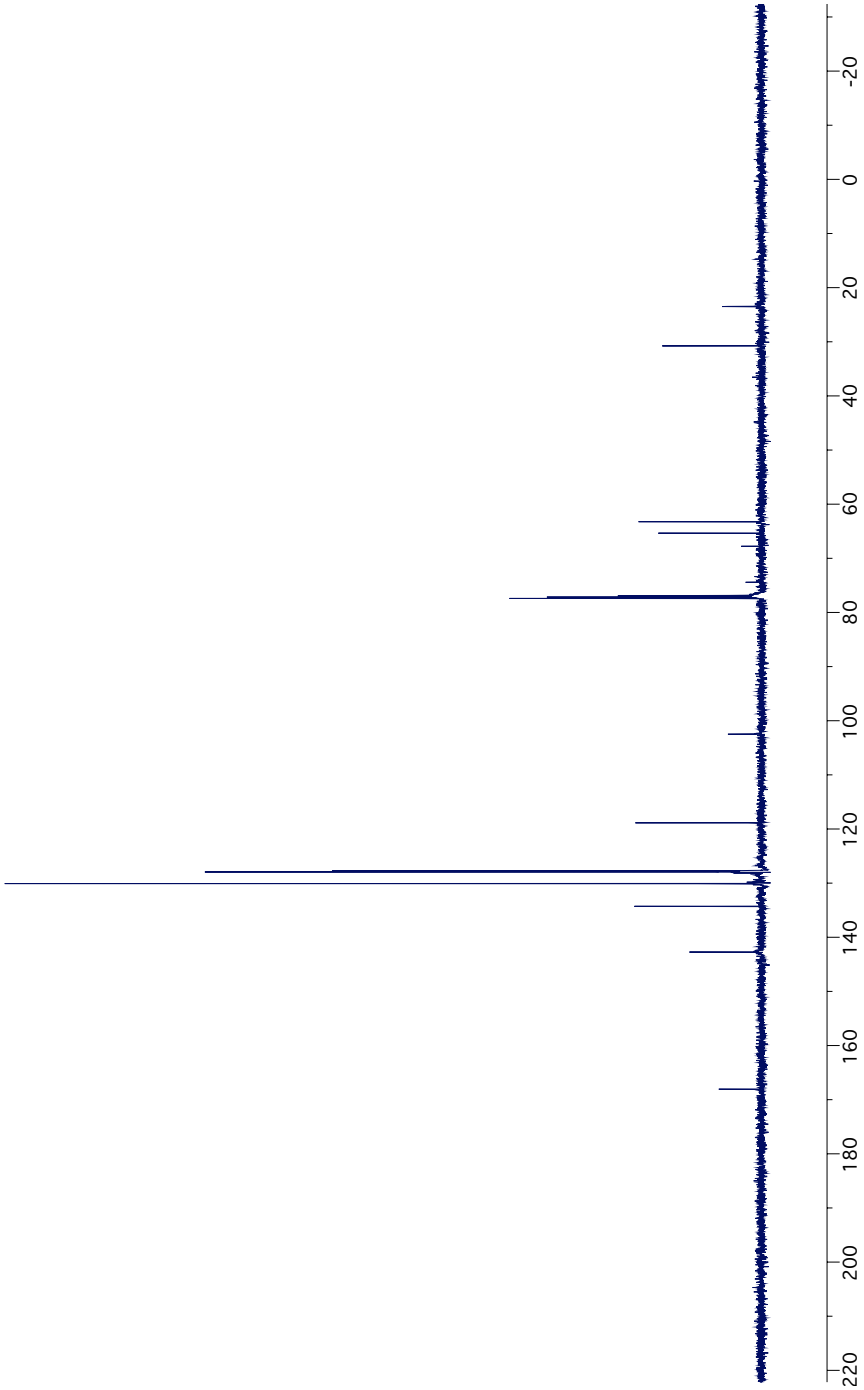

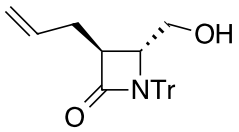

1.49

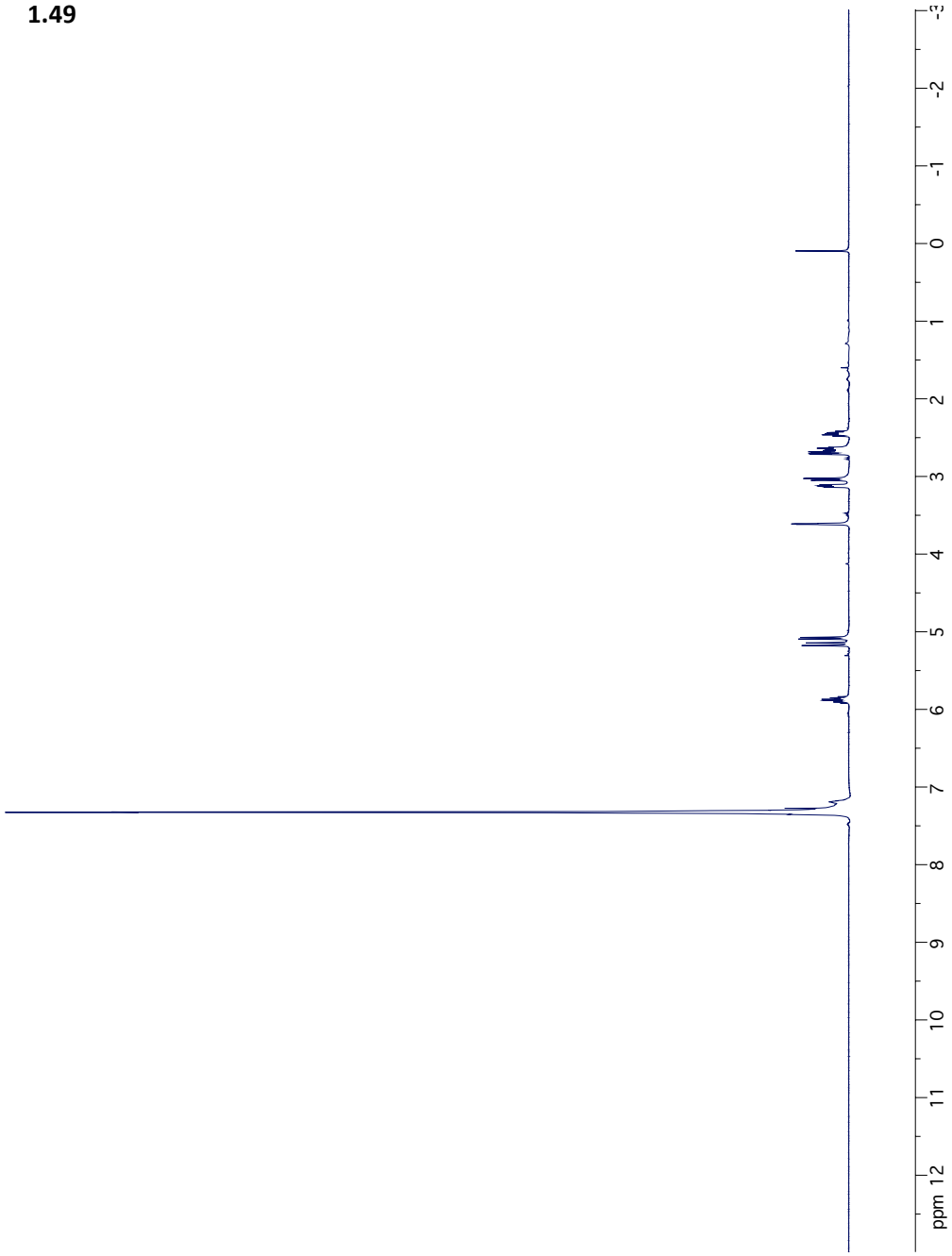

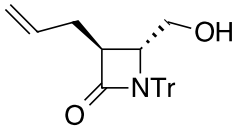

1.49

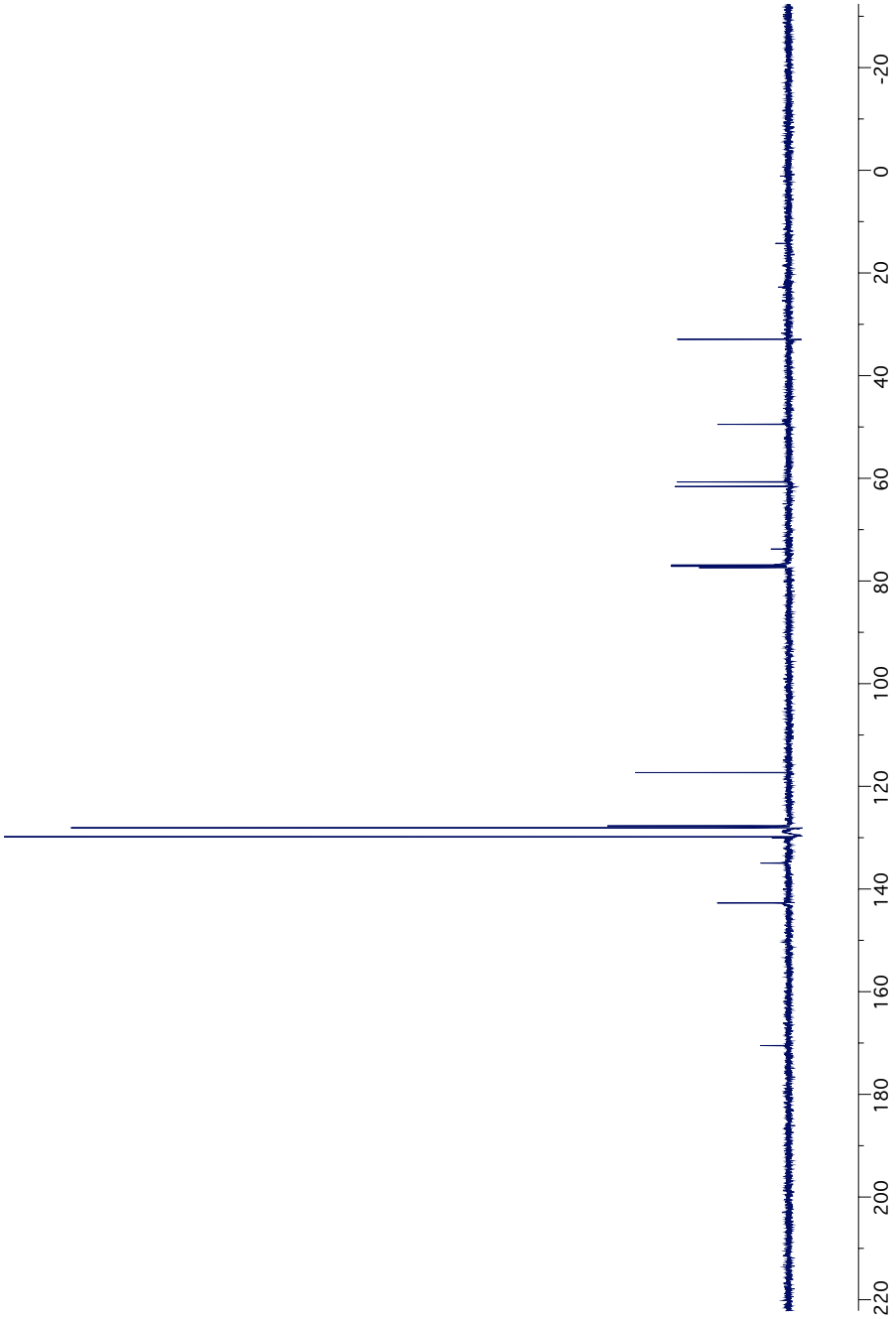

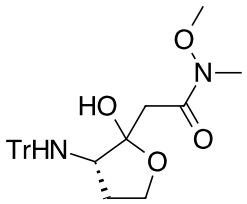
O
N
HO
O
TrHN
O

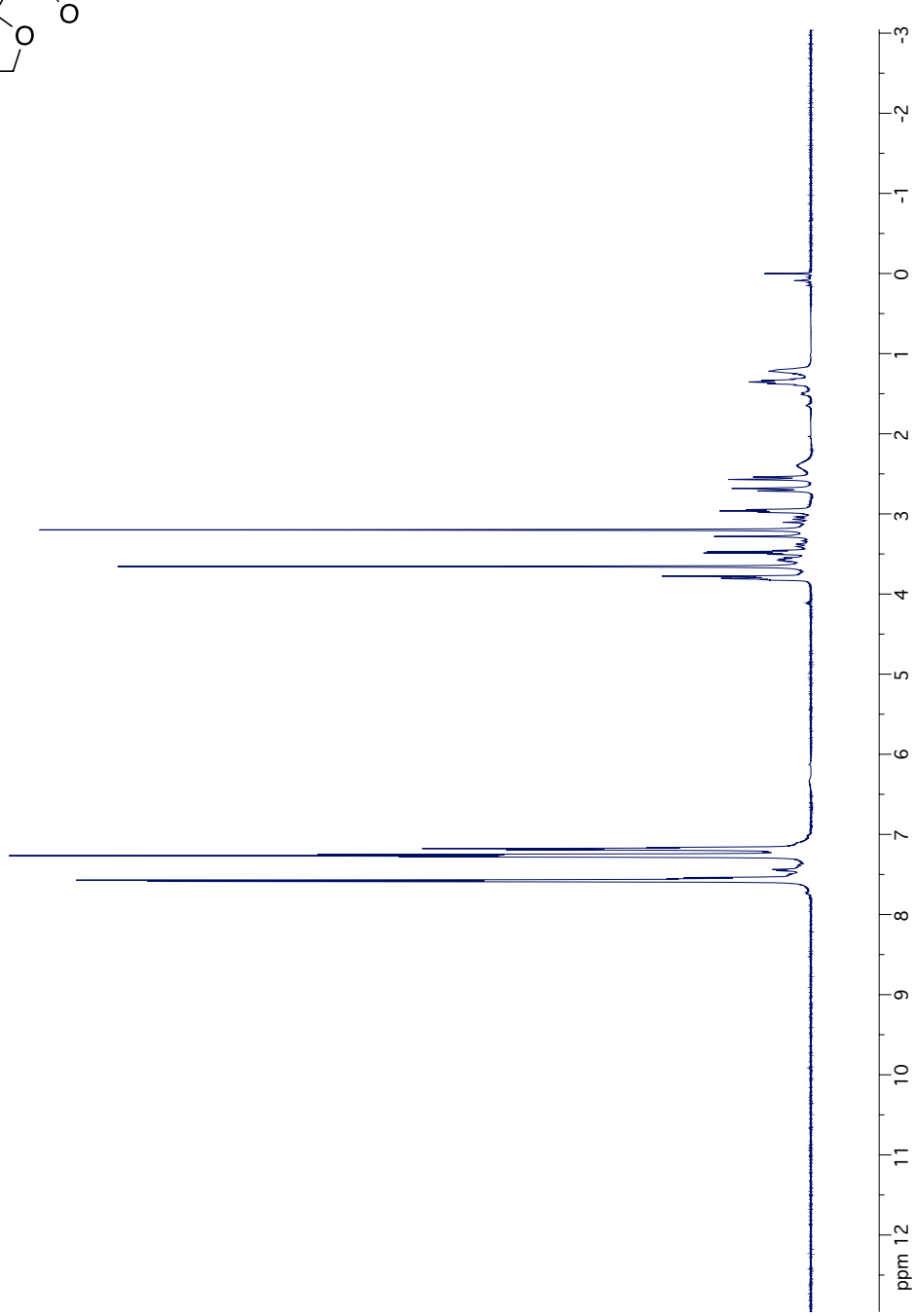
-3
-2
-1
0
1
2
3
4
5
6
7
8
9
10
11
ppm 12

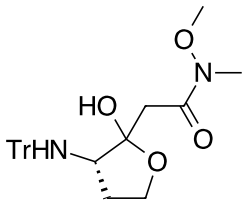
O
N
HO
O
TrHN
O

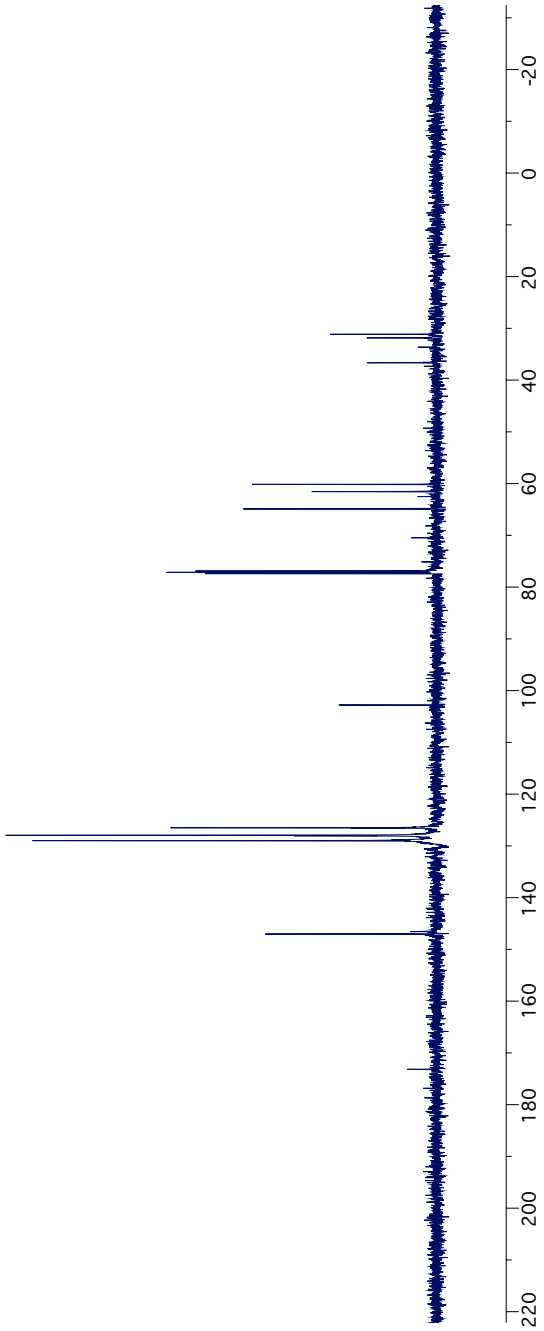
-20
0
20
40
60
80
100
120
140
160
180
200
220

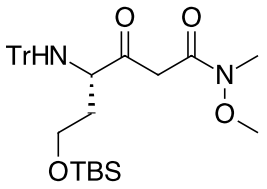
TrHN
O
O
N
O
OTBS

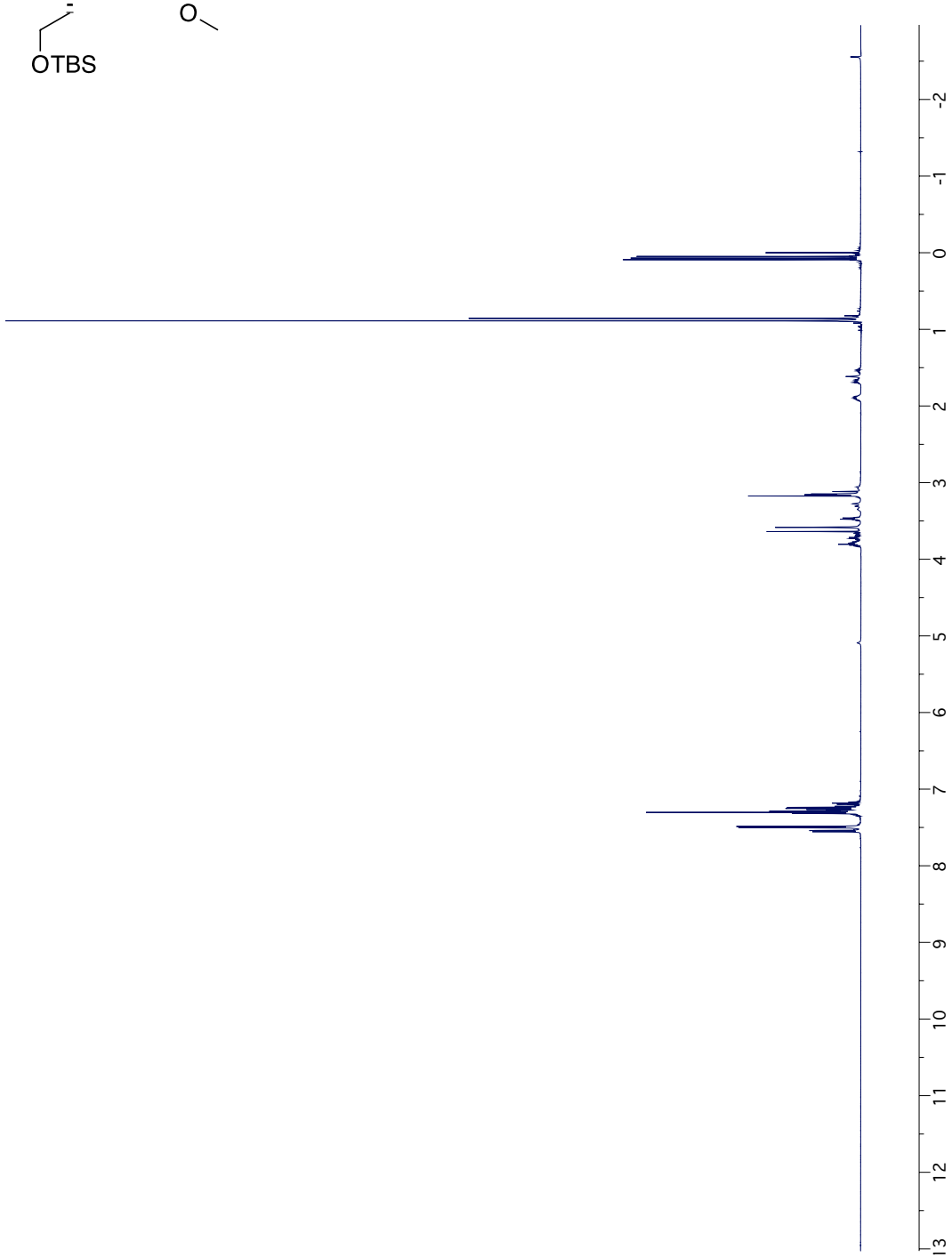
13
12
11
10
9
8
7
6
5
4
3
2
1
0
-1
-2

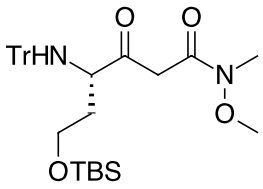
TrHN
O
O
N
O
OTBS

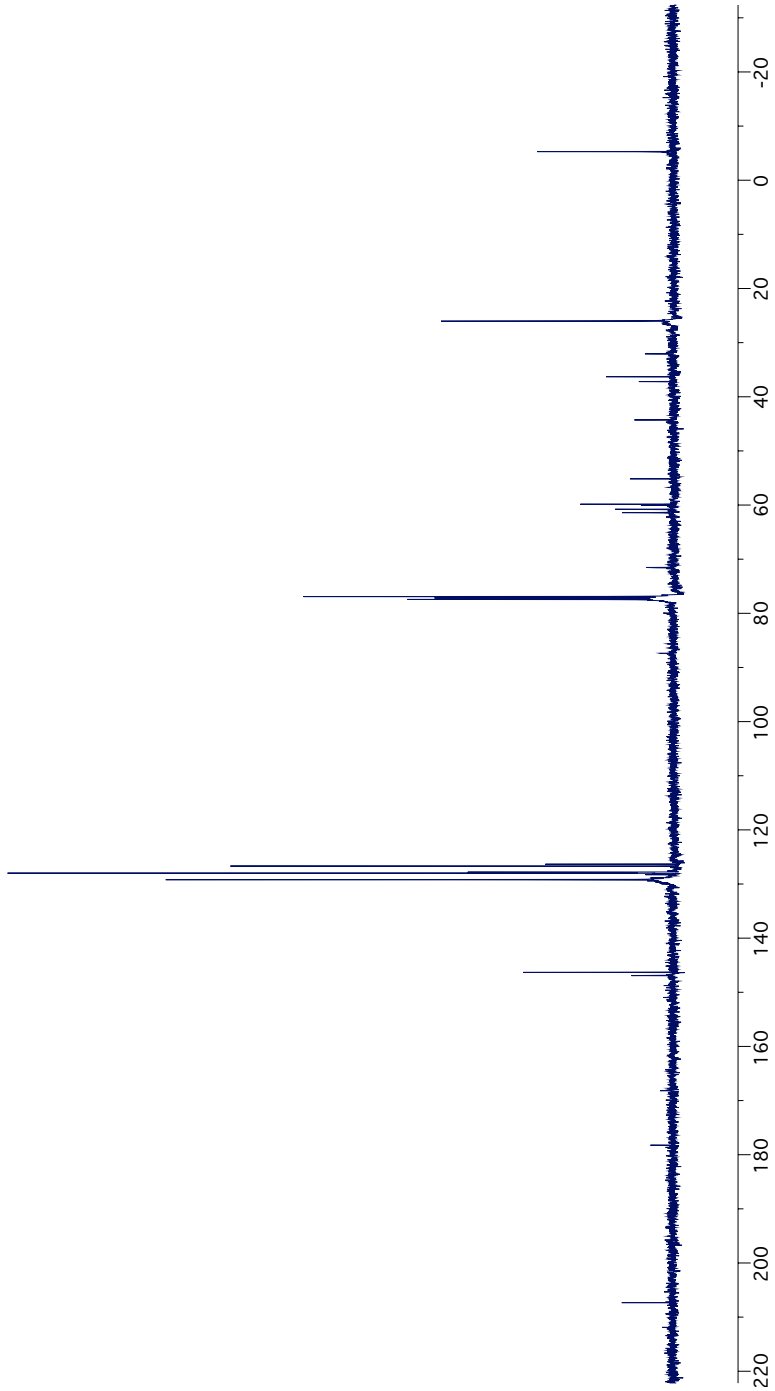
-20
0
20
40
60
80
100
120
140
160
180
200
220

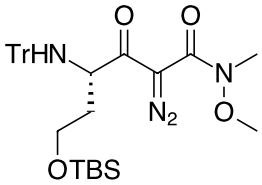

1.58

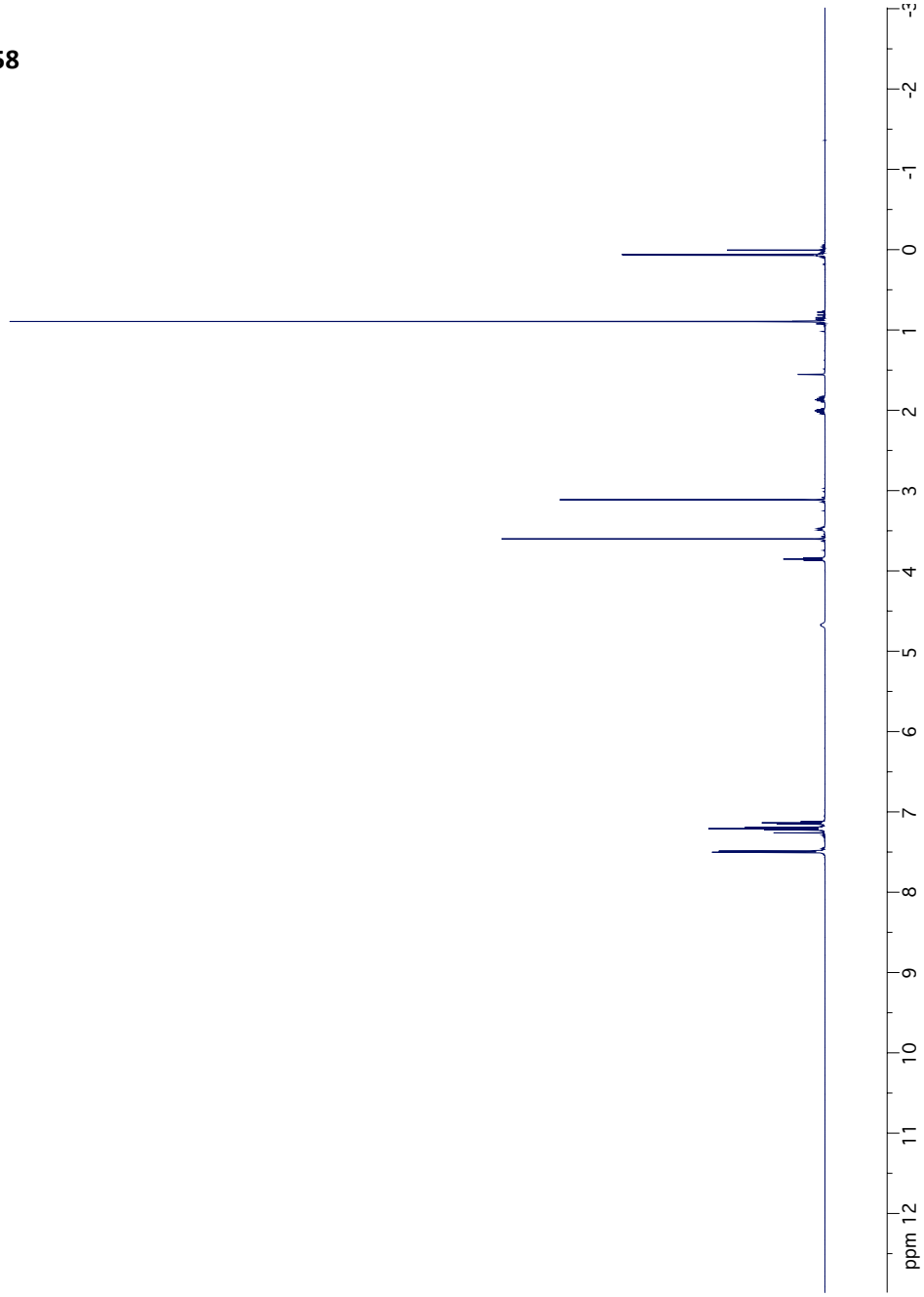

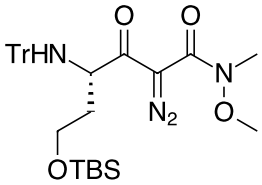

1.58

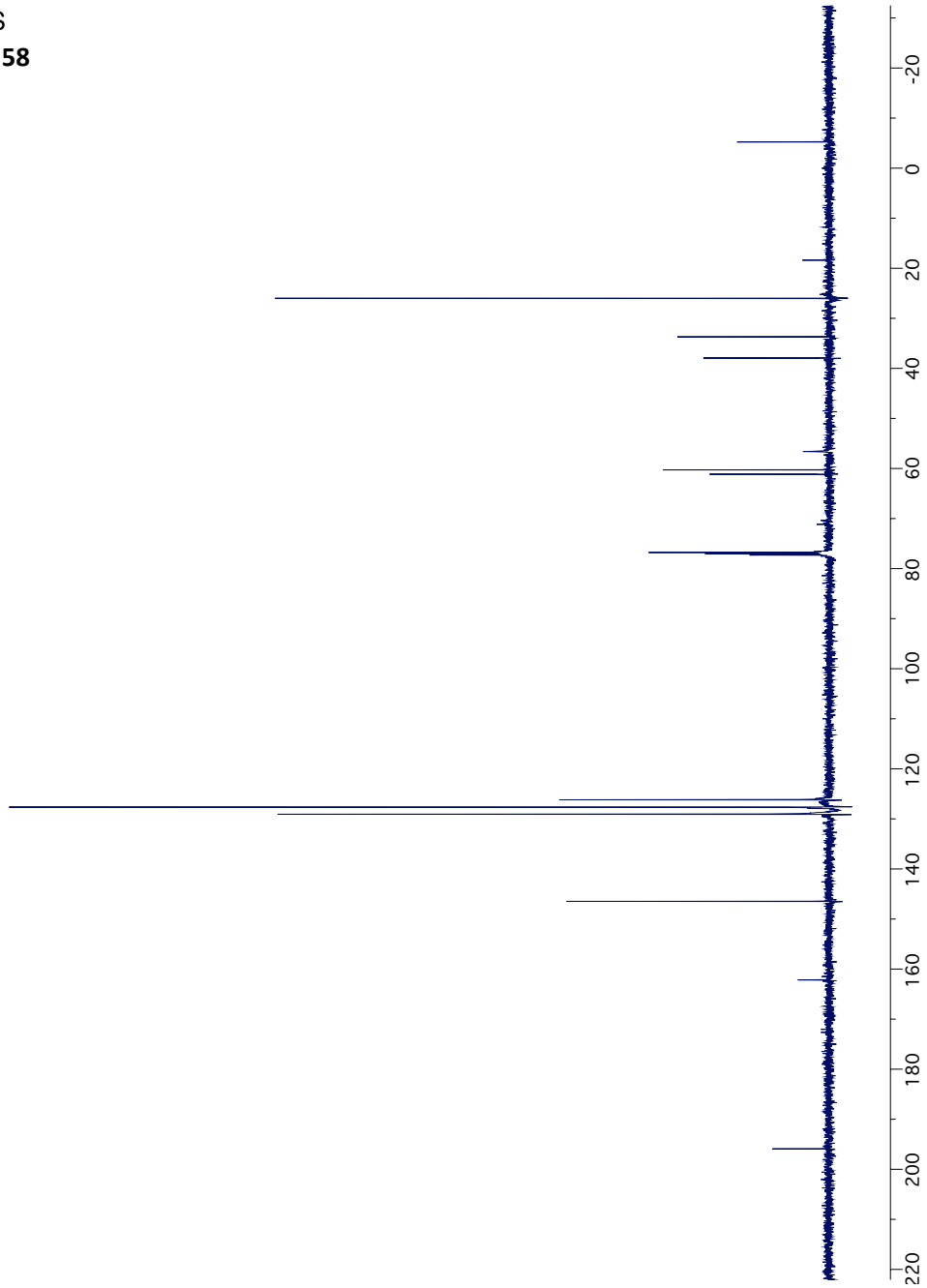

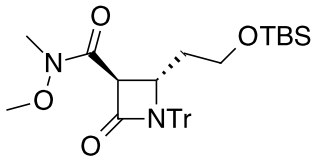

1.55

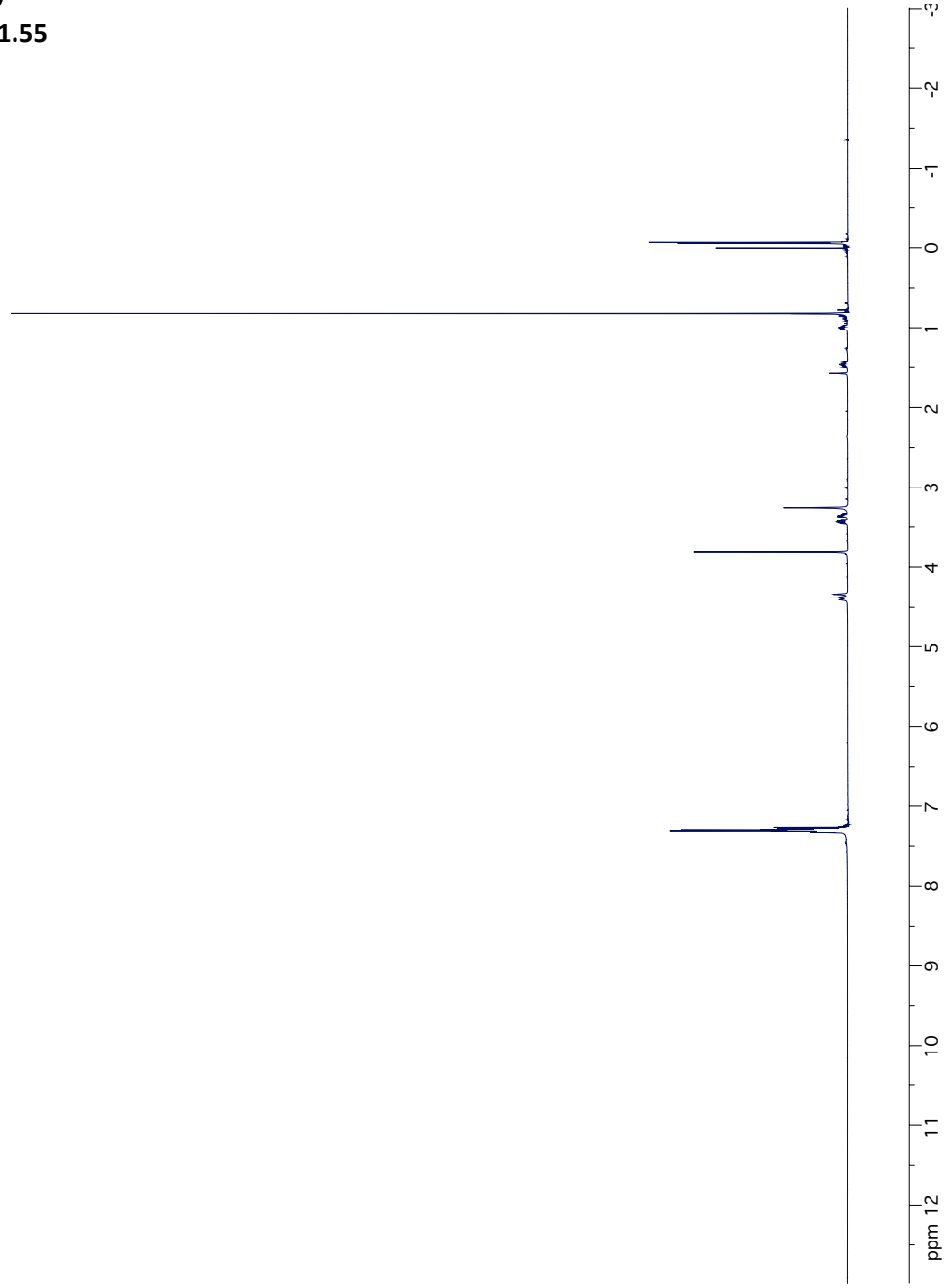

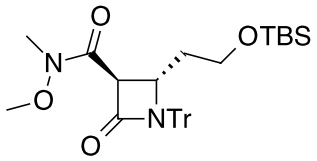

1.55

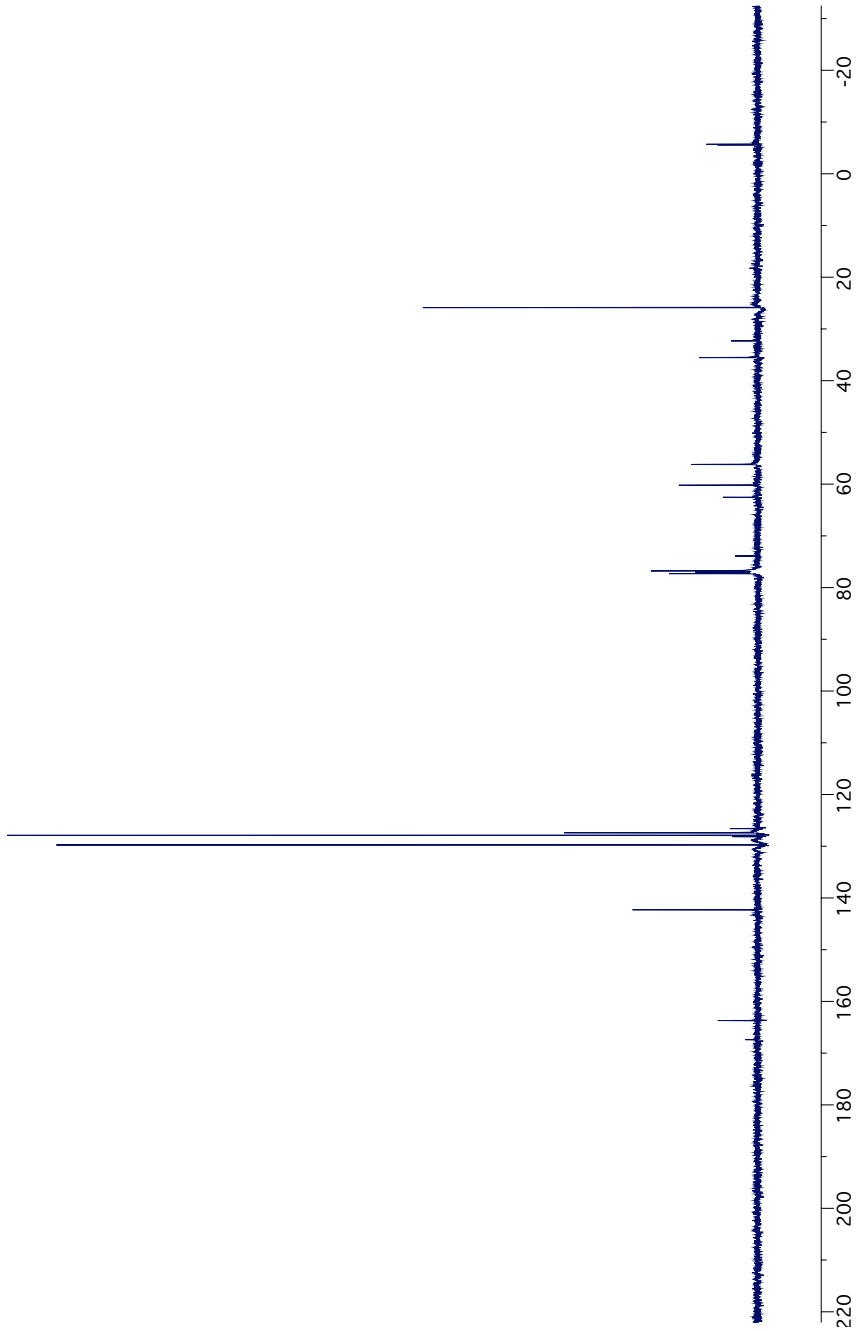

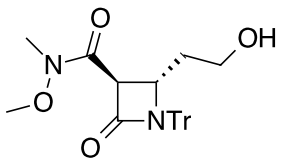
O
N
O
OH
NTr
O

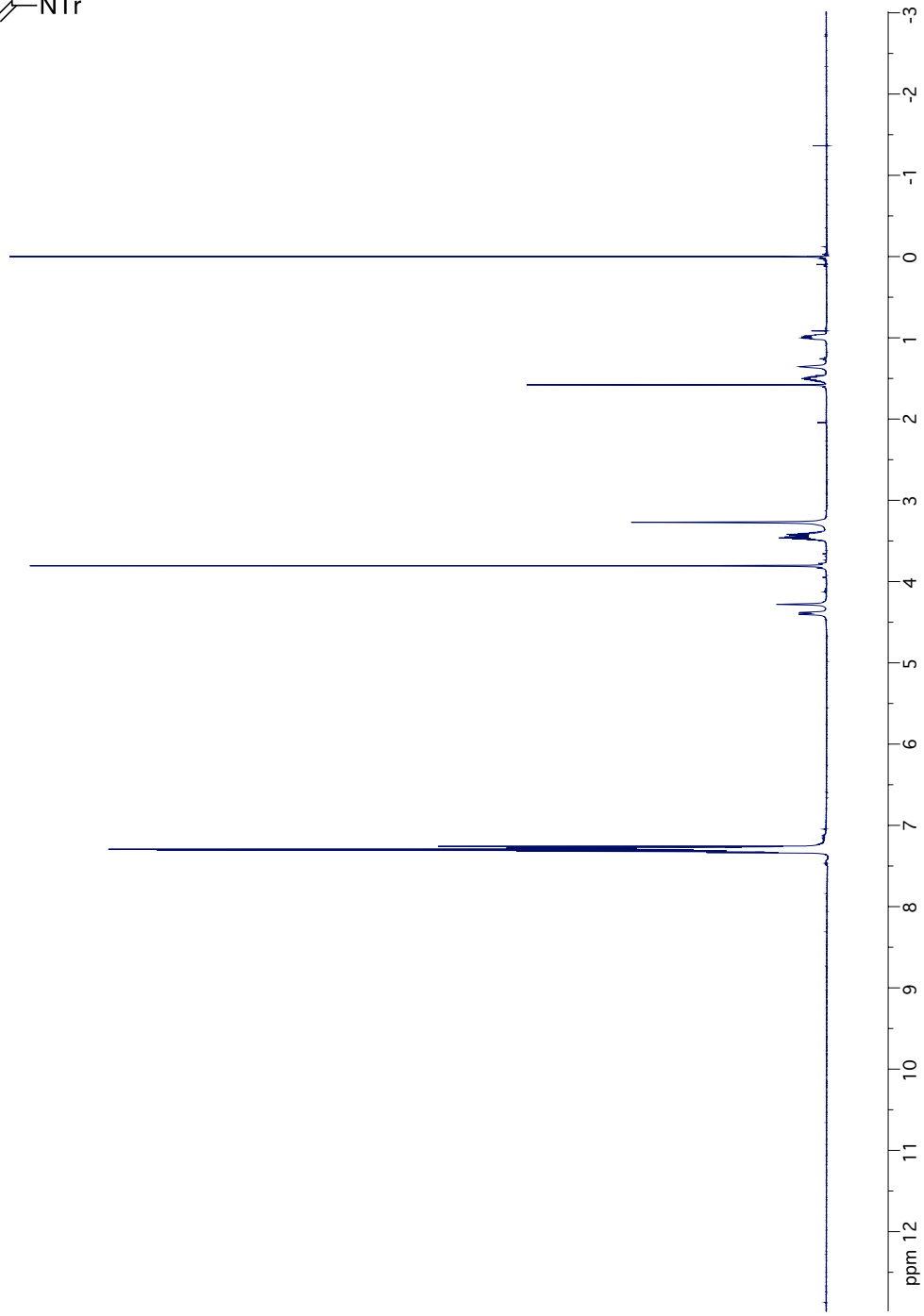
ppm
12
11
10
9
8
7
6
5
4
3
2
1
0
-1
-2
-3

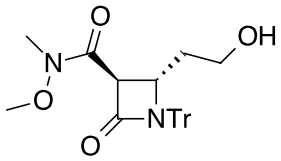
O
N
O
OH
NTr
O

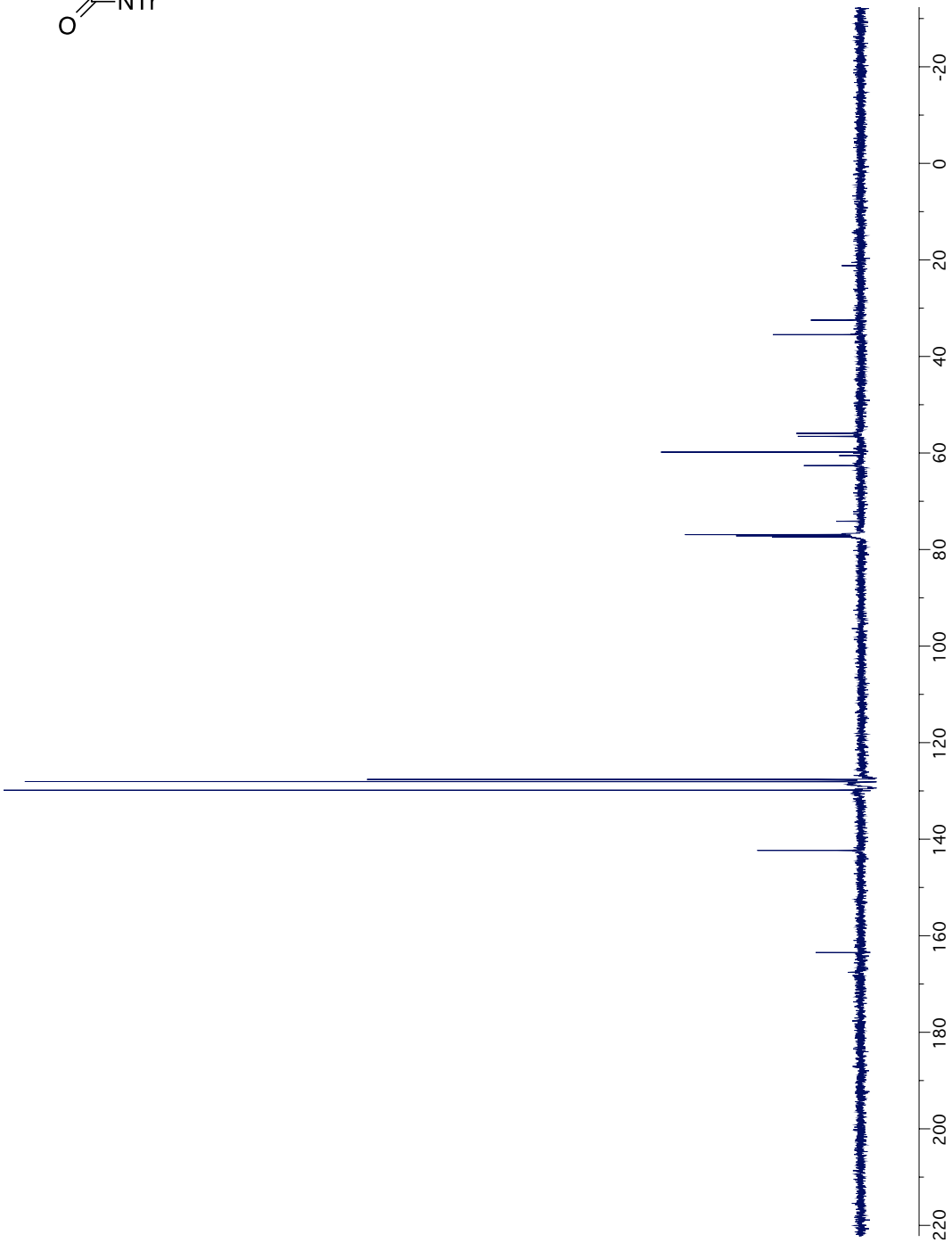
-20
0
20
40
60
80
100
120
140
160
180
200
220

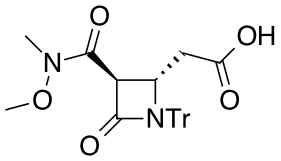
O
N
O
OH
O
NTr
O

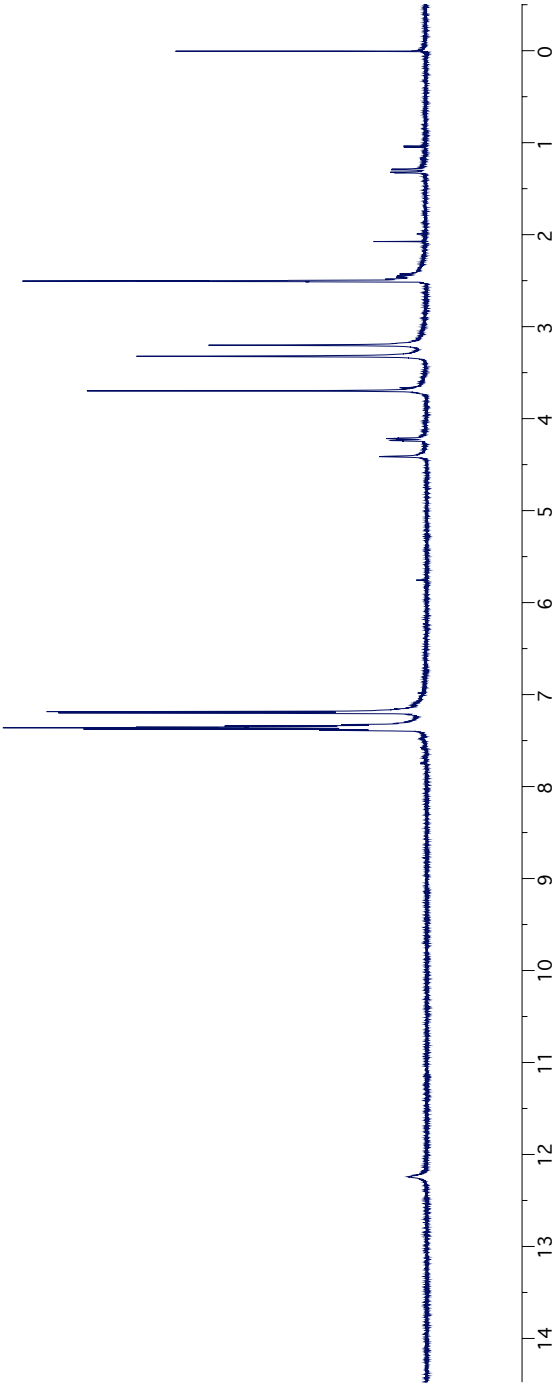
0
1
2
3
4
5
6
7
8
9
10
11
12
13
14

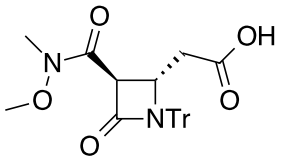
O
N
O
OH
O
NTr
O

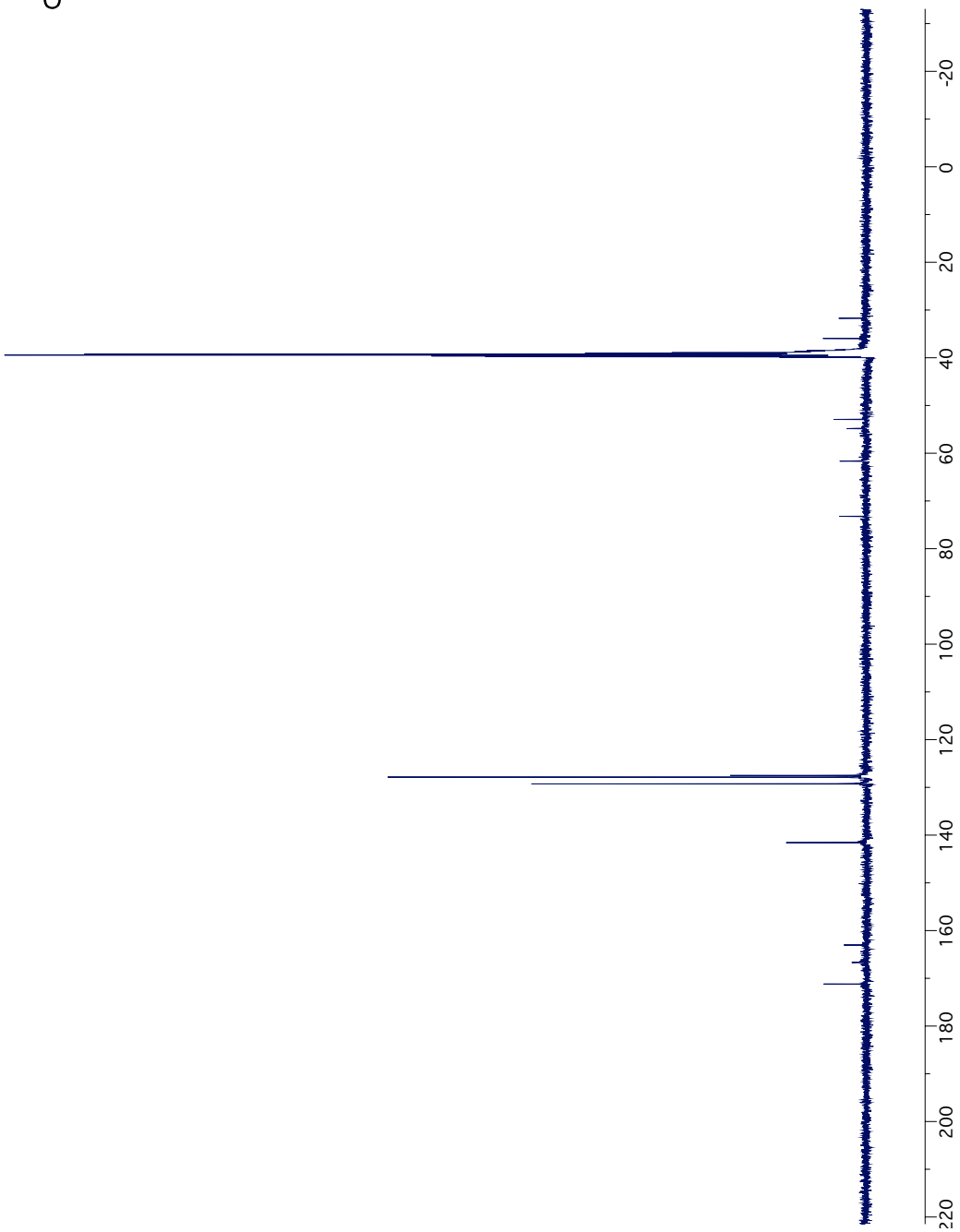
-20
0
20
40
60
80
100
120
140
160
180
200
220

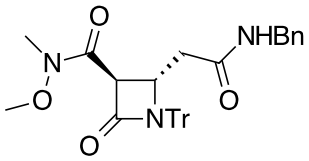

1.54

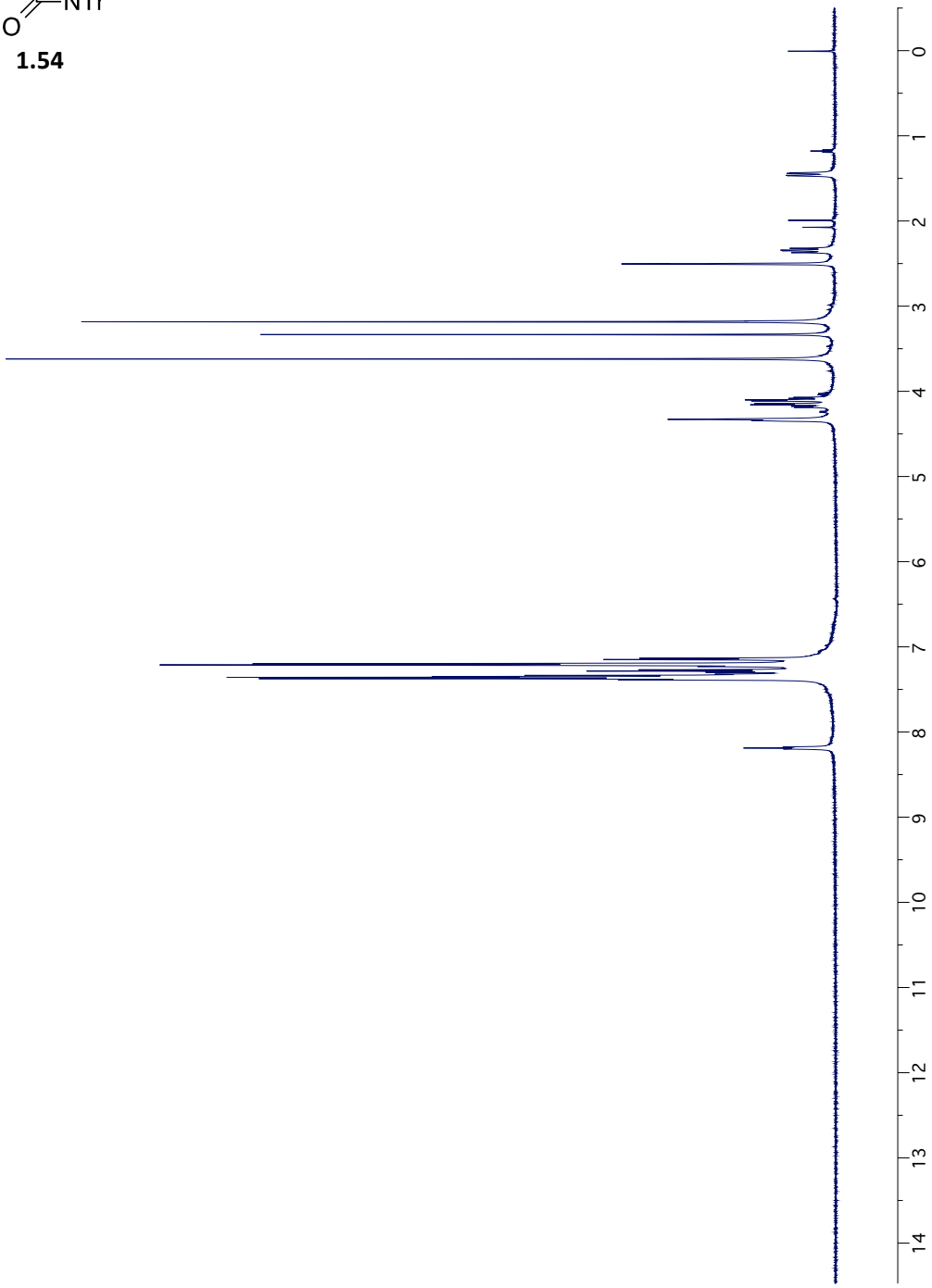

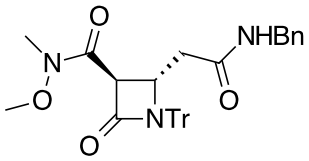

1.54

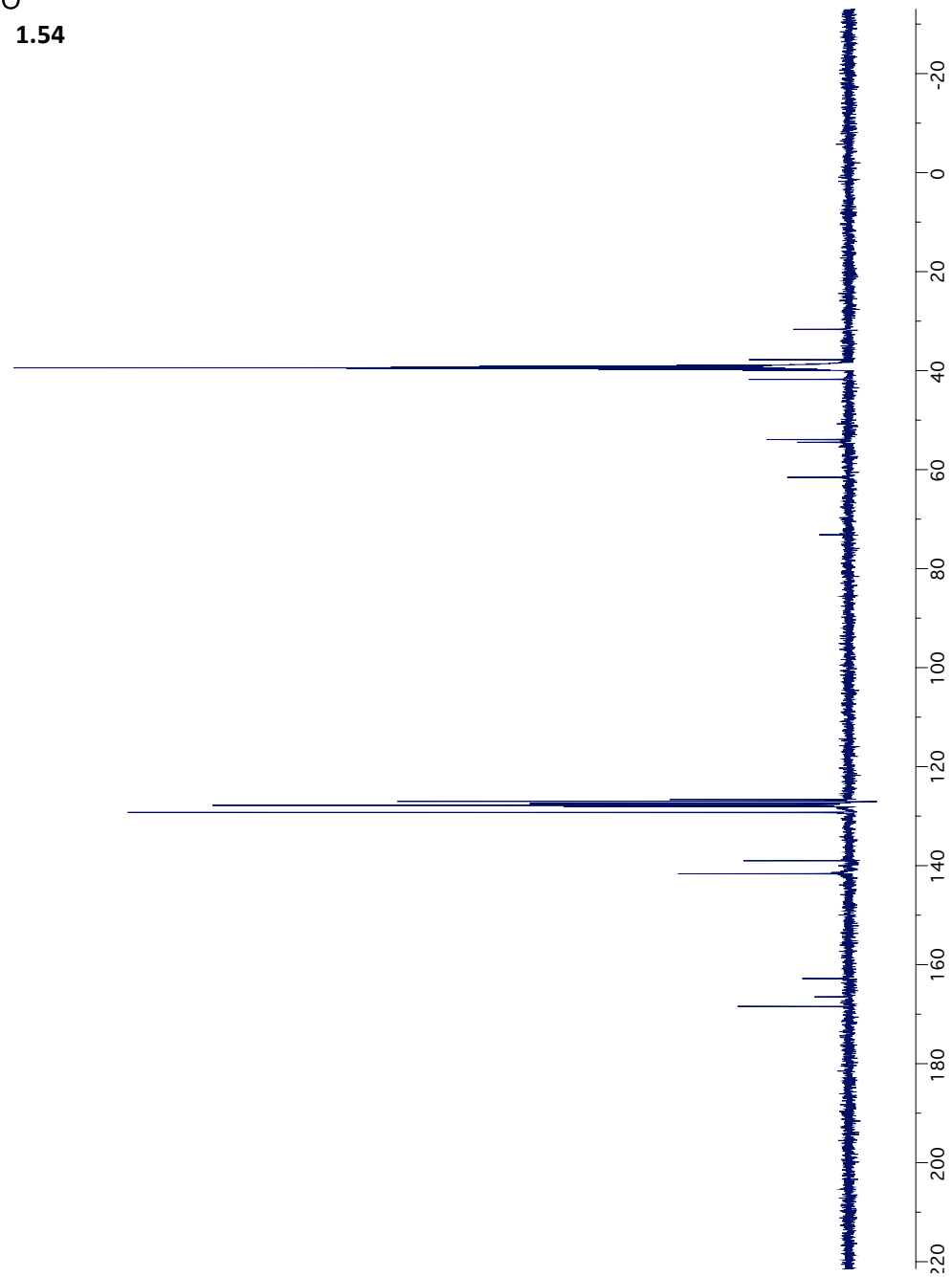

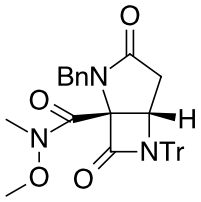

1.59

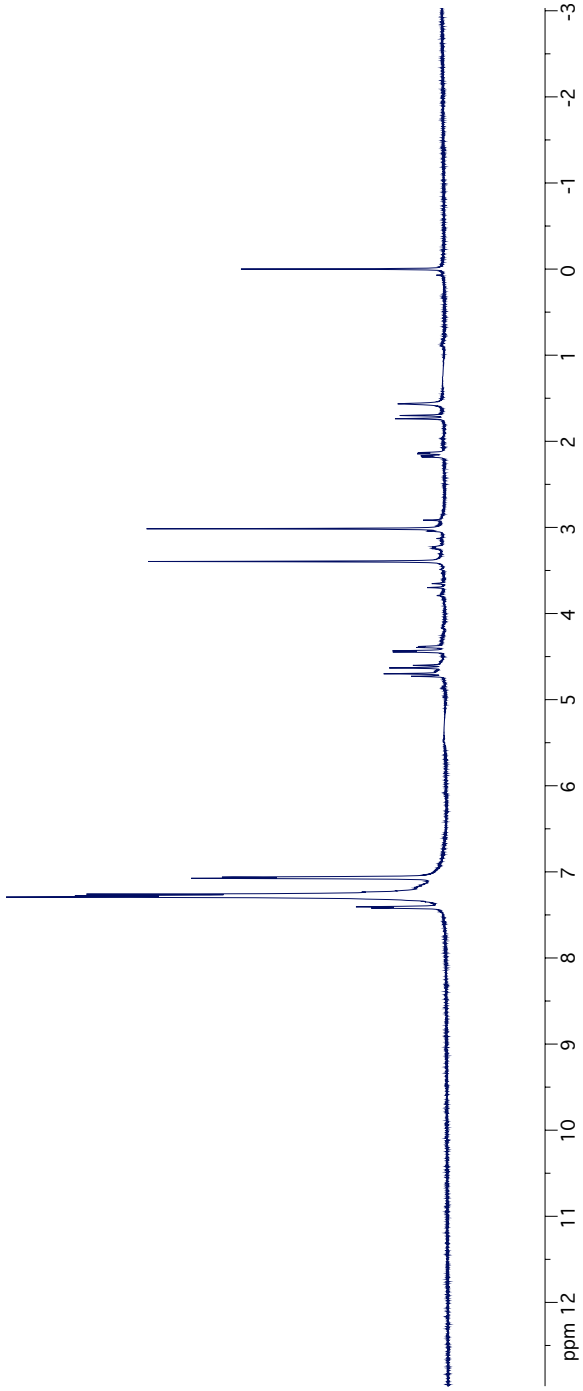

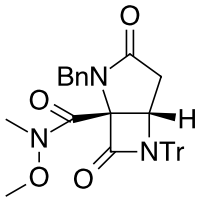

1.59

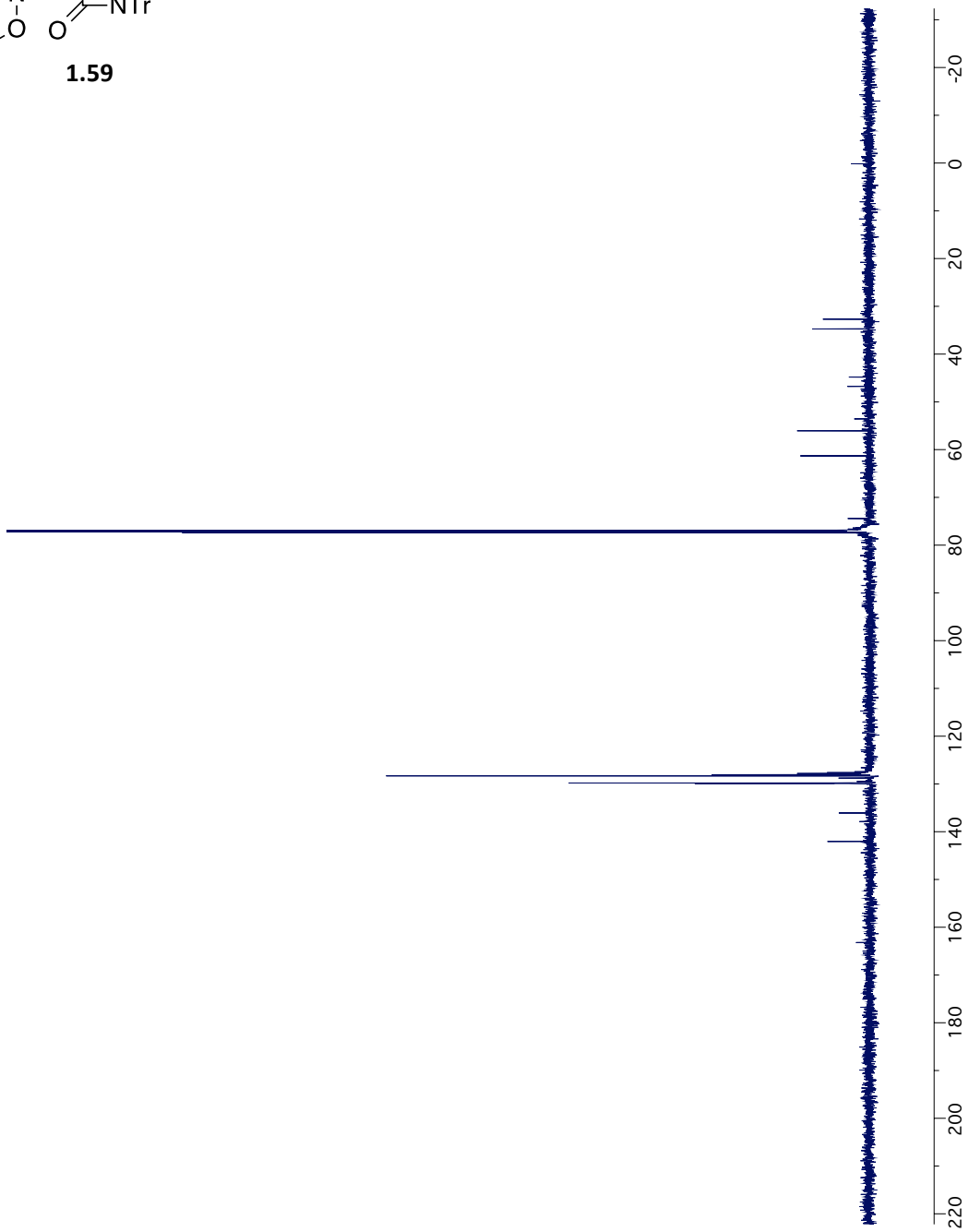

Chapter 2: Cell-permeable cyclic peptides from synthetic libraries inspired by natural products.

Introduction

Recent biomedical advances have produced a wave of candidate therapeutic targets, many of which are intracellular protein-DNA, protein-RNA, and protein-protein interactions (PPI's) whose binding interfaces are larger and less pocket-like than typical drug targets.[1,2] While many larger binding sites are considered "undruggable" by small molecules, they can often be inhibited by larger, more complex molecules such as intracellularly expressed antibodies (intrabodies)[3-5] as well as natural and synthetic cyclic peptides.[6-11] Indeed, the prevalence of potent, PPI-disrupting cyclic peptides highlights the potential utility of these compounds as therapeutics.[12-14] However, this increased MW and complexity comes at a cost, as larger, more functionally rich molecules often fail to meet the physicochemical requirements (captured by rough bioavailability predictors such as Lipinski's "Rule of 5")[15,16] for cell permeability, thus limiting them in most cases to parenteral delivery against extracellular targets.

Nonetheless, there is a class of compounds exemplified by the cyclic peptide cyclosporine A (CSA; MW 1202 Da) that exhibit drug-like cell permeability and, in some cases, oral bioavailability, despite molecular weights that lie well outside the range of typical small molecule drugs (i.e., ~ 500 – 700 Da). While physical models of permeability for conventional drug-like molecules are well established[17], the determinants of passive membrane diffusion in molecules at the larger end of the MW continuum are somewhat less well understood[18], hindering the rational design of cell-permeable, "beyond-Rule-of-5" molecules as therapeutic agents. As interest grows in designing cyclic peptides and other

macrocycles against intracellular targets[19,20] understanding the relationship between structure and permeability in these "beyond-Rules-of-5" molecules will be vital.

Previously we reported model cyclic peptides[21-23] whose passive permeabilities, like CSA, depend on conformation-determining backbone elements such as stereochemistry and *N*-methylation.[24] Here, we describe the synthesis of an exhaustive library of 1152 cyclic hexapeptide stereoisomers and *N*-methyl variants—prepared and screened as twelve sublibraries consisting of 96 cyclic peptides—inspired by the diverse backbone geometries found in cyclic peptide natural products (i.e. guangomide A,[25] baceridin,[26] Figure 2.1a), and investigations into the relationship between conformation and permeability across small sets of structures present in the library. Our results confirm the importance of side chain orientation and steric factors in determining membrane permeability in cyclic peptides, with implications for the design of synthetic, cell-permeable macrocycles.

Experimental Design

In order to access a relatively large conformational space, we designed a split-pool library[27] based on a cyclic hexapeptide template that would sample all possible stereoisomers and *N*-methyl variants, translating into diverse backbone geometries and conformational preferences. We employed the generic sequence Pro-$(Xaa)_4$-Tyr, incorporating L- and D-Leu, and L- and D-MeLeu at the variable positions X^2-X^5 (Figure 2.1b), and included Gly and MeGly (Sar) at positions X^2 and X^4 to investigate the impact of overall lipophilicity and backbone flexibility on permeability. Following library synthesis, LCMS analysis showed that although impurities were observed, all expected masses were present in appropriate ratios predicted by the statistical representation of each isomeric series.

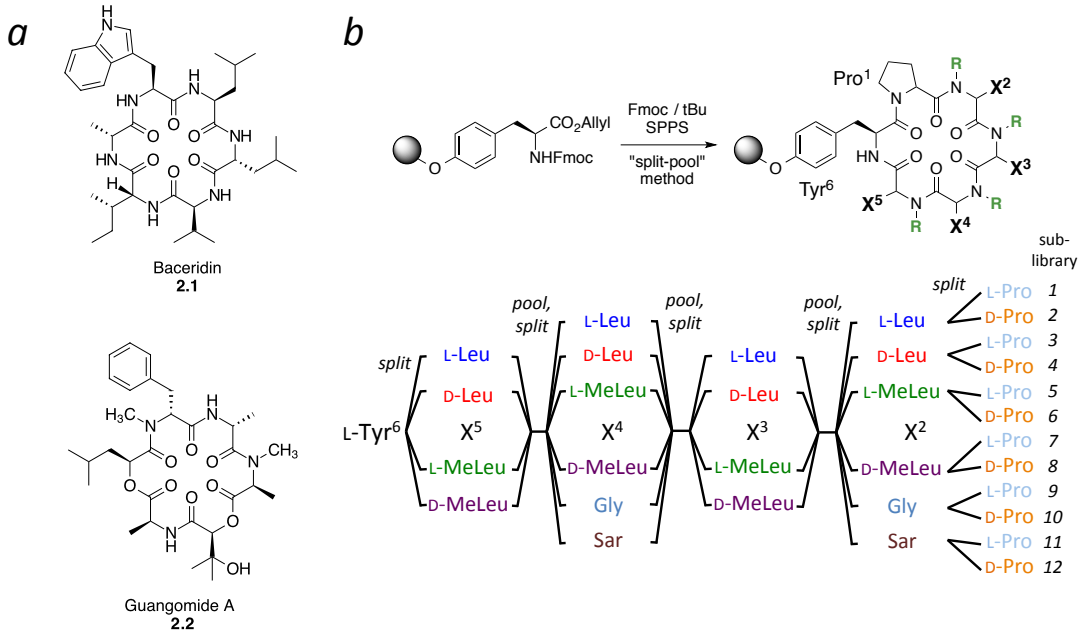

Figure 2.1. a) Natural products similar to library members synthesized in this study. b) Overall design of split-pool library of geometrically diverse cyclic hexapeptides.

The library design allowed unambiguous assignment of the composition (i.e., specifying the number of Leu vs. Gly residues and the number of *N*-methyls) of each set of stereo- and constitutional isomers to an observed parent mass. Within each isomeric series there was good chromatographic separation of the individual compounds.

Passive membrane diffusion was quantified initially using the parallel artificial membrane permeability assay (PAMPA), an established cell-free membrane permeability system comprised of a donor and acceptor well separated by a filter impregnated with 1% lecithin in dodecane (Figure 2.2a).[28,29] After a period of incubation, compound flux across the dodecane layer was measured by LCMS analysis of the acceptor wells using selected ion monitoring (SIM), which allowed for the acquisition of mass-separated chromatogram traces (Figure 2.2b) corresponding to the different isomeric series.

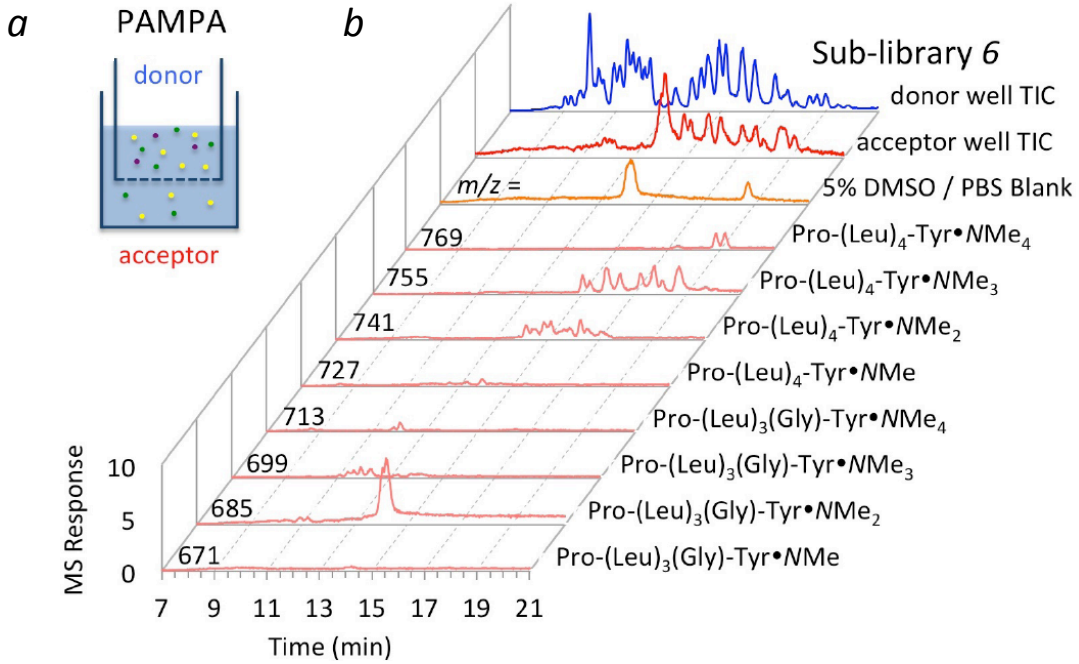

Figure 2.2. a) Schematic of PAMPA in vitro permeability assay system. b) LCMS traces from PAMPA analysis of sub-library 6, showing extracted-ion chromatograms from acceptor well at m/z values corresponding to compositional variants.

Results and Discussion

Initial analysis of the cyclic peptide libraries revealed an average of ~47 distinct peaks from each sub-library, or 567 peaks for the entire library. After PAMPA, ~240 distinct peaks appeared in the acceptor wells. Although differences in the amounts of each species present in the donor wells precludes a quantitative assessment of the individual permeabilities at this stage in the analysis, nearly half of these peaks (~105) showed significant intensity in their respective acceptor wells by rough MS quantitation (Figure 2.3a). A significant portion of these peaks with high apparent permeability were concentrated in sub-libraries *4* and *6*. In general, however, sub-libraries with more *N*-methyl

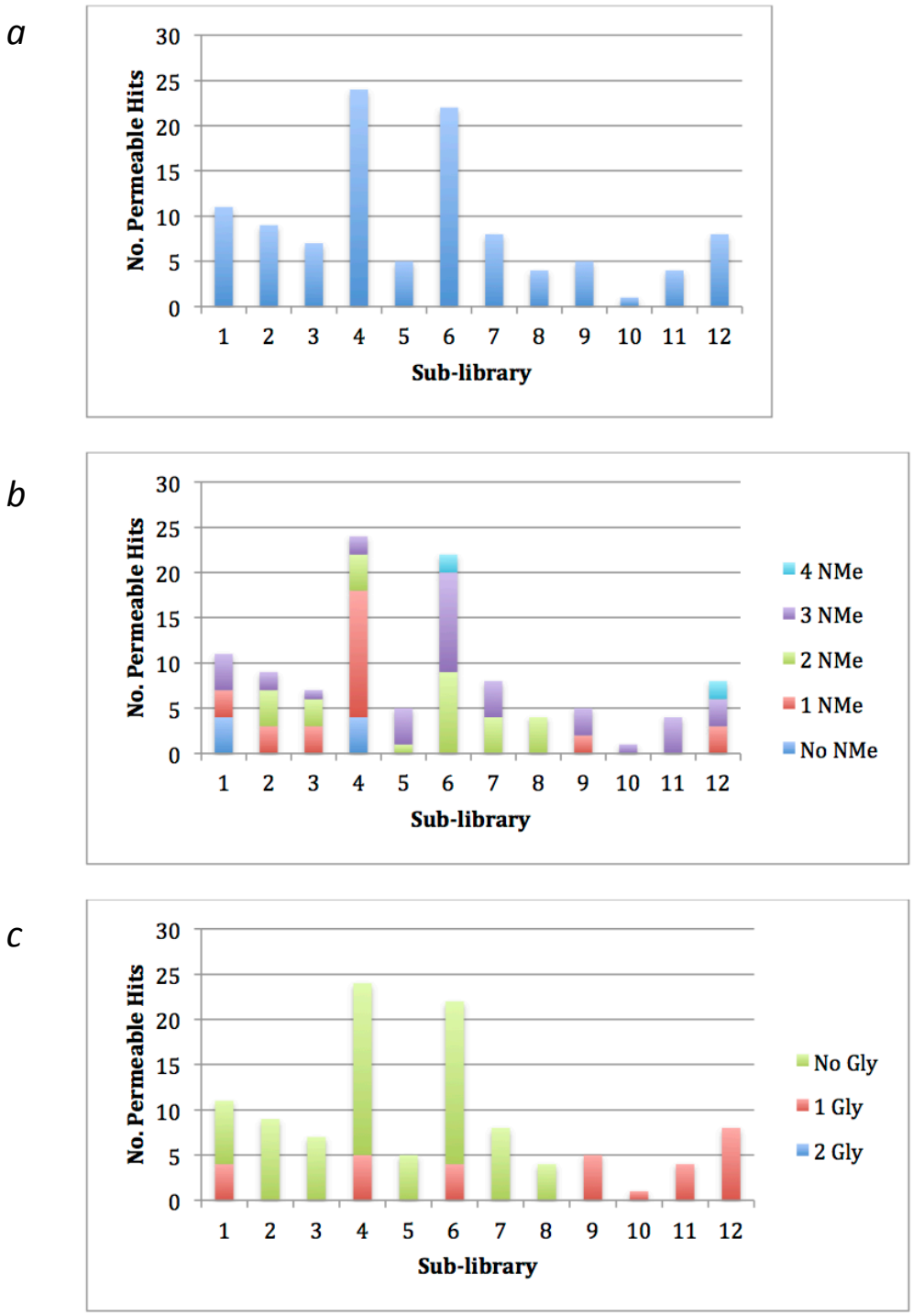

Figure 2.3. a) Total number of compounds above an intensity threshold of 1 x 10^4 in the LCMS trace acceptor wells of each sub-library. These hits are further classified by b) number of *N*-methyl amides and c) glycine incorporation.

groups showed a greater overall enrichment in permeable compounds compared to sub-libraries with fewer *N*-methyls (Figure 2.3b), and sub-libraries with Gly or Sar residues were on average less permeable than the corresponding all-Leu-containing sub-libraries, with no permeable compounds detected containing two Gly / Sar residues (Figure 2.3c). There were exceptions to these trends, for example, some compounds with 4 *N*-Me groups showed very low permeability, while some non-*N*-methylated compounds appeared to be highly permeable (see below). Also, several Gly- and Sar-containing compounds showed strong enrichment in the PAMPA acceptor wells, suggesting that these scaffolds can adopt particularly permeable conformations that compensate for the decrease in lipophilicity resulting from the loss of a Leu side chain.

Following this initial analysis, we then set out to identify specific, membrane permeable scaffolds from the twelve sub-libraries, initially focusing on sub-library *6* with the consensus sequence cyclo[D-Pro^1 – L-MeLeu^2 – X^3 – X^4 – X^5 – L-Tyr^6] (Figure 2.4, top chromatogram). LCMS analysis of this sub-library showed a large number of permeable scaffolds in the *m/z* = 755 trace corresponding to cyclic peptides with three backbone *N*-methyl groups. Rather than synthesizing and testing all twenty-four tri-*N*-methylated stereochemical and *N*-methyl positional isomers in sub-library *6* , we used a recursive deconvolution strategy[30] to identify selected peaks. Thus, four new "tier-2" sub-libraries with X^3 defined (as L-Leu, D-Leu, L-MeLeu, or D-MeLeu) (Figure 2.4) were synthesized and submitted to PAMPA analysis. The resulting mixtures (simplified as expected compared to the parent sub-library) showed compounds with varying degrees of permeability, and

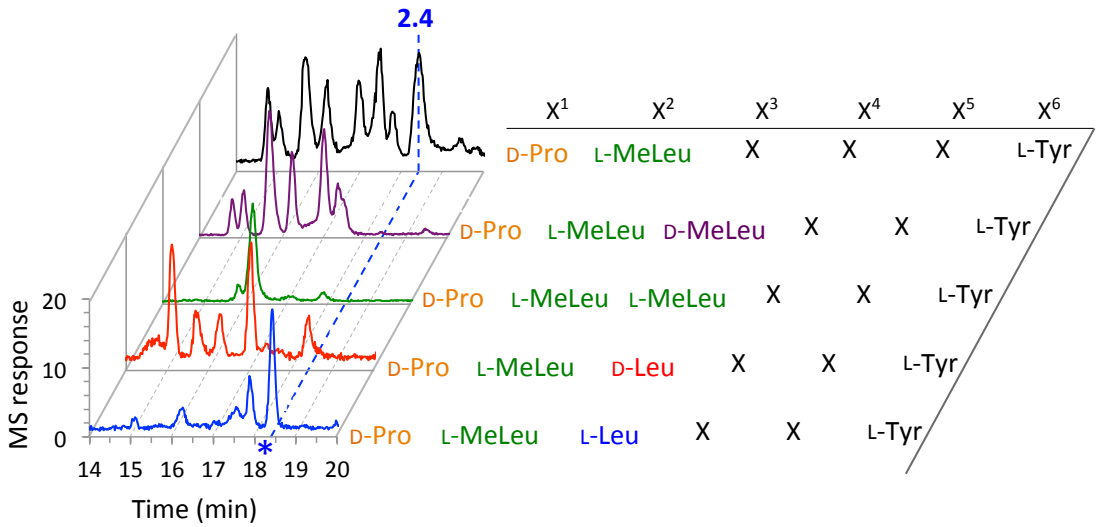

Figure 2.4. Deconvolution of sub-library *6* by resynthesis of tier-2 sub-libraries in which X^3 is known. The major permeable component of the X^3 = L-Leu is shown with an asterix and was identified as **2.4**, a sequence analog of the previously identified (ref. 23), highly permeable compound **2.3** (Figure 2.5).

follow-up studies on individual compounds led to scaffolds of known permeability, as well as novel scaffolds that revealed interesting structure-permeability relationships.

In the tier-2 sub-library in which X^3 = L-Leu (Figure 2.4, blue chromatogram), the major permeable component was **2.4**, an analog that shares the same backbone scaffold as a compound (**2.3**) which we had identified previously using independent methods as a highly permeable and orally bioavailable scaffold (*F* = 28% in rat) (Figure 2.5a,b).[23] Compounds **2.3** and **2.4** share the same stereochemistry and *N*-methylation pattern, differing only in the side chains of the two amino acids on either side of the Pro. Indeed the low-dielectric conformation of **2.4** was predicted to be identical to the NMR solution conformation determined for **2.3** (Figure 2.5c). The permeabilities of **2.3** and **2.4** were measured in the Caco-2 epithelial cell line and were found to be nearly identical (Figure 2.5).

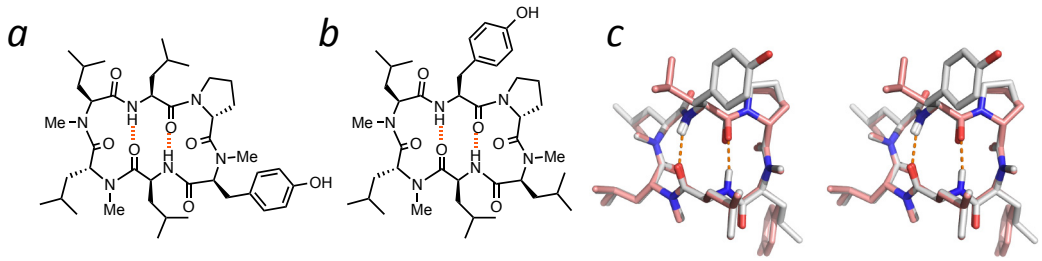

2.3
18 × 10^{-6} cm/s

2.4
20 × 10^{-6} cm/s

Figure 2.5. Structures of a) **2.3** (discovered in a previous study, ref. 23) and b) **2.4**; c) Stereoview of NMR structure of **2.3** (salmon) overlaid with calculated structure of **2.4** (white) showing that they have the same conformation and hydrogen bonding pattern. Permeabilities shown below the structures were determined in Caco-2 cells.

Additionally, we observed a high frequency of permeable compounds in the X^3 = D-MeLeu tier-2 sub-library. Rather than performing an additional round of recursive deconvolution, we chose to resynthesize all eight possible diastereomeric and *N*-methyl variants. Through this process, we discovered several additional novel scaffolds with moderate to excellent permeation rates as measured by Caco-2 assay (Table 2.1).

Table 2.1. Sequence and permeation rates for selected compounds from sub-library *6*

	Sequence[a]			
Compound	X^3	X^4	X^5	P_e[b]
2.4	L-Leu	D-MeLeu	L-MeLeu	20.0
2.5	D-MeLeu	L-Leu	L-MeLeu	2.1
2.6	D-MeLeu	L-Leu	D-MeLeu	1.11
2.7	D-MeLeu	D-Leu	L-MeLeu	0.55
2.8	D-MeLeu	D-Leu	D-MeLeu	0.4
2.9	D-MeLeu	L-MeLeu	L-Leu	0.380
2.10	D-MeLeu	L-MeLeu	D-Leu	23.3
2.11	D-MeLeu	D-MeLeu	L-Leu	2.14
2.12	D-MeLeu	D-MeLeu	D-Leu	16.4

[a]All compounds share the generic sequence D-Pro[1] - D-MeLeu[2] - X^3 - X^4 - X^5 - L-Tyr[6]. [b]As measured in Caco-2 assay, reported in units of 10^{-6} cm/s

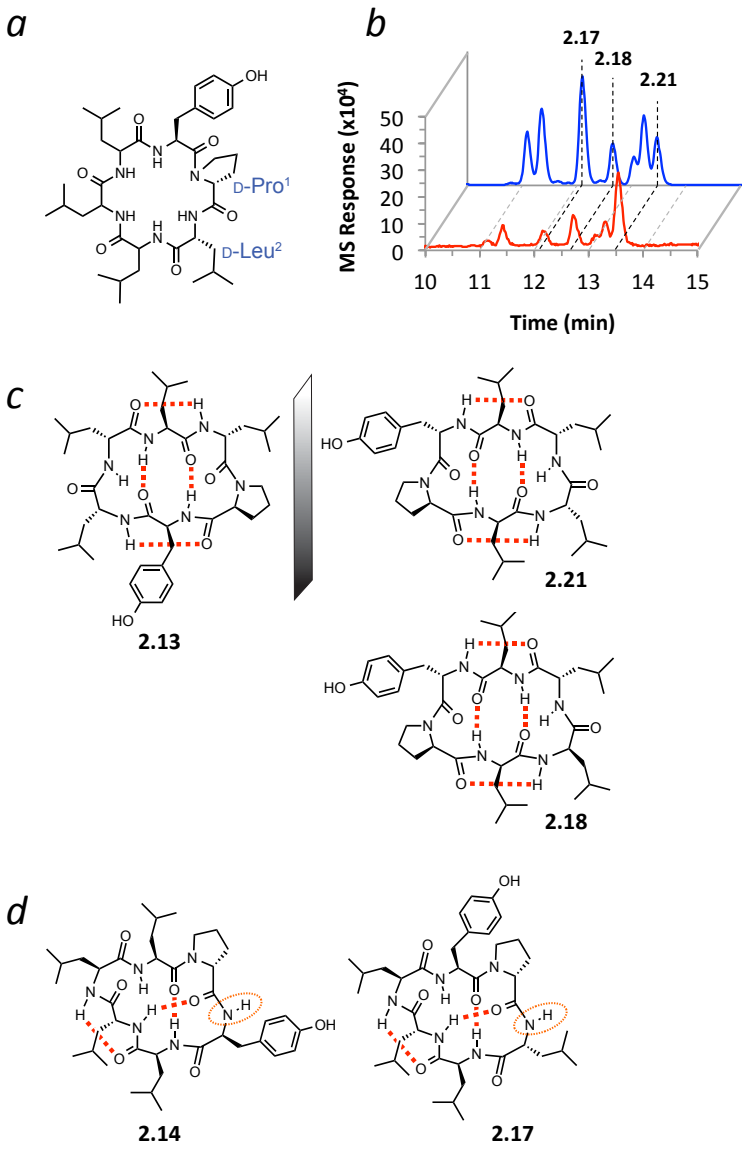

Figure 2.6. a) General structure of sub-library *4* at *m/z* = 713, corresponding to non-*N*-methylated scaffolds. b) HPLC traces of chromatogram (extracted ion monitoring at *m/z* = 713) for donor (blue) and acceptor (red) wells following PAMPA analysis of sub-library *4*. c) Structures of compound **2.13** from an earlier study (ref. 22) and two pseudo-enantiomers from this study, **2.18** and **2.21**. d) Structures of compound **2.14** from the same previous study and analog **2.17**, highlighting their most solvent-exposed NH group.

Most cyclic peptide natural products that are known to be cell permeable by passive diffusion contain at least one *N*-methylated backbone amide,[24] although synthetic cyclic hexapeptide scaffolds have been reported with no *N*-methyl groups that also show drug-like passive membrane permeability[21,22] and even oral bioavailability.[31] In the 1152-member library reported here, excluding compounds with glycine there are 32 non-*N*-methylated cyclic peptides distributed exclusively among sub-libraries *1-4*. The combined extracted ion chromatograms from these sub-libraries showed 31 distinct peaks (at *m/z* = 713 corresponding to the non-*N*-methyl, non-Gly-containing isomers) in the PAMPA donor wells. At least 6 of these compounds showed significant enrichment in the PAMPA acceptor wells, with the most permeable species concentrated in sub-libraries *1* and *4*. In sub-library *4* (Figure 2.6a), seven out of the eight possible diastereomers were visible in the acceptor well chromatogram, with strong enrichment observed for two of the peaks (Figure 2.6b). All eight

Table 2.2. Sequence, retention times, and permeation rates for selected compounds from sub-library *4*

		Sequence[a]			
Compound	R_t (min)	X^3	X^4	X^5	P_e[b]
2.15	11.1	D-Leu	L-Leu	L-Leu	0.257
2.16	11.3	L-Leu	L-Leu	L-Leu	0.43
2.17	12.1	L-Leu	D-Leu	L-Leu	0.143
2.18	12.7	D-Leu	L-Leu	D-Leu	7.9
2.19	13.1	D-Leu	D-Leu	D-Leu	0.045
2.20	13.2	L-Leu	D-Leu	D-Leu	0.5
2.21	13.5	L-Leu	L-Leu	D-Leu	3.6
2.22	ND[c]	D-Leu	D-Leu	L-Leu	0.228

[a]All compounds share the generic sequence D-Pro^1 - D-Leu^2 - X^3 - X^4 - X^5 - L-Tyr^6. [b]As measured in Caco-2 assay, reported in units of 10^{-6} cm/s.
[c]Not determined due to inconclusive results.

isomers from sub-library *4* were synthesized individually and the identities of the peaks from the original mixture were confirmed by separate co-injections with each of the pure compounds.

Caco-2 permeability studies on the 8 non-*N*-methylated stereoisomers from sub-library *4* confirmed that the two most permeable isomers were **2.18** and **2.21** (Table 2.2). The predicted backbone conformations of these compounds are near mirror images of the NMR-derived solution conformation of compound **2.13**, which we had previously identified as having drug-like passive permeability by PAMPA.[22] At the backbone level, **2.13** and **2.21** are indeed enantiomers, and **2.18** differs from **2.21** by a single stereocenter (position X^3). Moreover, among the least permeable isomers in the series was **2.17** (Figure 2.6d, Table 2.2) in which both the X^4 and X^5 stereocenters are inverted with respect to compounds **2.18** and **2.21**. The predicted conformation for **2.17** was nearly identical to the NMR solution structure in $CDCl_3$ of **2.14**, revealing the highly exposed amide NH that is most likely responsible for the poor permeability of both compounds. Variable temperature ^{1}H NMR (VT-NMR), which has been used as a tool to provide evidence of hydrogen bonding or solvent exclusion within proteins[32,33], supports these interpretations (Table 2.3). The small

Table 2.3. Permeation rates and temperature coefficients for selected compounds from sub-library *4.*

		Δδ/ΔT (ppb/K)				
Compound	P_e[a]	NH1	NH2	NH3	NH4	NH5
2.17	0.143	-2.7	-0.8	-2.9	**-5.5**	**-13.8**
2.18	7.9	-0.7	-0.3	-1.3	-1.1	-1.5
2.21	3.6	-1.5	-0.3	-1.3	-1.1	-1.1

[a]As measured in Caco-2 assay, reported in units of 10^{-6} cm/s.

temperature shift coefficients (< 4 ppb/K) of all NH groups in **2.18** and **2.21** are consistent with their relatively high cell permeabilities, and also with the prediction, based on computational studies and their structural similarity to compound **2.13**, that all amides in these compounds are protected from solvent (either through intramolecular hydrogen bonding or, in the case of L-Leu^4, by steric occlusion).[22] On the other hand, two of the temperature shift coefficients in **2.17** are greater than 4 ppb/K, consistent with the two solvent-exposed amides found in the solution NMR structure (in $CDCl_3$) of its congener, **2.14**, and also consistent with the relatively low cell permeabilities of both **2.14** and **2.17**. Thus, this screening/deconvolution approach not only independently identified the enantiomer of a scaffold known to have good membrane permeability, but it also suggests that the stereocenter at Leu^3 can be inverted without changing the backbone conformation or compromising permeability.

In both series of compounds discussed thus far, the tri-*N*-methylated scaffold of **2.4** and the non-*N*-methylated scaffolds of **2.18** and **2.21**, the major conformation-defining features are the overlapping β-turns that enforce two strong, transannular hydrogen bonds. In **2.4**, the other three solvent-exposed amide NH groups are N-methylated, whereas in **2.18**, two of the solvent-exposed amides are forced into extra-annular γ-turns, creating a bowl-shaped structure that orients the remaining free NH into the center of the bowl and away from solvent. Upon further deconvolution of the tri-*N*-methylated compounds from sub-library *6*, we were intrigued to find that among the most permeable compounds in one of the tier-2 sub-libraries were compounds corresponding to the consensus sequence cyclo[D-Pro^1 – L-MeLeu^2 – D-MeLeu^3 – D/L-MeLeu^4 – D/L-Leu^5 – L-Tyr^6] (Figure 2.4, purple

chromatogram), in which the two non-*N*-methylated residues were contiguous. Since this arrangement of *N*-Me and NH groups would appear to preclude the type of β-turn architecture found in **2.4**, **2.18**, and **2.21**, we set out to investigate this scaffold further by synthesizing and testing all eight permutations within the X^3 = D-MeLeu tier-2 sub-library. The two most cell permeable compounds in this series, **2.10** and **2.12**, differed only in the configuration at $MeLeu^4$, while the most- and least-permeable compounds, **2.10** and **2.9**, also differed by a single stereocenter at Leu^5 despite a 60-fold difference in Caco-2 permeabilities (Table 2.4).

We used a combination of computational and NMR approaches to investigate the underlying structural/conformational basis for the large variation in permeability among the closely related stereoisomeric series **2.9** – **2.12**. First, 2D ROESY NMR experiments (in the low dielectric solvent $CDCl_3$) of **2.12**, one of the two most permeable compounds in the series, revealed that the two contiguous, non-*N*-methylated residues enforce two overlapping, somewhat distorted γ-turns. Because of this distortion, neither of the amide NH groups in **2.12** are involved in a classic hydrogen bond.[34,35] The computationally predicted conformation of **2.12** was also consistent with its NMR structure, with a backbone RMSD of 0.27 Å between the two structures (Figure 2.7a). Indeed, while the four stereoisomers **2.9** – **2.12** were predicted to adopt very similar backbone conformations (average RMSD = 0.5 Å, Figure 2.7b), classically defined intramolecular hydrogen bonds were observed in only two of the compounds, **2.9** and **2.11** (as γ-turns between $MeLeu^4$ and Leu^5). Paradoxically, these compounds are the two *least* permeable compounds in the series, while neither of the most permeable compounds, **2.10** and **2.12**, showed any intramolecular hydrogen bonding. Nonetheless, in all four isomers, both NH groups point

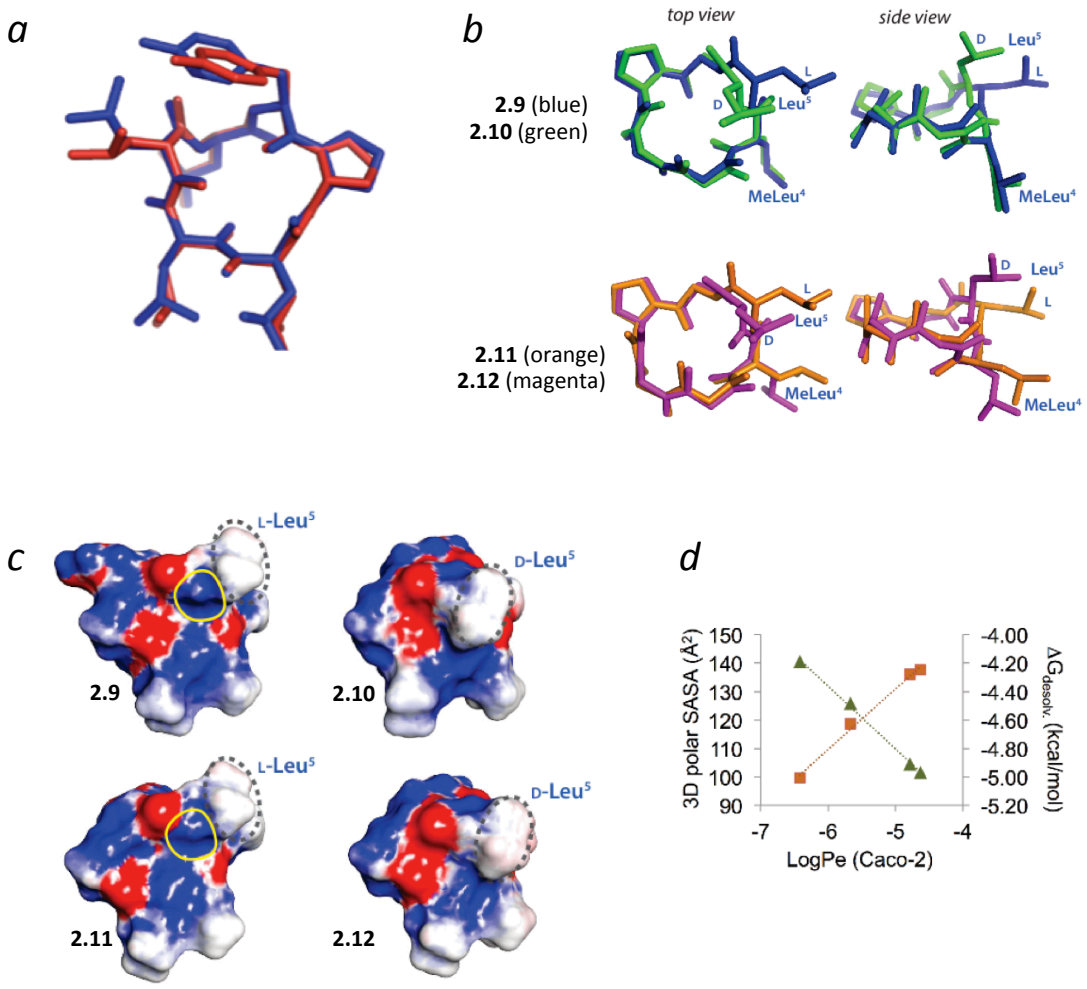

Figure 2.7. a) overlay of calculated (red) and solution NMR (blue) structures for compound **2.12**; b) Top and side views of compounds **2.9** (blue); **2.10** (green), **2.11** (orange), and **2.12** (magenta) overlaid (for clarity, only the side chains of residues MeLeu^4 and Leu^5 are shown); c) electrostatic surfaces (red = δ-, blue = δ+, white = neutral) of predicted low-dielectric conformers of **2.9** – **2.12** with the orientation of the Leu^5 side chains highlighted in grey dashed ovals. Outlined in yellow is the portion of the polar surface in **6.6** and **6.8** that is effectively masked by the D-Leu^5 side chains in **2.9** and **2.11**; d) plot of predicted desolvation energy (orange) and 3D polar SASA (green) vs. Caco-2 permeabilities of the four compounds.

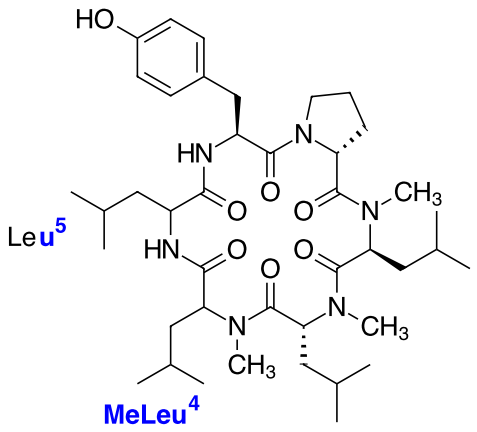

Table 2.4. Various experimental and calculated values for compounds **2.9** - **2.12**

Compound	Position MeLeu^4	Position Leu^5	P_e (× 10^{-6} cm/s)^a	Calc. ΔG_{desolv} (kcal/mol)	3D polar SASA (Å^2)	No. H-bonds^b
2.9	L	L	0.38	5.01	140.5	1
2.10	L	D	23.3	4.25	101.6	0
2.11	D	L	2.4	4.63	125.7	1
2.12	D	D	16.4	4.28	104.5	0

^{a}As measured by Caco-2 assay. ^{b}Refers to classical intramolecular hydrogen bonds as defined by ref. 34,35.

well into the interior of the macrocycle, shielding all of the amides from solvent, including those not involved in hydrogen bonds.

The cell permeabilities in **2.9** – **2.12** are most influenced by the configuration at Leu^5: In **2.10** and **2.12** the D-Leu^5 side chains project over the macrocycle center, while the L-Leu^5 side chains of **2.9** and **2.11** project away from the ring (Figure 2.7b). In contrast, permeabilities are much less sensitive to the configuration at MeLeu^4, where the side chains orient away from the macrocycle, irrespective of stereochemistry at that position. The different side chain orientations give rise to different calculated 3D solvent accessible surface areas (SASA), as the projection of the Leu^5 side chains in **2.10** and **2.12** over one face of the macrocycle partially shield its polar interior from solvent (Figure 2.7c). This variation

in 3D SASA (Table 2.4) in turn gives rise to corresponding differences in calculated desolvation energies (ΔG_{desolv}), and indeed both 3D SASA and ΔG_{desolv} are highly correlated with Caco-2 permeabilities in this set (Figure 2.7d). These results highlight the existence of "permeability cliffs" among closely related cyclic peptide scaffolds that differ only by relative stereochemistry, and also demonstrate that steric occlusion of polar groups from solvent can outweigh intramolecular hydrogen bonding in the relationship between structure and permeability in cyclic peptides.

Having discovered several cyclic peptides with measurable membrane permeability, we wanted to investigate whether one of these scaffolds could be diversified at the side chain level while retaining favorable membrane permeability. Therefore, we used our split-pool approach to generate side chain variants based on the permeable scaffold **2.21** and tested their permeabilities by PAMPA, including the parent scaffold as an internal control. Three new libraries were synthesized in which positions 3, 4 and 5 were varied among amino acids with a variety of side chain functionalities, including a basic residue (Orn), a hydrogen bond donor (Thr) and acceptor (4-Pal), and various nonpolar residues of natural and non-natural origin (Ala, Abu, Val, Phe, 2-Nal, and Cha) (Figure 2.8). In general, substitutions that led to a decrease in lipophilicity were detrimental to permeability, while those that retained or increased lipophilicity showed similar or improved permeability compared to the parent **2.21** (Figure 2.9). For the highly lipophilic substitution Nal, the variability in PAMPA values could be attributable to the low recovery, most likely due to solubility or aggregation issues. The permeability trends among the side chain variants were the same for each substituted position. These results suggest that diverse libraries

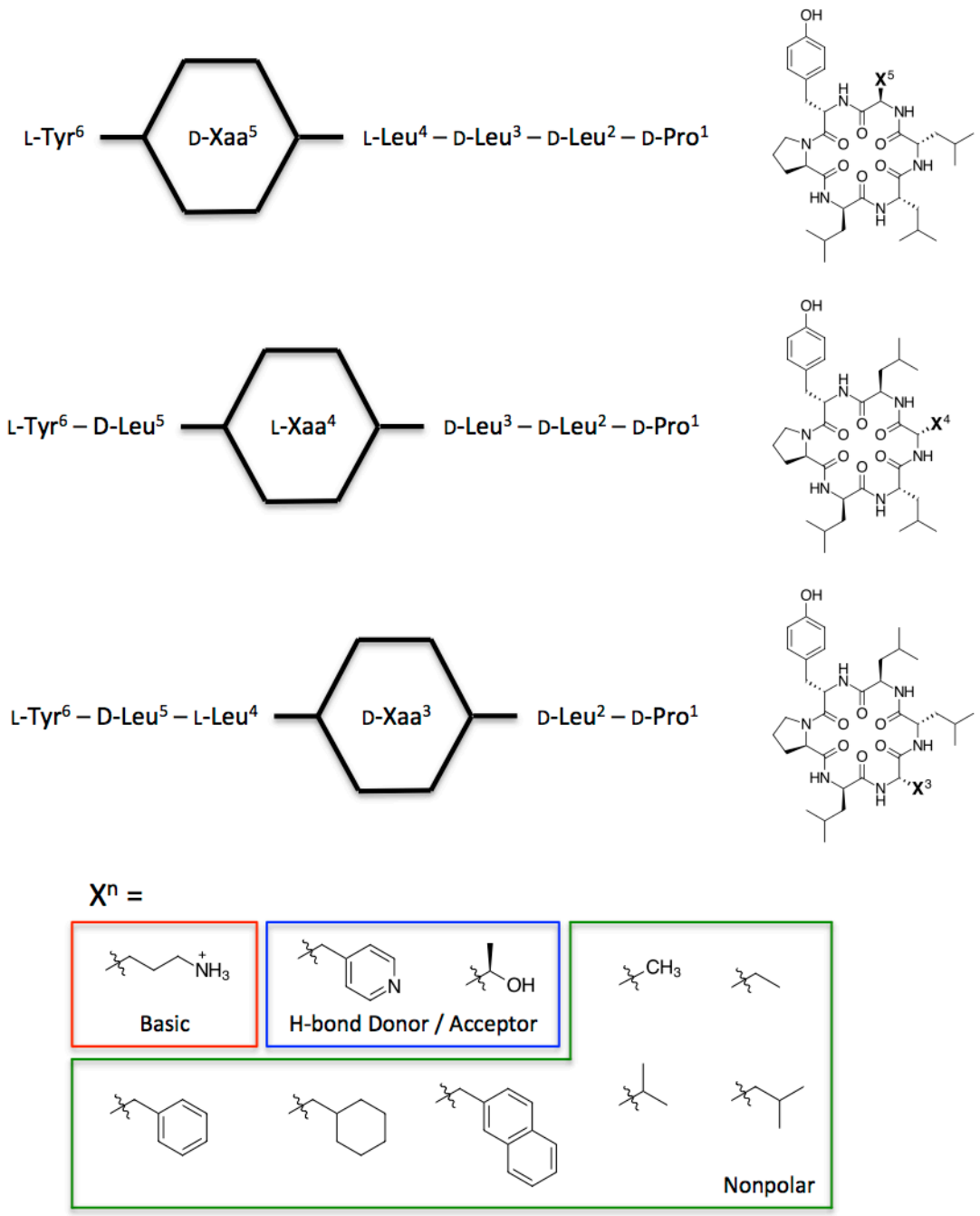

Figure 2.8. Design of single-point diversity (SPD) libraries based on **2.21**.

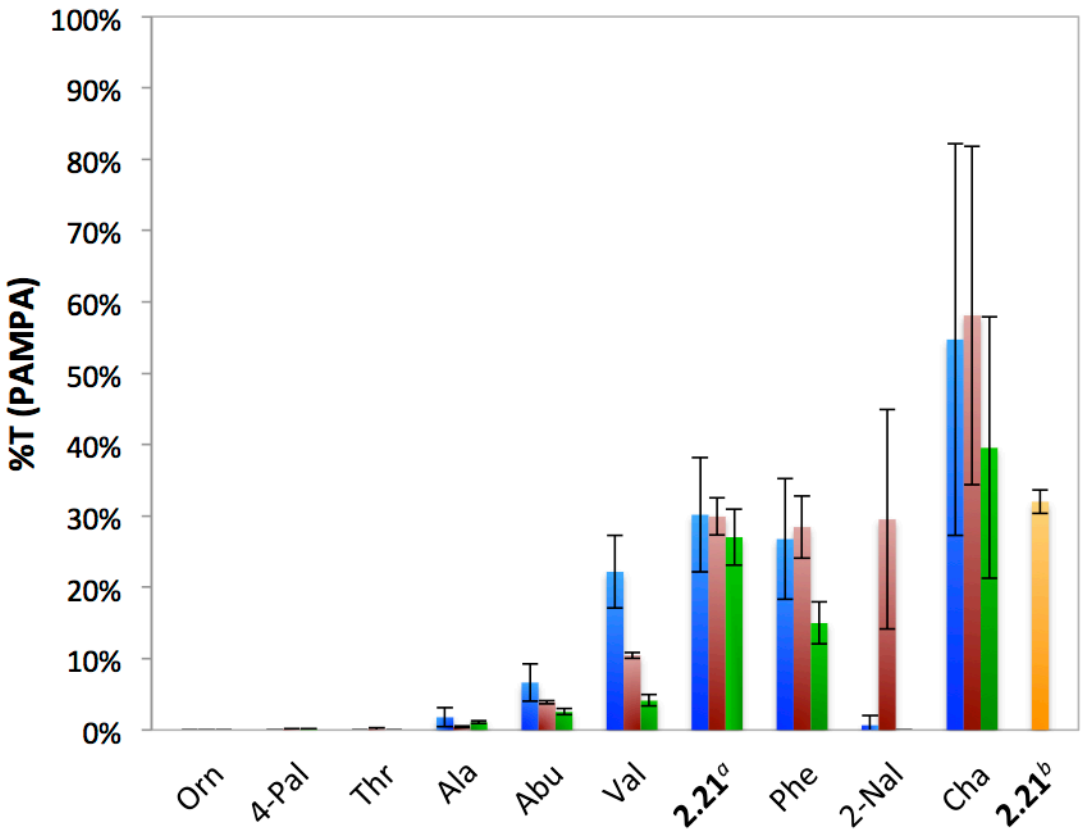

Figure 2.9. PAMPA permeability of Leu[3]Xaa (blue), Leu[4]Xaa (red), and Leu[5]Xaa (green) diversified analogs of compound **2.21** within split-pool single-point-diversity libraries. [a]Refers to compound **2.21** synthesized within each library. [b]Refers to the permeability of **2.21** as an external reference.

generated from side chain variants of permeable scaffolds such as **2.21** (e.g., for use as input into biochemical screens) can maintain the permeability of the parent scaffold at least within a reasonable lipophilicity window.[36]

Conclusion

We have described a combinatorial library/deconvolution approach to the discovery of cell permeable cyclic peptide scaffolds. The methodology reported here, based on the synthesis and direct permeability analysis of complex cyclic peptide mixtures, was validated

by the discovery of analogs of two cyclic peptides known to be passively permeable and, in one case, orally bioavailable. We have also found, consistent with studies in other systems,[31,37] that subtle factors such as side chain orientation can significantly impact permeability by sterically masking polar backbone atoms. Indeed, in our earlier studies on **2.13** and **2.14**, we found that the steric occlusion of backbone amides could be as effective as internal hydrogen bonding in increasing permeability,[22] which was corroborated by later computational studies demonstrating that intramolecular hydrogen bond counts are not as predictive of permeability as more quantitative descriptors such as 3D polar SASA.[21] However, to our knowledge this is the first example in which the relationship between stereochemistry and permeability has been specifically attributed to differences in side chain orientation. Our results also raise the question as to whether steric factors related to side chain positioning are also at play in the extraordinary permeability of other cyclic peptide natural products such as CSA.

Additionally, we have shown that the cell permeability of a particular scaffold can be maintained upon side chain substitution, which provides precedence towards the development of a permeability-biased library for biochemical screening based on side-chain variation of a particular permeable scaffold, provided that side chains are selected to maintain an appropriate level of lipophilicity. Variations on scaffold **2.21**, which is not *N*-methylated and has only a moderate Caco-2 permeability, suggest that any decrease in lipophilicity is detrimental to permeability in this scaffold. We predict that the same substitutions performed on more intrinsically permeable, *N*-methylated scaffolds such as **2.10**, will show a wider "lipophilicity window" within which permeability can be achieved. Work is now underway to further deconvolute the permeable species in the library reported

here, and to quantify in more detail the impact of side chain lipohilicity on permeability in the context of other scaffolds.

General Materials and Methods

Dry dichloromethane (DCM) and tetrahydrofuran (THF) were obtained from an activated alumina-based solvent purification system. *N*-Fluorenylmethyloxycarbonyl-*N*-methylamino acids were prepared according to literature procedures.[38] All other chemicals were purchased and used without further purification.

All HPLC/MS chromatograms were obtained on a Waters MicromassZQ mass spectrometer equipped with a Waters 1525 binary HPLC pump and a Waters 2998 photodiode array detector. To determine identity and purity, individually synthesized cyclic peptides were analyzed via reverse phase HPLC through a 3.5 µm C18 (XBridge, 50 mm x 4.6 mm) column at 1.2 mL/min eluting with acetonitrile (ACN) / water, with 0.1% formic acid.

All NMR spectra were recorded at 298 K in chloroform-*d* or dimethylsulfoxide-*d*6 on a 600-MHz Varian Inova spectrometer equipped with a 5-mm inverse detection probe. Spectra were referenced to residual solvent proton signals (^{1}H 7.26 for chloroform-*d*, 2.50 for dimethylsulfoxide-*d*6).

Synthesis of Pure Cyclic Hexapeptides

Cyclic peptides were synthesized starting with the allyl ester of *N*-fluorenylmethyloxycarbonyl (Fmoc)-protected tyrosine linked via the phenolic hydroxyl group to 2-chlorotrityl polystyrene resin (0.4 mmol/g loading value) according to published procedures.[39] The peptide sequences were synthesized and cyclized using an automated peptide synthesizer (Prelude, Protein Technologies). In general, couplings were performed using 4 eq Fmoc-protected amino acid, 3.8 eq O-(azabenzotriazol-1-yl)- *N*,*N*,*N*',*N*'-tetramethyluronium hexafluorophosphate (HATU) and 6 eq *N*,*N*-diisopropylethylamine

(DIPEA) in *N*,*N*-dimethylformamide (DMF, 0.1 M with respect to amino acid) for 1 h. Fmoc deprotections were carried out with 2% 1,8-diazabicycloundec-7-ene (DBU) and 2% piperidine in DMF for 15 min.

After each coupling and deprotection step, the resin was washed with DMF (3×), DCM (3×) and DMF (3×). After the addition of the final residue, deallylation and final Fmoc removal were performed simultaneously with a solution of 1 eq $Pd(Ph_3P)_4$ in THF containing 10% (v/v) piperidine for 3 h. A chelating wash was performed to remove traces of palladium using 5% (w/v) sodium diethyldithiocarbamate and 5% (v/v) DIPEA in DMF, followed by the normal DMF-DCM-DMF resin wash sequence. Cyclization was performed with 3 eq (Benzotriazol-1-yloxy)tripyrrolidinophosphonium hexafluorophosphate (PyBOP), 3 eq 1-hydroxy-7-azabenzotriazole (HOAt), and 6 eq DIPEA in DMF for 3 h, followed by resin washing with five final DCM washes to remove residual DMF. Peptides were cleaved following cyclization with a 5% (v/v) trifluoroacetic acid (TFA) in DCM solution. The filtrate was concentrated and the crude residue was then purified by reverse phase automated flash chromatography (Isolera Prime, Biotage) and lyophilized.

Synthesis of Cyclic Peptide Library

The 1,152-member cyclic hexapeptide library was synthesized using the "split-pool" strategy[25] (Figure 2.1b), starting with the allyl ester of *N*-fluorenylmethyloxycarbonyl (Fmoc)-protected tyrosine linked via the phenolic hydroxyl group to 2-chlorotrityl polystyrene resin (0.4 mmol/g loading value) according to published procedures.[39] Standard Fmoc / tBu SPPS techniques were utilized as outlined in the synthesis of pure cyclic hexapeptides. For the coupling of *N*-Fmoc-L-leucine, *N*-Fmoc-D-leucine, *N*-Fmoc-glycine, and

N-Fmoc-sarcosine, a coupling solution was prepared by dissolving 4 eq of the amino acid and 3.8 eq of HATU in DMF (0.2 M with respect to amino acid). DIPEA (6 eq) was added and the solution was allowed to preactivate for 30 min, then added to the deprotected resin.

For the coupling of *N*-Fmoc-*N*-methyl-L-leucine , *N*-Fmoc-*N*-methyl-D-leucine, *N*-Fmoc-L-proline, and *N*-Fmoc-D-proline, an acid chloride method[40] was adapted to ensure complete coupling of *N*-Fmoc-*N*-methyl amino acids onto free *N*-methylamines of the resin-bound peptide. In general, a coupling solution was prepared by dissolving 4 eq of the *N*-methylamino acid and 1.25 eq of bis(trichloromethyl)carbonate (BTC) in dry THF (0.2 M with respect to amino acid) and adding 6 eq of 2,6-lutidine. The solution was allowed to preactivate for 30 s, then immediately added to the deprotected resin (prewashed with THF 3x).

One gram of resin loaded with Fmoc-L-Tyr-OAllyl was segregated into four separate polypropylene SPPS vessels and deprotected for 30 min. The resin was washed with DMF (3x), MeOH (3x), DCM (3x), and DMF (3x), then coupled with either *N*-Fmoc-L-leucine, *N*-Fmoc-D-leucine, *N*-Fmoc-*N*-methyl-L-leucine, or *N*-Fmoc-*N*-methyl-D-leucine as outlined above. The resin was washed, pooled into a single vessel, thoroughly mixed, reapportioned into six separate SPPS vessels, and deprotected. Each portion of resin was washed, then coupled as before with either *N*-Fmoc-L-leucine, *N*-Fmoc-D-leucine, *N*-Fmoc-*N*-methyl-L-leucine, *N*-Fmoc-*N*-methyl-D-leucine, *N*-Fmoc-glycine, or *N*-Fmoc-sarcosine.

The resin was washed, pooled into a single vessel, thoroughly mixed, reapportioned into four separate SPPS vessels, and deprotected. Each portion of resin was washed, then coupled as before with either *N*-Fmoc-L-leucine, *N*-Fmoc-D-leucine, *N*-Fmoc-*N*-methyl-L-leucine, or *N*-Fmoc-*N*-methyl-D-leucine .

The resin was pooled into a single vessel, thoroughly mixed, reapportioned into six separate SPPS vessels, and deprotected. Each portion of resin was washed, then coupled as before with either *N*-Fmoc-L-leucine, *N*-Fmoc-D-leucine, *N*-Fmoc-*N*-methyl-L-leucine, *N*-Fmoc-*N*-methyl-D-leucine, *N*-Fmoc-glycine, or *N*-Fmoc-sarcosine.

Each portion of resin was washed and, without pooling, deprotected and divided into two vessels, then coupled with either *N*-Fmoc-L-proline or *N*-Fmoc-D-proline, providing a total of twelve vessels. After the final coupling, each portion of resin was washed and subjected to the simultaneous N/C-terminus deprotection. After deprotection, the resin was washed, cyclized as previously described, washed again, and cleaved with a 5% solution of TFA in DCM. The collected filtrates were concentrated and the residue redissolved in DMSO at a concentration of 100 mg/mL to give stock solutions of the twelve 96-member sublibraries.

Computational Analysis of Cyclic Peptide Library

Conformational prediction of cyclic peptides The computational method for modeling conformations of cyclic peptides has been described in detail previously.[21-23,41] Using PLOP in conjunction with the OPLS force field,[42,43] the protein-loop prediction algorithm, which employed a semi-exhaustive search in torsional space, was utilized here . The concept of this approach is to treat cyclic peptides as a closed protein loop without the protein. One of the amide bonds in the cyclic peptide is defined as an anchoring point and the rest of the molecule is treated as a protein loop. The loop prediction algorithm essentially considers the backbone of the cyclic peptides as linear with the anchoring amide as the mid-point. Via a systematic search of the backbone dihedral angles of the amino acid

Table 2.5. The input sequences of compound **2.10**, cyclo-[D-Pro, L-Me-Leu, D-Me-Leu, L-Me-Leu, L-Leu, L-Tyr], for conformational predictions using multiple sequence orders.

Calc. No.	Segment 1			Segment 2		
	Residue 1	Residue 2	Residue 3	Residue 4	Residue 5	Residue 6
1	D-Pro	L-MeLeu	D-MeLeu	L-MeLeu	D-Leu	L-Tyr
2	L-MeLeu	D-MeLeu	L-MeLeu	D-Leu	L-Tyr	D-Pro
3	D-MeLeu	L-MeLeu	D-Leu	L-Tyr	D-Pro	L-MeLeu
4	L-MeLeu	D-Leu	L-Tyr	D-Pro	L-MeLeu	D-MeLeu
5	D-Leu	L-Tyr	D-Pro	L-MeLeu	D-MeLeu	L-MeLeu
6	L-Tyr	D-Pro	L-MeLeu	D-MeLeu	L-MeLeu	D-Leu

segment on each side of the anchoring amide, the algorithm identifies conformations that will satisfy the loop closure condition. Side chains are subsequently built on these "cyclized" backbone conformations, followed by energy minimization of the whole molecule to determine favorable conformations.

To improve sampling, a multiple sequence orders approach was implemented in the current protocol in which *n* individual calculations were performed on a cyclic peptide with *n* amino acids. For example, as illustrated in Table 2.5, six individual calculations were performed on a cyclic hexapeptide and the results were combined to identify the lowest energy conformation and the corresponding low energy conformational ensemble. By allowing the loop to be built with amino acid segments of different combinations, this approach improves sampling efficiency, especially for those contain amino acids that can impose high strain on the molecule, such as proline and *N*-methyl amino acids. The membrane environment was represented by an implicit solvent model of chloroform.

NMR Solution Structure Generation for Compound 2.12

A 2D ROESY spectrum of compound **2.12** was obtained at 298K in chloroform-*d* with a mixing time of 200 ms, which was in the linear range in cross-relaxation ROESY buildup curve as determined by performing separate ROESY experiment mixing times of 75, 150, 200, 300, and 500 ms. The crosspeaks were integrated and normalized to their respective diagonal signal, and the peak volumes were converted to atomic distances using the initial rate approximation and a calibration distance between Pro-γ geminal protons of 1.76 Å (Table 2.6). Neither of the amide NH resonances were sharp enough to obtain reliable HN-Hα *J*-coupling values for calculating dihedral restraints.

To determine the solution structure of **2.12**, we used the NMR analysis of molecular flexibility in solution (NAMFIS) strategy,[44,45] as implemented in the "distribution of solution conformations" (DISCON) algorithm[46,47] using the Janocchio program interface.[48] Broadly, rather than using distance-restrained molecular dynamics or distance geometry calculations to arrive at a single conformer (or family of related conformers) that best fits the NOE/ROE data, NAMFIS uses a least-squares approach to determine a mole fraction-weighted ensemble that best fits the NMR data. To obtain starting conformations for input into DISCON, the Nanoscale Molecular Dynamics (NAMD) protocol[49] was used, beginning with an arbitrary conformation, to generate a diverse family of minimized conformers. We used the CHARMM forcefield with MMFF94 partial charge estimation for the molecular dynamics (MD) simulation, which was carried out for 1 ns at 2000˚ K with a 1 fs time step. Snapshots were saved every 5 ps, leading to an ensemble of 200 snapshots. The resulting high temperature snapshots were energy minimized using the generalized Born implicit solvent model with a dielectric of 4. The 100 snapshots with the lowest CHARMM energies were

Table 2.6. ROESY Correlations Used for Solution Structure Generation

Atom 1[a]	Atom 2	Experimental Atomic Distance (Å)[b]	Predicted Atomic Distance (Å)	Difference
3	2	2.43	2.72	0.29
3	8	3.09	2.77	0.32
10	8	2.64	2.48	0.16
15	10	2.85	2.98	0.13
17	15	3.08	3.31	0.23
15	22	3.11	3.76	0.65
17	18	2.80	2.61	0.19
17	22	2.13	2.72	0.59
15	18	2.46	3.85	1.39
17	19	2.91	3.16	0.25
18	19	2.58	2.71	0.13
22	19	3.48	3.55	0.07
22	18	4.69	4.69	0.00
22	24	2.42	2.77	0.35
22	8	5.50	4.74	0.76
31	36	3.29	4.05	0.76
36	38	2.35	2.63	0.28
38	39a	3.59	2.36	1.23
38	39b	3.78	3.02	0.76
39b	41b	3.05	2.98	0.07
40a	41a	2.43	2.35	0.08
40a	41b	3.20	3.03	0.17
40a	38	3.74	2.96	0.78
41a	39a	3.00	4.14	1.14
41a	39b	3.30	3.90	0.60
41b	41a	1.76	1.78	0.02
41a	2	2.22	2.32	0.10
5	10	4.43	4.56	0.13
5	41a	4.40	3.51	0.89
5	3	2.35	2.72	0.37
6	2	4.00	5.15	1.15
17	6	5.73	6.67	0.94
6	41a	4.80	6.06	1.26
6	3	4.23	4.96	0.73

[a]See Figure 2.10. [b]Calculated using the initial rate approximation and an internal calibration distance between geminal γ-CH_2 hydrogens of Pro as 1.76 Å.

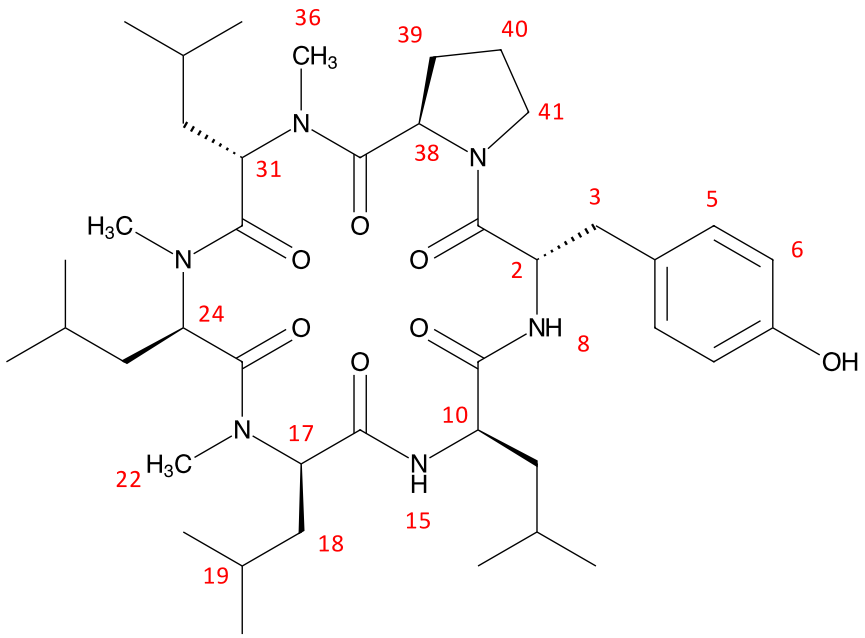

Figure 2.10. Structure and atomic numbering for compound **2.12**

taken forward into the DISCON calculations. We have found that these MD parameters adequately sample conformational space in cyclic hexapeptides with multiple *N*-methyl groups and are able to recapitulate the independently calculated NMR solution structures of well studied cyclic peptides such as **2.3**,[23] including the ability to sample all *N*-Me and Pro cis-trans rotamers. The resulting energy-minimized conformers were used as input into the DISCON protocol (using the ROESY crosspeak volumes to provide experimental distances) for 5000 iterations at a cluster level of 10 (Table 2.6). The best fit (in terms of the fewest ROE violations) was obtained with a single conformer (Figure 2.11a), which was in the

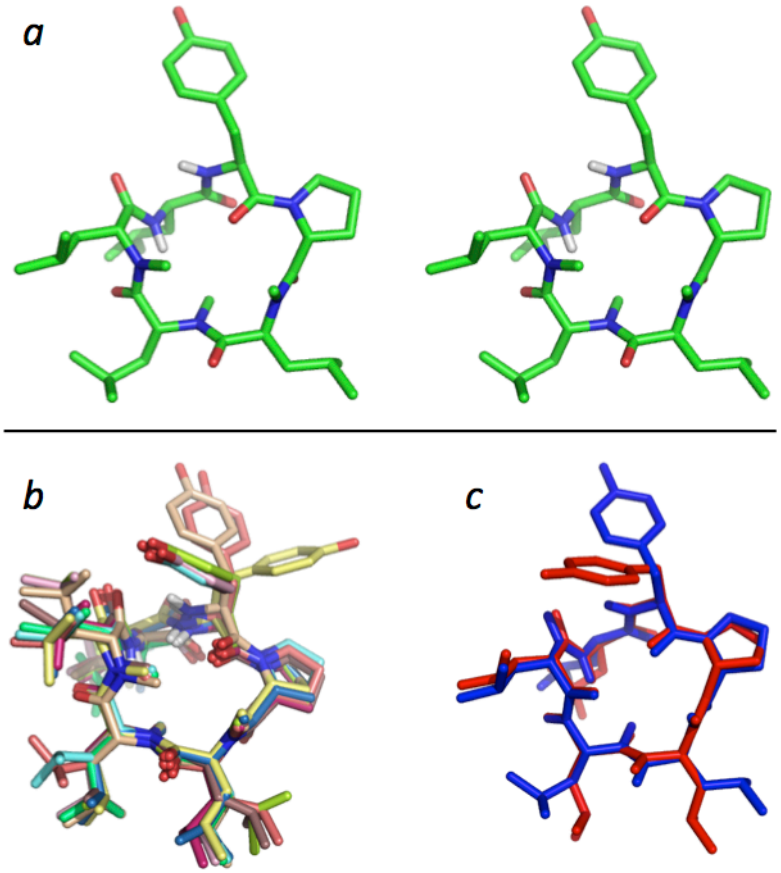

Figure 2.11. a) Stereoview of the NMR solution structure for **2.12**. b) The 10 lowest-energy conformers from the high temperature molecular dynamics run. c) Backbone overlay of the NMR solution structure and the independendly generated computational low dielectric conformation.

bottom 10th percentile of the 100 MD-derived conformers in terms of CHARMM energy. All the 10 lowest-energy conformers from the MD run, including the DISCON-derived conformer, had virtually identical backbone conformations (Figure 2.11b). Thus, the NMR-derived solution structure of **2.12** also represents the lowest energy conformer family derived from the CHARMM-minimized high-temperature MD snapshots. This conformation also had a nearly identical backbone conformation (within 0.2 Å RMSD) to the

independently calculated low energy conformer of **2.12** using the PLOP-directed conformational search algorithm implementing the OPLS forcefield (Figure 2.11c).

Permeability Analysis of Cyclic Peptide Mixtures by PAMPA

A 96-well donor plate with 0.45 µ hydrophobic Immobilon-P membrane supports (Millipore) and a 96-well Teflon acceptor plate were used in the PAMPA permeability test. The acceptor plate was prepared by adding 300 µL of 5% DMSO in pH=7.4 phosphate-buffered saline (PBS) to each well. Donor well solutions of the cyclic peptide libraries were prepared by diluting 10 µL of the DMSO stock solutions prepared above to a final volume of 200 µL with PBS. A 1% (w/v) solution of lecithin in dodecane was prepared and sonicated before use. 5 µL of the dodecane / lecithin solution was carefully applied to the membrane supports in the wells of the donor plate, with care being taken to not touch the pipet tip to the membrane. Without allowing this solution to evaporate, 150 µL of the peptide solutions were added to the donor wells. The donor plate was then placed on top of the acceptor plate so that the artificial membrane was in contact with the buffer solution below. A lid was placed on the donor well, and the system was covered with a glass evaporating dish and left overnight (18 h) at room temperature. A wet paper towel was placed on the inside of the chamber to prevent evaporation.

Donor well solutions before (t = 0 h) and after (t = 18 h) PAMPA as well as acceptor well solutions after PAMPA were diluted in acetonitrile (1:1) and were analyzed by LCMS (Waters Micromass ZQ) through a 5 µm C18 column (Alltech, 150 mm x 4.6 mm) using selected ion monitoring (SIM) mode. Selected peaks present in acceptor well chromatograms were then chosen for deconvolution and resynthesis.

Direct Inject Mass Spectrum of Sublibrary 1

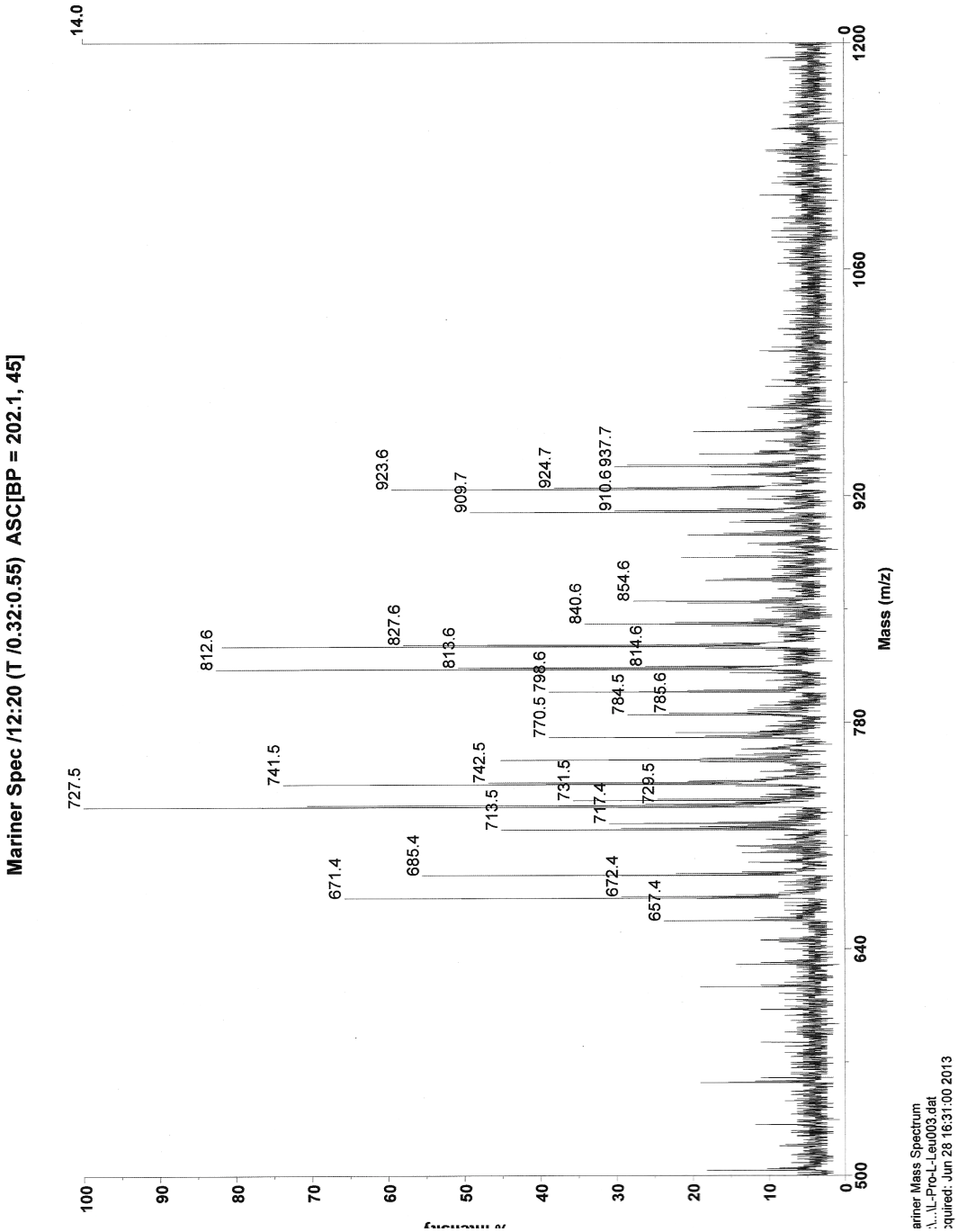

Direct Inject Mass Spectrum of Sublibrary 2

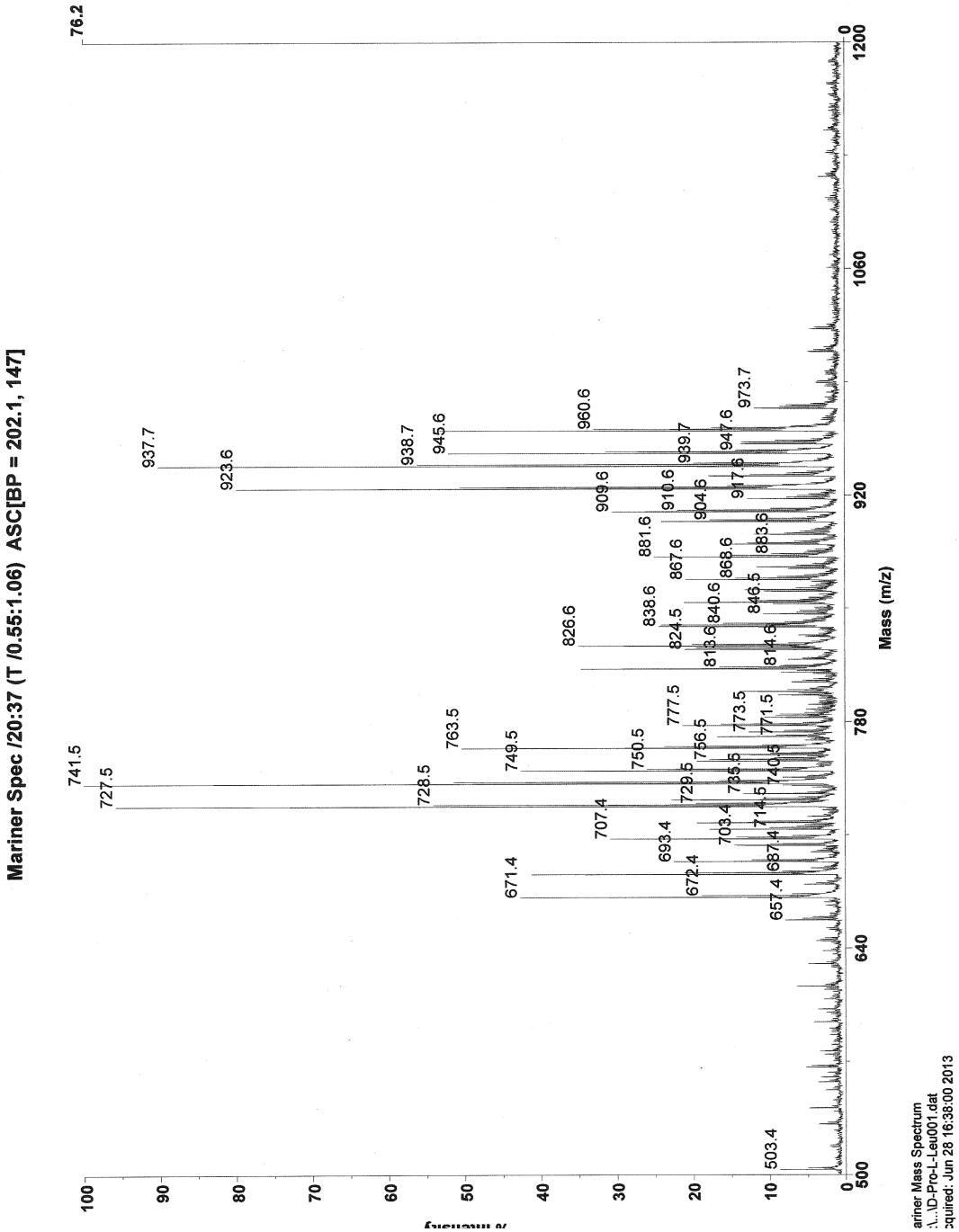

Direct Inject Mass Spectrum of Sublibrary 3

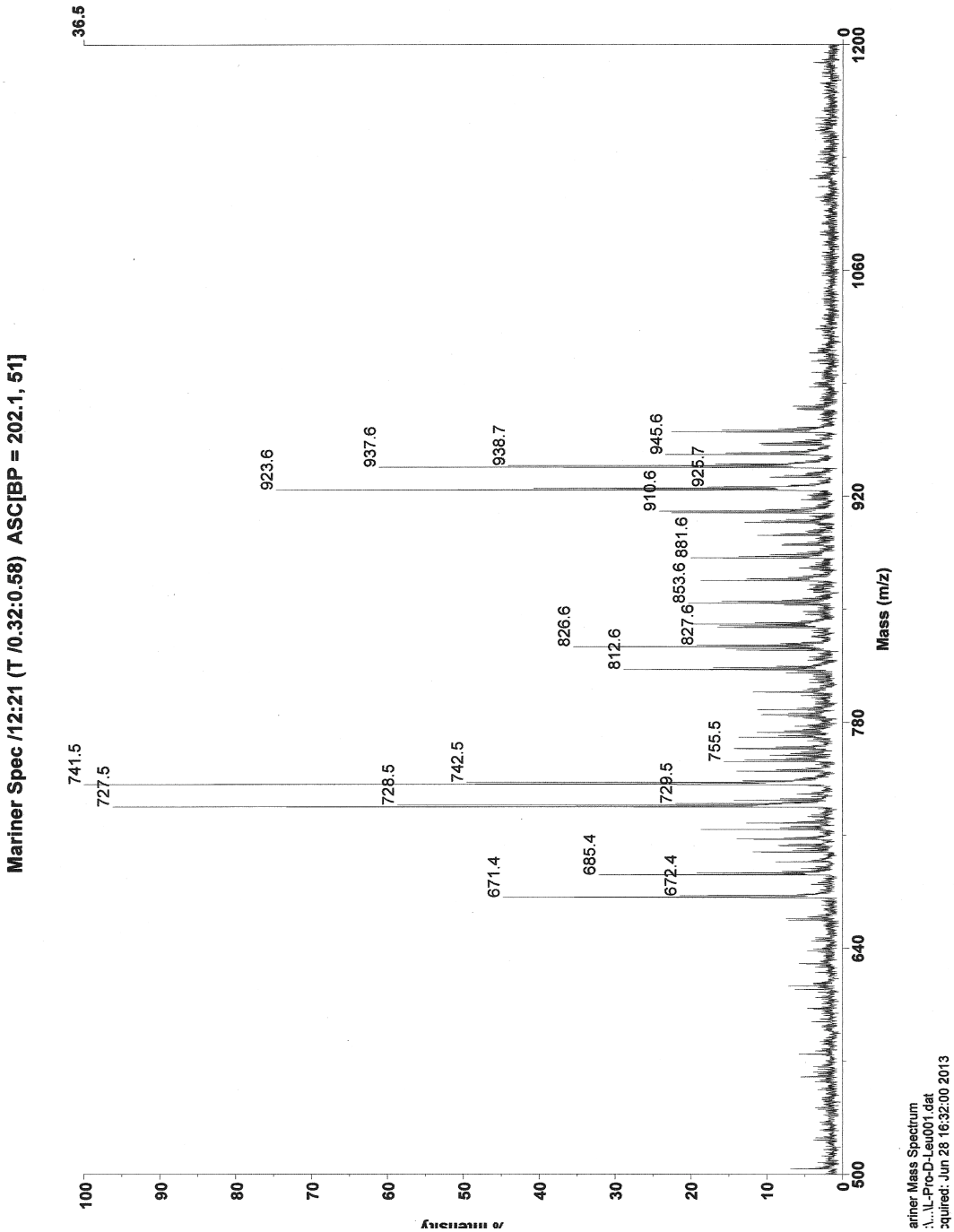

Direct Inject Mass Spectrum of Sublibrary 4

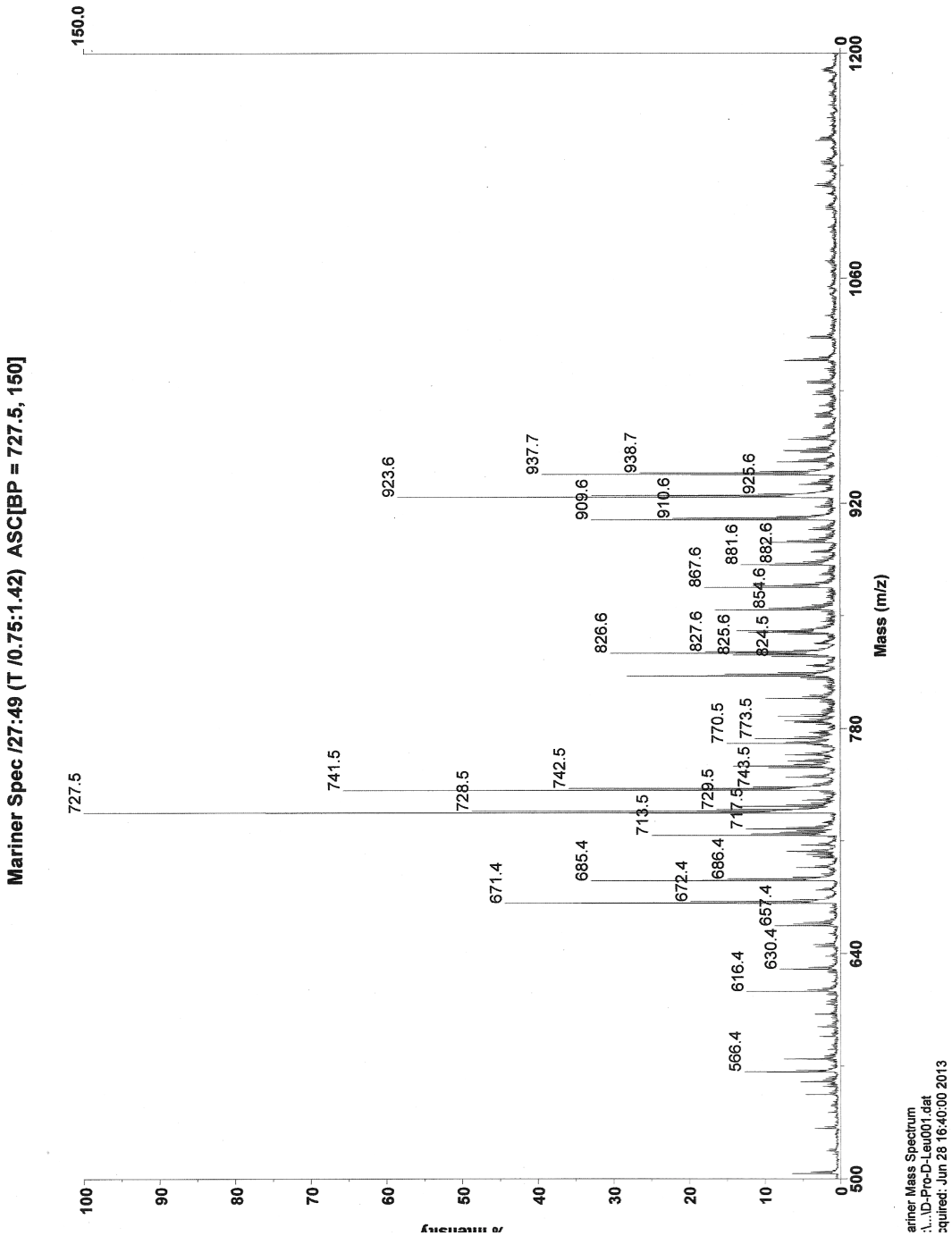

Direct Inject Mass Spectrum of Sublibrary 5

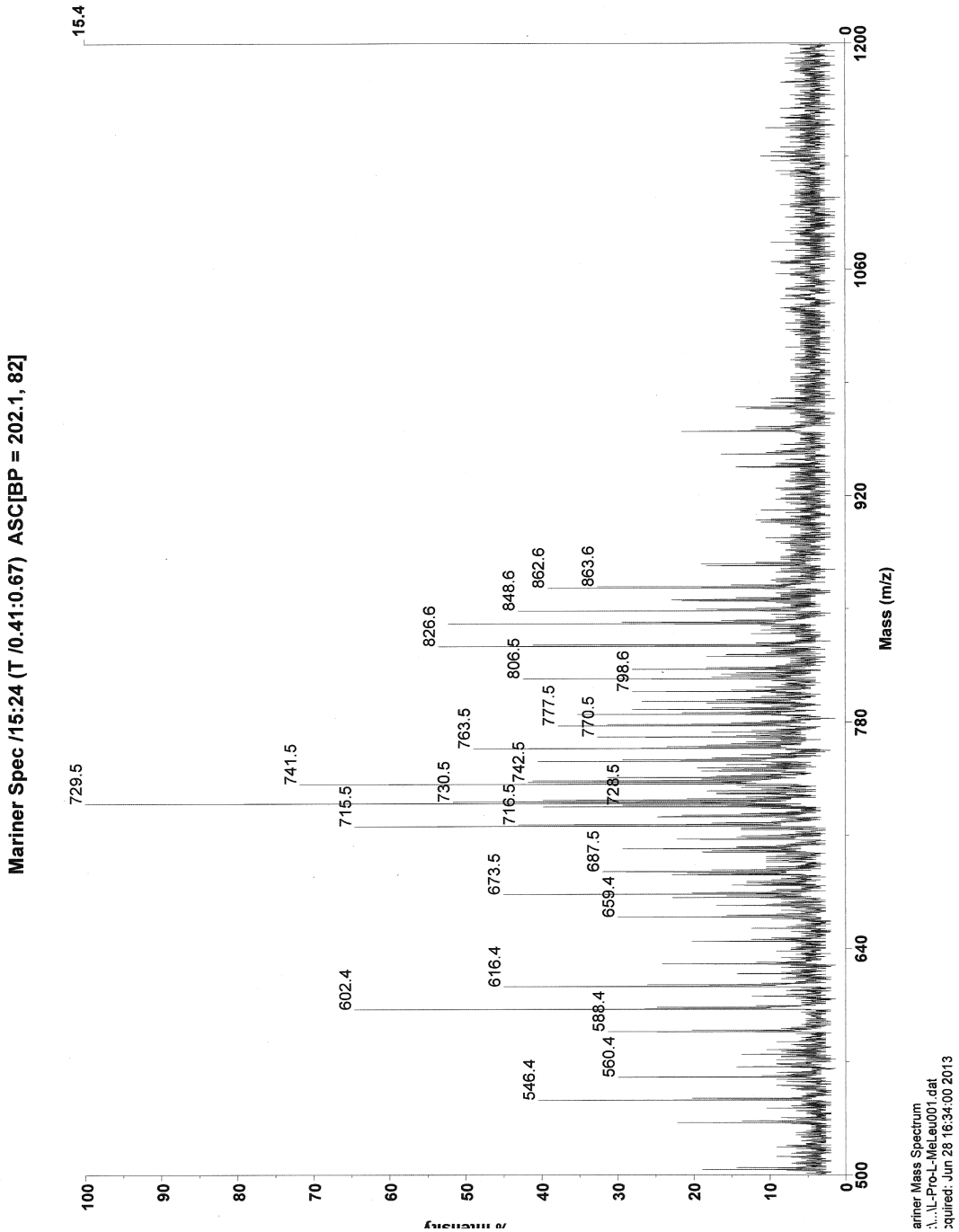

Direct Inject Mass Spectrum of Sublibrary 6

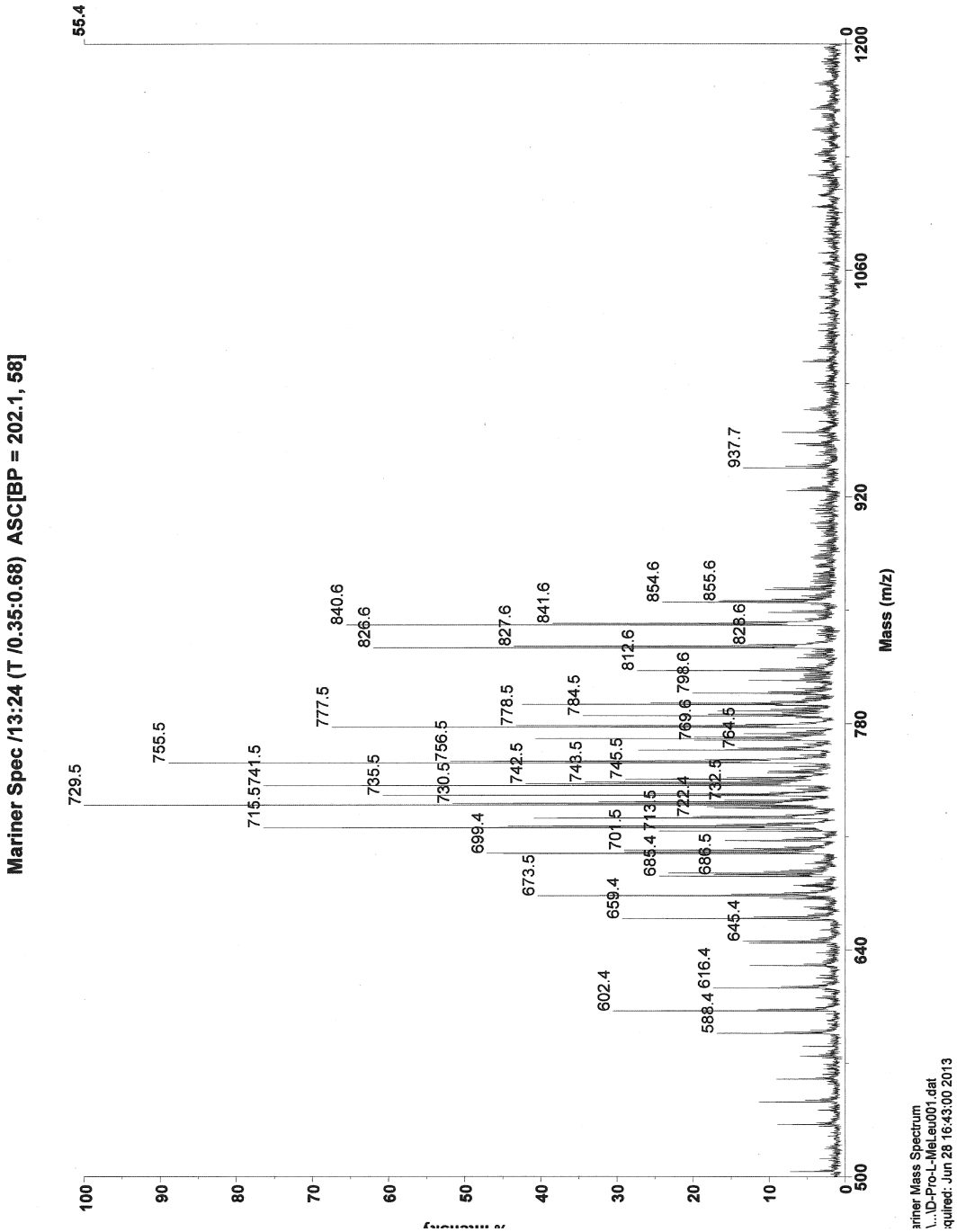

Direct Inject Mass Spectrum of Sublibrary 7

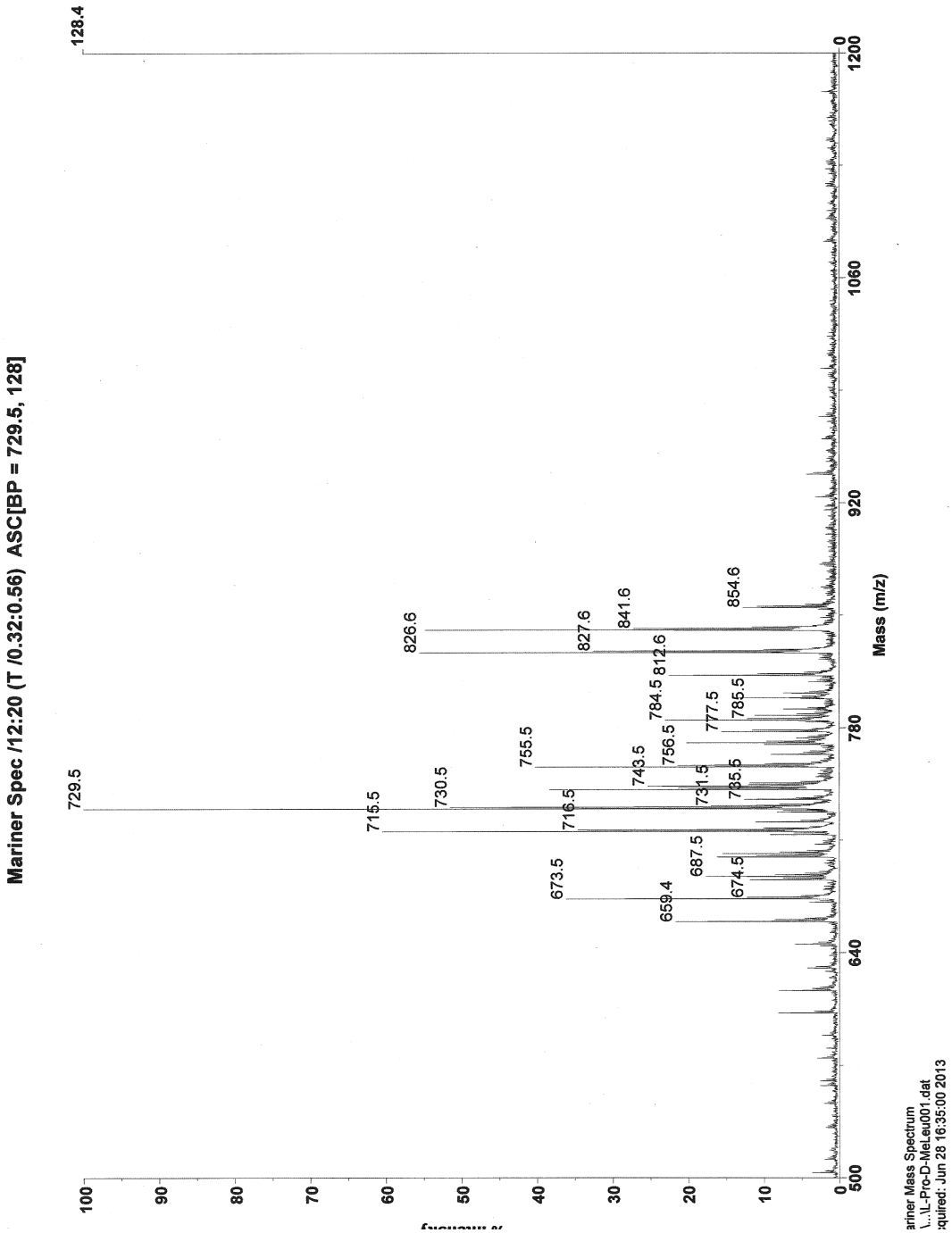

Direct Inject Mass Spectrum of Sublibrary 8

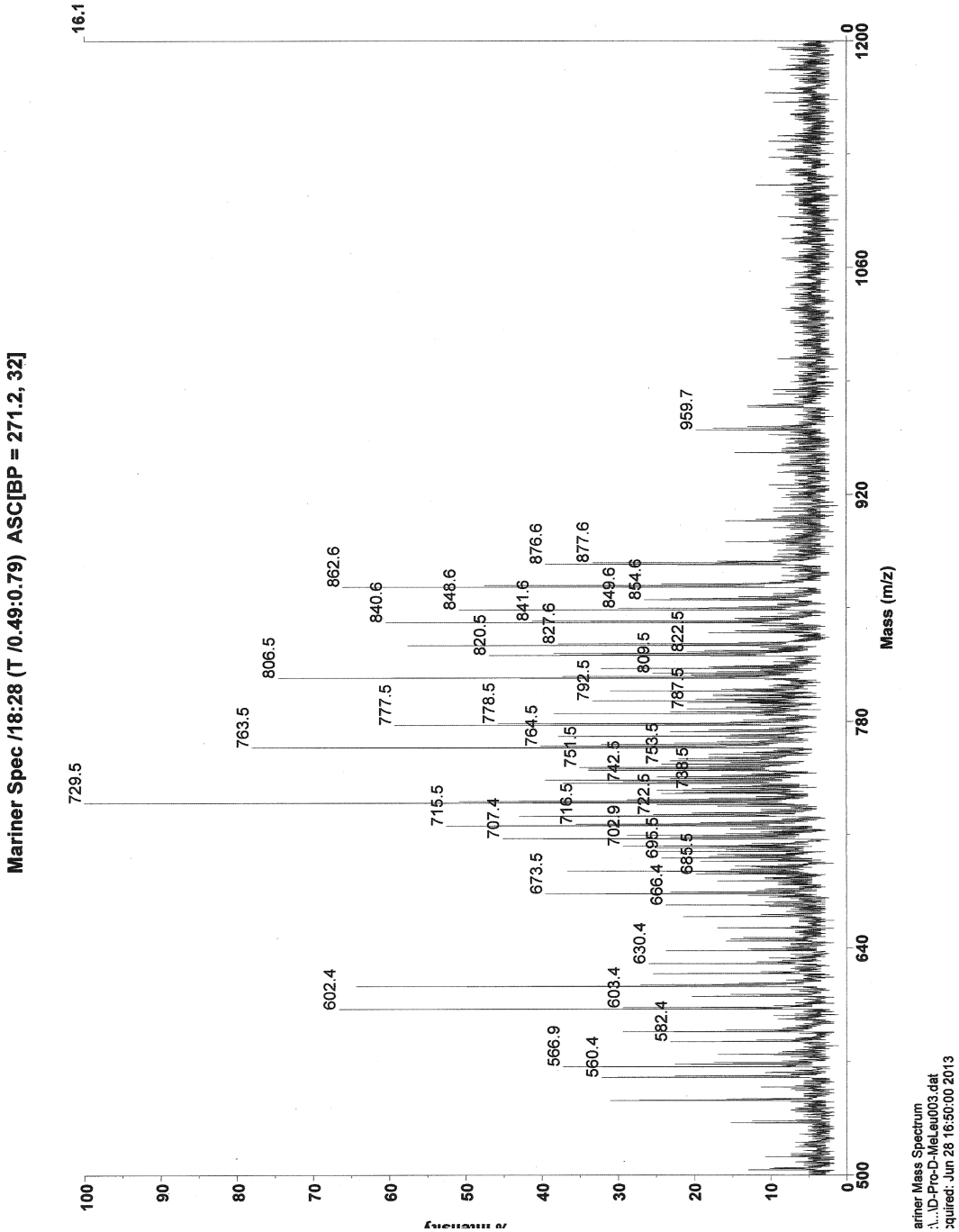

Direct Inject Mass Spectrum of Sublibrary 9

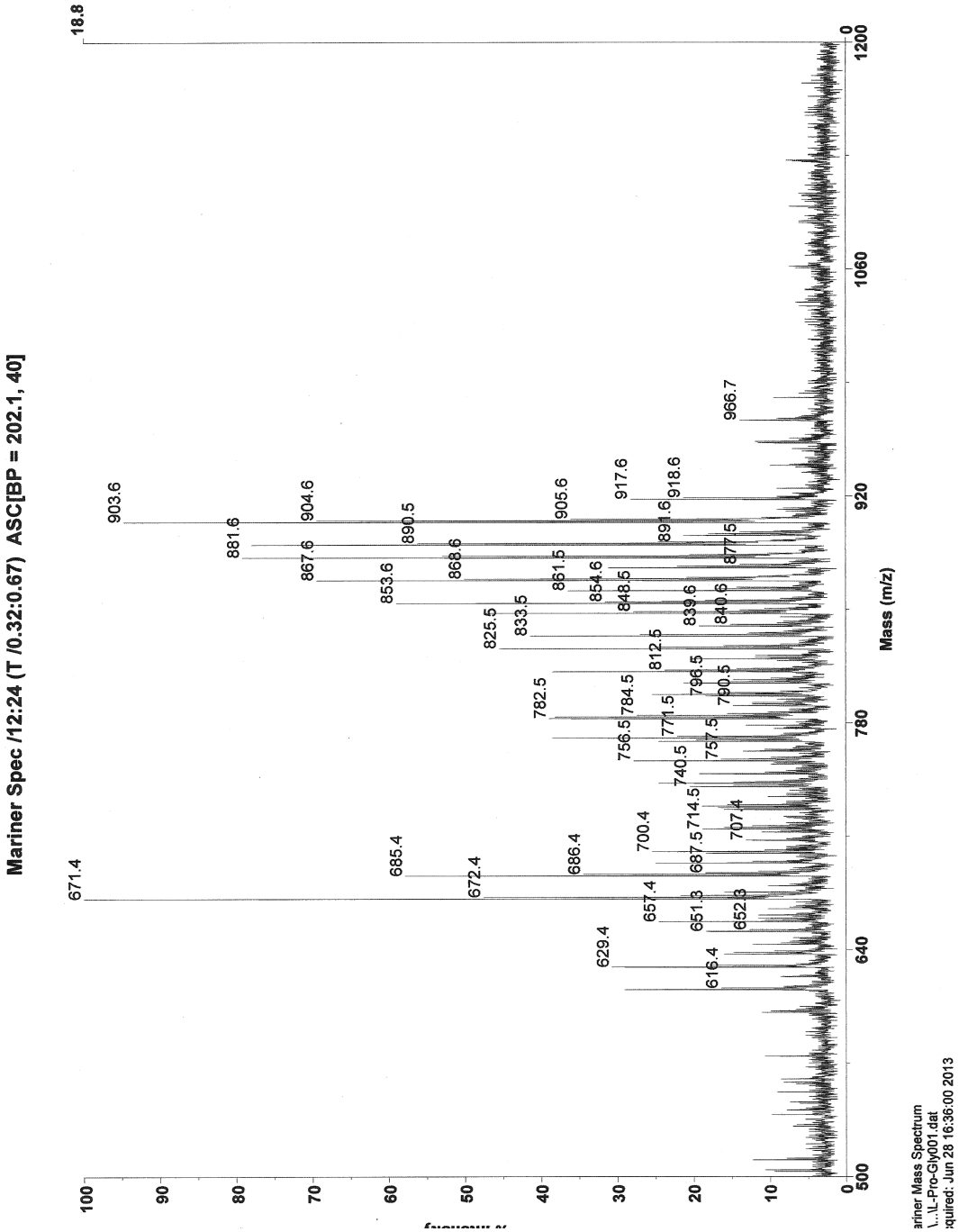

Direct Inject Mass Spectrum of Sublibrary 10

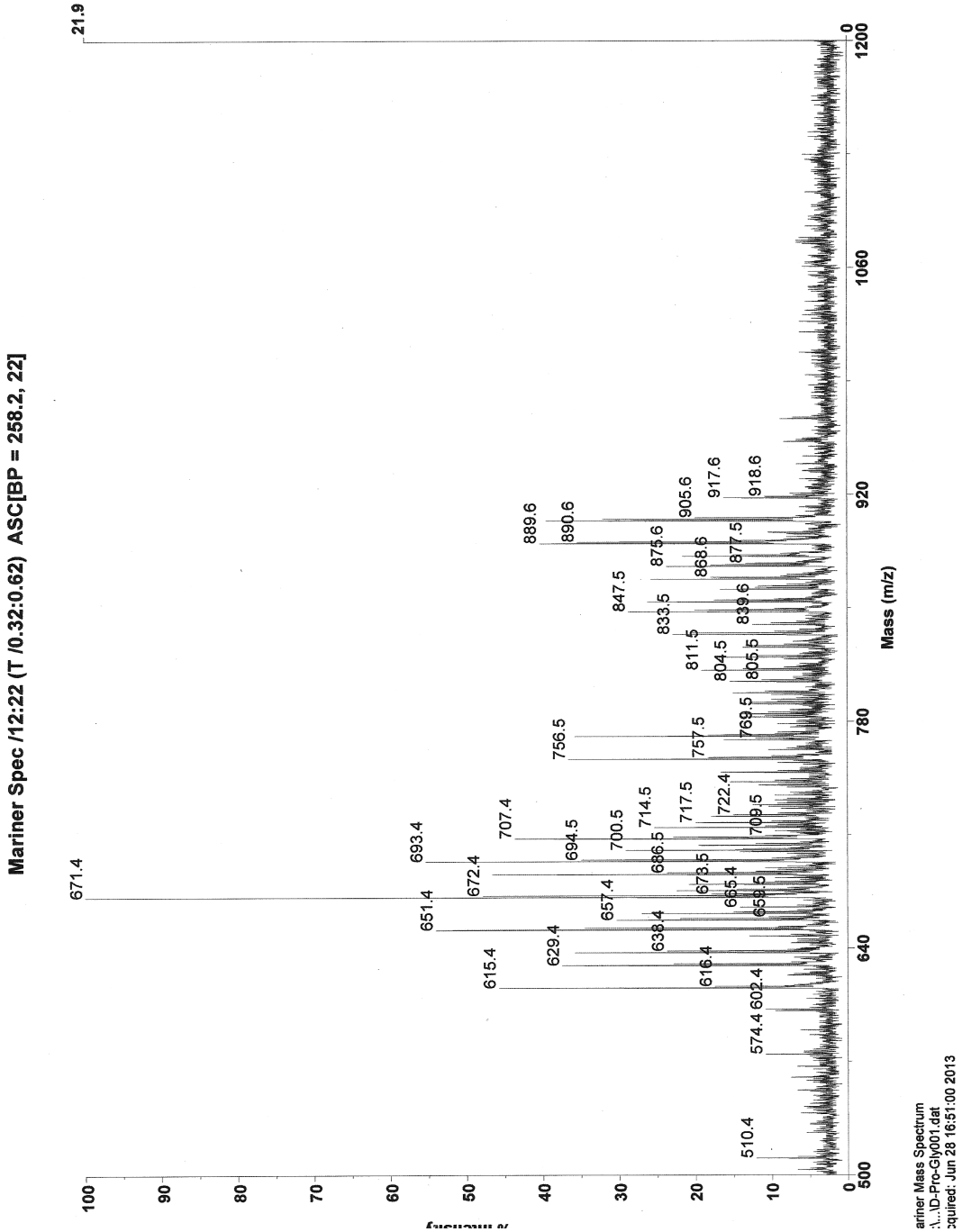

Direct Inject Mass Spectrum of Sublibrary 11

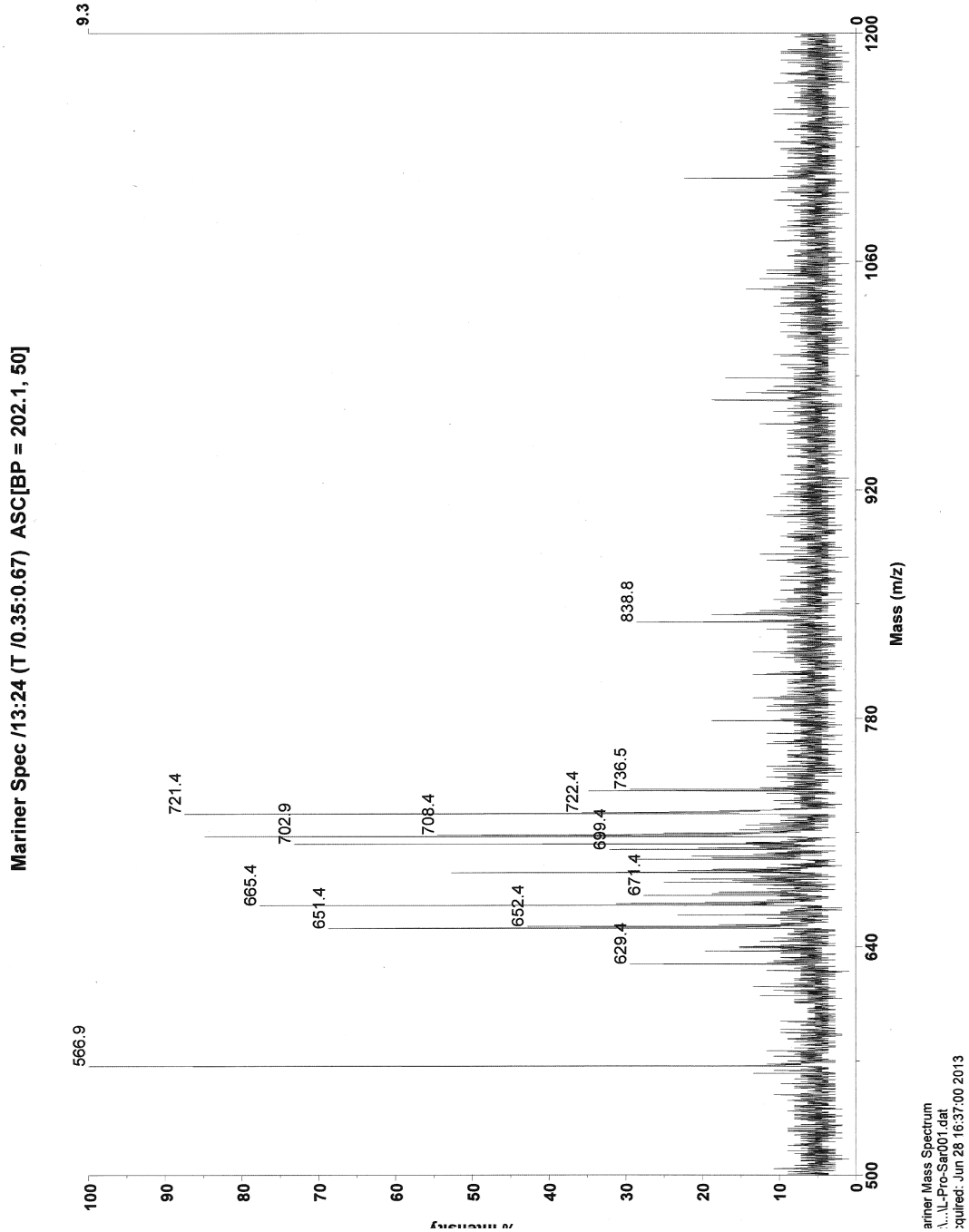

Direct Inject Mass Spectrum of Sublibrary 12

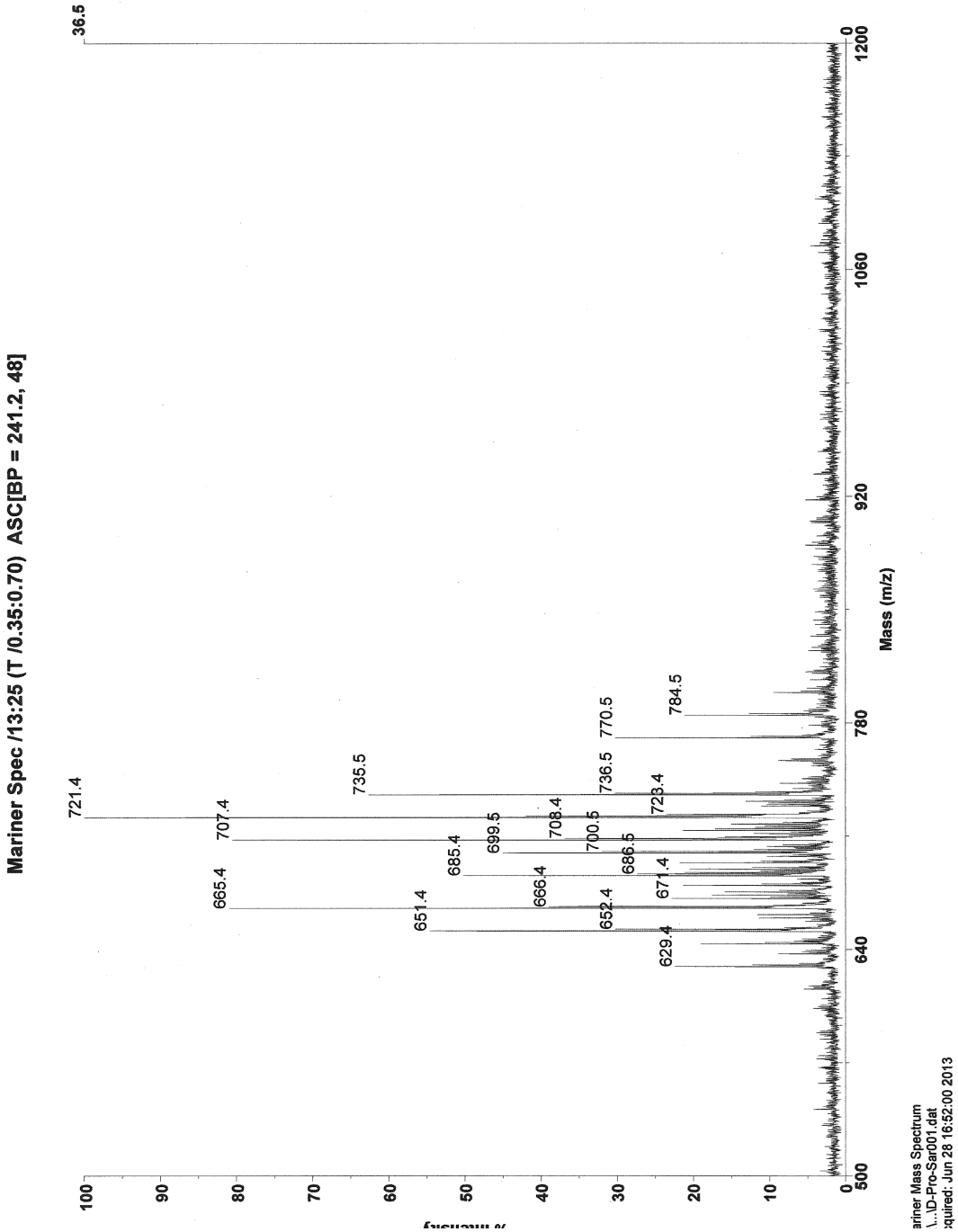

Table 2.7. Expected Masses and Relative Ratios for Pro-Leu-$(Xaa)_3$-Tyr Sublibraries (**1**-**4**)

Amino Acid Composition			Expected *m/z*				No.	Relative
			Cyclic Peptide		Linear[b]	Pyrrolidide[c]		
No. Leu	No. Gly[a]	No. *N*-Me	$(M+H)^+$	$(M+Na)^+$	$(M+H)^+$	$(M+H)^+$	Isomers	Ratio
3	1	0	657.4	679.4	675.4	728.5	4	1
3	1	1	671.4	693.4	689.4	742.5	12	3
3	1	2	685.4	707.4	703.4	756.5	12	3
3	1	3	699.4	721.4	717.4	770.5	4	1
4	0	0	713.5	735.5	731.5	784.6	8	2
4	0	1	727.5	749.5	745.5	798.6	24	6
4	0	2	741.5	763.5	759.5	812.6	24	6
4	0	3	755.5	777.5	773.5	826.6	8	2

Table 2.8. Expected Masses and Relative Ratios for Pro-MeLeu-$(Xaa)_3$-Tyr Sublibraries (**5**-**8**)

Amino Acid Composition			Expected *m/z* (M+H)				No.	Relative
			Cyclic Peptide		Linear[b]	Pyrrolidide[c]		
No. Leu	No. Gly[a]	No. *N*-Me	$(M+H)^+$	$(M+Na)^+$	$(M+H)^+$	$(M+H)^+$	Isomers	Ratio
3	1	1	671.4	693.4	689.4	742.5	4	1
3	1	2	685.4	707.4	703.4	756.5	12	3
3	1	3	699.4	721.4	717.4	770.5	12	3
3	1	4	713.5	735.5	731.5	784.6	4	1
4	0	1	727.5	749.5	745.5	798.6	8	2
4	0	2	741.5	763.5	759.5	812.6	24	6
4	0	3	755.5	777.5	773.5	826.6	24	6
4	0	4	769.5	791.5	787.5	840.6	8	2

Table 2.9. Expected Masses and Relative Ratios for Pro-Gly-$(Xaa)_3$-Tyr Sublibraries (**9**-**10**)

Amino Acid Composition			Expected *m/z*				No.	Relative
			Cyclic Peptide		Linear[b]	Pyrrolidide[c]		
No. Leu	No. Gly[a]	No. *N*-Me	$(M+H)^+$	$(M+Na)^+$	$(M+H)^+$	$(M+H)^+$	Isomers	Ratio
2	2	0	601.3	623.3	619.3	672.4	4	1
2	2	1	615.4	637.4	633.4	686.5	12	3
2	2	2	629.4	651.4	647.4	700.5	12	3
2	2	3	643.4	665.4	661.4	714.5	4	1
3	1	0	657.4	679.4	675.4	728.5	4	2
3	1	1	671.4	693.4	689.4	742.5	12	6
3	1	2	685.4	707.4	703.4	756.5	12	6
3	1	3	699.4	721.4	717.4	770.5	4	2

Table 2.10. Expected Masses and Relative Ratios for Pro-Sar-$(Xaa)_3$-Tyr Sublibraries (**11**-**12**)

Amino Acid Composition			Expected *m/z*				No.	Relative
			Cyclic Peptide		Linear[b]	Pyrrolidide[c]		
No. Leu	No. Gly[a]	No. *N*-Me	$(M+H)^+$	$(M+Na)^+$	$(M+H)^+$	$(M+H)^+$	Isomers	Ratio
2	2	1	615.4	637.4	633.4	686.5	4	1
2	2	2	629.4	651.4	647.4	700.5	12	3
2	2	3	643.4	665.4	661.4	714.5	12	3
2	2	4	657.4	679.4	675.4	728.5	4	1
3	1	1	671.4	693.4	689.4	742.5	4	2
3	1	2	685.4	707.4	703.4	756.5	12	6
3	1	3	699.4	721.4	717.4	770.5	12	6
3	1	4	713.5	735.5	731.5	784.6	4	2

[a]For purpose of clarity, sarcosine is classified as *N*-methylglycine in this table. [b]Resulting from inefficient cyclization. [c]Resulting from c-terminal coupling of linear peptide with pyrrolidine.

Sublibrary 1 Donor Well (t = 0 h)

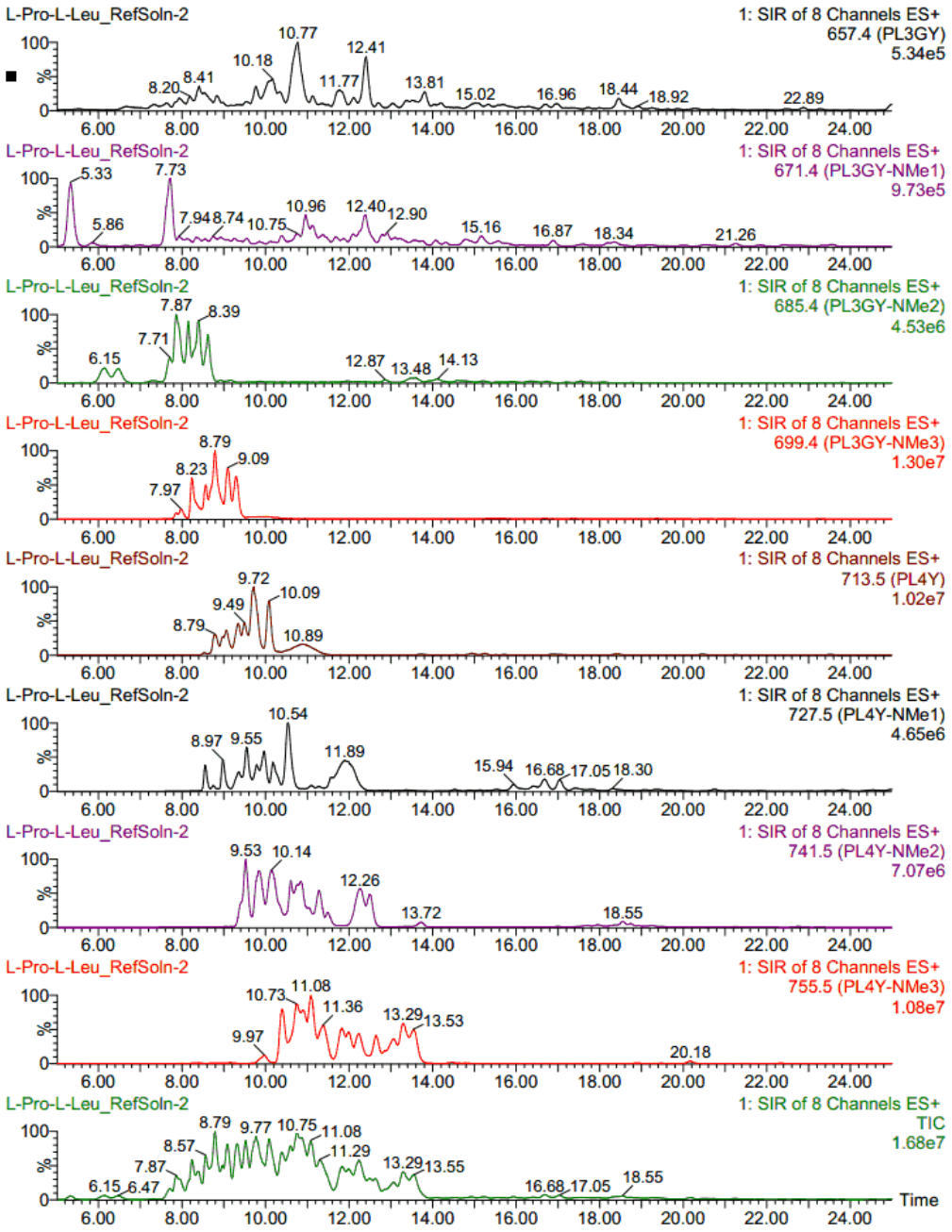

Sublibrary 1 Acceptor Well (t = 18 h)

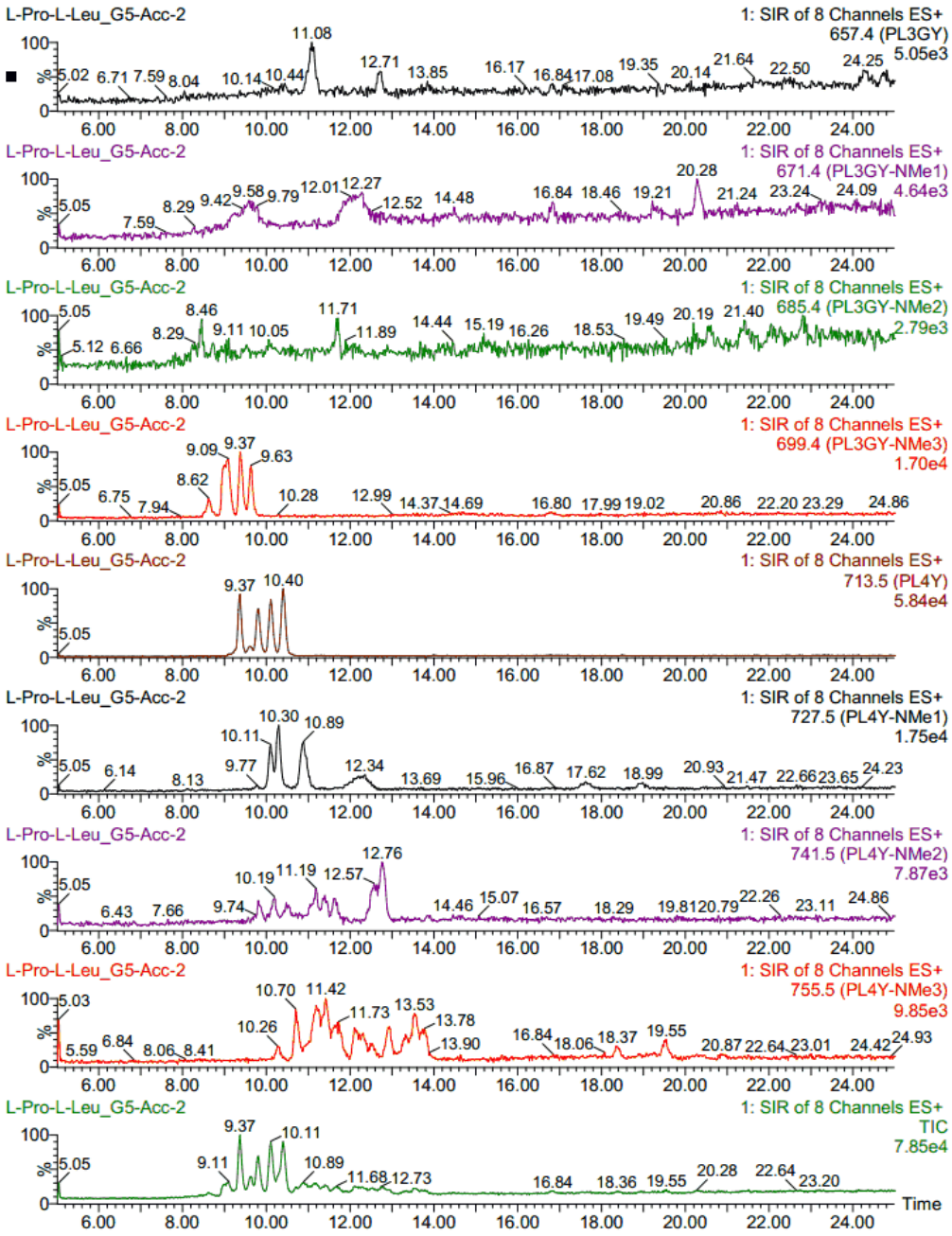

Sublibrary 1 Blank

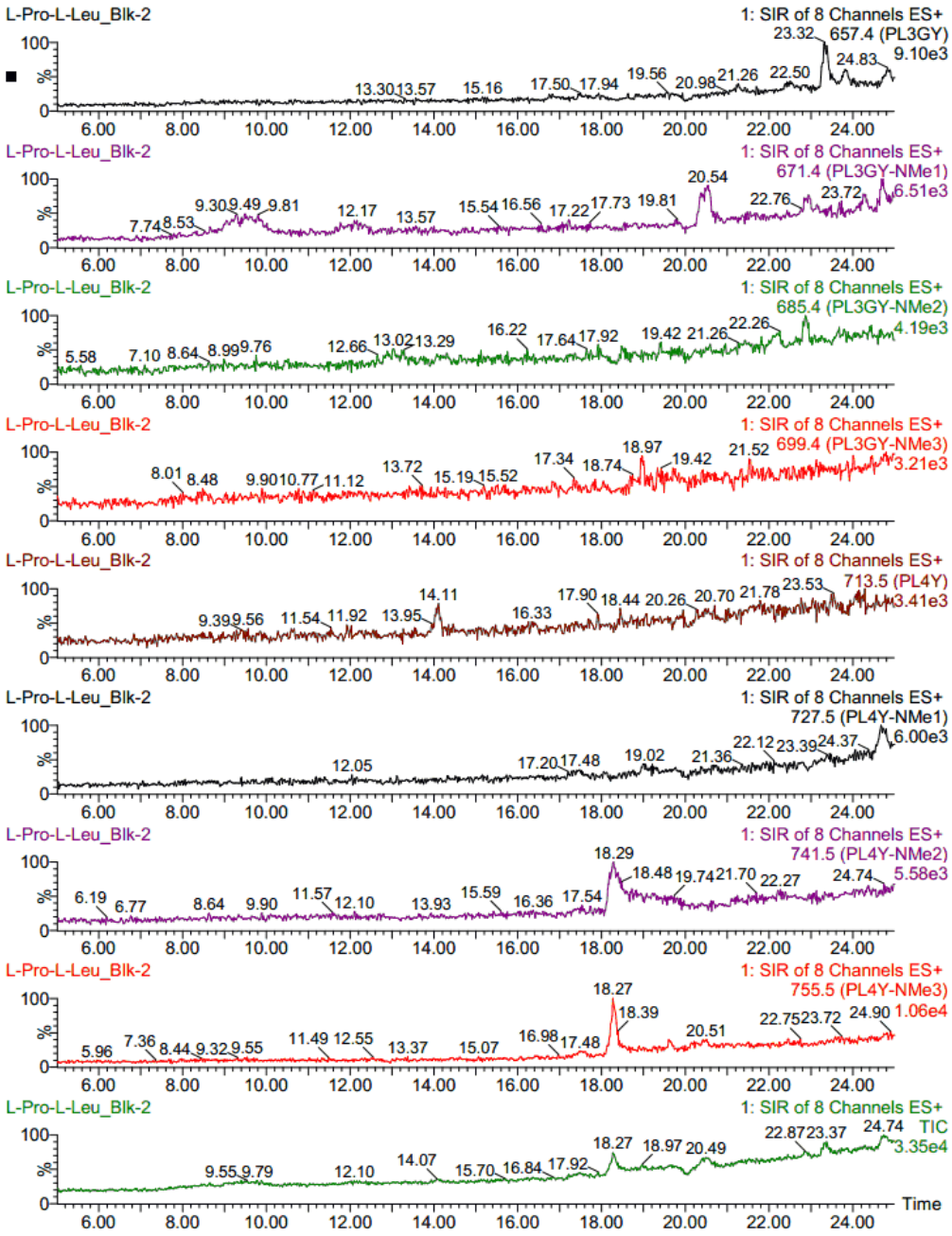

Sublibrary 2 Donor Well (t = 0 h)

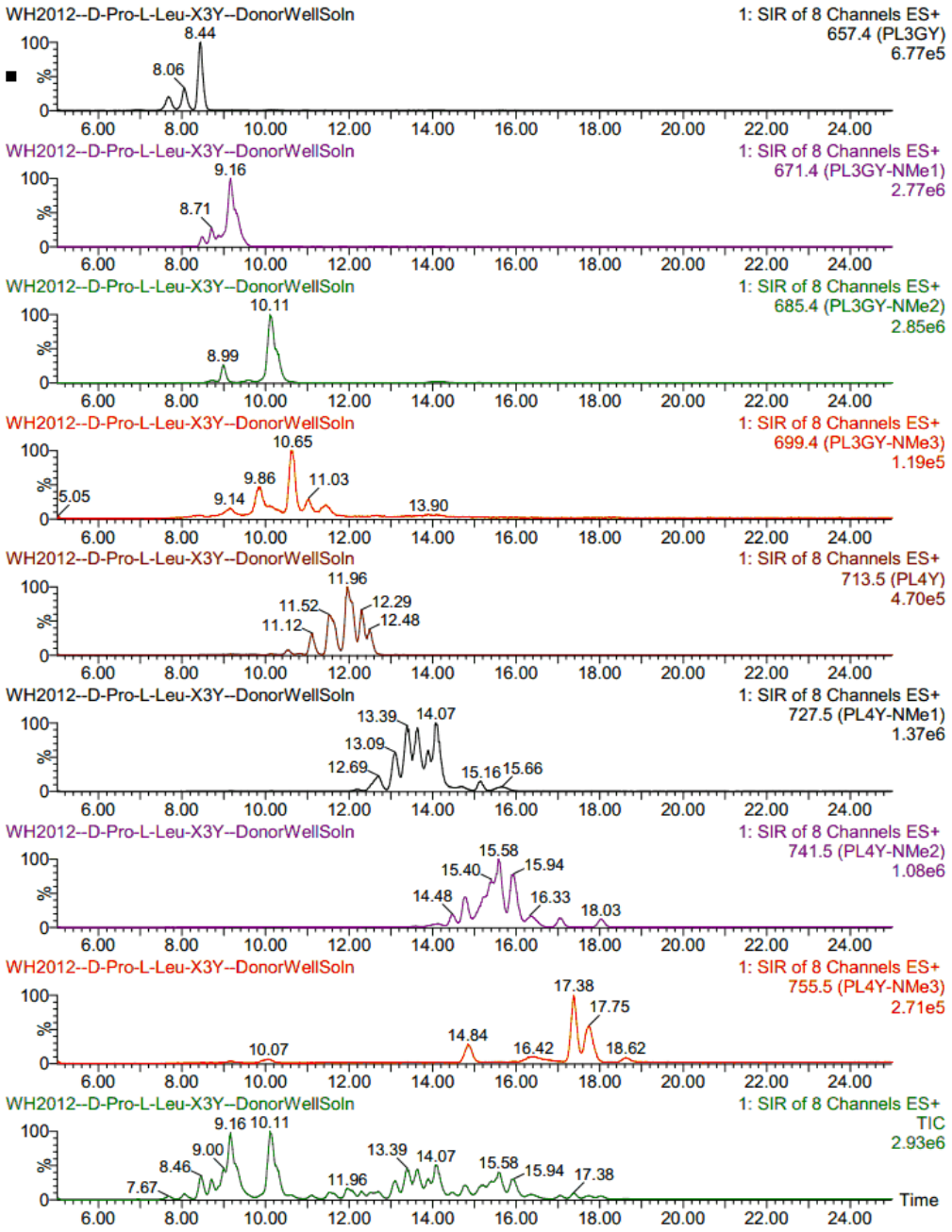

Sublibrary 2 Acceptor Well (t = 18 h)

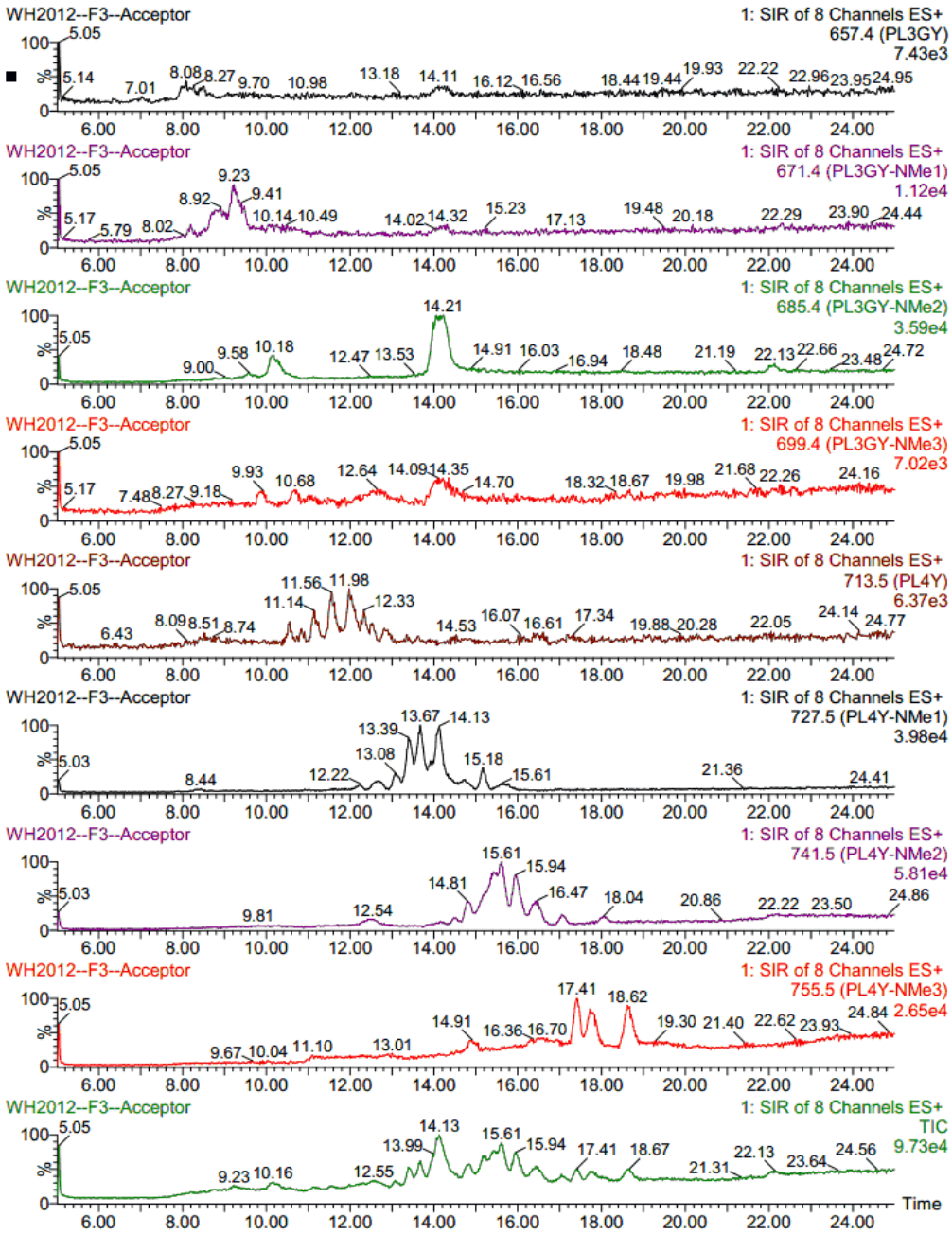

Sublibrary 2 Blank

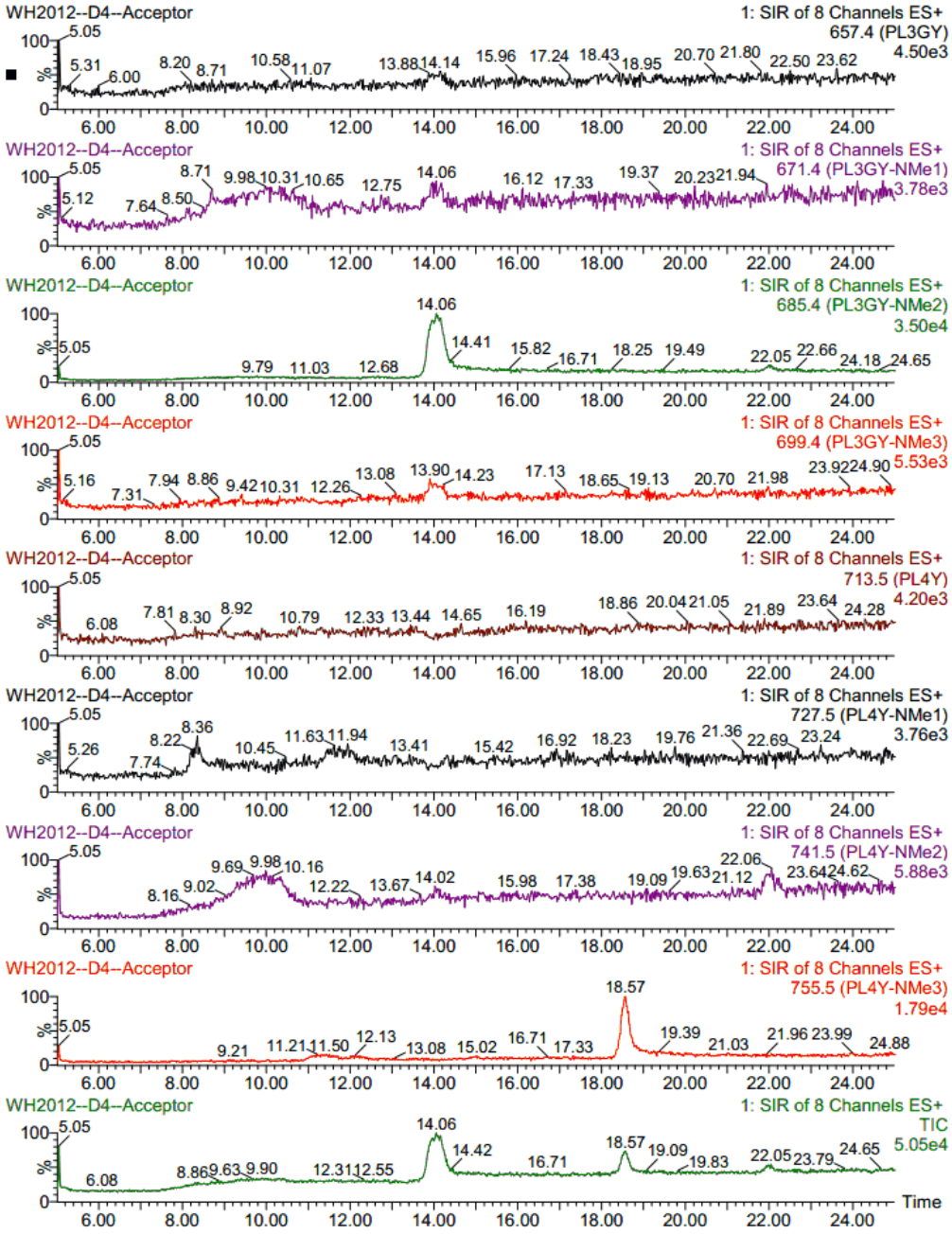

Sublibrary 3 Donor Well (t = 0 h)

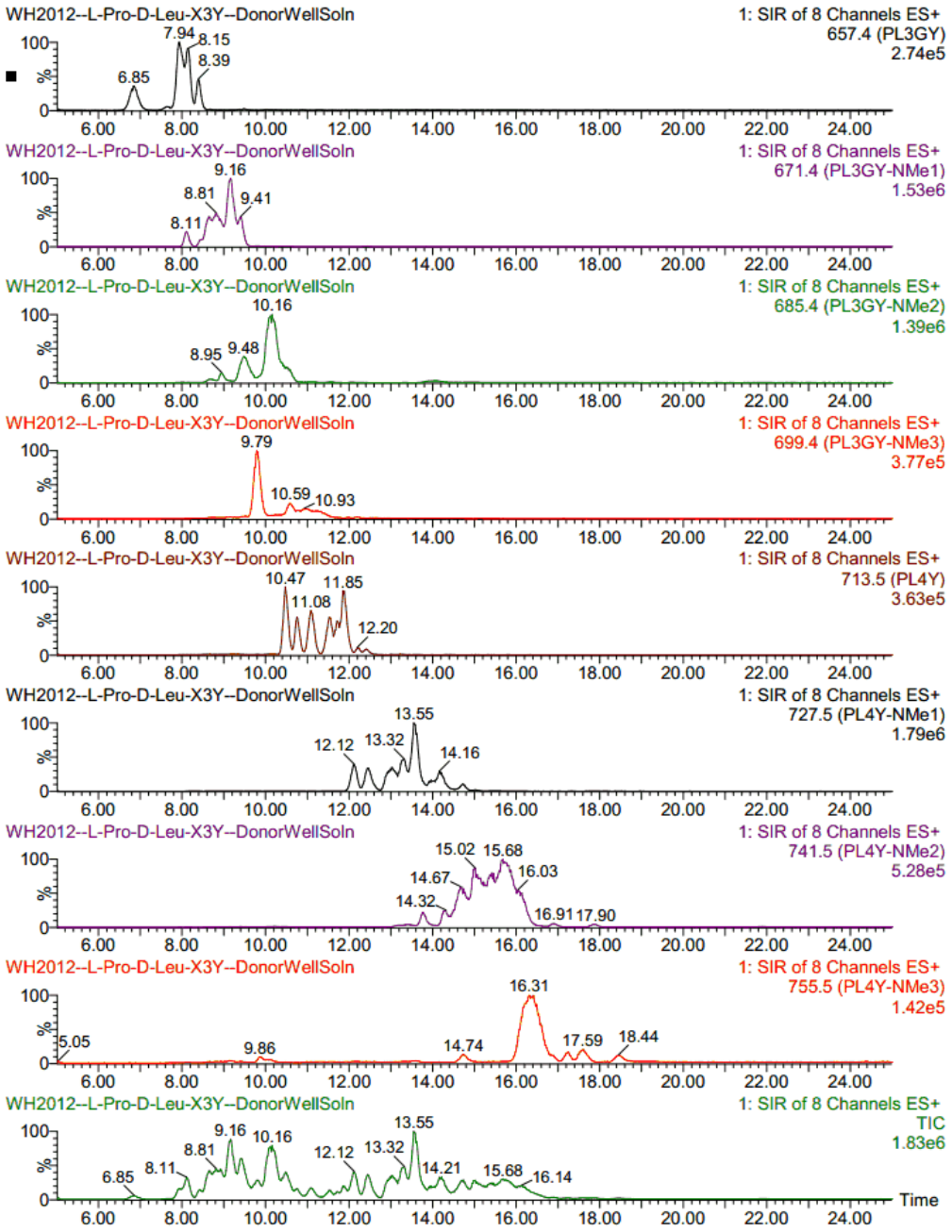

Sublibrary 3 Acceptor Well (t = 18 h)

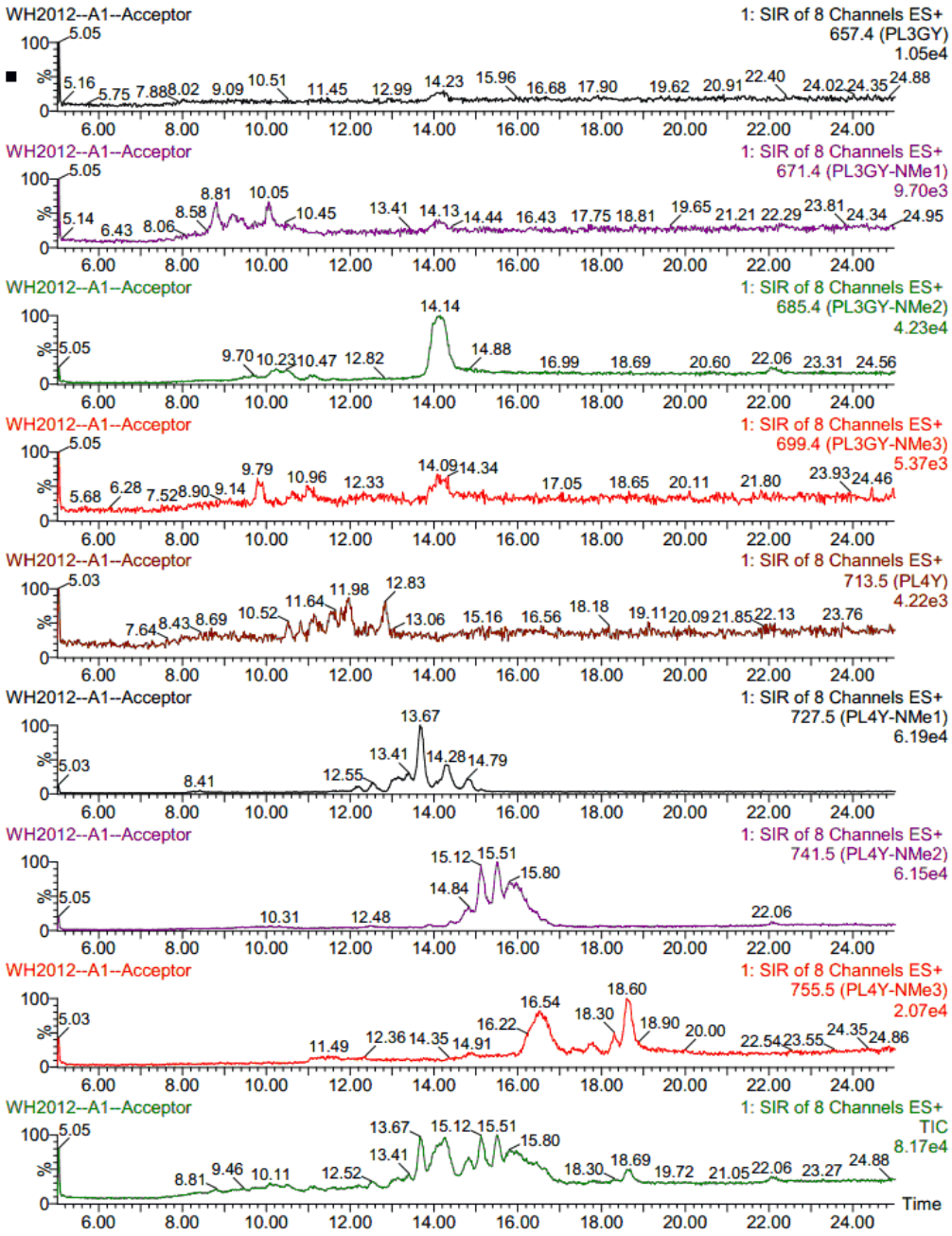

Sublibrary 3 Blank

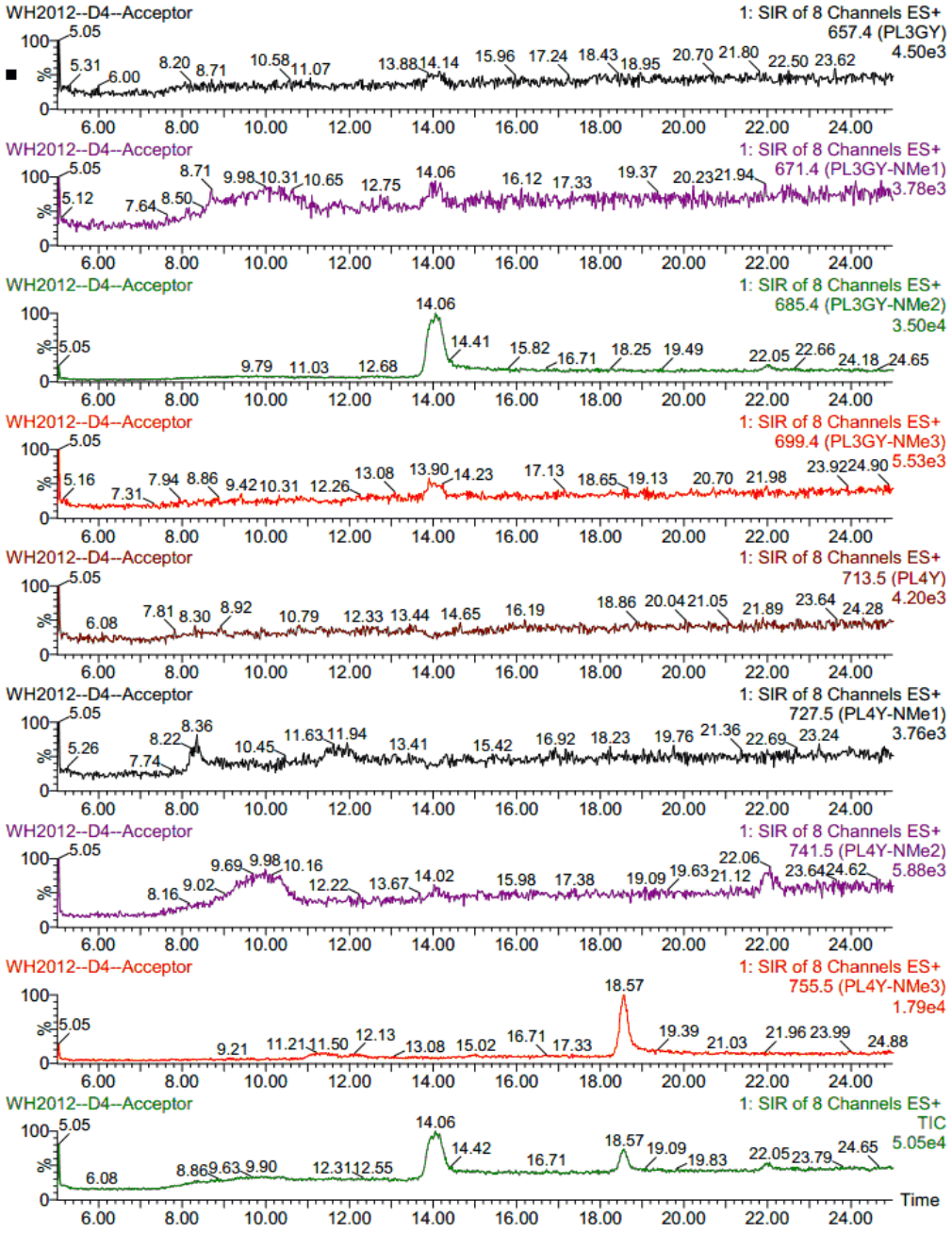

Sublibrary 4 Donor Well (t = 0 h)

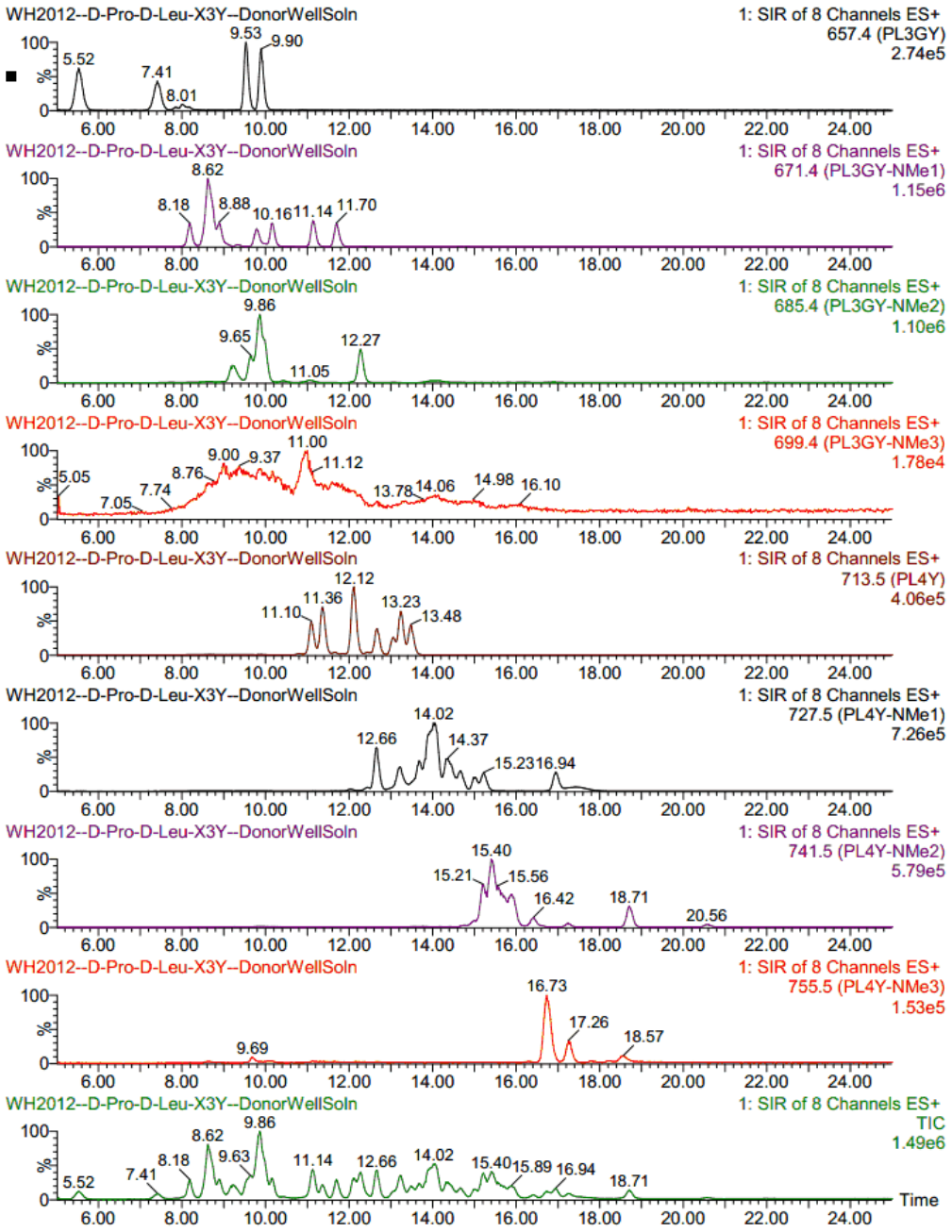

Sublibrary 4 Acceptor Well (t = 18 h)

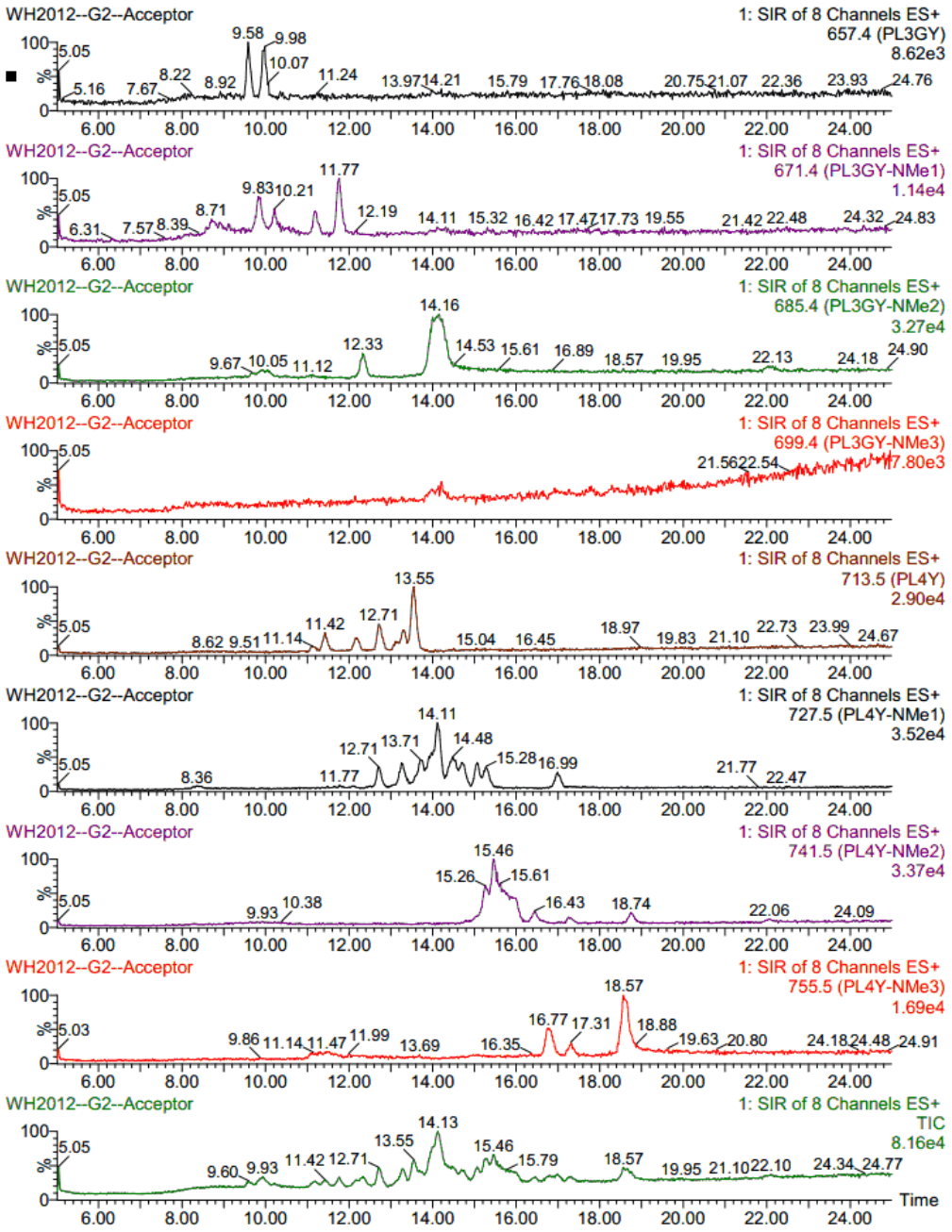

Sublibrary 4 Blank

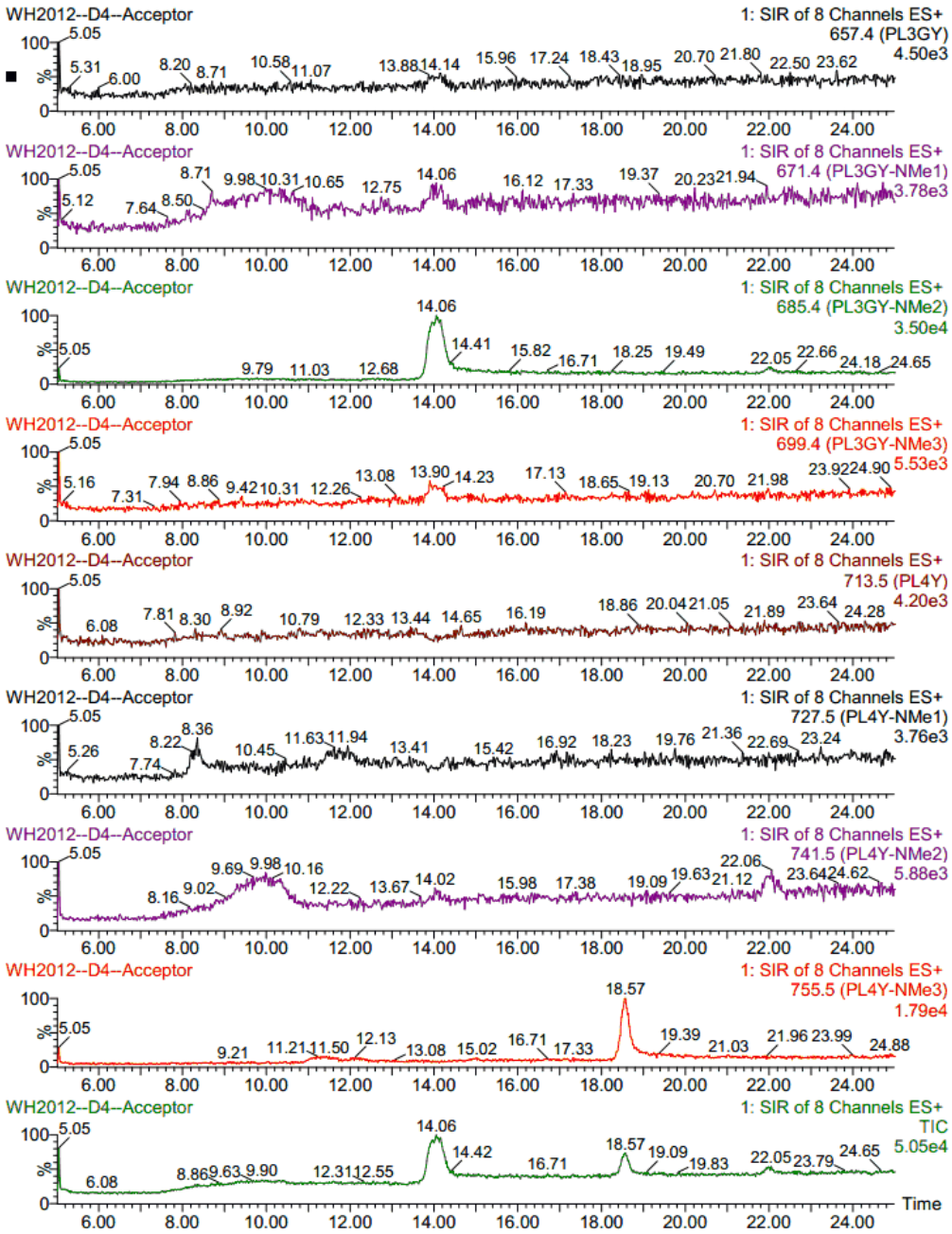

Sublibrary 5 Donor Well (t = 0 h)

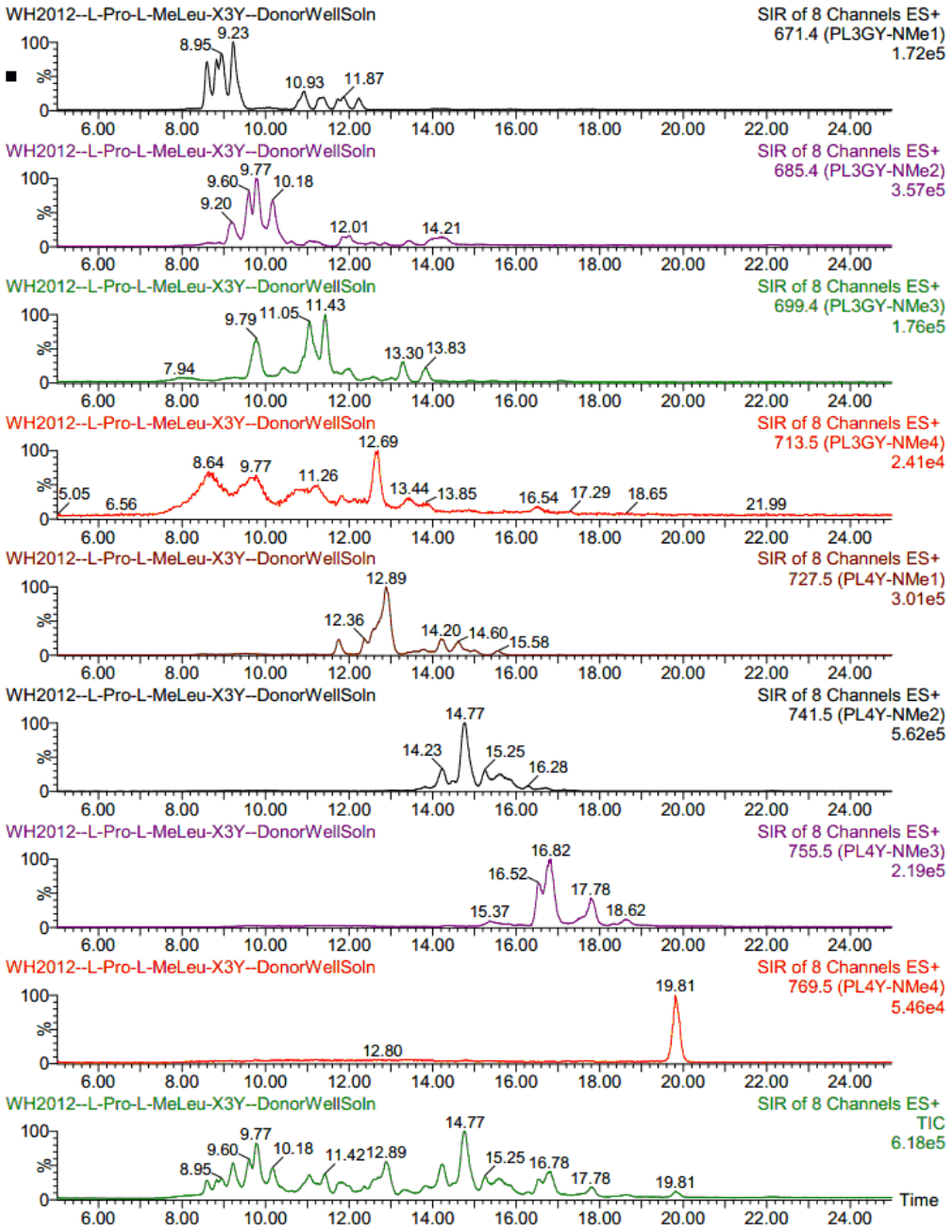

Sublibrary 5 Acceptor Well (t = 18 h)

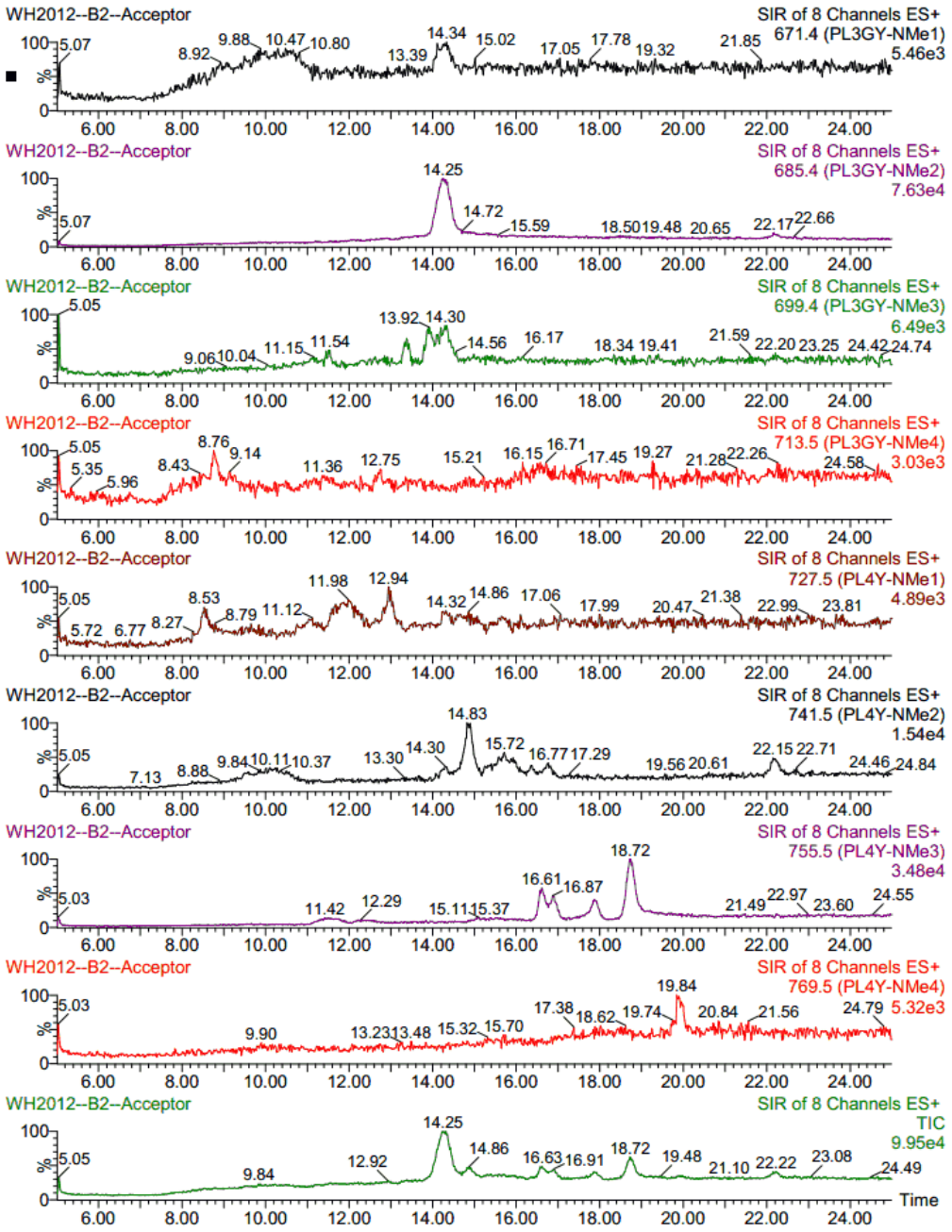

Sublibrary 5 Blank

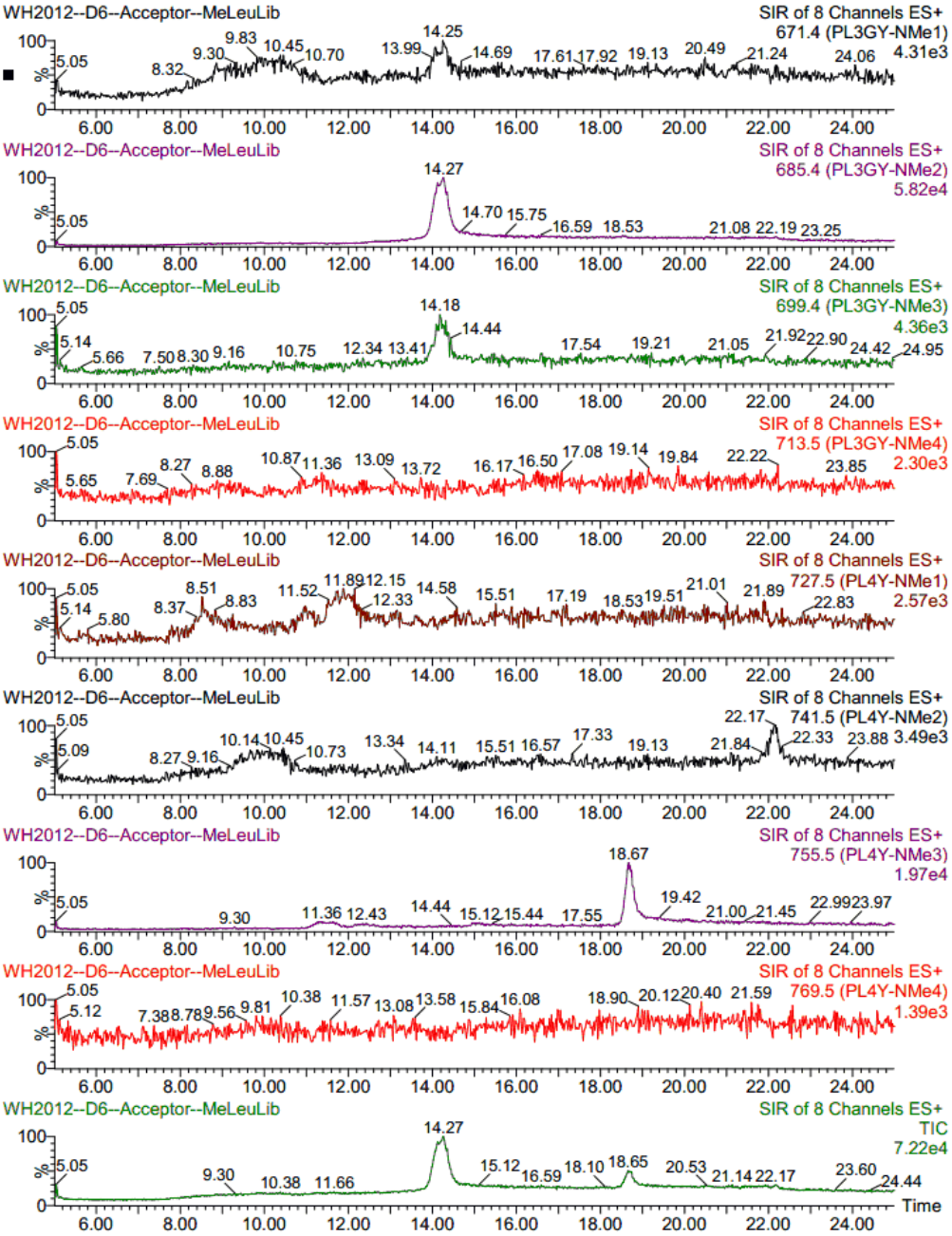

Sublibrary 6 Donor Well (t = 0 h)

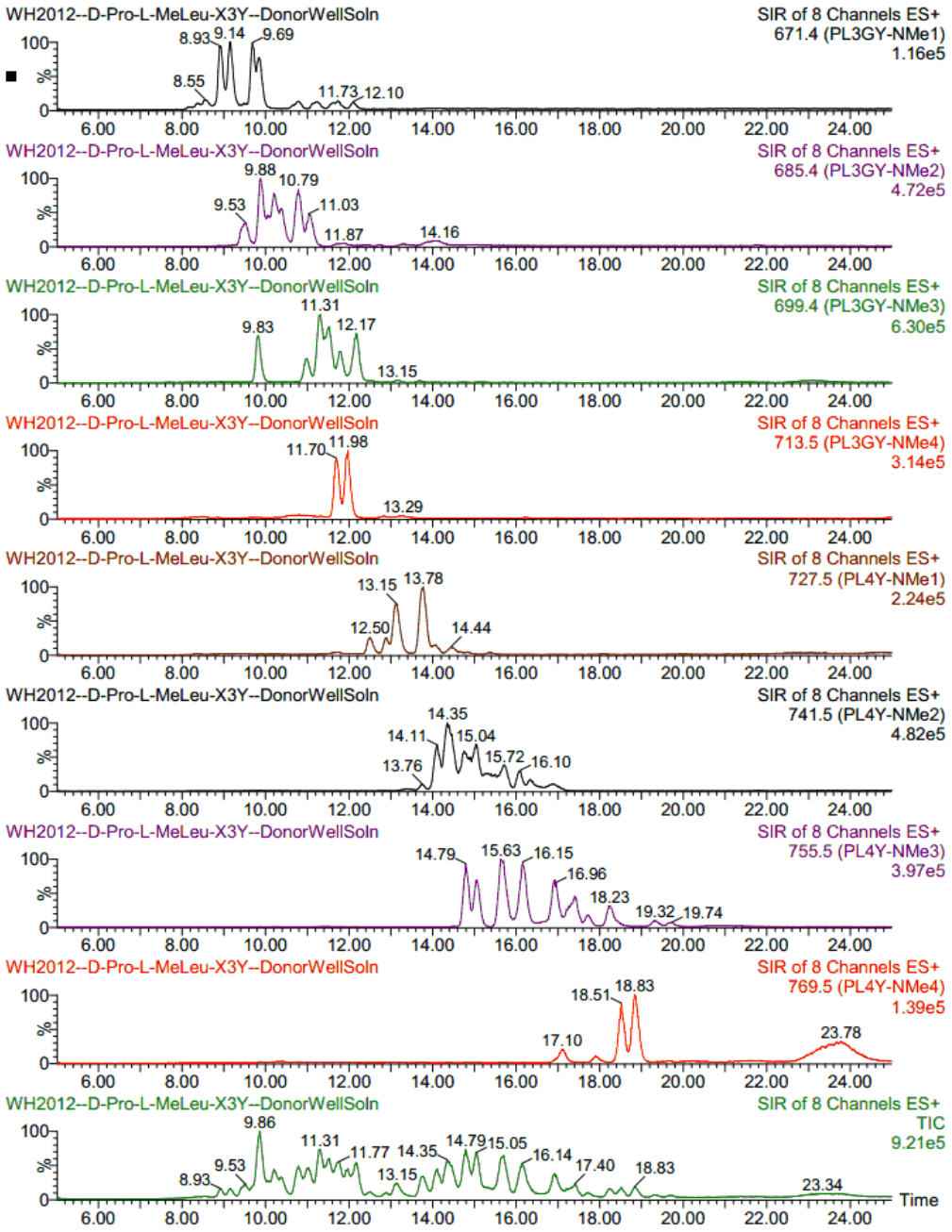

Sublibrary 6 Acceptor Well (t = 18 h)

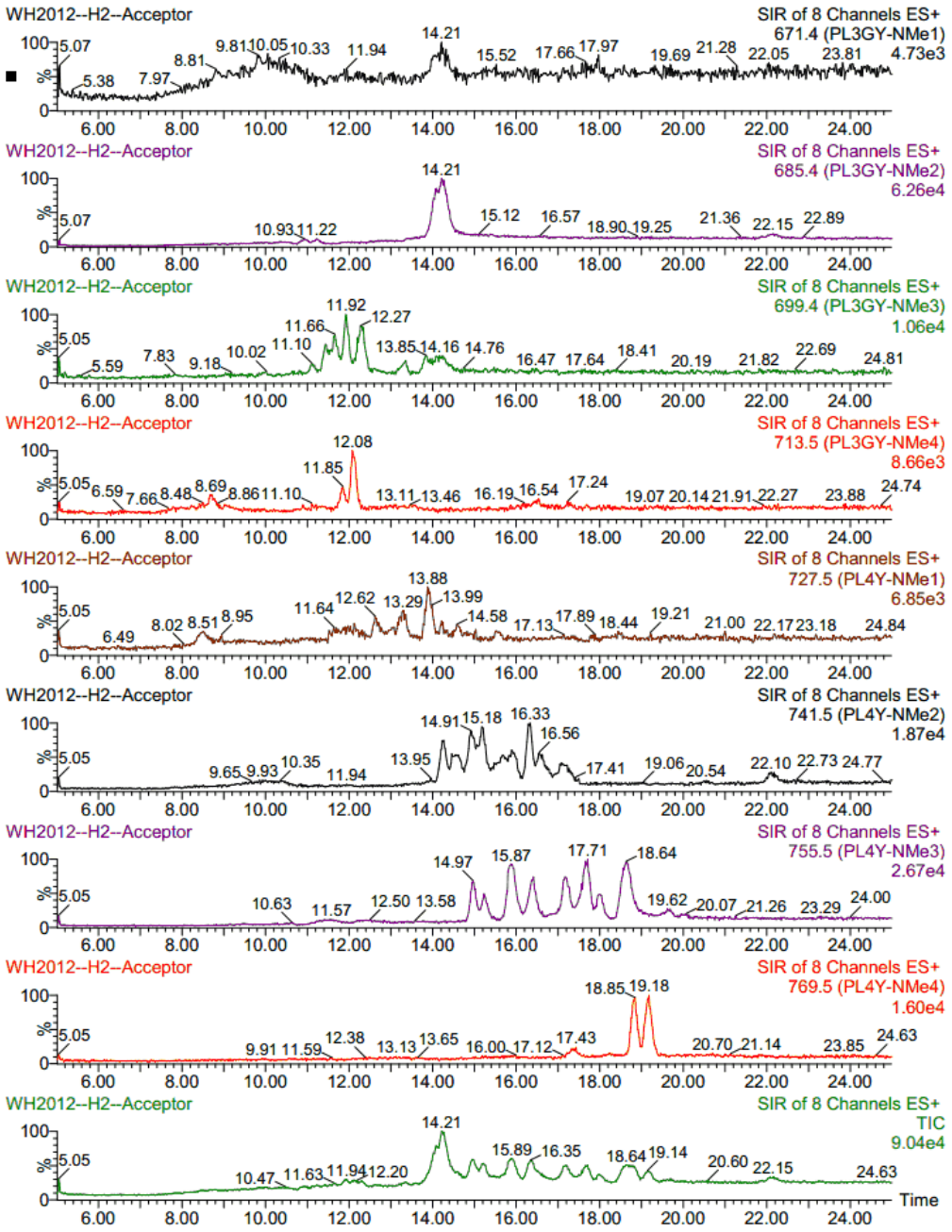

Sublibrary 6 Blank

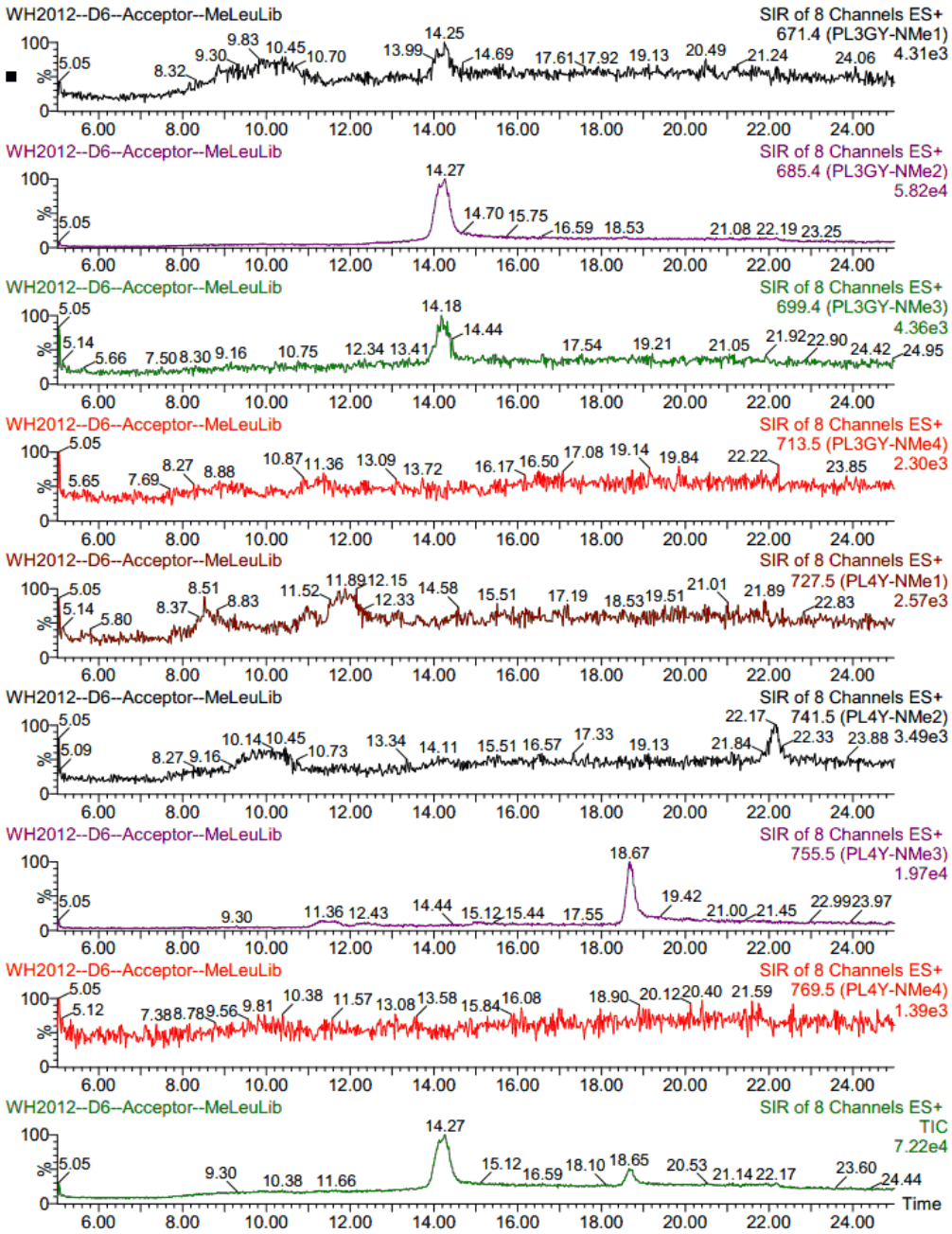

Sublibrary 7 Donor Well (t = 0 h)

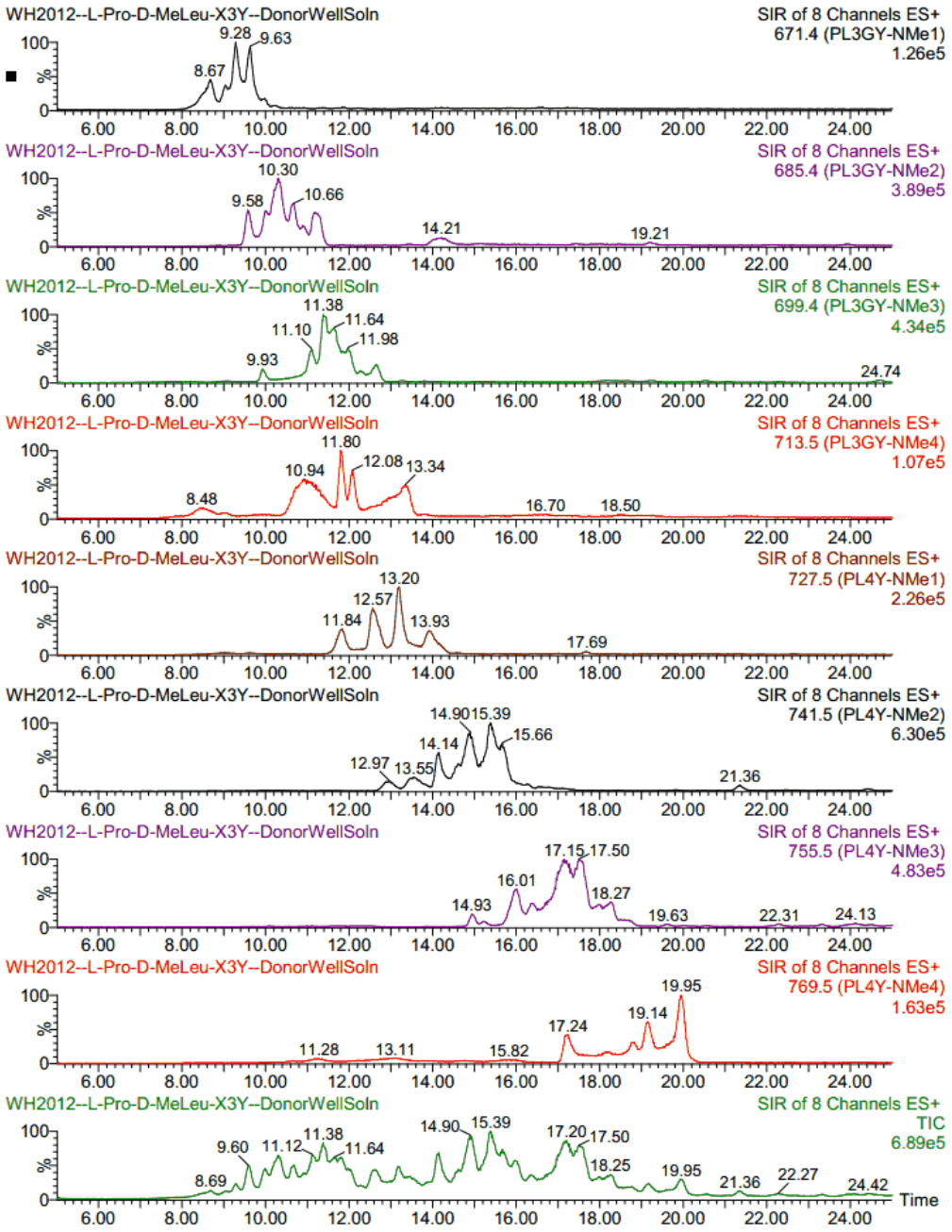

Sublibrary 7 Acceptor Well (t = 18 h)

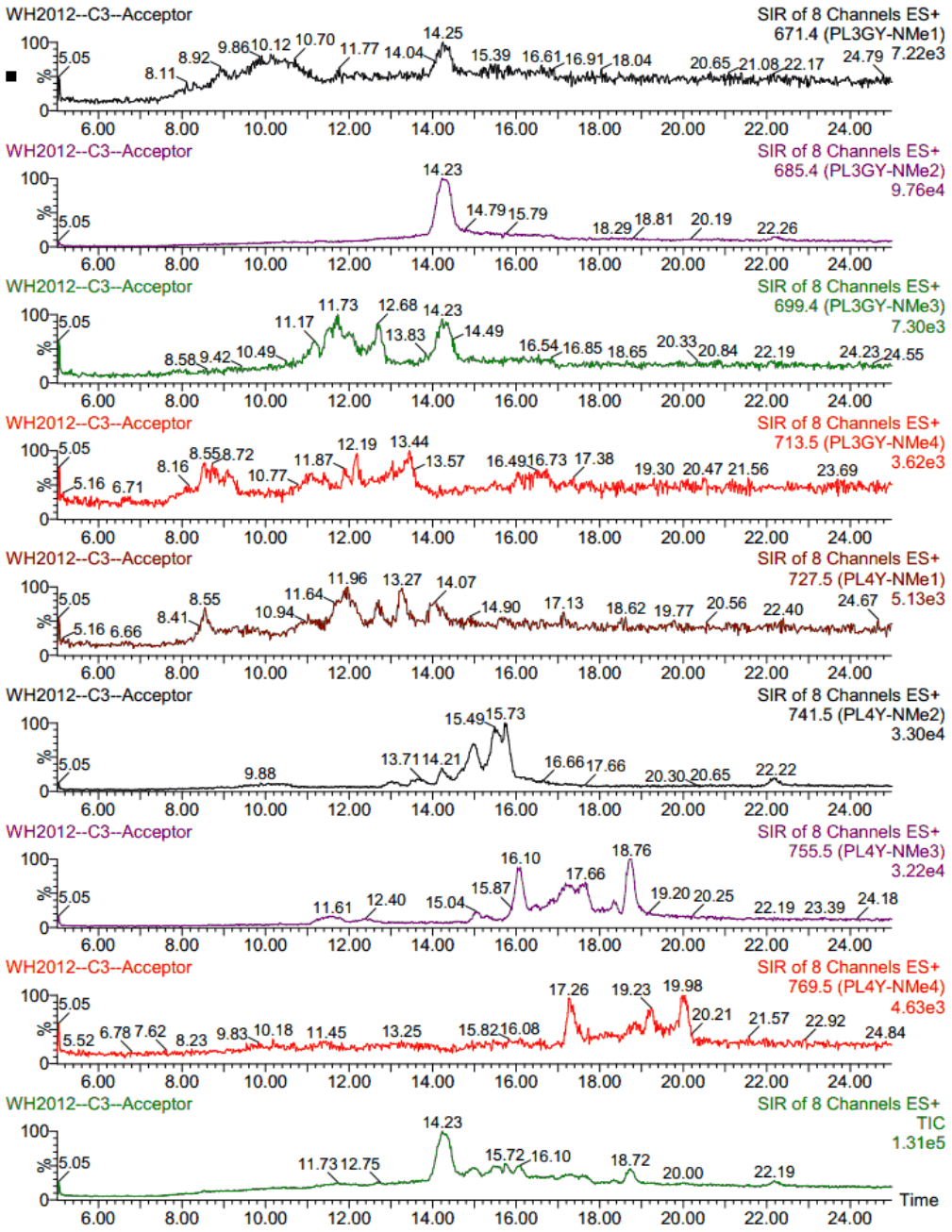

Sublibrary 7 Blank

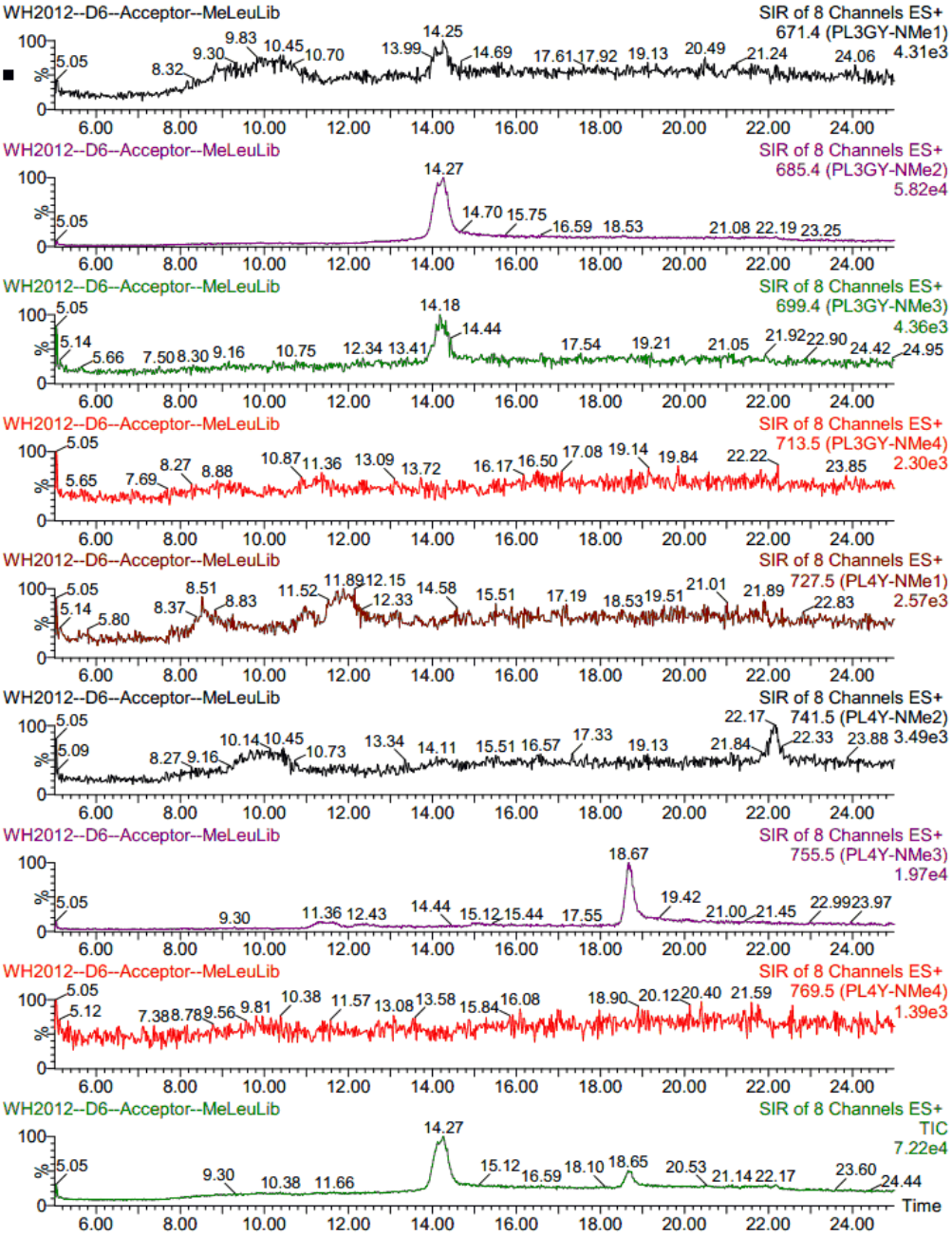

Sublibrary 8 Donor Well (t = 0 h)

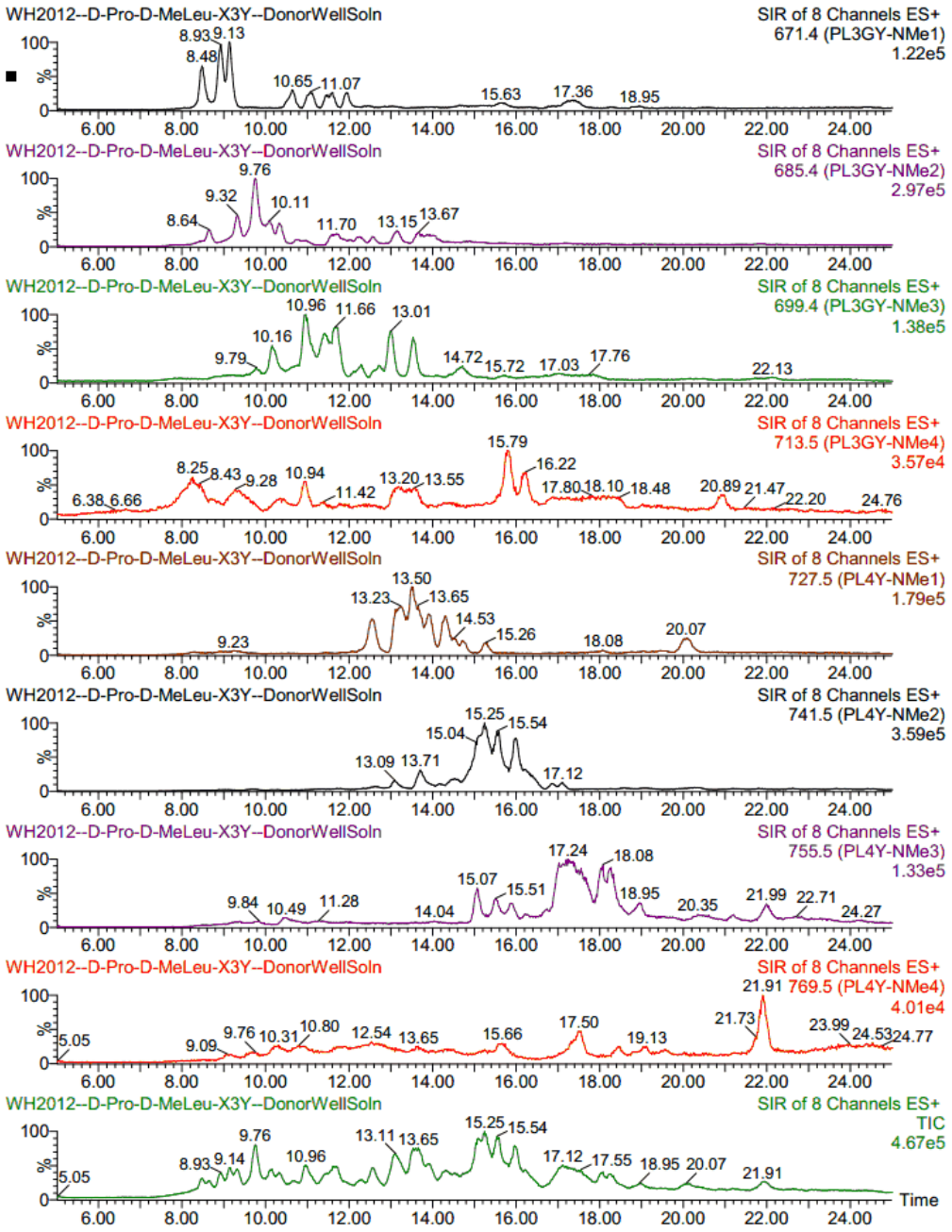

Sublibrary 8 Acceptor Well (t = 18 h)

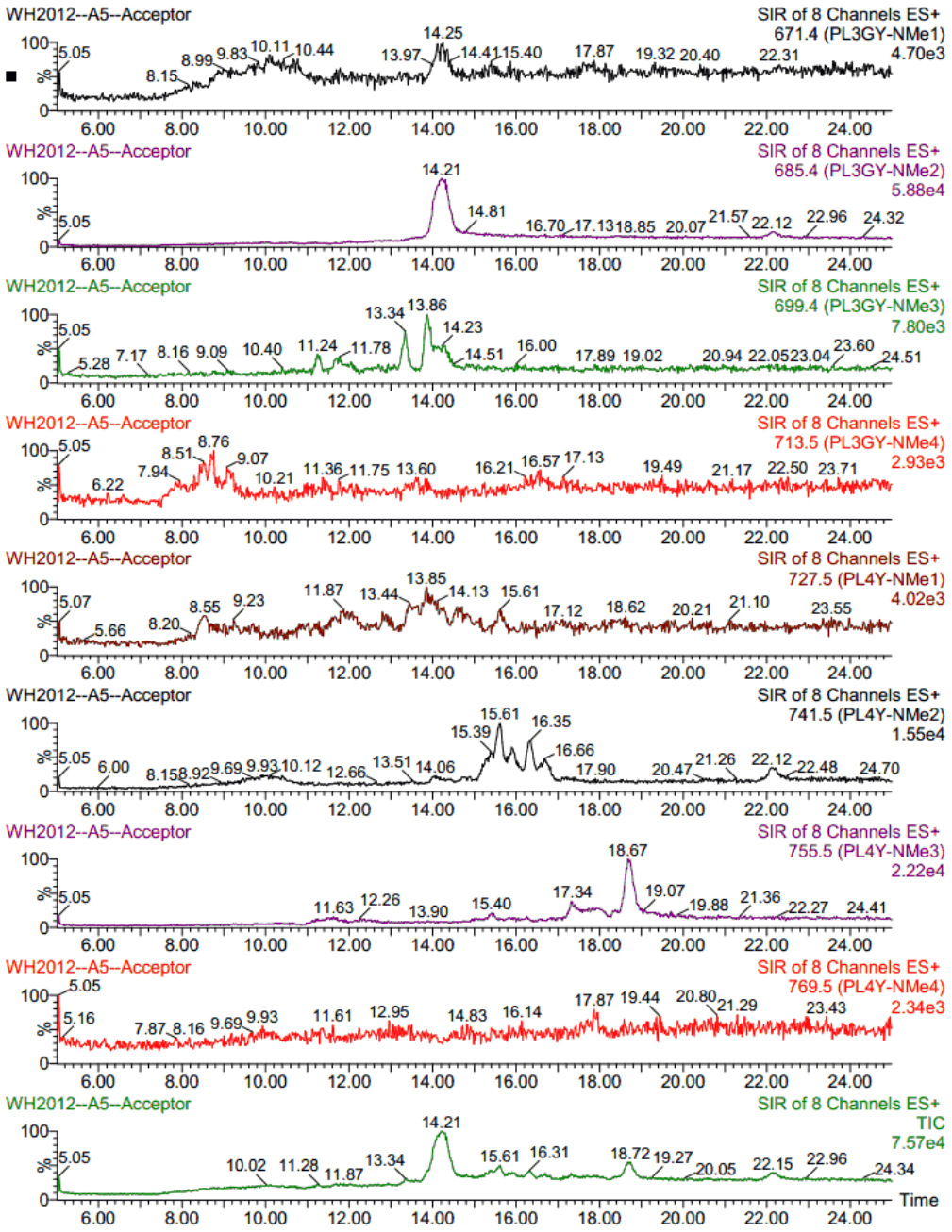

Sublibrary 8 Blank

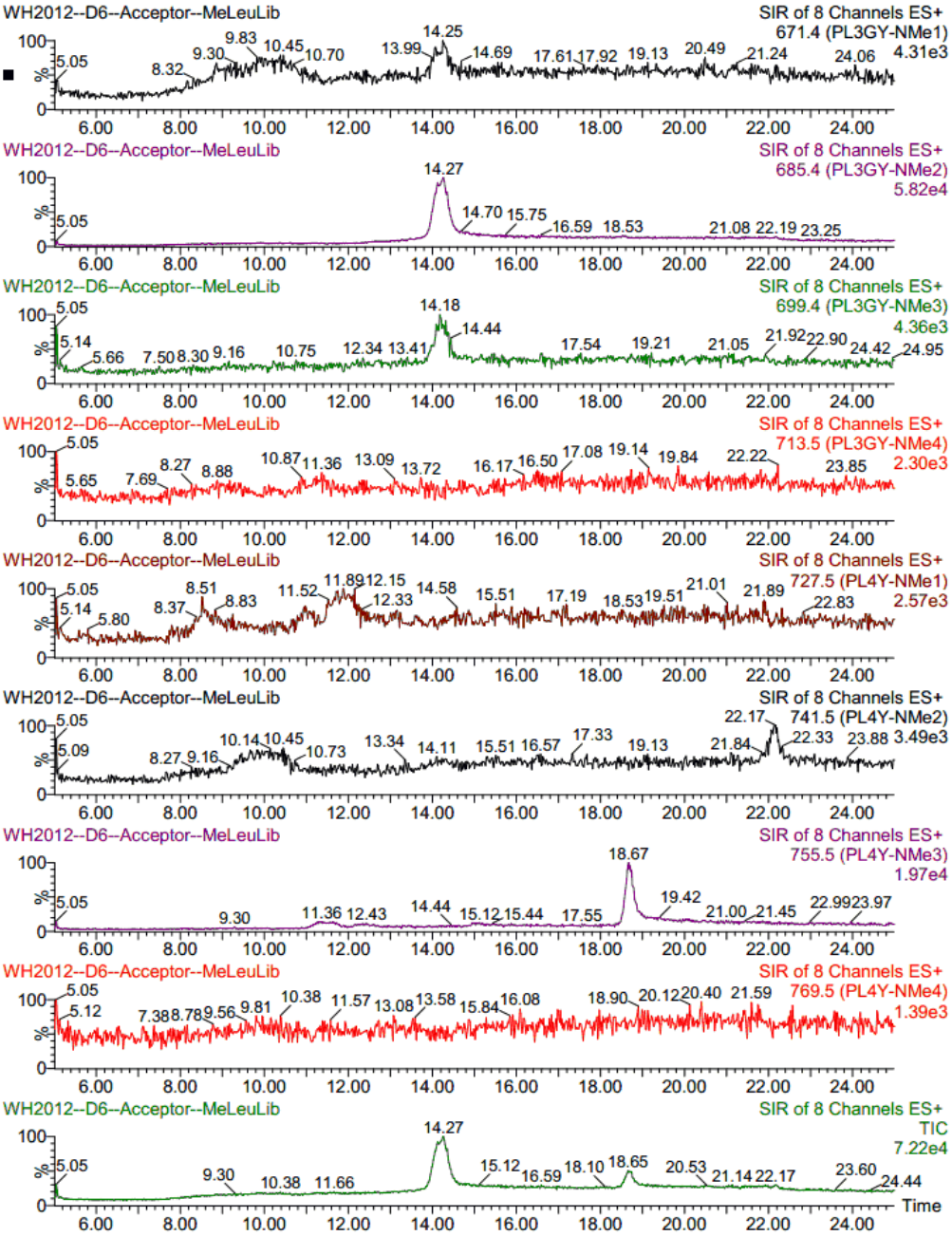

Sublibrary 9 Donor Well (t = 0 h)

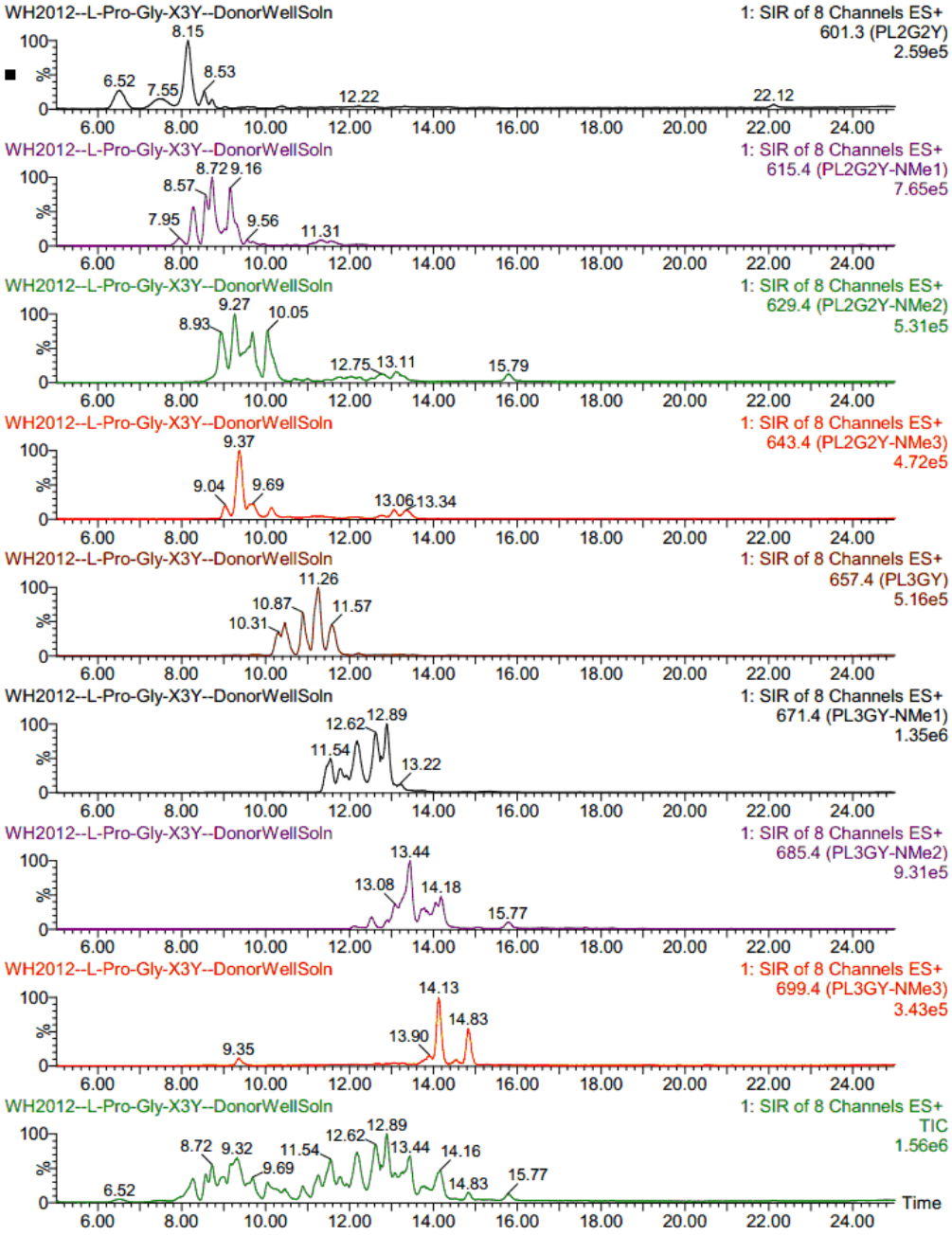

Sublibrary 9 Acceptor Well (t = 18 h)

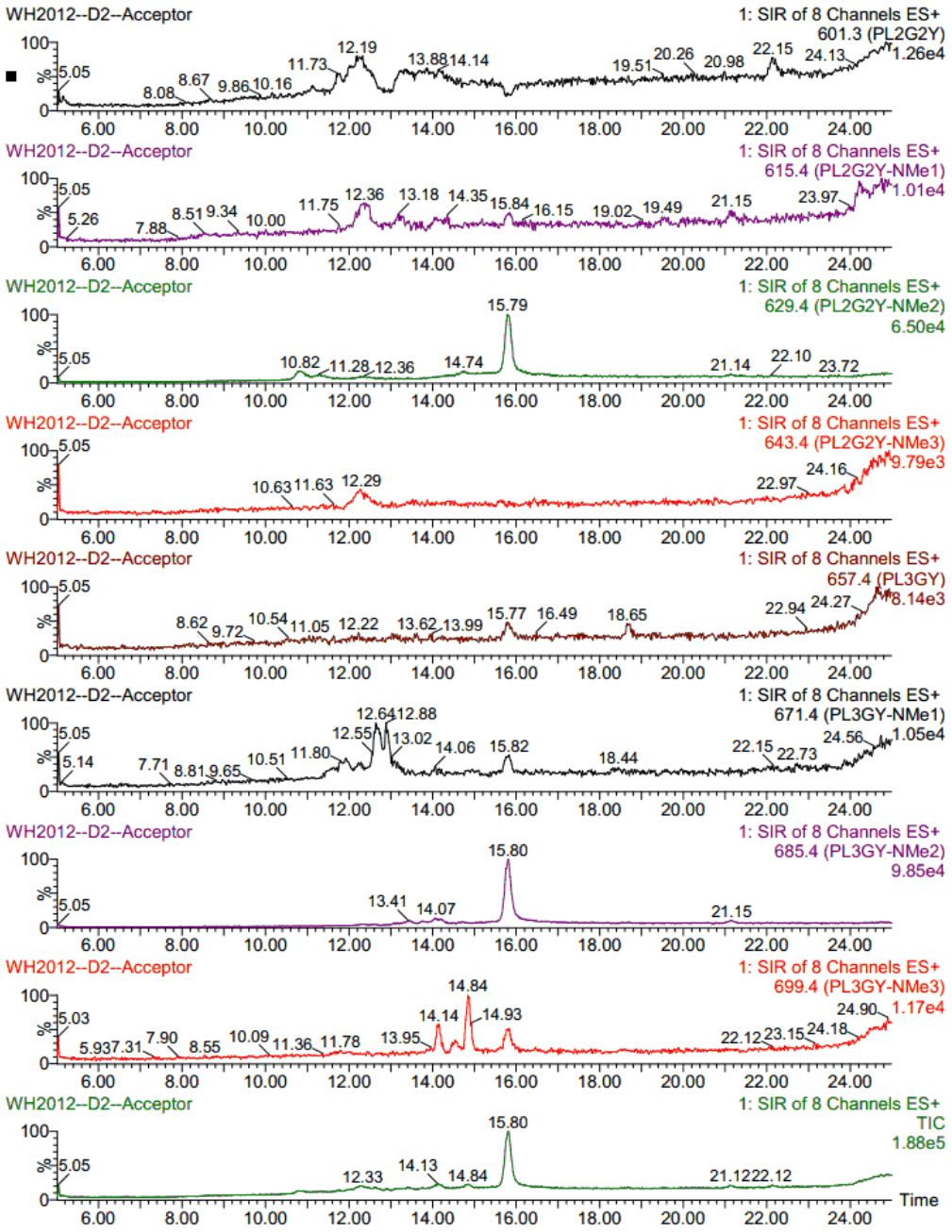

Sublibrary 9 Blank

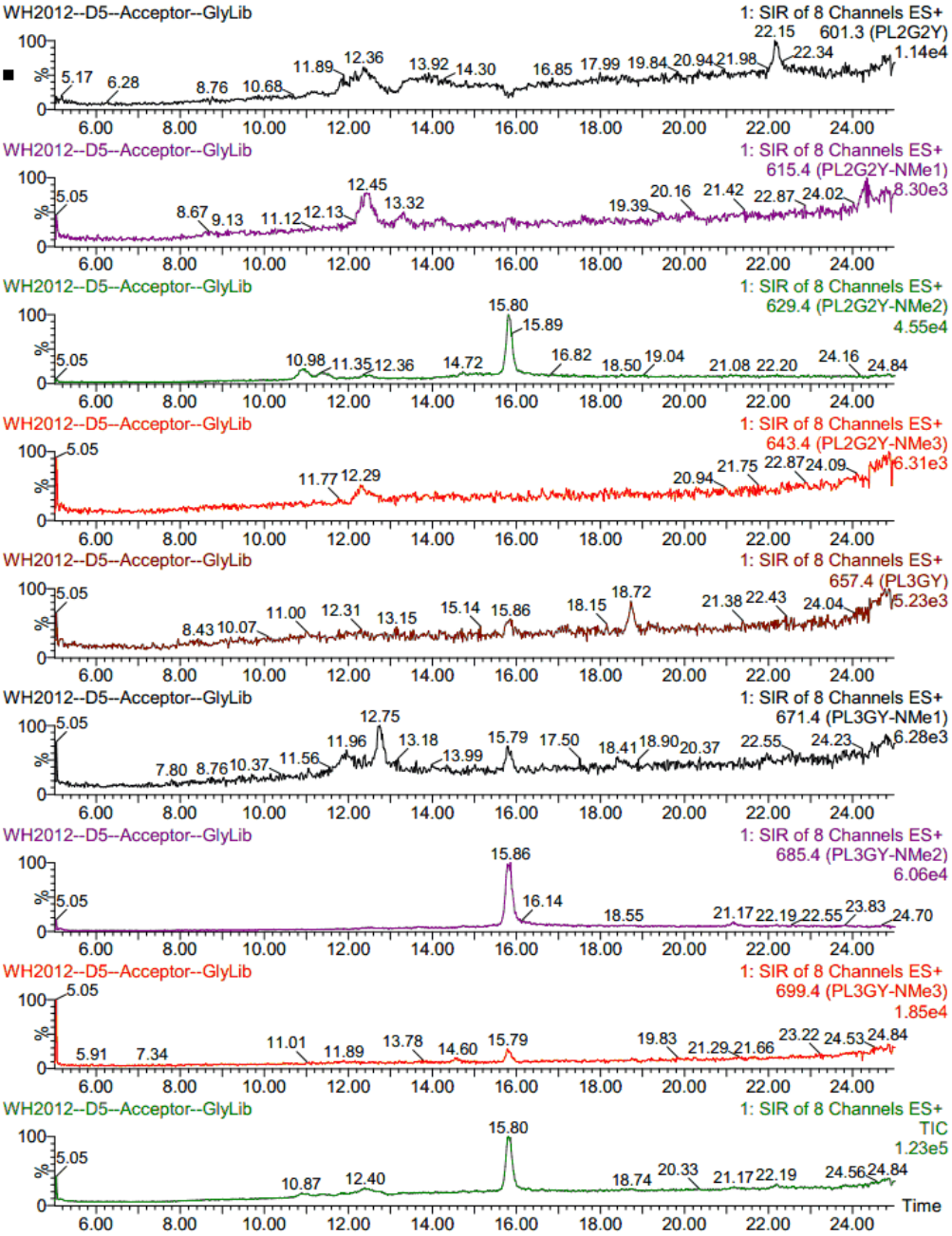

Sublibrary 10 Donor Well (t = 0 h)

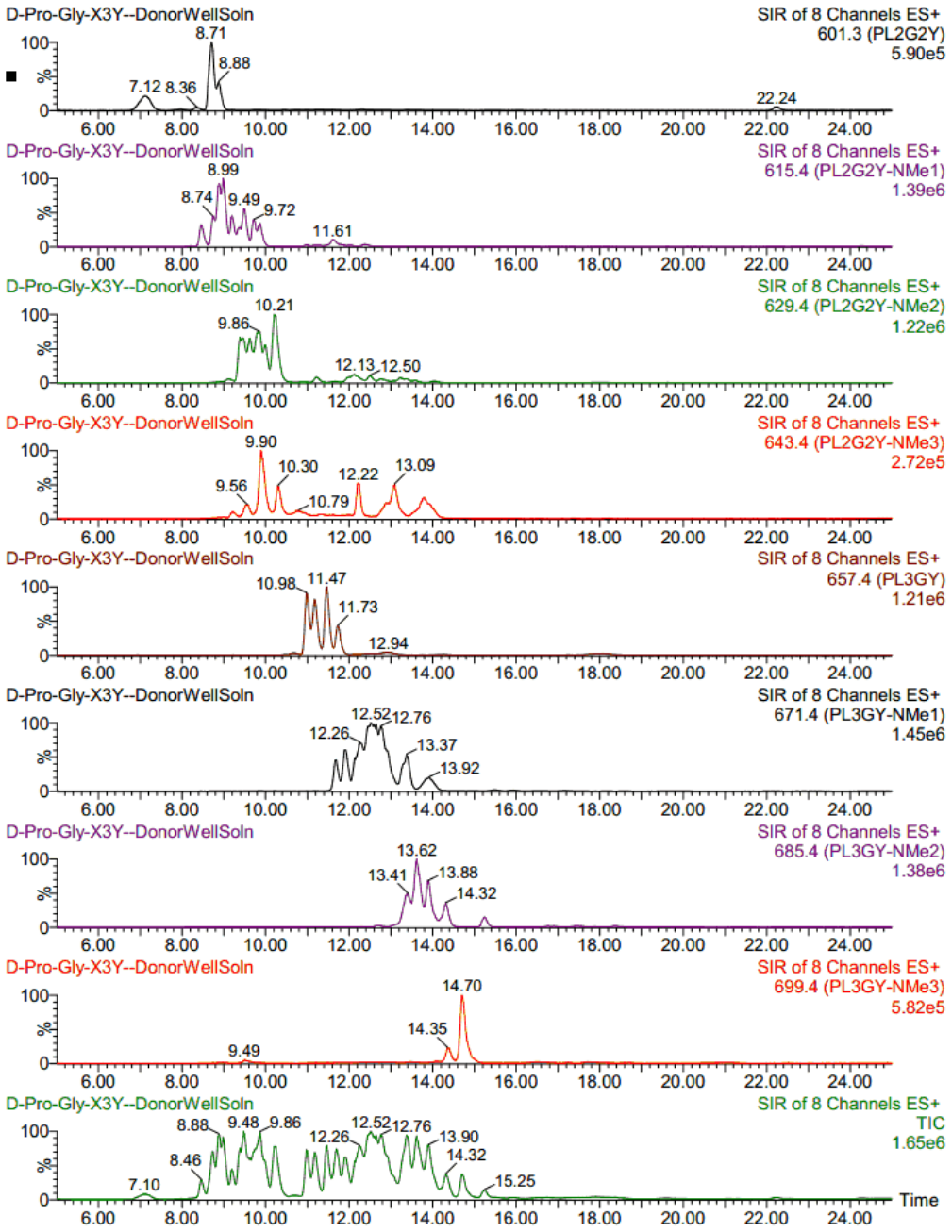

Sublibrary 10 Acceptor Well (t = 18 h)

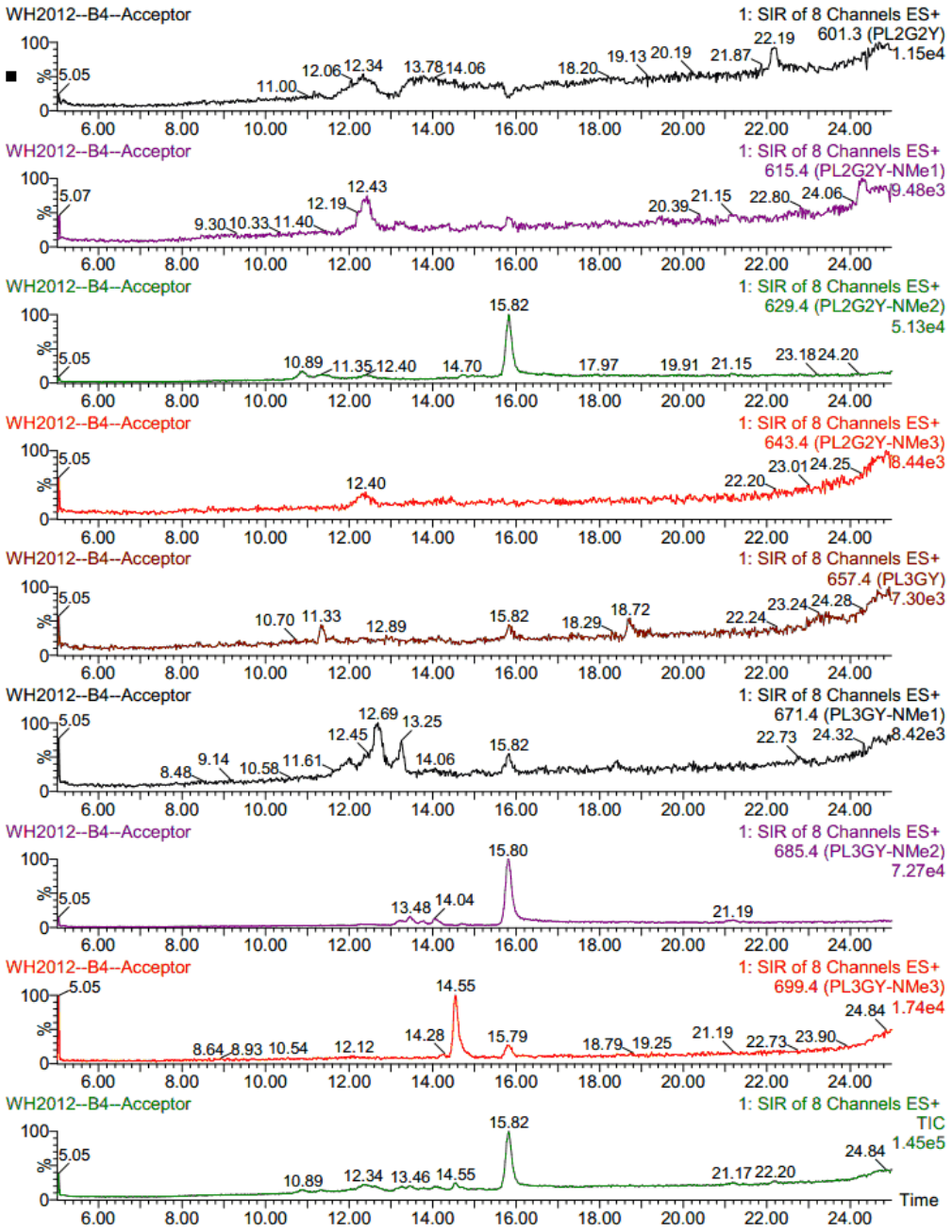

Sublibrary 10 Blank

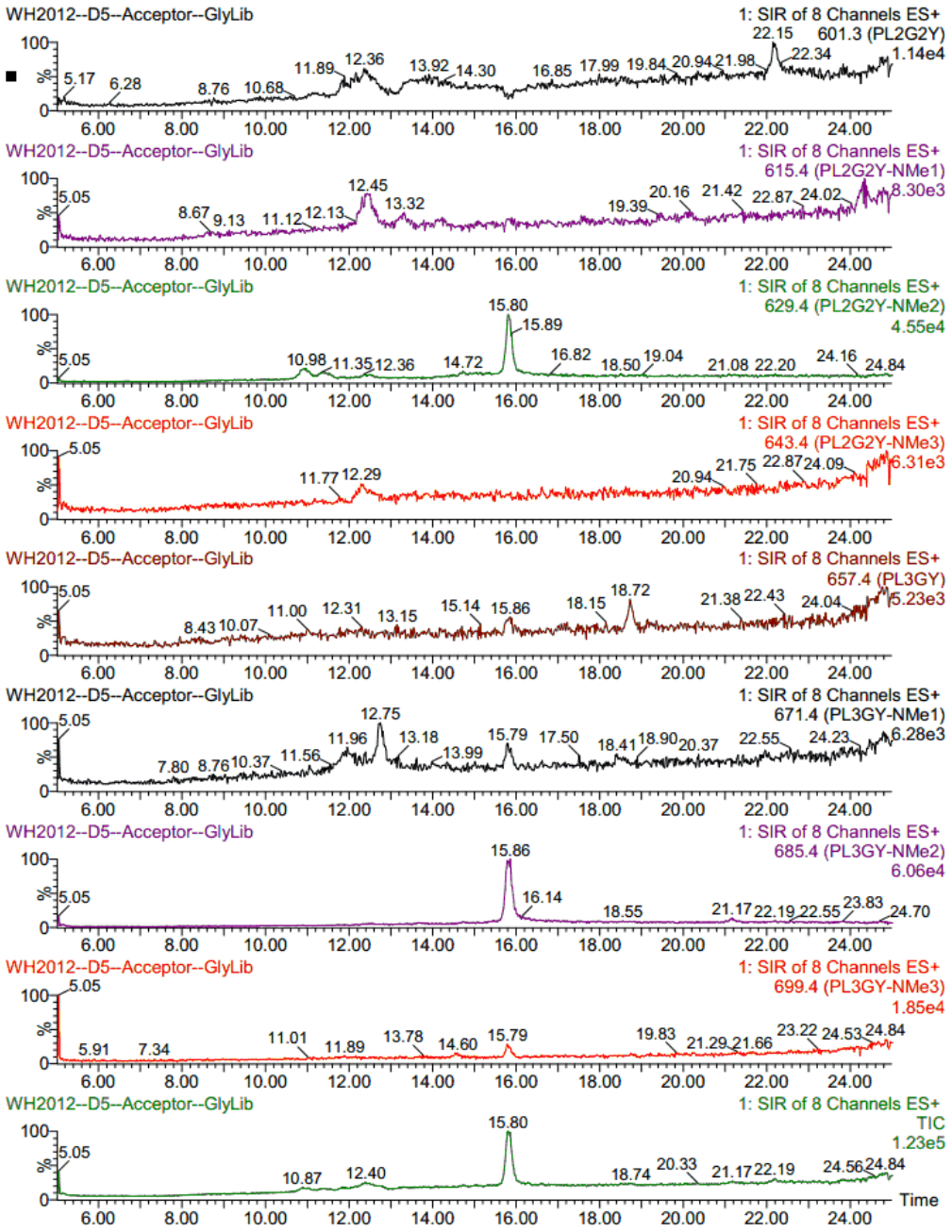

Sublibrary 11 Donor Well (t = 0 h)

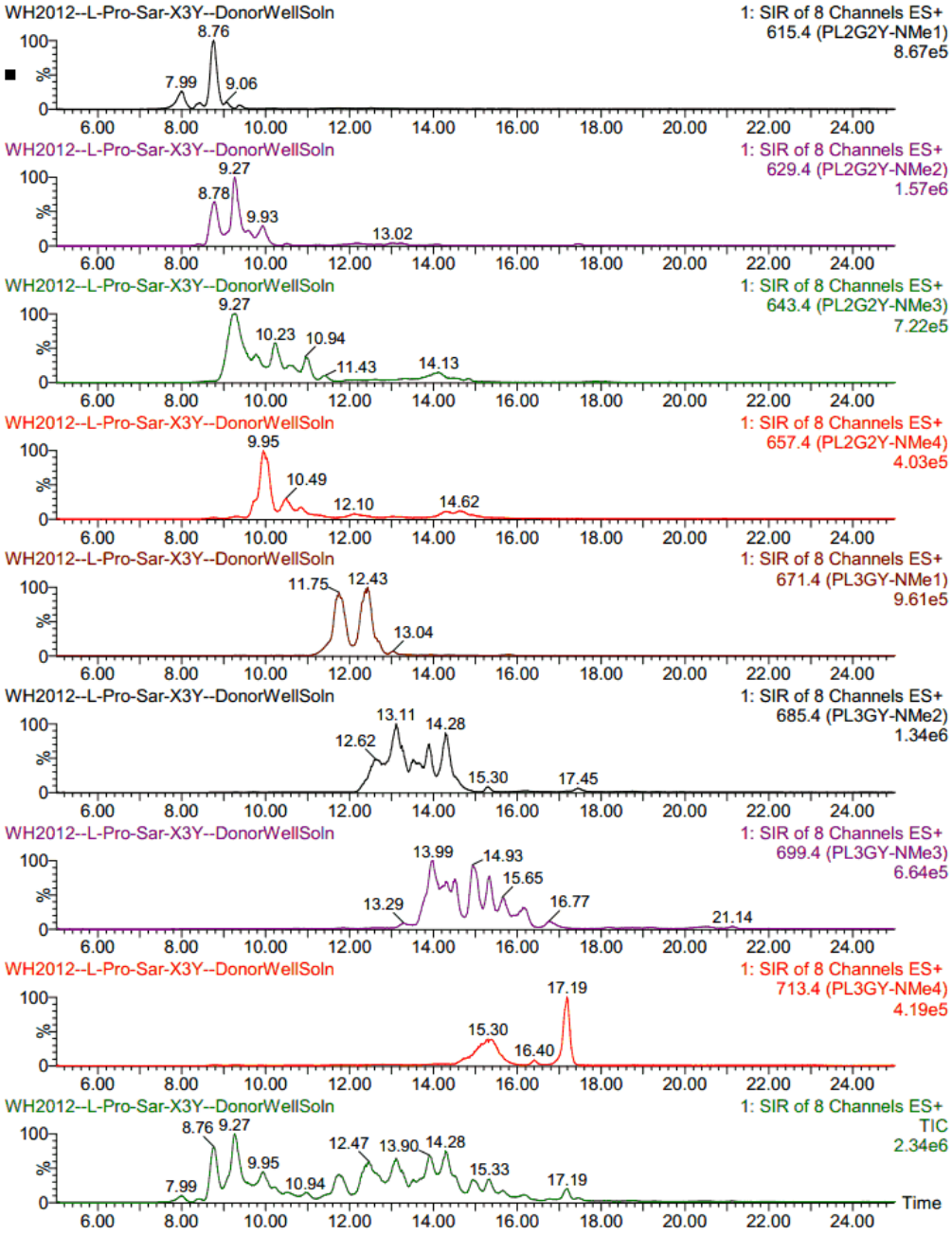

Sublibrary 11 Acceptor Well (t = 18 h)

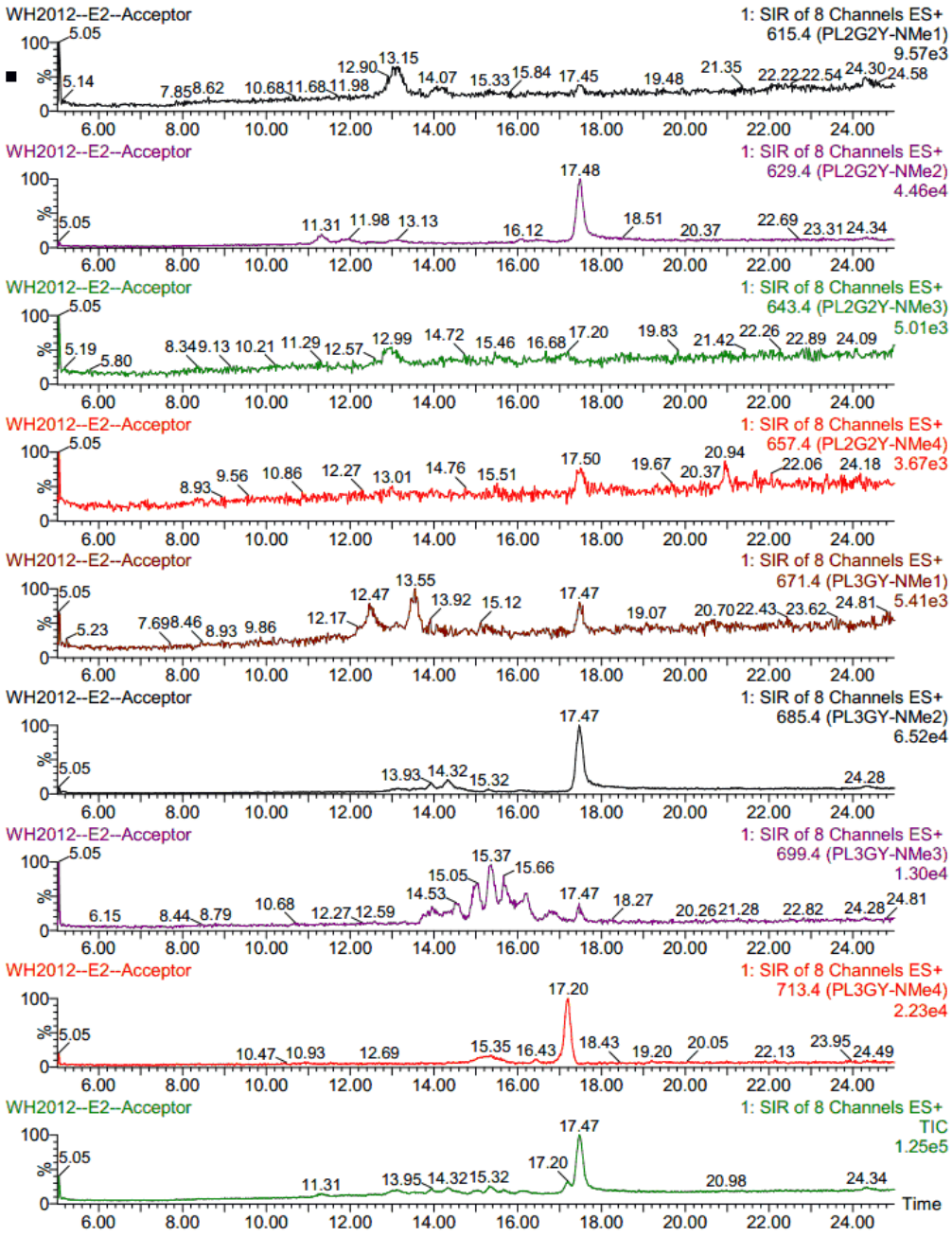

Sublibrary 11 Blank

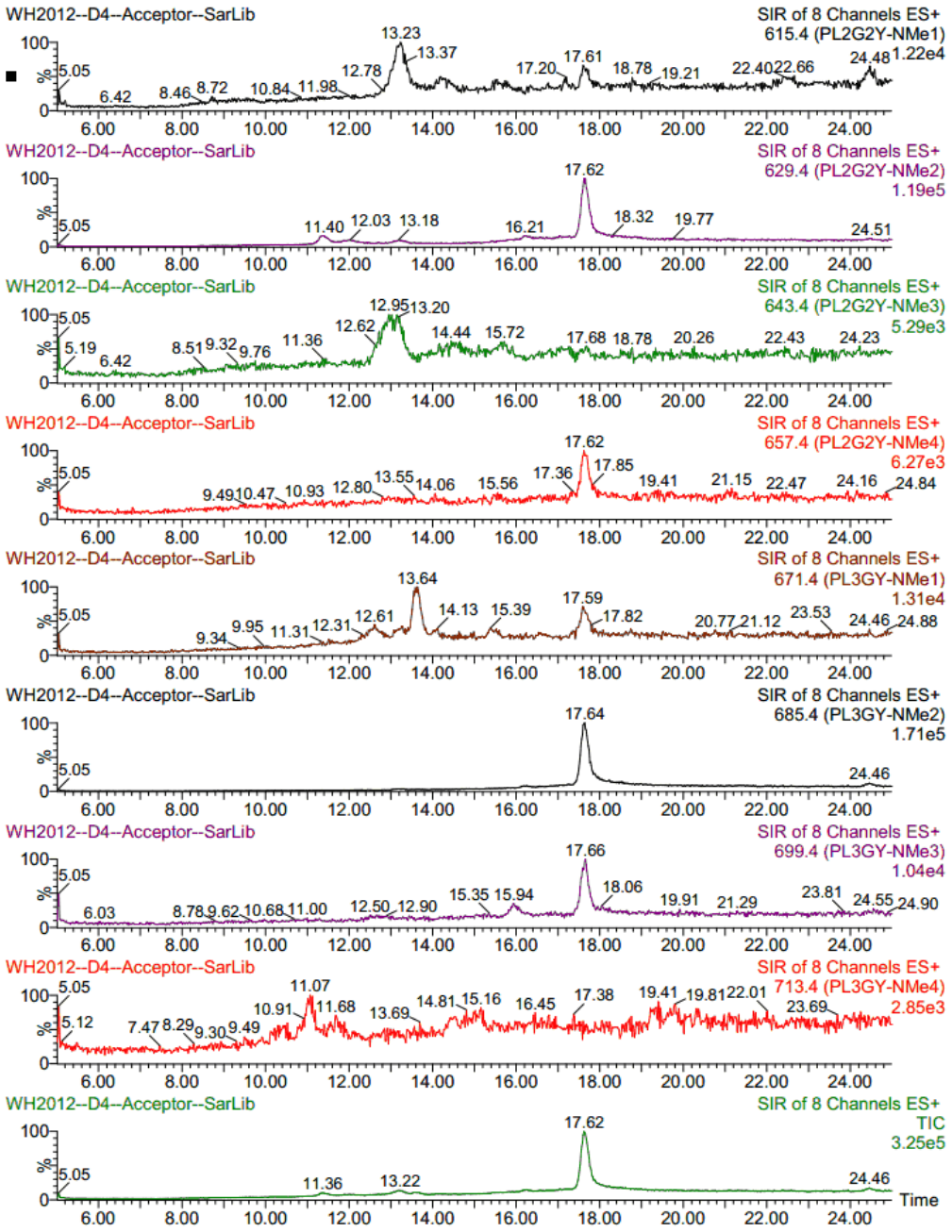

Sublibrary 12 Donor Well (t = 0 h)

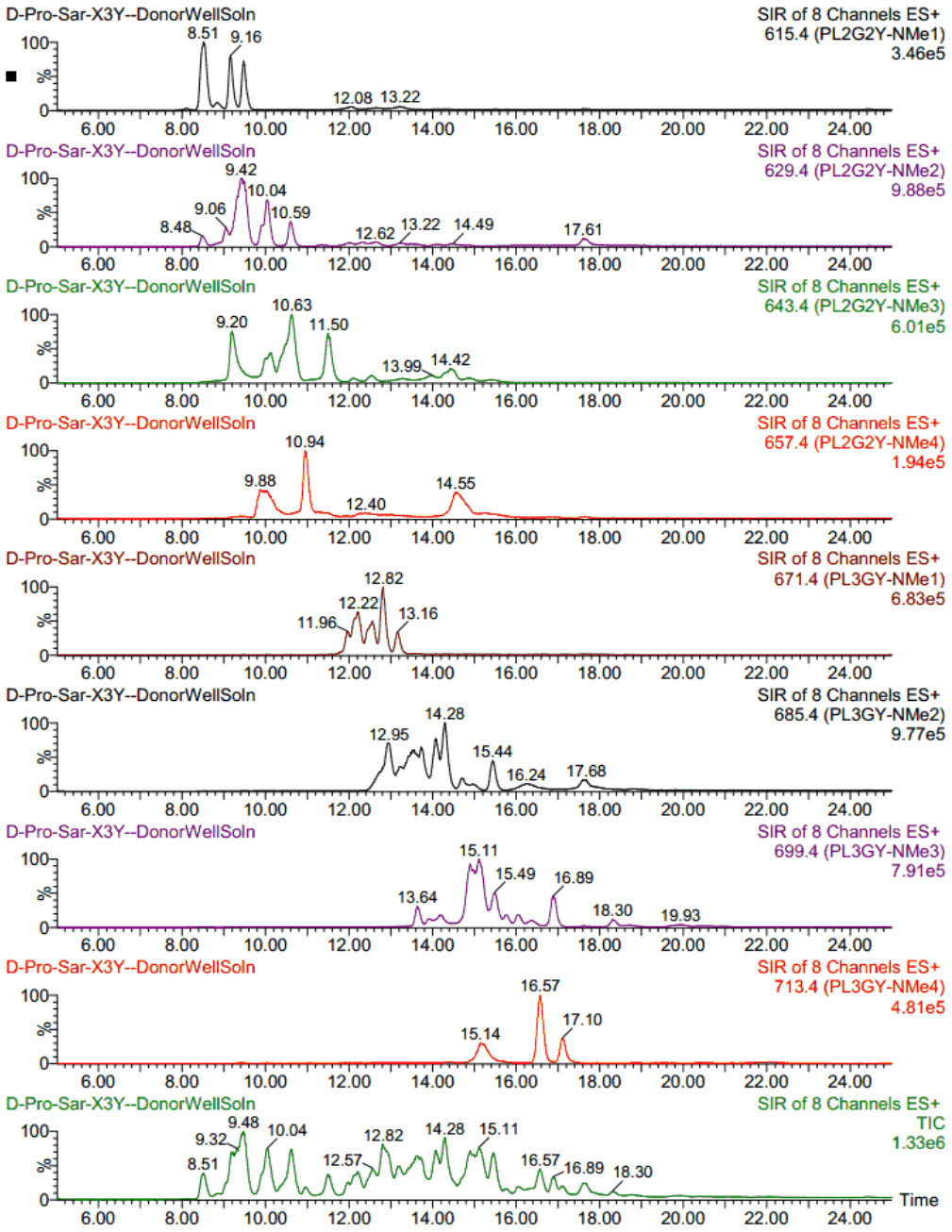

Sublibrary 12 Acceptor Well (t = 18 h)

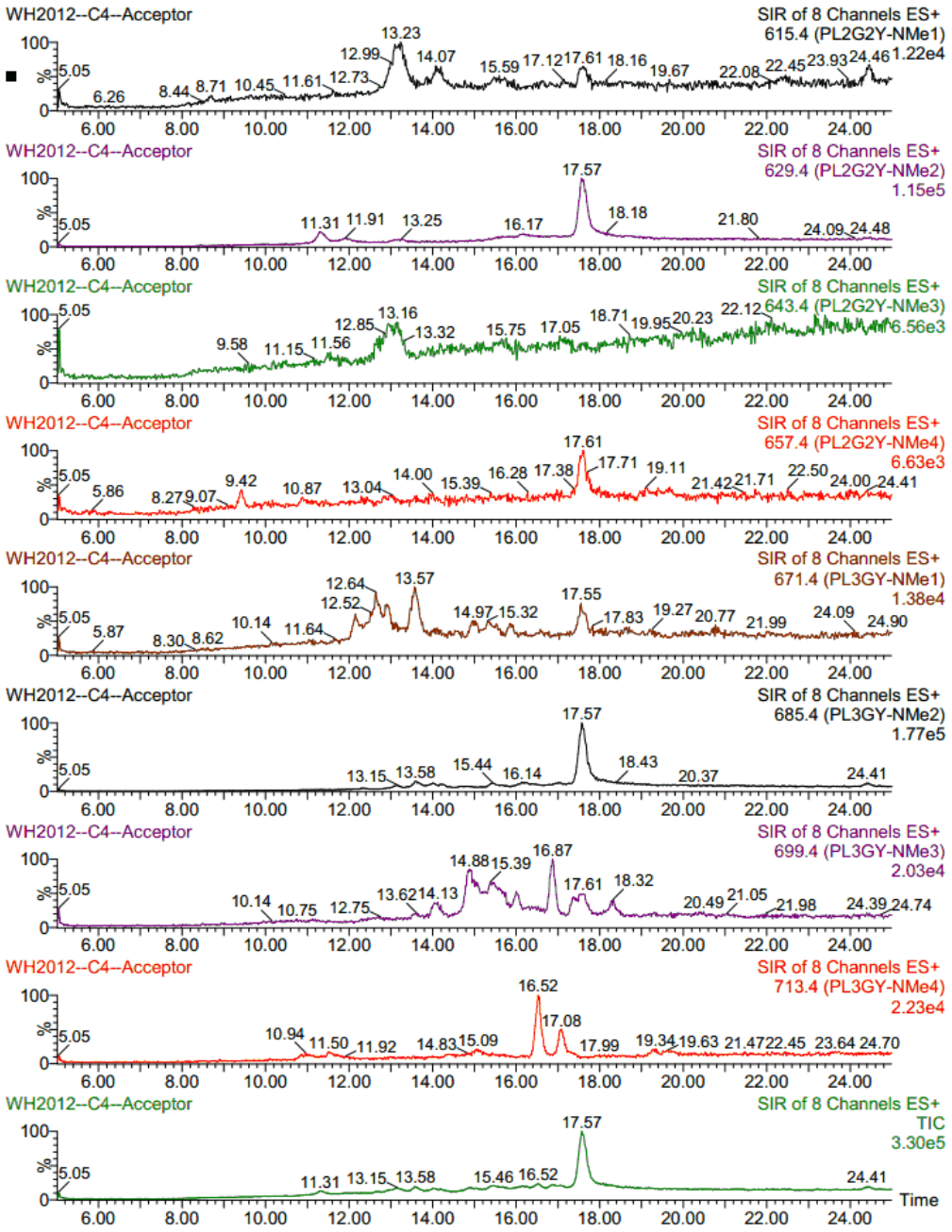

Sublibrary 12 Blank

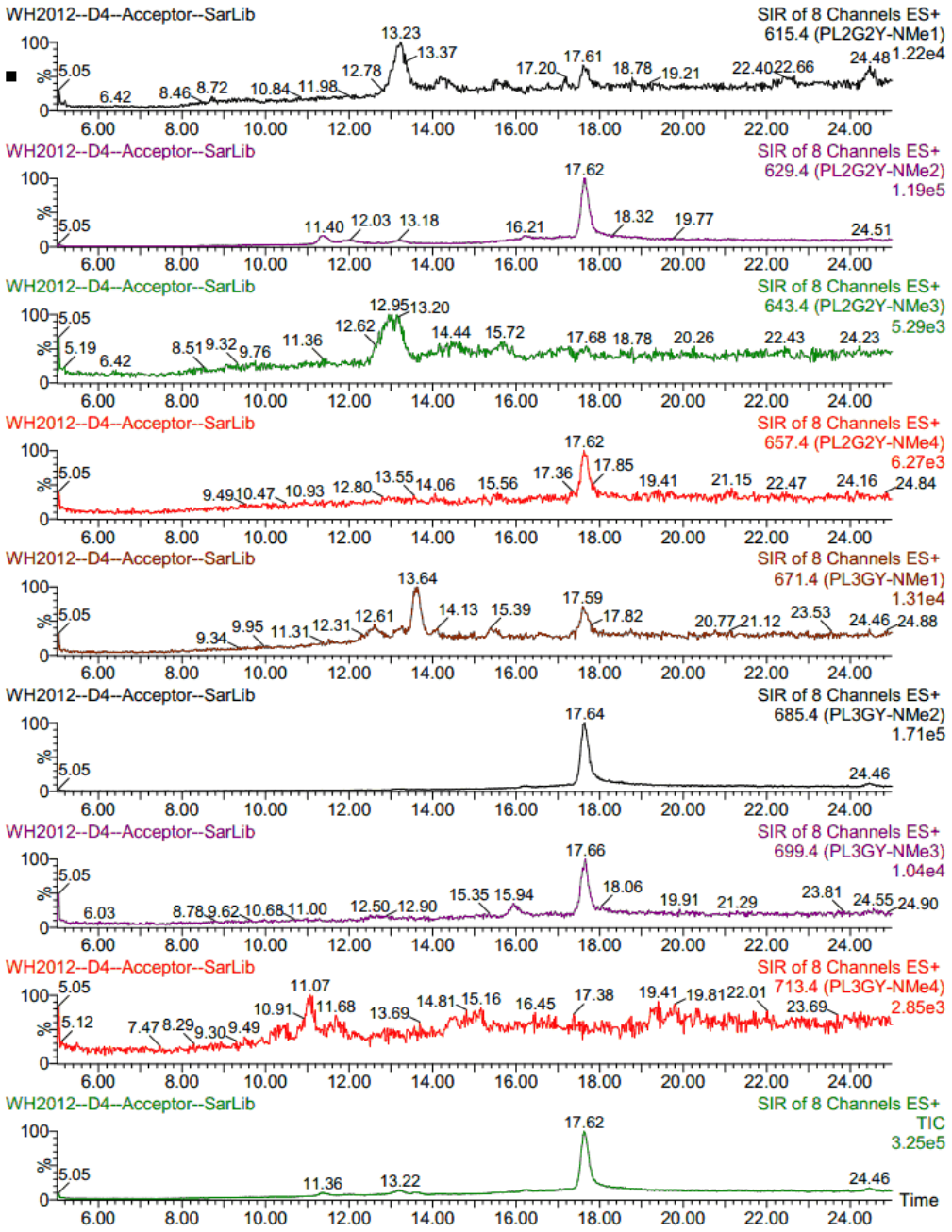

LCMS Spectra for Compound 2.4

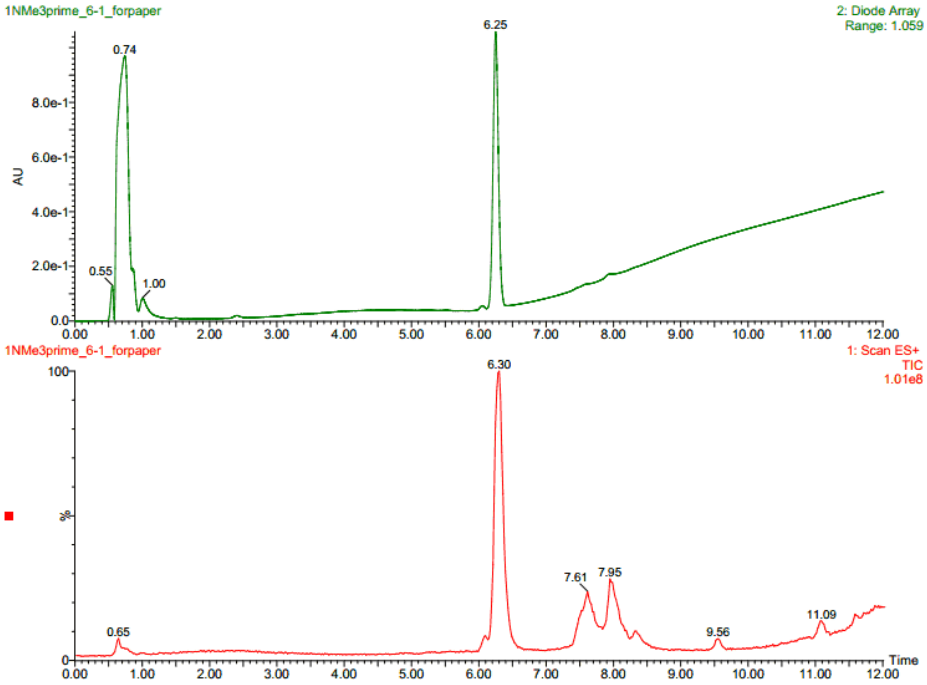

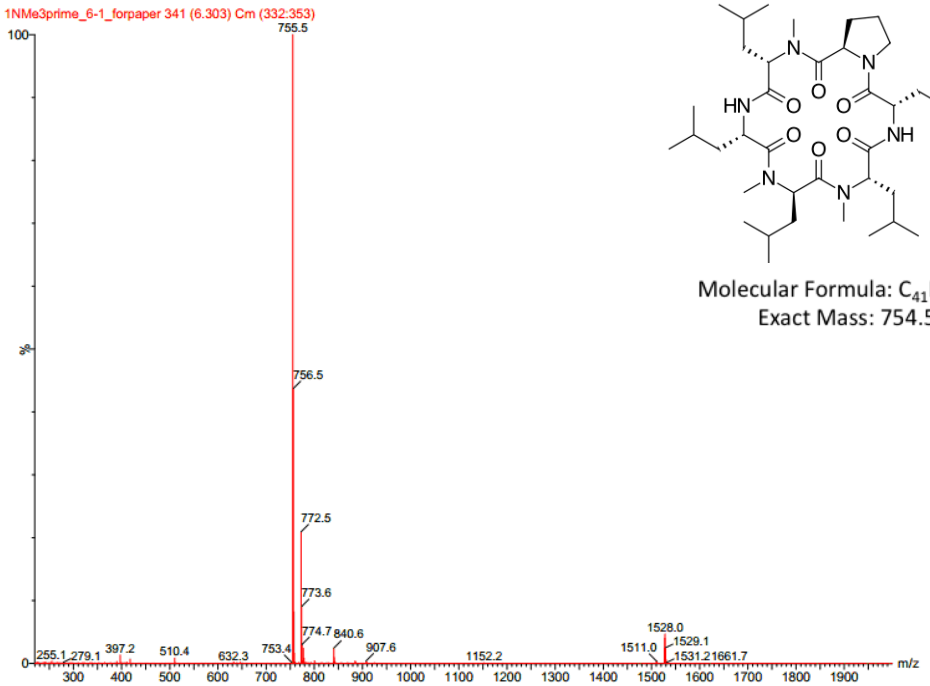

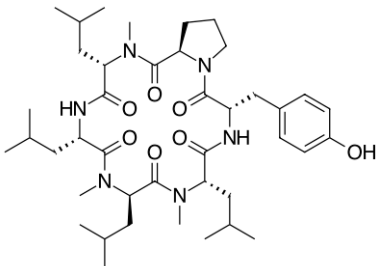

Molecular Formula: $C_{41}H_{66}N_6O_7$
Exact Mass: 754.50

HNMR Spectrum for Compound 2.4

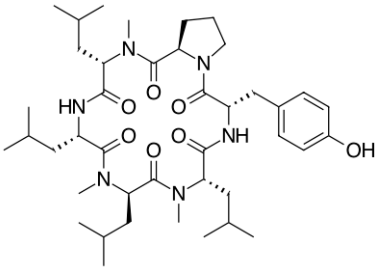

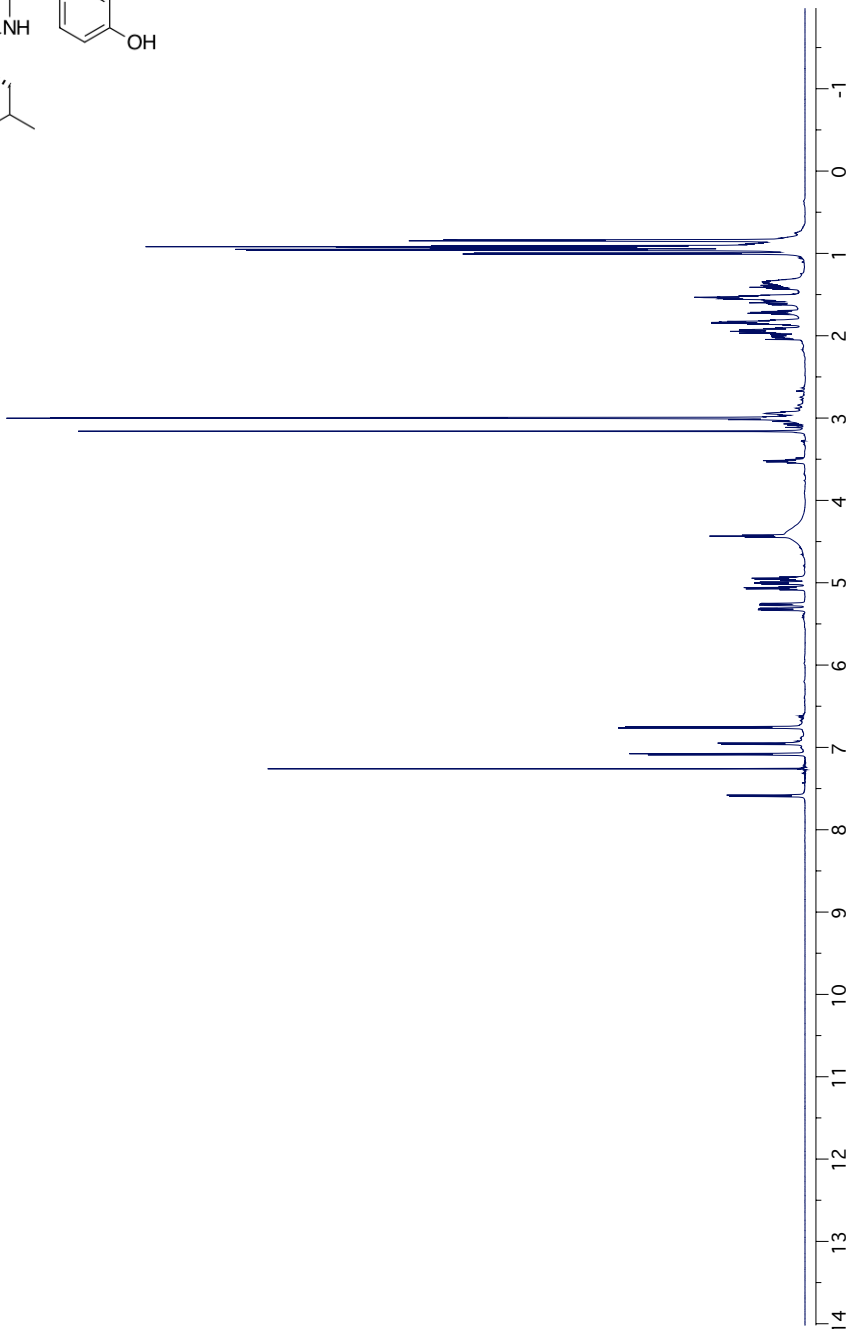

LCMS Spectra for Compound 2.5

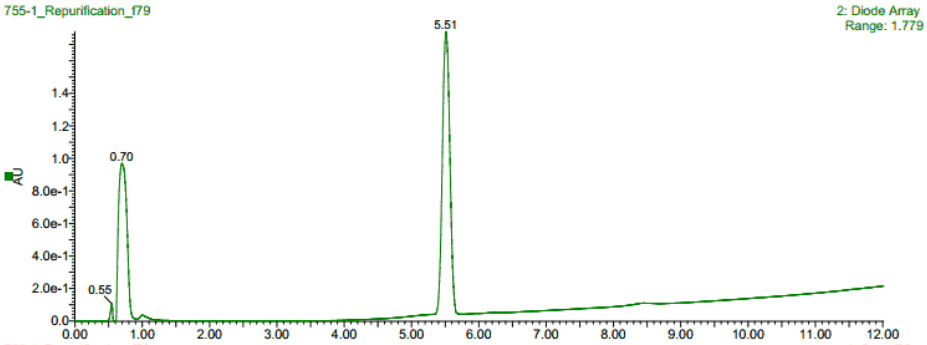

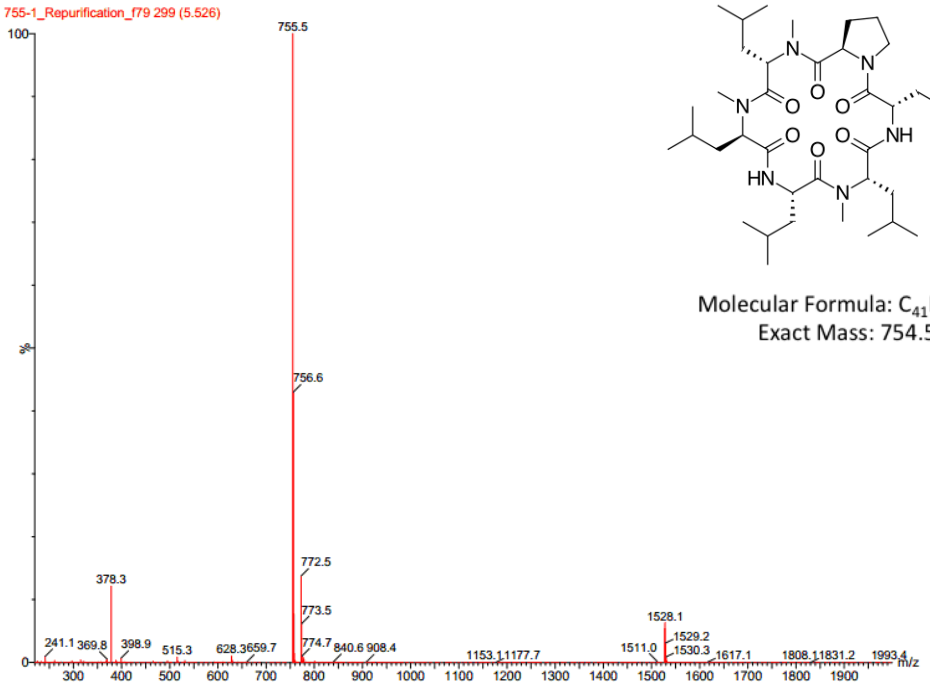

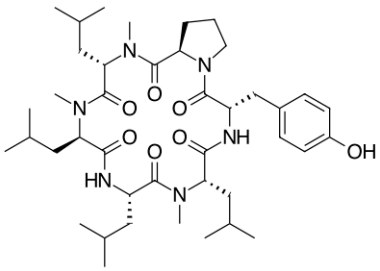

Molecular Formula: $C_{41}H_{66}N_6O_7$
Exact Mass: 754.50

HNMR Spectrum for Compound 2.5

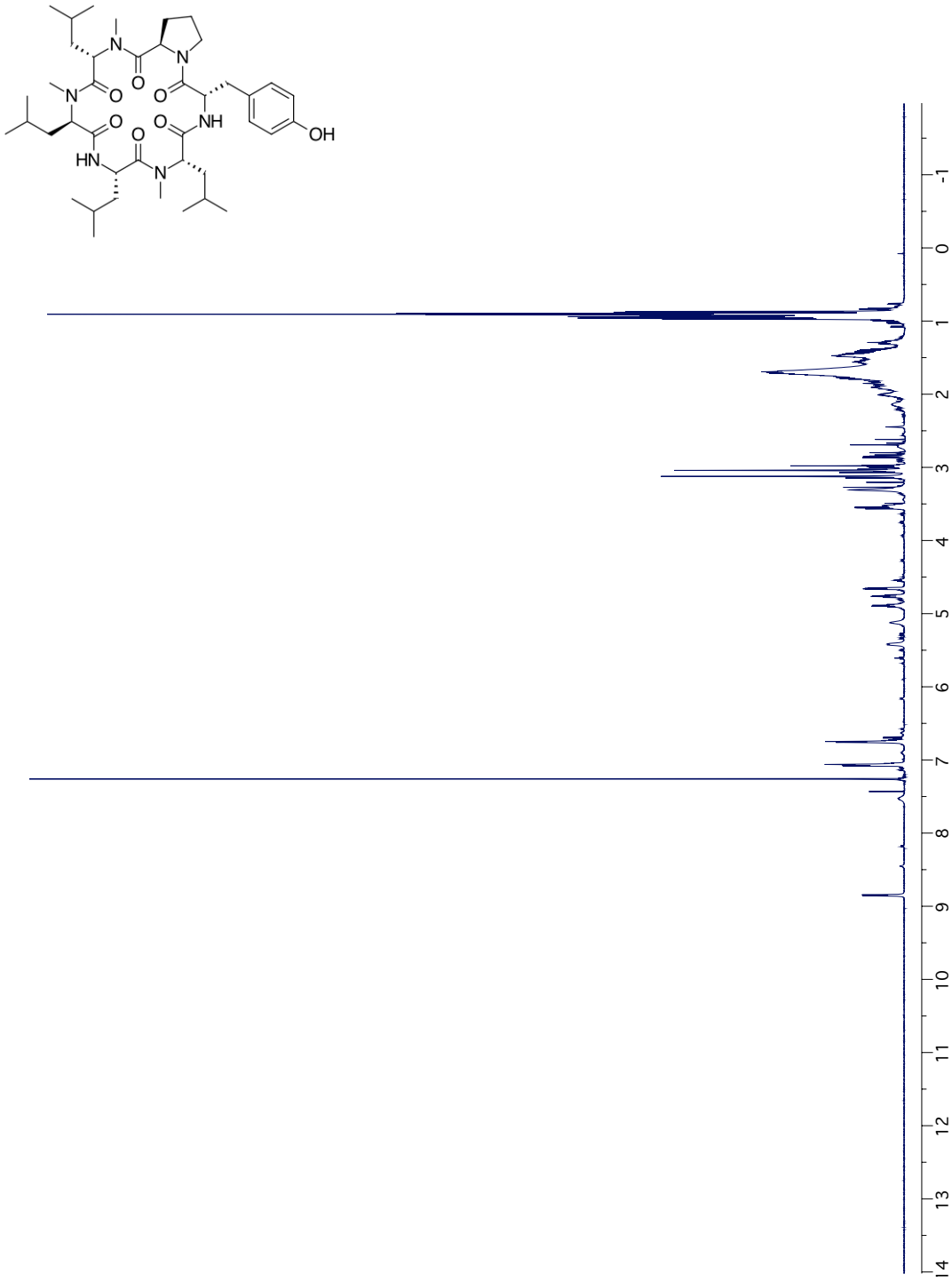

LCMS Spectra for Compound 2.6

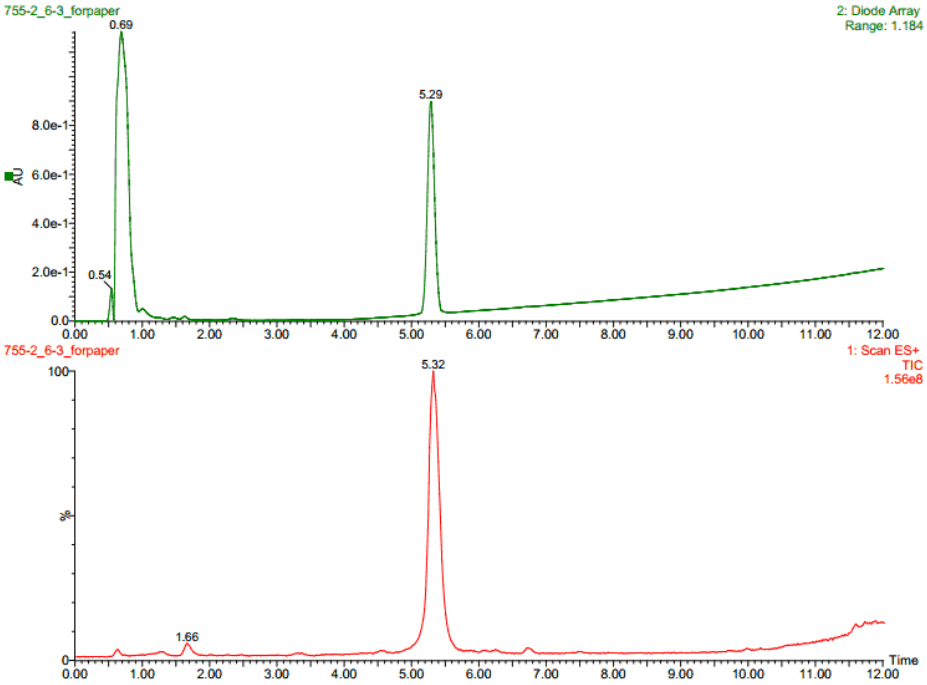

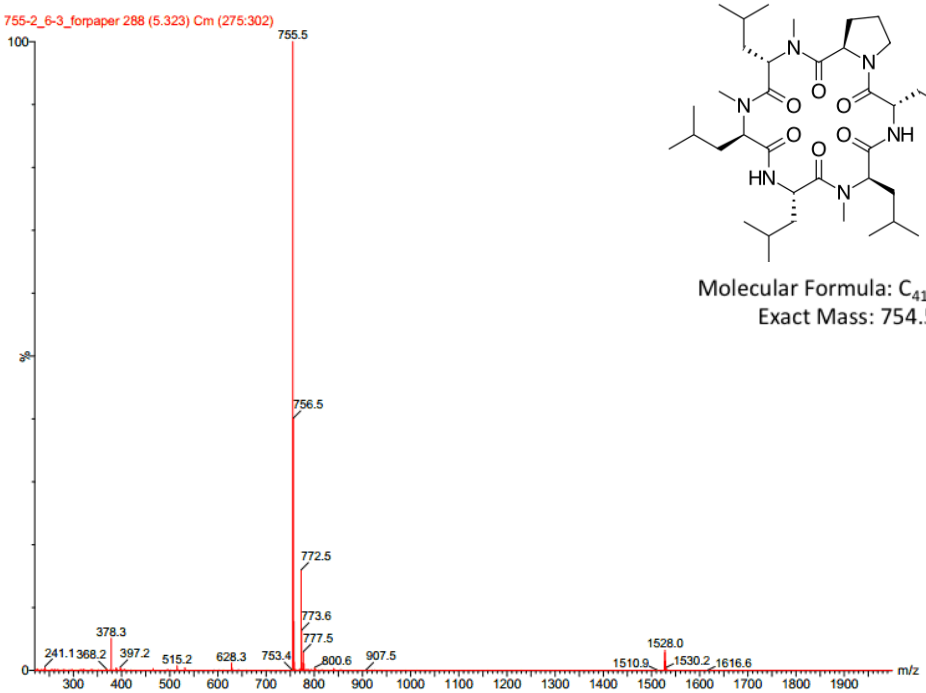

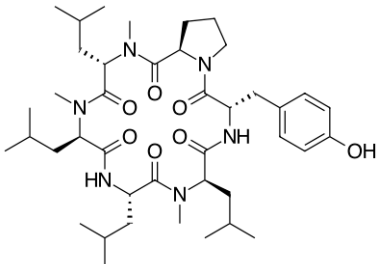

Molecular Formula: $C_{41}H_{66}N_6O_7$
Exact Mass: 754.50

HNMR Spectrum for Compound 2.6

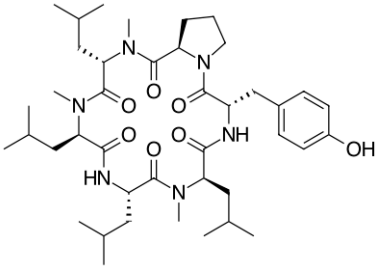

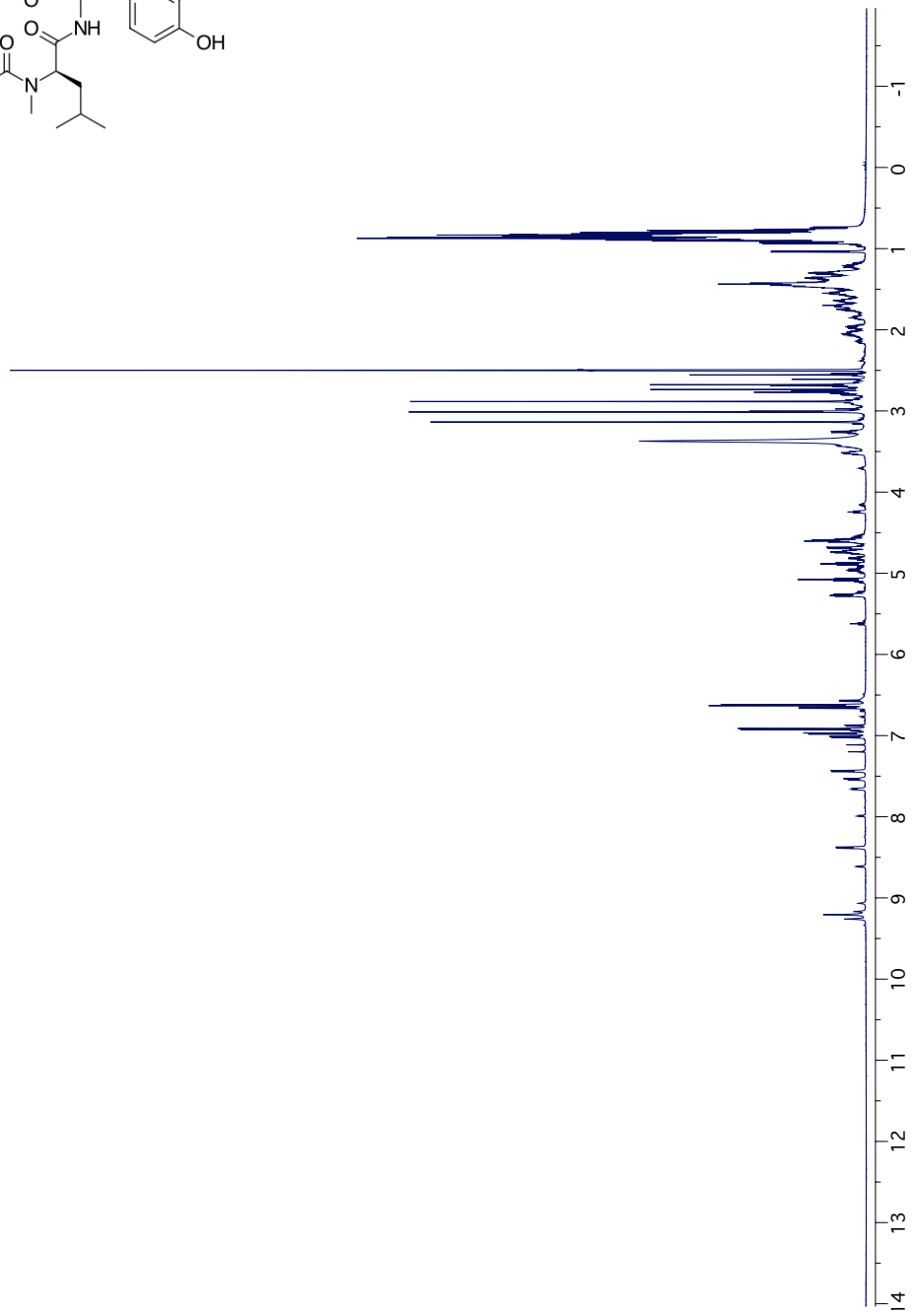

LCMS Spectra for Compound 2.7

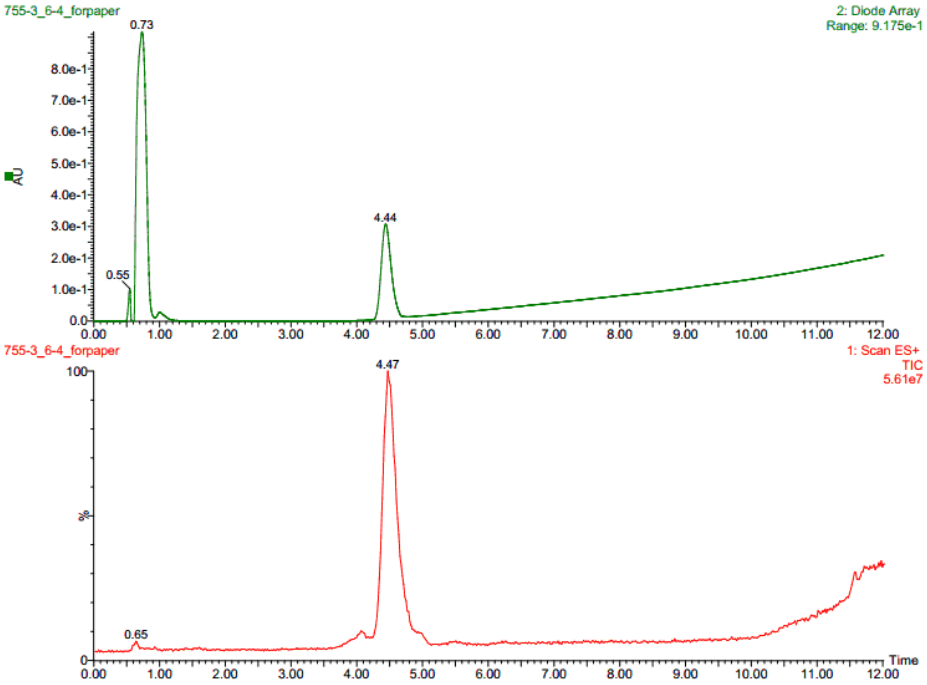

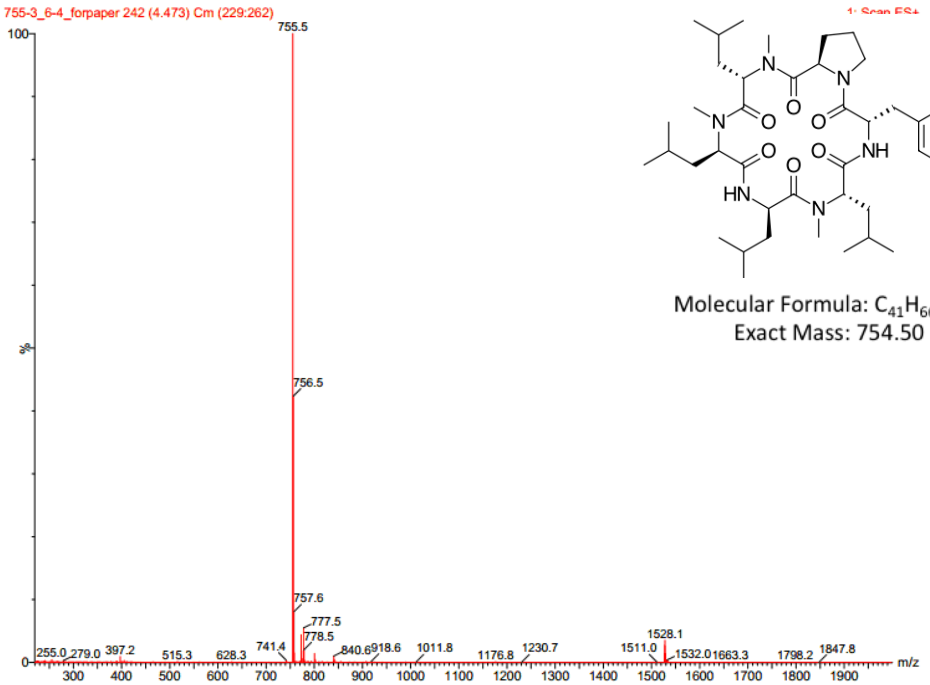

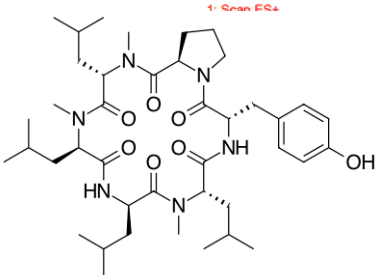

Molecular Formula: $C_{41}H_{66}N_6O_7$
Exact Mass: 754.50

HNMR Spectrum for Compound 2.7

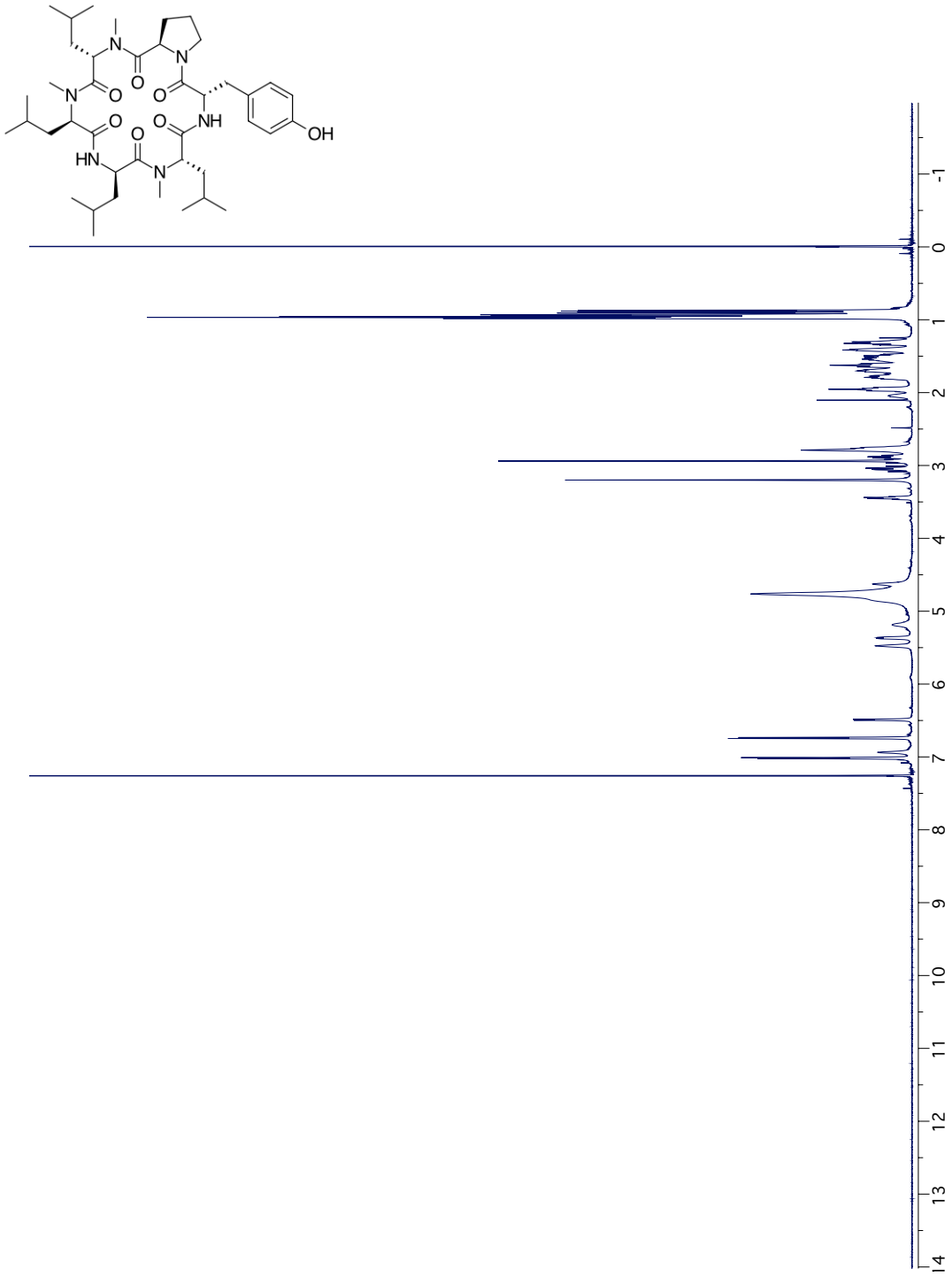

LCMS Spectra for Compound 2.8

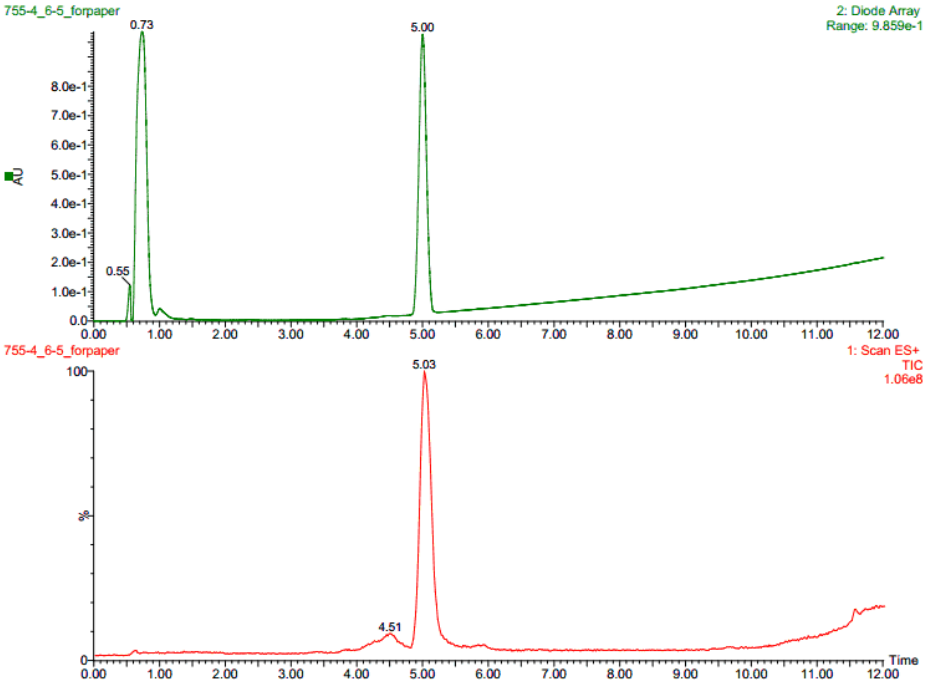

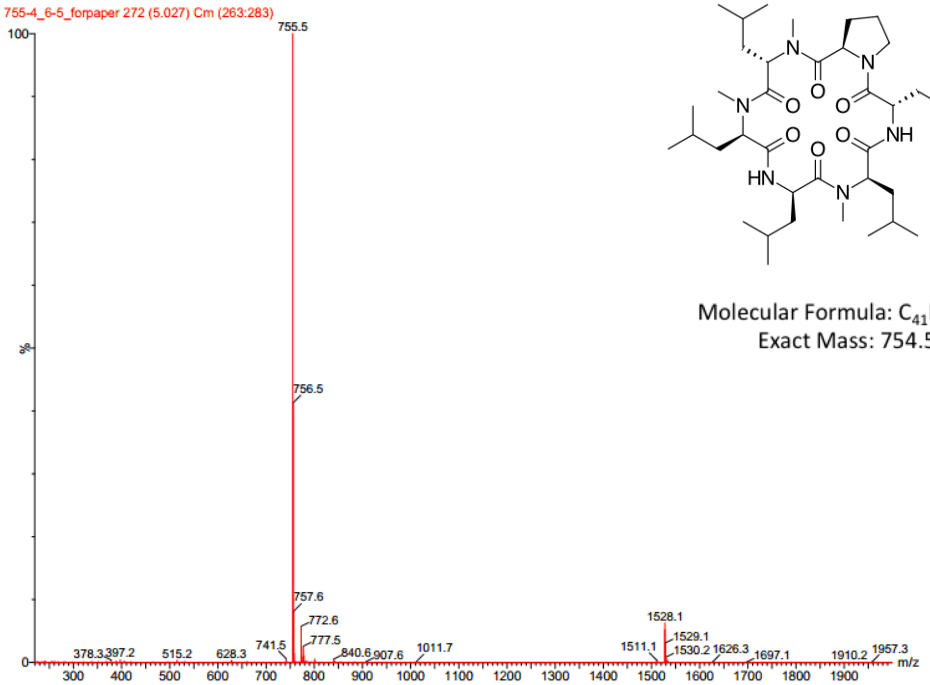

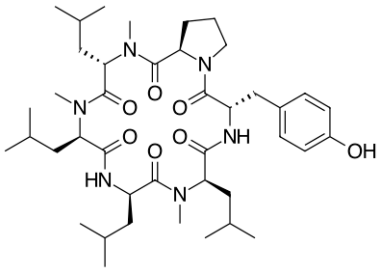

Molecular Formula: $C_{41}H_{66}N_6O_7$
Exact Mass: 754.50

HNMR Spectrum for Compound 2.8

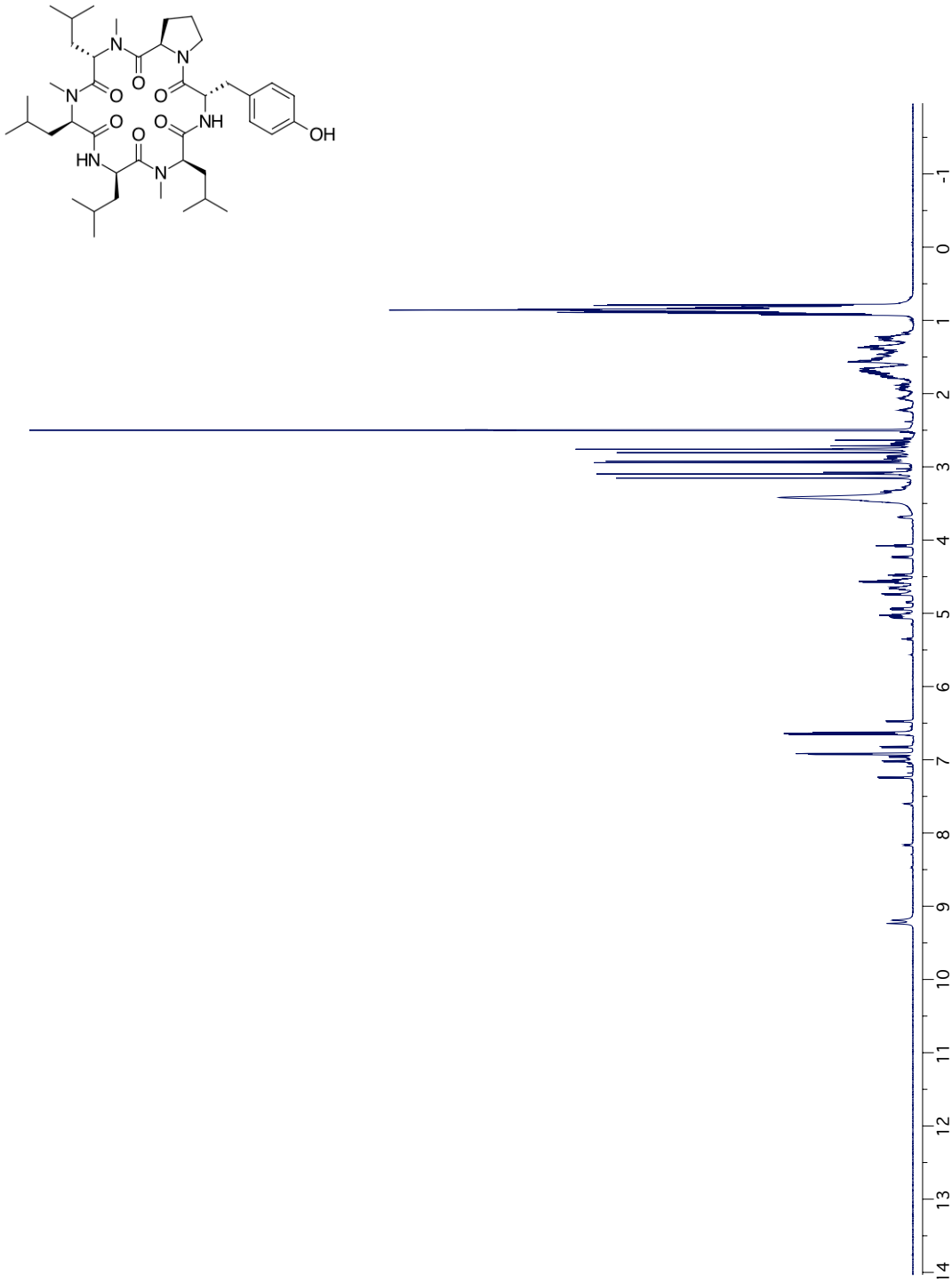

LCMS Spectra of Compound 2.9

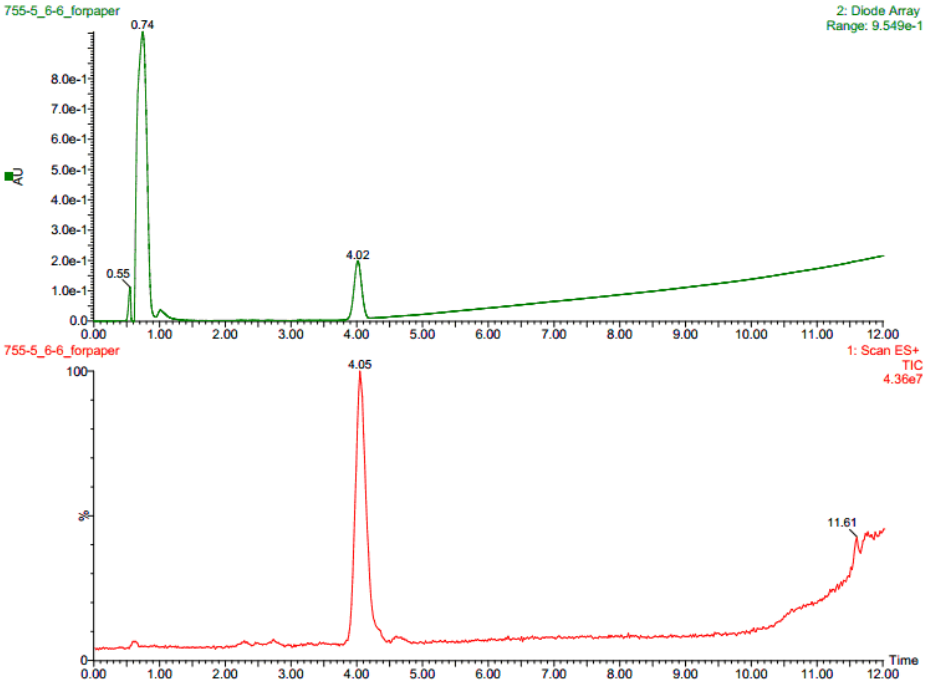

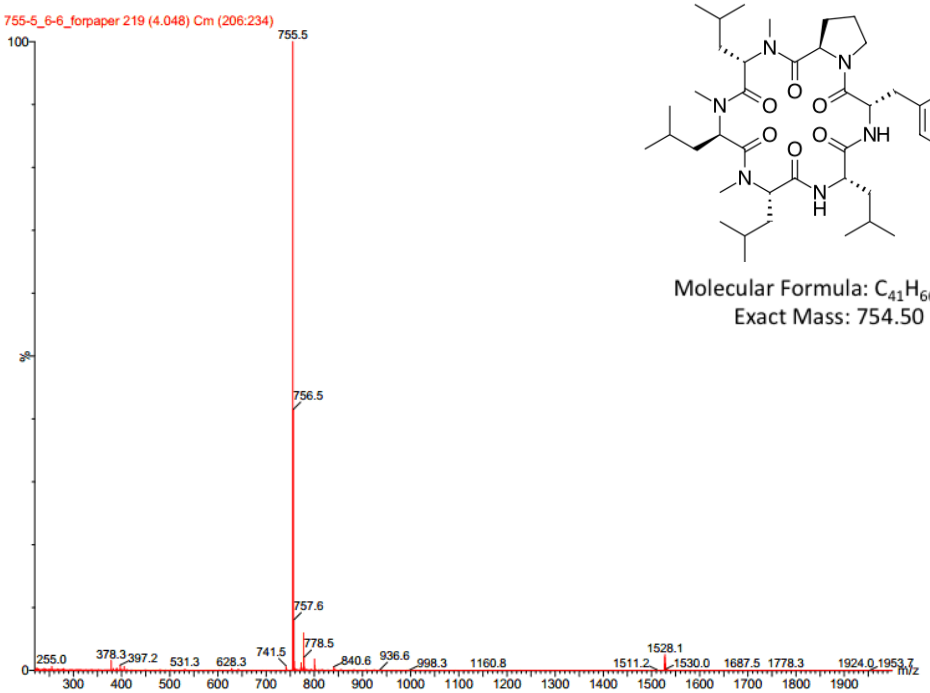

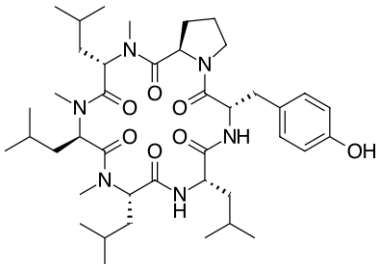

Molecular Formula: $C_{41}H_{66}N_6O_7$
Exact Mass: 754.50

HNMR Spectrum for Compound 2.9

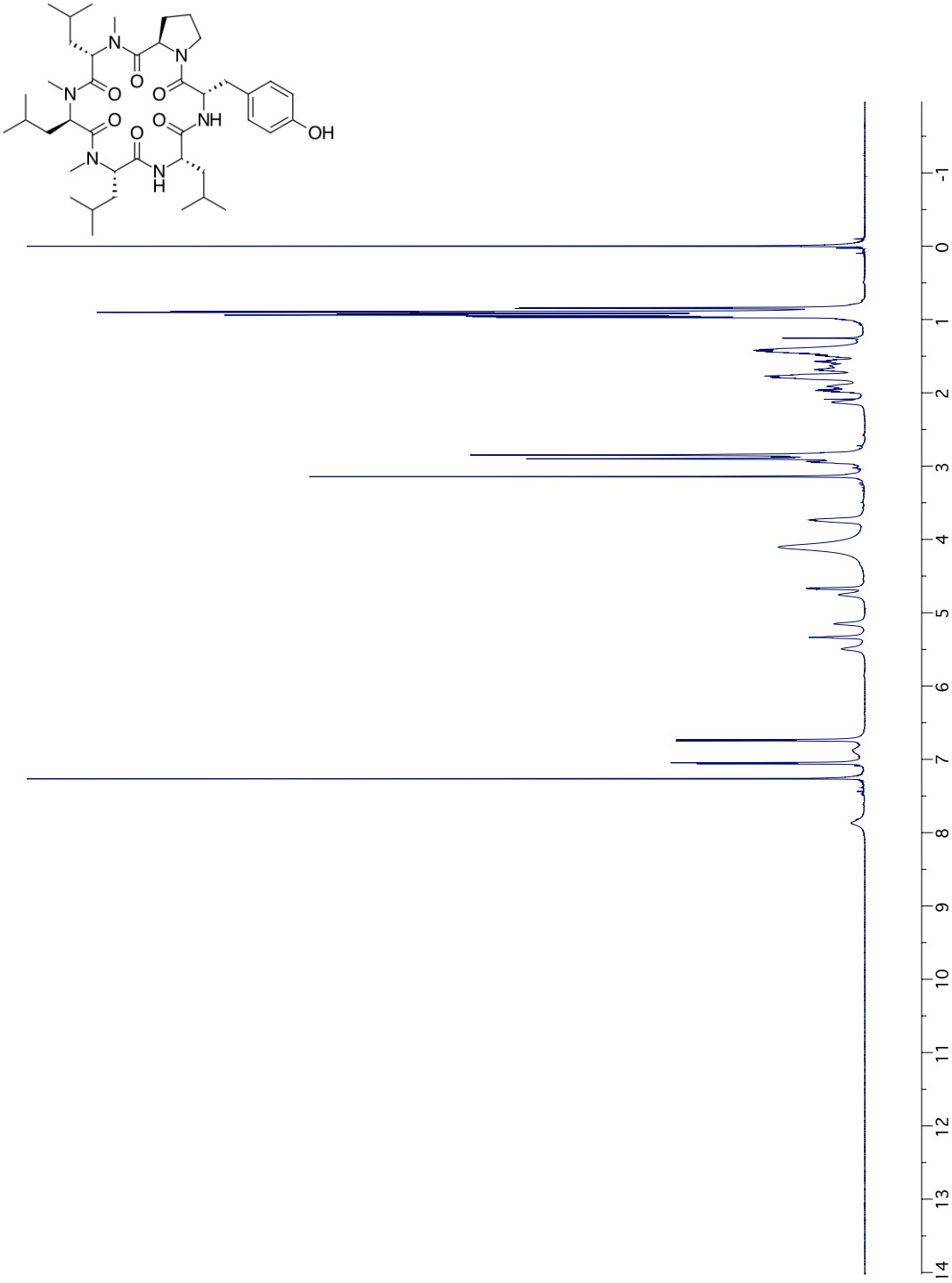

LCMS Spectra for Compound 2.10

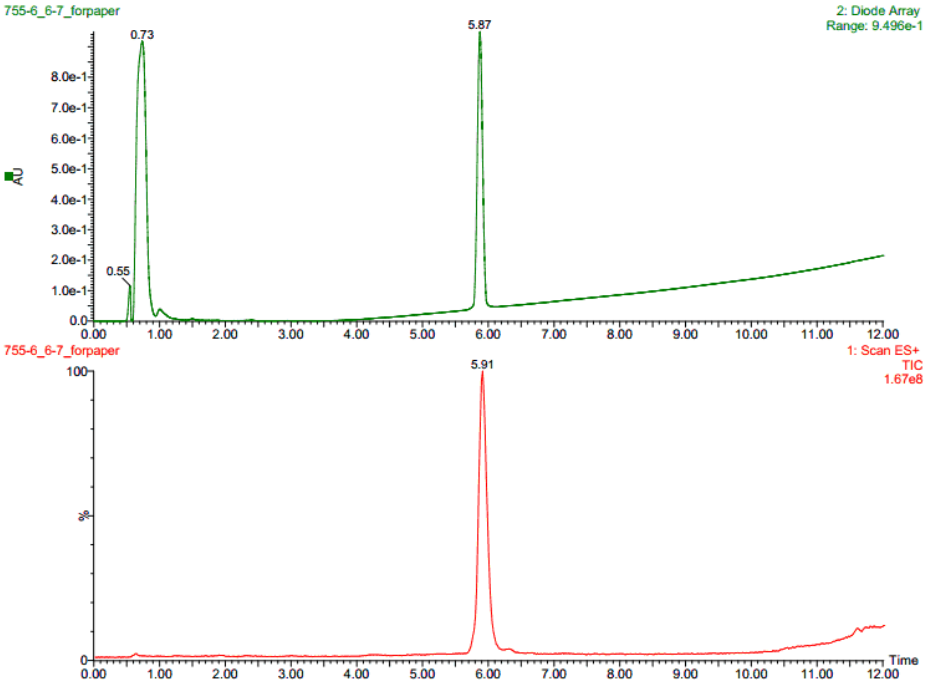

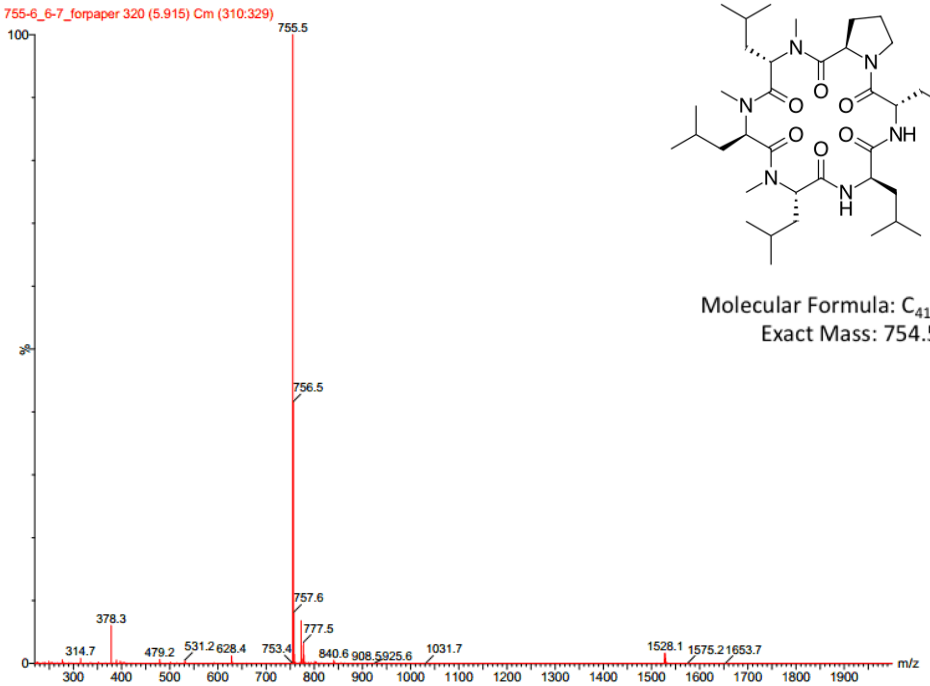

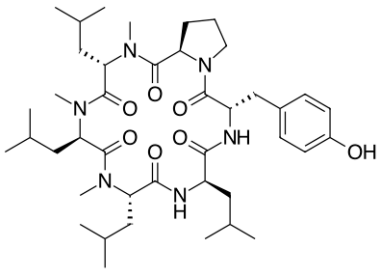

Molecular Formula: $C_{41}H_{66}N_6O_7$
Exact Mass: 754.50

HNMR Spectrum for Compound 2.10

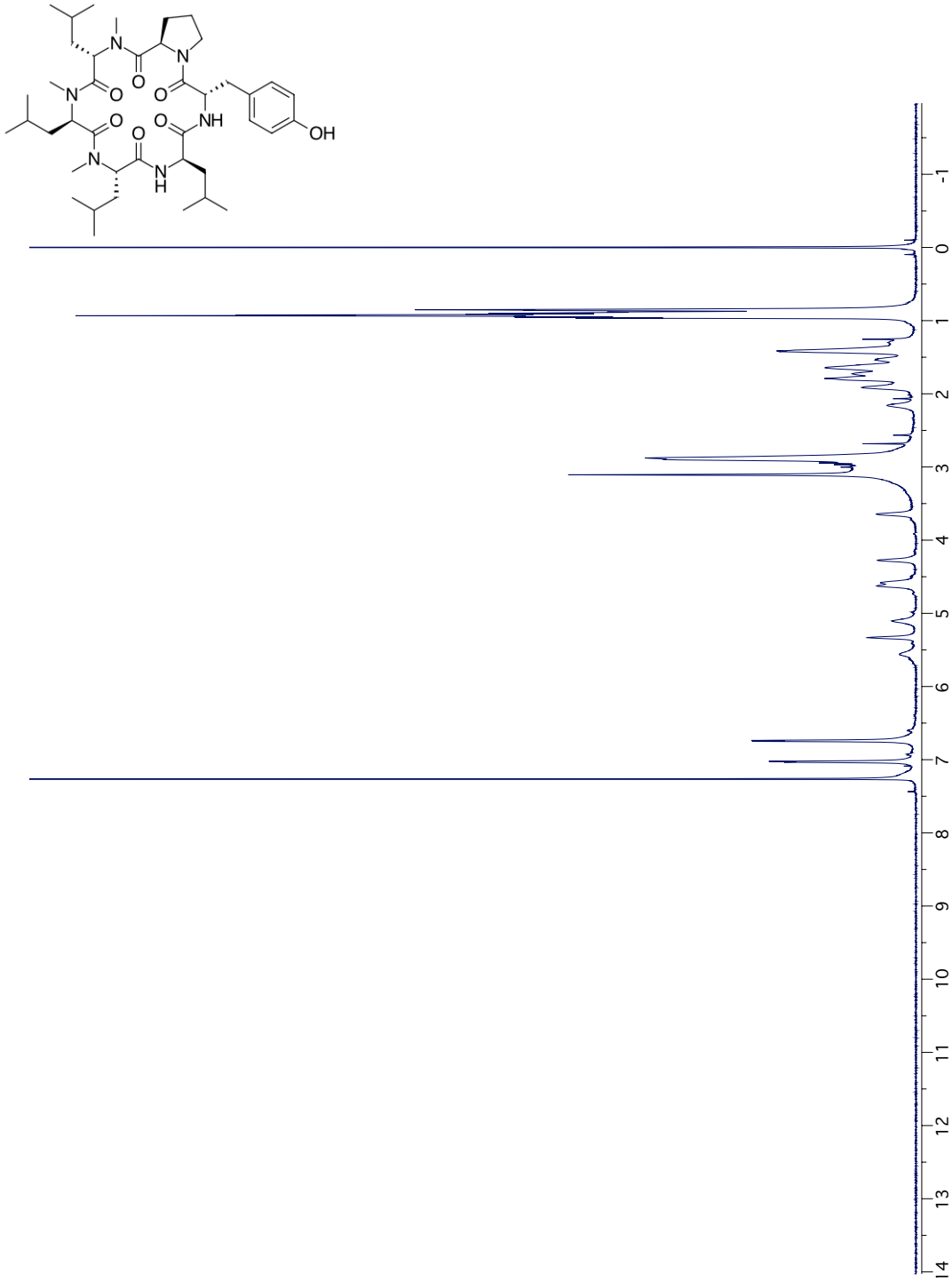

LCMS Spectra for Compound 2.11

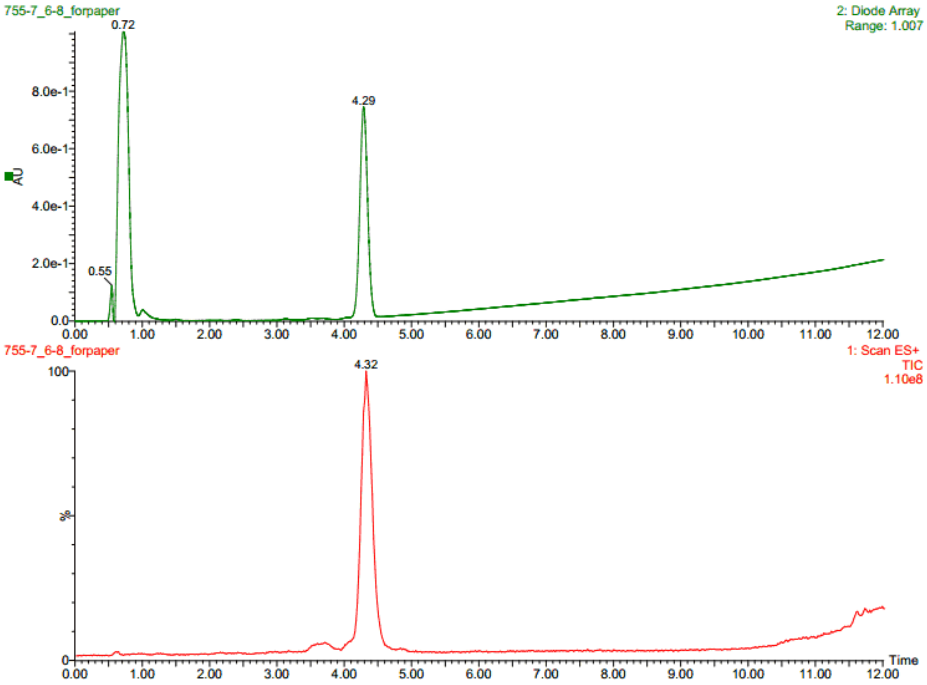

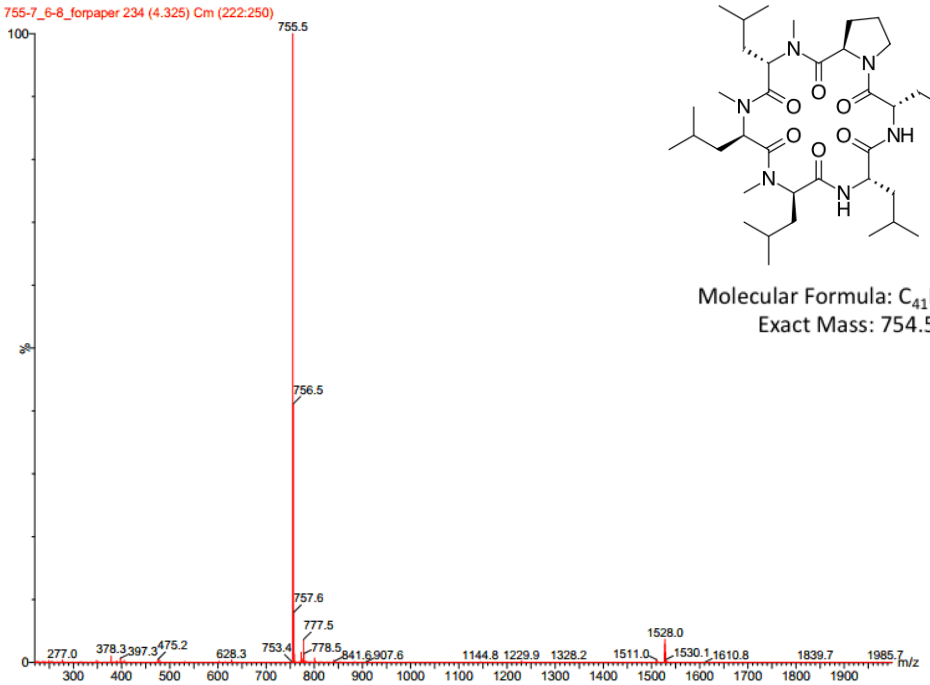

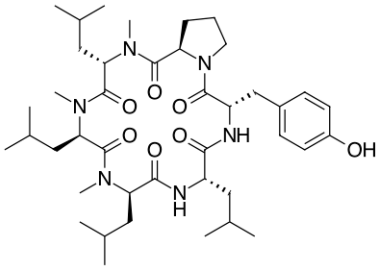

Molecular Formula: $C_{41}H_{66}N_6O_7$
Exact Mass: 754.50

HNMR Spectrum for Compound 2.11

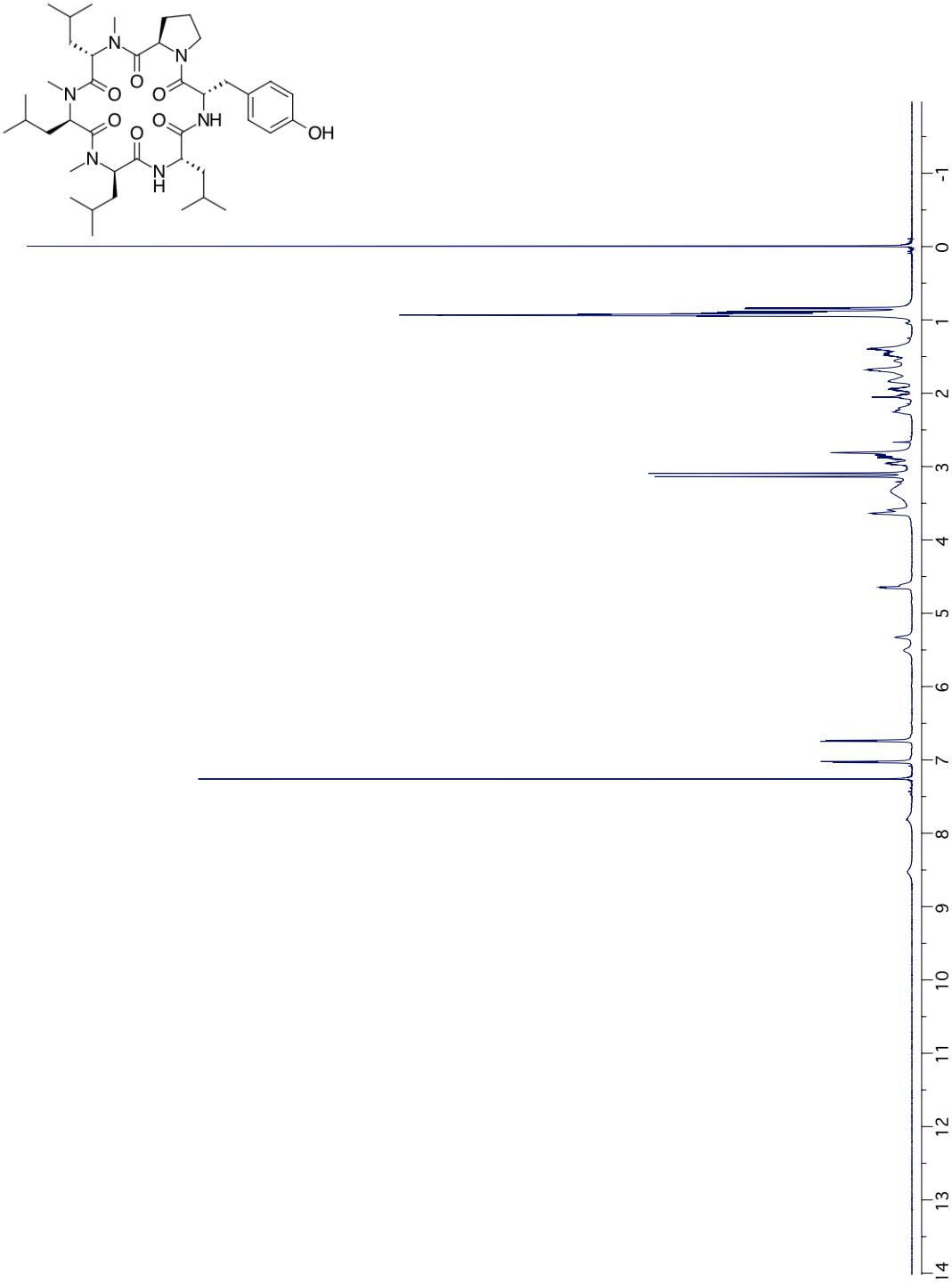

LCMS Spectra for Compound 2.12

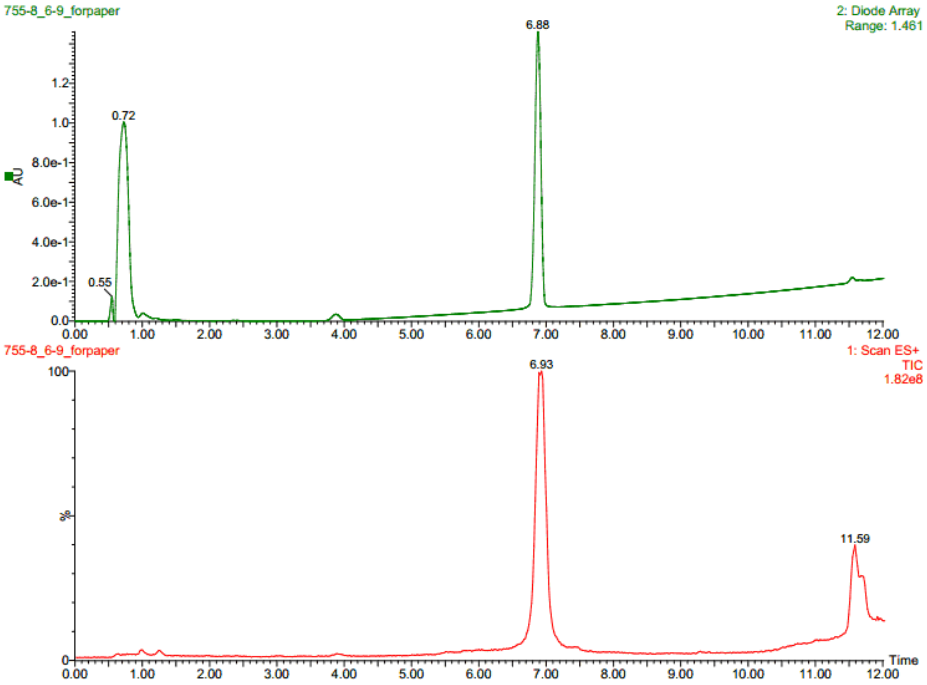

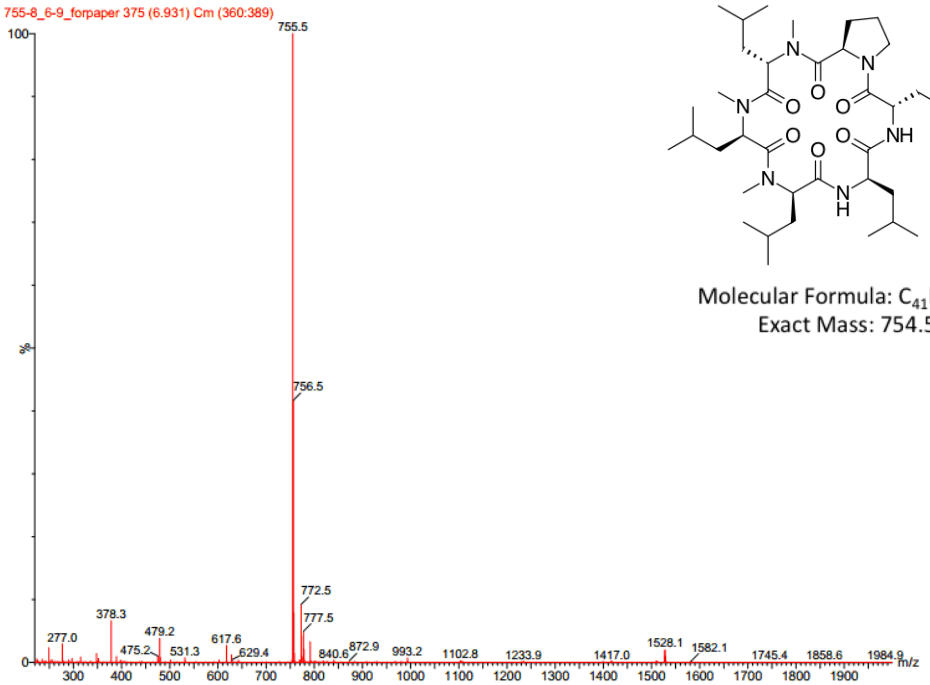

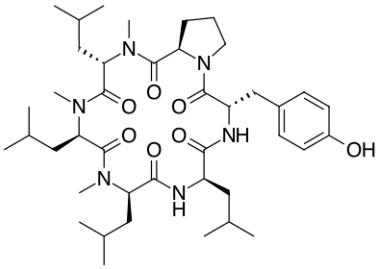

Molecular Formula: $C_{41}H_{66}N_6O_7$
Exact Mass: 754.50

HNMR Spectrum for Compound 2.12

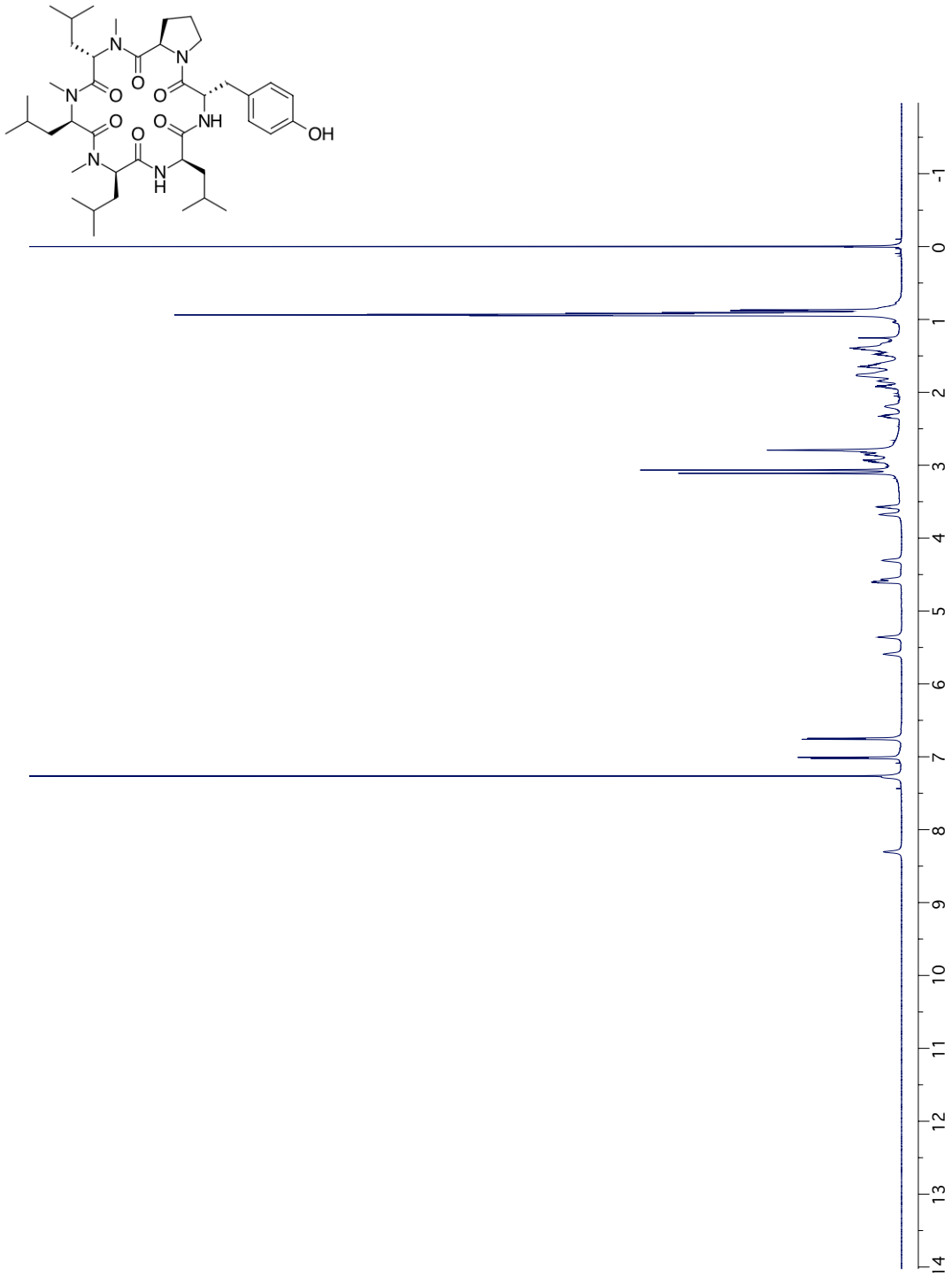

COSY for Compound 2.12

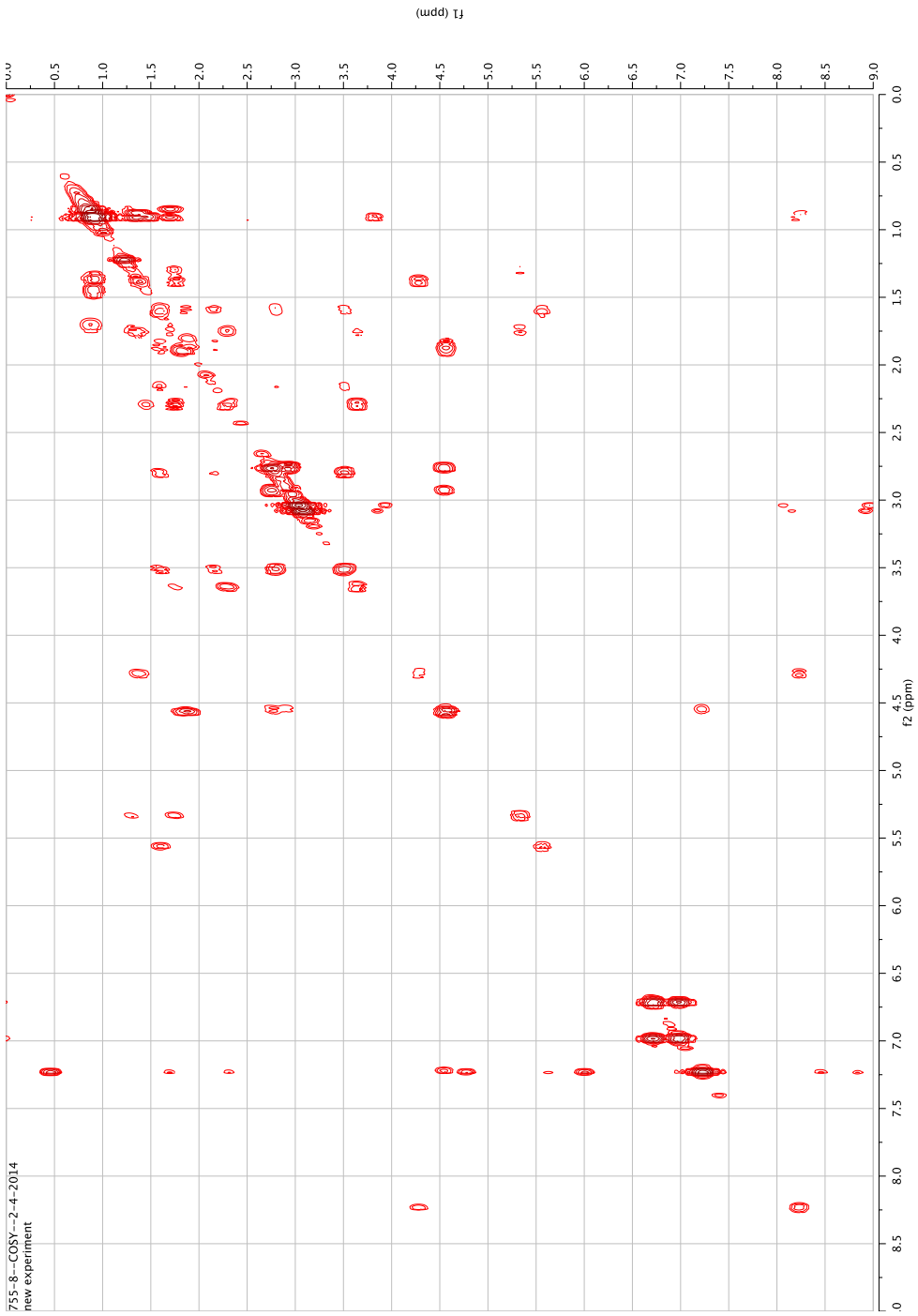

TOCSY for Compound 2.12

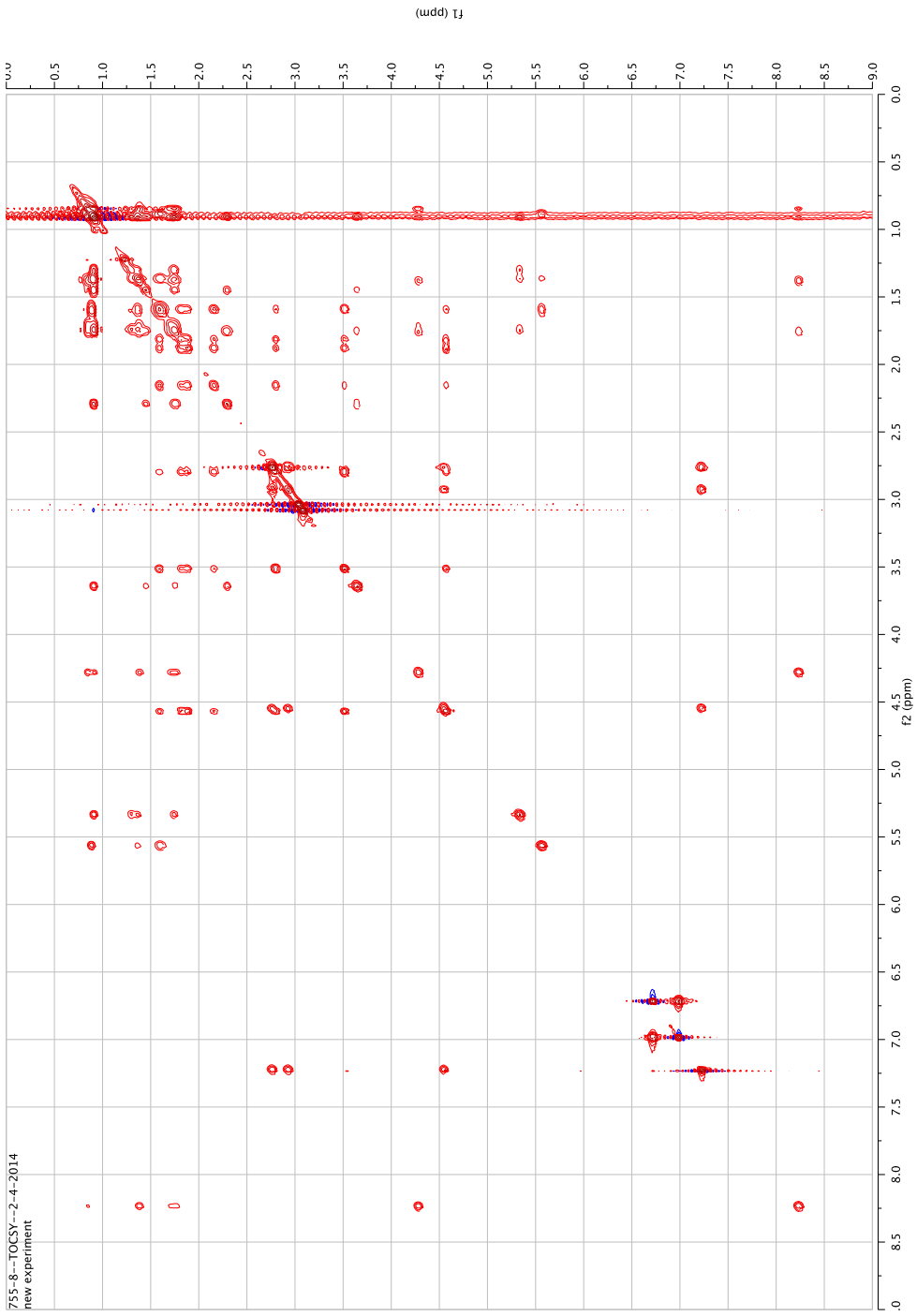

HSQC for Compound 2.12

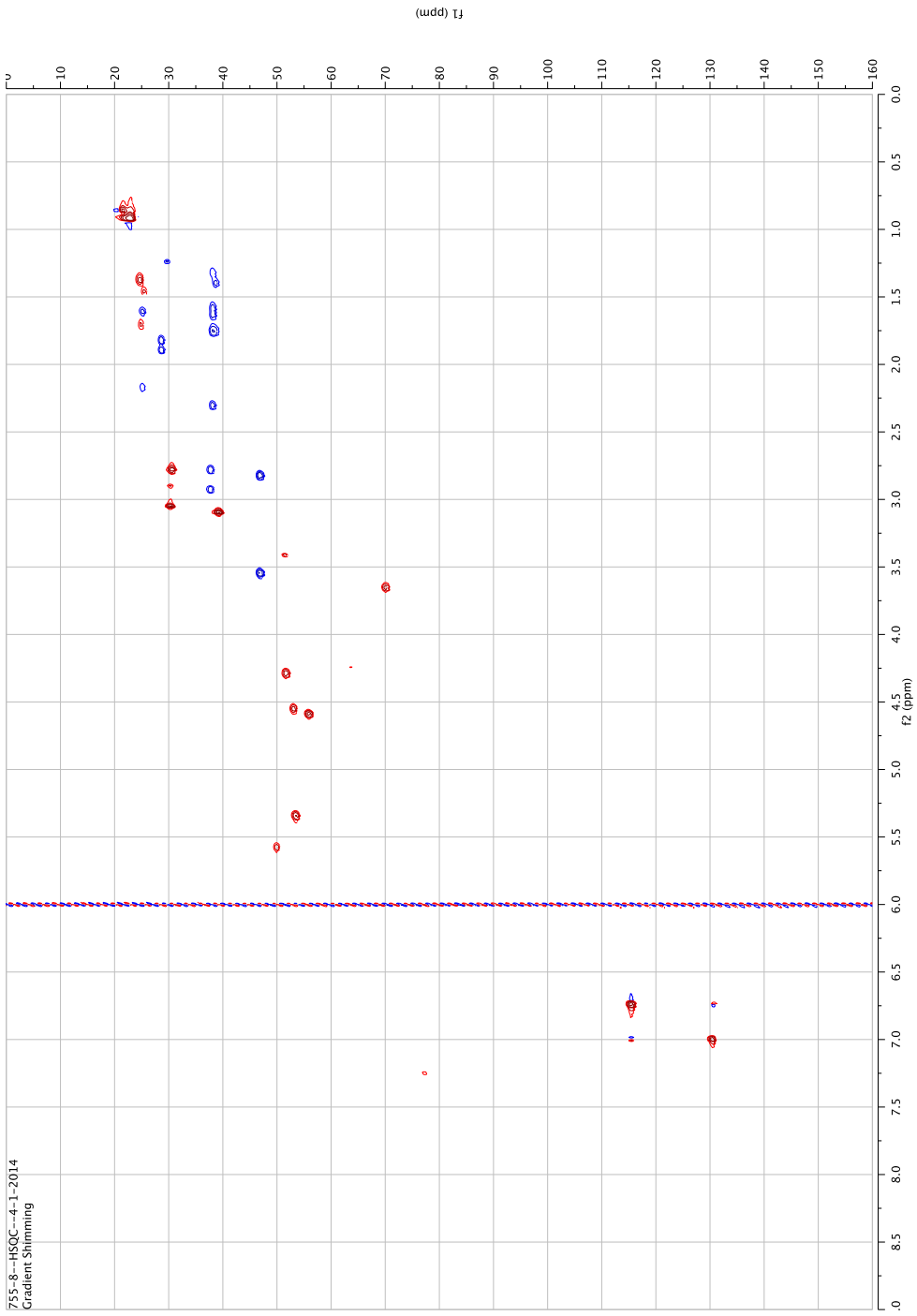

HMBC for Compound 2.12

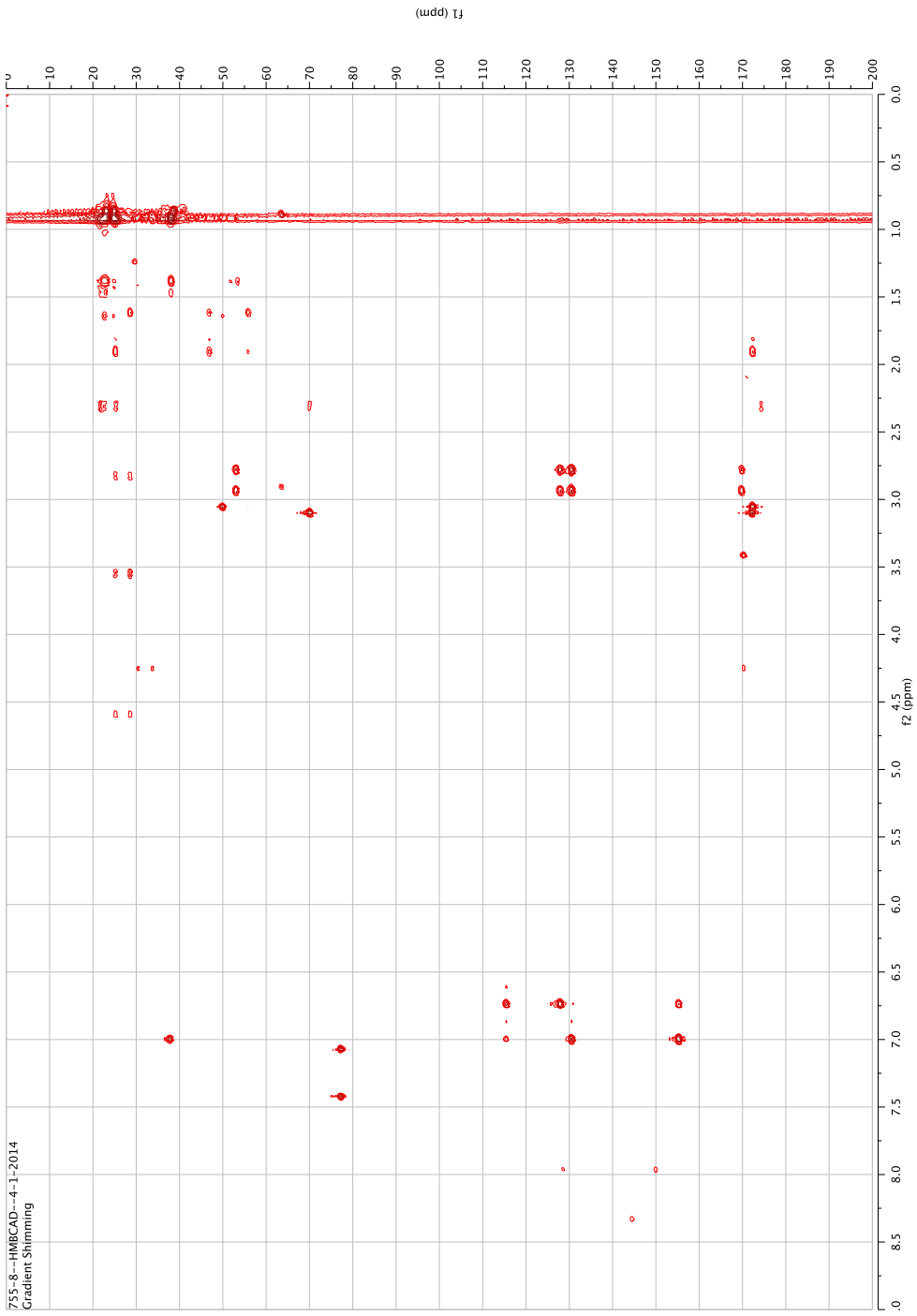

ROESY for Compound 2.12

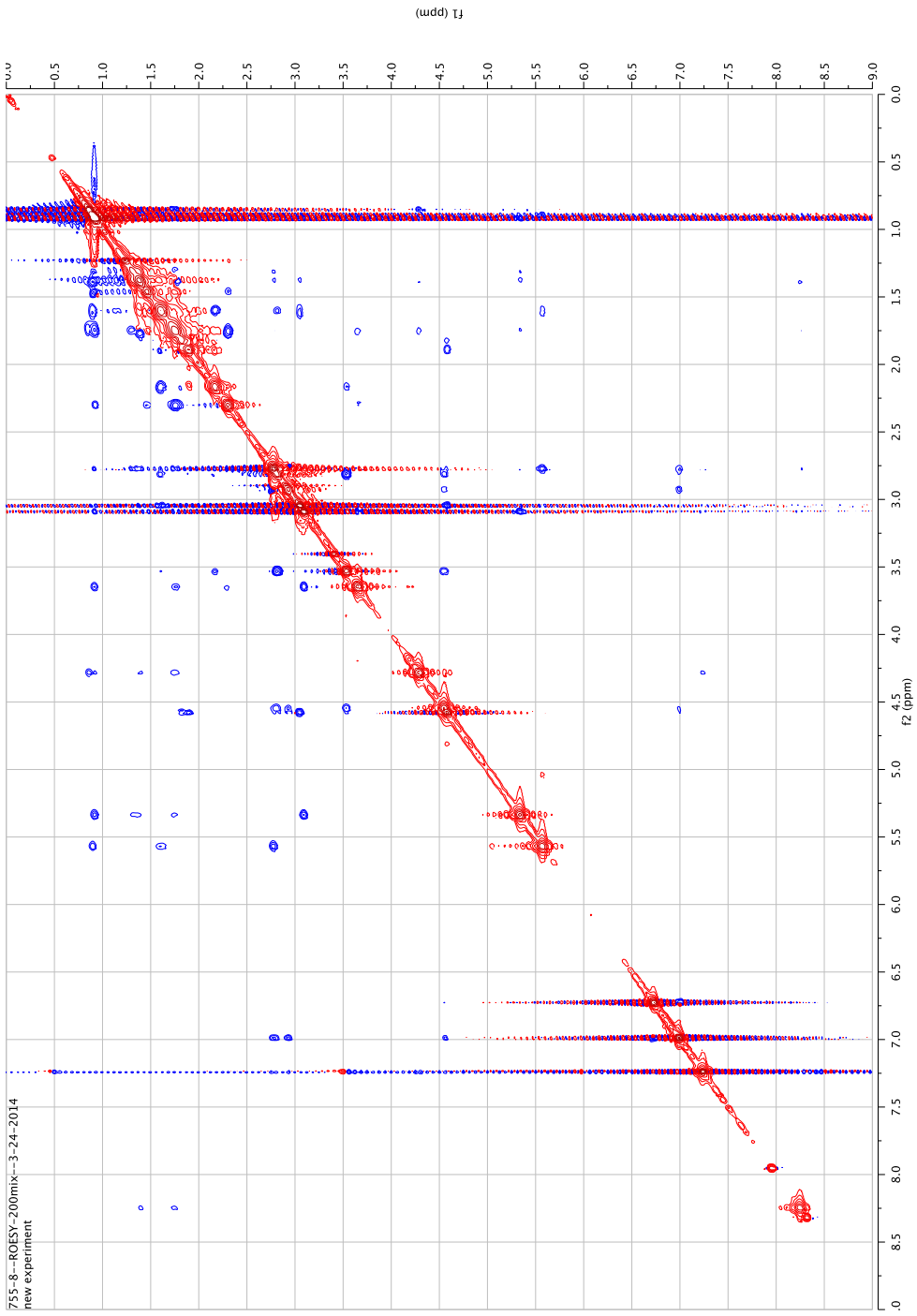

LCMS Spectra for Compound 2.15

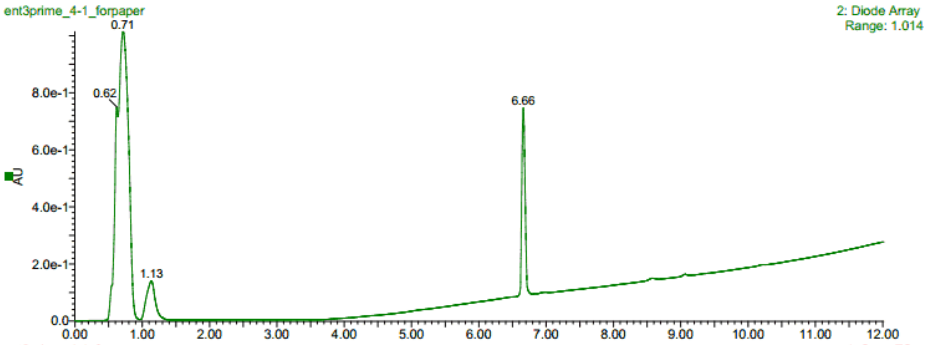

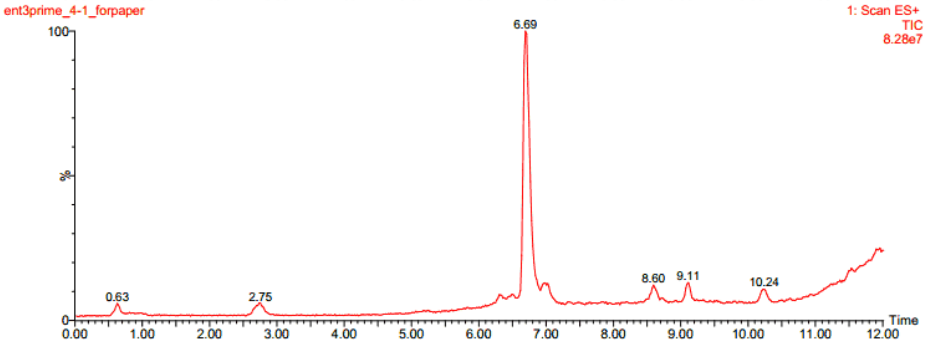

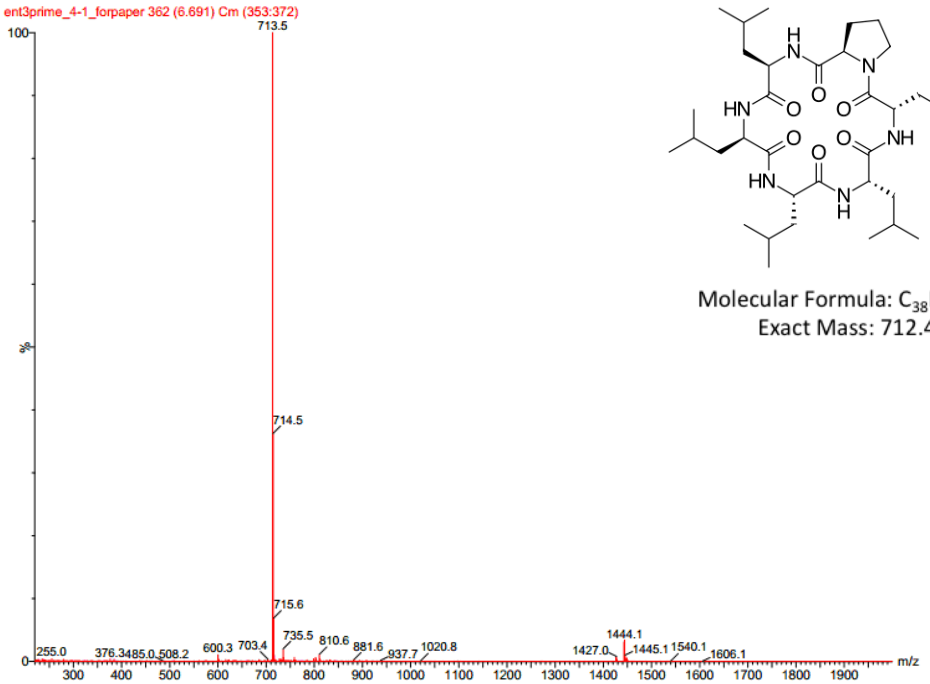

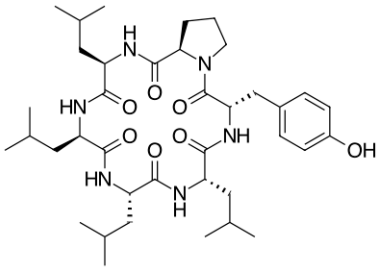

Molecular Formula: $C_{38}H_{60}N_6O_7$
Exact Mass: 712.45

HNMR Spectrum for Compound 2.15

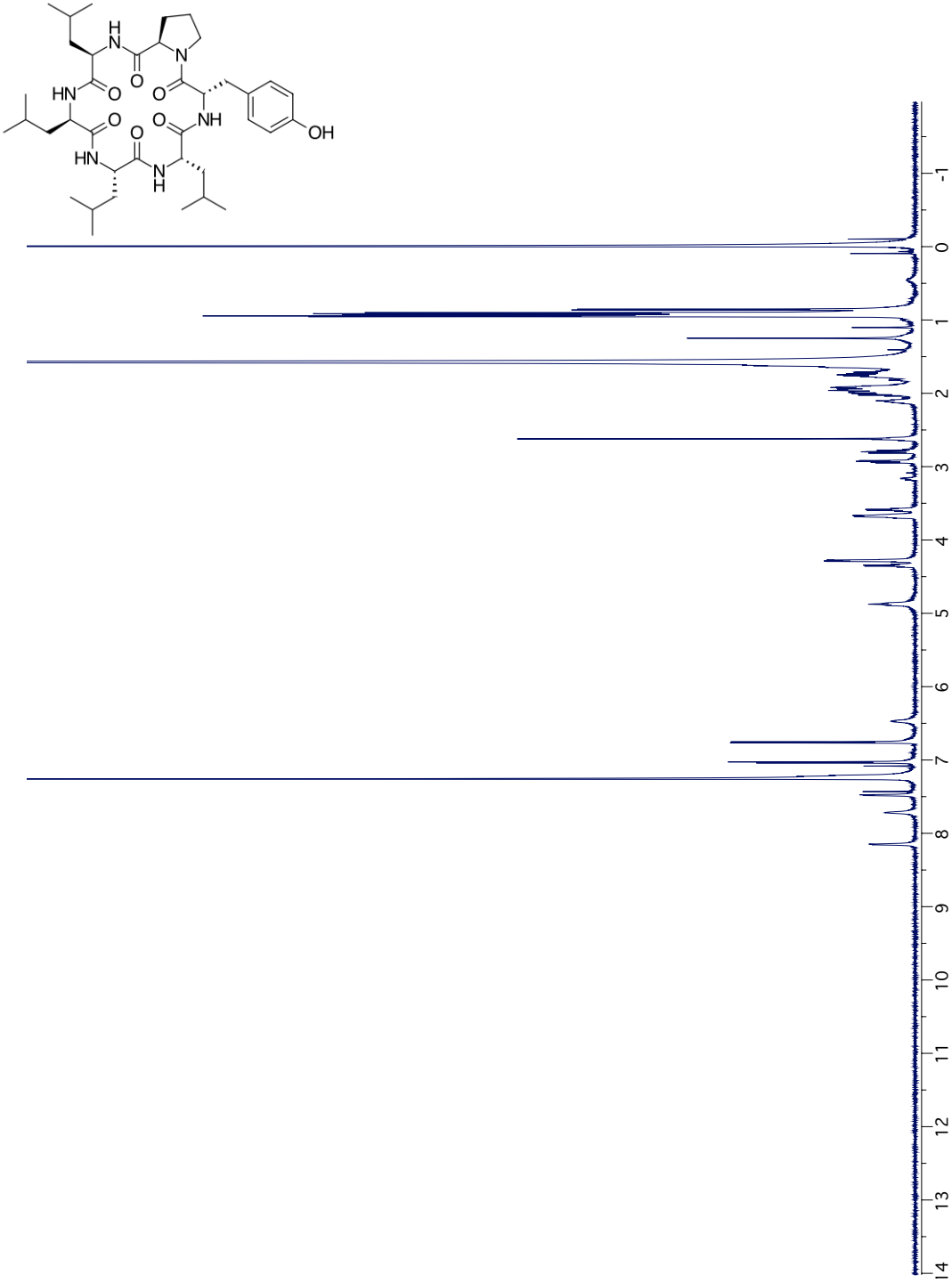

LCMS Spectra for Compound 2.16

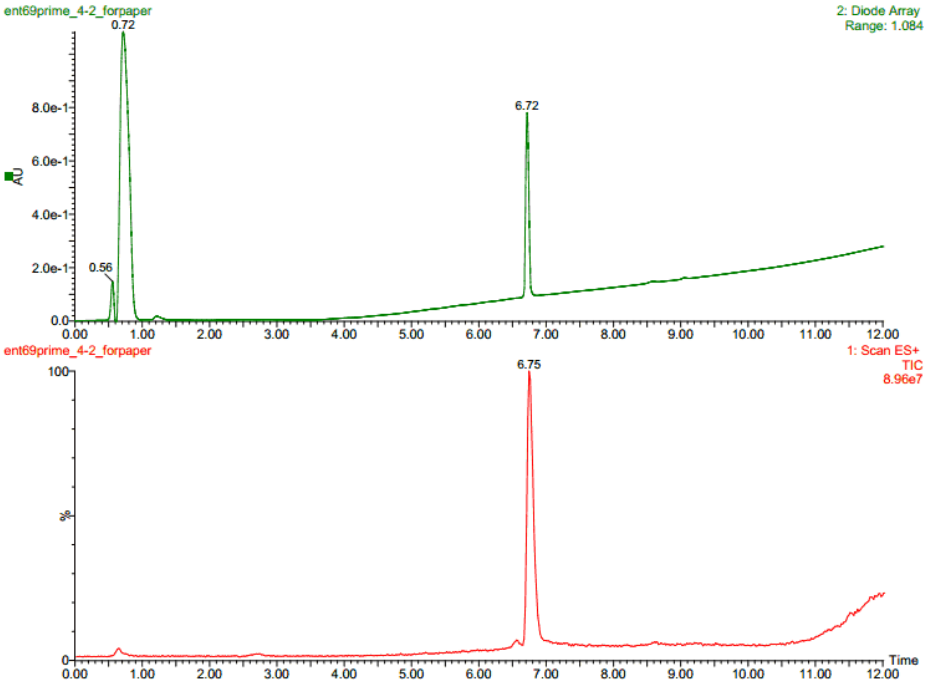

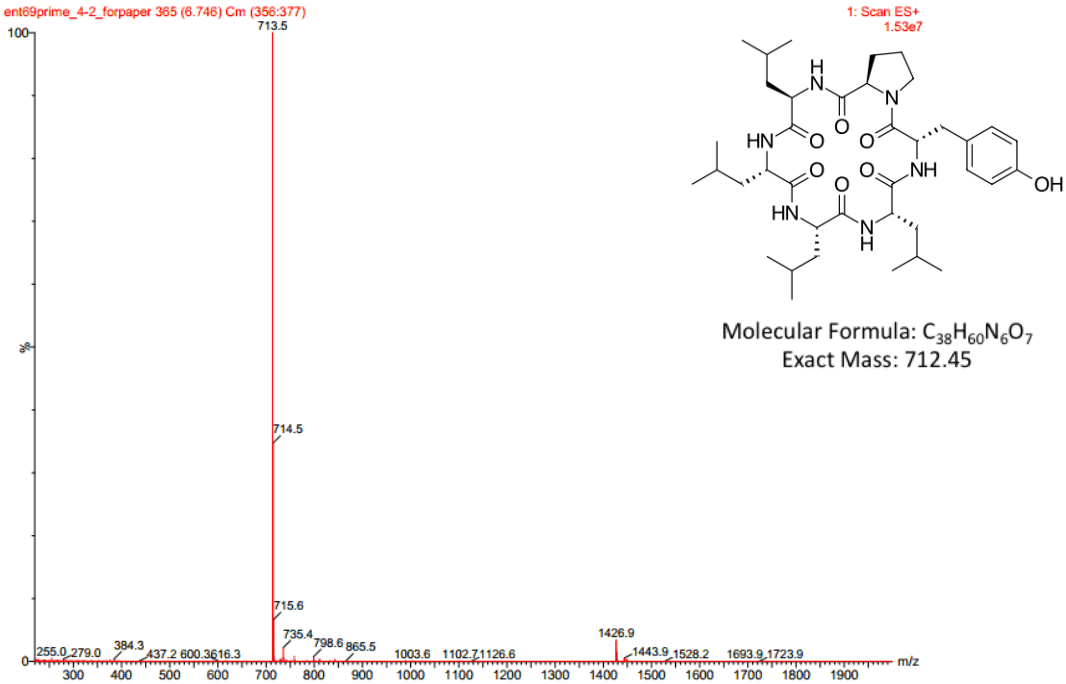

HNMR Spectrum for Compound 2.16

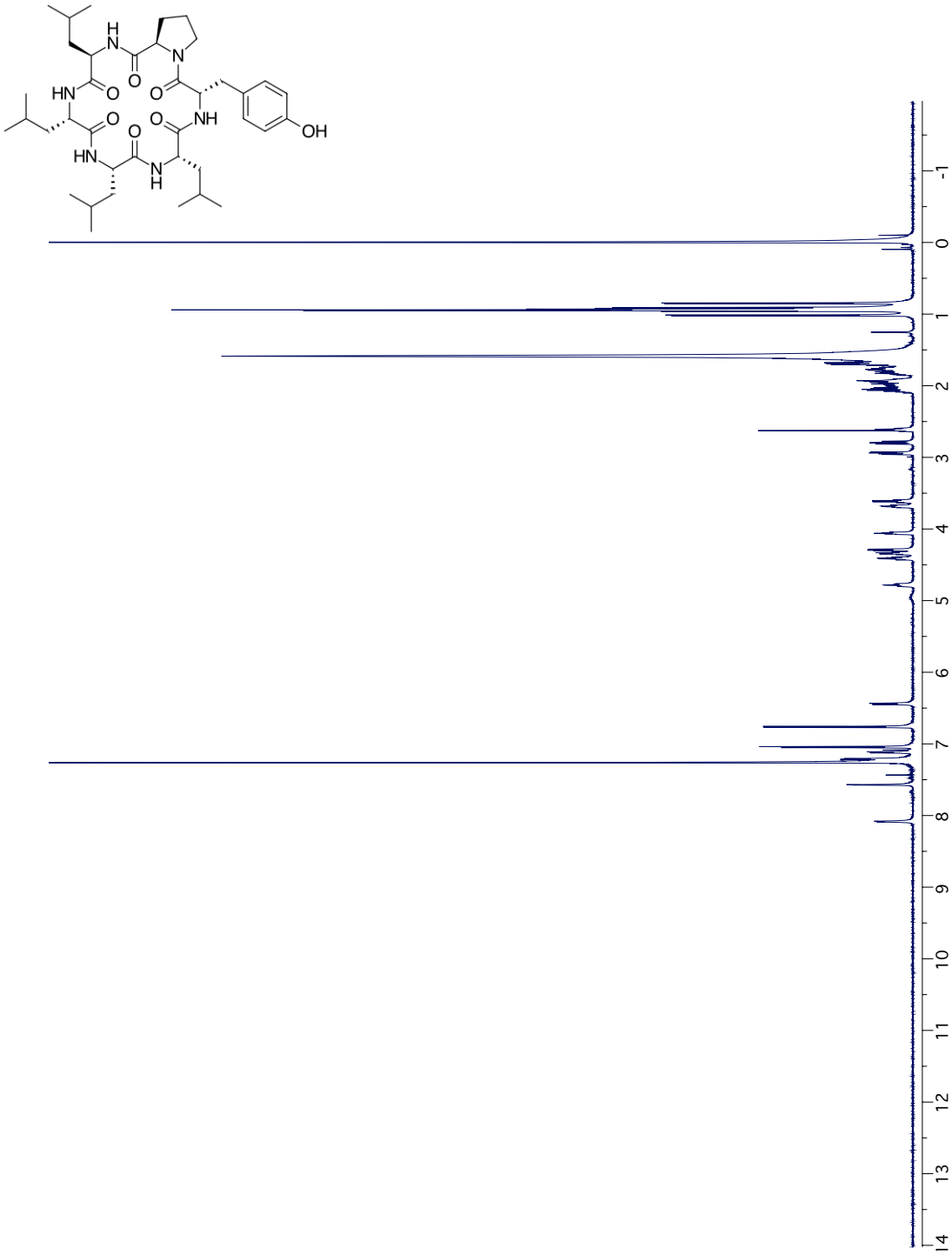

LCMS Spectra for Compound 2.17

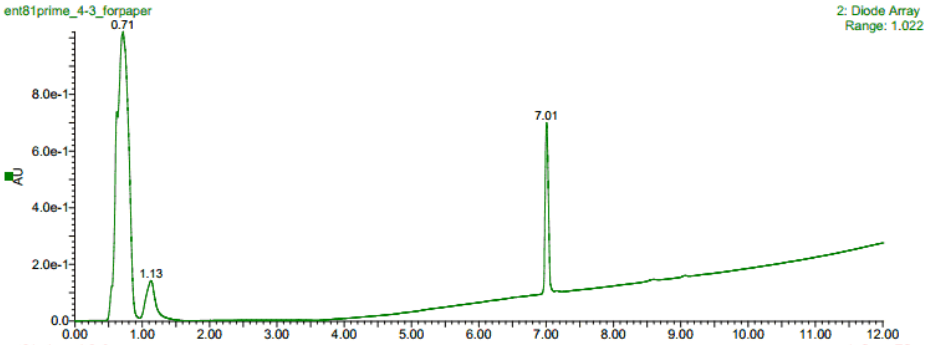

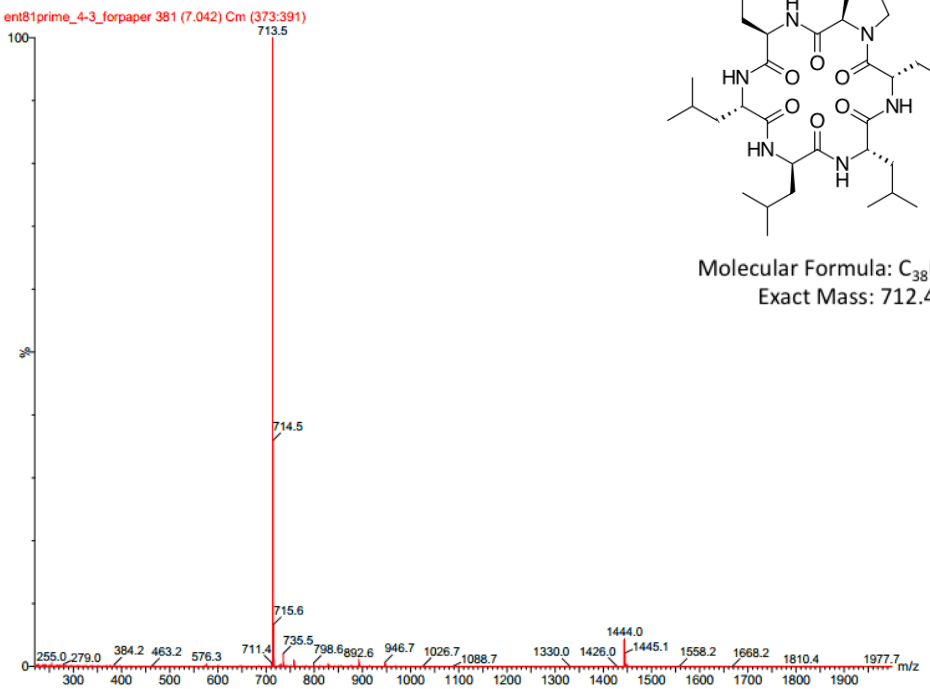

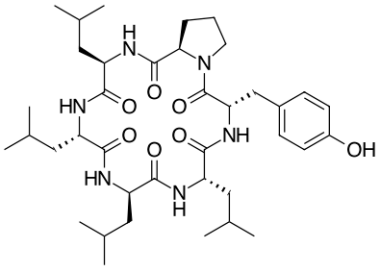

Molecular Formula: $C_{38}H_{60}N_6O_7$
Exact Mass: 712.45

HNMR Spectrum for Compound 2.17

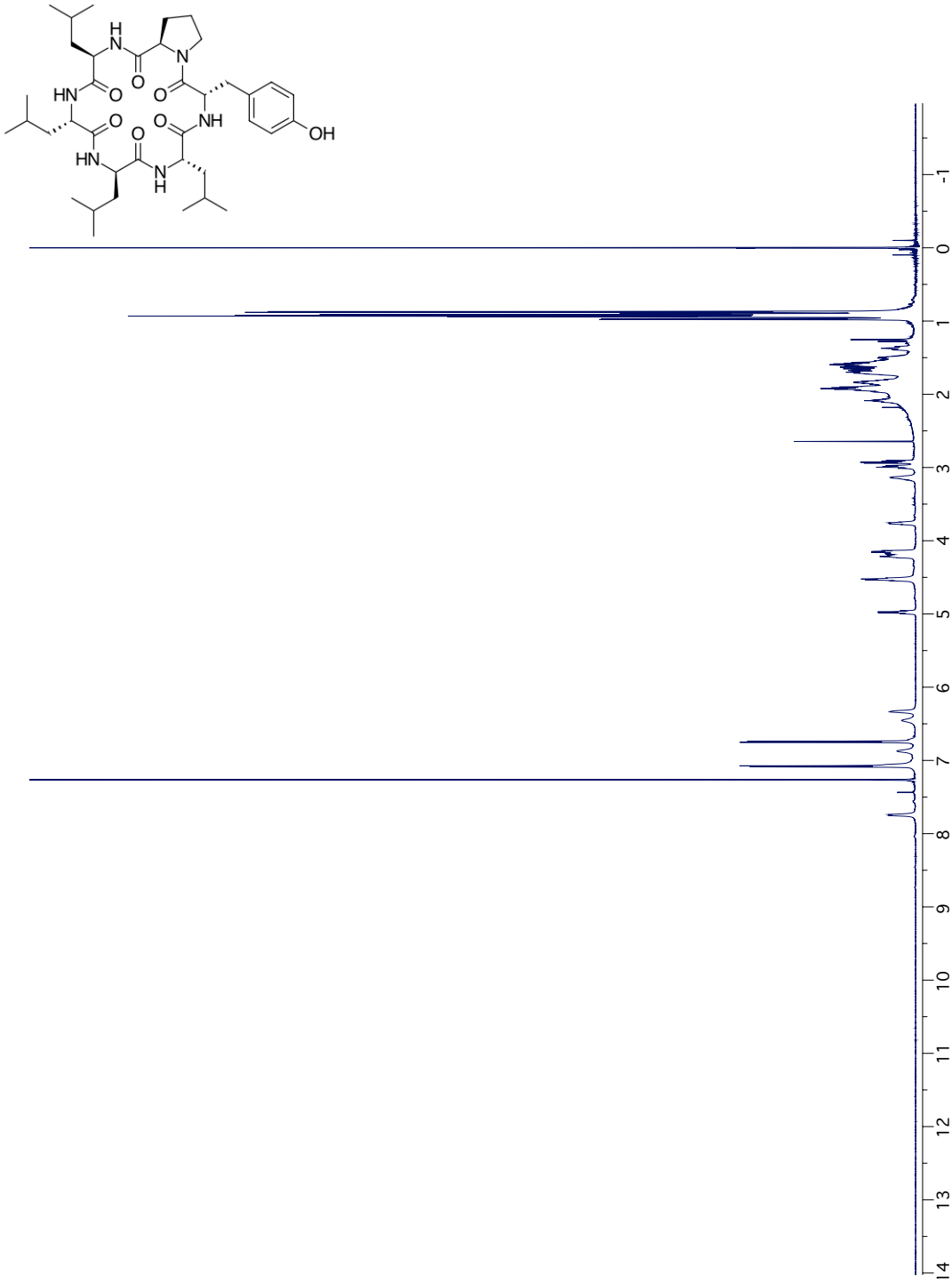

LCMS Spectra for Compound 2.18

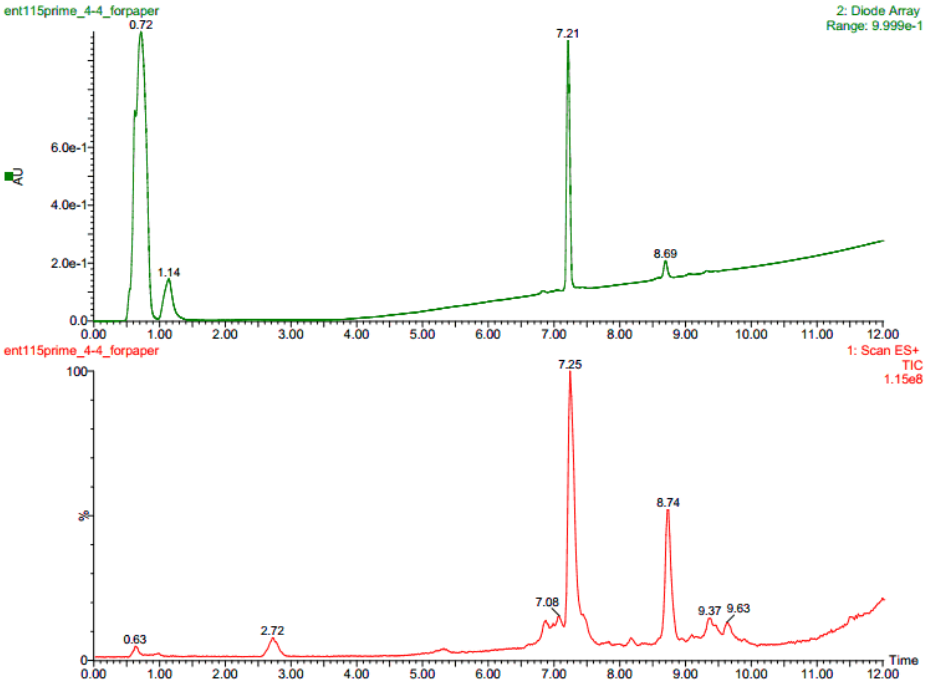

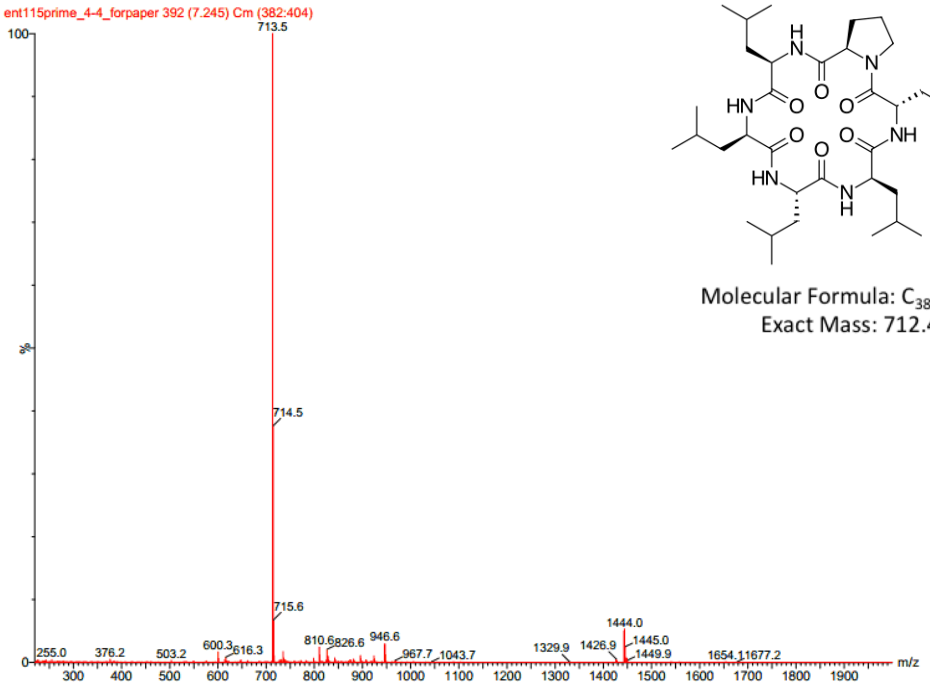

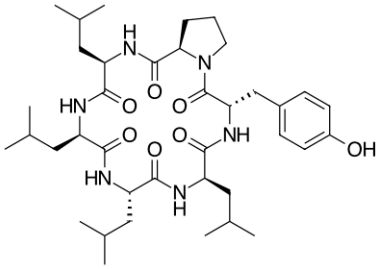

Molecular Formula: $C_{38}H_{60}N_6O_7$
Exact Mass: 712.45

HNMR Spectrum for Compound 2.18

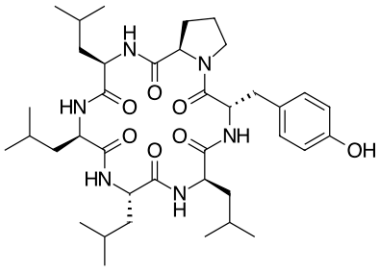

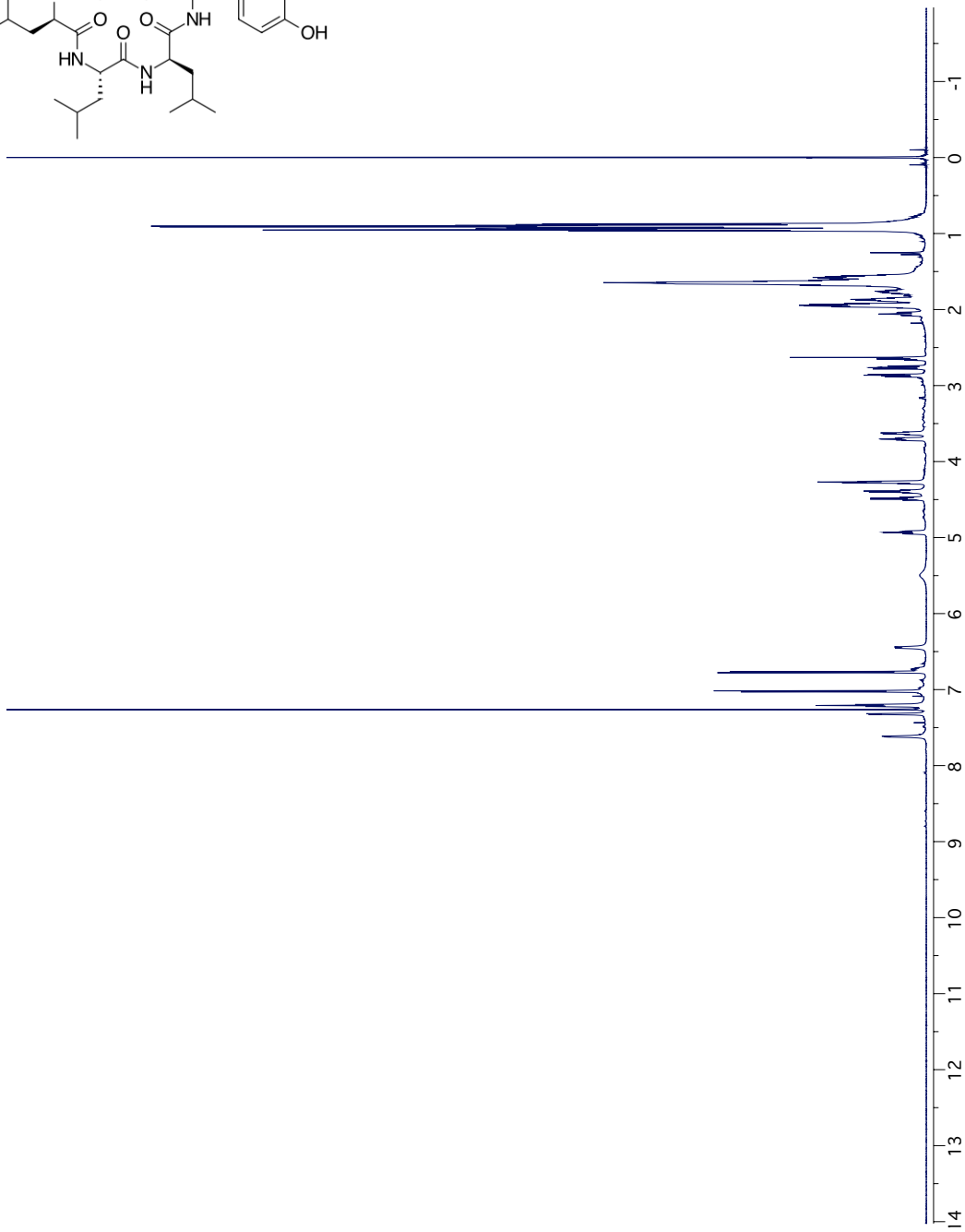

LCMS Spectra for Compound 2.19

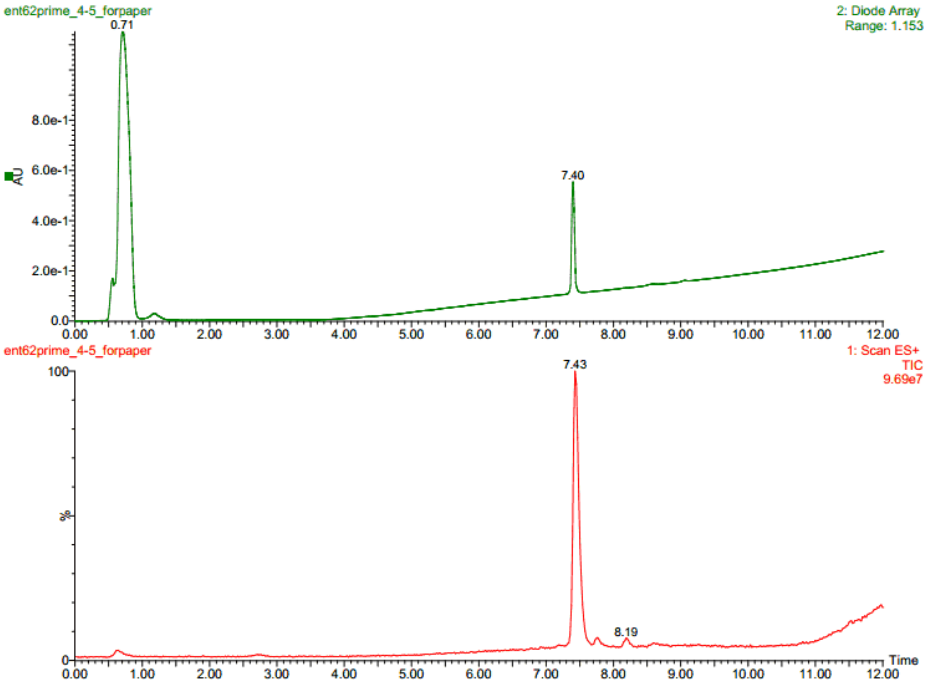

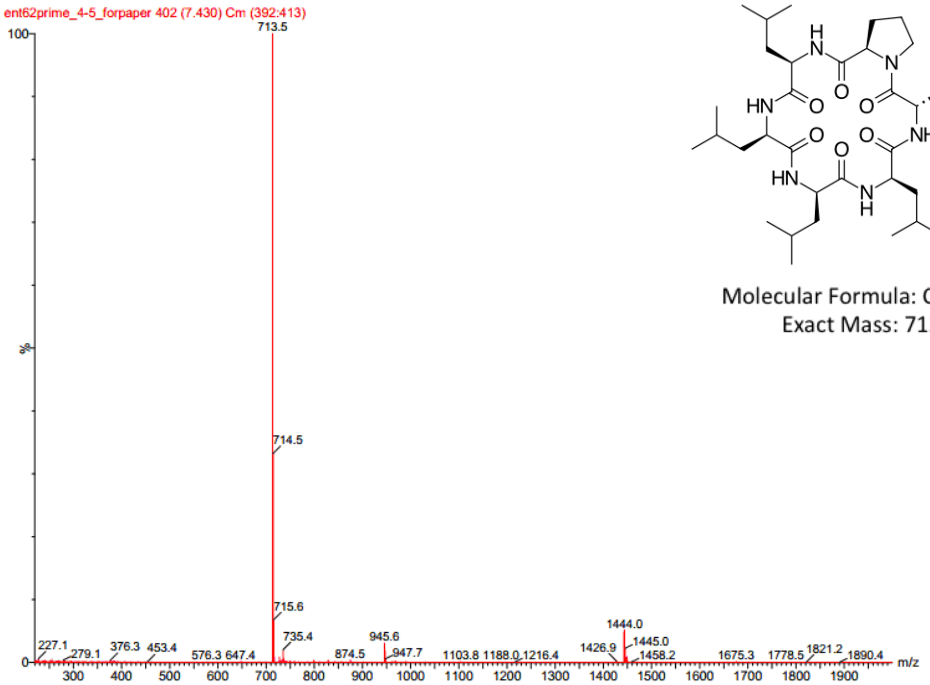

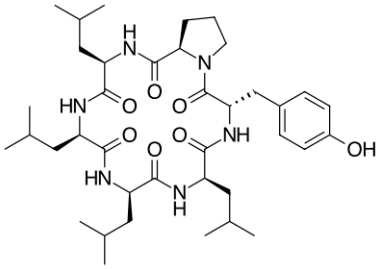

Molecular Formula: $C_{38}H_{60}N_6O_7$
Exact Mass: 712.45

HNMR Spectrum for Compound 2.19

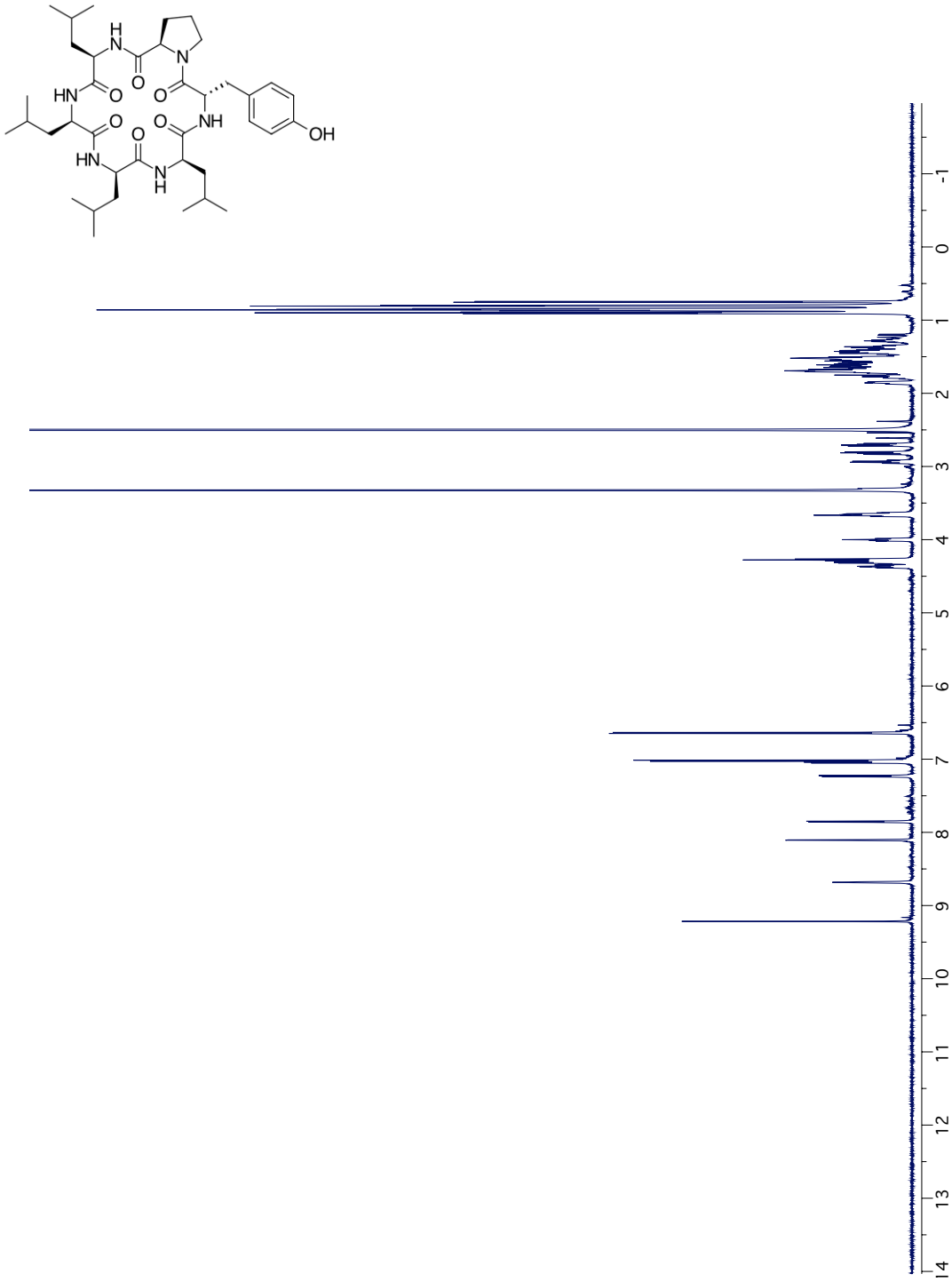

LCMS Spectra for Compound 2.20

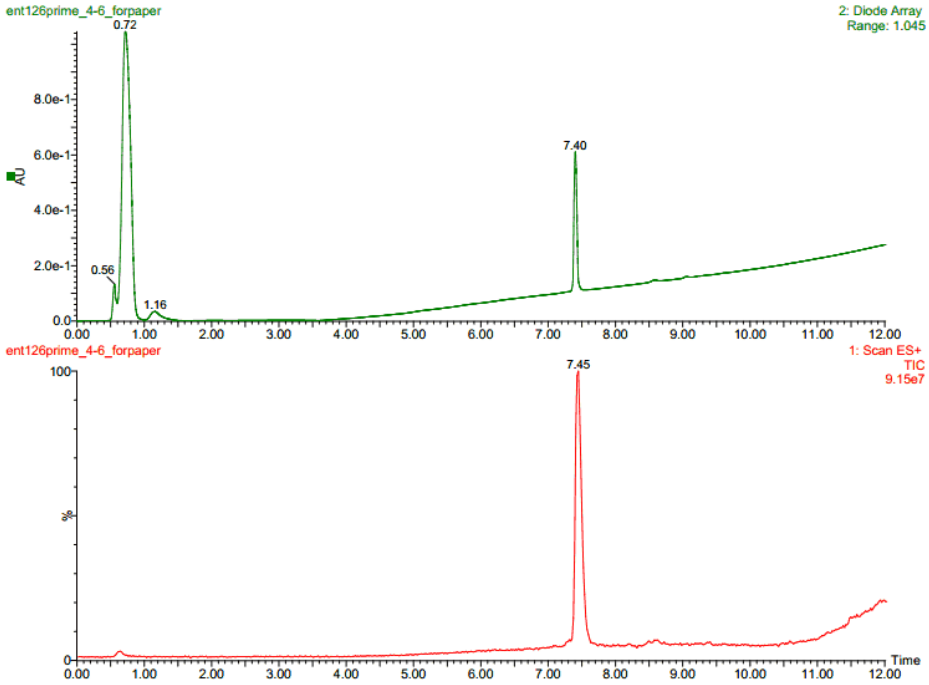

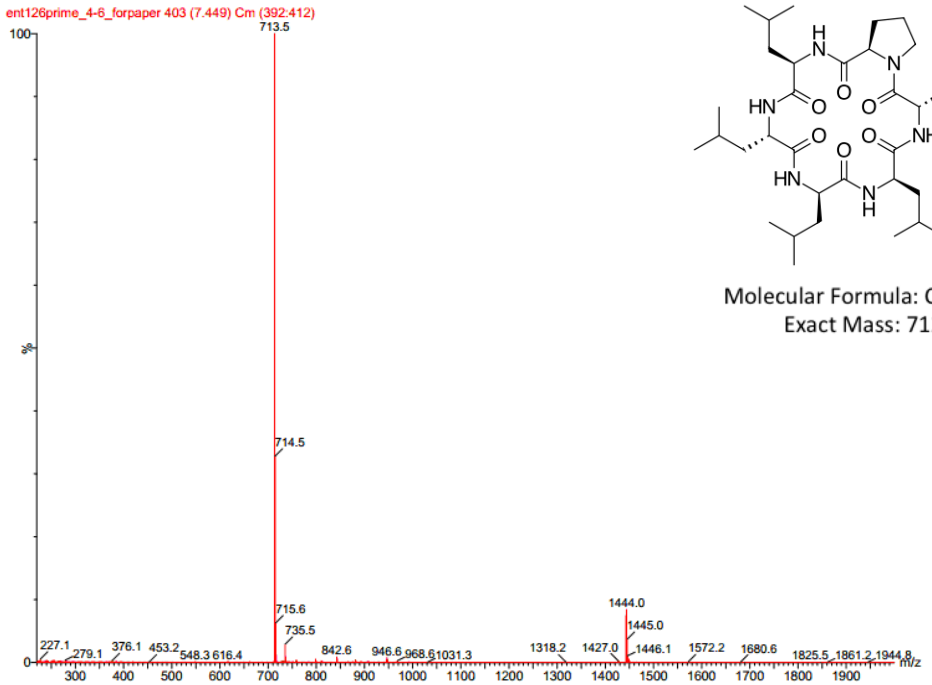

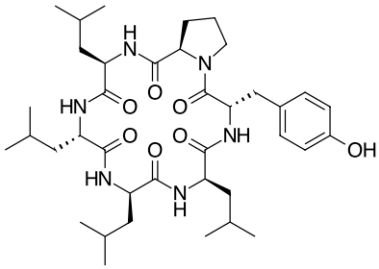

Molecular Formula: $C_{38}H_{60}N_6O_7$
Exact Mass: 712.45

HNMR Spectrum for Compound 2.20

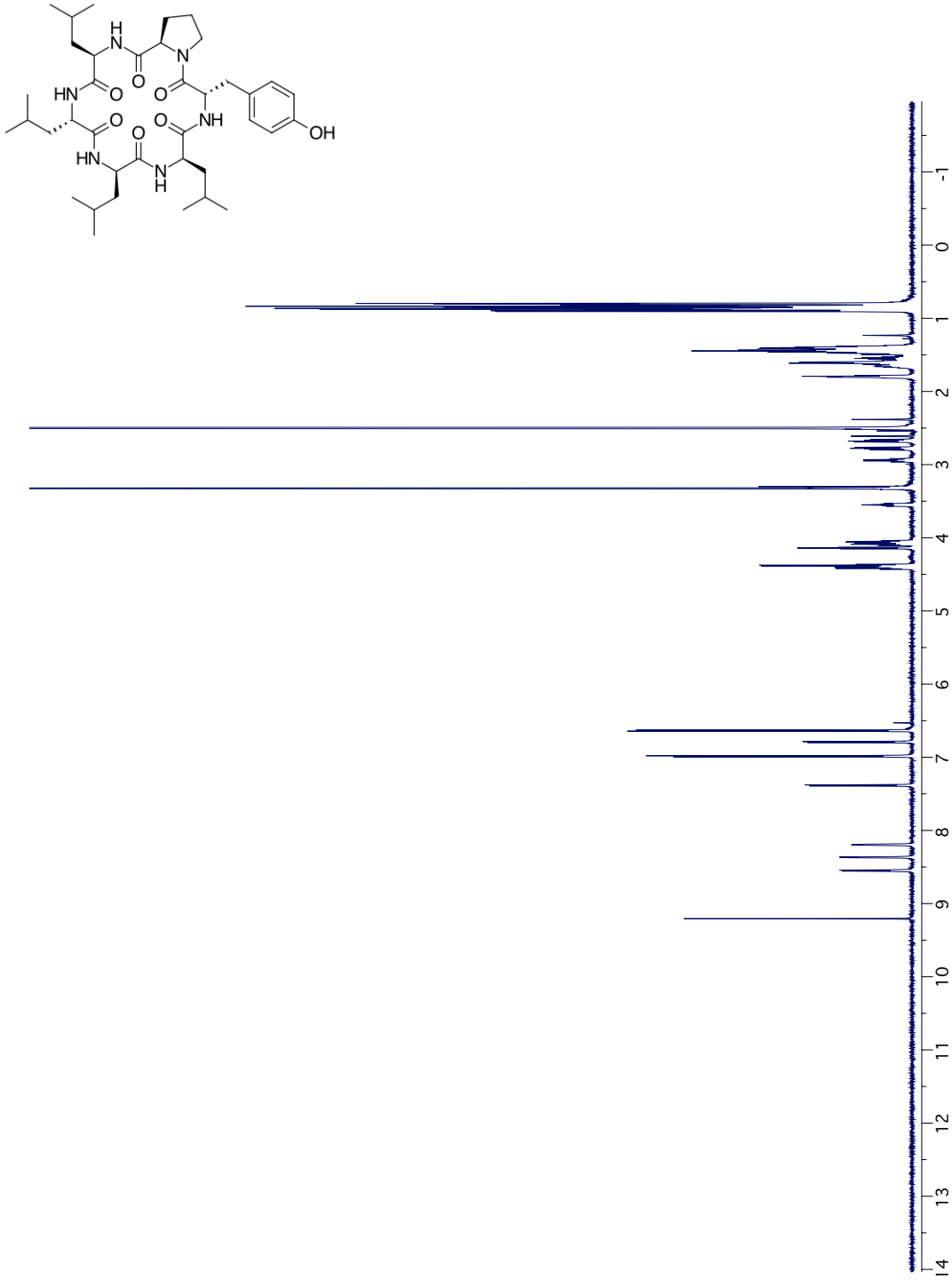

LCMS Spectra for Compound 2.21

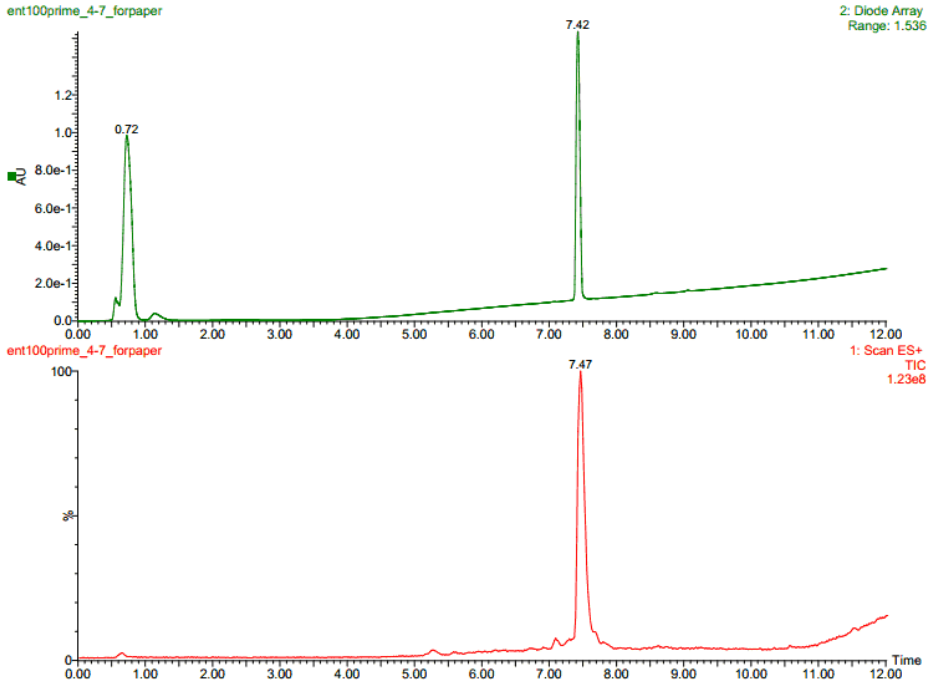

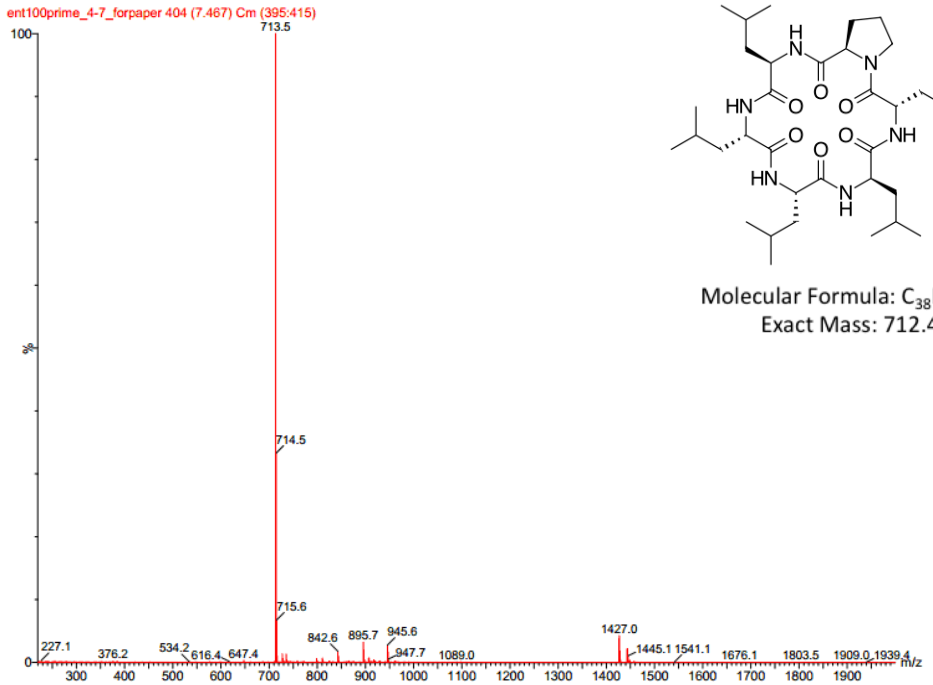

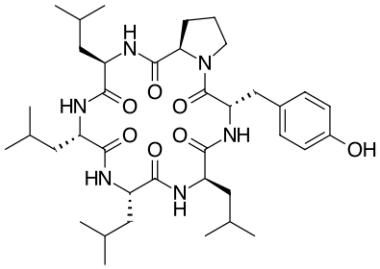

Molecular Formula: $C_{38}H_{60}N_6O_7$
Exact Mass: 712.45

HNMR Spectrum for Compound 2.21

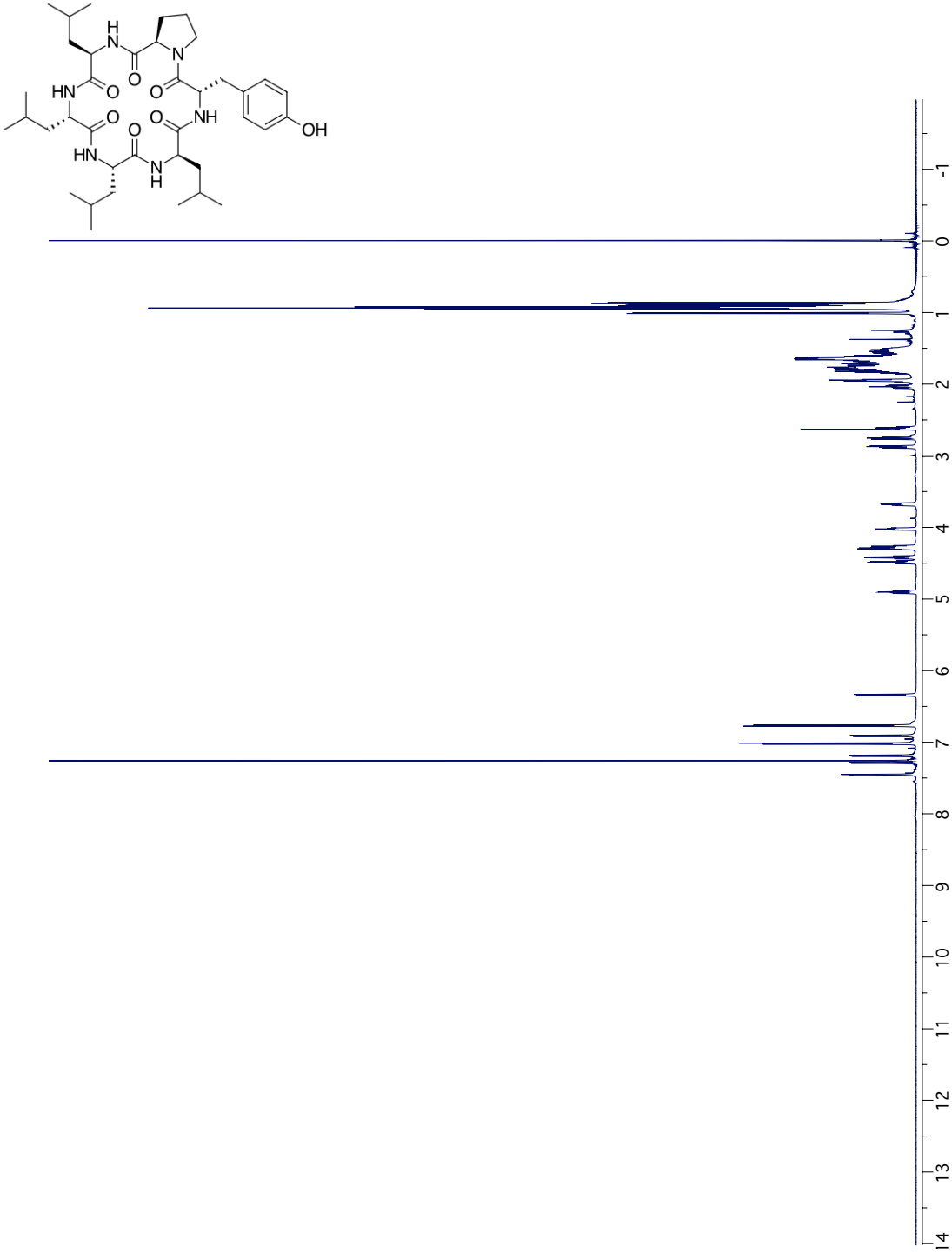

LCMS Spectra for Compound 2.22

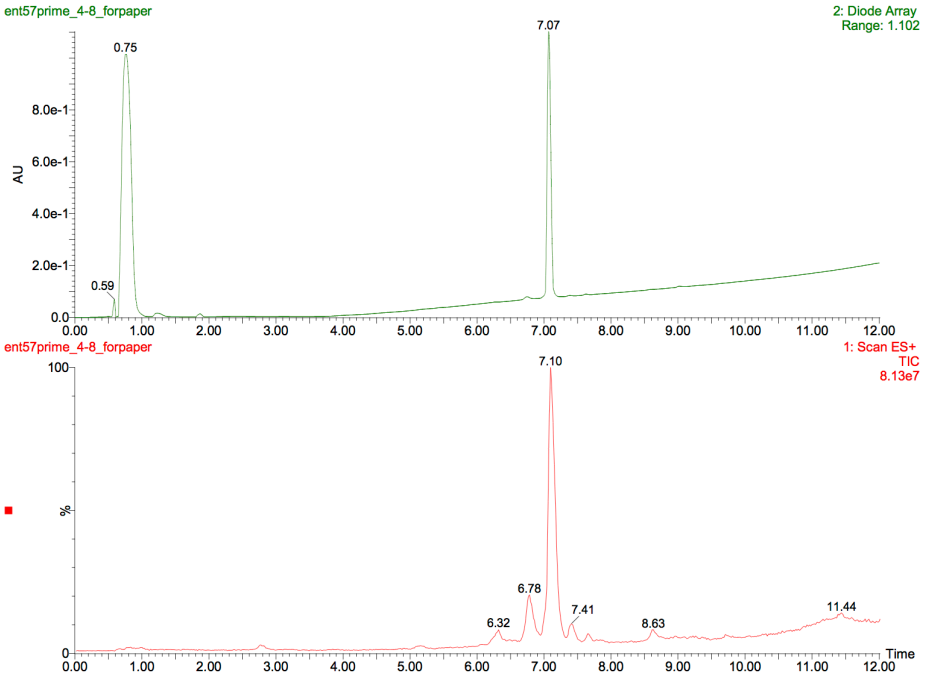

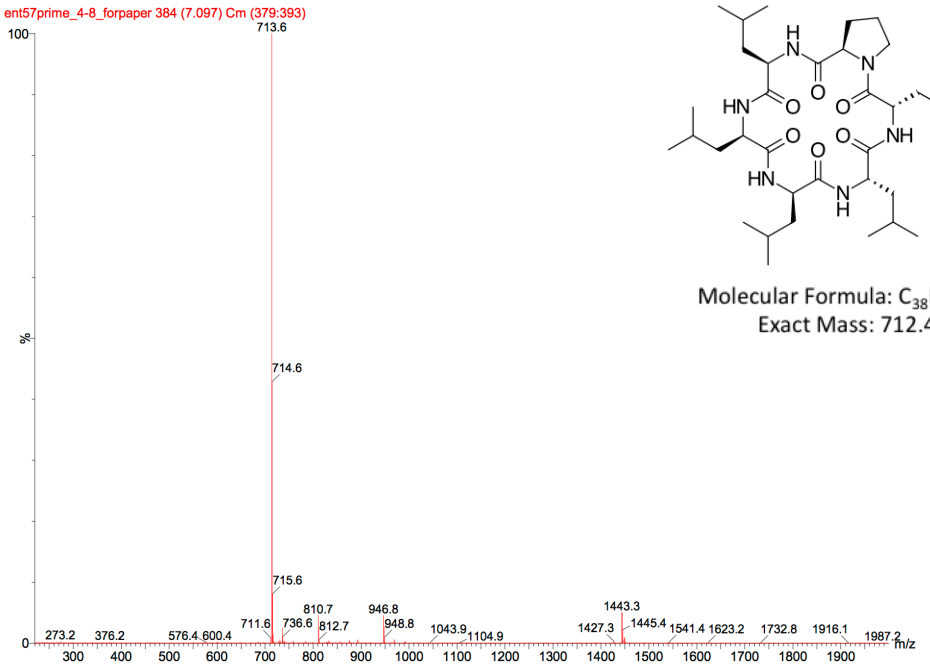

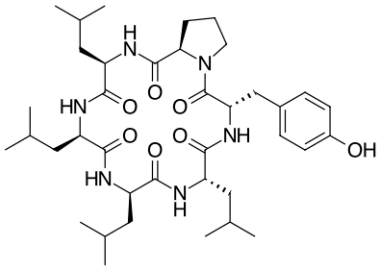

Molecular Formula: $C_{38}H_{60}N_6O_7$
Exact Mass: 712.45

HNMR Spectrum for Compound 2.22

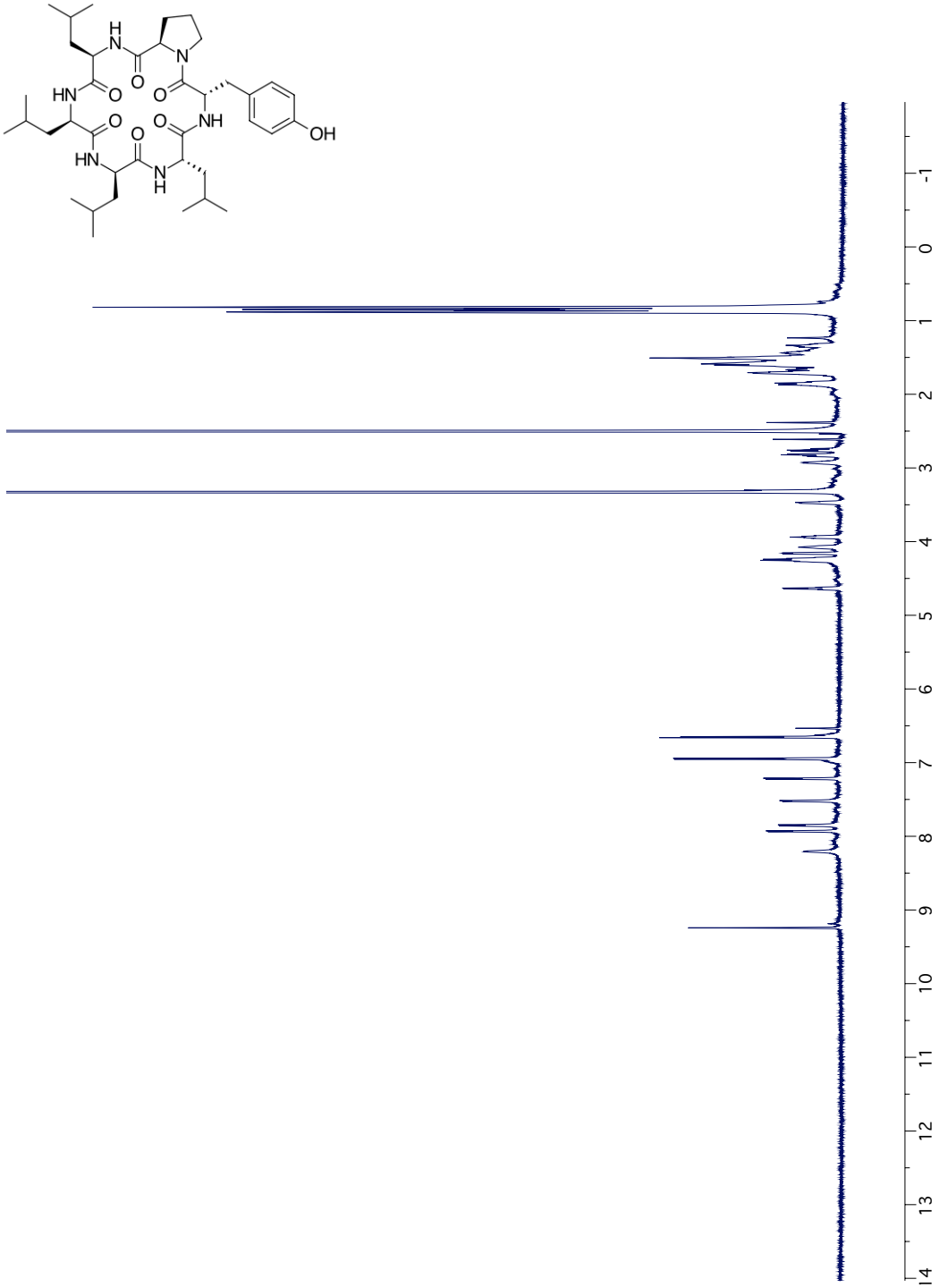

References

1. Overington, J. P.; Al-Lazikani, B.; Hopkins, A. L. *Nat Rev Drug Discov* **2006**, *5*, 993.
2. Malovannaya, A.; Lanz, R. B.; Jung, S. Y.; Bulynko, Y.; Le, N. T.; Chan, D. W.; Ding, C.; Shi, Y.; Yucer, N.; Krenciute, G.; Kim, B. J.; Li, C.; Chen, R.; Li, W.; Wang, Y.; O'Malley, B. W.; Qin, J. *Cell* **2011**, *145*, 787.
3. Colby, D. W.; Chu, Y.; Cassady, J. P.; Duennwald, M.; Zazulak, H.; Webster, J. M.; Messer, A.; Lindquist, S.; Ingram, V. M.; Wittrup, K. D. *Proc. Natl. Acad. Sci. U. S. A.* **2004**, *101*, 17616.
4. Kenne, E.; Renne, T. *Drug Discov Today* **2014**, *9*, 1459.
5. Reichert, J. M.; Dhimolea, E. *Drug Discov Today* **2012**, *17*, 954.
6. Passioura, T.; Katoh, T.; Goto, Y.; Suga, H. *Annu. Rev. Biochem.* **2014**, *83*, 727.
7. Kawamoto, S. A.; Coleska, A.; Ran, X.; Yi, H.; Yang, C. Y.; Wang, S. *J. Med. Chem.* **2012**, *55*, 1137.
8. Madden, M. M.; Muppidi, A.; Li, Z.; Li, X.; Chen, J.; Lin, Q. *Bioorg. Med. Chem. Lett.* **2011**, *21*, 1472.
9. Moellering, R. E.; Cornejo, M.; Davis, T. N.; Del Bianco, C.; Aster, J. C.; Blacklow, S. C.; Kung, A. L.; Gilliland, D. G.; Verdine, G. L.; Bradner, J. E. *Nature* **2009**, *462*, 182.
10. Liu, T.; Joo, S. H.; Voorhees, J. L.; Brooks, C. L.; Pei, D. *Bioorg. Med. Chem.* **2009**, *17*, 1026.
11. Gavenonis, J.; Sheneman, B. A.; Siegert, T. R.; Eshelman, M. R.; Kritzer, J. A. *Nat Chem Biol* **2014**, *10*, 716.
12. Passioura, T.; Suga, H. *Chemistry* **2013**, *19*, 6530.
13. Quartararo, J. S.; Wu, P.; Kritzer, J. A. *ChemBioChem* **2012**, *13*, 1490.

14. Wrighton, N. C.; Farrell, F. X.; Chang, R.; Kashyap, A. K.; Barbone, F. P.; Mulcahy, L. S.; Johnson, D. L.; Barrett, R. W.; Jolliffe, L. K.; Dower, W. J. *Science* **1996**, *273*, 458.
15. Lipinski, C.; Lombardo, F.; Dominy, B.; Feeney, P. *Adv. Drug Del. Rev.* **1997**, *23*, 3.
16. Lipinski, C. A. *J Pharmacol Toxicol Methods* **2000**, *44*, 235.
17. Swift, R. V.; Amaro, R. E. *Chem Biol Drug Des* **2013**, *81*, 61.
18. Guimaraes, C. R.; Mathiowetz, A. M.; Shalaeva, M.; Goetz, G.; Liras, S. *J Chem Inf Model* **2012**, *52*, 882.
19. Kotz, J. *SciBX* **2012**, *5*, 1.
20. Villar, E. A.; Beglov, D.; Chennamadhavuni, S.; Porco, J. A., Jr.; Kozakov, D.; Vajda, S.; Whitty, A. *Nat Chem Biol* **2014**, *10*, 723.
21. Rezai, T.; Bock, J.; Zhou, M.; Kalyanaraman, C.; Lokey, R.; Jacobson, M. *J. Am. Chem. Soc.* **2006**, *128*, 14073.
22. Rezai, T.; Yu, B.; Millhauser, G.; Jacobson, M.; Lokey, R. *J. Am. Chem. Soc.* **2006**, *128*, 2510.
23. White, T. R.; Renzelman, C. M.; Rand, A. C.; Rezai, T.; McEwen, C. M.; Gelev, V. M.; Turner, R. A.; Linington, R. G.; Leung, S. S.; Kalgutkar, A. S.; Bauman, J. N.; Zhang, Y.; Liras, S.; Price, D. A.; Mathiowetz, A. M.; Jacobson, M. P.; Lokey, R. S. *Nat Chem Biol* **2011**, *7*, 810.
24. Bockus, A. T.; McEwen, C. M.; Lokey, R. S. *Curr. Top. Med. Chem.* **2013**, *13*, 821.
25. Amagata, T.; Morinaka, B. I.; Amagata, A.; Tenney, K.; Valeriote, F. A.; Lobkovsky, E.; Clardy, J.; Crews, P. *J. Nat. Prod.* **2006**, *69*, 1560.

26. Niggemann, J.; Bozko, P.; Bruns, N.; Wodtke, A.; Gieseler, M. T.; Thomas, K.; Jahns, C.; Nimtz, M.; Reupke, I.; Bruser, T.; Auling, G.; Malek, N.; Kalesse, M. *ChemBioChem* **2014**, *15*, 1021.
27. Lam, K. S.; Salmon, S. E.; Hersh, E. M.; Hruby, V. J.; Kazmierski, W. M.; Knapp, R. J. *Nature (London, United Kingdom)* **1991**, *354*, 82.
28. Avdeef, A.; Bendels, S.; Di, L.; Faller, B.; Kansy, M.; Sugano, K.; Yamauchi, Y. *J. Pharm. Sci.* **2007**, *96*, 2893.
29. Kansy, M.; Senner, F.; Gubernator, K. *J. Med. Chem.* **1998**, *41*, 1007.
30. Erb, E.; Janda, K. D.; Brenner, S. *Proc. Natl. Acad. Sci. U. S. A.* **1994**, *91*, 11422.
31. Hill, T. A.; Lohman, R.-J.; Hoang, H. N.; Nielsen, D. S.; Scully, C. C. G.; Kok, W. M.; Liu, L.; Lucke, A. J.; Stoermer, M. J.; Schroeder, C. I.; Chaousis, S.; Colless, B.; Bernhardt, P. V.; Edmonds, D. J.; Griffith, D. A.; Rotter, C. J.; Ruggeri, R. B.; Price, D. A.; Liras, S.; Craik, D. J.; Fairlie, D. P. *ACS Medicinal Chemistry Letters* **2014**, *10*, 1148.
32. Hong, J.; Jing, Q.; Yao, L. *J. Biomol. NMR* **2013**, *55*, 71.
33. Cordier, F.; Grzesiek, S. *J. Mol. Biol.* **2002**, *317*, 739.
34. Baker, E. N.; Hubbard, R. E. *Prog. Biophys. Mol. Biol.* **1984**, *44*, 97.
35. Bissantz, C.; Kuhn, B.; Stahl, M. *J. Med. Chem.* **2010**, *53*, 5061.
36. Waring, M.J. Bioorg. Med. Chem. Lett. 2009, 19, 2844.
37. Nielsen, D. S.; Hoang, H. N.; Lohman, R. J.; Diness, F.; Fairlie, D. P. *Org Lett* **2012**, *14*, 5720.
38. Zhang, S.; Govender, T.; Norström, T.; Arvidsson, P.I. *J. Org. Chem.* **2005**, *70*, 6918-6920
39. Rizzi, L.; Cendic, K.; Vaiana, N.; Romeo, S. *Tetrahedron Lett.* **2011**, *52*, 2808-2811

40. Falb, E.; Yechezkel, T; Salitra, Y.; Gilon, C. *J. Pept. Res.* **1999**, *53*, 507-517

41. Rand, A. C.; Leung, S. S. F.; Eng, H.; Rotter, C. J.; Sharma, R.; Kalgutkar, A. S.; Zhang, Y.; Varma, M. V.; Farley, K. A.; Khunte, B.; Limberakis, C.; Price, D. A.; Liras, S.; Mathiowetz, A. M.; Jacobson, M. P.; Lokey, R. S. *Med. Chem. Commun.* **2012**, *3*, 1282-1289.

42. Jacobson, M. P.; Pincus, D. L.; Rapp, C. S.; Day, T. J. F.; Honig, B.; Shaw, D. E.; Friesner, R. A. *Proteins: Struct., Funct., Bioinf.* **2004**, *55*, 351.

43. Jorgensen, W. L.; Maxwell, D. S.; TiradoRives, J. *J. Am. Chem. Soc.* **1996**, *118*, 11225.

44. Cicero, D.O.; Barbato, G.; Bazzo, R. *J. Am. Chem. Soc.* **1995**, *117*, 1027-1033

45. Thepchatri, P.; Cicero, D.O.; Monteagudo, E.; Ghosh, A.K.; Cornett, B.; Weeks, E.R.; Snyder, J.P. *J. Am. Chem. Soc.* **2005**, *127*, 12838-12846

46. Lai, X.N.; Chen, C.P.; Andersen, N.H. *J. Magn. Reson., Ser. B* **1993**, *101*, 271-288

47. Atasoylu, O.; Furst, G.; Risatti, C.; Smith, A.B. *Org. Lett.* **2010**, *12*, 1788-1791

48. Evans, D.A.; Bodkin, M.J.; Baker, S.R.; Sharman, G.J. *Magn. Reson. Chem.* **2007**, *45*, 595-600

49. Phillips, J.C.; Braun, R.; Wang, W.; Gumbart, J.; Tajkhorshid, E.; Villa, E.; Chipot, C.; Skeel, R.D.; Kale, L.; Schulten, K. *J. Comput. Chem.* **2005**, *26*, 1781-1802

Chapter 3: Investigation of the Influence of Lipophilicity and Molecular Weight on Passive Membrane Permeation of Cyclic Peptides

Introduction

` One of the most common metrics developed and utilized for the qualitative assessment of "drug likeness" is Lipinski's rule of five (Ro5).[1] These criteria have been the basis for the development of small molecule drugs with good pharmacokinetic (PK) properties such as solubility and oral bioavailability for over a decade. However, a new class of macrocyclic drugs have emerged which seem to defy these qualitative rules—so called "beyond Rule of five" (bRo5) compounds. A recent survey of FDA approved drugs showed 19 of the 68 marketed macrocyclic drugs are orally bioavailable, all of which lie well beyond the traditionally accepted 500 Da molecular weight limit.[2] The largest of these is a partially *N*-methylated undecapeptide of 1202 Da—cyclosporin A (CSA).[3] It's oral bioavailability is attributed to its ability to passively permeate biological membranes, as it has appreciable permeability values in various permeation assays.[4-6] Although extensively studied,[7-15] the underlying physical features which contribute to the permeability of CSA and other large macrocycles are still poorly understood.

One approach to understanding permeation of small molecules has been the development of physical models of passive permeation. Extensive work has been made in this area involving the barrier-domain model.[16-18] The basis of this model involves an assumption that the rate limiting step of membrane permeation is passive diffusion through a so-called "barrier region" of the lipid bilayer. This barrier region is an area of highly ordered lipid hydrocarbon chains residing between the hydrophilic phosphate head groups and the highly disordered bilayer center. Based on Equation 3.1:

$$P_m = \frac{K_{barrier} D_{barrier}}{\delta} \tag{3.1}$$

the permeation rate of a solute is based on the intrinsic values of $K_{barrier}$—the size-dependent partition coefficient between an aqueous environment and the barrier domain—and $D_{barrier}$, defined as the size-dependent diffusion constant of a permeant through this barrier region. $K_{barrier}$ can be estimated by equation 3.2 as:

$$K_{barrier} = K_{hc/w}\, \xi \tag{3.2}$$

where $K_{hc/w}$ is the hydrocarbon / water partition coefficient, and ξ is the size dependent coefficient for partitioning, defined by equation 3.3:

$$\xi = e^{-2(p_{\perp} - p_{\parallel})V/3k_BT} = e^{-\alpha V} \tag{3.3}$$

in which $p_{\perp}$ and $p_{||}$ are the lateral and normal pressures within a bilayer membrane, respectively, k_B is the Boltzmann constant, T is temperature in Kelvin, and V is the molecular volume of the permeant in square angstroms. Similarly, $D_{barrier}$ can be estimated by equation 3.4:

$$D_{barrier} = \frac{D_o}{V^n} \tag{3.4}$$

where D_0 is the diffusion coefficient of the permeant through bulk solvent, V is the molecular volume in square angstroms, and n is an experimentally derived size dependence factor. Alternatively, $D_{barrier}$ can be estimated by the application of the Stokes-Einstein equation, as in equation 3.5:

$$D_{barrier} = \frac{k_B T}{6\pi\eta r} \tag{3.5}$$

where r is the radius of the (assumed) spherical permeant, calculated from the molecular volume as in equation 3.6:

$$r = \left(\frac{3V}{4\pi}\right)^{1/3} \tag{3.6}$$

Although simplistic, this model has been successfully applied to very small solutes and small molecule drugs with reasonable correlation.

More recently, similar computational models have been applied to small molecules and cyclic peptides.[19,20] These models take in to account additional factors such as conformational penalties for flexible molecules, applying a rigorous computational approach to model these conformations both in an aqueous environment as well as in a low dielectric solvent, similar to that found in the hydrophobic bilayer center. Although the authors report good correlation to published permeability data, this system has yet to be applied to larger macrocycles <750 Da. Successful extension of these and other theoretical models towards larger molecules and macrocycles would be a considerable contribution towards

the understanding of bRo5 molecule permeability and would aide in the design of such bRo5-based drugs.

We previously described the direct permeability analysis via the well established parallel artificial membrane permeability assay (PAMPA) of a synthetic split-pool library of 1152 cyclic hexapeptides representing all diastereomeric and *N*-methyl variants (see chapter 2). Through this methodology, we discovered several novel cyclic hexapeptides with good to excellent membrane permeability. We also extended this library approach to investigate the impact of side-chain identity on a membrane permeable scaffold. We observed that hexapeptides with either extremely high or low cLogP values displayed very low permeability via PAMPA, suggesting a notion that cyclic peptides must have an optimal lipophilicity residing a "lipophilicity window" in order to passively permeate—highly hydrophilic compounds will not permeate due to high desolvation energy (ΔG_{desolv}) costs to enter the nonpolar lipid bilayer, whereas highly lipophilic compounds will be insoluble or prone to aggregation. Herein, we report the application of our synthetic library approach towards the understanding of the impact lipophilicity and molecular size on intrinsic permeability of peptidic macrocycles.

Background and Experimental Design

In previous unpublished work, compound **3.1** was identified in a computationally generated library of 16,384 octapeptides as a potentially permeable compound. Upon resynthesis, however, the compound showed poor permeability by both passive and cell-based permeability assays (Table 3.1). However, permeability analysis of an analogue involving two leucine residues substituted with alanines (**3.2**) showed drastic improvement.

Table 3.1. Permeability of Previously Studied Permethylated Octapeptides.

Cpd	Substitution relative to **3.1**[b]	P_e (x 10^{-6} cm/s) PAMPA	RRCK (Tier 1)[c]	SFLogD[d]	cLogP[e]
3.1[a]	L_6PY	0.033	<0.1	ND	6.85
3.2	L(2,6)A	19	2.76	5.1	4.32
3.3	L(1,3,5,6)A	1	0.38	2.7	1.78
3.4	A_6PY	0.023	0.66	0.6	-0.76

[a]Linear N-to-C sequence is D-MeLeu[1] – L-MeLeu[2] – D-MeLeu[3] – D-MeLeu[4] – L-MeLeu[5] – D-MeLeu[6] – D-MePro[7] – L-MeTyr[8]. [b]Denotes which leucines in the linear sequence of **3.1** (see footnote *a*) are substituted for alanines, with retention of stereochemistry. [c]Ref. 22. [d]LogD via shake-flask method. [e]Calculated LogP, via Osiris Molecular Properties Calculator.

Additional leucine-to-alanine substitutions, however, proved detrimental to the permeability of this permethylated octapeptide. Dynamic light scattering (DLS) analysis[21] showed aggregation to be the major factor in limiting the solubility of **3.1**, whereas high desolvation energies was hypothesized to be responsible for the poor permeability of **3.3**

Table 3.2. Permeability of Sequence Isomers of Compound **3.2**.

Cpd	Substitution relative to **3.1**[a]	P_e (x 10^{-6} cm/s) PAMPA	RRCK (Tier 1)[b]	SFLogD[c]	cLogP[d]
3.5	L(1,2)A	8	10.31	4.9	4.32
3.6	L(3,4)A	4	4.47	4.2	4.32
3.7	L(5,6)A	6	7.3	ND	4.32
3.8	L(1,6)A	11	8.96	4.8	4.32
3.9	L(2,5)A	19	12.72	4.8	4.32
3.10	L(2,4)A	24	9.68	ND	4.32

[a]Denotes which leucines in the linear sequence of **3.1** (see footnote *a*) are substituted for alanines, with retention of stereochemistry. [b]Ref. 22. [c]LogD via shake-flask method. [d]Calculated LogP, via Osiris Molecular Properties Calculator.

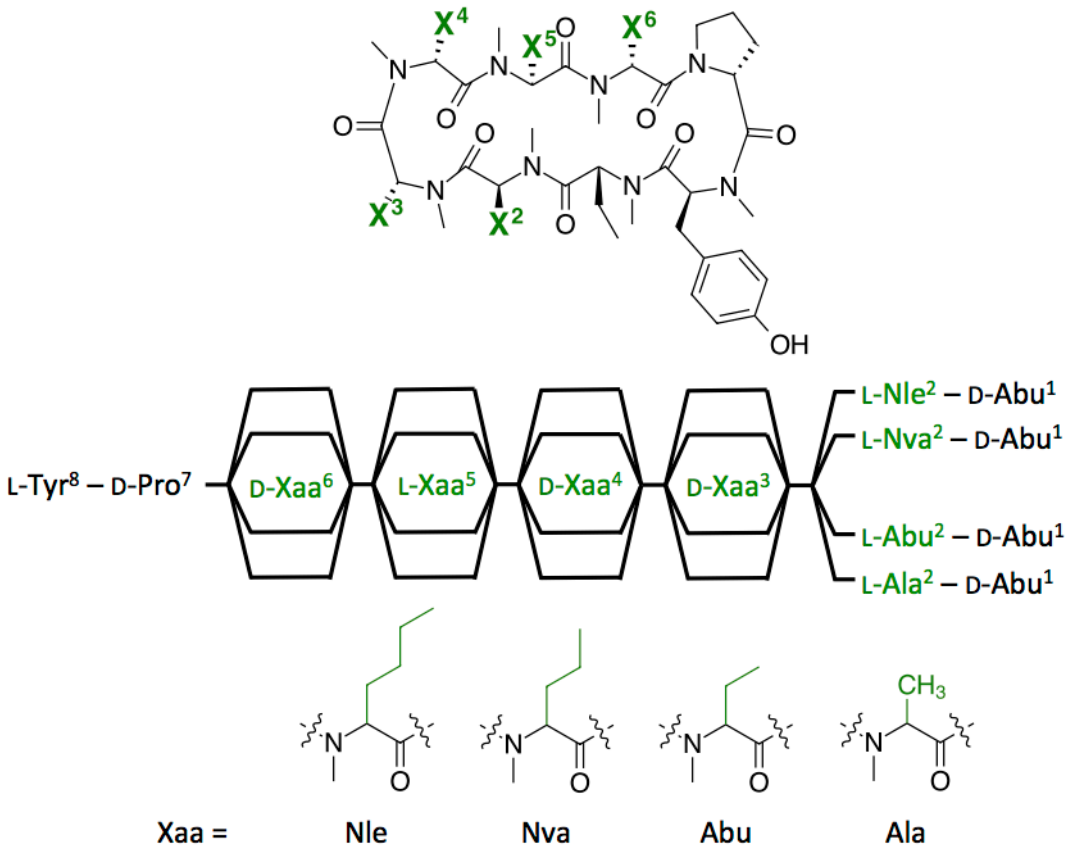

Figure 3.1. Synthesis of a lipophilicity scan library based on a permethylated octapeptide scaffold.

and **3.4**. Additionally, we synthesized a small number of isomers (Table 3.2) to investigate the sequence-dependence of permeability for **3.2** and found that all positional variants showed reasonable permeability in both PAMPA and the live-cell RRCK assay.[22]

To further investigate the generality of the lipophilicity-permeability relationship in this macrocyclic system, we sought to design a split-pool synthetic library (Figure 3.1) that would sample a maximum number of lipophilicity values within this scaffold. We chose to utilize Ala, aminobutyric acid (Abu), norvaline (Nva) and norleucine (Nle) as monomers.

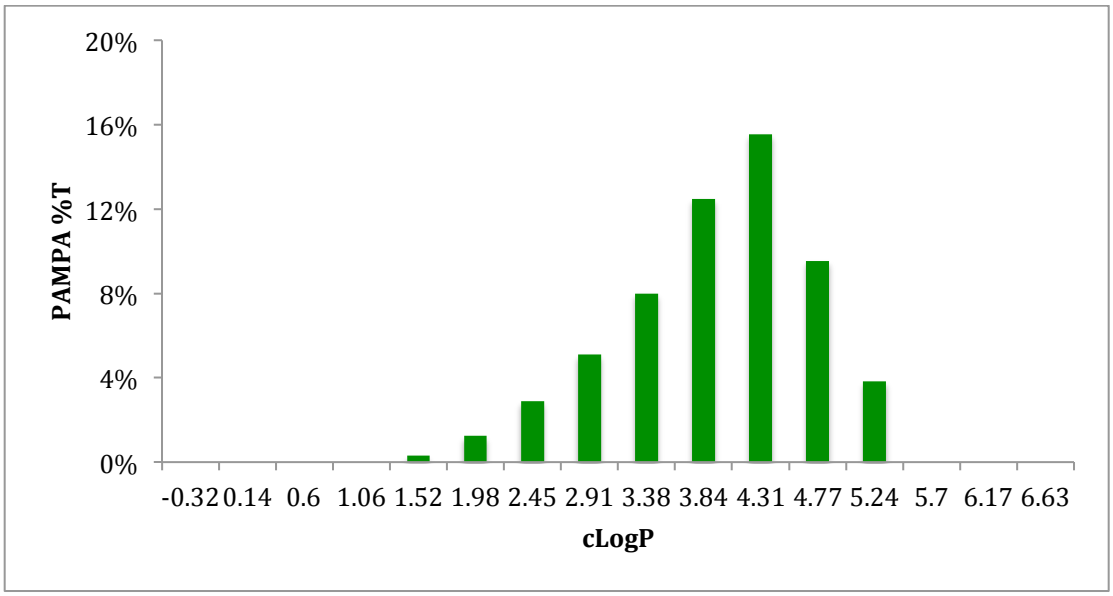

Figure 3.2. Permeability analysis of the lipophilicity scan library of permethylated octapeptides, showing an optimal cLogP value of 4.3.

With each side-chain differing by only a single methylene unit, this design allows sampling of a large number of lipophilicities.

Results and Discussion

After synthesis and permeability analysis of the library (Figure 3.2), we observed permeability within a "lipophilicity window," with an optimal permeation rate corresponding to a cLogP equivalent to that of **3.2**. These results were supported through resynthesis and analysis of a small subset of compounds found within this library (Table 3.3). As is suggestive of the high cLogP value for **3.14**, the low permeability is attributed to aggregation factors, though this needs confirmation by DLS analysis.

Having developed an understanding of the overall impact of lipophilicity on passive permeabilities within this macrocyclic framework, we sought to extend this work to larger-

Table 3.3. Permeability and Lipophilicity Values for Selected Permethylated Cyclic Peptides

	Sequence										P_e (x 10^{-6} cm/s)			
Cpd	1	2	3	4	5	6	7	8	9	10	PAMPA	RRCK (Tier 1)[a]	SFLogD[b]	cLogP[c]
3.11	D-MeAbu	L-MeAla	D-MeAla	D-MeNle	L-MeAla	D-MeAla	D-Pro	L-MeTyr	---	---	0.24	0.22	2.04	1.06
3.12	D-MeAbu	L-MeNle	D-MeAla	D-MeNva	L-MeNle	D-MeAla	D-Pro	L-MeTyr	---	---	3.3	4.02	4.25	3.38
3.13	D-MeAbu	L-MeNva	D-MeNva	D-MeNva	L-MeNva	D-MeNva	D-Pro	L-MeTyr	---	---	4	7.29	4.81	4.31
3.14	D-MeAbu	L-MeNle	D-MeNle	D-MeNle	L-MeNle	D-MeNle	D-Pro	L-MeTyr	---	---	Below LOD	<0.1	ND	6.63
3.15	L-MeNva	D-MeAbu	L-MeAla	D-MeAbu	D-MeAla	L-MeAla	D-MeAbu	D-Pro	L-MeTyr	---	0.05	ND	ND	1.21
3.16	L-MeNva	D-MeAbu	L-MeAla	D-MeNle	D-MeAla	L-MeNle	D-MeAla	D-Pro	L-MeTyr	---	0.8	ND	ND	3.06
3.17	L-MeNva	D-MeAbu	L-MeNva	D-MeNva	D-MeNva	L-MeAbu	D-MeNva	D-Pro	L-MeTyr	---	4.5	ND	ND	4.45
3.18	L-MeNva	D-MeAbu	L-MeNle	D-MeNle	D-MeNle	L-MeNle	D-MeNle	D-Pro	L-MeTyr	---	Below LOD	<0.1	ND	7.24
3.19	D-MeAla	L-MeNva	D-MeAbu	L-MeAla	D-MeAbu	D-MeAbu	L-MeAla	D-MeAbu	D-Pro	L-MeTyr	0.12	<0.1	2.47	1.37
3.20	D-MeAla	L-MeNva	D-MeAbu	L-MeNle	D-MeAbu	D-MeAla	L-MeNva	D-MeAbu	D-Pro	L-MeTyr	1.4	0.58	4.27	3.22
3.21	D-MeAla	L-MeNva	D-MeAbu	L-MeNle	D-MeAbu	D-MeNle	L-MeNle	D-MeAbu	D-Pro	L-MeTyr	0.8		ND	5.07

[a]Ref. 22. [b]LogD via shake-flask method. [c]Calculated LogP, via Osiris Molecular Properties Calculator.

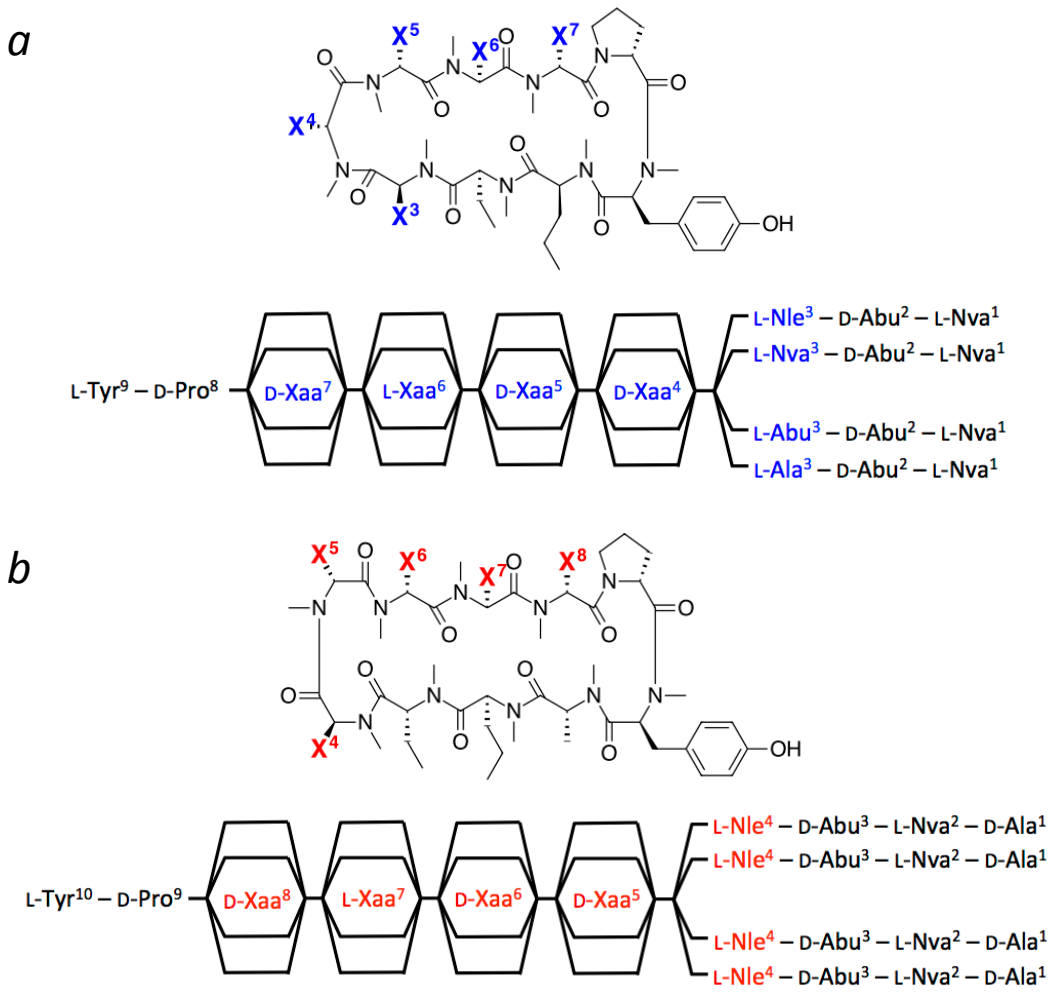

Figure 3.3. Schematic representation of library design for permethylated a) nonapeptides and b) decapeptides of varying lipophilicities.

sized ring systems. To this end, we designed two additional libraries of nonapeptides and decapeptides (Figure 3.3). The results (Figure 3.4) show a similar trend in that both these larger systems show an optimal lipophilicity window. However, additional correlations are also observed; the size of this window seems to decrease with increasing ring size / molecular weight, as does the overall permeation rates. Again, resynthesis and permeability analysis of a small subset from each macrocycle library confirmed these trends (Table 3.3).

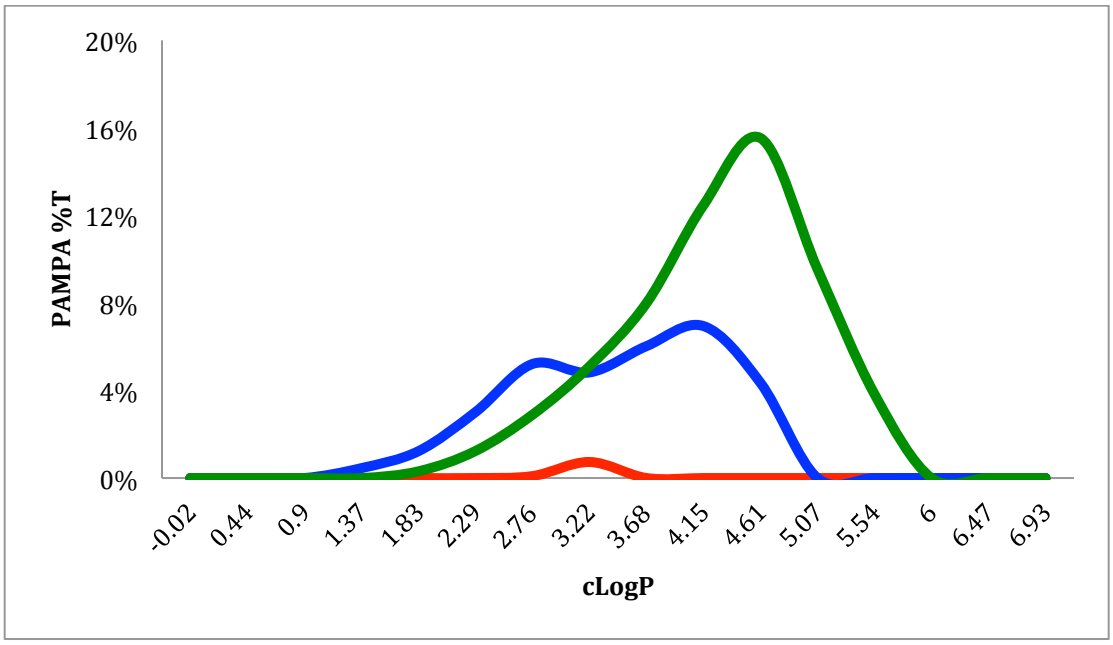

Figure 3.4. Permeabilities via PAMPA (as %T) of permethylated octapeptide (green), nonapeptide (blue) and decapeptide (red) lipophilicity scan libraries.

Overall, these results show that for these large macrocycles, permeability is governed by both lipophilicity and size. On the lower end, increasing lipophilicity leads to an increase in permeability, as is suggested by physical models of membrane permeation; increases in lipophilicity lead to higher hydrocarbon / water partition coefficients and lower desolvation energy costs. However, this is limited by solubility as well. On the higher end, permeability is governed by solubility and/or aggregation propensity of these highly hydrophobic molecules. This suggests an advantage to incorporate aggregation predictors into current computational models, studies of which have been performed computationally on known small molecule aggregators, but not coupled with permeability of macrocycles.[23] In addition, as size increases for these macrocycles, so does the energy cost of passive

membrane permeation, again predicted by the barrier domain model of passive membrane diffusion.

Conclusions and Future Directions

We have successfully demonstrated the impact of both lipophilicity and molecular size on the permeability of large bRo5 macrocycles. We have shown that a balance of both side-chain lipophilicity and solubility must be found to allow membrane permeation of these large molecules. Additionally, we have illustrated the deleterious impact of increased molecular weight on permeability. These results are supported through the synthesis and analysis of individual cyclic peptides in both passive and live-cell permeability assays. Additional experimentation—i.e. solubility, hydrocarbon / water partition coefficients—should be performed to attempt to fit these macrocycles to physical models of membrane permeation, such as the barrier domain model.

However, we recognize these results still leave several questions unanswered. With molecular size having such a detrimental effect on the permeability of large molecules, it begs the question as to how CSA and other bRo5 achieve such optimal permeation rates. Work is currently underway to explain this phenomenon.

General Materials and Methods

Dry tetrahydrofuran (THF) was obtained from an activated alumina-based solvent purification system. Dimethylsulfoxide (DMSO) was dried by storage over 3Å molecular sieves before use. All other chemicals were purchased and used without further purification.

All HPLC/MS chromatograms were obtained on a Waters MicromassZQ mass spectrometer equipped with a Waters 1525 binary HPLC pump and a Waters 2998 photodiode array detector. To determine identity and purity, individually synthesized cyclic peptides were analyzed via reverse phase HPLC through a 3.5 µm C18 (XBridge, 50 mm x 4.6 mm) column at 1.2 mL/min eluting with acetonitrile (ACN) / water, with 0.1% formic acid.

All NMR spectra were recorded at 298 K in chloroform-*d* or dimethylsulfoxide-*d*6 on a 600-MHz Varian Inova spectrometer equipped with a 5-mm inverse detection probe. Spectra were referenced to residual solvent proton signals (^{1}H 7.26 for chloroform-*d*, 2.50 for dimethylsulfoxide-*d*6).

Synthesis of Pure Cyclic Permethylated Peptides

Cyclic peptides were synthesized starting with the allyl ester of *N*-fluorenylmethyloxycarbonyl (Fmoc)-protected tyrosine linked via the phenolic hydroxyl group to 2-chlorotrityl polystyrene resin (0.4 mmol/g loading value) according to published procedures [24] The linear peptide sequences were synthesized and cyclized using an automated peptide synthesizer (Prelude, Protein Technologies). In general, couplings were performed using 4 eq Fmoc-protected amino acid, 3.8 eq O-(azabenzotriazol-1-yl)-*N*,*N*,*N*',*N*'-tetramethyluronium hexafluorophosphate (HATU) and 6 eq *N*,*N*-diisopropylethylamine (DIPEA) in *N*,*N*-dimethylformamide (DMF, 0.1 M with respect to amino acid) for 1 h. Fmoc deprotections were carried out with 2% 1,8-diazabicycloundec-7-ene (DBU) and 2% piperidine in DMF for 15 min.

After each coupling and deprotection step, the resin was washed with DMF (3×), DCM (3×) and DMF (3×). After the addition of the final residue, deallylation and final Fmoc

removal were performed simultaneously with a solution of 1 eq $Pd(Ph_3P)_4$ in THF containing 10% (v/v) piperidine for 3 h. A chelating wash was performed to remove traces of palladium using 5% (w/v) sodium diethyldithiocarbamate and 5% (v/v) DIPEA in DMF, followed by the normal DMF-DCM-DMF resin wash sequence. Cyclization was performed with 3 eq (Benzotriazol-1-yloxy)tripyrrolidinophosphonium hexafluorophosphate (PyBOP), 3 eq 1-hydroxy-7-azabenzotriazole (HOAt), and 6 eq DIPEA in DMF for 3 h, followed by resin washing with five final DCM washes to remove residual DMF.

Following cyclization, cyclic peptides were subjected to an on-resin permethylation step.[25] In short, to the resin-bound peptides were added lithium tert-butoxide (3 equiv / NH) in DMSO / THF (1:1). The resin was agitated for 15 min, after which methyl iodide was added. After an additional 15 min agitation, the resin was washed exhaustively with water, followed by washings with DMF (3x), MeOH (3x), and DCM (3x). Peptides were cleaved with a 5% (v/v) trifluoroacetic acid (TFA) in DCM solution. The filtrate was concentrated and the crude residue was then purified by reverse phase automated flash chromatography (Isolera Prime, Biotage) and lyophilized.

Synthesis of Cyclic Peptide Libraries

The permethylated libraries were synthesized using the "split-pool" strategy[26] (Figure 1b), starting with the allyl ester of *N*-fluorenylmethyloxycarbonyl (Fmoc)-protected tyrosine linked via the phenolic hydroxyl group to 2-chlorotrityl polystyrene resin (0.4 mmol/g loading value) according to published procedures.[24] Standard Fmoc / tBu SPPS techniques were utilized as outlined in the synthesis of pure cyclic hexapeptides. For all couplings, a coupling solution was prepared by dissolving 4 eq of the amino acid and 3.8 eq

of HATU in DMF (0.2 M with respect to amino acid). DIPEA (6 eq) was added and the solution was allowed to preactivate for 30 min, then added to the deprotected resin.

One gram of resin loaded with Fmoc-L-Tyr-OAllyl was coupled with Fmoc-D-proline as outlined above, then segregated into four separate polypropylene SPPS vessels and deprotected for 30 min. The resin was washed with DMF (3x), MeOH (3x), DCM (3x), and DMF (3x), then coupled with either *N*-Fmoc-D-norleucine, *N*-Fmoc-D-norvaline, *N*-Fmoc-D-aminobutyric acid, or *N*-Fmoc-D-alanine as outlined above. The resin was washed, pooled into a single vessel, thoroughly mixed, and the split-pool process repeated (following the same stereochemistry as compound **3.1**-**3.4**) to generate four sub-libraries of 256 linear heptapeptides. To keep the library size relatively small, all sub-libraries were coupled with *N*-Fmoc-D-aminobutyric acid.

After the final coupling, each portion of resin was washed and subjected to the simultaneous N/C-terminus deprotection. After deprotection, the resin was washed, cyclized as previously described, washed again, and subjected to the described on-resin permethylation conditions. The resin-bound sub-libraries were cleaved with a 5% solution of TFA in DCM. The collected filtrates were concentrated and the residue redissolved in DMSO at a concentration of 100 mg/mL to give stock solutions of four 256-member sublibraries of permethylated octapeptides.

Libraries of permethylated nonapeptides were generated in a similar manner except after coupling of the final Abu residue, an additional coupling of *N*-Fmoc-L-norvaline was performed to give four sub-libraries of 256 linear nonapeptides, which were cyclized, permethylated, cleaved, and reconstituted in DMSO as described above.

Libraries of permethylated decapeptides were generated in a similar manner except after the coupling of the final Nva residue (in the preparation of nonapeptides), an additional coupling of *N*-Fmoc-D-alanine was performed to give four sub-libraries of 256 linear decapeptides, which were cyclized, permethylated, cleaved, and reconstituted in DMSO as described above.

Permeability Analysis of Cyclic Peptide Mixtures by PAMPA

A 96-well donor plate with 0.45 µ hydrophobic Immobilon-P membrane supports (Millipore) and a 96-well Teflon acceptor plate were used in the PAMPA permeability test. The acceptor plate was prepared by adding 300 µL of 5% DMSO in pH=7.4 phosphate-buffered saline (PBS) to each well. Donor well solutions of the cyclic peptide libraries were prepared by diluting 10 µL of the DMSO stock solutions prepared above to a final volume of 200 µL with PBS. The suspensions were centrifuged to remove any insoluble material. A 1% (w/v) solution of lecithin in dodecane was prepared and sonicated before use. 5 µL of the dodecane / lecithin solution was carefully applied to the membrane supports in the wells of the donor plate, with care being taken to not touch the pipet tip to the membrane. Without allowing this solution to evaporate, 150 µL of the peptide solutions were added to the donor wells. The donor plate was then placed on top of the acceptor plate so that the artificial membrane was in contact with the buffer solution below. A lid was placed on the donor well, and the system was covered with a glass evaporating dish and left overnight (18 h) at room temperature. A wet paper towel was placed on the inside of the chamber to prevent evaporation.

Donor well solutions before (t = 0 h) and after (t = 18 h) PAMPA as well as acceptor well solutions after PAMPA were prepared by combining 25 uL of each solution with 25 uL of an aqueous 100 μM H-Tyr(OtBu)-OH solution (as an internal standard) and 50 μL of methanol. These solutions were analyzed by LCMS (Waters Micromass ZQ) through a 5 μm C18 column (Alltech, 150 mm x 4.6 mm) using selected ion monitoring (SIM) mode. Permeability (%T) was quantified as the ratio of analyte-to-standard areas in the acceptor well divided by a theoretical equilibrium ratio based on amounts of combined analyte found in the donor and acceptor wells as follows:

$$\%T = \frac{R_A}{\left(\frac{R_A V_A + R_D V_D}{V_A + V_D}\right)} \tag{3.7}$$

Where R_A and R_D are the ratio of analyte to internal standard in the acceptor and donor wells, respectively, and V_A and V_D are the volumes of the acceptor (300 uL) and donor (150) wells, respectively.

Permeability Analysis of Pure Cyclic Peptides by PAMPA

Pure compounds were analyzed via PAMPA as outlined above. Permeation rates (P_e) were calculated from %T by the following equations:

$$P_e = -\frac{V_A V_D}{V_A + V_D} \times \frac{\ln(1 - \%T)}{At} \tag{3.8}$$

Where A is the surface area of the filter support (0.24 cm^2), and t is time of the incubation period in seconds.

LCMS Spectra for 3.1

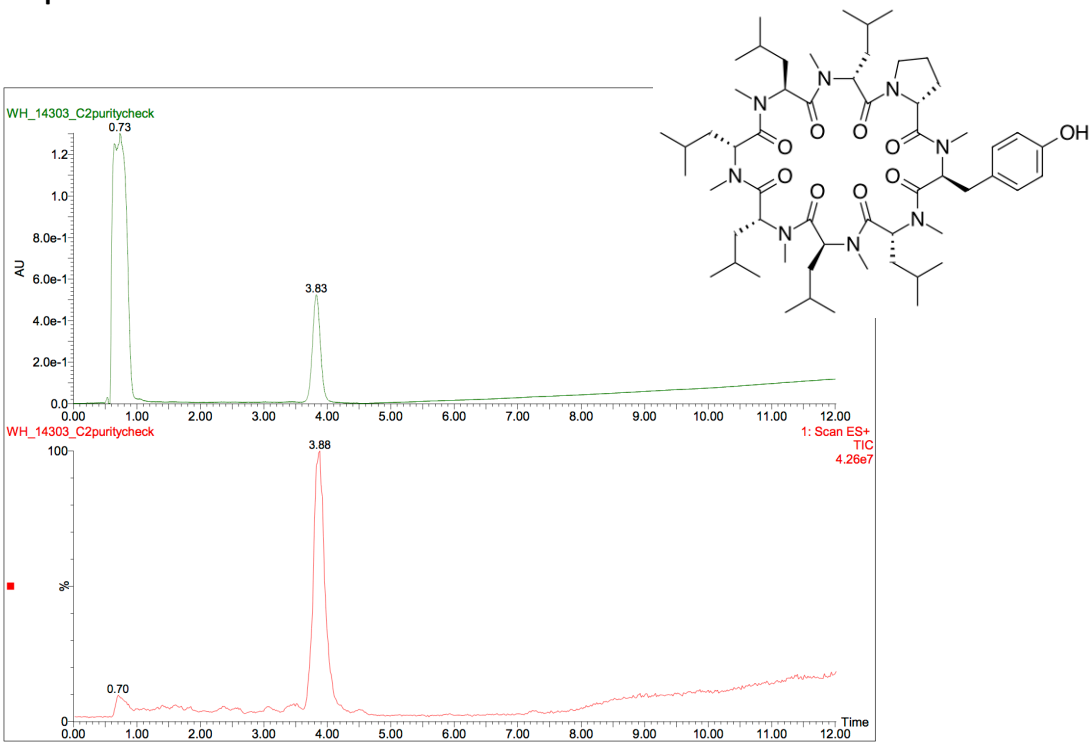

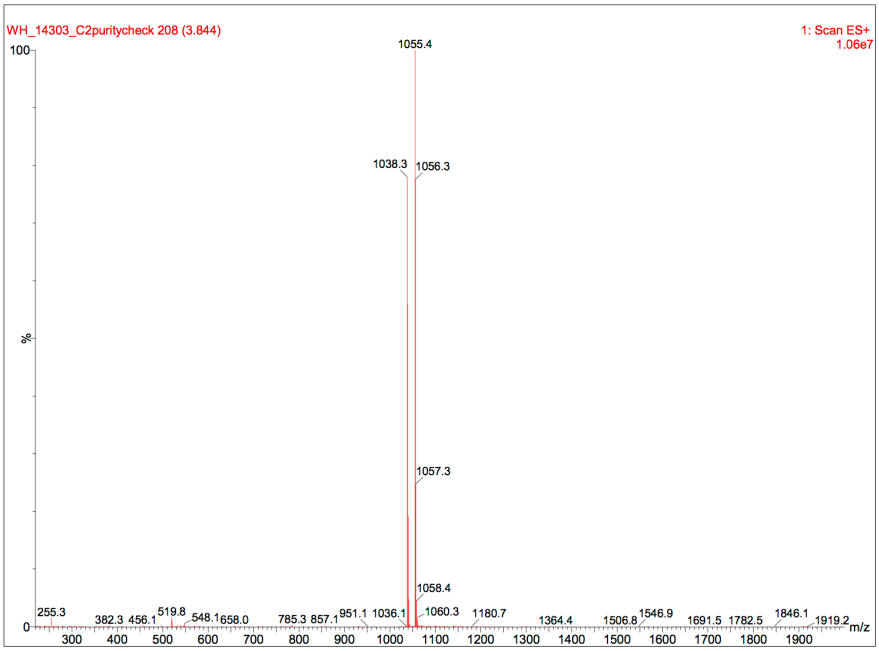

LCMS Spectra for 3.2

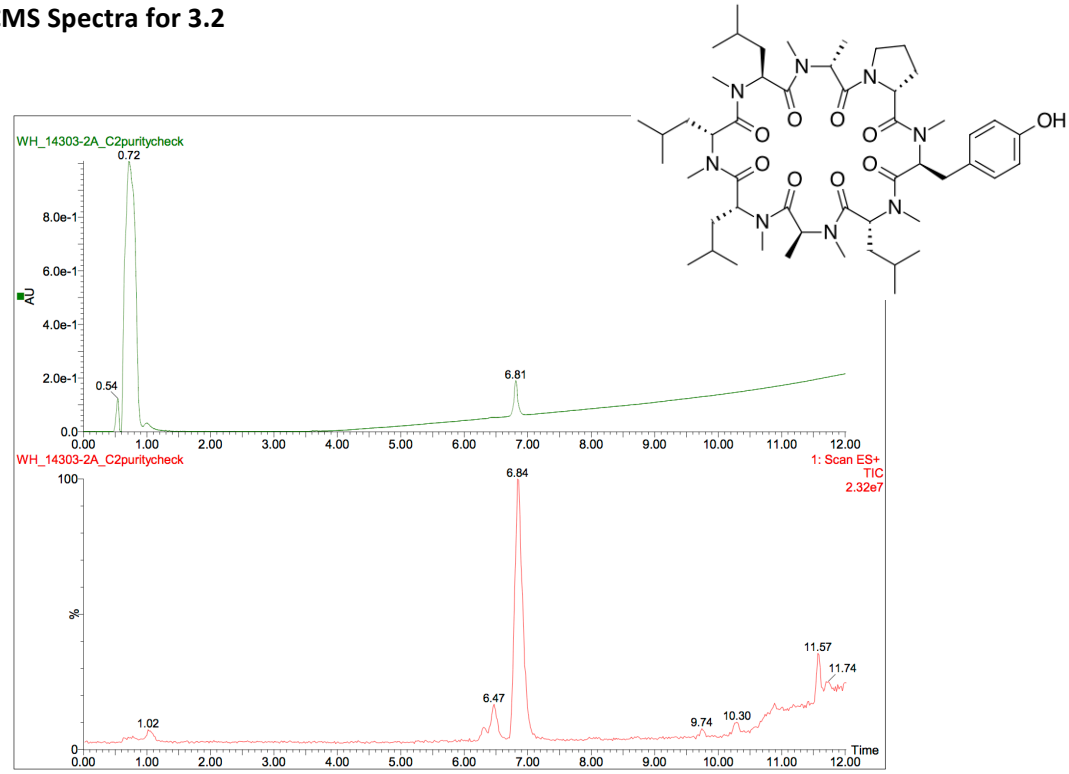

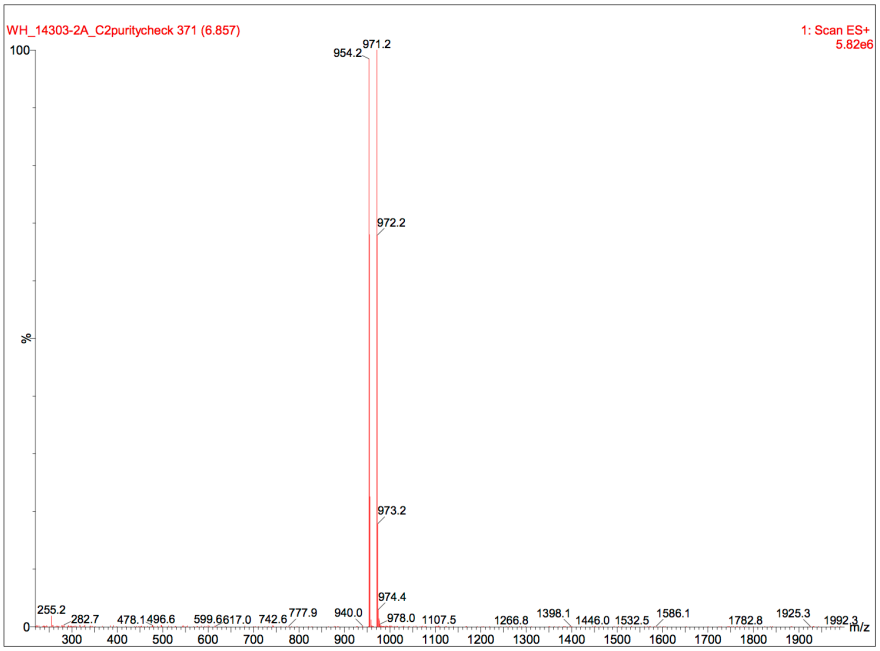

LCMS Spectra for 3.3

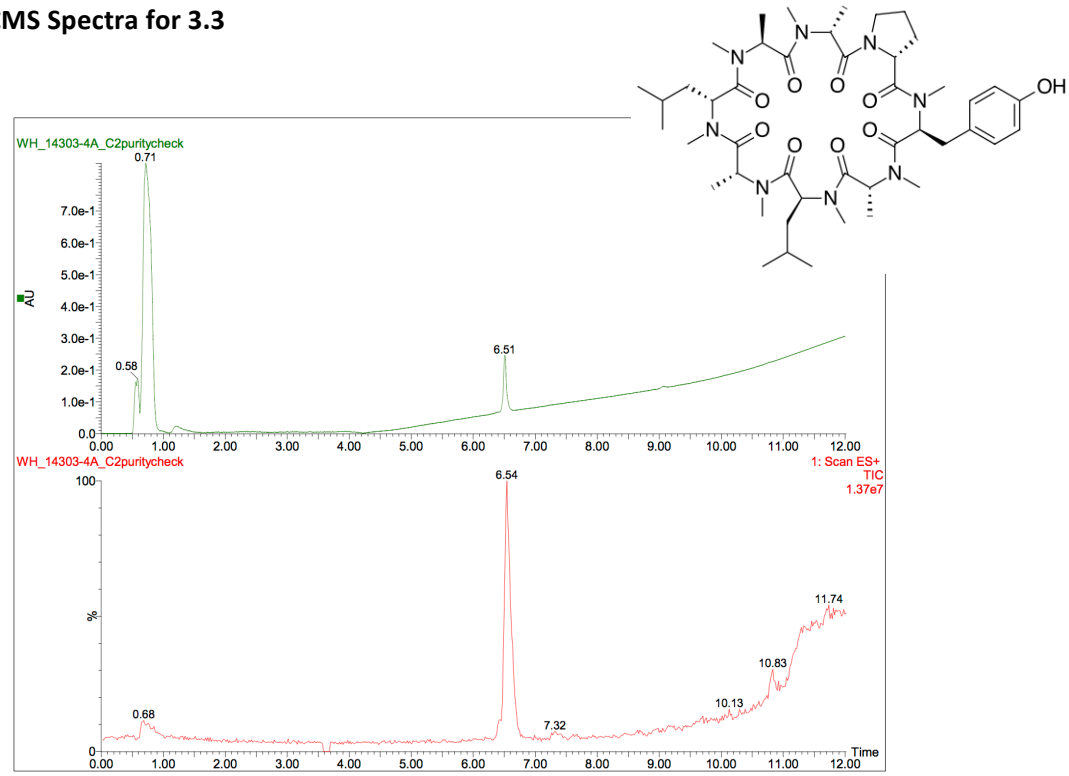

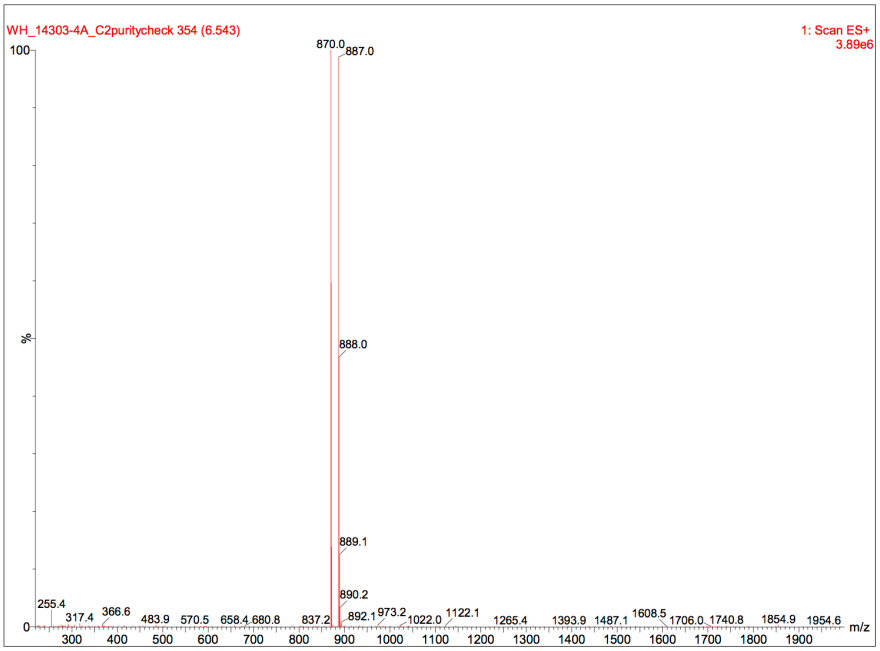

LCMS Spectra for 3.4

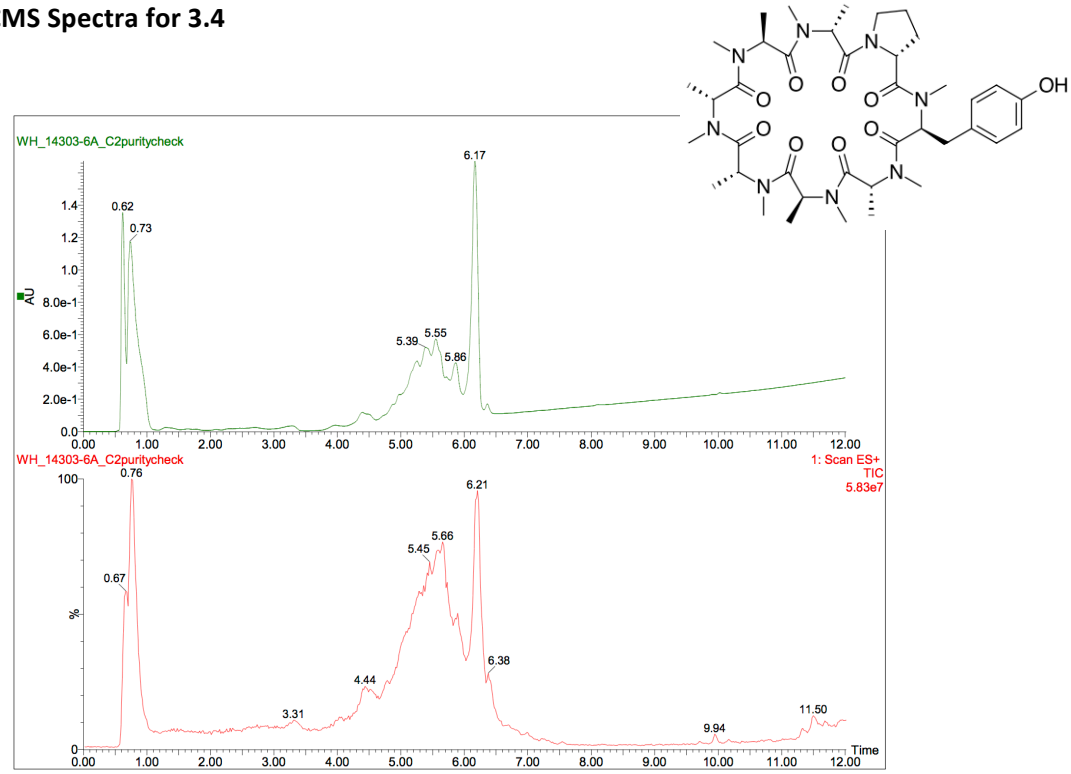

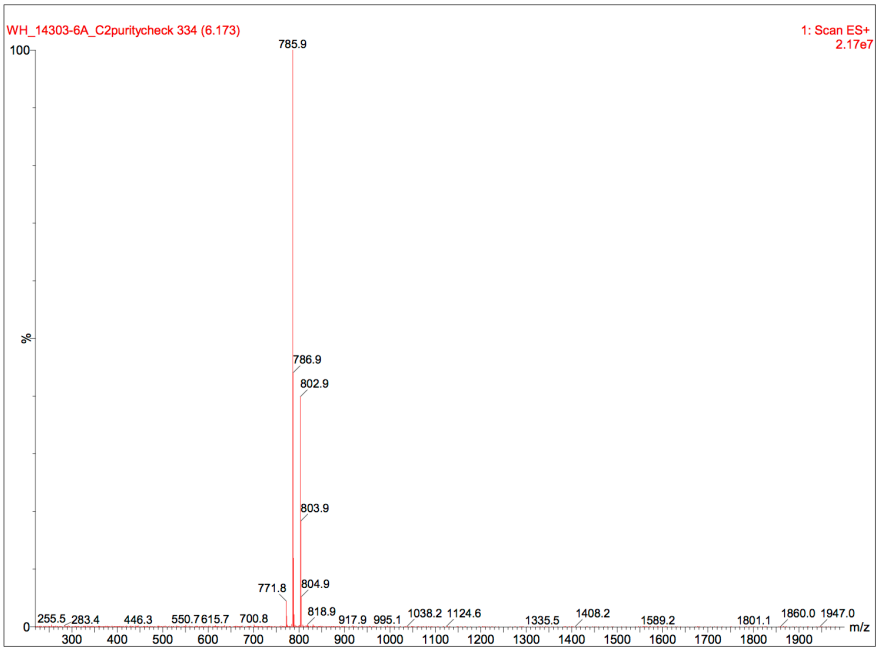

LCMS Spectra for 3.5

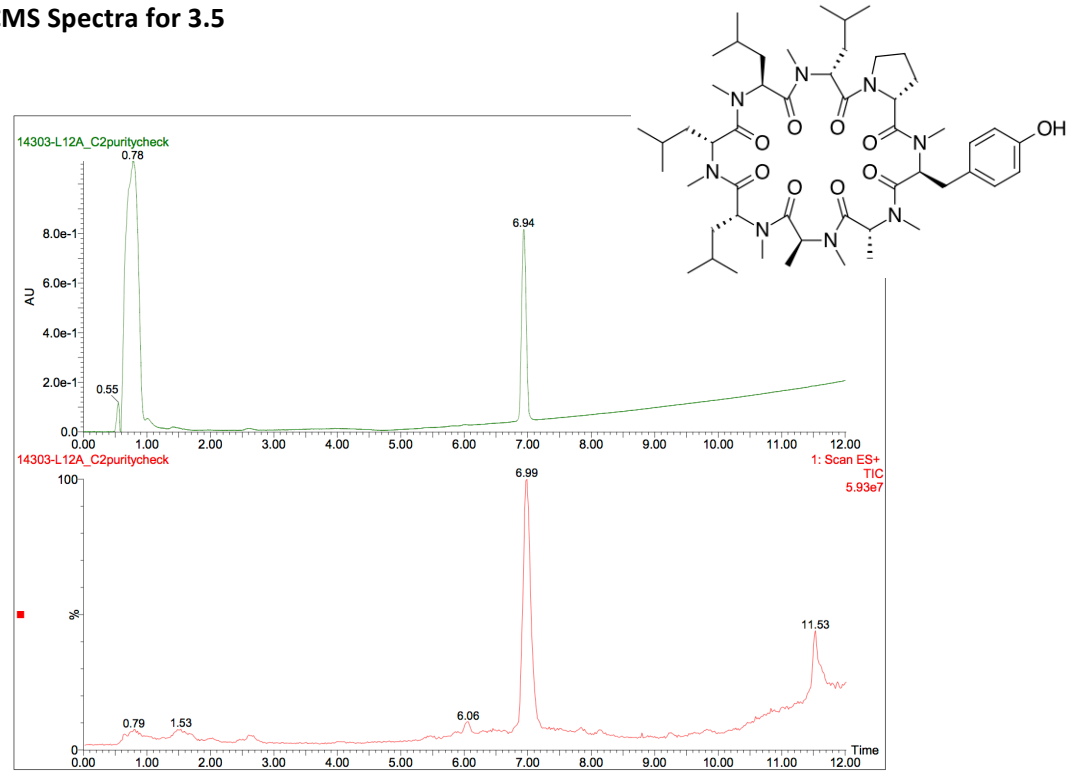

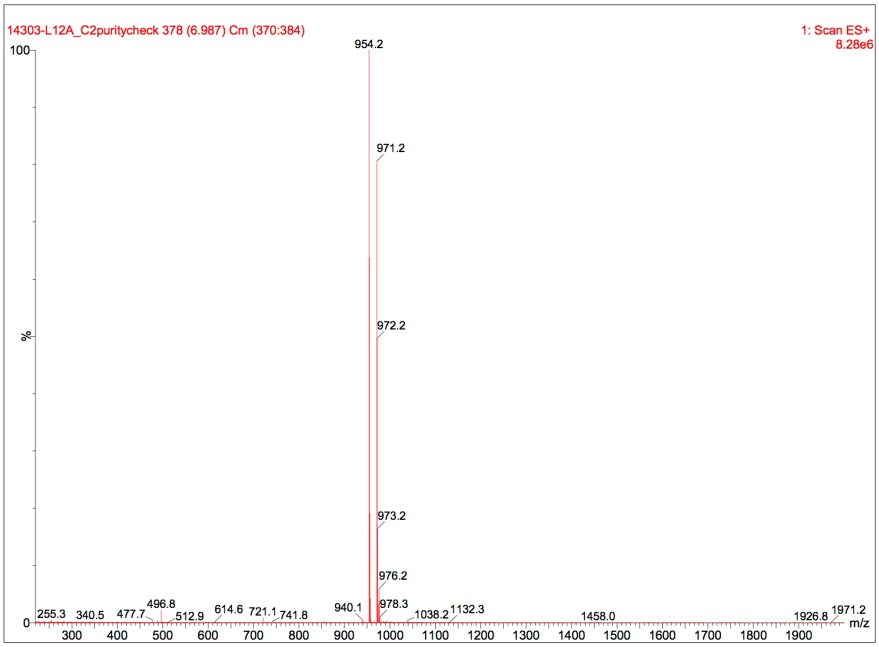

LCMS Spectra for 3.6

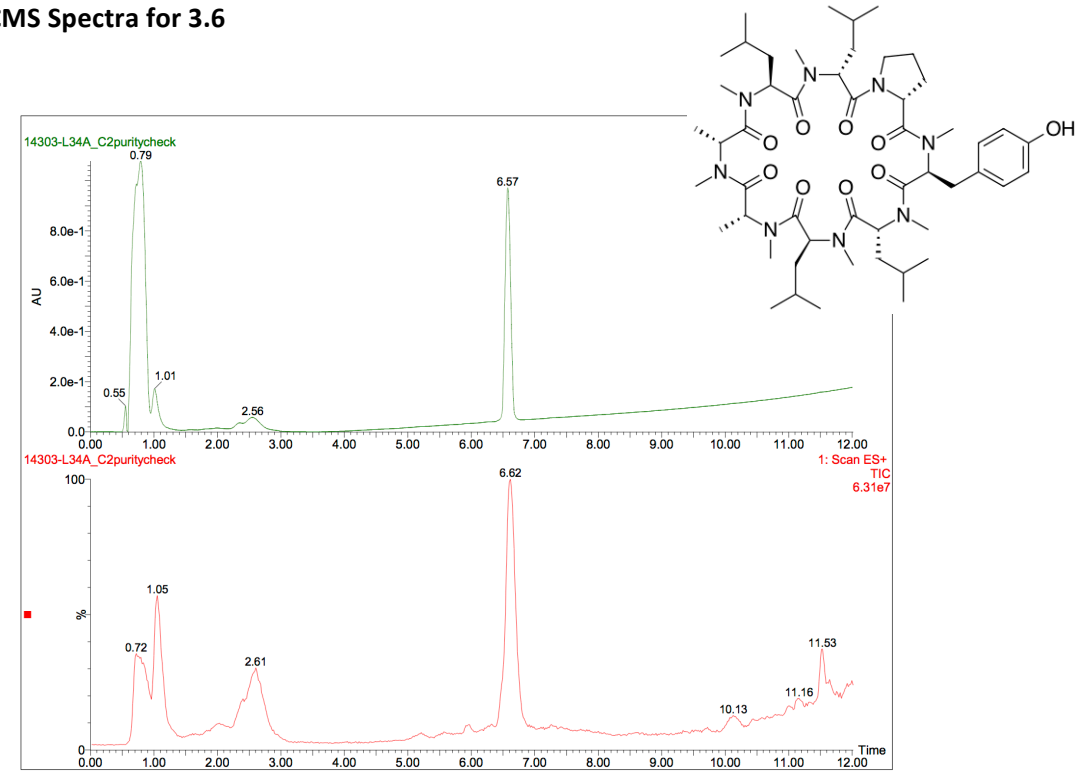

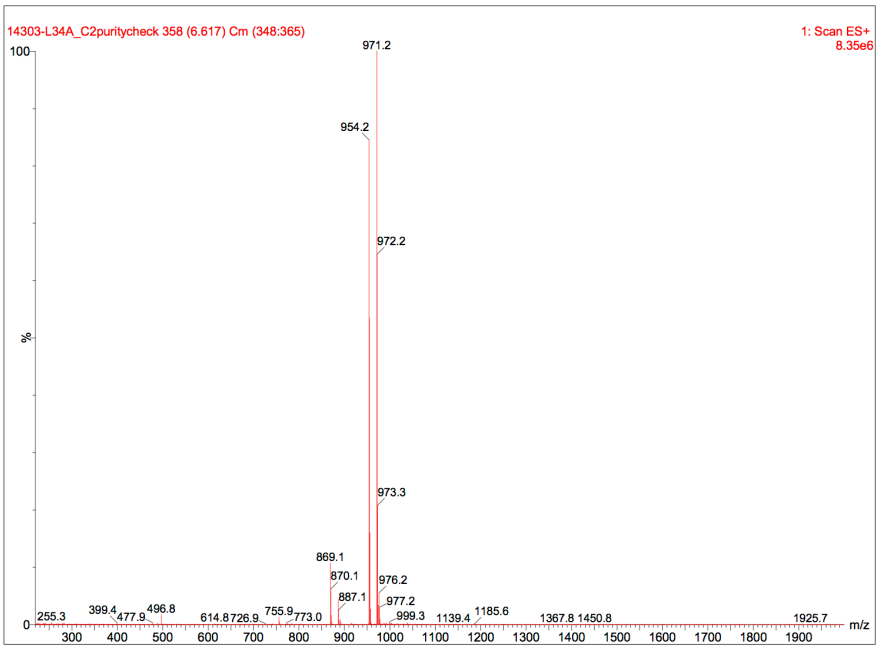

LCMS Spectra for 3.7

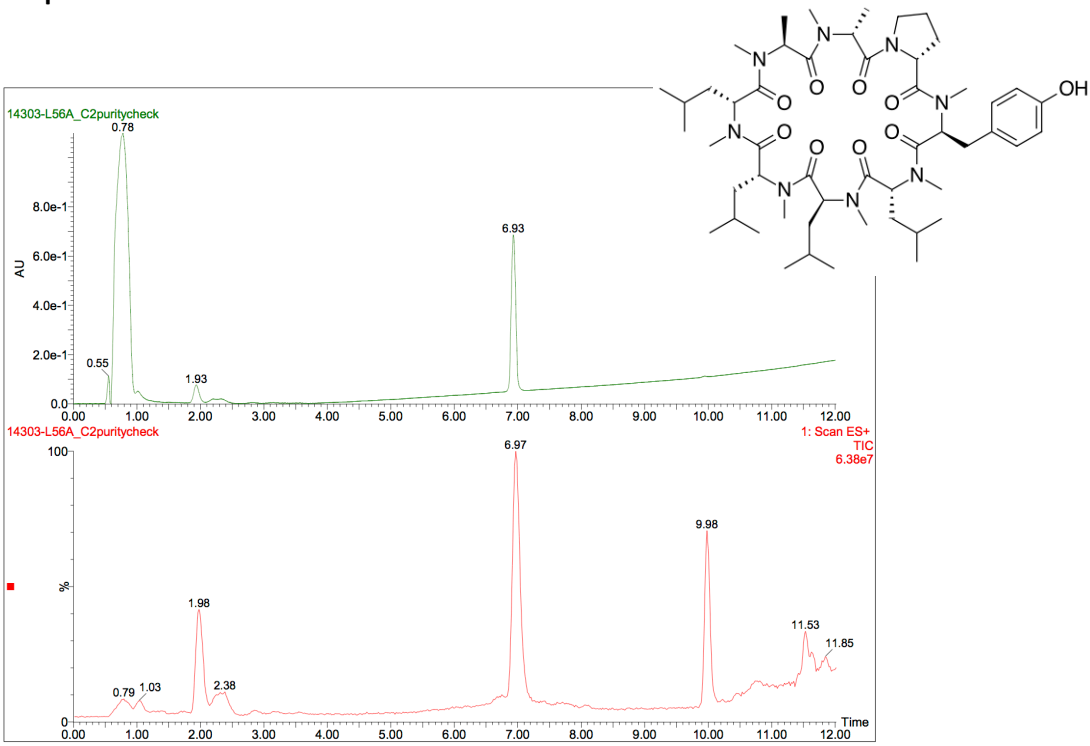

LCMS Spectra for 3.8

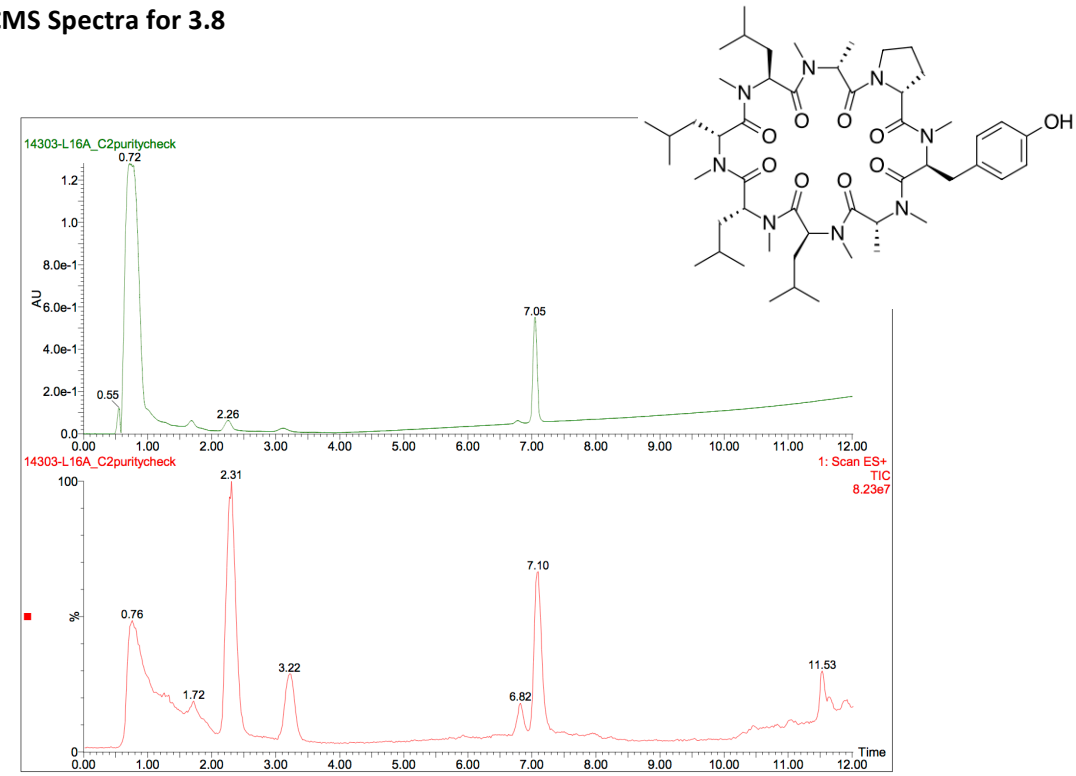

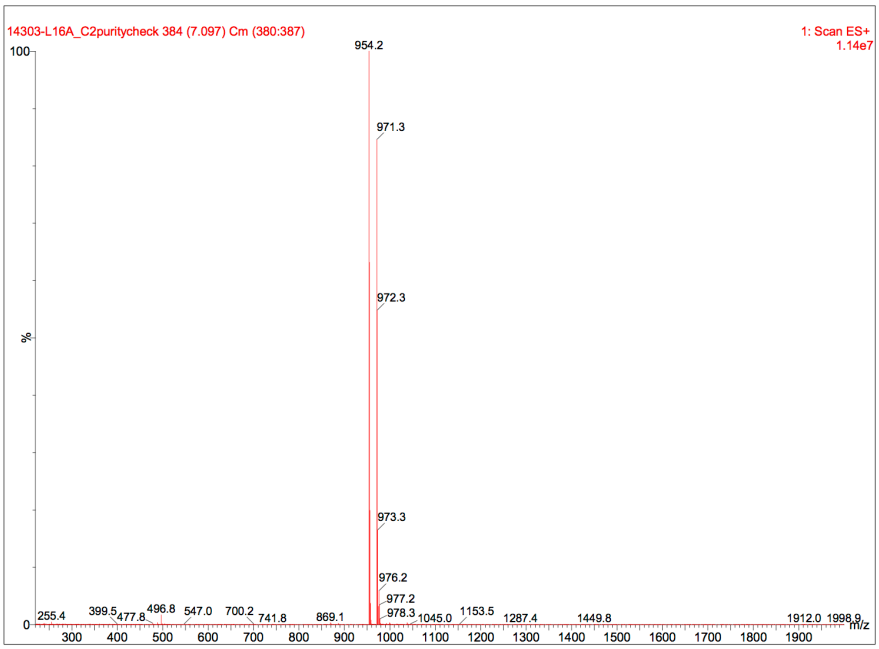

LCMS Spectra for 3.9

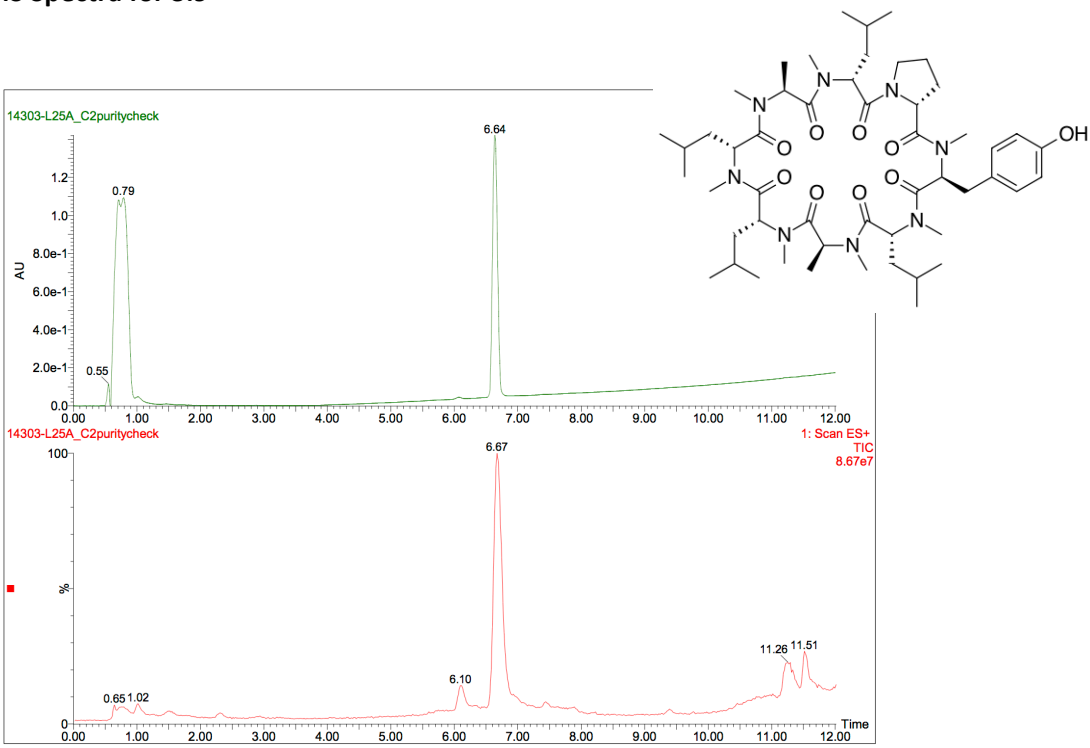

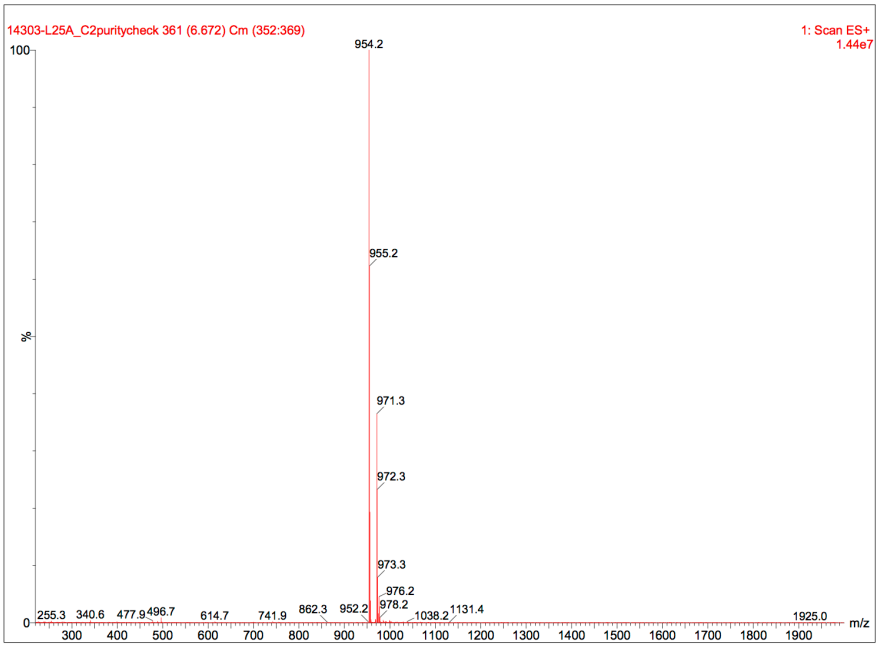

LCMS Spectra for 3.10

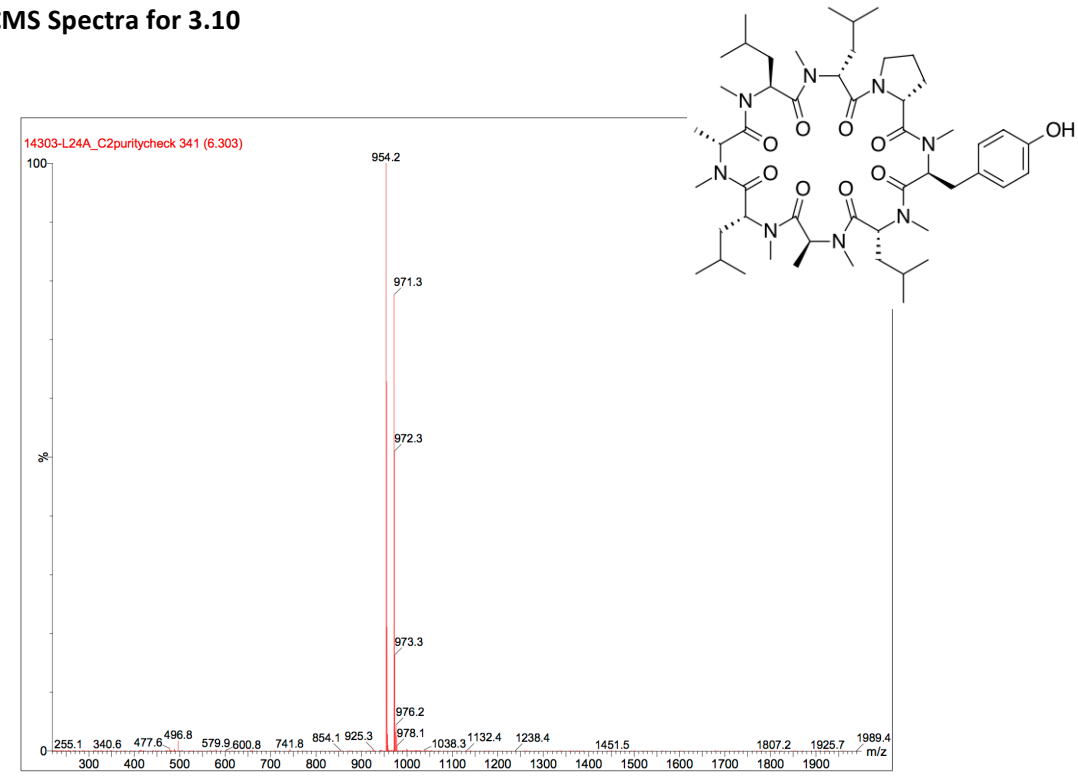

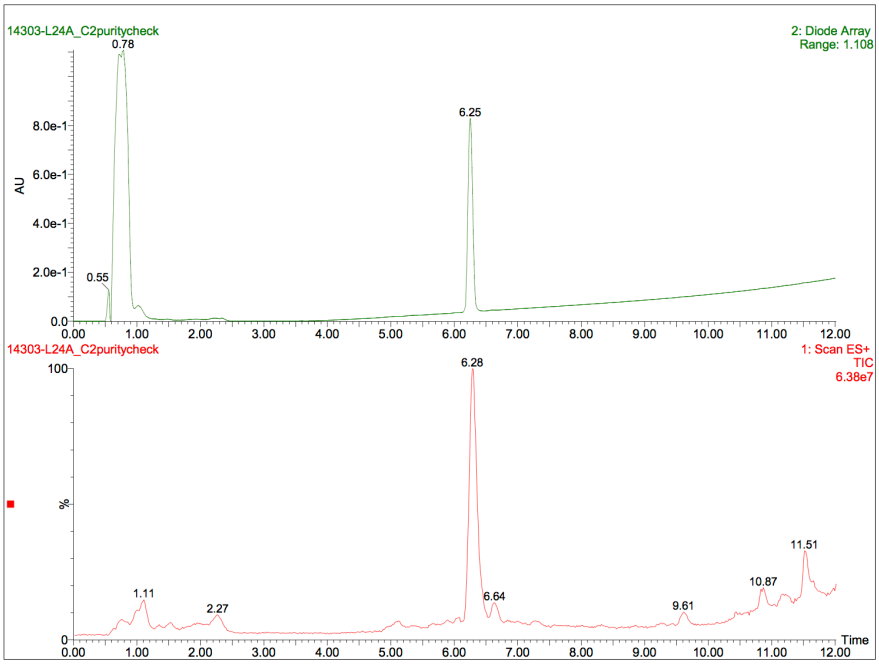

LCMS Spectra for 3.11

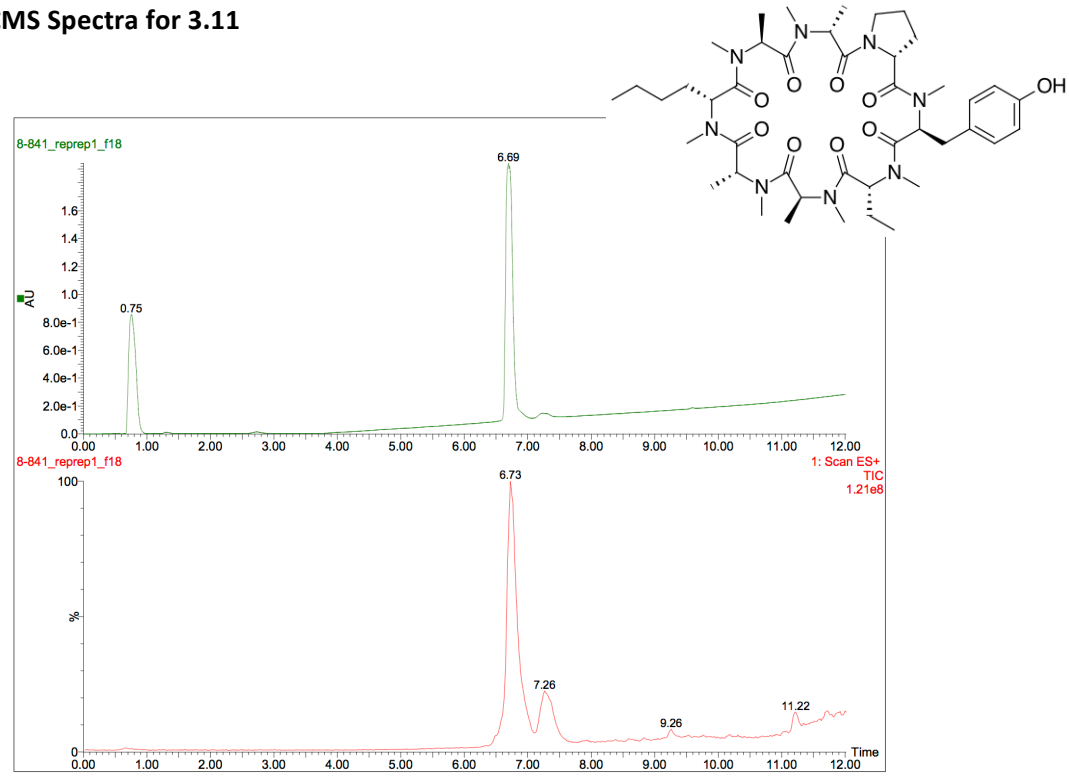

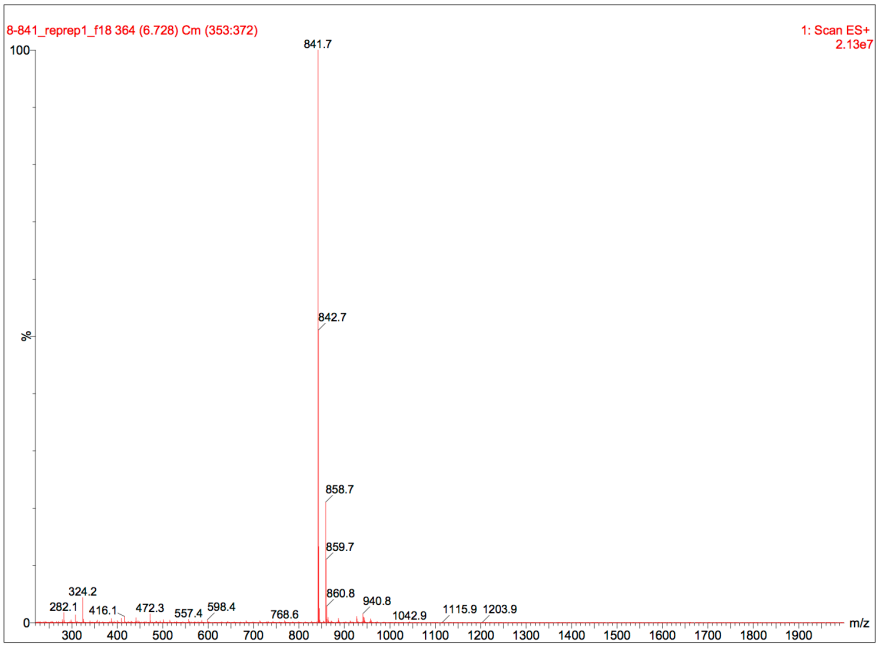

LCMS Spectra for 3.12

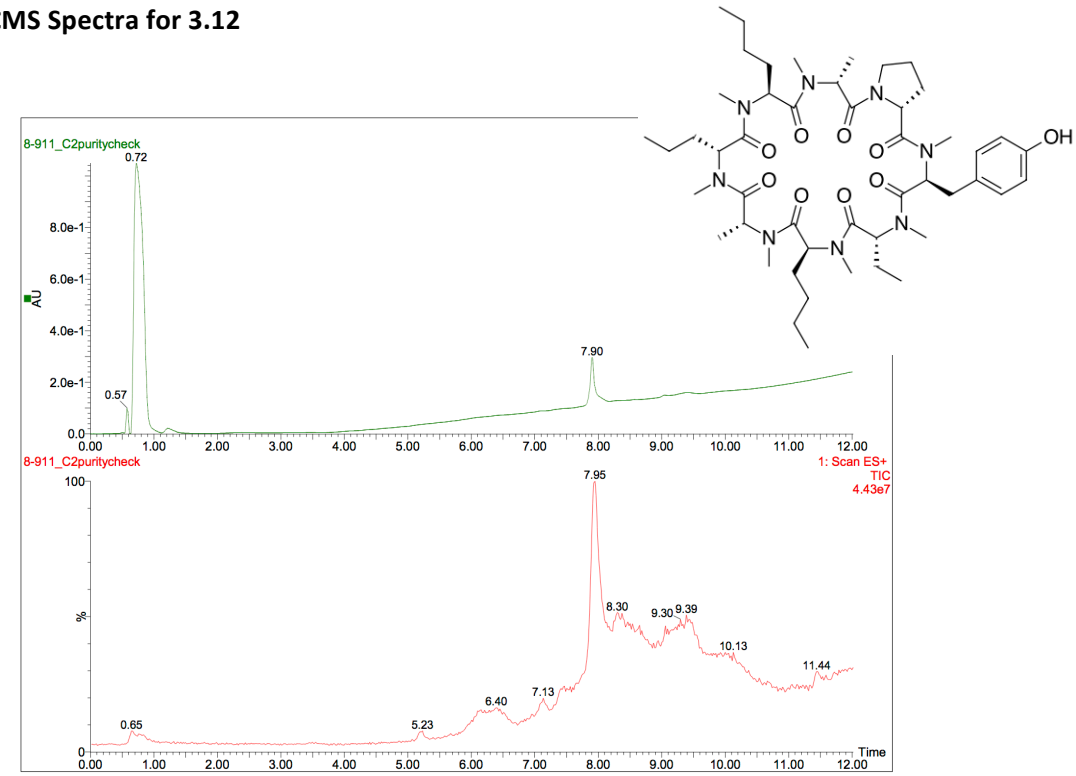

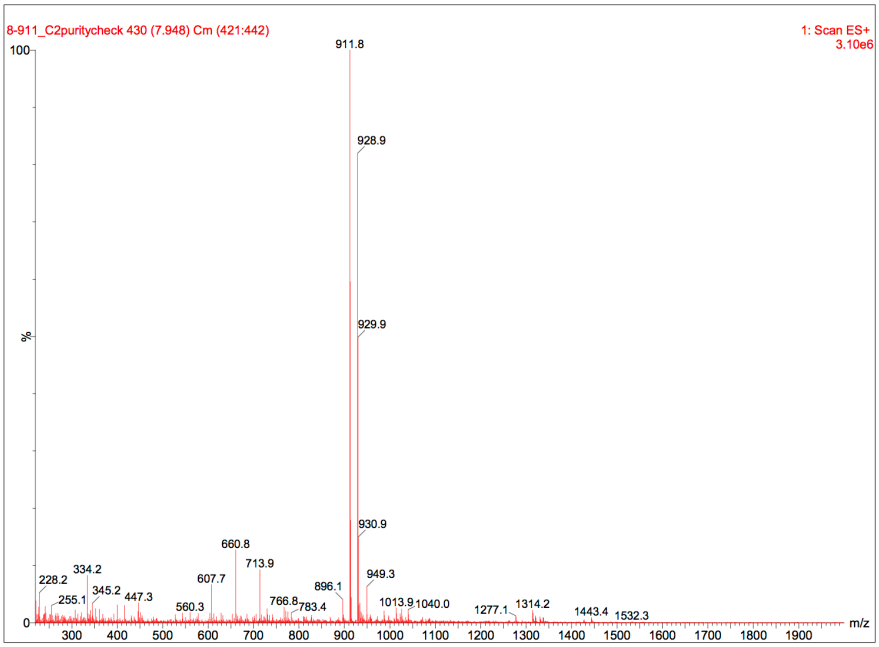

LCMS Spectra for 3.13

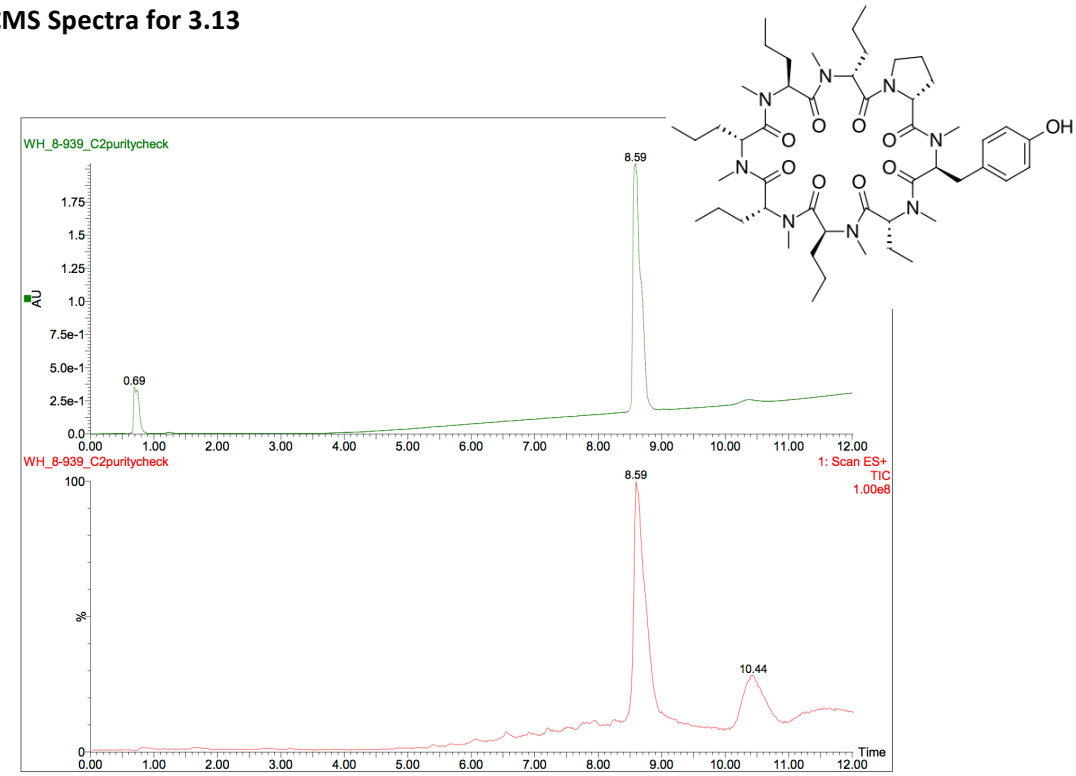

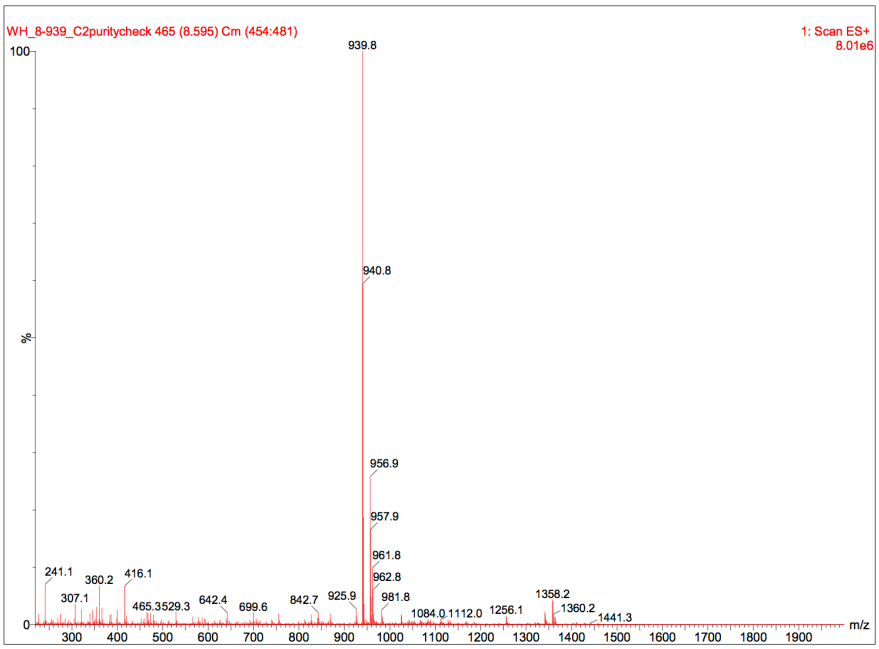

LCMS Spectra for 3.14

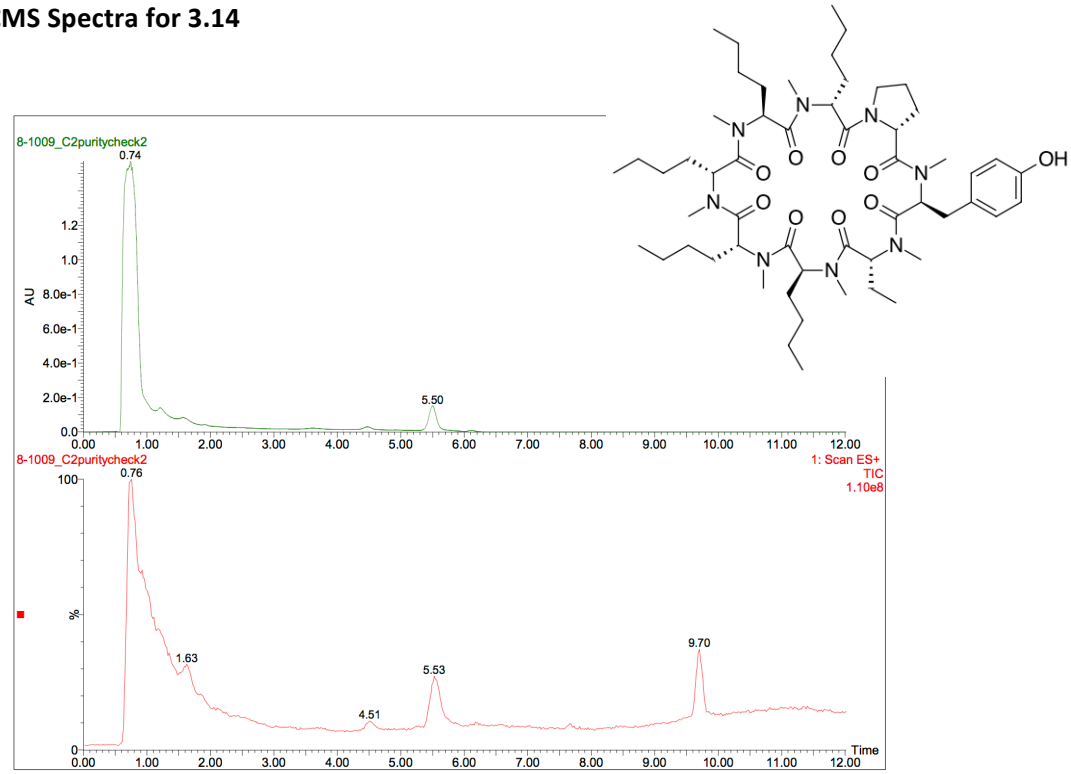

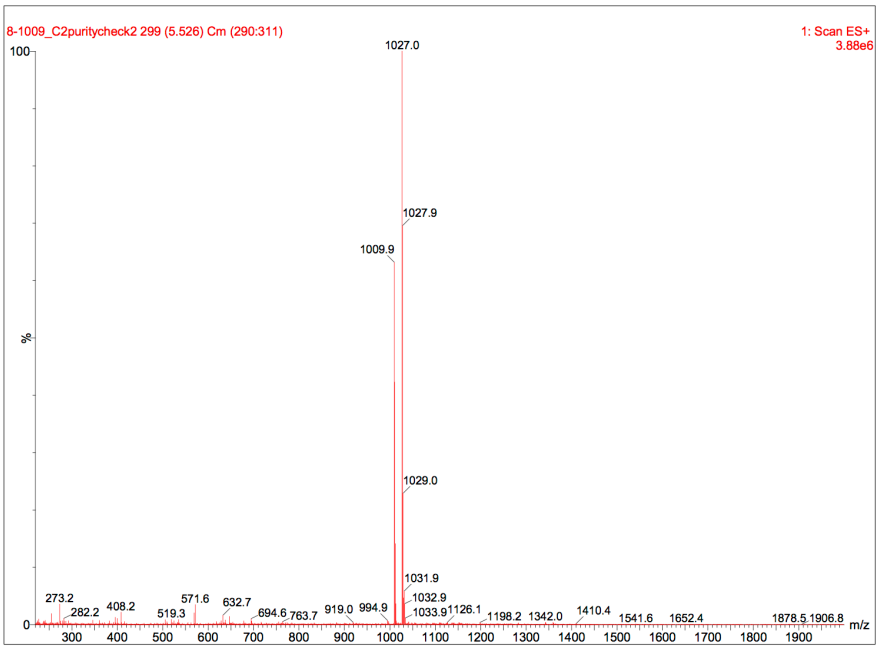

LCMS Spectra for 3.15

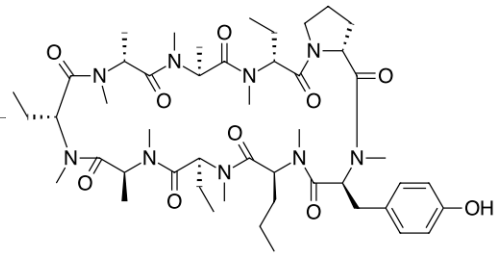

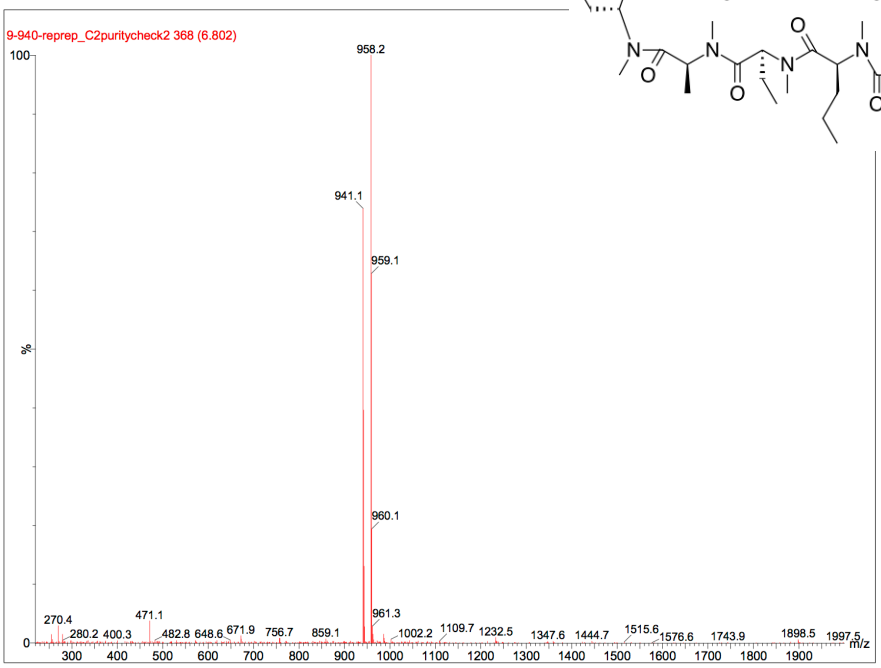

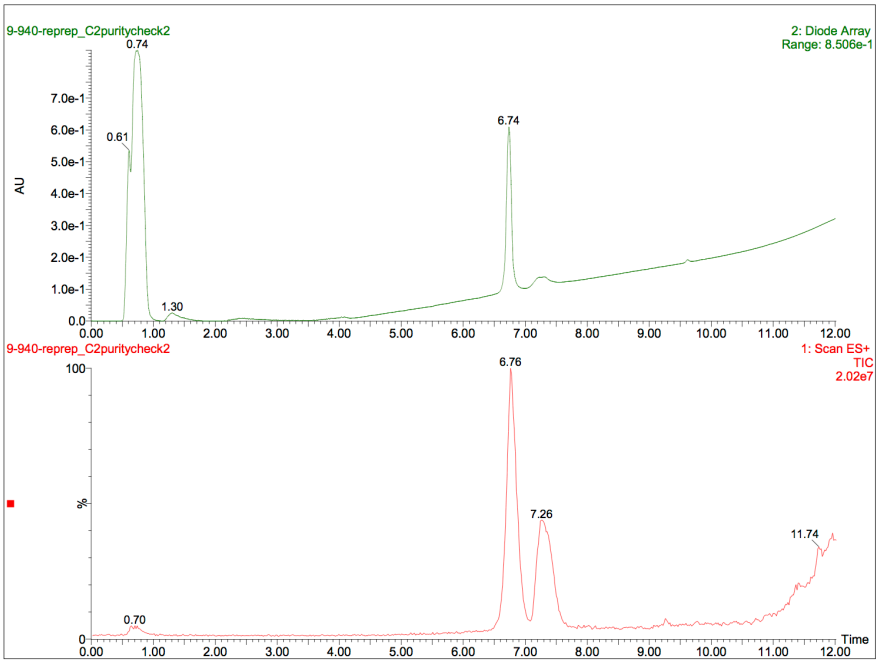

LCMS Spectra for 3.16

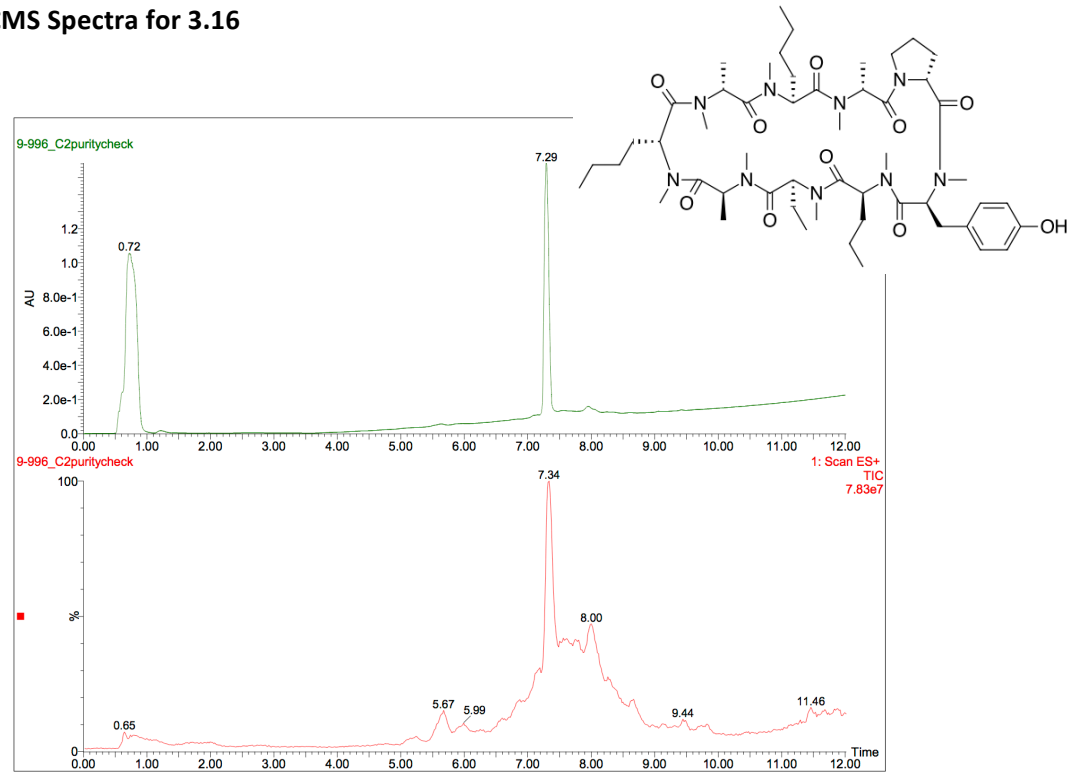

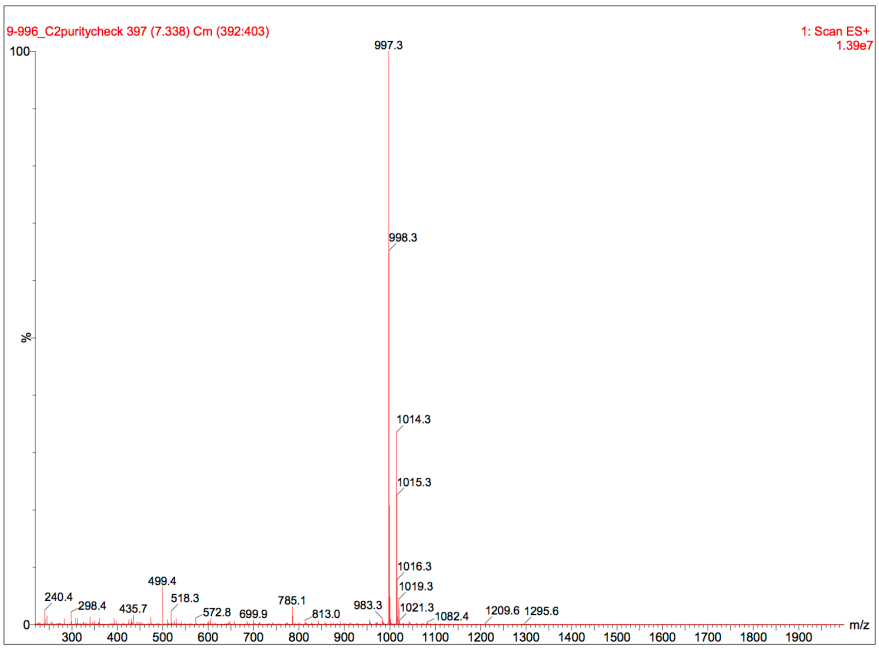

LCMS Spectra for 3.17

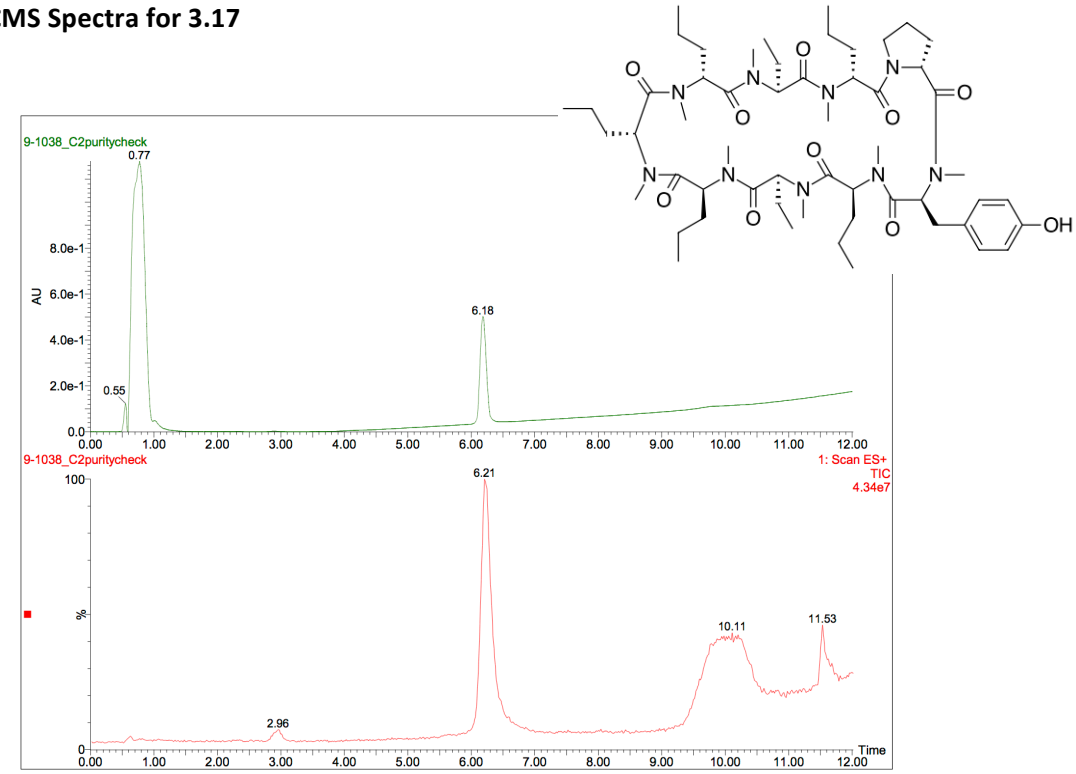

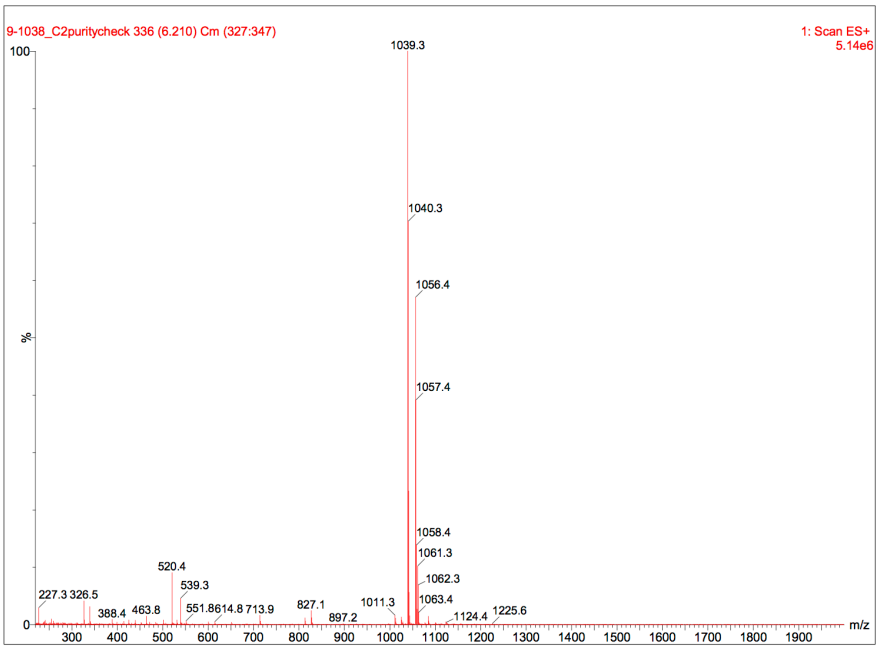

LCMS Spectra for 3.18

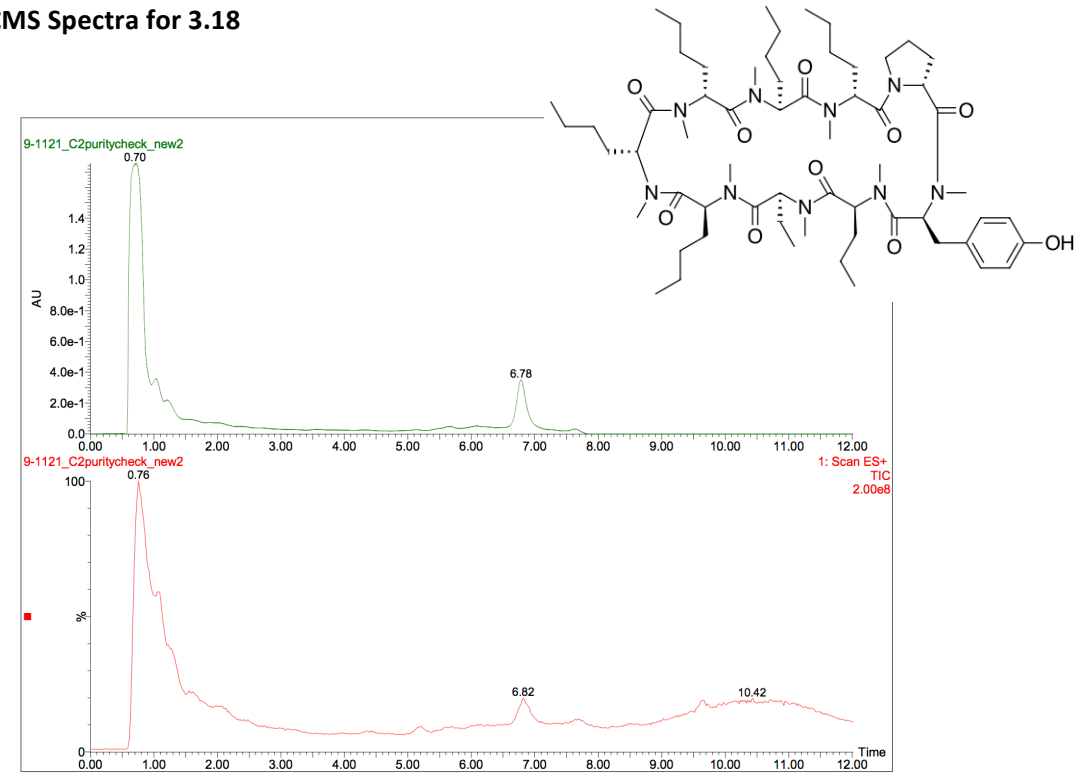

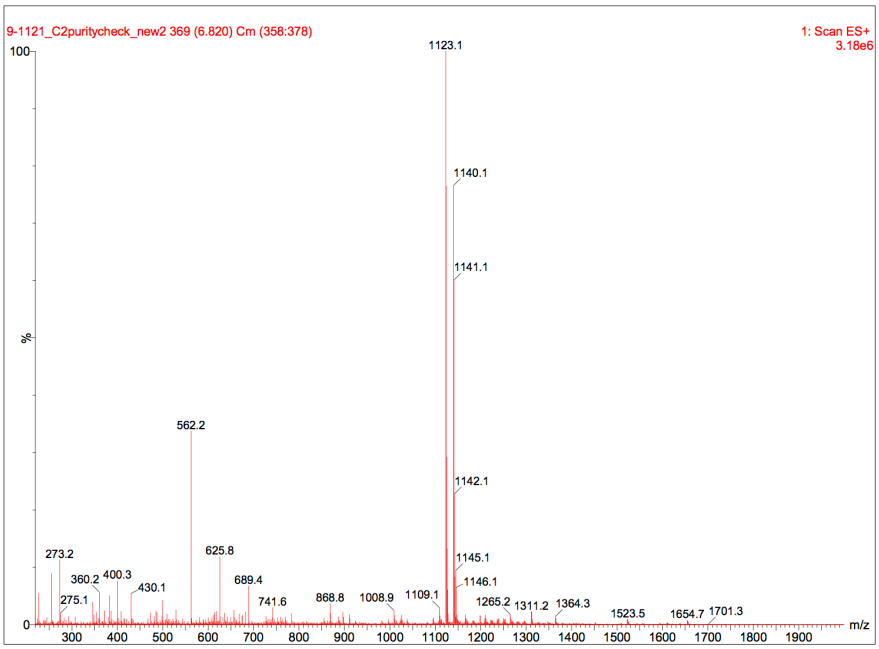

LCMS Spectra for 3.19

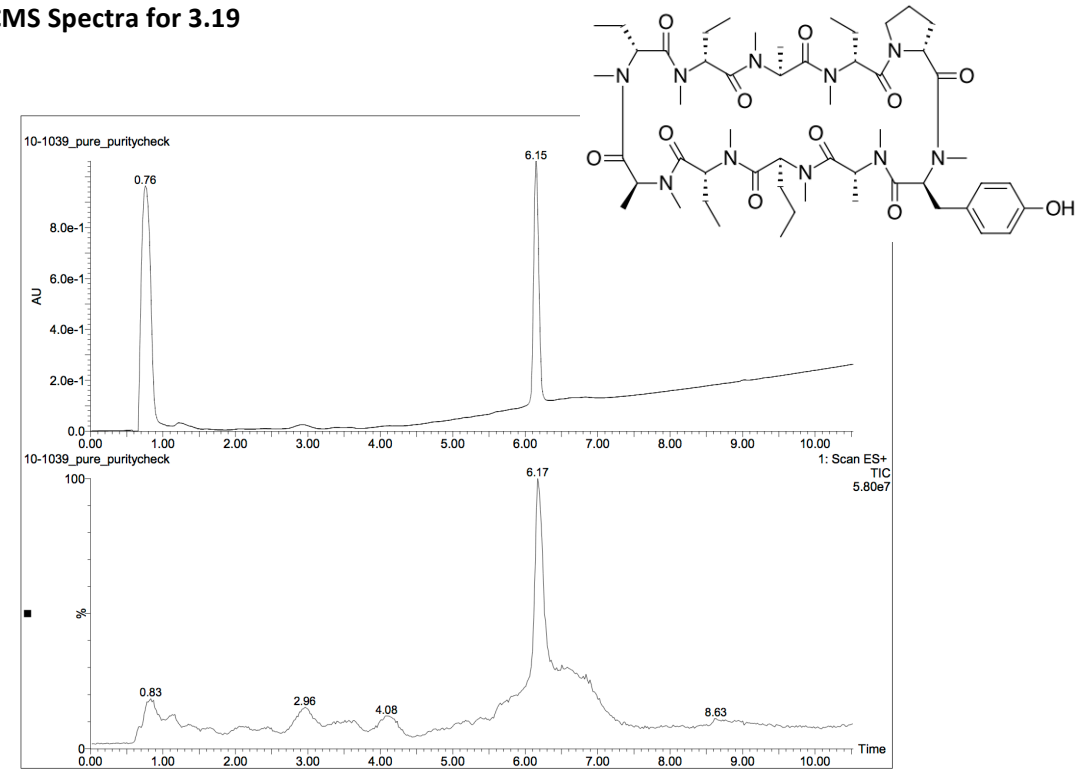

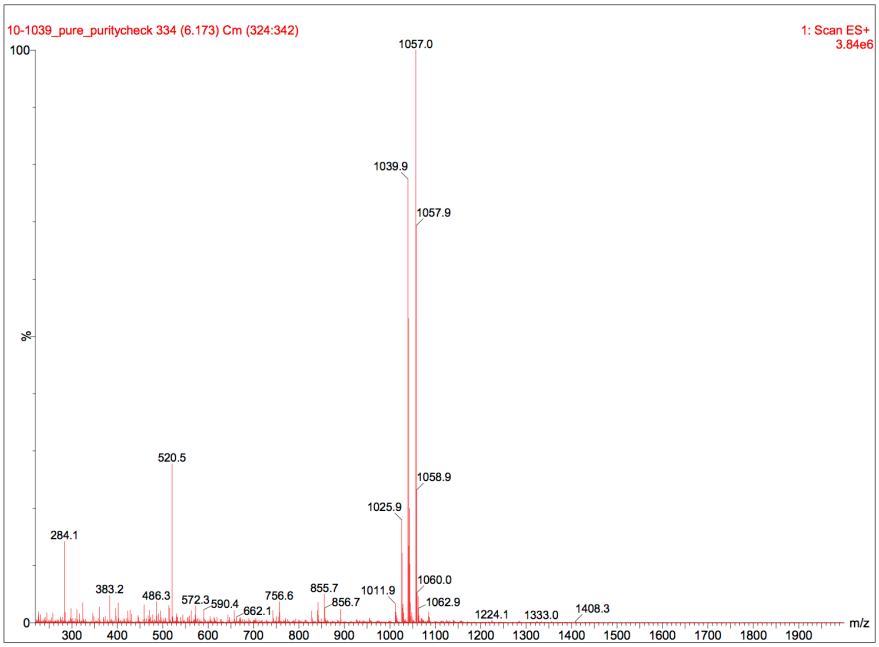

LCMS Spectra for 3.20

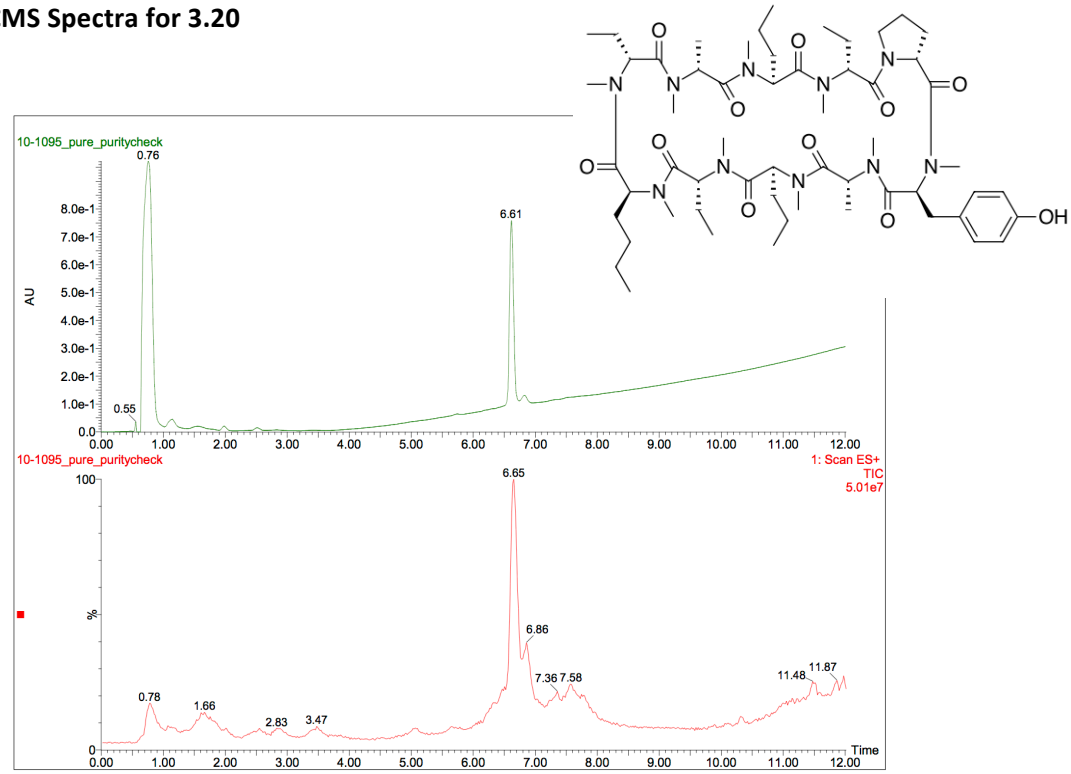

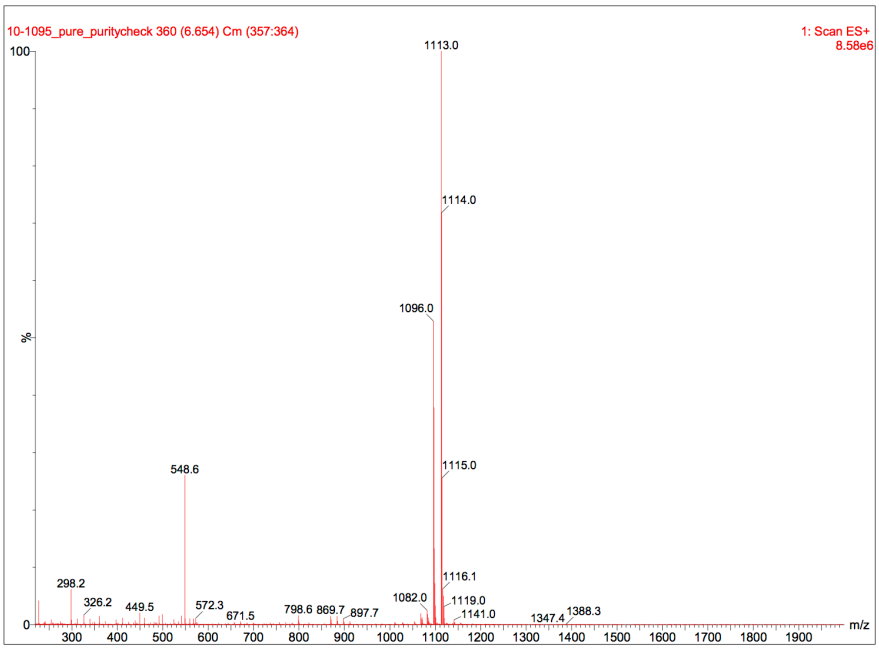

LCMS Spectra for 3.21

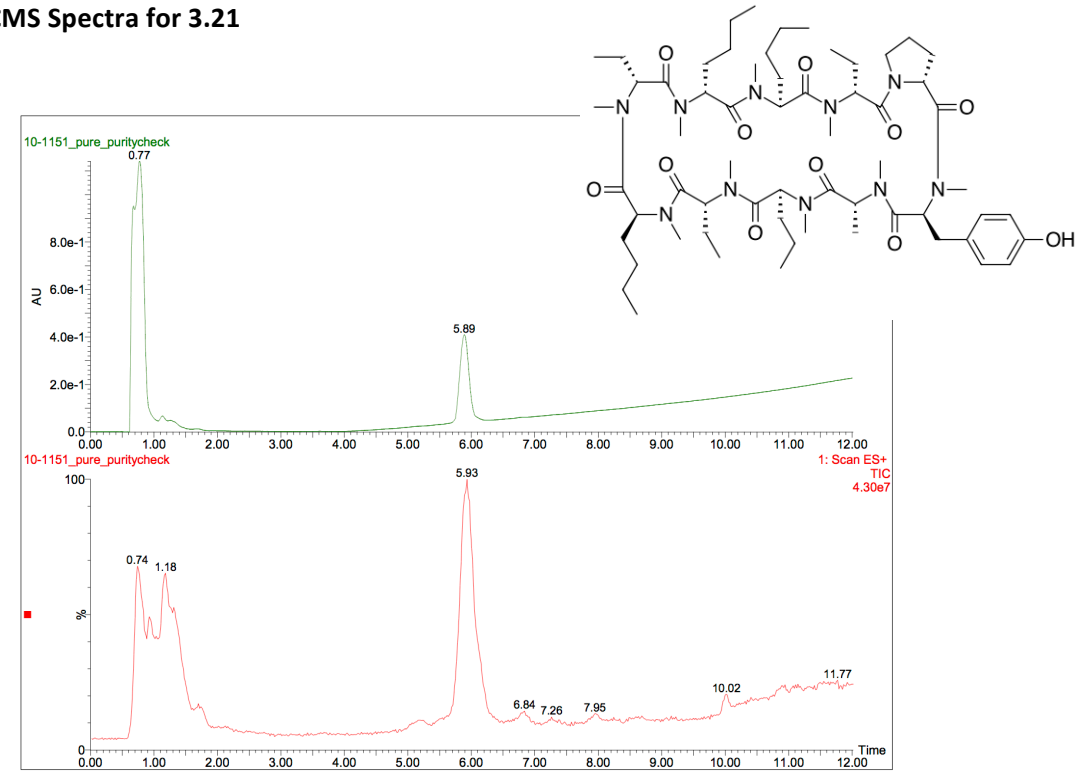

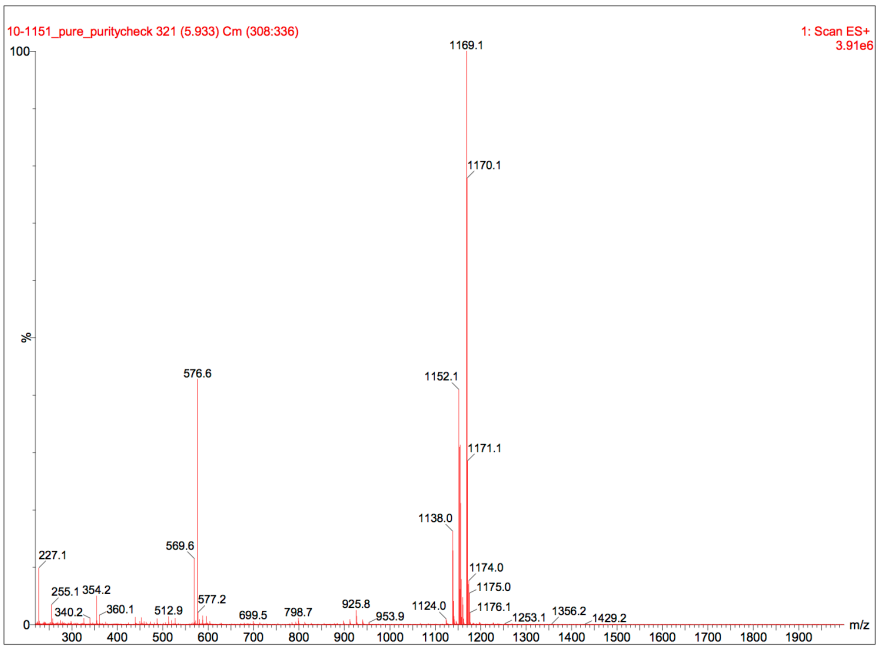

References

1. Lipinski, C. A.; Lombardo, F.; Dominy, B. W.; Feeney, P. J. *Adv. Drug Delivery Rev.* **1997**, *23*, 3–25.
2. Giordanetto, F.; Kihlberg, J. *J. Med. Chem.* **2014**, *57*, 278-295
3. Svarstad, H.; Bugge, H.C.; Dhillion, S.S. *Biodivers. Conserv.*, **2000**, *9* 1521–1541.
4. Lindholm, A.; Henricsson, S.; Lind, M.; Dahlqvist, R. *Eur. J. Clin. Pharmacol.*, **1988**, *34*, 461-464.
5. Augustijns, P.F.; Bradshaw, T.P.; Gan, L.S.L.; Hendren, R.W.; Thakker, D.R. *Biochem. Biophys. Res. Commun.*, **1993**, *197*, 360-365.
6. Chiu, Y.Y.; Higaki, K.; Neudeck, B.L.; Barnett, J.L.; Welage, L.S.; Amidon, G.L. *Pharm. Res.*, **2003**, *20*, 749-756.
7. Loosli, H.R.; Kessler, H.; Oschkinat, H.; Weber, H.P.; Petcher, T.J.; Widmer, A. *Helv. Chim. Acta*, **1985**, *68*, 682-704
8. Hyung, S.J.; Feng, X.; Che, Y.; Stroh, J.G.; Sapiro, M. *Anal. Bioanal. Chem.*, **2014**, *406*, 5785-5794.
9. Efimov, S.V.; Karataeva, F.K.; Aganov, A.V.; Berger, S.; Klochkov, V.V. *J. Mol. Struct.*, **2013**, *1036*, 298-304.
10. Lambros, M.P.; Rahman, Y.E. *Chem. Phys. Lipids*, **2004**, *131*, 63-69.
11. Krarochvil, B.; Husak, M.; Jegorov, A. *Chem. Listy*, **2001**, *95*, 9-17.
12. Augustijns, P.F.; Brown, S.C.; Wilard, D.H.; Consler, T.G.; Annaert, P.P.; Hendren, R.W.; Bradshaw, T.P. *Biochemistry*, **2000**, *39*, 7621-7630.
13. Ke, H.M.; Zhao, Y.D.; Luo, F.; Weissman, I.; Friedman, J. *Proc. Natl. Acad. Sci. U.S.A.*, **1993**, *90*, 11850-11854.

14. Shaw, R.A.; Mantsch, H.H.; Chowdhry, B.Z. *Can. J. Chem.*, **1993**, *71*, 1334-1339.

15. Ko, S.Y.; Dalvit, C. *Int. J. Pept. Protein Res.*, **1992**, *40*, 380-382.

16. Xiang, T.X.; Chen, X.; Anderson, B.D. *Biophys. J.*, **1992**, *63*, 78-88.

17. Xiang, T.X.; Anderson, B.D. *J. Chem. Phys.*, **1995**, *103*, 8666-8678.

18. Xiang, T.X.; Xu, Y.H.; Anderson, B.D. *J. Membr. Biol.*, **1998**, *165*, 77-90.

19. Leung, S.S.F.; Mijalkovic, J.; Borellie, K.; Jacobson, M.P. *J. Chem. Inf. Model*, **2012**, *52*, 1621-1636.

20. Swift, R.V.; Amaro, R.E. *J. Comput. Aided Mol. Des.*, **2011**, *11*, 1007-1017.

21. Seidler, J.; McGovern, S.L.; Doman, T.N.; Shoichet, B.K. *J. Med. Chem.*, **2003**, *46*, 4477-4486

22. Di, L.; Whitney-Pickett, C.; Umland, J.P.; Zhang, H.; Zhang, X.; Gebhard, D.F.; Lai, Y.; Federico, J.J.; Davidson, R.E.; Smith, R.; Reyner, E.L.; Lee, C.; Feng, B.; Rotter, C.; Varma, M.V.; Kempshall, S.; Fenner, K.; El-Kattan, A.F.; Liston, T.E.; Troutman, M.D. *J. Pharm. Sci.*, **2011**, *100*, 4974-4985.

23. Raschke, T.M.; Tsai, J.; Levitt, M. *Proc. Natl. Acad. Sci. U.S.A.*, **2001**, *98*, 5965-5969

24. Rizzi, L.; Cendic, K.; Vaiana, N.; Romeo, S. *Tetrahedron Lett.* **2011**, *52*, 2808-2811

25. White, T. R.; Renzelman, C. M.; Rand, A. C.; Rezai, T.; McEwen, C. M.; Gelev, V. M.; Turner, R. A.; Linington, R. G.; Leung, S. S.; Kalgutkar, A. S.; Bauman, J. N.; Zhang, Y.; Liras, S.; Price, D. A.; Mathiowetz, A. M.; Jacobson, M. P.; Lokey, R. S. *Nat Chem Biol* **2011**, *7*, 810.

26. Lam, K. S.; Salmon, S. E.; Hersh, E. M.; Hruby, V. J.; Kazmierski, W. M.; Knapp, R. J. *Nature (London, United Kingdom)* **1991**, *354*, 82.

Bibliography

Alcaide, B.; Almendros, P. *Chem. Soc. Rev.* **2001**, *30*, 226-240.

Alcaide, B.; Almendros, P.; Aragoncillo, C. *Chem Rev.* **2007**, 107, 4437-4492.

Amagata, T.; Morinaka, B. I.; Amagata, A.; Tenney, K.; Valeriote, F. A.; Lobkovsky, E.; Clardy, J.; Crews, P. *J. Nat. Prod.* **2006**, *69*, 1560.

Argoudelis, A.D.; Jahnke, H.K.; Fox, J.A. *Antimicrob. Agents Chemother.* **1961**, 191-197.

Atasoylu, O.; Furst, G.; Risatti, C.; Smith, A.B. *Org. Lett.* **2010**, *12*, 1788-1791

Augustijns, P.F.; Bradshaw, T.P.; Gan, L.S.L.; Hendren, R.W.; Thakker, D.R. *Biochem. Biophys. Res. Commun.*, **1993**, *197*, 360-365.

Augustijns, P.F.; Brown, S.C.; Wilard, D.H.; Consler, T.G.; Annaert, P.P.; Hendren, R.W.; Bradshaw, T.P. *Biochemistry*, **2000**, *39*, 7621-7630.

Avdeef, A.; Bendels, S.; Di, L.; Faller, B.; Kansy, M.; Sugano, K.; Yamauchi, Y. *J. Pharm. Sci.* **2007**, *96*, 2893.

Baker, E. N.; Hubbard, R. E. *Prog. Biophys. Mol. Biol.* **1984**, *44*, 97.

Baldwin, S.W.; Doll, T.J. *Tetrahedron Lett.* **1979**, *20*, 3275-3278.

Baldwin, J. E.; North, M.; Flinn, A. *Tetrahedron* **1988**, *44*, 637-642.

Ban, Y.; Kimura, M.; Oishi, T. *Chem. Pharm. Bull.* **1976**, *24*, 1490-1496.

Betancor, C.; Conceptión, J.I.; Hernández, R.; Salazar, J.A.; Suárez, E. *J. Org. Chem.* **1983**, *48*, 4430-4432.

Bhuyan, B.K.; Dietz, A.; Smith, C.G. *Antimicrob. Agents Chemother.* **1961**, 184-190.

Bissantz, C.; Kuhn, B.; Stahl, M. *J. Med. Chem.* **2010**, *53*, 5061.

Bockus, A. T.; McEwen, C. M.; Lokey, R. S. *Curr. Top. Med. Chem.* **2013**, *13*, 821.

Brodasky, T.F.; Lummis, W.L. *Antimicrob. Agents Chemother.* **1961**, 198-204.

Brodersen, D.E.; Clemons, W.M. Jr.; Carter, A.P.; Morgan-Warren, R.J.; Wimberly, B.T.; Ramakrishnan, V. *Cell* **2000**, *103*, 1143-1154.

Bourgeois, D.; Craig, D.; Grellepois, F.; Mondford, D.M.; Stewart, A.J.W. *Tetrahedron* **2006**, *62*, 483-495.

Carrau, R.; Hernández, R.; Suárez, E.; Betancor, C. *J. Chem. Soc. Perkin Trans.* **1987**, *1*, 937-943.

Chiu, Y.Y.; Higaki, K.; Neudeck, B.L.; Barnett, J.L.; Welage, L.S.; Amidon, G.L. *Pharm. Res.*, **2003**, *20*, 749-756.

Chow, Y.L.; Mojelsky, T.W.; Magdzinski, L.J.; Tichy, M. *Can. J. Chem.* **1985**, *63*, 2197-2202.

Cicero, D.O.; Barbato, G.; Bazzo, R. *J. Am. Chem. Soc.* **1995**, *117*, 1027-1033

Colby, D. W.; Chu, Y.; Cassady, J. P.; Duennwald, M.; Zazulak, H.; Webster, J. M.; Messer, A.; Lindquist, S.; Ingram, V. M.; Wittrup, K. D. *Proc. Natl. Acad. Sci. U. S. A.* **2004**, *101*, 17616.

Cordier, F.; Grzesiek, S. *J. Mol. Biol.* **2002**, *317*, 739.

Davies, S. G.; Fletcher, A. M.; Thomson, J. E. *Chem Commun.* **2013**, *49*, 8586-8598.

De Armas, P.; Carrau, R.; Conceptión, J.I.; Francisco, C.G.; Hernández, R.; Suárez, E. *Tetrahedron Lett.* **1985**, *26*, 2493-2496.

De Armas, P.; Francisco, C.G.; Hernández, R.; Salazar, J.A.; Suárez, E. *J. Chem. Soc. Perkin Trans.* **1988**, *1*, 3255-3265.

Dekeukeleire, S.; D'hooghe, M.; De Kimpe, N. *Pure Appl. Chem.* **2005**, *77*, 2061.

D'hooghe, M.' Dekeukeleire, S.; Leemans, E.; De Kimpe, N. *Pure Appl. Chem.* **2010**, *82*, 1749-1759.

Di, L.; Whitney-Pickett, C.; Umland, J.P.; Zhang, H.; Zhang, X.; Gebhard, D.F.; Lai, Y.; Federico, J.J.; Davidson, R.E.; Smith, R.; Reyner, E.L.; Lee, C.; Feng, B.; Rotter, C.; Varma, M.V.; Kempshall, S.; Fenner, K.; El-Kattan, A.F.; Liston, T.E.; Troutman, M.D. *J. Pharm. Sci.*, **2011**, *100*, 4974-4985.

Dinos, G.; Wilson, D.N.; Teraoka, Y.; Szaflarski, W.; Fucini, P.; Kalpaxis, D.; Nierhaus, K.H. *Mol. Cell* **2004**, *13*, 113-124.

Dobashi, K. *et al.*; *J. Antibiot.* **1986**, *39*, 1779.

Duchamp, D.J. abstract no. 23 presented at the American Crystallographic Association Winter Meeting, Albuquerque, NM, 3 to 7 April 1972.

Efimov, S.V.; Karataeva, F.K.; Aganov, A.V.; Berger, S.; Klochkov, V.V. *J. Mol. Struct.*, **2013**, *1036*, 298-304.

Erb, E.; Janda, K. D.; Brenner, S. *Proc. Natl. Acad. Sci. U. S. A.* **1994**, *91*, 11422.

Evans, D.A.; Bodkin, M.J.; Baker, S.R.; Sharman, G.J. *Magn. Reson. Chem.* **2007**, *45*, 595-600

Falb, E.; Yechezkel, T; Salitra, Y.; Gilon, C. *J. Pept. Res.* **1999**, *53*, 507-517

Feling, R.H.; Buchanan, G.O.; Mincer, T.J.; Kauffman, C.A.; Jensen, P.R.; Fenical, W. *Angew. Chem. Int. Ed.* **2003**, *42*, 355-357.

France, S.; Weatherwax, A.; Taggi, A. E.; Lectka, T. *Acc. Chem. Res.* **2004**, *37*, 592-600.

Francisco, C.G.; Herrera, A.J.; Suárez, E. *J. Org. Chem.* **2003**, *68*, 1012-1017.

Fülöp, F.; Forró, E.; Tóth, G. K. *Org. Lett.* **2004**, *6*, 4239-4241.

Gavenonis, J.; Sheneman, B. A.; Siegert, T. R.; Eshelman, M. R.; Kritzer, J. A. *Nat Chem Biol* **2014**, *10*, 716.

Gerona-Navarro, G.; de Vega, M. J. P.; García-López, M. T.; Andrei, G.; Snoeck, R.; De Clercq, E.; Balzarini, J.; González-Muñiz, R. *J. Med. Chem.* **2005**, *48*, 2612-2621.

Giordanetto, F.; Kihlberg, J. *J. Med. Chem.* **2014**, *57*, 278-295

Guimaraes, C. R.; Mathiowetz, A. M.; Shalaeva, M.; Goetz, G.; Liras, S. *J Chem Inf Model* **2012**, *52*, 882.

Hanessian, S.; Vakiti, R.R.; Dorich, S.; Banerjee, S.; Lecomte, F.; DelValle, J.R.; Zhang, J.; Deschênes-Simard, B. *Angew. Chem. Int. Ed.* **2011**, *50*, 3497-3500.

Hanessian, S.; Vakiti, R.R.; Dorich, S.; Banerjee, S.; Deschênes-Simard, B. *J. Org. Chem.* **2012**, *77*, 9458-9472.

Hernández, R.; Rivera, A.; Salazar, J.A.; Suárez, E. *Chem. Commun.* **1980**, *20*, 958-959.

Hill, T. A.; Lohman, R.-J.; Hoang, H. N.; Nielsen, D. S.; Scully, C. C. G.; Kok, W. M.; Liu, L.; Lucke, A. J.; Stoermer, M. J.; Schroeder, C. I.; Chaousis, S.; Colless, B.; Bernhardt, P. V.; Edmonds, D. J.; Griffith, D. A.; Rotter, C. J.; Ruggeri, R. B.; Price, D. A.; Liras, S.; Craik, D. J.; Fairlie, D. P. *ACS Medicinal Chemistry Letters* **2014**, *10*, 1148.

Hogan, P. C.; Corey, E. J., *J. Am. Chem. Soc.* **2005**, *127*, 15386-15387.

Hong, J.; Jing, Q.; Yao, L. *J. Biomol. NMR* **2013**, *55*, 71.

Hotoda, H.; Takahashi, M.; Tanzawa, K.; Takahashi, S.; Kaneko, M. *Tetrahedron Lett.* **1995**, *36*, 5037.

Hyung, S.J.; Feng, X.; Che, Y.; Stroh, J.G.; Sapiro, M. *Anal. Bioanal. Chem.*, **2014**, *406*, 5785-5794.

Iwatsuki, M.; Nishihara-Tsukashima, A.; Ishiyama, A.; Namatame, M.; Watanabe, Y.; Handasah, S.; Pranamuda, H.; Marwota, B.; Matsumoto, A.; Takahashi, Y.; Otoguro, K.; Ŏmura, S. *J. Antibiot.* **2012**, *65*, 169.

Jacobson, M. P.; Pincus, D. L.; Rapp, C. S.; Day, T. J. F.; Honig, B.; Shaw, D. E.; Friesner, R. A. *Proteins: Struct., Funct., Bioinf.* **2004**, *55*, 351.

Jeffrey, J.L.; Bartlett, E.S.; Sarpong, R. *Angew. Chem. Int. Ed.* **2013**, *52*, 2194–2197.

Jorgensen, W. L.; Maxwell, D. S.; TiradoRives, J. *J. Am. Chem. Soc.* **1996**, *118*, 11225.

Juraisti, E. *Enantioselective Synthesis of* β*-Amino Acids*, Wiley-VCH: New York, 1997.

Juraisti, E.; Soloshonok, V. *Enantioselective Synthesis of* β*-Amino Acids*, 2nd ed.; Wiley: New York, 2005.

Kansy, M.; Senner, F.; Gubernator, K. *J. Med. Chem.* **1998**, *41*, 1007.

Kawamoto, S. A.; Coleska, A.; Ran, X.; Yi, H.; Yang, C. Y.; Wang, S. *J. Med. Chem.* **2012**, *55*, 1137.

Ke, H.M.; Zhao, Y.D.; Luo, F.; Weissman, I.; Friedman, J. *Proc. Natl. Acad. Sci. U.S.A.*, **1993**, *90*, 11850-11854.

Kenne, E.; Renne, T. *Drug Discov Today* **2014**, *9*, 1459.

Kimura, M.; Ban, Y. *Synthesis* **1976**, 201-202.

Kisunzu, J.K.; Sarpong, R. *Angew. Chem. Int. Ed.* **2013**, *52*, 10694-10696.

Knapp, S.; Yu, Y. *Org. Lett.* **2007**, *9*, 1359-1362.

Ko, S.Y.; Dalvit, C. *Int. J. Pept. Protein Res.*, **1992**, *40*, 380-382.

Konopelski, J. P.; Boehler, M. A. *J. Am. Chem. Soc.* **1989**, *111*, 4515-4517.

Kotz, J. *SciBX* **2012**, *5*, 1.

Krarochvil, B.; Husak, M.; Jegorov, A. *Chem. Listy*, **2001**, *95*, 9-17.

Kværnø, L.; Werder, M.; Hauser, H.; Carreira, E. *J. Med. Chem.* **2005**, *48*, 6035-6053.

Lai, X.N.; Chen, C.P.; Andersen, N.H. *J. Magn. Reson., Ser. B* **1993**, *101*, 271-288

Lam, K. S.; Salmon, S. E.; Hersh, E. M.; Hruby, V. J.; Kazmierski, W. M.; Knapp, R. J. *Nature (London, United Kingdom)* **1991**, *354*, 82.

Lambros, M.P.; Rahman, Y.E. *Chem. Phys. Lipids*, **2004**, *131*, 63-69.

Lee, J.-H.; Evans, B. S.; Li, G.; Kelleher, N. L.; van der Donk, W. A. *Biochemistry* **2009**, *48*, 5054-5056.

Leemans, E.; D'hooghe, M.; Dejaegher, Y.; Törnroos, K.W.; De Kimpe, N. *J. Org Chem.* **2008**, *73*, 1422.

Leemans, E.; D'hooghe, M.; Dejaegher, Y.; Törnroos, K.W.; De Kimpe, N. *Eur. J. Org. Chem.* **2010**, 352.

Leung, S.S.F.; Mijalkovic, J.; Borellie, K.; Jacobson, M.P. *J. Chem. Inf. Model*, **2012**, *52*, 1621-1636.

Lindholm, A.; Henricsson, S.; Lind, M.; Dahlqvist, R. *Eur. J. Clin. Pharmacol.*, **1988**, *34*, 461-464.

Lipinski, C. A. *J Pharmacol Toxicol Methods* **2000**, *44*, 235.

Lipinski, C. A.; Lombardo, F.; Dominy, B. W.; Feeney, P. J. *Adv. Drug Delivery Rev.* **1997**, *23*, 3–25.

Liu, T.; Joo, S. H.; Voorhees, J. L.; Brooks, C. L.; Pei, D. *Bioorg. Med. Chem.* **2009**, *17*, 1026.

Looper, R.E.; Haussener, T.J. *Org. Lett.* **2012**, *14*, 3632-3635.

Loosli, H.R.; Kessler, H.; Oschkinat, H.; Weber, H.P.; Petcher, T.J.; Widmer, A. *Helv. Chim. Acta*, **1985**, *68*, 682-704

Lu, W.; Roongsawang, N.; Mahmud, T. *Chem. Biol.* **2011**, *18*, 425.

Ma, Y.; Qu, L.; Liu, Z.; Zhang, L.; Yang, Z.; Zhang, L. *Curr. Top. Med. Chem.* **2011**, *11*, 2906-2922.

Madden, M. M.; Muppidi, A.; Li, Z.; Li, X.; Chen, J.; Lin, Q. *Bioorg. Med. Chem. Lett.* **2011**, *21*, 1472.

Maier, T. C.; Frey, W. U.; Podlech, J. *Eur. J. Org. Chem.* **2002**, 2686-2689.

Malinowski, J.T.; McCarver, S.J.; Johnson, J.S. *Org. Lett.* **2012**, *14*, 2878-2881.

Malinowski, J.T.; Sharpe, R.J.; Johnson, J.S. *Science* **2013**, *340*, 180-182.

Malovannaya, A.; Lanz, R. B.; Jung, S. Y.; Bulynko, Y.; Le, N. T.; Chan, D. W.; Ding, C.; Shi, Y.; Yucer, N.; Krenciute, G.; Kim, B. J.; Li, C.; Chen, R.; Li, W.; Wang, Y.; O'Malley, B. W.; Qin, J. *Cell* **2011**, *145*, 787.

Matsumoto, N.; Tsujimoto, T.; Nakazaki, A.; Isobe, M.; Nishikawa, T. *RSC Adv.* **2012**, *2*, 9448-9462.

Mimieux Vaske, Y. S.; Mahoney, M. E.; Konopelski, J. P.; Rogow, D. L.; McDonald, W. J. *J. Am. Chem. Soc.* **2010**, *132*, 11379-11385.

Moellering, R. E.; Cornejo, M.; Davis, T. N.; Del Bianco, C.; Aster, J. C.; Blacklow, S. C.; Kung, A. L.; Gilliland, D. G.; Verdine, G. L.; Bradner, J. E. *Nature* **2009**, *462*, 182.

Nielsen, D. S.; Hoang, H. N.; Lohman, R. J.; Diness, F.; Fairlie, D. P. *Org Lett* **2012**, *14*, 5720.

Niggemann, J.; Bozko, P.; Bruns, N.; Wodtke, A.; Gieseler, M. T.; Thomas, K.; Jahns, C.; Nimtz, M.; Reupke, I.; Bruser, T.; Auling, G.; Malek, N.; Kalesse, M. *ChemBioChem* **2014**, *15*, 1021.

Nikishin, G.I.; Troyansky, E.I.; Lazareva, M.I. *Tetrahedron Lett.* **1985**, *26*, 3743-3744.

Ojima, I. *The Organic Chemistry of β-Lactams*; Georg, G. I., Ed.; VCH Publishers: New York, 1992; 197-255.

Ojima, I. *Acc. Chem. Res.* **1995**, *28*, 383-389.

Otoguro, K.; Iwatsuki, M.; Ishiyama, A.; Namatame, M.; Nishihara-Tukashima, A.; Shibahara, S.; Kondo, S.; Yamada, H.; Ŏmura, S. *J. Antibiot.* **2010**, *63*, 381.

Overington, J. P.; Al-Lazikani, B.; Hopkins, A. L. *Nat Rev Drug Discov* **2006**, *5*, 993.

Palomo, C.; Aizpurua, J. M.; Balentová, E.; Jimenez, A.; Oyarbide, J.; Fratila, R. M.; Miranda, J. I. *Org. Lett.* **2007**, *9*, 101-104.

Passioura, T.; Katoh, T.; Goto, Y.; Suga, H. *Annu. Rev. Biochem.* **2014**, *83*, 727.

Passioura, T.; Suga, H. *Chemistry* **2013**, *19*, 6530.

Phillips, J.C.; Braun, R.; Wang, W.; Gumbart, J.; Tajkhorshid, E.; Villa, E.; Chipot, C.; Skeel, R.D.; Kale, L.; Schulten, K. *J. Comput. Chem.* **2005**, *26*, 1781-1802

Quartararo, J. S.; Wu, P.; Kritzer, J. A. *ChemBioChem* **2012**, *13*, 1490.

Rand, A. C.; Leung, S. S. F.; Eng, H.; Rotter, C. J.; Sharma, R.; Kalgutkar, A. S.; Zhang, Y.; Varma, M. V.; Farley, K. A.; Khunte, B.; Limberakis, C.; Price, D. A.; Liras, S.; Mathiowetz, A. M.; Jacobson, M. P.; Lokey, R. S. *Med. Chem. Commun.* **2012**, *3*, 1282-1289.

Raschke, T.M.; Tsai, J.; Levitt, M. *Proc. Natl. Acad. Sci. U.S.A.*, **2001**, *98*, 5965-5969

Reddy, L.R.; Saravanan, P.; Corey, E.J. *J. Am. Chem. Soc.* **2004**, *126*, 6230-6231.

Reichert, J. M.; Dhimolea, E. *Drug Discov Today* **2012**, *17*, 954.

Rezai, T.; Bock, J.; Zhou, M.; Kalyanaraman, C.; Lokey, R.; Jacobson, M. *J. Am. Chem. Soc.* **2006**, *128*, 14073.

Rezai, T.; Yu, B.; Millhauser, G.; Jacobson, M.; Lokey, R. *J. Am. Chem. Soc.* **2006**, *128*, 2510.

Rizzi, L.; Cendic, K.; Vaiana, N.; Romeo, S. *Tetrahedron Lett.* **2011**, *52*, 2808-2811

Sax, M.; Ebert, K.; Schepmann, D.; Wibbeling, B.; Wünsch, B. *Bioorg. Med. Chem.* **2006**, *14*, 5955.

Seebach, D.; Kimmerlin, T.; Šebesta, R.; Campo, M. A.; Beck, A. K. *Tetrahedron* **2004**, *60*, 7455-7506.

Seidler, J.; McGovern, S.L.; Doman, T.N.; Shoichet, B.K. *J. Med. Chem.*, **2003**, *46*, 4477-4486

Sharpe, R.J.; Malinowski, J.T.; Johnson, J.S. *J. Am. Chem. Soc.* **2013**, *135*, 17990-17998.

Shaw, R.A.; Mantsch, H.H.; Chowdhry, B.Z. *Can. J. Chem.*, **1993**, *71*, 1334-1339.

Singh, G. S. *Tetrahedron* **2003**, *59*, 7631-7649.

Svarstad, H.; Bugge, H.C.; Dhillion, S.S. *Biodivers. Conserv.*, **2000**, *9* 1521–1541.

Swift, R.V.; Amaro, R.E. *J. Comput. Aided Mol. Des.*, **2011**, *11*, 1007-1017.

Swift, R. V.; Amaro, R. E. *Chem Biol Drug Des* **2013**, *81*, 61.

Thepchatri, P.; Cicero, D.O.; Monteagudo, E.; Ghosh, A.K.; Cornett, B.; Weeks, E.R.; Snyder, J.P. *J. Am. Chem. Soc.* **2005**, *127*, 12838-12846

Thurkauf, A.; Mattson, M.V.; Huguenin, P.N.; Rice, K.C.; Jacobson, A.E. *FEBS Lett.* **1988**, *238*, 369.

Tsujimoto, T.; Nishikawa, T.; Urabe, D.; Isobe, M. *Synlett* **2005**, *3*, 433-436.

Van Brabandt, W.; Vanwalleghem, M.; D'hooghe, M.; De Kimpe, N. *J. Org. Chem.* **2006**, *71*, 7083.

Verron, J.; Malherbe, P.; Prinssen, E.; Thomas, A.W.; Nock, N.; Masciadri, R. *Tetrahedron Lett.* **2007**, *48*, 377-380.

Villar, E. A.; Beglov, D.; Chennamadhavuni, S.; Porco, J. A., Jr.; Kozakov, D.; Vajda, S.; Whitty, A. *Nat Chem Biol* **2014**, *10*, 723.

Von Nussbaum, F.; Brands, M.; Hinzen, B.; Weigand, S.; Häbich, D. *Angew. Chem. Int. Ed.* **2006**, *45*, 5072-5129.

Waring, M.J. Bioorg. Med. Chem. Lett. 2009, 19, 2844.

Weller, D.D.; Haber, A.; Rinehart, K.L. Jr.; Wiley, P.F. *J. Antibiot.* **1978**, *31*, 997.

White, T. R.; Renzelman, C. M.; Rand, A. C.; Rezai, T.; McEwen, C. M.; Gelev, V. M.; Turner, R. A.; Linington, R. G.; Leung, S. S.; Kalgutkar, A. S.; Bauman, J. N.; Zhang, Y.; Liras, S.; Price, D. A.; Mathiowetz, A. M.; Jacobson, M. P.; Lokey, R. S. *Nat Chem Biol* **2011**, *7*, 810.

Wiley, P.F.; Jahnke, H.K.; MacKellar, F.; Kelly, R.B., Argoudelis, A.D. *J. Org. Chem.* **1970**, *35*, 1420.

Wolff, M.E. *Chem. Rev.* **1963**, *63*, 55-64.

Wrighton, N. C.; Farrell, F. X.; Chang, R.; Kashyap, A. K.; Barbone, F. P.; Mulcahy, L. S.; Johnson, D. L.; Barrett, R. W.; Jolliffe, L. K.; Dower, W. J. *Science* **1996**, *273*, 458.

Xiang, T.X.; Anderson, B.D. *J. Chem. Phys.*, **1995**, *103*, 8666-8678.

Xiang, T.X.; Chen, X.; Anderson, B.D. *Biophys. J.*, **1992**, *63*, 78-88.

Xiang, T.X.; Xu, Y.H.; Anderson, B.D. *J. Membr. Biol.*, **1998**, *165*, 77-90.

Yamashita, M.; Tsurumi, Y.; Hosoda, J.; Komori, T.; Kohsaka, M.; Imanaka, H. *J. Antibiot.* **1984**, *37*, 1279.

Yeung, C.S.; Dong, V.M. *Chem. Rev.*, **2011**, *111*, 1215–1292.

Zhang, S.; Govender, T.; Norström, T.; Arvidsson, P.I. *J. Org. Chem.* **2005**, *70*, 6918-6920

Zuckerman, N. B.; Myers, A. S.; Quan, T. K.; Bray, W. M.; Lokey, R. S.; Hartzog, G. A.; Konopelski, J. P. *ChemMedChem* **2012**, *7*, 761-765.